VNIVERSITAT DE VALÈNCIA

Aplicacions de Mètodes no Pertorbatius a la Dinàmica del Sabor

Vicent Mateu Barreda

IFIC, Departament de Física Teòrica

Tesi doctoral, Octubre de 2008

Director: Antonio Pich Zardoya

To Teresa

Contents

Introducció

Una descripció adequada per a la física no pertorbativa

Encara que pot semblar estrany començar l'escriptura d'una tesi que tracta la Cromodinàmica Cuàntica (QCD) a energies baixes sense parlar d'aspectes tals com simetria quiral, teories efectives o semblants, crec que és fonamental assentar la base sobre la qual es construiran tots els càlculs discutits en este treball.

La física no pertorbativa no es pot estudiar amb els mètodes habituals de la Teoria Quàntica de Camps (QFT), és a dir, teoria de pertorbacions. En este últim cas els diferents observables admeten una expansió en potències de la costant d'acoblament, que si se suposa petita (comparada amb la unitat) permet establir una jerarquia entre els termes de l'expansió: els termes amb potències més altes de la constant d'acoblament estan suprimits i per tant podem tallar l'expansió a un ordre donat. La QFT garanteix que els observables acompleixen tots els requisits d'una teoria quàntica relativista: microcausalitat, unitarietat, analiticitat, invariància *Poincaré*, teorema spin–estadística i descomposició en *clusters*. Estos prerequisits no defineixen unívocament la QFT, però qualsevol teoria que pretenga donar una descripció adequada de la física deu complir–los. El fet de que la física no pertorbativa no es puga estudiar amb teoria de pertorbacions a QFT no vol dir que dega ser descrita amb altres teories que no complisquen els nostres prerequisits. Per tant en esta tesi no es consideraran models per als hadrons tals com el model de quarks constituents no relativista (per suposat no es pretén fer una crítica destructiva d'estos models, que en alguns casos donen resultats sorprenenment en acord amb l'experiment).

Quina és doncs la manera adequada per a estudiar la física no pertorbativa? En principi hom pot partir dels principis fonamentals abans esmentats i amb el seu sol ús tractar d'obtindre la màxima informació possible de l'objecte que s'està estudiant. Encara que este mètode és el més general i no es compromet amb ninguna teoria, sol ser molt poc restrictiu, de tal manera que dóna propietats molt generals de l'objecte sota estudi i requereix de molta informació experimental adicional per a fer una predicció. Per tant esta idea no és gaire atractiva. Per un altra banda, tenint en compte la reflexió que fa Weinberg al seu llibre [1], a energies suficientment baixes la física quàntica relativista (a la que ens referirem genèricament com física de partícules) necessàriament ve descrita per la QFT. Per tant, encara que no es

puga aplicar la teoria de pertorbacions estàndard a la física no pertorbativa, la QFT segueix sent la descripció adequada (i pot ser, l'única possible).

El que hem discutit al paràgraf anterior sembla un poc contradictori. Tenim que emprar QFT però no el mètod estàndard de QFT. Com podem doncs fer càlculs? Ens calen els mètodes no pertorbatius de la QFT. La manera més directa de fer açò és definint la QFT desde el formalisme d'integrals de camí, però és prou més fàcil de dir que de fer. En este formalisme tots els observables es defineixen a partir d'integrals sobre totes les possibles configuracions dels camps de la teoria, pesades per l'acció clàsica exponenciada. Estes integrals (integrals de camí) són inabordables analíticament i per tant tan sols mètodes numèrics poden calcular–les (estos mètodes es coneixen com càlcus en el retícle o *lattice*). Tot i així es requereixen ordinadors molt potents, que empren grans quantitats de temps per a fer estos càlculs. Les aproximacions que es deuen fer per a aconseguir reduir el temps de computació fan que els errors associats a estos càlculs siguen grans. Este mètode és per tant, insatisfactori (encara que nous ordinadors més potents i refinaments en les tècniques de càlcul el fan més i més precís).

Hi ha doncs alguna altra possibilitat a banda de *lattice*? Afortunadament la resposta és sí. Encara que la teoria fonamental siga essencialment no pertorbativa, quan restringim el nostre estudi a un sector determinat es poden trobar paràmetres que romanen menuts en este sector. Per tant podem organitzar el nostre càlcul com una expanxió en potències creixents d'estos paràmetres i establir una jerarquia entre ells. Esta idea es manifesta plenament a les *teories efectives de camps* (EFT). En un règim (d'energies, per exemple) donat, no tots els graus de llibertat (*i.e.*, partícules) de la teoria necessiten ser considerats. Els modes pesats deuen ser integrats funcionalment de l'acció i els seus efectes es manifestaran en les constants de energies baixes (LECs). Per tant, el primer pas per a afrontar l'estudi de la física no pertorbativa és trobar els graus de llibertat efectius adients. Esta elecció normalment determina també quin és el paràmetre d'expansió.

Esta última possibilitat serà la que en la majoria dels casos emprarem per a afrontar els càlculs d'esta tesi, encara que quan calga, els combinarem adequadament amb principis axiomàtics i altres tècniques.

La teoria de les interaccions fortes

La Cromodinàmica Cuàntica (QCD) es considera la teoria fonamental que governa les interaccions fortes. Hi ha un bon grapat d'evidències teòriques i experimentals que suporten esta afirmació [2]. QCD és la teoria gauge $SU(3)_C$, és a dir una teoria que roman invariant sota transformacions *locals* del grup $SU(3)$ de color. Esta invariància implica que els transmisors de la interacció són vuit gluons, bosons de gauge sense massa d'spin 1, que es transformen com la representació adjunta del grup de gauge. El caràcter no abelià del grup $SU(3)$ implica que els gluons interactuen entre ells, o dit d'un altra manera, els gluons són portadors de la càrrega de color (al contrari que en electromagnetisme, on el fotó es elèctricament neutre). El contingut

material de la teoria són els quarks (antiquarks), partícules d'spin $\frac{1}{2}$ (fermions) que es transformen com la representació fonamental (antifonamental) del grup de gauge, i per tant es manifesten en tres colors diferents. Estos fermions són en general massius. Mentre el contingut en bosons de gauge de la teoria ve fixat pel grup de gauge, el contingut material deu ser inferit de la fenomenologia (per exemple no hi ha cap impediment teòric a incloure bosons d'spin zero transformant–se com la representació fonamental, com tampoc seria inconsistent incloure camps transformant–se com altres representacions irreductibles del grup de gauge). El nombre de quarks en la teoria (nombre de famílies) tampoc ve fixat. El model estàndard (SM) prediu que deuen aparèixer sempre en doblets [3], i experimentalment s'han trobat tres famílies:

$$\begin{pmatrix} u \\ d \end{pmatrix}, \qquad \begin{pmatrix} c \\ s \end{pmatrix}, \qquad \begin{pmatrix} t \\ b \end{pmatrix}. \tag{1}$$

El fet que siguen precisament tres famílies és un fet que encara no ha trobat una explicació teòrica satisfactòria. Nosaltres acceptarem que hi ha tres famílies i no ens preocuparem dels motius fonamentals que impliquen una (inexistent) teoria del sabor. Segons la seua massa, els quarks es poden separar en lleugers (u, d i s) i pesats (c, b i t). L'escala que separa els dos sectors es coneix com $\Lambda_{\mathrm{QCD}} \sim 1\,\mathrm{GeV}$ i es discutirà a continuació.

Concentrem–nos en el sector lleuger de QCD. En este sector és una bona aproximació suposar que la massa dels quarks és zero. D'esta manera la teoria tan sols depén d'un paràmetre, la constant d'acoblament α_s. Encara podem dir més: no hi ha en el Lagrangià de QCD cap paràmetre amb dimensions de massa. Per tant no tenim ninguna escala per a distingir energies altes de baixes (la teoria és per tant clàssicament *conforme*). Clarament la fenomenologia distingeix energies baixes (física hadrònica) d'altes (física de *jets*). La solució d'este trencaclosques la tenen els efectes quàntics. El caràcter no abelià del grup de gauge $SU(3)$ no es manifesta tan sols en les particules transmisores de la interacció. És també responsable dels fenòmens de llibertat assimptòtica i confinament. Correccions quàntiques fan que la constant d'acoblament no siga "constant" en el sentit estricte, sino més bé que depenga de l'escala d'energia. Açò soluciona els problemes anteriors: la dependència en energia d'α_s genera una escala d'energia, Λ_{QCD} (este fenòmen va ser batejat com *transmutació dimensional*) que a més trenca la simetria conforme que apareixia a nivell clàssic (a nivell del Lagrangià); el caràcter no abelià fa que α_s siga menuda per a energies altes (llibertat assimptòtica) i gran per a baixes (confinament). Per tant a energies menors que Λ_{QCD} la interacció es fa tan intensa que quarks i gluons no poden existir com a partícules lliures i es veuen "confinats" en hadrons, partícules que *sempre* es transformen com la representació trivial de $SU(3)$ (és a dir, no tenen color). Estos són els graus de llibertat assimptòtics que són observats experimentalment a energies baixes i són els que tractarem en esta tesi.

Una consequència de la grandària d'α_s a energies baixes és que no podem emprar el Lagrangià de QCD directament per als nostres càlculs en una expansió pertorbativa estàndard. Els mètodes no pertorbatius seran la ferramenta clau per a poder

calcular fenòmens relacionats amb les interaccions fortes.

Teories efectives: teoria de pertorbacions quiral

Trets fonamentals de les teories efectives

Seria correcte afirmar que les lleis de Newton son *incorrectes*? Sabem que no tenen en compte ni la relativitat especial ni la física quàntica. I les equacions de Maxwell? Ignoren els efectes quàntics de la natura. I l'equació d'Schrödinger? Encara que és una teoria quàntica considera que la velocitat de la llum és infinita. Inclús la teoria de la relativitat general, el gran llegat d'Einstein seria una teoria *errònia* al no considerar efectes quàntics, si som tant restrictius en els nostres criteris. De fet, seguint amb el mateix criteri, seria molt atrevit dir que la QFT és correcta, ja que ningú ens pot assegurar que no hi ha un altra teoria més fonamental que es manifesta plenament a energies més altes.

En esta tesi, per descomptat, no adoptarem este punt de vista tan intransigent. La mecànica clàssica newtoniana és vàlida si considerem $c = \infty$ i $\hbar = 0$, l'electrodinàmica clàssica i la relativitat assumeixen $\hbar = 0$ i la mecànica quàntica considera $c = \infty$. Per tant considerarem estes aproximacions com *teories efectives* [4, 5] d'una teoria més fonamental, més que considerar–les incorrectes. De fet, en els règims en els que estes teories són vàlides constitueixen la menera més eficient de calcular qualsevol procés físic. Al cap i a la fi no hi ha que oblidar que la física és una descripció de la natura (ens diu *com* ocorren les coses més que dir *perquè* ocorren). Per tant el terme efectiu no deu ser despreciatiu, sino més bé deu fer referència a la conveniència del càlcul.

Inclús en un escenari donat, en el que optem per una d'estes teories, podem desitjar assolir un nivell de precissió tal que els efectes quantics (o relativistes) no poden ser ignorats. Per tant hom pot, en lloc de calcular en la teoria fonamental (generalment molt més complicada) considerar correccions petites degudes a esta teoria. Per tant estes correccions es manifestaran com potències creixents de $\hbar$ (o $1/c$) de manera que podem truncar la sèrie segons la precissió desitjada. Esta és l'essència i un dels trets més fonamentals de les teories efectives: la possibilitat d'incorporar de manera organitzada correccions per a millorar la pressició dels càlculs. De fet, la teoria de pertorbacions en la constant d'acoblament es pot veure com una teoria efectiva on els efectes relativistes són exactes i els efectes quàntics apareixen com una sèrie de potències en $\hbar$.

En el marc d'una QFT, les teories efectives s'obtenen integrant funcionalment els camps pesats de l'acció. Si estem estudiant procesos a energies $E \ll \Lambda$ integrarem els graus de llibertat amb massa $M \gg \Lambda$. Els càlculs s'organitzaran com potències creixents d'energia sobre l'escala Λ. Els acoblaments dels operadors a la teoria efectiva s'obtenen pertorbativament de la teoria més fonamental. Este procediment que *a priori* pot pareixer senzill, es complica en els casos de teories fortament acoblades, com és el cas de QCD. En este cas, per sota de l'escala Λ la teoria esdevé una transició de fase, i per tant l'espectre canvia. Aixídoncs tan sols podem guiar–nos

per arguments generals com simetria : la teoria efectiva ha de tindre les mateixes simetries que la teoria fonamental, i els acoblaments del operadors no poden fixar–se.

La simetria quiral

Restringint–nos al sector lleuger de QCD, podem considerar quarks sense massa, $m_u = m_d = m_s = 0$. En este límit, el Lagrangià de QCD té una simetria (global) accidental de sabor que involucra tan sols els camps de quark. El Lagrangià és invariant sota el grup quiral $G = SU(3)_L \otimes SU(3)_R$, que transforma de manera independent els camps de quark dretans q_R i esquerrans q_L (estos camps de *Weyl* són en realitat els camps fermiònics fonamentals, que pertanyen a representacions irreductibles del grup de *Poincaré*).

Esta simetria deuria tindre un efecte sobre l'espectre de la teoria, classificant les partícules en multiplets amb aproximadament la mateixa massa corresponents a representacions irreductibles de G. En particular açò implicaria que els multiplets deurien apareixer per parells amb igual massa i paritat oposada. En la natura sí trobem multiplets aproximadament degenerats en massa, però els multiplets de paritat oposada tenen masses prou diferents. Açò fa pensar que el buit de QCD *no* és invariant sota G, fenòmen conegut com trencament espontani de la simetria. El fet de que sí es troben multiplets corresponents al grup $H = SU(3)_V$ indica que la simetria no està totalment trencada : el buit és invariant sota este subgrup $H \subset G$. Este fenòmen implica l'aparició en la teoria de vuit partícules sense massa conegudes com els bosons de Goldstone, π, K i η [6], una per cada generador que no deixa el buit invariant (corresponent als vuit generadors axials). Encara que realment els quarks tenen massa, esta és prou menuda i pot considerar–se una perturbació del cas sense masses. Açò fa que els bosons de Goldstone adquirisquen una massa (la simetria quiral està explícitament trencada per les masses dels quarks), que és molt menor que la de la resta dels hadrons de l'espectre.

A energies suficientment baixes, els bosons de Goldstone són els únics graus de llibertat dinàmics i per tant podem construir una teoria efectiva que tinga les mateixes simetries que QCD (simetria quiral espontàniament trencada, paritat i conjugació de càrrega) tan sols amb estes partícules. El formalisme general per a parametritzar els camps describint els bosons de Goldstone va ser desenvolupat per Callan, Coleman Wess i Zumino [7]. Com que les masses dels Goldstones són menudes i les energies baixes, organitzarem el càlcul en potències creixents de moments i masses sobre $\Lambda_{\rm QCD}$. Açò es tradueix en una organització del Lagrangià efectiu en termes creixents de derivades i masses, on en principi hi ha un nombre infinit de termes multiplicats per constants desconegudes. Esta teoria es coneix com Teoria de Pertorbacions Quiral (χPT) i va ser desenvolupada en les Refs. [8, 9].

Un dels trets característics de les teories efectives és que no són renormalitzables en el sentit clàssic. Calen un nombre infinit de termes per a poder absorbir les divergències generades pels loops. Com que d'entrada tenim un nombre infinit d'operadors a la nostra teoria efectiva, podem obtindre resultats finits treballant a un ordre donat en l'expansió quiral.

Expansió en $1/N_C$: Resonàncies i barions

Teoria quiral de resonàncies

Si volem extendre el rang d'energies de χPT per damunt de la ressonància més lleugera (el mesò ρ, d'spin 1), necessitem incloure explícitament camps dinàmics que creen esta i altres resonàncies. En principi açò es pot fer de manera relativament fàcil, però perdem una de les propietats més importants de χPT: l'existència d'un paràmetre menut per a organitzar el nostre càlcul. En este rang d'energies E/Λ_{QCD} no és menut, i en principi no tenim un criteri clar per a consider un operador subdominant respectre d'un altre pel fet de tindre més derivades. Tots els operadors són igualment importants. Açò és un desastre desde el punt de vista fenomenològic, ja que no hi ha manera de tindre la més mínima capacitat predictiva.

Part de la solució la trobem a l'expansió de QCD en $1/N_C$, on N_C representa el nombre de colors. 't Hooft [10] va suggerir que la teoria gauge $SU(N_C)$ amb N_C tendint a infinit presentaria simplificacions notables i al mateix temps podria descriure la fenomenologia de QCD amb tres sabors. En general hom pot estudiar este límit com una expansió en termes de $1/N_C$ on el primer terme representa el límit $N_C \to \infty$. Entre altres coses, en este límit els loops d'hadrons estan suprimits i poden en primera aproximació ser ignorats. Altres consequències son [11]:

1. Hi ha un nombre infinit de resonàncies per cada conjunt de nombres quàntics. Estes resonàncies són estables i no interactuen entre elles.

2. Els vertex d'interacció dels estats hadrònics estan suprimits com $1/\sqrt{N_C}$ per cada estat adicional.

3. A l'ordre dominant la dinàmica hadrònica es descriu mitjançant un Lagrangià efectiu amb hadrons com a graus de llibertat actius, on només contribucions a nivell arbre deuen ser considerades.

4. La anòmalia axial dessapareix i QCD és invariant sota $U(3)_L \otimes U(3)_R$.

5. Es pot demostrar que en este límit la simetria quiral es trenca espontàniament [12].

6. Els mesons són estats purs $\bar{q}q$.

Per tant, tenim un criteri d'ordenació dels operadors en el Lagrangià efectiu per a les resonàncies. Termes amb més traces de sabor i càlculs a un loop són subdominants. Encara tenim, però, un problema: no tenim cap criteri per a ordenar termes amb diferent nombre de derivades. Per a resoldre este problema tenim que imposar que la nostra teoria amb resonàncies, que en principi descriu la física en qualsevol règim energètic, empalme bé amb QCD a energies altes. Funcions de Green, factors de forma i amplituts de dispersió tendeixen a zero quan els moments es fan grans. Per tant exigirem que la descripció en termes de paràmetres hadrònics tendisquen a zero

de la mateixa manera. Este procediment es coneix com empalmament amb curtes distàncies. D'esta manera termes amb moltes derivades produiran contribucions que no tendeixen a zero en el límit de grans moments, i per tant el corresponent coeficient deu ser zero.

En la majoria de les ocasions, tractar amb un nombre infinit de resonàncies és massa ambiciós, i s'opta per considerar tan sols un nombre de resonàncies suficient per a satisfer tots els lligams que s'estan estudiant. Este procediment es coneix com *Minimal Hadronic Ansatz* (MHA). En esta tesi considerarem la torre sencera de resonàncies en alguns casos particulars. Una volta que hem exigit que els paràmetres hadrònics satisfacen QCD, podem integrar funcionalment les resonàncies per a obtindre una predicció per a les LECs del Lagrangià de χPT. Esta predicció s'anomena per saturació amb resonàncies, procediment que va ser aplicat per primera volta en Ref. [13].

Barions en l'expansió $1/\mathrm{N}_C$

Podem aprofitar l'expansió de QCD en $1/N_C$ per aprendre física bariònica? La resposta és afirmativa. L'estudi conjunt de les regles de contatge en N_C de QCD i el procés de dispersió pio–nucleó a energies baixes permet trobar relacions de consistència que deuen ser satisfetes pels operadors d'spin–sabor en el sector bariònic de QCD. Com a resultat es troba que en el límit de $N_C \to \infty$ els barions deuen satisfer una algebra $SU(2\,n_f)_c$ contreta. n_f fa referència al nombre de sabors lleugers i el 2 denota l'spin. El paràmetre que contrau l'algebra és precisament $1/N_C$. L'estudi de les relacions de consistència és pot fer emprant una representació explícita de l'algebra contreta. La base òptima per a este estudi és la donada pel model quark no relativista (encara que esta elecció no suposa cap hipòtesi del caràcter relativista dels quarks que formen el barió). Este estudi ens permet expresar propietats estàtiques de barions (tals com masses, factors de forma, moments magnètics ...) com una expansió en operadors de l'algebra d'spin–sabor, ordenats en potències creixents de $1/N_C$. I el que és més interesant, podem estudiar el trencament de simetria $SU(3)$ de sabor de manera conjunta a les correccions en $1/N_C$, ja que els dos efectes són aproximadament del mateix ordre [12].

Funcions de Green

Com ja hem comentat, a energies baixes i intermèdies els graus de llibertat efectius no són quarks i gluons, sino més bé hadrons. Per tant un càlcul on els estats assimptòtics són quarks, encara que siga a energies baixes, no té gaire trellat. El càlcul en principi és pot fer (si es troben els mètodes necessaris), però no ens ajudarà a tindre una millor comprensió de la física hadrònica a energies baixes. En l'esperit de la fórmula de reducció LSZ, podem calcular el valor esperat en el buit del producte temporalment ordenat de corrents en QCD. Estos corrents són de la forma $J_\Gamma = \bar{q}\,\Gamma\,q$, on Γ és una matriu de Dirac i de sabor (però singlet de colour), i per tant involucren

el producte de dos camps en el mateix punt de l'espai–temps. Γ determina els nombres quàntics d'spin, paritat i conjugació de càrrega, i com el corrent J_Γ conecta una determinada ressonància amb el buit, pot fer de camp interpolador per a esta. El métode més eficient per a calcular funcions de Green es coneix com el *métode dels corrents externs.*

Una manera d'obtindre informació del món hadrònic és fer un estudi de les funcions de Green en diferents règims energètics i exigir que empalmen suaument. Per a energies baixes i intermèdies ja hem discutit com afrontar estos càlculs, però, com procedir a energies altes? Hom podria pensar que a energies altes, on la constant d'acoblament és prou menuda, un càlcul pertorbatiu proporciona un resultat satisfactori, però açò no és cert. Les contribucions no pertorbatives també es manifesten a energies altes i a més d'una forma que no pot ser mai simulada per la part pertorbativa. Per exemple, per a una família de funcions de Green coneguda com a paràmetres d'ordre del trencament espontani de la simetria quiral, el càlcul pertorbatiu és zero en el límit quiral (massa dels quarks nul·la) a tots els ordres d'α_s, però açò no pot ser tota la veritat. Són precisament els efectes no pertorbatius els que fan que estes funcions de Green no siguen idénticament nul·les.

El métode emprat per a estudiar les correccions no pertorbatives a transferència de moment alta es basa en l'expansió en producte d'operadors (OPE) [15]. Esta expansió permet escriure el producte de dos (o més) operadors situats en diferents punts de l'espai–temps x i y, com una sèrie d'operadors locals definits a el punt de l'espai–temps x multiplicats per coefficients (anomenats de Wilson) que depenen de la diferència $x - y$. El primer operador de l'expansió és la identitat, que correspon al resultat pertorbatiu. Normalment hom tracta les funcions de Green a l'espai de moments, de manera que l'OPE es transforma en una expanssió en potències inverses del moment. En prendre el valor d'expectació en el buit dels operadors, en teories pertorbatives tan sols l'operador identitat dóna una contribució no nul·la. La idea de les regles de suma [16] va ser considerar que el buit de QCD és essencialment no pertorbatiu i per tant el valor d'expectació en el buit d'operadors n–ordenats no és zero. Estos elements de matriu s'anomenen condensats de buit i parametritzen el nostre desconeixement dels mecanismes no pertorbatius.

Així doncs ja tenim les ferramentes adequades per a calcular les funcions de Green en les diferents regions energètiques. Després d'exigir un empalmament suau a les regions intermèdies podrem obtindre molta informació rellevant del mecanisme d'hadronització.

Relacions de dispersió

Tal i com hem esmentat prèviament, la descripció teòrica adequada per als fenòmens no pertorbatius és la QFT. No obstant això, en moltes ocasions els principis axiomàtics de la física de partícules poden complementar la descripció en termes d'una teoria de camps. Açò pot pareixer a primera vista un poc contradictori. Com es poden complementar si tota la informació dels principis axiomàtics ja està au-

tomàticament inclosa en la QFT? La resposta és senzilla : en la majoria dels casos tan sols sabem calcular en teories de camps mitjançant una expansió (no necessàriament en la constant d'acoblament), de tal manera que els principis axiomàtics tan sols es compleixen de manera pertorbativa. Els principis axiomàtics ens proporcionen propietats que deuen complir (per exemple) les amplituts de dispersió a tots els ordres i en tots el règims energètics : són essencialment resultats no pertorbatius. Certament aquesta informació és massa suculenta per a deixar de considerar–la. En esta tesi emprarem els següents principis :

1. Simetria Poincaré. Este és el requeriment més bàsic. En primer lloc implica que en tots els processos energia i moment (és a dir, tetra–moment) són magnituds conservades. En segon lloc considerem la simetria de Lorentz (subgrup del grup de Poincaré). Tal i com deia Einstein, les equacions que governen la física s'escriuen de la mateixa manera en qualsevol sistema de referència inercial. Açò es tradueix en que l'amplitut de dispersió tan sols pot dependre de quantitats invariants Lorentz (és a dir, productes escalars).

2. Unitarietat. És el principi més intuïtiu, i bàsicament ens diu que de la probabilitat de que de la col·lisió de dos (o més) partícules es produïsca algun estat final és del 100%; i a l'inrevés, que donat un estat final, hi ha una probabilitat màxima de que es puga produir de la col·lisió d'algunes partícules. Estos requeriments es tradueixen en que la matriu de dispersió és unitària :

$$S\,S^\dagger \;=\; S^\dagger\,S \;=\; \mathbb{1}\,, \tag{2}$$

3. Simetria de creuament. Este principi relaciona les amplituts de dispersió dels processos obtesos intercanviant partícules de l'estat inicial i final (convertint–les en antipartícules). Els processos així obtesos s'anomenen canals creuats.

4. Analiticitat. Este principi és el menys intuïtiu, però és molt i molt útil. Donada una amplitut de dispersió per a un procés de dos partícules anant a dos partícules podem extraure les diferents ones parcials. Mentre l'amplitud de dispersió depén de l'energia i angles, les ones parcials tan sols depenen de l'energia (normalment emprarem l'energia total en el centre de masses, o equivalentment l'invariant relativista s). Suposant que s és una variable complexa, les ones parcials passen a ser funcions definides en el pla complex $\mathbb{C}$. Analiticitat imposa que cadascuna de les ones parcials és una funció analítica de s excepte per un tall a l'eix real positiu, necessari per a satisfer unitarietat. Com que una amplitud parcial en el canal s conté a totes les ones parcials dels canals t i u, la condició d'analiticitat es pot traduir en una condició per a l'amplitut de dispersió com a funció de s i t.

Per tant l'ús conjunt de la QFT (com a teories efectives) i els principis axiomàtics és una ferramenta fonamental per a la física no pertorbativa.

Objectius de la tesi

Totes estes tècniques tenen com a primer objectiu una major comprensió dels fenòmens no pertorbatius en general i de l'hadronització en particular. Un segon objectiu és obtindre valuosa informació de la dinàmica del sabor. Encara que en QCD el sabor és sempre conservat, les interaccions electrofebles en general violen el sabor (i també simetries discretes tals com P, C i CP) [3]. Encara que el model estàndard s'escriga en termes de quarks (i per suposat també leptons), els procesos físics ocorren entre hadrons. Normalment les interaccions febles descriuen la dessintegració d'un quark (per exemple s) en un altre quark (u) i un parell de leptons, mitjançant corrents vectorials i vector–axials. Com ja hem discutit, els estats assimptòtics son hadrons, i per tant hem de calcular elements de matriu hadrònics de corrents de quarks. El mètode dels corrents externs aplicat a les teories efectives és idoni per al seu càlcul. És per tant essencial controlar el fenòmen de l'hadronització per a poder entendre correctament les interaccions electrofebles.

Al Capítol 1 es fa una introducció a la χPT i en particular es discutirà com incloure corrents i fonts tensorials en QCD i en teories efectives. Estos corrents, a més de codificar informació important per a entendre l'estructura bariónica i la dessintegració de mesons pesats amb bellesa, apareixen de manera natural en escenaris més enllà del SM. En particular es construirà la base d'operadors d'ordres $\mathcal{O}(p^4)$ i $\mathcal{O}(p^6)$, discutint els mecanismes que fan que siga mínima i no redundant. Al Capítol 2 s'introduirà l'expansió en $1/N_C$ de QCD i com dóna lloc a la teoria de resonàncies quiral (RχT). En particular s'introduiran les fonts tensorials i les resonàncies amb nombres quàntics $J^{PC} = 1^{+-}$. També s'escriurà la base d'operadors en el sector de paritat intrínseca negativa. Al Capítol 3 s'aplicaran les tècniques de $1/N_C$ en el sector bariònic. Es trobaran les relacions de consistència i les identitats entre operadors de l'algebra d'spin–sabor. Com a aplicació calcularem els factors de forma vectorial i vector–axial tenint en compte el trencament de simetria $SU(3)$. Al Capítol 4 introduirem les funcions de Green i derivarem les diferents identitats de Ward. Es discutirà l'OPE i es calcularan les funcions de Green rellevants per a la fenomenologia en els diferents règims energètics. Al Capítol 5 emprarem els resultats anteriors per a dues aplicacions fenomenòlogiques : la desintegració radiativa del pio carregat i la determinació del paràmetre V_{us} en desintegracions semileptòniques d'hiperons. Finalment, al Capítol 6 es discutiran àmpliament les aplicacions dels principis axiomàtics de la física de partícules. Fent una anàlisi combinada amb teories efectives obtindrem, per una banda, cotes per a les LECs de χPT, i per un altra obtindrem la descripció òptima de la producció de mesons mitjançant fotons sota el llindar de producció de quatre pions.

Chapter 1

Chiral Perturbation Theory

1.1 Introduction to effective field theories

Although the ultimate goal of physics is a description of nature in terms of a fundamental theory (let us say, the theory of everything), this does not mean that in order to get a prediction for a given phenomenon we necessarily need to know that theory. Even if that theory were known (which is very unlikely to happen), it would not be sensible to employ it for describing any process that one may imagine. Moreover, the knowledge of this ultimate theory does not necessarily invalidate less fundamental theories (however, a model can indeed be invalidated by a more fundamental theory). This less fundamental theory must be regarded as a valid theory that only applies under certain conditions.

Let us illustrate this with an example. If we are interested in the description of the translational movement of the Earth around the Sun, it is of little sense to use quantum mechanics. For instance the radial excitation quantum number would have a value $n \approx 3 \times 10^{68}$, clearly pointing out that the system is utterly classic (although in principle it is not forbidden at all, it seems more sensible to use the Schrödinger equation for describing the hydrogen atom, where the radial excitation number lies between one and ten). It seems more reasonable then to assume $\hbar = 0$ and use classical mechanics. It is also an excellent approximation to use the Newtonian description (assuming then $c = \infty$) for the gravitational force and use Newton's laws (this will give us a description which is valid within a 5% accuracy). But if we want to beat that precision we need to include relativistic corrections due to the finiteness of the speed of light and the curvature of the space–time. Since this problem possesses spherical symmetry the exact analytic solution can be obtained easily, but in general this is not the case. For those more complicated cases, one can employ numerical methods and obtain the exact solution, but the lack of an analytic structure will translate into less insight into the physical situation. If the corrections are expected to be small, as it is the case for our example, there is another approach which yields to analytic solutions. We can identify a small quantity that can qualify as an expansion parameter, as for example $1/c$ (since it is more desirable to have dimensionless quantities one might choose $\beta = v/c$ with v the speed of the object

under study). Then the first term in the expansion would correspond to $c = \infty$ ($\beta = 0$) representing the Newtonian description, and the rest of the terms would correspond to the relativistic corrections. The more accurate we want our result to be, the more terms in the expansion we need to include. And what it is more important, the magnitude of the corrections decreases with the number of powers (so corrections are under control). Other usual expansion parameters are $\hbar$, $\alpha_{\rm em}$, m_e/m_p ...

From the example discussed above we learn that the appropriate choice of the theory is essential. In the case of Quantum Field Theory, though, it is compulsory to make the optimum choice of the degrees of freedom. This is so because any particle existing in the spectrum of nature, no matter how heavy it is, enters our calculations as virtual excitations from the vacuum. Since it is impossible to know the whole spectrum of particles (let alone the details of their interactions with the particles we are interested in) we need a smart way of tackling this problem. The concepts of symmetry and Effective Field Theory are the key to solve it and constitute the main tool to study the physics at energies much smaller than a typical scale. Using a more technical language, if we are interested in an energy scale $E \ll \Lambda$ we should integrate out of the action those degrees of freedom heavier than Λ (typically particles with mass higher than Λ). Those local operators remaining after the integration (in general an infinite number of them) will have the same symmetries as the underlying more fundamental theory and the effects of the degrees of freedom that have been integrated out will be encoded in the couplings. The Applequist–Carazonne theorem is the rigorous formulation of this result [17]. For the cases where the theory is known and it is weakly coupled, this integration can be performed analytically. In those cases where the fundamental theory is not known, or where the theory is strongly coupled, symmetry will be the only guidance for building the Effective Field Theory.

As a last remark, Effective Field Theories are not renormalizable in the usual, strict sense, because they have operators with dimension higher than four. This is not however a drawback, as from the very beginning we are dealing with an infinite number of operators. For the case of theories built only from symmetry principles the coefficients accompanying each operator are a priory unknown, in such a way that if we want to increase the precision of the calculations we will face more and more unknown parameters.

The theoretical issues discussed in this chapters are nicely explained in Refs. [4, 5, 18, 19].

1.2 The QCD Lagrangian and its symmetries

Nowadays Quantum Chromodynamics (QCD for short) is regarded as the theory of the strong interactions. It is the gauge theory associated to the Lie group $SU(N_C)$ where N_C stands for the number of colours. The colour degree of freedom was first introduced to account for the apparent violation of the Pauli principle in hadronic states with spin 3/2 such as $\Delta^{++}(u\,u\,u)$; then it played the röle of a quantum

number associated to a *global* symmetry (it restricts the form of the interaction). The gauge principle assumes that this symmetry is *local* and this local invariance *dictates* the form of the interacction. Gauge symmetry is a successful method to generate interactions between matter fields carried by gauge bosons (massless in the case of unbroken symmetry) ensuring its renormalizability. Furthermore, in the case of non–Abelian theories the full lot of processes is governed by a single coupling per each gauge group, for instance α_s in the case of the strong interactions. There are plenty of arguments pointing out that the number of colours is indeed three [2].

Once the symmetry group and matter content is specified, the Lagrangian is unique. In our case the building blocks are N_f (number of flavours) massive spin–1/2 particles called quarks. We will use a rather compact notation and use a single symbol q to denote an N_f–component vector column, each component having N_C different colours. The QCD Lagrangian then reads :

$$\begin{aligned}
\mathcal{L}_{QCD} &= \overline{q}\,(i\not{D} - \mathcal{M})\,q \,-\, \frac{1}{4}\,G^a_{\mu\nu}\,G^{\mu\nu}_a \,+\, \mathcal{L}_{FP} \,+\, \mathcal{L}_{GF}\,, \\
D_\mu &= \partial_\mu \,-\, i\,g_s\,G^a_\mu\,\frac{\lambda_a}{2}\,, \\
G^a_{\mu\nu} &= \partial_\mu G^a_\nu \,-\, \partial_\nu G^a_\mu \,+\, g_s\,f^{abc}\,G^b_\mu\,G^c_\nu\,, \\
\alpha_s &\equiv \frac{g_s^2}{4\,\pi}\,, \qquad a_s \equiv \frac{\alpha_s}{\pi}\,,
\end{aligned} \tag{1.1}$$

where G^a_μ are the $N_C^2 - 1$ spin–one massless gluon fields, g_s is the strong coupling constant, f^{abc} are the structure constants of the $SU(N_C)$ group and λ^a are its generators. $\mathcal{L}_{FP}$ stands for the Faddeev–Popov term and $\mathcal{L}_{GF}$ for the Gauge Fixing term, both required for a correct quantization of the theory. Two nice features of this Lagrangian are that a mass term for the gluons is forbidden and that their coupling to the fermions does not depend on the particular flavour. $\mathcal{M} = \mathrm{diag}\{m_u, m_d, m_s \ldots\}$ stands for the mass matrix, which without loss of generality can be chosen to be diagonal. Unfortunately symmetry does not constrain the value of the masses.

In order to discuss the (accidental) global symmetries of (1.1) we will restrict ourselves to the so called light sector of QCD with n_f light flavours. It comprises the u, d and s (light) quarks whose mass is much lighter than the so called *heavy* quarks (c, b and t), which will not be discussed in this thesis. It is not a bad approximation to consider their mass equal to zero (the so called chiral limit), being (1.1) reduced to

$$\mathcal{L}^0_{QCD} \,=\, i\,\overline{q}_L \not{D}\, q_L \,+\, i\,\overline{q}_R \not{D}\, q_R \,-\, \frac{1}{4}\,G^a_{\mu\nu}G^{\mu\nu}_a \,+\, \mathcal{L}_{FP} \,+\, \mathcal{L}_{GF}\,, \tag{1.2}$$

where q_L and q_R correspond to the left– and right–handed quark fields defined as [1]

$$q_{L,R} \,=\, P_{L,R}\,q\,, \qquad P_{L,R} \,=\, \frac{1}{2}\,(1 \mp \gamma_5)\,. \tag{1.3}$$

[1] In our conventions $\gamma_5 = i\,\gamma^0\gamma^1\gamma^2\gamma^3$ and $\sigma^{\mu\nu} = \frac{i}{2}\,[\gamma^\mu, \gamma^\nu]$.

Since the left– and right–handed quarks do not mix among each other, (1.2) is invariant under independent phase redefinitions and rotations for each set of chiral fields, what can be expressed in group theoretical language as an invariance under the action of the group $U_V(1) \otimes U_A(1) \otimes SU(n_f)_L \otimes SU(n_f)_R$. Quantum effects (anomalies) break the $U(1)_A$ transformations and the $U(1)_V$ symmetry is trivially realized as the baryonic number. The remaining transformations belong to the so called chiral group $G = SU(n_f)_L \otimes SU(n_f)_R$ whose elements can be written as

$$\begin{aligned} g &= \begin{pmatrix} g_L & 0 \\ 0 & g_R \end{pmatrix} = \exp \begin{pmatrix} i\,\alpha_L^a\, T_L^a & 0 \\ 0 & i\,\alpha_R^a\, T_R^a \end{pmatrix} \\ &\equiv (g_L,\, g_R) = \left[\exp\left(i\,\alpha_L^a\, T_L^a\right), \exp\left(i\,\alpha_R^a\, T_R^a\right) \right], \end{aligned} \tag{1.4}$$

being $T_{L,R}^a = \frac{\lambda^a}{2}$ the generators of the subgroups $SU(3)_{L,R}$. Its action on the quark fields is

$$q_{L,R}(x) \to g_{L,R}\, q_{L,R}(x)\,. \tag{1.5}$$

The chiral group has two obvious *invariant* subgroups $SU(3)_L$ and $SU(3)_R$ whose elements are of the type $(g_L, \mathbb{1})$ and $(\mathbb{1}, g_R)$, respectively. There is another *non–invariant* but interesting subgroup, $H = SU(3)_V$, whose elements are defined as (g_V, g_V) or equivalently $\alpha_L^a = \alpha_R^a$. We can define the *set* of axial transformations defined as $\Xi = (g_A, g_A^\dagger)$ or $\alpha_L^a = -\alpha_R^a$ that *do not* form a subgroup of G. One can take the quotient G/H but since H is not invariant the result has not the structure of a group. There is, however, a one to one correspondence between the elements of the quotient space and the elements of either $SU(3)_L$, $SU(3)_R$ or Ξ. This freedom will be exploited to find the building blocks of Chiral Perturbation Theory (χPT for short). The $2 \times (n_f^2 - 1)$ associated Noether currents, L_μ^a and R_μ^a are conserved and the corresponding charges $Q_X^a = \int \mathrm{d}^3\vec{x}\, X_0^a$ are time–independent. They satisfy the group algebra of a direct product space:

$$\left[Q_X^a, Q_Y^b\right] = i\,\delta_{XY}\, f^{abc}\, Q_X^c\,. \tag{1.6}$$

For future purposes it is better to use linear combinations of them, called the octets of vector and axial–vector currents, associated to the sets of vector and axial–vector transformations:

$$V_\mu^a(x) = R_\mu^a + L_\mu^a = \bar{q}(x)\,\frac{\lambda^a}{2}\,\gamma_\mu\, q(x)\,, \quad A_\mu^a(x) = R_\mu^a - L_\mu^a = \bar{q}(x)\,\frac{\lambda^a}{2}\,\gamma_\mu\gamma_5\, q(x)\,, \tag{1.7}$$

their associated charges satisfying the group algebra structure

$$\left[Q_{V(A)}^a, Q_{V(A)}^b\right] = i\, f^{abc}\, Q_V^c\,, \qquad \left[Q_A^a, Q_V^b\right] = i\, f^{abc}\, Q_A^c\,, \tag{1.8}$$

transforming under parity as

$$\mathcal{P}\, Q_V^a\, \mathcal{P}^{-1} = Q_V^a\,, \qquad \mathcal{P}\, Q_A^a\, \mathcal{P}^{-1} = -\, Q_A^a\,. \tag{1.9}$$

Of course they commute with the Hamiltonian of massless QCD $[Q_V^a, \mathcal{H}^0_{QCD}] = [Q_A^a, \mathcal{H}^0_{QCD}] = 0$. The electromagnetic current and the electric charge can be written as linear combinations of the octet of vector currents and charges :

$$J^\mu_{\rm em} \,=\, V_3^\mu \,+\, \frac{1}{\sqrt{3}} V_8^\mu \,\equiv\, V^\mu_{3+\frac{8}{\sqrt{3}}}\,, \qquad Q_{\rm em} = Q_3 \,+\, \frac{1}{\sqrt{3}}\, Q_8 \,\equiv\, Q_{3+\frac{8}{\sqrt{3}}}\,. \tag{1.10}$$

The vector and axial–vector currents that mediate the weak decay of hadrons are also linear combinations of the octet of currents :

$$\begin{aligned} &V_\mu^{1-i\,2}\,,\; A_\mu^{1-i\,2}\,, \qquad u \to d \quad , \\ &V_\mu^{4+i\,5}\,,\; A_\mu^{4+i\,5}\,, \qquad s \to u \quad . \end{aligned} \tag{1.11}$$

We will introduce now for future use the rest of the QCD octets of currents : scalar, pseudo–scalar and tensor currents

$$\begin{aligned} S^a(x) \,&=\, \bar q(x)\,\lambda^a\, q(x)\,, \qquad & P^a(x) \,&=\, i\,\bar q(x)\,\lambda^a\,\gamma_5\, q(x)\,, \\ T^a_{\mu\nu}(x) \,&=\, \bar q(x)\,\frac{\lambda^a}{2}\,\sigma_{\mu\nu}\, q(x)\,, \end{aligned} \tag{1.12}$$

and the singlet currents

$$\begin{aligned} V_\mu(x) \,&=\, \bar q(x)\,\gamma_\mu\, q(x)\,, \qquad & A_\mu(x) \,&=\, \bar q(x)\,\gamma_\mu\,\gamma_5\, q(x)\,, \\ S(x) \,&=\, \bar q(x)\, q(x)\,, & P(x) \,&=\, i\,\bar q(x)\,\gamma_5\, q(x)\,, \\ T_{\mu\nu}(x) \,&=\, \bar q(x)\,\sigma_{\mu\nu}\, q(x)\,. \end{aligned} \tag{1.13}$$

These comprise all independent sources because we have used a complete basis of the Dirac Algebra. We remind the reader that there is no pseudo–tensor current because of the identity [2] :

$$\sigma^{\mu\nu}\,\gamma_5 \,=\, \frac{i}{2}\,\varepsilon^{\mu\nu\lambda\rho}\,\sigma_{\lambda\rho}\,. \tag{1.14}$$

Of course one can handle with octets and singlets of currents within a single expression allowing a to take the value 0 and defining $\lambda^0 = \sqrt{2/n_f}\,\mathbb{1}_{3\times3}$. It will turn out useful to define the left– and right–handed scalar and tensor currents

$$\begin{aligned} S^a_L \,&=\, \frac{1}{2}\,(S^a + i\,P^a)\,, \qquad & T^{\mu\nu\,a}_L \,&=\, P^{\mu\nu\alpha\beta}_L\, T^a_{\alpha\beta}\,, \\ S^a_R \,&=\, \frac{1}{2}\,(S^a - i\,P^a)\,, & T^{\mu\nu\,a}_R \,&=\, P^{\mu\nu\alpha\beta}_R\, T^a_{\alpha\beta}\,, \end{aligned} \tag{1.15}$$

where $P_{L,R}$ are defined later in Eq. (1.24). It is interesting to know the derivatives of the vector and axial–vector currents when the chiral symmetry is explicitly broken. Using the identities

$$\partial_\mu(\bar q_j\,\gamma^\mu\, q_i) \,=\, i\,(m_j - m_i)\,\bar q_j\, q_i\,, \qquad \partial_\mu(\bar q_j\,\gamma^\mu\,\gamma_5\, q_i) \,=\, (m_j + m_i)\,\bar q_j\, i\,\gamma_5\, q_i\,, \tag{1.16}$$

[2] We will use the convention $\epsilon^{0123} = +1$ for the Levi–Civitá tensor $\epsilon^{\mu\nu\alpha\beta}$ throughout this thesis.

inferred from the equations of motion we get:

$$\begin{aligned}
\partial^\mu V^a_\mu(x) &= i\,\bar q(x)\left[\mathcal{M},\frac{\lambda^a}{2}\right] q(x)\,, \qquad \partial^\mu V_\mu(x) \,=\, 0\,,\\
\partial^\mu A^a_\mu(x) &= i\,\bar q(x)\left\{\mathcal{M},\frac{\lambda^a}{2}\right\}\gamma_5\, q(x)\,,\\
\partial^\mu A_\mu(x) &= 2\,i\,\bar q(x)\,\mathcal{M}\,\gamma_5\, q(x) \,+\, \frac{n_f\, g_s^2}{32\,\pi^2}\,\varepsilon_{\mu\nu\alpha\beta}\, G^{\mu\nu}_a(x)\, G^{\alpha\beta}_a(x)\,, \qquad (1.17)
\end{aligned}$$

where the gluon term in the last divergence comes from the axial anomaly. Note that in the special case of $\mathcal{M} \,=\, m\,\mathbb{1}_{n_f\times n_f}$ [that is, having exact $SU(n_f)$ symmetry] the octet–vector current is still conserved and

$$\begin{aligned}
\partial^\mu A^a_\mu(x) &= 2\,m\,P^a(x)\,,\\
\partial^\mu A_\mu(x) &= 2\,m\,P(x) \,+\, \frac{n_f\, g_s^2}{32\,\pi^2}\,\varepsilon_{\mu\nu\alpha\beta}\, G^{\mu\nu}_a(x)\, G^{\alpha\beta}_a(x)\,. \qquad (1.18)
\end{aligned}$$

1.3 The running of α_s: non–perturbative regime and confinement

In the chiral limit the QCD Lagrangian (1.2) has no energy scale. Naïvely one can think then that there is no possible distinction between long and short distances, since there is no mass scale to compare with. This is in clear contradiction with the phenomenology, which shows that at energies below one GeV QCD is a confining theory and at high energies the quarks and gluons are almost free (this is the celebrated asymptotic freedom of QCD [20, 21]). The quantum behaviour of QCD is generating an energy scale, usually denoted by $\Lambda_{\rm QCD}$.

To get a firmer grip on that idea let us have a look at the renormalization group equation of QCD at the one–loop level:

$$\begin{aligned}
-\,\frac{\mu}{\pi}\,\frac{\mathrm{d}\alpha_s}{\mathrm{d}\mu} &= \beta_{QCD}(\alpha_s) \,=\, \beta^{(1)}_{\rm QCD}\,\left(\frac{\alpha_s}{\pi}\right)^2 \,+\, \mathcal{O}(\alpha_s^3)\,,\\
\beta^{(1)}_{\rm QCD} &= \frac{11}{6}\,N_C - \frac{n_f}{3}\,. \qquad (1.19)
\end{aligned}$$

This equation is only valid in perturbation theory, that is, as we shall see, at high energies. For the physical values of n_f and N_C $\beta_{\rm QCD} > 0$, what points out that the strength of the interaction increases at low energies and decreases at high energies (a distinctive feature of non–Abelian theories). The solution of (1.19) is widely known:

$$\alpha_s(\mu) \,=\, \frac{\alpha_s(\mu_0)}{1+\dfrac{\beta^{(1)}_{\rm QCD}}{\pi}\,\alpha_s(\mu_0)\,\log\left(\dfrac{\mu}{\mu_0}\right)} \,\equiv\, \frac{\pi}{\beta^{(1)}_{\rm QCD}\,\log\left(\dfrac{\mu}{\Lambda_{QCD}}\right)}\,, \qquad (1.20)$$

where a new scale $\Lambda_{\rm QCD} \,\equiv\, \mu_0\,\exp\left[-\frac{\pi}{\beta_{QCD}\,\alpha_S(\mu_0)}\right]$ has emerged due to quantum effects. Now we have a scale to compare with and thence we are able to distinguish

between long and short distances. At the scale $\mu = M_Z = 91.12\,\text{GeV}$ the strong coupling constant has a value of $\alpha_s(M_Z) = 0.119$ small enough for perturbation theory to work. Applying the four–loop running equation and taking into account the matching factors when quark thresholds are crossed, at a typical low–energy scale $m_p \approx 1\,\text{GeV}$ one gets $\alpha_s(1\,\text{GeV}) = 0.5$. Then at low energies the coupling constant is so big that the theory becomes non–perturbative and confining. Of course in such regime Eq. (1.19) no longer applies, but we can extrapolate its behaviour to conclude that the theory becomes strongly coupled. Being non–perturbative implies that the mathematical expression of the observables does not admit an expansion as a power series in the coupling constant. Confinement means that the degrees of freedom are not quark and gluons any more, but rather hadrons.

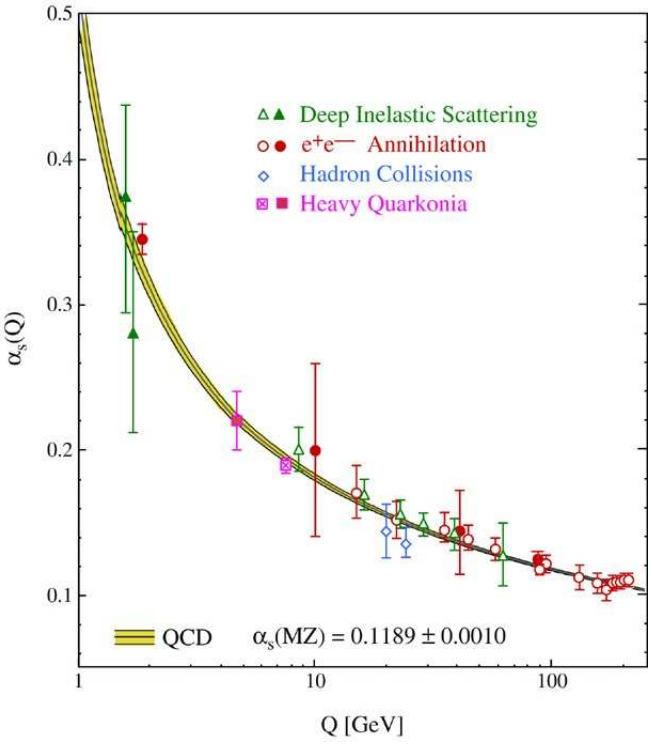

Figure 1.1: Running of the QCD strong coupling constant α_s.

1.4 QCD in the presence of external sources : transformation properties of the tensor source

As explained in this chapter, the asymptotic states of QCD are not quarks and gluons, but hadrons. Then it is of little use to calculate matrix elements with quarks as initial or final states. It makes more sense to calculate vacuum expectation values of colour singlet operators having the same quantum numbers as the hadronic states.

This objects are usually called Green functions and their discussion is relegated to Chapter 4.

There is a powerful method for computing matrix elements of operators made of quark fields in the same space–time point called the *external field method* [22]. At the same time this method ensures that the chiral Ward identities are automatically satisfied for any Green function (the concept of Ward identities will be explained in detail in Chapter 4). The idea is to extend the massless QCD Lagrangian (1.2) with external sources coupled to the different quark bilinears :

$$\begin{aligned}
\mathcal{L}_{QCD} &= \mathcal{L}^0_{QCD} + \mathcal{L}_{ext}\,, \\
\mathcal{L}_{ext} &= \bar{q}\,\gamma_\mu(v^\mu + \gamma_5\, a^\mu)\, q - \bar{q}\,(s - i\,\gamma_5\, p)\, q + \bar{q}\,\sigma_{\mu\nu}\,\bar{t}^{\,\mu\nu}\, q \\
&= \bar{q}_R\,\gamma_\mu\, r^\mu\, q_R + \bar{q}_L\,\gamma_\mu\,\ell^\mu\, q_L - \bar{q}_R\,(s + i\,p)\, q_L - \bar{q}_L(s - i\,p)\, q_R + \\
&\quad \bar{q}_L\,\sigma^{\mu\nu}\, t^\dagger_{\mu\nu}\, q_R + \bar{q}_R\,\sigma^{\mu\nu}\, t_{\mu\nu}\, q_L\,, \qquad (1.21)
\end{aligned}$$

where we have defined $r_\mu \equiv v_\mu + a_\mu$ and $\ell_\mu \equiv v_\mu - a_\mu$. The vector and axial–vector external fields are chosen to be traceless in flavour space, but the rest of them will in general have a non–vanishing trace; for instance

$$\bar{t}^{\,\mu\nu} = \sum_{a=0}^{8} \frac{\lambda^a}{2}\, \bar{t}^{\,\mu\nu}_a\,, \qquad (1.22)$$

The scalar current has been introduced with a minus sign for latter convenience (it has the same sign as the mass term). It is well known that an antisymmetric tensor $\bar{t}^{\mu\nu}$ does not correspond to an irreducible representation of the Lorentz group, moreover, it is completely reducible. So it can be decomposed into two irreducible representations using the identity [23]

$$\bar{t}^{\,\mu\nu} = P_L^{\mu\nu\lambda\rho}\, t_{\lambda\rho} + P_R^{\mu\nu\lambda\rho}\, t^\dagger_{\lambda\rho}\,, \qquad t^{\mu\nu} = P_L^{\mu\nu\lambda\rho}\, \bar{t}_{\lambda\rho}\,, \qquad (1.23)$$

where $P^{\mu\nu\lambda\rho}_{L,R}$ are the analogs of $P_{L,R}$ in Eq. (1.3) for the tensor fields, given by

$$P_R^{\mu\nu\lambda\rho} = \frac{1}{4}\,(g^{\mu\lambda}\, g^{\nu\rho} - g^{\nu\lambda}\, g^{\mu\rho} + i\,\varepsilon^{\mu\nu\lambda\rho})\,, \qquad P_L^{\mu\nu\lambda\rho} = \left(P_R^{\mu\nu\lambda\rho}\right)^\dagger\,. \qquad (1.24)$$

Actually one can check that indeed they satisfy the usual properties of chiral projectors

$$P^{\mu\nu\lambda\rho}_{R(L)}\, P_{R(L)\,\lambda\rho}^{\quad\alpha\beta} = P^{\mu\nu\alpha\beta}_{R(L)}\,, \qquad P^{\mu\nu\lambda\rho}_{L(R)}\, P_{R(L)\,\lambda\rho}^{\quad\alpha\beta} = 0\,. \qquad (1.25)$$

Eq. (1.23) above just states the fact that $t_{\mu\nu}$ and $t^\dagger_{\mu\nu}$ are the left– and right–handed projections of the tensor field and can be seen as the analog of Eq. (1.3). The six independent components of $\bar{t}^{\,\mu\nu}$ can be split in a covariant way into three left– and three right–handed components. A chiral rotation could mix v_μ with a_μ, s with p and the tensor with itself. This is precisely what one expects, since γ_5 acting on $\sigma^{\mu\nu}$ is not an independent Dirac matrix, but decomposable in terms of $\sigma^{\mu\nu}$ alone.

These external sources are $n_f \times n_f$ hermitian matrices. They are not operators but rather functions, hence they are not quantized and do not propagate. We want (1.21) to have the same symmetries as (1.2) and this imposes restrictions in the way this sources transform under either discrete symmetries (parity and charge conjugation) and the chiral group. Furthermore, we can now impose the invariance of (1.21) under *local* chiral transformations, where the transformation matrices $g_{R,L}$ now depend on the space–time point in which they are applied. Something similar is impossible to be satisfied in (1.2). It is precisely this local invariance what makes chiral Ward identities to be satisfied for any Green function at any order [22]. These transformation properties are sketched in Table 1.1.

	$G(x) = SU(3)_L \otimes SU(3)_R$	$\mathcal{P}$	$\mathcal{C}$
$s + ip$	$g_R(s + i\,p)g_L^\dagger$	$s - i\,p$	$(s - i\,p)^\top$
ℓ_μ	$g_L \ell_\mu g_L^\dagger + i\,g_L \partial_\mu g_L^\dagger$	r_μ	$-r_\mu^\top$
r_μ	$g_R r_\mu g_R^\dagger + i\,g_R \partial_\mu g_R^\dagger$	ℓ_μ	$-\ell_\mu^\top$
$t_{\mu\nu}$	$g_R\, t_{\mu\nu}\, g_L^\dagger$	$t_{\mu\nu}^\dagger$	$-t_{\mu\nu}^\top$

Table 1.1: Transformation properties of the external sources.

If one defines the generating functional, which can be regarded as the vacuum–to–vacuum transition amplitude in the presence of external fields

$$\begin{aligned}
\exp\left(i\,Z[v_\mu, a_\mu, s, p, \bar{t}_{\mu\nu}]\right) &= \int \mathcal{D}\bar{q}\,\mathcal{D}q\,\mathcal{D}G_\mu \exp\left[i \int d^4x \left\{\mathcal{L}^0_{QCD} + \mathcal{L}_{ext}(v_\mu, a_\mu, s, p, \bar{t}_{\mu\nu})\right\}\right] \\
&= \langle\, 0 \,|\, T \exp\left[\, i\,\mathcal{L}_{g.f.}(v_\mu, a_\mu, s, p, \bar{t}_{\mu\nu})\right] |\, 0 \,\rangle \\
&= \int \mathcal{D}\bar{q}\,\mathcal{D}q\,\mathcal{D}G_\mu \exp\left[i \int d^4x \mathcal{L}^0_{QCD}\right] \langle 0_{out} |\, 0_{in}\rangle_{v_\mu, a_\mu, s, p, \bar{t}_{\mu\nu}}, \qquad (1.26)
\end{aligned}$$

then Green functions are computed by functional derivatives taken with respect to the external sources.

As a last comment, we can use the external source s to explicitly introduce a symmetry breaking term due to the non–zero masses of the quarks and the external sources r_μ and ℓ_μ to break explicitly the symmetry due to electromagnetic and weak interactions :

$$\begin{aligned}
r_\mu &\to r_\mu + e\,\mathcal{Q}\,A_\mu\,, \\
\ell_\mu &\to \ell_\mu + e\,\mathcal{Q}\,A_\mu + \frac{2\,e}{\sqrt{2}\,\sin\theta_W}\left(W^\dagger\,T_+ + \text{h.c.}\right)\,, \\
s &\to s + \mathcal{M}\,, \qquad (1.27)
\end{aligned}$$

being

$$\mathcal{Q} = \begin{pmatrix} \frac{2}{3} & 0 & 0 \\ 0 & -\frac{1}{3} & 0 \\ 0 & 0 & -\frac{1}{3} \end{pmatrix}, \quad T_+ = \begin{pmatrix} 0 & V_{ud} & V_{us} \\ 0 & 0 & 0 \\ 0 & 0 & 0 \end{pmatrix}. \tag{1.28}$$

1.5 Spontaneous chiral symmetry breaking and the CCWZ formalism

Since (1.2) is invariant under global transformations of the G group, we expect the hadronic spectrum to organize itself according to irreducible representations of G. This implies the existence of an equal–mass parity partner for each particle, a situation that does not seem to occur in nature. The hadronic spectrum is however, organized as a series of irreducible representation of the group $SU(3)_V$. This indicates that we are facing the phenomenon of spontaneous breakdown of the symmetry group G into a smaller subgroup $H \subset G$, where some generators of the group G do not annihilate the vacuum of the theory (so the interaction is indeed invariant but the vacuum is not).

1.5.1 The appearance of the Goldstone bosons

In Ref. [24] it was shown that for massless QCD the ground state must be invariant under vector transformations (much as happens in quantum mechanics: the ground state of a system described by a symmetric potential has even parity) and then the vacuum is annihilated by their corresponding operators. So the chiral group $G = SU(3)_L \otimes SU(3)_R$ is spontaneously broken to $SU(3)_V$ and we can choose the axial generators to be the ones not annihilating the vacuum:

$$Q_V^a \,|\, 0 \,\rangle = 0\,, \qquad Q_A^a \,|\, 0 \,\rangle \neq 0\,. \tag{1.29}$$

The Goldstone theorem [6] tells us that there must appear a number of massless particles (the so called Goldstone bosons) equal to the number of operators that do not annihilate the vacuum (broken generators), eight in our case. We can associate these particles to the lightest pseudoscalar octet.

Let us show now that the existence of a non–vanishing scalar quark condensate implies Eq. (1.29). It can be shown that (the procedure to reach this result is relegated to the next chapters)

$$\left[Q_V^a, S^b(x)\right] = i\, f^{abc}\, S_c(x)\,, \tag{1.30}$$

and taking vacuum expectation value of this expression and using (1.29) we arrive at $\langle S_c \rangle = 0$ or $\langle \bar{u}u \rangle = \langle \bar{d}d \rangle = \langle \bar{s}s \rangle \equiv \langle \bar{q}q \rangle$. With this result we can show that

$$\left\langle\, 0 \,\middle|\, i\left[Q_A^a, P^b(x)\right] \middle|\, 0 \,\right\rangle = \frac{2}{3}\,\delta_{ab}\,\langle \bar{q}q \rangle \neq 0\,, \tag{1.31}$$

being the right–hand side of (1.31) the *order parameter* of the spontaneous breakdown of the chiral symmetry. Then the Goldstone theorem tells that there exists a set of massless states ϕ^a such that (no summation implied)

$$\langle\, 0 \,|\, A_0^a \,|\, \phi^a \,\rangle \,\langle\, \phi^a \,|\, P^a \,|\, 0 \,\rangle \;\neq\; 0\,, \tag{1.32}$$

being the quantum numbers of these states are determined by this expression. Let us first determine the parity of the Goldstone bosons [3]

$$\begin{aligned} \langle\, 0 \,|\, Q_A^a \,|\, \phi^a \,\rangle \;&=\; \big\langle\, 0 \,\big|\, \mathcal{P}^{-1}\,\mathcal{P}\,Q_A^a\,\mathcal{P}^{-1}\,\mathcal{P} \,\big|\, \phi^a \big\rangle \;=\; -\,\langle\, 0 \,|\, Q_A^a\,\mathcal{P} \,|\, \phi^a \rangle\,, \\ \mathcal{P}\,|\, \phi^a \,\rangle \;&=\; -\,|\, \phi^a \,\rangle\,, \end{aligned} \tag{1.33}$$

and now we concentrate in their transformation behaviour under an infinitesimal transformation of $SU(3)_V$:

$$\begin{aligned} \langle\, 0 \,|Q_A^a|\, \phi^a \,\rangle \;&=\; \langle\, 0 \,|\, g_V^\dagger\, g_V\, Q_A^a\, g_V^\dagger\, g_V \,|\, \phi^a \,\rangle \\ &=\; \big\langle\, 0 \,\big|\big(1 - i\,\alpha_b\, Q_V^b\big)\big(1 + i\,\alpha_b\, Q_V^b\big) Q_A^a \big(1 - i\,\alpha_b\, Q_V^b\big)\big(1 + i\,\alpha_b\, Q_V^b\big) \,\big|\, \phi^a \,\big\rangle \\ &=\; \langle\, 0 \,|Q_A^a|\, \phi^a \,\rangle \;+\; \alpha_b\, f^{abc}\, \langle\, 0 \,|Q_A^c|\, \phi^a \,\rangle + i\,\alpha_b \big\langle\, 0 \,\big|Q_A^a\, Q_V^b\big|\, \phi^a \,\big\rangle\,, \\ \big\langle\, 0 \,\big|Q_A^a Q_V^b\big|\, \phi^a \,\big\rangle \;&=\; i\, f^{abc}\, \langle\, 0 \,|Q_A^c|\, \phi^a \,\rangle \;=\; -\,i\, f^{abc}\, \langle\, 0 \,|Q_A^a|\, \phi^c \,\rangle\,, \\ Q_V^a \,\big|\phi^b\big\rangle \;&=\; i\, f^{abc}\, |\phi^c \,\rangle\,. \end{aligned} \tag{1.34}$$

So they form an octet of pseudoscalar mesons. We can parametrize the non–vanishing matrix element in Eq. (1.32) as

$$\big\langle\, 0 \,\big|\, A_\mu^a(0) \big|\, \phi^b(p) \,\big\rangle \;=\; i\, p_\mu\, F\, \delta^{ab}\,, \tag{1.35}$$

where F has dimensions of energy and its approximate value is $F \approx 92.4\,\mathrm{MeV}$. Since the axial–vector current is conserved, its matrix element between the Goldstone bosons and the vacuum must be zero

$$\big\langle\, 0 \,\big|\, \partial^\mu A_\mu^a(0) \big|\, \phi^b(p) \,\big\rangle \;=\; m^2\, F\, \delta^{ab} \;= 0\,, \tag{1.36}$$

what points out that either m or F is zero. The latter case corresponds to a symmetry realized *a la* Wigner–Weyl whereas the former corresponds to the Nambu–Goldstone realization. So, if (1.35) is not zero then the Goldstone bosons are massless.

1.5.2 The Callan–Coleman–Wess–Zumino formalism

The general formalism to parametrize the set of fields describing the dynamics of the Goldstone bosons of a system suffering spontaneous breakdown of a continuous symmetry was developed by Callan, Coleman, Wess and Zumino (CCWZ prescription) [7]. We review here the most relevant aspects. Let us consider a dimension–n_G group G being spontaneously broken to one dimension–n_H (non–invariant) subgroup

[3] We assume our vacuum state invariant under parity and transformations generated by H.

H, giving rise to $n_G - n_H$ massless Goldstone bosons. First let us show that there is an isomorphism between the Goldstone boson fields manifold $\mathcal{M}_1$ and the quotient space G/H. Let us define the transformation φ of the set of fields (or vector) ϕ of the Goldstone bosons under one element g of the group G (it will be shown that it is not a linear transformation)

$$\begin{aligned} \varphi \;&:\; G \times \mathcal{M}_1 \to \mathcal{M}_1 \,, \\ &\quad \varphi\,(g,\phi) = \phi' \,, \end{aligned} \tag{1.37}$$

satisfying [4]

$$\begin{aligned} \varphi\,(e,\phi) &= \phi \quad \forall \phi \in \mathcal{M}_1 \,, \\ \varphi\,(g_1, \varphi\,(g_2,\phi)) &= \varphi\,(g_1\, g_2, \phi) \quad \forall g_1, g_2 \in G \,,\ \forall \phi \in \mathcal{M}_1 \,. \end{aligned} \tag{1.38}$$

We then require that the origin $\phi = 0$ of $\mathcal{M}_1$ (ground state configuration) is mapped onto itself when transformed by elements $h \in H$ or $\varphi(h,0) = 0$ (and so H constitutes the little group of $\phi = 0$). With this it is clear that the origin is mapped into the same configuration field by all elements satisfying $g_1\, g_2^{-1} \in H$, that is, all elements belonging to the same left coset of H, which is one element of the quotient space G/H : $\varphi(gH,0) = \varphi(g,0)$. This defines a *one to one* (it can be shown to be invertible) mapping between the coset space and the vector space of the Goldstone bosons fields : $\phi = \varphi(f,0) = \varphi(gH,0)$ where $f \in G/H$ and can be chosen to be represented by an element $g \in f$. Then the transformation properties of the Goldstone fields under an element $\tilde{g} \in G$ read $\varphi(\tilde{g},\phi) = \varphi(\tilde{g}, \varphi(f,0)) = \varphi(\tilde{g}gH,0) = \varphi(\bar{g}H,0)$ where $\bar{g} = \tilde{g}gh$ is the representative of the element of the coset space $g\tilde{g}H$ (in general different from $g\tilde{g}$).

An easy way of understanding the formal procedure followed above is to consider the parametrization of the vector of Goldstone boson fields $\phi(x)$ as a local rotation under an element $g(x) \in G$ of the constant vacuum state $\langle\phi\rangle$ vector : $\phi(x) = g(x)\,\langle\phi\rangle$. Then the Goldstone fields are specified by $g(x)$. But since by assumption $h\,\langle\phi\rangle = \langle\phi\rangle$ for $h \in H$, two elements g_1 and g_2 satisfying $g_1 g_2^{-1} \in H$ render the same $\phi(x)$, $g_2\,\langle\phi\rangle = g_1 h\,\langle\phi\rangle = g_1\,\langle\phi\rangle$. We only need then to consider elements of G belonging to the same left coset gH to fully specify a given $\phi(x)$ configuration. Then, as stated above, to each element of G/H corresponds one field configuration ϕ.

The CCWZ prescription consists in picking a set of eight broken generators $\{A^a\}$ such that $A^a\,\langle\phi\rangle \neq 0$ and choose as a representative for each element of G/H the following $SU(3)_L \times SU(3)_R$ matrix :

$$\Xi(x) \;=\; e^{iA^a \pi^a(x)} \;=\; [\,\xi_L(x), \xi_R(x)\,] \to \phi(x) \;=\; \Xi\,(x)\,\langle\phi\rangle \;. \tag{1.39}$$

Once we select from the continuum of degenerate states with equal minimal energy one to be the vacuum, we are at the same time spontaneously breaking the symmetry and specifying the broken generators. But of course this choice is completely arbitrary and so are the broken generators (as far as we do not choose the

[4] We do not require the linear condition $\varphi(g, \lambda\,\phi) = \lambda\,\varphi(g,\phi)$.

ones generating H !). Under a global $g \in G$ transformation the $\Xi(x)$ rotates to another matrix which is not necessarily of the form (1.39), but can be written as $g\,\Xi(x) = \Xi'(x)\,h^{-1}(g,\Xi(x))$ where $\Xi'(x)$ has the form (1.39) and $h(g,\Xi(x)) \in H$ is denoted as the compensating field. It is clear that $g\,\Xi(x)\,\langle\phi\rangle = \Xi'(x)\,\langle\phi\rangle$. $h(g,\Xi(x))$ has an implicit x dependence through its dependence on $\Xi(x)$ and since it is a vector transformation can be written as $h(g,\Xi(x)) = [\,\tilde{h}(g,\Xi(x)), \tilde{h}(g,\Xi(x))\,]$. Then we can write the transformation of $\Xi(x)$ as

$$\begin{aligned} \varphi(g,\Xi(x)) &= g\,\Xi(x)\,h^{-1}(g,\Xi(x))\,, \\ \varphi_{L(R)}(g,\xi_{L(R)}(x)) &= g_{L(R)}\,\xi_{L(R)}(x)\,\tilde{h}^{-1}(g,\Xi(x))\,. \end{aligned} \tag{1.40}$$

We comment on passing that the mapping φ is a non–linear realization of the group because the matrices $\Xi(x)$ do not form a vector space (the sum of two unitary matrices is no longer unitary). The vacuum state (that is, the configuration with the Goldstone boson fields equal to zero) according to (1.39) is represented by $\Xi = \mathbb{1}$ ($\xi_L = \xi_R = \mathbb{1}$). Since we want the vacuum to be mapped onto itself by vector transformations $g_H = (g_V, g_V)$, according to (1.40) $h(g_H, \mathbb{1}) = g_H$ or $\tilde{h}(g_H, \mathbb{1}) = g_V$. One can get rid of the compensating field combining the relations of (1.40) into the simpler form $U(x) = \xi_R(x)\,\xi_L^\dagger(x)$ transforming under g as $U(x) \to g_R\,U(x)\,g_L^\dagger$, which is equivalent to choose as broken generators T_R^a or $\xi_L(x) = \mathbb{1}$, $\xi_R(x) = U(x)$ and the compensating field $\tilde{h}(g,x) = g_L$. This is denoted as the U–basis. Another possibility is to take $\Sigma(x) = U^\dagger(x) = \xi_L(x)\,\xi_R^\dagger(x)$ transforming under g as $\Sigma(x) \to g_L\,\Sigma(x)\,g_R^\dagger$, which is equivalent to choose as broken generators T_L^a or $\xi_R(x) = \mathbb{1}$, $\xi_L = \Sigma(x)$ and $\tilde{h}(g,x) = g_R$. These is to the so called Σ–basis and corresponds to the choice $\xi_R(x) = \mathbb{1}$, $\xi_L(x) = U(x)$ and the compensating field $\tilde{h}(g,x) = g_R$. Choosing the axial generators $T_L^a - T_R^a$ as the broken ones (the so called ξ–basis) corresponds to $\xi_L(x) = \xi_R^\dagger(x) \equiv \xi(x)$ transforming under g as $\xi(x) \to g_L\,\xi(x)\,\tilde{h}^{-1}(g,x) = \tilde{h}(g,x)\,\xi(x)\,g_R^\dagger$. This transformation implies that if $g_L = g_R \equiv g_V$ then $\tilde{h}(g,x) \equiv g_V$ and it is independent of $\Xi(x)$, as it happens also in the U–basis. Our preferred choice is the u–basis corresponding to the choice $T_R^a - T_L^a$ for broken generators, and $u(x) = \xi_R(x) = \xi_L^\dagger(x) = \xi^\dagger(x)$ transforming as $u(x) \to g_R\,u(x)\,\tilde{h}^{-1}(g,x) = \tilde{h}(g,x)\,u(x)\,g_L^\dagger$.

The Goldstone boson fields are angular variables and hence dimensionless. However for a field theoretical description we want them to have dimension one and so we write

$$u(x) = \exp\left[i\,\frac{\Phi(x)}{\sqrt{2}\,F}\right]\,, \tag{1.41}$$

where it can be shown that at lowest order F equals that of Eq. (1.35). The matrix $\Phi(x)$ in terms of physical fields reads

$$\Phi(x) \;=\; \sqrt{2}\sum_{a=1}^{8} T_a\,\pi^a(x) \;=\; \begin{pmatrix} \frac{1}{\sqrt{2}}\pi^0 + \frac{1}{\sqrt{6}}\eta_8 & \pi^+ & K^+ \\ \pi^- & -\frac{1}{\sqrt{2}}\pi^0 + \frac{1}{\sqrt{6}}\eta_8 & K^0 \\ K^- & \overline{K}^0 & -\sqrt{\frac{2}{3}}\eta_8 \end{pmatrix}\,. \tag{1.42}$$

Under a vector transformation of the fields $u(x) \to g_V\, u(x)\, g_V^\dagger$, the $\Phi(x) \to g_V\, \Phi\,(x) g_V^\dagger$ undergoes the same transformation, pointing it transforms as an octet. For the case of a general transformation (*e.g.* an axial transformation) the Goldstone bosons are transformed as a non–linear function of the fields.

As a final comment in the U–basis representation we can identify

$$U(x) \;=\; u(x)^2 \;=\; \exp\left[\, i\,\frac{\sqrt{2}\,\Phi(x)}{F}\right]\,, \tag{1.43}$$

and of course in the Σ–basis, $\Sigma(x) = \xi(x)^2$.

1.6 Effective Lagrangians of order $\mathcal{O}(p^2)$ and $\mathcal{O}(p^4)$

If one restricts oneself to very low energies then the only interacting particles will be the Goldstone bosons. With the ingredients discussed in the preceding section one can build a theory made only of the Goldstone boson fields as active degrees of freedom. This theory is known as Chiral Perturbation Theory and was developed in Ref. [9]. In this range of energies one can expand the observables in increasing powers of both the external momentum and quark masses, what translates into an organization of the Lagrangian in terms of an increasing number of derivatives and mass operators

$$\mathcal{L}_{\chi PT} \;=\; \sum_{n=1} \mathcal{L}_{2n}\,. \tag{1.44}$$

The range of validity of the theory is provided by a characteristic chiral symmetry breaking scale Λ_χ. When computing the chiral expansion each loop correction is accompanied by a factor $1/(4\,\pi F)^2$ giving us an estimate $\Lambda_\chi \sim 4\,\pi F \sim 1.2\,\mathrm{GeV}$ [25]. Counterterms have a typical size of the inverse of the mass of a resonance, what gives us $\Lambda_\chi \sim m_R \sim 1\,\mathrm{GeV}$. So the radius of convergence of the power expansion corresponds to the mass of the lightest resonance $m_\rho = 775\,\mathrm{MeV}$.

The calculations performed in χPT are organized in the so called Weinberg power counting [8]. Given a diagram with N_{2n} vertices from $\mathcal{L}_{2n}$ and L loops it has a chiral dimension

$$D_\chi \;=\; 2\,L \;+\; 2 \;+\; 2\sum_n N_{2n}(n-1)\,. \tag{1.45}$$

Since $n \geq 1$, D_χ is always positive. Expression (1.45) makes clear that only a finite number of terms in the Lagrangian (1.44) is needed to a given order in the chiral expansion, and then the Lagrangian behaves as a regular renormalizable theory.

1.6.1 Building blocks and $\mathcal{L}_2$

Our strategy is to find the most general Lagrangian having the same symmetries as (1.21) (local chiral symmetry, parity and charge conjugation) built with Goldstone fields described as in (1.41) and the external sources. Then the QCD generating functional (1.26) when restricted to low energies will read

$$Z(v_\mu, a_\mu, s, p, \bar{t}_{\mu\nu}) = \int \mathcal{D}U\, \mathcal{D}U^\dagger \exp\left[i \int d^4x\, \mathcal{L}_\chi(U, v_\mu, a_\mu, s, p, \bar{t}_{\mu\nu}) \right] , \qquad (1.46)$$

and the Green functions will be obtained by functional differentiation. If one works in the U–basis, the building blocks are the $U(x)$ matrix with a covariant derivative for the pion fields

$$\begin{aligned} D_\mu U = \partial_\mu U - i\, r_\mu\, U + i\, U\, l_\mu \quad &, \quad D_\mu U \to g_R\, D_\mu U\, g_L^\dagger , \\ D_\mu U^\dagger = \partial_\mu U^\dagger + i\, U^\dagger\, r_\mu - i\, \ell_\mu\, U^\dagger \quad &, \quad D_\mu U^\dagger \to g_L\, D_\mu U^\dagger\, g_R , \end{aligned} \qquad (1.47)$$

and $\chi = 2\, B_0\, (s + i\, p)$. For the right– and left–handed fields, field strength tensors arise naturally

$$\begin{aligned} &[D^\mu, D^\nu]\, X = i\, X F_L^{\mu\nu} - i\, F_R^{\mu\nu} X , \\ &F_L^{\mu\nu} = \partial^\mu \ell^\nu - \partial^\nu \ell^\mu - i\, [\ell^\mu, \ell^\nu] , \qquad F_R^{\mu\nu} = \partial^\mu r^\nu - \partial^\nu r^\mu - i\, [r^\mu, r^\nu] . \end{aligned} \qquad (1.48)$$

The set $(U, F_{L,R}^{\mu\nu}, \chi, t_{\mu\nu})$ along with their adjoints and covariant derivatives, are the building blocks to construct a theory with chiral symmetry. The next step would be to assemble them together in chiral invariant combinations which respect parity, charge conjugation and hermiticity. However, the building blocks listed above transform differently under the chiral group. This is not a problem when one is dealing with the lowest orders in the chiral expansion, where the combinatorics are simple and only a small number of operators result. However, already at next–to–leading order the number of operators involved recommends to deal with building blocks in a more efficient way. In order to easily identify the invariant operators it is better to use the ξ–basis and use a set of building blocks that transform under the G group as

$$X \to h(g, \Phi) X\, h\, (g, \Phi)^\dagger , \qquad (1.49)$$

and under discrete symmetries they transform onto $(-1)^p$ times themselves. As a result, one can define a unique covariant derivative for objects transforming as (1.49),

$$\nabla_\rho X = \partial_\rho X + [\, \Gamma_\rho, X] , \qquad \Gamma_\rho = \frac{1}{2} \left\{ u^\dagger\, (\partial_\rho - i\, r_\rho)\, u + u\, (\partial_\rho - i\, l_\rho)\, u^\dagger \right\} , \qquad (1.50)$$

where the last term is the chiral connection. The set of building blocks used in this thesis follows and their transformation properties are sketched in Table 1.2

$$\begin{aligned} u_\mu &= i \left\{ u^\dagger\, (\partial_\mu - i\, r_\mu)\, u - u\, (\partial_\mu - i\, l_\mu)\, u^\dagger \right\} \equiv i\, u^\dagger\, D_\mu U\, u^\dagger , \\ h_{\mu\nu} &= \nabla_\mu u_\nu + \nabla_\nu u_\mu , \qquad f_\pm^{\mu\nu} = u\, F_L^{\mu\nu}\, u^\dagger \pm u^\dagger\, F_R^{\mu\nu}\, u , \\ t_\pm^{\mu\nu} &= u^\dagger\, t^{\mu\nu}\, u^\dagger \pm u\, t^{\mu\nu\,\dagger}\, u , \qquad \chi_\pm = u^\dagger\, \chi\, u^\dagger \pm u\, \chi^\dagger\, u . \end{aligned} \qquad (1.51)$$

There is a field strength tensor associated to the covariant derivative, namely

$$[\nabla_\mu, \nabla_\nu]\, X \,=\, [\,\Gamma_{\mu\nu},\, X]\,, \tag{1.52}$$

with

$$\Gamma_{\mu\nu} \,=\, \partial_\mu \Gamma_\nu \,-\, \partial_\nu \Gamma_\mu \,+ [\,\Gamma_\mu, \Gamma_\nu] \,=\, \frac{1}{4}\,[u_\mu, u_\nu] \,-\, \frac{i}{2}\, f_{+\mu\nu}\,. \tag{1.53}$$

The list of elements in the left–hand side of Eq. (1.51) is complete : u_μ is self–adjoint and the combination $\nabla_\mu u_\nu - \nabla_\nu u_\mu = f_{-\nu\mu}$ is redundant. All along our analysis we will make extensive use of the tracelessness properties $\langle r_\mu \rangle = 0 = \langle F_R^{\mu\nu} \rangle$, $\langle \ell_\mu \rangle = 0 = \langle F_L^{\mu\nu} \rangle$ and $\langle u_\mu \rangle = 0 = \langle f_\pm^{\mu\nu} \rangle$.

$\mathcal{O}$	$\mathcal{P}$	$\mathcal{C}$	h.c.
u^μ	$-\,u_\mu$	$(u^\mu)^T$	u^μ
$h^{\mu\nu}$	$-\,h_{\mu\nu}$	$(h^{\mu\nu})^T$	$h^{\mu\nu}$
$\chi_\pm$	$\pm\,\chi_\pm$	$(\chi_\pm)^T$	$\pm\,\chi_\pm$
$f_\pm^{\mu\nu}$	$\pm\, f_{\pm\mu\nu}$	$\mp\,(f_\pm^{\mu\nu})^T$	$f_\pm^{\mu\nu}$
$t_\pm^{\mu\nu}$	$\pm\, t_{\pm\mu\nu}$	$-\,(t_\pm^{\mu\nu})^T$	$\pm\, t_\pm^{\mu\nu}$

Table 1.2: Various transformation properties of the elements of Eq. (1.51)

Then the lowest order Lagrangian has the simple form

$$\mathcal{L}_2 \,=\, \frac{F^2}{4}\,\langle\, u_\mu\, u^\mu + \chi_+ \,\rangle\ , \tag{1.54}$$

where $\langle \cdots \rangle$ stands for the trace in n_f flavour space. At this point several comments are in order. The tensor does not appear at this order, the vector and axial–vector sources only appear through u^μ and there is only one operator involving the scalar source. Expanding (1.54) and identifying the mass term for the Goldstone bosons we get (we assume exact isospin symmetry in this thesis)

$$2\,B_0\,\mathcal{M} \,=\, \begin{pmatrix} M_\pi^2 & 0 & 0 \\ 0 & M_\pi^2 & 0 \\ 0 & 0 & 2\,M_K^2 - M_\pi^2 \end{pmatrix}\ , \tag{1.55}$$

and computing the quark condensate we get the relation $B_0 = -\,\dfrac{\langle \overline{q} q \rangle}{F^2}$. The equations of motion at this order read

$$\nabla_\mu u^\mu \,=\, \frac{1}{2\,i}\left(\frac{\langle \chi_- \rangle}{n_f} \,-\, \chi_-\right)\ . \tag{1.56}$$

and will be used to remove redundant operators from the basis of the Lagrangians of higher dimension.

1.6.2 On the power counting for the tensor source

Let us begin by briefly reviewing the chiral counting for the remaining Dirac external fields. We have motivated the introduction of external fields coupled to QCD currents as a way to automatically ensure the chiral Ward identities when computing Green functions. For this to happen, the global chiral symmetry of the QCD Lagrangian has to be promoted to a local one. From the point of view of external fields, this step only affects the vector and axial–vector, which play the röle of chiral gauge fields entering the chiral covariant derivative, which replaces the ordinary derivative. One is then naturally led to make the chiral dimension of the vector and axial–vector sources coincide with that of the ordinary derivative, *i.e.*, v_μ, $a_\mu \sim \mathcal{O}(p)$. Furthermore, the combination $\bar{q}\,\gamma_\mu(v^\mu + \gamma_5\, a^\mu)\, q$ has no anomalous dimension [5] (as it is a piece of the QCD Lagrangian). Both vector and axial–vector currents are conserved (in the chiral limit), what in turn implies they have zero anomalous dimension. Then both vector and axial–vector sources have no anomalous dimension. Notice that no reference to the actual physical meaning of the sources was needed : gauge invariance is enough and the sources can be regarded as formal entities.

However, for scalar and pseudoscalar sources the situation changes. In order to motivate their chiral scaling contact has to be made with QCD through quark masses. Quark masses are formally introduced as external scalar sources, and chiral invariance groups the scalar and pseudoscalar densities in the combination $\chi = 2\,B_0\,(s + i\,p)$ (and its hermitian conjugate), where B_0 can be seen as a coupling required by naïve dimensional analysis. At the sight of Eq. (1.55) one is naturally led to consider $\chi \sim m_\pi^2 \sim \mathcal{O}(p^2)$. This scaling assignment is of course subject to assuming $B_0 \gg F$, which seems to be the picture supported by phenomenology. Again the combination $\bar{q}\,(s - i\,\gamma_5\, p)\, q$ is renormalization invariant. The anomalous dimension of the scalar and pseudoscalar currents is known to be the opposite of that of the quark mass. Then the running of s and p coincides with the running of the quark mass. Since combination $B_0\, m_q$ is renormalization invariant $\chi = 2\,B_0(s + i\,p)$ is also invariant.

Therefore, gauge symmetry alone motivates the scaling for vector and axial–vector sources, whereas the momentum scaling for scalars and pseudoscalars is suggested by the way chiral symmetry is broken.

Let us examine the situation for tensor sources. The tensor field coupled to $\bar{q}\,\sigma_{\mu\nu}\, q$ induces a chirality flip (much like scalars and pseudoscalars do) and therefore transforms in the same way under a chiral transformation. However, unlike scalars and pseudoscalars, tensor fields do not have a physical realization as symmetry breaking terms in the chiral Lagrangian. Their chiral power counting is therefore not motivated by physical arguments and should be seen only as a formal theoretical tool to compute Green functions. Whatever choice is made for the chiral counting, however, it will only affect the way operators with different number of tensor sources are organized in the chiral expansion, but it will not affect the chiral expansion of each different Green function. A convenient choice is to assign the tensor source

[5] The concept of anomalous dimension will be discussed in Chapter 4.

with the same chiral counting as the scalar and pseudo–scalar sources, *i.e.*, $\mathcal{O}(p^2)$. This has two main advantages: (a) the tensor source only generates even terms in the chiral expansion, and therefore does not change the standard chiral counting scheme; (b) operators involving resonance exchange appear at $\mathcal{O}(p^4)$ [26], leaving only universal terms at $\mathcal{O}(p^2)$.

Since we are assigning the same chiral counting to all spin–flipping sources s, p and $t_{\mu\nu}$, one could equally well define, by analogy to $\chi = 2\,B_0\,(s+i\,p)$, a tensor chiral field $\tau_{\mu\nu}$ related to our tensor fields $t_{\mu\nu}$ by $\tau_{\mu\nu} = b_0\,t_{\mu\nu}$. Here b_0 would be the analog of B_0 for tensor fields. Another advantage of introducing the dimensionful parameter b_0 is that all the low–energy couplings at a given order in the chiral expansion then have the same mass dimension. For instance, at $\mathcal{O}(p^4)$, the complete set of chiral low energy couplings

$$L_i,\;\; i = 1, \cdots, 10\,; \qquad H_1,\, H_2\,; \qquad \lambda_j,\;\; j = 1, \cdots, 4, \tag{1.57}$$

are dimensionless, where λ_j are defined in terms of the Λ_j of Eq. (1.62) as $\Lambda_j \,=\, b_0^n\,\lambda_j$, n being the number of tensor sources in the associated operators. For instance, $\Lambda_1 \,=\, b_0\,\lambda_1$ but $\Lambda_3 \,=\, b_0^2\,\lambda_3$.

Again the combination $\bar{q}\,\sigma_{\mu\nu}\,\bar{t}^{\mu\nu}\,q$ has zero anomalous dimension, but unfortunately the running of the tensor current can only be calculated in the perturbative regime. This can be better understood by means of a renormalization group analysis (all these concepts will be explained in Chapter 4). For the tensor current,

$$\mu\,\frac{\mathrm{d}}{\mathrm{d}\mu}\,T^a_{\alpha\beta} \;=\; -\,\gamma_T\,T^a_{\alpha\beta}\,, \tag{1.58}$$

where γ_T is the tensor anomalous dimension. In the high–momentum transfer regime ($\mu \,\gg\, \Lambda_{QCD}$), the anomalous dimension can be computed at leading order to give (see Chapter 4)

$$\gamma_T \;=\; C_F\,\frac{\alpha_s}{2\,\pi} \,+\, \mathcal{O}(\alpha_s^2)\,. \tag{1.59}$$

Invariance of the QCD Lagrangian implies that the tensor external source $\bar{t}_{\mu\nu}$ has to evolve as

$$\mu\,\frac{\mathrm{d}}{\mathrm{d}\mu}\,\bar{t}^a_{\alpha\beta} \;=\; \gamma_T\,\bar{t}^a_{\alpha\beta}\,. \tag{1.60}$$

Consider now a term in the χPT Lagrangian with n tensor sources, $\Lambda^{(n)}\,\mathcal{A}_n(\bar{t}_{\mu\nu})$. When related to QCD parameters, the low energy coupling $\Lambda^{(n)}$ will pick the QCD scale dependence. Defining $\tau_{\mu\nu} = b_0\,\bar{t}_{\mu\nu}$, the term can now be written as $\Lambda^{(n)}\,\mathcal{A}_n(\bar{t}_{\mu\nu}) = \lambda^{(n)}\,\mathcal{A}_n(\tau_{\mu\nu}) = b_0^n\,\lambda^{(n)}\,\mathcal{A}_n(\bar{t}_{\mu\nu})$. Therefore $\Lambda^{(n)} = b_0^n\,\lambda^{(n)}$ and all the QCD scale dependence is contained in b_0, namely

$$\mu\,\frac{\mathrm{d}}{\mathrm{d}\mu}\,b_0 \;=\; -\,\gamma_T\,b_0\,. \tag{1.61}$$

This is in complete analogy to the röle played by B_0 in the scalar–pseudoscalar sector. This analogy can be best illustrated with the example of Section 1.9.

1.6.3 The order $\mathcal{O}(p^4)$ Lagrangian

Operators containing tensor sources appear for the first time at $\mathcal{O}(p^4)$, together with a new set of operators. At this order one obtains operators that only depend on the external sources and have no Goldstone boson dependence. These are called contact terms and contain no dynamics, are needed only to renormalize the theory. Also one gets a different number of independent operators depending on the number of flavours considered, due to the Cayley–Hamilton theorem discussed in Appendix A. For three flavours it reads:

$$\begin{aligned}
\mathcal{L}_4 \;=\;& L_1 \langle u_\mu u^\mu\rangle^2 + L_2 \langle u_\mu u^\nu\rangle\langle u^\mu u_\nu\rangle + L_3 \langle u_\mu u^\mu u_\nu u^\nu\rangle + L_4 \langle u_\mu u^\mu\rangle\langle\chi_+\rangle \\
&+ L_5 \langle u_\mu u^\mu \chi_+\rangle + L_6 \langle\chi_+\rangle^2 + L_7 \langle\chi_-\rangle^2 + L_8/2 \left\langle\chi_+^2+\chi_-^2\right\rangle \\
&- i\, L_9 \langle f_+^{\mu\nu} u_\mu u_\nu\rangle + L_{10}/4 \langle f_{+\mu\nu} f_+^{\mu\nu} - f_{-\mu\nu} f_-^{\mu\nu}\rangle \\
&+ i\, L_{11} \langle\chi_-(\nabla_\mu u^\mu + i/2\,\chi_-)\rangle - L_{12} \left\langle(\nabla_\mu u^\mu + i/2\,\chi_-)^2\right\rangle \\
&+ \Lambda_1 \langle t_+^{\mu\nu} f_{+\mu\nu}\rangle - i\,\Lambda_2 \langle t_+^{\mu\nu} u_\mu u_\nu\rangle + \Lambda_3 \langle t_+^{\mu\nu} t_{\mu\nu}^+\rangle + \Lambda_4 \langle t_+^{\mu\nu}\rangle^2 \\
&+ H_1/2 \langle f_{+\mu\nu} f_+^{\mu\nu} + f_{-\mu\nu} f_-^{\mu\nu}\rangle + H_2/4 \left\langle\chi_+^2 - \chi_-^2\right\rangle ,
\end{aligned} \tag{1.62}$$

where the operators proportional to L_{11} and L_{12} vanish when using the equations of motion and the terms proportional to H_1 and H_2 are contact terms. They can be rewritten in the U–basis to make them manifestly independent of the Goldstone boson fields: $H_1 \langle F_L^{\mu\nu} F_{L\mu\nu} + F_R^{\mu\nu} F_{R\mu\nu}\rangle + H_2 \left\langle\chi\chi^\dagger\right\rangle$. The terms Λ_{1-4} have tensor sources and since they appear for the first time do not require renormalization. It is interesting to remark that a potential contact term like $t^{\mu\nu} t^\dagger_{\mu\nu}$ cancels identically due to orthogonality of chiralities, as can be easily checked using the chiral projectors of Eq. (1.23). Hence, it follows that $t_+^{\mu\nu}\, t^+_{\mu\nu} = t_-^{\mu\nu}\, t^-_{\mu\nu}$ and $t_+^{\mu\nu}\, t^-_{\mu\nu} = t_-^{\mu\nu}\, t^+_{\mu\nu}$. These relations have been used in deriving Eq. (1.62) and will be used hereafter. When computing loop diagrams with the operators contained in the Lagrangian (1.54) divergences will occur and must be *regularized*. Using dimensional regularization one does not spoil the symmetries of the theory and then the counterterms needed to *renormalize* the divergences are contained in (1.62). This leads to a splitting of the couplings of (1.62) into a divergent part and a finite part, called renormalized coupling. Since this splitting is arbitrary it will lead to a dependence of the renormalized coupling on an arbitrary scale μ:

$$\begin{aligned}
L_i &= L_i^r(\mu) + \Gamma_i \frac{\mu^{D-4}}{32\,\pi^2}\left\{\frac{2}{D-4} + C\right\} \\
H_i &= H_i^r(\mu) + \tilde{\Gamma}_i \frac{\mu^{D-4}}{32\,\pi^2}\left\{\frac{2}{D-4} + C\right\} ,
\end{aligned} \tag{1.63}$$

where $D = 4 - 2\,\epsilon$ is the space–time dimension and C is a constant that fixes the renormalization scheme[6]. One has to take into account that in D dimensions, the $\mathcal{O}(p^4)$ L_i LECs have energy dimension of E^{D-4}. Since each term in Eq. (1.63) must

[6] In this thesis we will regularize loops in dimensional regularization, defining $\epsilon = \frac{4-D}{2}$.

have the same energy dimension, we have to multiply the second term by μ^{D-4}, where μ is an arbitrary parameter with mass dimension (the chiral scale). Since L_i does not depend on μ, the μ dependence of L_i^r is canceled by the divergent piece. In χPT the usual choice is $C = \gamma_E - \log(4\,\pi) - 1$ where $\gamma_E \simeq 0.5772$ is the Euler constant, and the so called $\overline{\rm MS}$ scheme is defined by the choice $C = \gamma_E - \log(4\pi)$. Eq. (1.63) also dictates the running of the renormalized piece:

$$\mu\,\frac{{\rm d}L_i^r(\mu)}{{\rm d}\mu} \;=\; -\,\Gamma_i\,\frac{1}{16\,\pi^2}\,. \tag{1.64}$$

The explicit calculation of the one–loop generating functional gives [9]:

$$\Gamma_1 = \tfrac{3}{32},\quad \Gamma_2 = \tfrac{3}{16},\quad \Gamma_3 = 0,\quad \Gamma_4 = \tfrac{1}{8},\qquad \Gamma_5 = \tfrac{3}{8},\qquad \Gamma_6 = \tfrac{11}{144},$$

$$\Gamma_7 = 0,\qquad \Gamma_8 = \tfrac{5}{48},\quad \Gamma_9 = \tfrac{1}{4},\quad \Gamma_{10} = -\,\tfrac{1}{4},\quad \tilde{\Gamma}_1 = -\,\tfrac{1}{8},\quad \tilde{\Gamma}_2 = \tfrac{5}{24}.$$

Observables are written in terms of the renormalized couplings $L_i^r(\mu)$ and are of course μ–independent.

1.7 The $\mathcal{O}(p^6)$ Lagrangian with tensor sources

At next–to–next–to–leading order $\mathcal{O}(p^6)$, the number of operators increases dramatically. For the sector without tensor sources the full set of operators in the U–basis was first found in [27]. Latter, in [28] it was found that the set was not minimal and a new one written in the u–basis for two and three flavours was given.

In Ref. [23] this list of operators was enlarged to include also operators with tensor sources. The purpose of this section is to sketch the steps followed in reaching the basis of chiral invariant operators listed in Table B.1, in Appendix B. In particular, we will outline the strategies followed to reduce the set of operators to a non–redundant minimal one, focusing on the results obtained rather than giving the technical details, which can be found in [27, 28].

The full set of $\mathcal{O}(p^6)$ operators which results from combining the building blocks of Eq. (1.51) and their covariant derivatives falls into one of the following generic groups

$$\begin{array}{ccc}
t_{\mu\nu}\,t^{\mu\nu}\,u_\alpha\,u^\alpha\,; & t_{\mu\nu}\,f^{\mu\nu}\,\chi\,; & t_{\mu\nu}\,t^{\mu\nu}\,\chi\,; \\
t_{\mu\nu}\,\chi\,u^\mu\,u^\nu\,; & t_{\mu\nu}\,f^{\mu\rho}\,f^\nu_{\ \rho}\,; & t_{\mu\nu}\,t^{\nu\rho}\,h^\mu_{\ \rho}\,; \\
t_{\mu\nu}\,h^{\nu\rho}\,u_\rho\,u^\mu\,; & t_{\mu\nu}\,h^{\mu\alpha}\,h^\nu_{\ \alpha}; & t_{\mu\nu}\,t^{\nu\rho}\,f^\mu_{\ \rho}\,; \\
t_{\mu\nu}\,f^{\mu\nu}\,u_\alpha\,u^\alpha\,; & t^{\mu\nu}\,\chi_\mu\,u_\nu\,; & t_{\mu\nu}\,t^{\mu\rho}\,t^\nu_{\ \rho}\,; \\
\nabla_\rho t_{\mu\nu}\,\nabla^\rho t^{\mu\nu}\,; & t_{\mu\nu}\,h^{\mu\alpha}\,f^\nu_{\ \alpha}\,; & \nabla_\mu t^{\mu\nu}\,\nabla^\alpha f_{\alpha\nu}\,; \\
\nabla_\rho t_{\mu\nu}\,h^{\mu\rho}\,u^\nu\,; & \nabla^\mu t_{\mu\nu}\,f^{\nu\rho}\,u_\rho\,; & \nabla_\lambda t^{\mu\nu}\,t_{\mu\nu}\,u^\lambda\,; \\
 & t_{\mu\nu}\,u_\alpha\,u^\mu\,u^\nu\,u_\alpha\,; &
\end{array} \tag{1.65}$$

where emphasis has been placed only on operator combinations, *i.e.*, traces and i factors have been omitted and $\pm$ subscripts have been skipped for simplicity. The previous list is however complete in the sense that it contains all the independent operator combinations. For instance, operators like $\nabla^\lambda t_{\mu\nu}\,\nabla_\lambda\chi$ are generically C–violating and $\nabla^\mu t_{\mu\nu}\,u^\nu\,u_\alpha\,u^\alpha$ or $t^{\mu\nu}\,\nabla^\lambda f_{\mu\nu}\,u_\lambda$ can be shown to be redundant using partial integration and the chain rule.

Table B.1 lists the full set of hermitian operators invariant under parity and charge conjugation, organized in blocks of operators below each of the representatives of Eq. (1.65).

Obviously, the most challenging task in going from Eq. (1.65) above to our final set of operators in Table B.1 is to make sure that the set is minimal, *i.e.*, linearly dependent operators have been removed and we can talk of a true chiral basis of operators. In the following we will discuss the commonly used strategies, namely integration by parts, use of the equations of motion [7] and the Bianchi identity.

1.7.1 Partial integration and equations of motion

Integration by parts was already used to obtain Eq. (1.65). The list can be further reduced, however, if one notices that the covariant derivatives of u_μ satisfy

$$\nabla_\mu u_\nu \;=\; \frac{1}{2}\,(h_{\mu\nu} - f_{-\mu\nu})\;. \tag{1.66}$$

If we combine Eqs. (1.66) and (1.56) with integration by parts we find the following relations,

$$\begin{aligned}
i\,\{\nabla_\lambda t_-^{\mu\nu}, t_{+\mu\nu}\}\,u^\lambda &= -\,i\,\{\nabla_\lambda t_+^{\mu\nu}, t_{-\mu\nu}\}\,u^\lambda + t_+^{\mu\nu}\,t_{-\mu\nu}\,\chi_- - \frac{1}{n_f}\,t_+^{\mu\nu}\,t_{-\mu\nu}\langle\,\chi_-\rangle\,,\\
i\,\{\nabla_\mu t_-^{\mu\nu}, t_{+\nu\lambda}\}\,u^\lambda &= -\,i\,\{\nabla^\lambda t_+^{\mu\nu}, t_{-\nu\lambda}\}\,u_\mu + \frac{i}{2}\,\{t_{+\nu}^\mu, t_{-\mu\alpha}\}\,h^{\nu\alpha} + \frac{i}{2}\,\{t_{+\nu}^\mu, t_{-\mu\alpha}\}\,f_-^{\nu\alpha}\,,\\
i\,\{\nabla_\mu t_+^{\mu\nu}, t_{-\nu\lambda}\}\,u^\lambda &= -\,i\,\{\nabla^\lambda t_-^{\mu\nu}, t_{+\nu\lambda}\}\,u_\mu + \frac{i}{2}\,\{t_{+\nu}^\mu, t_{-\mu\alpha}\}\,h^{\nu\alpha} - \frac{i}{2}\,\{t_{+\nu}^\mu, t_{-\mu\alpha}\}\,f_-^{\nu\alpha}\,,
\end{aligned} \tag{1.67}$$

where in the first line the lowest–order equations of motion of Eq. (1.56) were used. The second and third relations follow from Eq. (1.66).

Further relations can be found using the properties of the chiral connection listed in Eqs. (1.52) and (1.53). In particular,

$$\begin{aligned}
\nabla^\lambda t_{\lambda\nu}^+\nabla_\rho t_+^{\rho\nu} - \nabla^\rho t_{\lambda\nu}^+\nabla^\lambda t_+^{\rho\nu} &= [\,\Gamma^{\lambda\rho}, t_\lambda^{+\nu}\,]\,t_{\rho\nu}^+ \;=\; -\,\frac{1}{2}\,Y_{11} + \frac{1}{2}\,Y_{12} + Y_{89}\,,\\
\nabla^\lambda t_{\lambda\nu}^-\nabla_\rho t_-^{\rho\nu} - \nabla^\rho t_{\lambda\nu}^-\nabla^\lambda t_-^{\rho\nu} &= [\,\Gamma^{\lambda\rho}, t_\lambda^{-\nu}\,]\,t_{\rho\nu}^- \;=\; -\,\frac{1}{2}\,Y_{23} + \frac{1}{2}\,Y_{24} + Y_{90}\,,\\
\nabla^\lambda t_{\lambda\nu}^+\nabla_\rho f_+^{\rho\nu} - \nabla^\rho t_{\lambda\nu}^+\nabla^\lambda f_+^{\rho\nu} &= [\,\Gamma^{\lambda\rho}, t_\lambda^{+\nu}\,]\,f_{\rho\nu}^+ \;=\; \frac{1}{4}\,Y_{58} - \frac{1}{4}\,Y_{59} - Y_{84}\,.
\end{aligned} \tag{1.68}$$

[7] In determining the higher order terms in the chiral expansion the equations of motion for the leading order can be used. As discussed in [28], its enforcement is equivalent to a transformation of fields and therefore physics is left invariant.

In a similar fashion (but after a more involved calculation), one can show that $i\,\langle\,\nabla_\rho t_{+\mu\nu}\,\{f_-^{\mu\nu},u^\rho\}\rangle$ and $i\,\langle\,\nabla_\rho t_{+\mu\nu}\,\{f_-^{\mu\rho},u^\nu\}\rangle$ are also redundant.

1.7.2 Bianchi identity

In Eqs. (1.50)–(1.53) we introduced the chiral connection and the field strength $\Gamma_{\mu\nu}$ that naturally stems from it. There is also an associated Bianchi identity, which in this case takes the form

$$\nabla_\mu\Gamma_{\nu\rho}\,+\,\nabla_\nu\Gamma_{\rho\mu}\,+\,\nabla_\rho\Gamma_{\mu\nu}\,=\,0\,. \tag{1.69}$$

and reads

$$\nabla_\mu f_{+\nu\alpha}+\nabla_\nu f_{+\alpha\mu}+\nabla_\alpha f_{+\mu\nu}\,=\,\frac{i}{2}\left([\,f_{-\mu\nu},u_\alpha\,]+[\,f_{-\nu\alpha},u_\mu\,]+[\,f_{-\alpha\mu},u_\nu\,]\right)\,. \tag{1.70}$$

Tracing this equation with $\nabla^\rho t_+^{\mu\nu}$ and integrating by parts we get one additional relation between operators. We choose to remove from our list the operator $i\,\langle\nabla^\mu t_{\mu\nu}\nabla_\rho f_+^{\rho\nu}\rangle$. There is a second Bianchi identity

$$\nabla_\mu f_{-\nu\alpha}+\nabla_\nu f_{-\alpha\mu}+\nabla_\alpha f_{-\mu\nu}\,=\,\frac{i}{2}\left([\,f_{+\mu\nu},u_\alpha\,]+[\,f_{+\nu\alpha},u_\mu\,]+[\,f_{+\alpha\mu},u_\nu\,]\right)\,, \tag{1.71}$$

that does not lead to further reduction of our basis.

1.7.3 Contact terms

So far, to the best of our knowledge the number of operators for general n_f is complete and minimal. However, in our list there are contact terms, *i.e.*, combinations of operators which only depend on external sources. Since they do not contain the pion field, they cannot be determined from phenomenology, but are necessary to correctly account for the ultraviolet behaviour of Green functions.

In the u–basis we have been using, contact terms do not arise in a natural way, but are hidden in linear combinations of operators. It is easier to express them in the U–basis. As we already discussed, chirality prevents a contact term like $t^{\mu\nu}\,t^\dagger_{\mu\nu}$

at order $\mathcal{O}(p^4)$. At the next order, one finds the following ones

$$\begin{aligned}
\left\langle D_\mu t^{\mu\nu}\, D^\alpha t^\dagger_{\alpha\nu}\right\rangle &= \frac{1}{4}\left\langle \nabla_\mu t_+^{\mu\nu}\, \nabla^\alpha t_{+\alpha\nu}\right\rangle - \frac{1}{4}\left\langle \nabla_\mu t_-^{\mu\nu}\, \nabla^\alpha t_{-\alpha\nu}\right\rangle - \frac{i}{4}\left\langle \nabla_\mu t_+^{\mu\nu}\, \{t_{-\alpha\nu}, u^\alpha\}\right\rangle \\
&\quad + \frac{1}{16}\left\langle t_{+\mu\nu}\,(u^\nu\, t_+^{\mu\alpha}\, u_\alpha + u_\alpha\, t_+^{\mu\alpha}\, u^\nu)\right\rangle + \frac{1}{8}\left\langle t_{+\mu\nu}\, t_+^{\mu\alpha}\, u_\alpha\, u^\nu\right\rangle \\
&\quad - \frac{1}{16}\left\langle t_{-\mu\nu}\,(u^\nu\, t_-^{\mu\alpha}\, u_\alpha + u_\alpha\, t_-^{\mu\alpha}\, u^\nu)\right\rangle - \frac{1}{8}\left\langle t_{-\mu\nu}\, t_-^{\mu\alpha}\, u_\alpha\, u^\nu\right\rangle \\
&\quad + \frac{i}{4}\left\langle \nabla_\mu t_-^{\mu\nu}\, \{t_{+\alpha\nu}, u^\alpha\}\right\rangle , \\
\left\langle t^{\dagger\nu\rho}\, t^\mu_{\ \rho}\, F_{L\mu\nu} + t^{\nu\rho}\, t^{\dagger\mu}_{\ \ \rho}\, F_{R\mu\nu}\right\rangle &= \frac{1}{4}\left\langle t_+^{\nu\rho}\, t^\mu_{+\rho}\, f_{+\mu\nu}\right\rangle - \frac{1}{4}\left\langle t_-^{\nu\rho}\, t^\mu_{-\rho}\, f_{+\mu\nu}\right\rangle \\
&\quad + \frac{1}{4}\left\langle \left\{t_+^{\nu\rho}, t^\mu_{-\rho}\right\} f_{-\mu\nu}\right\rangle , \\
\left\langle t_{\mu\nu}\, \chi^\dagger\, F_R^{\mu\nu} + \chi^\dagger\, t_{\mu\nu}\, F_L^{\mu\nu} + \text{h.c.}\right\rangle &= \frac{1}{4}\left\langle t_{+\mu\nu}\, \{f_+^{\mu\nu}, \chi_+\}\right\rangle + \frac{1}{4}\left\langle t_{-\mu\nu}\, [f_-^{\mu\nu}, \chi_+]\right\rangle \\
&\quad - \frac{1}{4}\left\langle t_{-\mu\nu}\, \{f_+^{\mu\nu}, \chi_-\}\right\rangle - \frac{1}{4}\left\langle t_{+\mu\nu}\, [f_-^{\mu\nu}, \chi_-]\right\rangle . \qquad (1.72)
\end{aligned}$$

where $\nabla_\mu t_\pm^{\mu\nu} = (D_\mu t^{\mu\nu})_\pm + \frac{i}{2}\{u_\mu, t_\mp^{\mu\nu}\}$ has been used in the first relation. We will incorporate the previous contact terms in our basis, and accordingly remove the following monomials, which otherwise would be redundant:

$$\begin{aligned}
i\left\langle \left\{t_+^{\nu\rho}, t^\mu_{-\rho}\right\} f_{-\mu\nu}\right\rangle &= -Y_{89} + Y_{90} + 4\, Y_{119} , \\
\left\langle\, \nabla_\mu t_-^{\mu\nu}\, \nabla^\alpha t_{-\alpha\nu}\,\right\rangle &= \frac{1}{2}\, Y_{11} + \frac{1}{4}\, Y_{13} - \frac{1}{2}\, Y_{23} - \frac{1}{4}\, Y_{25} + Y_{52} - Y_{104} + Y_{105} - 4\, Y_{118} , \\
\left\langle\, t_{+\mu\nu}\, [f_-^{\mu\nu}, \chi_-]\,\right\rangle &= Y_{73} - Y_{74} + Y_{75} - 4\, Y_{120} . \qquad (1.73)
\end{aligned}$$

All the relations discussed above finally reduce the number of operators to 117 and 3 contact terms. This is the number of independent operators for any number of flavours. However, only $n_f = 2, 3$ are phenomenologically relevant. For such cases, the Cayley–Hamilton theorem provides further relations between traces. For reference, we list them in Appendix B. We end up with 110+3 independent operators for three flavours and 77+3 for two flavours.

In order to have a minimal basis of $\mathcal{O}(p^6)$ chiral invariant monomials with tensor sources, we have followed the same procedure as in Ref. [28]. However, a recent paper [29] has pointed out that the basis of [28] for two flavours is not yet minimal: an identity among several operators of that basis was found, which does not become trivial when setting to zero the external sources. Interestingly, such identity does not require new algebraic manipulations other than the Cayley–Hamilton relations, Bianchi identities, partial integration and equations of motion. The fact that even after the sophisticated analysis of [28] an additional relation was found shows that reaching a minimal set of operators at higher orders in the chiral expansion is quite a challenging task. With tensor sources, however, highly nontrivial relations such as the one reported in Ref. [29] are unlikely to be found, mainly because: (a) the tensor source does not enter the lowest order equations of motion and (b) there is no

Bianchi identity associated with it. As a result, algebraic manipulations are simpler and we do not expect our basis to suffer further reduction.

1.8 Odd–intrinsic–parity sector

So far we have restricted our analysis to the even–intrinsic–parity sector of the chiral expansion. The Lagrangians discussed exhibit a larger symmetry than the "real world". For instance, if we switch off the external sources, our Lagrangians are invariant under the substitution $\phi(x) \to -\phi(x)$ (they contain terms with an even number of Goldstone bosons only). There is no odd–intrinsic–parity chiral invariant operator of dimension lower than six. But QCD suffers an anomaly that affects the whole $U(3)_L \otimes U(3)_R$ symmetry group and has its origin in the fact that it is not possible to preserve the simultaneous invariance of the generating functional under vector and axial–vector transformations. This anomaly translates into a dimension four piece of the chiral Lagrangian which is not chiral invariant : the Wess–Zumino term. So the odd–intrinsic–parity sector starts already at $\mathcal{O}(p^4)$ with the non chiral invariant anomalous term and contains an infinite number of chiral invariant operators of higher dimension.

1.8.1 Wess–Zumino–Witten functional

Wess and Zumino were the first to derive a functional involving only pseudoscalar fields generating this anomaly [30]. For pions alone, its form is fixed by cohomology theory and is expressible in a 5–dimensional manifold. They emphasized that these interaction Lagrangians cannot be chiral invariant. However, the terms that involve external sources can be cast as a four–dimensional integral proportional to the Levi–Civitá tensor $\varepsilon_{\mu\nu\sigma\rho}$. It is more convenient to use the functional derived by Witten [31] and here we will follow the discussion of [32].

The fermionic determinant does not allow for a chiral invariant regularization. Given the transformations

$$g_R \,=\, 1 \,+\, i\,[\alpha(x) + \beta(x)]\ , \qquad g_L \,=\, 1 \,+\, i\,[\alpha(x) - \beta(x)]\ , \tag{1.74}$$

the conventions in the definition of the fermionic determinant may be chosen to preserve the invariance of the generating functional Z, either under vector transformations, or under the axial ones; but not both simultaneously. Choosing to preserve invariance under the transformations generated by the vector currents, the change

in Z only involves the difference $\beta(x)$ between g_R and g_L.

$$\begin{aligned}
\delta Z &= -\int \mathrm{d}x \, \langle \beta(x)\, \Omega(x) \rangle \ , \\
\Omega(x) &= \frac{N_C}{16\,\pi^2}\, \varepsilon^{\alpha\beta\mu\nu} \Big[v_{\alpha\beta}\, v_{\mu\nu} \, + \, \frac{4}{3}\, D_\alpha a_\beta \, D_\mu a_\nu \, + \frac{2\,i}{3}\, \{ v_{\alpha\beta}, a_\mu\, a_\nu \} \\
&\qquad + \frac{8\,i}{3}\, a_\mu\, v_{\alpha\beta}\, a_\nu \, + \, \frac{4}{3}\, a_\alpha\, a_\beta\, a_\mu\, a_\nu \Big] \ , \\
v_{\alpha\beta} &= \partial_\alpha v_\beta \, - \, \partial_\beta v_\alpha \, - \, i\, [v_\alpha, v_\beta] \ , \\
D_\alpha a_\beta &= \partial_\alpha a_\beta \, - \, i\, [v_\alpha, a_\beta] \ .
\end{aligned} \tag{1.75}$$

Notice that Ω only depends of the external sources v_μ and a_μ and that the quark mass matrix does not play any röle. The explicit form for the functional is:

$$\begin{aligned}
Z\,[U,\,l,\,r]_{\mathrm{WZW}} &= -\frac{i\,N_C}{240\,\pi^2} \int_{M^5} \mathrm{d}^5 x\, \varepsilon^{ijklm}\, \langle \Sigma_i^L\, \Sigma_j^L\, \Sigma_k^L\, \Sigma_l^L\, \Sigma_m^L \rangle \\
&\quad - \frac{i\,N_C}{48\,\pi^2} \int \mathrm{d}^4 x\, \varepsilon_{\mu\nu\alpha\beta} \left(W(U,\,l,\,r)^{\mu\nu\alpha\beta} \, - \, W(\mathbb{1},\,l,\,r)^{\mu\nu\alpha\beta} \right) \ , \\
W(U,\,l,\,r)_{\mu\nu\alpha\beta} &= \Big\langle U\, l_\mu\, l_\nu\, l_\alpha\, U^\dagger\, r_\beta \, + \, \frac{1}{4}\, U\, l_\mu\, U^\dagger\, r_\nu\, U\, l_\alpha\, U^\dagger\, r_\beta \, + \, i\, U\, \partial_\mu l_\nu\, l_\alpha\, U^\dagger\, r_\beta \\
&\quad + i\, \partial_\mu r_\nu\, U\, l_\alpha\, U^\dagger\, r_\beta \, - \, i\, \Sigma_\mu^L\, l_\nu\, U^\dagger\, r_\alpha\, U\, l_\beta \, + \, \Sigma_\mu^L\, U^\dagger\, \partial_\nu r_\alpha\, U\, l_\beta \\
&\quad - \Sigma_\mu^L\, \Sigma_\nu^L\, U^\dagger\, r_\alpha\, U\, l_\beta \, + \, \Sigma_\mu^L\, l_\nu\, \partial_\alpha\, l_\beta \, + \, \Sigma_\mu^L\, \partial_\nu\, l_\alpha\, l_\beta \\
&\quad - i\, \Sigma_\mu^L\, l_\nu\, l_\alpha\, l_\beta \, + \, \frac{1}{2}\, \Sigma_\mu^L\, l_\nu\, \Sigma_\alpha^L\, l_\beta \, - \, i\, \Sigma_\mu^L\, \Sigma_\nu^L\, \Sigma_\alpha^L\, l_\beta \Big\rangle \\
&\quad - (L \, \longleftrightarrow \, R) \ , \ N_C \, = \, 3 \, , \\
\Sigma_\mu^L &= U^\dagger\, \partial_\mu U \qquad \Sigma_\mu^R \, = \, U\, \partial_\mu U^\dagger \, ,
\end{aligned} \tag{1.76}$$

where $(L \, \longleftrightarrow \, R)$ stands for the exchange

$$U \, \longleftrightarrow \, U^\dagger \ , \ l_\mu \, \longleftrightarrow \, r_\mu \ , \ \Sigma_\mu^L \, \longleftrightarrow \, \Sigma_\mu^R \, . \tag{1.77}$$

This functional governs processes such as $K^+K^- \to \pi^+\pi^-\pi^0$, $\pi^0 \to \gamma\,\gamma$, $\pi^0 \to \gamma\, e^+ e^-$ and $\pi \to e\,\nu\,\gamma$. The last two processes are discussed in this thesis in Chapter 5.

For the calculation of the $\langle VVP \rangle$ Green function and the radiative pion decay process it suffices to work with the following piece of the anomalous Lagrangian:

$$\mathcal{L}_{\mathrm{WZW}}^{(4)} \, = \, -\frac{\sqrt{2}\,N_C}{8\,\pi^2\,F}\, \epsilon_{\mu\nu\alpha\beta}\, \langle \Phi\, \partial^\mu v^\nu\, \partial^\alpha v^\beta \, \rangle \, . \tag{1.78}$$

1.8.2 Odd–intrinsic–parity sector with tensor sources

The Wess–Zumino–Witten functional is of odd–intrinsic–parity and it enters in $\mathcal{L}_4$, so it constitutes the lowest order odd–intrinsic–parity Lagrangian. But of course at higher orders this sector appears and it is not related to the anomaly any more. In

Ref. [33,34] it was explicitly calculated for $\mathcal{L}_6$. In this thesis we will make use of two of the operators of this sector, namely

$$\mathcal{L}_6^{odd} \doteq i\,\varepsilon_{\mu\nu\alpha\beta}\left\{C_7^W\left\langle\chi_- f_+^{\mu\nu} f_+^{\alpha\beta}\right\rangle + i\,C_{22}^W\left\langle\nabla_\lambda f_+^{\lambda\mu}\left\{f_+^{\alpha\beta}, u^\nu\right\}\right\rangle\right\} . \tag{1.79}$$

In the following we will argue that such terms for the tensor source only arise at the order p^8.

In order to obtain the lowest order odd–intrinsic–parity operators in the chiral expansion, the tensor source must have some indices contracted with the Levi–Civitá symbol. It is straightforward to show that they all vanish.

Consider first the case when both tensor indices are paired to the Levi–Civitá symbol, *e.g.*

$$\varepsilon_{\mu\nu\sigma\rho}\, t_\pm^{\mu\nu}\, B^{\sigma\rho} , \tag{1.80}$$

where $B^{\sigma\rho}$ stands for any antisymmetric tensor structure compatible with chiral and discrete symmetries. From the definition of the chiral projectors, Eq. (1.3), one can write

$$\varepsilon^{\mu\nu\alpha\beta} = 2\,i\left(P_L^{\mu\nu\alpha\beta} - P_R^{\mu\nu\alpha\beta}\right) , \tag{1.81}$$

whence it follows that

$$\epsilon_{\mu\nu\alpha\beta}\, t_\pm^{\alpha\beta} = -\,2\,i\, t_{\mp\mu\nu} , \tag{1.82}$$

and therefore, such terms will not show up in the odd–intrinsic–parity sector. Notice that this is a consequence of the fact that the tensor source has no chiral partner, or equivalently that $\gamma_5\,\sigma_{\alpha\beta}$ is not an independent Dirac structure.

Consider now the case when only one of the indices of the tensor operator is contracted with the Levi–Civitá density, namely [8]

$$\epsilon_{\mu\nu\alpha\beta}\, t_\pm^{\mu\gamma}\, B_\gamma{}^{\nu\alpha\beta} , \tag{1.83}$$

where $B_\gamma{}^{\nu\alpha\beta}$ stands for any generic chiral tensor (completely antisymmetric in ν, α and β) made out of the elements of Eq. (1.51). We will use the Schouten identity:

$$g^{\rho\gamma}\,\epsilon^{\mu\nu\alpha\beta} - g^{\rho\mu}\,\epsilon^{\gamma\nu\alpha\beta} - g^{\rho\nu}\,\epsilon^{\mu\gamma\alpha\beta} - g^{\rho\alpha}\,\epsilon^{\mu\nu\gamma\beta} - g^{\rho\beta}\,\epsilon^{\mu\nu\alpha\gamma} = 0 , \tag{1.84}$$

which stems from the fact that any 5–form vanishes in 4 dimensions. Contracting it with $t_\pm^{\mu\gamma}\, B_\gamma{}^{\nu\alpha\beta}$ it is not difficult to show [with the use of Eq. (1.82)] that it can be rewritten in the following way:

$$\epsilon_{\mu\nu\alpha\beta}\, t_\pm^{\mu\gamma}\, B_\gamma{}^{\nu\alpha\beta} = 3\,i\, t_{\mp\alpha\beta}\, B_\nu{}^{\nu\alpha\beta} , \tag{1.85}$$

and then once more the Levi–Civitá density vanishes.

[8] All other contractions can be rendered equivalent by means of partial integration.

Obviously, when none of the indices of the tensor source is contracted with the Levi–Civitá density, these identities are no longer useful and odd–intrinsic–parity operators will arise. If we take, for instance, any of the operators of our basis at $\mathcal{O}(p^4)$ and multiply it by any of the $\mathcal{O}(p^4)$ odd–intrinsic–parity operators of Ref. [33] we will get an odd–intrinsic–parity operator involving tensor currents. But this operator will be at least of $\mathcal{O}(p^8)$ and thus falls beyond the scope of the present work.

1.9 A simple application : One loop corrections to Π_{VT}

Consider the following two–point correlator in the chiral limit

$$\Pi^{VT}_{\mu;\nu\rho}(q) \,=\, i\int \mathrm{d}^4x\, e^{iq\cdot x}\,\langle\, 0\,\big|\, T\left\{V_\mu(x)\, T^\dagger_{\nu\rho}(0)\right\}\big|\,0\,\rangle \,=\, i\,(q^\rho g^{\mu\nu} - q^\nu g^{\mu\rho})\,\Pi_{VT}(q^2)\,, \tag{1.86}$$

where $T_{\mu\nu}(x) = \bar{u}(x)\,\sigma_{\mu\nu}\,d(x)$ and $V_\mu(x) = \bar{u}(x)\,\gamma_\mu\,d(x)$.
Using dimensional regularization with minimal subtraction, a straightforward computation of the diagrams of Fig. 4.12 leads to

$$\Pi_{VT}(q^2) \,=\, -\,2\,\Lambda_1 \,-\, \Omega_{94}\,q^2 \,+\, \frac{\Lambda_2}{32\,\pi^2 F^2}\left[\frac{1}{\hat{\epsilon}} - \log(-\,q^2) + \frac{8}{3}\right] q^2\,, \tag{1.87}$$

where

$$\frac{1}{\hat{\epsilon}} \,=\, \frac{1}{\epsilon} \,-\, \gamma_E + \log(4\,\pi)\,. \tag{1.88}$$

The coupling Ω_{94} is the LEC coefficient of the operator Y_{94} of the chiral basis with tensor sources, that can be found in Appendix B. In χPT, renormalization proceeds order by order in the chiral expansion. This means that the logarithmic divergence of Fig. 4.12 (b) has to be absorbed by the counterterm Ω_{94} of Fig. 4.12(c) to render $\Pi_{VT}(q^2)$ finite. This defines the renormalized coupling Ω^R_{94} to be

$$\Omega_{94} \,=\, \Omega^R_{94}(\mu) \,-\, \frac{\Lambda_2}{32\,\pi^2 F^2}\mu^{-\,2\,\epsilon}\left\{\frac{2}{D-4} + C\right\}\,. \tag{1.89}$$

in D dimensions Ω_i and consequently Ω^R_i, have energy dimension of E^{D-5}; Λ_i and F_π have E^{D-3} and $E^{D/2-1}$, respectively. Since each term in Eq. (1.89) must have the same energy dimension, we have to multiply the second term by μ^{D-4}. Addopting the usual choice $C = \gamma_E - \log(4\,\pi) - 1$ the fully renormalized Green function therefore reads

$$\Pi_{VT}(q^2) \,=\, -\,2\,\Lambda_1 \,-\, \Omega^R_{94}(\mu)\,q^2 \,+\, \frac{\Lambda_2}{32\,\pi^2 F^2}\left[\frac{5}{3} - \log\left(-\,\frac{q^2}{\mu^2}\right)\right] q^2\,. \tag{1.90}$$

So far, the scale dependence associated to the tensor current has been implicitly stored into Λ_1, Ω_{94} and Λ_2. If we now introduce the aforementioned parameter b_0, we find $\Lambda_{1,2} = b_0\,\lambda_{1,2}$ and $\Omega_{94} = b_0\,\omega_{94}$ and as a result

$$\Pi_{VT}(q^2) \;=\; -\,2\,\lambda_1\,b_0 - \omega_{94}^R(\mu)\,b_0\,q^2 \;+\; \frac{\lambda_2\,b_0}{32\,\pi^2 F_\pi^2}\left[\frac{5}{3} - \log\left(-\,\frac{q^2}{\mu^2}\right)\right] q^2\,. \qquad (1.91)$$

Notice that with the b_0 parameter, the chiral scale and the QCD scale factorize.

For comparison consider now the following scalar–pseudoscalar two–point Green function:

$$\Pi_{SS-PP}(q) \;=\; i\int \mathrm{d}^4x\, e^{iq\cdot x}\,\big\langle\, 0\,\big|\,T\left\{S(x)S^\dagger(0) \;-\; P(x)P^\dagger(0)\right\}\big|\,0\,\big\rangle\;, \qquad (1.92)$$

where $S(x) = \bar{u}(x)\,d(x)$ and $P(x) = \bar{u}(x)\,i\,\gamma_5\,d(x)$. After evaluating the corresponding Feynman diagrams, one obtains, in the chiral limit,

$$\Pi_{SS-PP}(q^2) \;=\; \frac{2\,F_0^2\,B_0^2}{q^2} \;+\; 32\,B_0^2\,L_8 \;+\; \frac{5\,B_0^2}{48\,\pi^2}\left[\frac{1}{\hat{\epsilon}} - \log(-\,q^2) + 2\right]. \qquad (1.93)$$

The previous equation is finite when using Eq. (1.63), which also determines the (chiral) scale dependence of the renormalized coupling:

$$L_8 \;=\; L_8^R(\mu) \;-\; \frac{5}{48}\,\frac{1}{32\,\pi^2}\,\mu^{-\,\epsilon}\left\{\frac{2}{D-4} + C\right\}, \qquad (1.94)$$

leading to the one–loop renormalized two–point Green function

$$\Pi_{SS-PP}(q^2) \;=\; \frac{2\,F_0^2\,B_0^2}{q^2} \;+\; 32\,B_0^2\,L_8^R(\mu) \;+\; \frac{5\,B_0^2}{48\,\pi^2}\left[1 - \log\left(-\,\frac{q^2}{\mu^2}\right)\right]. \qquad (1.95)$$

All the QCD scale dependence, arising from the non–conservation of the scalar and pseudoscalar currents, is factored out in B_0, whereas $L_8^R(\mu)$ shows the running with the chiral scale. Notice the analogy with Eq. (1.91).

Unfortunately, b_0 cannot be matched onto the QCD Lagrangian in a way similar to what is done for B_0: the lowest dimension operators linear in the tensor source (and consequently in b_0) are coupled to the low–energy couplings Λ_1 and Λ_2. These couplings are insensitive to pion dynamics and instead do receive contributions from vector meson resonances (see Chapter 2). Therefore, there is an inherent ambiguity in the determination of b_0, because it cannot be decoupled from Λ_1 and Λ_2. The dimensionful coupling b_0 should not contain information on the hadronic resonances integrated out of the theory, but otherwise it remains unspecified. To avoid confusion, we have omitted in our treatment any reference to b_0.

As a result, one should keep in mind that, besides the chirally renormalized low–energy couplings, each operator with n tensor sources bears a non–vanishing anomalous dimension, namely $n\,\gamma_T$.

Chapter 2

The $1/N_C$ expansion I: Resonance Chiral Theory

2.1 Introduction

Many years ago, 't Hooft [10] proposed that many features of QCD at low and intermediate energies could be understood if considering a gauge theory $SU(N_C)$ of quarks and gluons when the limit $N_C \to \infty$ is taken. Even though one may thing that this theory has little to do with reality, this limit can always be regarded as the first term of an expansion in terms of the "small" parameter $1/N_C$. As we will see, this expansion is equivalent to a semiclassical expansion for an effective theory having colour–singlet hadrons as asymptotic degrees of freedom.

It could be thought that a large number of colours, since we are enhancing the gauge group and the number of degrees of freedom, would instead of simplify, complicate the understanding of QCD. In fact this is not the case and many simplifications will occur. Finally one may wonder if the parameter $1/N_C$ is small enough to qualify as an expansion parameter and how fast the convergence is. In QED the expansion parameter is not e but rather $\alpha_{\rm em} = e^2/4\pi \sim 10^{-3}$ meaning that $e \sim 1/3$. Although something similar does not happen in QCD, still $1/N_C$ is a useful expansion parameter. On the other hand, $1/N_C$ corrections are of the same order as the corrections due to the $SU(3)_V$ symmetry breaking, and an expansion of QCD in terms of the breaking parameter of this symmetry works fine. As a last comment, in certain observables the $1/N_C$ correction vanishes being the first non–zero corrections $1/N_C^2 \sim 10\,\%$.

Although at low energies we can make a perturbative expansion in small momenta, it would be desirable to have a more direct connection with the fundamental theory. χPT only exploits the global (accidental) symmetries of QCD, and any other theory with the same symmetries (and with the phenomenon of spontaneous chiral symmetry breaking) would have the same low–energy effective theory (with different coefficients). The $1/N_C$ expansion allows us to have the number of colours as a free parameter of χPT directly related to QCD.

Finally, for several features of the low–energy phenomenology of the strong inter-

actions, the $1/N_C$ expansion is the only satisfactory explanation from a fundamental point of view. Moreover, in the intermediate energy region where the resonances lie (above the ρ mass but below the perturbative regime) there is no other expansion parameter than $1/N_C$, since the quark masses can be set to zero and the strong coupling constant still is far too large. These reasons constitute additional motivations to take this expansion seriously.

For the elaboration of this chapter I have followed Refs. [11, 35–37].

2.2 Large–N_C QCD: counting rules

One may think that the renormalization group equation (1.19) behaves badly in the $N_C \to \infty$ limit. We can cure this by rescaling the coupling constant $g = \tilde{g}/\sqrt{N_C}$ to obtain:

$$\mu \frac{d\tilde{g}}{d\mu} = -\left(\frac{11}{3} - \frac{2}{3}\frac{N_F}{N_C}\right)\frac{\tilde{g}^3}{16\pi^2} + \mathcal{O}\left(\tilde{g}^5\right). \tag{2.1}$$

In this way we keep the hadronization scale $\Lambda_{\rm QCD}$ independent of the number of colours when N_C is big enough. It is convenient to define

$$(G_\mu)^\alpha_\beta = G^a_\mu\,(T^a)^\alpha_\beta\,, \qquad (G_{\mu\nu})^\alpha_\beta = G^a_{\mu\nu}\,(T^a)^\alpha_\beta\,, \tag{2.2}$$

in such a way that

$$\begin{aligned} D_\mu &= \partial_\mu + i\frac{\tilde{g}}{\sqrt{N_C}}G_\mu\,, \qquad \frac{1}{4}\left(G^a_{\mu\nu}\,G^{\mu\nu}_a\right) = \frac{1}{2}\,{\rm Tr}\left(G_{\mu\nu}\,G^{\mu\nu}\right), \\ G_{\mu\nu} &= \partial_\mu G_\nu - \partial_\nu G_\mu + i\frac{\tilde{g}}{\sqrt{N_C}}\left[G_\mu, G_\nu\right], \end{aligned} \tag{2.3}$$

reading the Lagrangian (1.1) then

$$\mathcal{L}_{QCD} = -\frac{1}{2}\,{\rm Tr}\,G_{\mu\nu}\,G^{\mu\nu} + \bar{q}\,(i\not{D} - \mathcal{M})\,q\,. \tag{2.4}$$

The large–N_C counting rules can be obtained using a trick developed by 't Hooft. The quark and gluon propagators read:

$$\left\langle q^\alpha(x)\,\bar{q}^{\,\beta}(y)\right\rangle = \delta^{\alpha\beta}S(x-y)\,, \qquad \left\langle G^a_\mu(x)\,G^b_\nu(y)\right\rangle = \delta^{ab}D_{\mu\nu}(x-y)\,, \tag{2.5}$$

and are represented as in Fig. 2.1 (a) and (b). Instead, using the $SU(N_C)$ Fierz identity

$$(T^a)^\alpha_\beta\,(T^a)^\gamma_\delta = \frac{1}{2}\,\delta^\alpha_\delta\,\delta^\gamma_\beta - \frac{1}{2\,N_C}\,\delta^\alpha_\beta\,\delta^\gamma_\delta\,, \tag{2.6}$$

we will use the representation of (2.2) to write:

$$\left\langle (G_\mu)^\alpha_\beta\,(x)\;(G_\nu)^\gamma_\delta\,(y)\right\rangle \;=\; D_{\mu\nu}\,(x-y)\left(\frac{1}{2}\,\delta^\alpha_\delta\,\delta^\gamma_\beta\;-\;\frac{1}{2\,N_C}\,\delta^\alpha_\beta\,\delta^\gamma_\delta\right)\,, \tag{2.7}$$

which in the limit $N_C \to \infty$ is reduced to

$$\left\langle (G_\mu)^\alpha_\beta\,(x)\;(G_\nu)^\gamma_\delta\,(y)\right\rangle \;=\; \frac{1}{2}\,D_{\mu\nu}\,(x-y)\;\delta^\alpha_\delta\,\delta^\gamma_\beta\,, \tag{2.8}$$

and admits the graphic representation of Fig. 2.1 (b). Any Feynman diagram can be drawn using the double line representation, as in Figs. 2.2 and 2.3. One can think of Feynman diagrams depicted in the double line representation as a surface obtained gluing together polygons in the double lines.

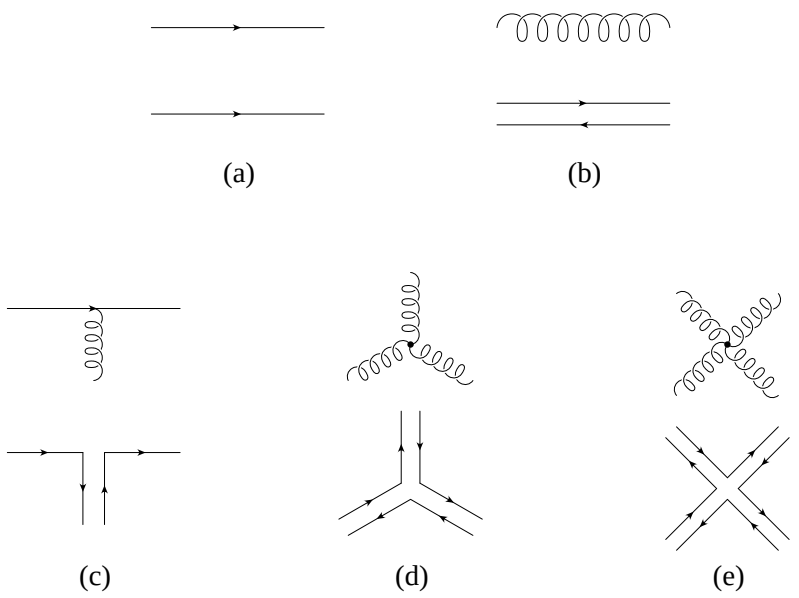

Figure 2.1: Double line representation for gluon fields.

For deriving the N_C–counting rules it is convenient to use a Lagrangian in which we redefine the quark and gluon fields :

$$\begin{aligned}
\hat{G}^\mu \;&=\; \frac{\tilde{g}}{\sqrt{N_C}}\,G^\mu \;=\; g\,G^\mu\,, \qquad D_\mu \;=\; \partial_\mu \;+\; i\,\hat{G}_\mu\,, \\
\hat{G}^{\mu\nu} \;&=\; \frac{\tilde{g}}{\sqrt{N_C}}\,G^{\mu\nu} \;=g\,G^{\mu\nu}\,, \qquad \hat{q} \;=\; \frac{1}{\sqrt{N_C}}\,q\,,
\end{aligned} \tag{2.9}$$

obtaining then

$$\mathcal{L}_{QCD} \;=\; N_C\left[\overline{\hat{q}}\left(i\hat{\not{D}}\;-\;\mathcal{M}\right)\hat{q}\;-\;\frac{1}{4\,\tilde{g}^2}\,\hat{G}^a_{\mu\nu}\,\hat{G}^{\mu\nu}_a\right]\,. \tag{2.10}$$

Although the Lagrangian (2.10) has now a global N_C factor it does not reduce to a semiclassical theory of quarks and gluons in the $N_C \to \infty$ limit because the number of quarks and gluons grows with N_C. Now it is easy to read the counting rules from (2.10) for vacuum self energy diagrams: each vertex has an N_C factor and each propagator $1/N_C$; in addition, each colour loop has an N_C factor. In the double line notation and considering the diagrams as polygons glued to form surfaces, each colour loop corresponds to the face of a polygon forming part of the surface and each propagator (either quark or gluon) corresponds to an edge of one polygon (two lines with arrows pointing in opposite directions are glued edges and count only as one). With this, the order of a vacuum connected diagram is

$$N_C^{V-E+F} \,=\, N_C^{\chi}\,, \tag{2.11}$$

where V stands for the number of vertices, E for the number of edges and F for the number of faces; and χ is a topological invariant known as the Euler character. For a connected orientable surface

$$\chi \,=\, 2-2\,h-b\,, \tag{2.12}$$

where b is the number of boundaries and h is the number of handles (or holes). Of course one can directly use Witten's counting rules [37] to obtain the correct N_C–counting rules: each colour loop gives an N_C factor and each interaction vertex gives a factor $1/\sqrt{N_C}$ or $1/N_C$ for quark–gluon and three–gluons or for four–gluons, respectively. But with these rules the connection with topology is more involved. In the case of unconnected diagrams the order is the product of the order of each connected diagram. For instance Fig. 2.2 has $V=4$, $E=6$ and $F=3$ giving $\chi=1$, correspondingly $h=0$ and $b=1$ and for Fig. 2.3 $V=4$, $E=6$ and $F=4$ giving $\chi=2$, correspondingly $h=0$ and $b=0$. A quark loop represents a hole and then it gives a $1/N_C$ suppression. The maximum N_C power we can reach is two and it corresponds to $h=b=0$, that is, connected vacuum diagrams with the topology of a sphere. Let as see how Fig. 2.3 has indeed the topology of a sphere. Let us start from a hollow sphere and cut it into two parts (two surfaces that can be chosen to be equal); one of them can be flatten to a plane giving Fig. 2.2. In order to glue the second surface we identify its center (or the "north" pole) with the border of a circle with infinity radius; that is, this second surface is the full $\Re^2$ plane with a circle removed in its origin. Now we can glue the two surfaces to get Fig. 2.3. So order N_C^2 diagrams are planar diagrams consisting only on gluons (they can be drawn on a sheet of paper without any gluon jumping on top of other).

If we are interested in correlation functions that depend on properties of quarks, such as masses, our diagram must have at least one quark loop that, without lose of generality can be pushed to the outermost edge. The leading diagrams with one quark loop are of order N_C and have the topology of a hollow sphere with one hole (the quark loop) on its surface, corresponding to $h=0$ and $b=1$. Then these diagrams are planar diagrams with a single quark loop which forms the outermost edge. An example of a subdominant diagram is Fig. 2.4: $F=1$, $V=4$, $E=6$ or

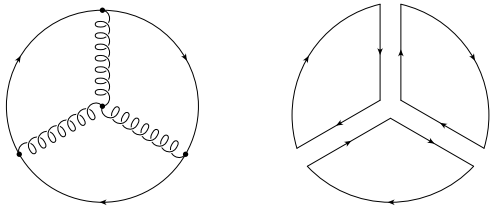

Figure 2.2: Flat diagram in both the ordinary and double line representations.

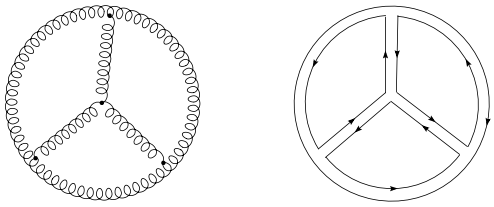

Figure 2.3: Flat diagram with the topology of a sphere in ordinary and double line representation.

$h = 1$, $b = 1$ corresponding to $\chi = -1$. In general a gluon that cannot be drawn in the same plane as the rest of the figure represents a handle and this corresponds to a $1/N_C^2$ suppression.

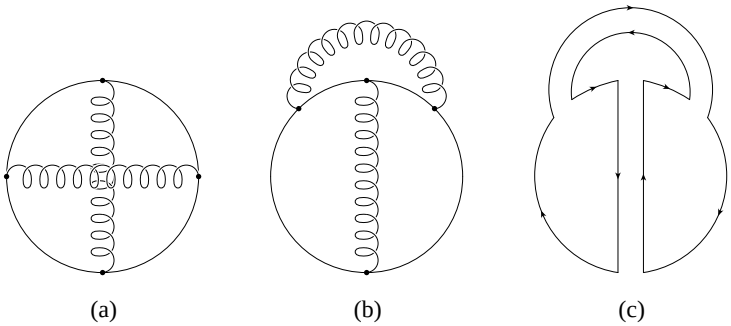

Figure 2.4: An example of a non–planar diagram.

It is important that we have been able to express the order of a given diagram in terms of a topological invariant, because this makes our results general, regardless of the number of gluons present in the diagram. To close this section, let us review the concept of the $1/N_C$ expansion of QCD. In a perturbative expansion in terms of the g_s coupling, each order corresponds to all Feynman diagrams having the same number of loops, and it comprises a finite number. On the other hand, each order in the $1/N_C$ expansion corresponds to all Feynman diagrams with a given topology described by (2.12) and it comprises an infinite number. This idea is sketched in Fig. 2.5.

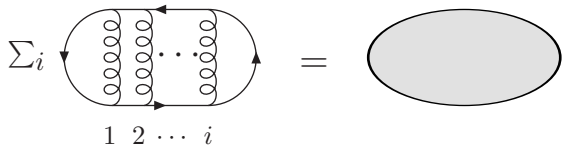

Figure 2.5: Representation of the Feynman diagrams contributing to a given order of the $1/N_C$ expansion.

2.3 N$_C$–counting rules for correlation functions

Using the counting rules derived for connected vacuum diagrams we can derive the counting rules for correlation functions of quark and gluon composite operators. We will concentrate on gauge invariant operators that cannot be split into separate gauge invariant pieces. This requires, for instance, that quark operators must be bilinear. We will use again the method of adding to the QCD Lagrangian external sources coupled to these operators. We need to express Eq. (1.21) in terms of the rescaled quark (and gluon) fields as in Eq. (2.9) and this adds an extra N_C factor to the source. We will add then to the QCD Lagrangian a source term as $N_C\, J_i(x)\, \hat{O}_i(x)$ where $\hat{O}_i(x)$ is one operator written in terms of the rescaled fields and $J_i(x)$ is the corresponding external source. Furthermore, the full extended Lagrangian again has a global N_C factor ensuring that the counting rule (2.11) still holds. To obtain the correlation functions we perform the appropriate functional derivatives:

$$\left\langle \hat{O}_1\, \hat{O}_2\, \ldots\, \hat{O}_r \right\rangle \;=\; \frac{1}{i\, N_C}\frac{\partial}{\partial J_1} \cdots \frac{1}{i\, N_C}\frac{\partial}{\partial J_r}\, W(J)\Big|_{J=0}\,, \tag{2.13}$$

from where it can be clearly established that each functional derivative (*i.e.* each source insertion) implies a $1/N_C$ suppression. The order N_C^2 contributions to $W(J)$ come from planar graphs with only gluons lines. They can contribute to correlation functions of purely gluonic operators. Thus pure–gluon r–point correlation functions are of order N_C^{2-r}. If we want to calculate correlation functions involving quark bilinears we will need order N_C contributions from $W(J)$ given by planar diagrams with a quark loop in the outermost border as shown in Fig. 2.6. Thus r–point correlation functions with quark bilinears are of order N_C^{1-r}. To obtain the counting rules for correlation functions made up from non–normalized quark fields we have to multiply the former result by N_C^r obtaining then that the order does not depend on the number of quark bilinear insertions and it is equal to N_C.

We can use the N_C–counting rules for correlation functions to derive the counting rules for meson and glueball scattering. We have to require that both meson and glueball are created with an amplitude independent of N_C (that is equivalent to making use of the LSZ formula). From now on, $\hat{H}_i$ will denote a quark bilinear operator and $\hat{G}_i$ a gluon operator, both expressed in terms of the rescaled fields (2.9), that qualify as interpolating fields for mesons or gluons. Generically we can

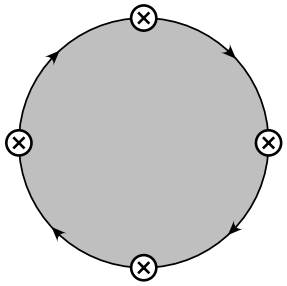

Figure 2.6: Dominant contribution to a 4–point correlation function involving quark bilinears.

write a meson field as a colour singlet made up of quarks and anti–quarks :

$$M_\Gamma \;=\; \frac{1}{\sqrt{N_C}} \sum_{i=1}^{N_C} \overline{q}_\alpha \, \Gamma \, q^\alpha \;=\; \sqrt{N_C} \sum_{i=1}^{N_C} \hat{\overline{q}}_\alpha \, \Gamma \, \hat{q}^\alpha \;=\; \sqrt{N_C}\, \hat{H}_\Gamma \,, \tag{2.14}$$

where the quantum numbers of the meson are specified by the Dirac and flavour matrix Γ and the factor $1/N_C$ is included to make the probability of creating a meson equal to one. The two point correlation function $\langle \hat{G}_1 \, \hat{G}_2 \rangle$ is of order unity and so $\hat{G}_i$ creates a glueball with unit amplitude. This could have been inferred from Eq. (2.9) since the rescaled gluon field is not rescaled by N_C powers. $\langle \hat{G}_1 \, \ldots \, \hat{G}_r \rangle$ is of order N_C^{2-r}, thus an r–glueball interaction vertex is of order N_C^{2-r}, and *each additional glueball* gives a $1/N_C$ suppression. The meson two point correlation function $\langle \hat{H}_1 \, \hat{H}_2 \rangle$ is of order $1/N_C$ and thus $\sqrt{N_C}\, \hat{H}_i$ creates a meson with unit amplitude, as shown in Eq. (2.14). The r–point correlation function $\langle \sqrt{N_C}\, \hat{H}_1 \, \ldots \, \sqrt{N_C}\, \hat{H}_r \rangle$ is of order $N_C^{1-\frac{r}{2}}$ as well as the r–meson interacting vertex, and *each additional meson* gives a $1/\sqrt{N_C}$ suppression. Mixed quark–meson vertices with r glueballs and s mesons are of order $N_C^{1-r-\frac{s}{2}}$. All these counting rules are summarized in Fig. 2.7.

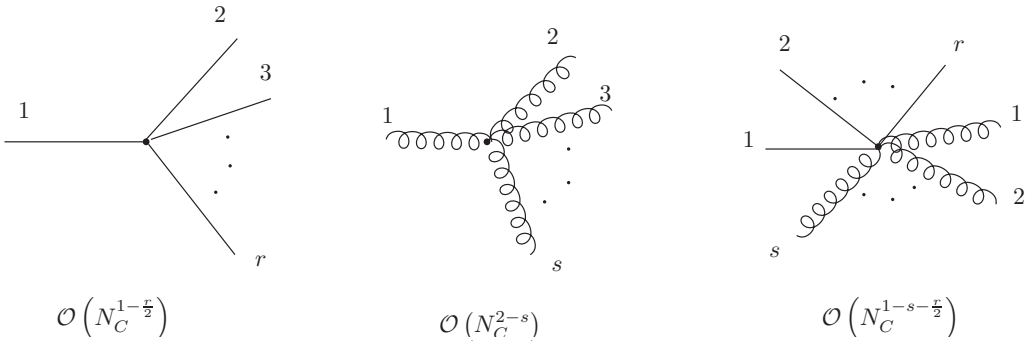

Figure 2.7: N_C–counting rules for the scattering of mesons (continuous line) and glueballs (wiggly line).

One important result is that the pion decay constant F is of order $\sqrt{N_C}$ as can be

read from Eq. (1.35) as this matrix element is of the type $\langle N_C \hat{H}_1 \sqrt{N_C}\, \hat{H}_2 \rangle \sim \sqrt{N_C}$ where the first N_C factor is added to write the axial current in terms of non–normalized quark fields and the second $\sqrt{N_C}$ factor to make the amplitude to create a pion unitary.

2.4 Phenomenology and main results

The N_C–counting rules imply that one has a weakly coupled theory of mesons and glueballs with a coupling constant $1/\sqrt{N_C}$. As a weakly interacting theory, one can perturbatively expand in the coupling constant $1/\sqrt{N_C}$. The leading–order graphs are tree–graphs, and the leading–order singularities are poles. QCD, a strongly interacting theory of quarks and gluons has been rewritten as a weakly interacting theory of hadrons. The leading N_C interactions bind the quarks and gluons into colour singlet hadrons. The residual interactions between these hadrons are $1/N_C$ suppressed. The $1/N_C$ expansion is also equivalent to a semiclassical expansion for the meson theory.

The spectrum of the theory contains an infinite number of narrow glueballs and meson resonances. They are narrow because their widths vanish as $N_C \to \infty$ (as their interaction vertices are $1/N_C$ suppressed). There must be an infinite number of resonances to match the logarithmic running of QCD correlation functions in the high–energy regime (see Chapter 4):

$$\int \mathrm{d}^4x\, e^{iq\cdot x} \langle Q(x)\, Q(0) \rangle \;=\; \sum_i^{\infty} \frac{f_i^2}{q^2 - m_i^2}\,, \tag{2.15}$$

where m_i is the mass of the i–th hadronic resonance H_i and it is $\sim \mathcal{O}(1)$, and $f_i \,=\, \langle\, 0\,|\, Q(0)\,|\, H_i\,\rangle$ is the decay constant of the resonance for the current Q , and it is $\sim \mathcal{O}(\sqrt{N_C})$. This can be seen in Fig. 2.8. The same argument can be applied to three–point Green functions, as shown in Fig. 2.9

Figure 2.8: Two–point correlation function in the large–N_C limit.

Other features ruled by the expansion are [35, 37]:

1. Mesons are pure $q\overline{q}$ states, that is, one finds a suppression of the $q\overline{q}$ sea at $N_C \to \infty$; suppression of exotic $qq\overline{qq}$ states.

2. Zweig's rule is exact in the large–N_C limit, that is, mesons should be classified as nonets rather than octets. The axial anomaly has disappeared and flavour $U(n_f)_L \otimes U(n_f)_R$ has been restored.

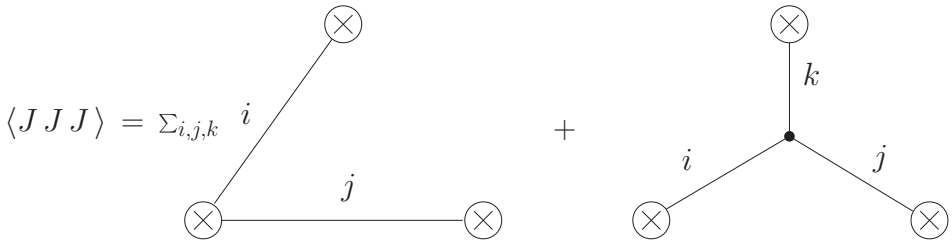

Figure 2.9: Three–point correlation functions in the large–N_C limit.

3. In the large–N_C limit and under reasonable assumptions, $U(n_f)_R \otimes U(n_f)_L$ symmetry must spontaneously break down to $U(n_f)_V$ [12].

4. Meson physics in the large–N_C limit is described by the tree diagrams of an effective local Lagrangian, with local vertices and local meson fields. This fact invites us quickly to think about the proper approach of the phenomenological Lagrangians.

2.5 The 1/N$_C$ expansion in χPT

We can use the N_C–counting rules obtained in the previous sections to derive useful results for the effective field theory of QCD at very low energies. It turns out to be a useful source of dynamical information [35,38], in the sense that it comes directly from QCD.

One can imagine computing the chiral Lagrangian by evaluating the QCD functional integral with sources (quark bilinears) for the Goldstone bosons. We have seen that the leading order diagrams contributing to correlation functions of quark bilinears are $\mathcal{O}(N_C)$ and contain a single quark loop, Fig. 2.6. This implies that the leading order terms in the Lagrangian are $\mathcal{O}(N_C)$. At the sight of this figure it is clear that the leading order terms can be written as a single flavour trace since the outgoing flavour quark in one vertex is the incoming flavour at the next vertex. Similarly terms with two quark loops are $\mathcal{O}(1)$ and consist in two traces and those with r loops have r flavour traces and are $\mathcal{O}(N_C^{1-r})$.

Since in the large–N_C limit the $U(n_f)_L \otimes U(n_f)_R$ symmetry is restored, we have nine Goldstone bosons which can be cast together in the matrix

$$\sum_{a=0}^{8} \frac{\lambda^a}{\sqrt{2}}\,\pi^a = \begin{pmatrix} \frac{1}{\sqrt{2}}\pi^0 + \frac{1}{\sqrt{6}}\eta_8 + \frac{1}{\sqrt{3}}\eta_1 & \pi^+ & K^+ \\ \pi^- & -\frac{1}{\sqrt{2}}\pi^0 + \frac{1}{\sqrt{6}}\eta_8 + \frac{1}{\sqrt{3}}\eta_1 & K^0 \\ K^- & \overline{K}^0 & -\sqrt{\frac{2}{3}}\eta_8 + \frac{1}{\sqrt{3}}\eta_1 \end{pmatrix}. \tag{2.16}$$

Let us concentrate first in the $\mathcal{L}_2$ Lagrangian (1.54). It has a global factor F^2 that translates into a global factor of N_C and it is split into two terms, the kinetic and

i	$L_i^r(M_\rho)$	$\mathcal{O}(N_C)$	source	$L_i^{N_C\to\infty}$
$2L_1 - L_2$	-0.6 ± 0.6	$\mathcal{O}(1)$	K_{e4}, $\pi\pi\to\pi\pi$	0.0
L_2	1.4 ± 0.3	$\mathcal{O}(N_C)$	K_{e4}, $\pi\pi\to\pi\pi$	1.8
L_3	-3.5 ± 1.1	$\mathcal{O}(N_C)$	K_{e4}, $\pi\pi\to\pi\pi$	-4.3
L_4	-0.3 ± 0.5	$\mathcal{O}(1)$	Zweig's rule	0.0
L_5	1.4 ± 0.5	$\mathcal{O}(N_C)$	$F_K : F_\pi$	2.1
L_6	-0.2 ± 0.3	$\mathcal{O}(1)$	Zweig's rule	0.0
L_7	-0.4 ± 0.2	$\mathcal{O}(1)$	GMO, L_5, L_8	-0.3
L_8	0.9 ± 0.3	$\mathcal{O}(N_C)$	M_ϕ, L_5	0.8
L_9	6.9 ± 0.7	$\mathcal{O}(N_C)$	$\langle r^2\rangle_V^\pi$	7.1
L_{10}	-5.5 ± 0.7	$\mathcal{O}(N_C)$	$\pi\to e\,\nu\,\gamma$	-5.4

Table 2.1: Experimental values of the coupling constants $L_i^r(M_\rho)$ in units of 10^{-3} [35]. The fourth column shows the experimental source employed. Predictions in the large–N_C limit are obtained in the one–resonance approximation working within $U(3)\otimes U(3)$.

the mass term. Since $\langle\overline{q}q\rangle = N_C\langle\hat{H}_i\rangle \sim \mathcal{O}(N_C)$ then $B_0 \sim \mathcal{O}(1)$ and both terms in (1.54) are $\mathcal{O}(N_C)$ as it corresponds to the fact that we have a single flavour trace. The u matrix has an expansion in powers of π/F and so each additional meson field has a factor $1/F \propto 1/\sqrt{N_C}$ as required by the N_C–counting rules. The Lagrangian (1.54) has an overall N_C factor and the u matrix is N_C independent, so the $1/N_C$ expansion is equivalent to a semiclassical expansion. Graphs computed using the chiral Lagrangian have a $1/N_C$ suppression for each loop as it implies an additional quark loop. It is reflected in the fact that each chiral loop in accompanied by a $1/(4\,\pi F)^2$ factor.

Let us have a look at the $\mathcal{L}_4$ Lagrangian (1.62). The terms with a single trace, $L_{3,5,8,9}$ should be $\mathcal{O}(N_C)$ and those with two traces $L_{1,2,4,6,7}$ should be $\mathcal{O}(1)$. However due to the Cayley–Hamilton relation for three flavours we can write

$$\langle u_\mu\,u_\nu\,u^\mu\,u^\nu\rangle \;=\; -\,2\,\langle u_\mu\,u^\mu\,u_\nu\,u^\nu\rangle \;+\; \frac{1}{2}\,\langle u_\mu\,u^\mu\rangle^2 \;+\; \langle u_\mu\,u_\nu\rangle\,\langle u^\mu\,u^\nu\rangle\;. \qquad (2.17)$$

The correct statement is then that L_1 and L_2 are $\mathcal{O}(N_C)$ but the linear combination $2\,L_1 - L_2$ is $\mathcal{O}(1)$. The full set of predictions is shown in Table 2.1.

2.6 Resonance Chiral Theory

2.6.1 General considerations

Already in the 50's and 60's, it was realized that in pion–nucleon scattering processes, for certain spin–isospin channels, peaks of probability showed up. Of course these peaks where pinning down the existence of a resonance as an intermediate state, and in the frame of the quark model it was given a $\bar{q}q$ content.

The aim of this section is to find an effective theory with these resonances as active degrees of freedom. The energy region where these resonances play an essential röle is $m_\rho \lesssim E \lesssim 2\,\mathrm{GeV}$. It has been already pointed out that at this range of energies the only known expansion parameter is $1/N_C$, and in this framework it was discussed that we can describe the physics by means of effective Lagrangians with hadronic degrees of freedom. In fact, at leading order in $1/N_C$ we will only consider tree–level diagrams given by terms with only one trace.

We have learned how to deal with theories suffering spontaneous breakdown of symmetries, and so we know how to parametrize the Goldstone fields. On the other hand, the $U(n_f)_L \otimes U(n_f)_R$ symmetry is restored and our resonance fields, as for the Goldstones, will be grouped in nonets rather than octets and singlets. The resonance fields do not know anything about the underlying chiral symmetry, and so they must have well defined transformation properties under the $U_V(3)$ subgroup. The fundamental work to develop this *Resonance Chiral Theory* (RχT) was performed in [13].

But the röle played by RχT is not only to describe the hadronic physics at the scale where resonances manifest themselves as active degrees of freedom. It will be an essential link between the very low–energy regime ruled by χPT and the high–energy regime ruled by the Operator Product Expansion (OPE). Since RχT is supposed to describe correctly physics at all energy regimes, we can find relations that must be satisfied by their parameters in order to match the asymptotic behaviour of QCD at high energies (RχT is not QCD for arbitrary values of its parameters). After a functional integration of the resonance fields (that is, restricting the energy below the lightest integrated resonance) we recover the χPT Lagrangian structure, but with predictions for its couplings in terms of the RχT parameters, those constrained by the asymptotic behaviour. So we can link the high– and low–energy regimes of QCD, and the missing link is precisely RχT. This matching procedure and functional integration can be better understood using the language of path integrals (1.26) and (1.46) :

$$
\begin{aligned}
e^{\,i\,Z} &= \int \mathcal{D}q\,\mathcal{D}\overline{q}\,\mathcal{D}G_\mu\, e^{\,i\int \mathrm{d}^4x\,\mathcal{L}_{QCD}} \\
&= \int \mathcal{D}u \prod_{i,j,q,l,m=1}^{\infty} \mathcal{D}V_i\,\mathcal{D}A_j\,\mathcal{D}S_k\,\mathcal{D}P_l\,\mathcal{D}B_m\, e^{\,i\int \mathrm{d}^4x\,\mathcal{L}_{R\chi T}(u,V_i,A_j,S_k,P_l,B_m)} \\
&= \int \mathcal{D}u\, e^{\,i\int \mathrm{d}^4x\,\mathcal{L}_{\chi PT}(u)}\,, \qquad (2.18)
\end{aligned}
$$

where V, A, S, P and B represent the vector, axial–vector, scalar, pseudoscalar and pseudovector resonance fields, respectively. As a last comment, although the large–N_C behaviour of QCD predicts an infinite number of resonances for any given set of quantum numbers, in most cases one only deals with the first multiplet, what is known as the *Single Resonance Approximation;* or if instead we take the minimum number of resonances in each channel such that we fulfill all the short distance requirements, the approach is known as the *Minimal Hadronic Ansatz* (MHA). Dealing with the infinite tower of resonances is complicated because their couplings are not a priory determined by QCD, and moreover, phenomenology supports the MHA approach. If we are far from the resonance pole, its influence is suppressed by the inverse of its mass.

2.6.2 The RχT Lagrangian

As discussed previously, the transformation properties of the resonance fields under the chiral group must ensure that they transform as nonets under the vector subgroup. The nine resonance fields are then grouped together in an $U(3)$ matrix, and for instance, for the first multiplet of vector mesons it takes the following form:

$$
V_{\mu\nu} = \frac{1}{\sqrt{2}}\sum_{a=0}^{8}\lambda_a V^a_{\mu\nu} =
$$

$$
\begin{pmatrix}
\frac{1}{\sqrt{2}}\rho^0 + \frac{1}{\sqrt{6}}\omega_8 + \sqrt{\frac{1}{3}}\omega_0 & \rho^+ & K^{*+} \\
\rho^- & -\frac{1}{\sqrt{2}}\rho^0 + \frac{1}{\sqrt{6}}\omega_8 + \sqrt{\frac{1}{3}}\omega_0 & K^{*0} \\
K^{*-} & \overline{K}^{*0} & -\sqrt{\frac{2}{3}}\omega_8 + \sqrt{\frac{1}{3}}\omega_0
\end{pmatrix}_{\mu\nu}, \qquad (2.19)
$$

where instead of the more familiar Proca formalism, we have used the antisymmetric one, to be discussed in Appendix C. This formalism will be used throughout this thesis for the spin–one resonance fields, unless otherwise stated. There are many possible ways to transform the resonance fields that lead to the same transformation

under the vector group, we give some examples

$$V \to \begin{cases} g_L\, V\, g_R^\dagger \\ g_L\, V\, g_L^\dagger \\ h(g,\Phi)\, V\, g_R^\dagger \\ g_L\, V\, h(g,\Phi)^\dagger \\ h(g,\Phi)\, V\, h(g,\Phi)^\dagger \\ \vdots \end{cases} , \tag{2.20}$$

but it can be shown that all of them are equivalent after a field redefinition. Working as we are in the u–basis, obviously the most convenient choice is $R \to h(g,\Phi)\, R\, h(g,\Phi)^\dagger$.

The RχT Lagrangian can be split in two parts :

$$\mathcal{L}_{R\,\chi T}(u,V,A,S,P,B) \,=\, \mathcal{L}_{\chi\mathrm{PT}\,n=2}(u) \,+\, \tilde{\mathcal{L}}_{\chi\mathrm{PT}\,n>2}(u) \,+\, \mathcal{L}_R(u,V,A,S,P,B)\,. \tag{2.21}$$

The first is the χPT Lagrangian describing the dynamics of the Goldstone bosons among themselves, but with different coupling constants, and the second contains the coupling of the mesonic resonances $R(J^{PC})$ of the type $V(1^{--})$, $A(1^{++})$, $B(1^{+-})$, $S(0^{++})$ and $P(0^{-+})$ to the Goldstone bosons. At this point a comment is in order : the values of the chiral LECs in $\tilde{\mathcal{L}}_{\chi PT}$ depend on the specific choice of the formalism for describing the spin–one resonance fields. Thus these LECs lack of physical meaning but are nevertheless necessary to ensure that the theory complies with the short–distance behaviour.

The discrete transformation properties of the fields describing the resonances are depicted in Table 2.2. Now using as building blocks the resonance fields plus the chiral tensors of (1.51) we have to write the most general Lagrangian being invariant under the $U(3)_L \otimes U(3)_R$ group and the discrete transformations $\mathcal{P}$ and $\mathcal{C}$ (and of course being hermitian and Lorentz invariant). Of course the problem now is that there are an infinite number of terms and we do not have a perturbative expansion in small momenta; so terms with many derivatives are not suppressed with respect to terms with less derivatives. However, if we want this Lagrangian to describe the high–energy regime, it cannot have many derivatives (at high energies form factors and Green functions vanish) and this limits the number of operators drastically. The usual way to proceed is to write those pieces of the Lagrangian needed for a given goal. In this section we provide the pieces necessary to calculate all the two–point Green functions yielding at the same time upon functional integration the chiral LECs of $\mathcal{L}_4$. These consist of the kinetic terms for the resonances (those are bilinear in the resonance fields) plus terms linear in the resonance fields times an $\mathcal{O}(p^2)$ chiral operator involving only Goldstone fields and external sources :

$$\mathcal{L}_R \,=\, \sum_{R=V,A,S,P,B} \{\mathcal{L}_{\mathrm{kin}}(R) \,+\, \mathcal{L}_2(R)\}\ , \tag{2.22}$$

with kinetic term [1]

$$\begin{aligned}
\mathcal{L}_{\rm kin}(R) &= -\frac{1}{2}\langle \nabla^\lambda R_{\lambda\mu}\nabla_\nu R^{\nu\mu} - \frac{1}{2}M_R^2\, R_{\mu\nu}\, R^{\mu\nu}\rangle\,, \quad R = V, A, B \quad , \\
\mathcal{L}_{\rm kin}(R) &= \frac{1}{2}\left\langle \nabla^\mu R\, \nabla_\mu R - M_R^2 R^2\right\rangle\,, \quad R = S, P \quad ,
\end{aligned} \tag{2.23}$$

where M_R is the corresponding mass in the chiral limit. The interaction term is given by

$$\begin{aligned}
\mathcal{L}_2[V(1^{--})] &= \frac{F_V}{2\sqrt{2}}\langle V_{\mu\nu}\, f_+^{\mu\nu}\rangle + \frac{i\,G_V}{2\sqrt{2}}\langle V_{\mu\nu}[u^\mu, u^\nu]\rangle + \sqrt{2}\,F_V^T\, m_V \langle V_{\mu\nu}\, t_+^{\mu\nu}\rangle\,, \\
\mathcal{L}_2[A(1^{++})] &= \frac{F_A}{2\sqrt{2}}\langle A_{\mu\nu}\, f_-^{\mu\nu}\rangle\,, \\
\mathcal{L}_2[B(1^{+-})] &= i\sqrt{2}\,F_B^T\, m_B \langle B_{\mu\nu}\, t_-^{\mu\nu}\rangle + \frac{F_B}{4\sqrt{2}}\langle B_{\mu\nu}\, f_{+\alpha\beta}\rangle\,\varepsilon^{\mu\nu\alpha\beta} + \frac{G_B}{\sqrt{2}}\langle B_{\mu\nu}\, u_\alpha\, u_\beta\rangle\,\varepsilon^{\mu\nu\alpha\beta}\,, \\
\mathcal{L}_2[S(0^{++})] &= c_d\,\langle S\, u_\mu\, u^\mu\rangle + c_m\,\langle S\,\chi_+\rangle\,, \\
\mathcal{L}_2[P(0^{-+})] &= i\,d_m\,\langle P\,\chi_-\rangle\,,
\end{aligned} \tag{2.24}$$

where all coupling constants are real. The interactions of the $B(1^{+-})$ resonances were first introduced in Ref. [39] and the interactions with tensor sources in Ref. [26]. The interaction of the $V(1^{--})$ with tensor sources was first introduced in Ref. [40]. It is remarkable that in the Proca formalism the $B(1^{+-})$ resonances decouple from vector sources:

$$\begin{aligned}
&\frac{F_B}{4\sqrt{2}\,m_B}\left\langle \hat{B}_{\mu\nu}\, f_{+\alpha\beta}\right\rangle \varepsilon^{\mu\nu\alpha\beta} = \frac{F_B}{2\sqrt{2}\,m_B}\left\langle \nabla_\mu \hat{B}_\nu\, f_{+\alpha\beta}\right\rangle \varepsilon^{\mu\nu\alpha\beta} \\
&\doteq -\frac{F_B}{2\sqrt{2}\,m_B}\left\langle \hat{B}_\nu\, \nabla_\mu f_{+\alpha\beta}\right\rangle \varepsilon^{\mu\nu\alpha\beta} = -\,i\,\frac{F_B}{4\sqrt{2}\,m_B}\left\langle \hat{B}_\nu\, [f_{+\mu\alpha}, u_\beta]\right\rangle \varepsilon^{\mu\nu\alpha\beta}\,,
\end{aligned} \tag{2.25}$$

where $\hat{B}_{\mu\nu} = \nabla_\mu \hat{B}_\nu - \nabla_\nu \hat{B}_\mu$ and $\hat{B}_\mu$ corresponds to the Proca field. Apart from integration by parts, in the last step we have used the first Bianchi identity, Eq. (1.70). From a physical point of view this fact can be easily understood, since the matrix element $\langle\, 0 \,|\, V_\mu^a(0) \,|\, b^b(p,\lambda)\rangle$ is identically zero.

2.7 Functional integration of the resonances

It is a common lore to believe that the dynamics of the Goldstone bosons is largely affected by the existence of the lowest mass resonances. Much as happens in the Fermi theory, at energies well below the pole of the corresponding resonance, we can substitute its propagator by a tower of local operators involving only light degrees of freedom. Since the lowest order χPT Lagrangian $\mathcal{L}_2$ (1.54) is universal, it cannot receive any influence from heavier degrees of freedom. Then we expect that the

[1] This kinetic term includes an interaction due to the covariant derivative.

Table 2.2: Discrete transformation properties of the resonance fields.

$\mathcal{O}$	$\mathcal{P}$	$\mathcal{C}$	h.c.
$V_{\mu\nu}$	$V^{\mu\nu}$	$-V_{\mu\nu}^{\top}$	$V_{\mu\nu}$
$A_{\mu\nu}$	$-A^{\mu\nu}$	$A_{\mu\nu}^{\top}$	$A_{\mu\nu}$
S	S	$S^{\top}$	S
P	$-P$	$P^{\top}$	P
$B_{\mu\nu}$	$-B^{\mu\nu}$	$-B_{\mu\nu}^{\top}$	$B_{\mu\nu}$

resonances will give a contribution to the LECs appearing at higher orders in the chiral expansion, namely $\mathcal{L}_4$ and $\mathcal{L}_6$. Of course, the formal procedure is to perform a functional integration of the resonance fields in the generating functional (2.18). In the large–N_C limit and after imposing that RχT matches the known short–distance behaviour, one can demonstrate that for almost all the cases, the LECs of χPT are fully determined by the resonance exchange; this phenomenon is known as *resonance saturation*.

In this section we will express the chiral LECs involving tensor currents in terms of the RχT parameters. In order for that, one must only integrate out the vector and pseudovector fields and pick the operators containing at least one tensor source.

We outline the general procedure. One can reexpress (2.24) for vectors and pseudo–vectors in the following way :

$$\mathcal{L}_2 \,=\, \langle\, V_{\mu\nu}\, J_V^{\mu\nu}\,\rangle \,+\, \langle\, B_{\mu\nu}\, J_B^{\mu\nu}\,\rangle\ , \tag{2.26}$$

The equation of motion then reads

$$\begin{aligned} \nabla^\mu\nabla_\alpha V_{cl}^{\alpha\nu} \,-\, \nabla^\nu\nabla_\alpha V_{cl}^{\alpha\mu} \,+\, m_V^2\, V_{cl}^{\mu\nu} \;&=\; -\,2\, J_V^{\mu\nu}\ , \\ \nabla^\mu\nabla_\alpha B_{cl}^{\alpha\nu} \,-\, \nabla^\nu\nabla_\alpha B_{cl}^{\alpha\mu} \,+\, m_B^2\, B_{cl}^{\mu\nu} \;&=\; -\,2\, J_B^{\mu\nu}\ . \end{aligned} \tag{2.27}$$

We can solve this equation iteratively and find the classical solution :

$$\begin{aligned} V_{cl}^{\mu\nu} \;&=\; -\,\frac{2}{m_V^2}\, J_V^{\mu\nu} \,+\, \frac{2}{m_V^4}\,(\nabla^\mu\nabla_\alpha J_V^{\alpha\nu} - \nabla^\nu\nabla_\alpha J_V^{\alpha\mu}) \,+\, \mathcal{O}\left(\frac{1}{m_V^6}\right)\ , \\ B_{cl}^{\mu\nu} \;&=\; -\,\frac{2}{m_B^2}\, J_B^{\mu\nu} \,+\, \frac{2}{m_B^4}\,(\nabla^\mu\nabla_\alpha J_B^{\alpha\nu} - \nabla^\nu\nabla_\alpha J_B^{\alpha\mu}) \,+\, \mathcal{O}\left(\frac{1}{m_B^6}\right)\ , \end{aligned} \tag{2.28}$$

when substituting back in (2.24) we find the effective Lagrangian :

$$\begin{aligned} \mathcal{L}_{\rm eff} \;&=\; \frac{1}{2}\,\langle V_{cl}^{\mu\nu}\, J_{V\mu\nu} + B_{cl}^{\mu\nu}\, J_{B\mu\nu}\rangle = -\,\frac{1}{m_V^2}\,\langle J_V^{\mu\nu}\, J_{V\mu\nu}\rangle \,-\, \frac{1}{m_B^2}\,\langle J_B^{\mu\nu}\, J_{B\mu\nu}\rangle \\ &\quad -\,\frac{2}{m_V^4}\,\langle \nabla^\mu J_{V\mu\nu}\,\nabla_\alpha J_V^{\alpha\nu}\rangle \,-\, \frac{2}{m_B^4}\,\langle \nabla^\mu J_{B\mu\nu}\,\nabla_\alpha J_B^{\alpha\nu}\rangle \,+\, \mathcal{O}\!\left(\frac{1}{m_R^6}\right). \end{aligned} \tag{2.29}$$

So considering terms having at least one tensor field we find (we only expand to $1/m_B^4$ those terms needed in this thesis):

$$\begin{aligned}\mathcal{L}_{\rm eff} &= \left(\frac{F_H F_B}{M_B} - \frac{F_V F_V^T}{M_V}\right)\langle f_{+\mu\nu}\, t_+^{\mu\nu}\rangle + \left(\frac{2\,i\,F_B G_H}{M_B} - \frac{2\,i\,F_V^T G_V}{M_V}\right)\langle t_{+\mu\nu}\, u^\mu\, u^\nu\rangle \\ &+ 2\left[F_B^2 - (F_V^T)^2\right]\langle t_{+\mu\nu}\, t_+^{\mu\nu}\rangle - \frac{4(F_V^T)^2}{M_V^2}\left\langle \nabla^\mu t_{+\mu\nu}\, \nabla_\alpha t_+^{\alpha\nu}\right\rangle \\ &+ \frac{4\,F_B^2}{M_B^2}\left\langle \nabla^\mu t_{-\mu\nu}\, \nabla_\alpha t_-^{\alpha\nu}\right\rangle - \frac{2\,F_V F_V^T}{M_V^3}\left\langle \nabla^\mu f_{+\mu\nu}\, \nabla_\alpha t_+^{\alpha\nu}\right\rangle . \end{aligned} \tag{2.30}$$

By comparison with the χPT Lagrangian of [23] shown in Eq. (1.62) and Table B.1 in Appendix A.2 and defining the chiral LECs as $L_i = \tilde{L}_i + L_i^R$ one concludes that

$$\begin{aligned}&\Lambda_1^R = \left(\frac{F_H F_B}{M_B} - \frac{F_V F_V^T}{M_V}\right), \quad \Lambda_2^R = \left(\frac{2\,F_V^T G_V}{M_V} - \frac{2\,F_B G_H}{M_B}\right), \\ &\Lambda_3^R = 2\left[F_B^2 - (F_V^T)^2\right], \quad \Omega_{51}^R = 0, \quad \Omega_{52}^R = -\frac{4(F_V^T)^2}{M_V^2}, \\ &\Omega_{53}^R = \frac{4\,F_B^2}{M_B^2}, \quad \Omega_{94}^R = -\frac{2F_V F_V^T}{M_V^3}, \quad H_{118}^R = 0 . \end{aligned} \tag{2.31}$$

Of course with (2.24) we cannot saturate all the LECs appearing in $\mathcal{L}_6$ of [23]. For these we would need to consider terms with more that one resonance.

To end with this subsection and for the sake of completeness we review the results obtained for the LECs of $\mathcal{L}_4$ not involving tensor sources [13]:

$$\begin{aligned}&L_1 = \frac{G_V^2}{8\,M_V^2}, && L_2 = \frac{G_V^2}{4\,M_V^2}, && L_3 = -\frac{3\,G_V^2}{4\,M_V^2} + \frac{c_d^2}{2\,M_S^2}, \\ &L_4 = 0, && L_5 = \frac{c_d\, c_m}{M_S^2}, && L_6 = 0, \\ &L_7 = 0, && L_8 = \frac{c_m^2}{2\,M_S^2} - \frac{d_m^2}{2\,M_P^2}, && L_9 = \frac{F_V G_V}{2\,M_V^2}, \\ &L_{10} = -\frac{F_V^2}{4M_V^2} + \frac{F_A^2}{4M_A^2}, && H_1 = -\frac{F_V^2}{8\,M_V^2} - \frac{F_A^2}{8\,M_A^2}, && H_2 = \frac{c_m}{M_S^2} + \frac{d_m^2}{M_P^2}. \end{aligned} \tag{2.32}$$

2.8 Odd–intrinsic–parity sector

If one wants to calculate three–point Green functions it is not enough to use the Lagrangian depicted in (2.22). One then would need terms with three resonance fields, terms with two resonance fields plus one $\mathcal{O}(p^2)$ chiral operator, and terms linear in the resonance fields times one $\mathcal{O}(p^4)$ tensor operator [typically this is achieved with the product of two $\mathcal{O}(p^2)$ chiral operators]. But this is not the only reason to go beyond the (2.22) Lagrangian. If we want to determine the $\mathcal{O}(p^6)$ LECs in terms of the resonance parameters, one might think that the procedure is

simply to use Eq. (2.29) up to the $\mathcal{O}(M_R^{-4})$ order. However this is not enough, since the complete set of $\mathcal{O}(M_R^{-4})$ operators is not totally rendered by the second order expansion of (2.22): one gets contributions of the same order precisely from the terms needed to calculate the three–point Green functions. The full set of operators needed to saturate the even–intrinsic–parity sector $\mathcal{O}(p^6)$ LECs not involving tensor currents can be found in Ref. [41].

For the phenomenological studies performed in this thesis, the only three–point Green function that we need to study in the framework of RχT is the $\langle VVP\rangle$. This function belongs to the odd–intrinsic–parity sector of QCD, and then upon functional integration it saturates the $\mathcal{O}(p^6)$ LECs corresponding to this sector [33]. We remind the reader that the first contribution to the odd–intrinsic–parity sector of the chiral Lagrangian is the WZW anomalous term, and it is $\mathcal{O}(p^4)$. This term is universal and does not receive any contribution from resonance exchange. Moreover, it must be explicitly included in the odd–intrinsic–parity RχT Lagrangian.

The contributions to the odd–intrinsic–parity sector consisting only on one multiplet of vector meson resonances was first worked out in Ref. [42] and we review here its expression. As we shall see, with only one multiplet of vector meson resonances, one fails to reproduce at the same time the OPE and Brodsky–Lepage constraints. Within the antisymmetric formalism, it consists of an independent set of odd–intrinsic–parity operators which comprise all possible vertices involving two vector resonances and one Goldstone (VVp), and vertices with one vector resonance and one external vector source plus one Goldstone (VJp). The basis reads:

VJp terms

$$\begin{aligned}
\mathcal{O}^1_{\rm VJp} &= \epsilon_{\mu\nu\rho\sigma}\left\langle \{V^{\mu\nu}, f_+^{\rho\alpha}\}\nabla_\alpha u^\sigma \right\rangle , & \mathcal{O}^2_{\rm VJp} &= \epsilon_{\mu\nu\rho\sigma}\left\langle \{V^{\mu\alpha}, f_+^{\rho\sigma}\}\nabla_\alpha u^\nu \right\rangle ,\\
\mathcal{O}^3_{\rm VJp} &= \epsilon_{\mu\nu\rho\sigma}\left\langle \{V^{\mu\nu}, f_+^{\rho\sigma}\}\,\chi_- \right\rangle , & \mathcal{O}^4_{\rm VJp} &= i\,\epsilon_{\mu\nu\rho\sigma}\left\langle V^{\mu\nu}\,[\,f_-^{\rho\sigma}, \chi_+]\right\rangle ,\\
\mathcal{O}^5_{\rm VJp} &= \epsilon_{\mu\nu\rho\sigma}\left\langle \{\nabla_\alpha V^{\mu\nu}, f_+^{\rho\alpha}\}\,u^\sigma \right\rangle , & \mathcal{O}^6_{\rm VJp} &= \epsilon_{\mu\nu\rho\sigma}\left\langle \{\nabla_\alpha V^{\mu\alpha}, f_+^{\rho\sigma}\}\,u^\nu \right\rangle ,\\
\mathcal{O}^7_{\rm VJp} &= \epsilon_{\mu\nu\rho\sigma}\left\langle \{\nabla^\sigma V^{\mu\nu}, f_+^{\rho\alpha}\}\,u_\alpha \right\rangle ,
\end{aligned} \tag{2.33}$$

VVp terms

$$\begin{aligned}
\mathcal{O}^1_{\rm VVp} &= \epsilon_{\mu\nu\rho\sigma}\left\langle \{V^{\mu\nu}, V^{\rho\alpha}\}\nabla_\alpha u^\sigma \right\rangle , & \mathcal{O}^2_{\rm VVp} &= i\,\epsilon_{\mu\nu\rho\sigma}\left\langle \{V^{\mu\nu}, V^{\rho\sigma}\}\,\chi_- \right\rangle ,\\
\mathcal{O}^3_{\rm VVp} &= \epsilon_{\mu\nu\rho\sigma}\left\langle \{\nabla_\alpha V^{\mu\nu}, V^{\rho\alpha}\}\,u^\sigma \right\rangle , & \mathcal{O}^4_{\rm VVp} &= \epsilon_{\mu\nu\rho\sigma}\left\langle \{\nabla^\sigma V^{\mu\nu}, V^{\rho\alpha}\}\,u_\alpha \right\rangle ,
\end{aligned} \tag{2.34}$$

And the Lagrangian has then the following form:

$$\begin{aligned}
\mathcal{L}_V^{\rm odd} &= \mathcal{L}_{\rm VJP} + \mathcal{L}_{\rm VVP} \ ,\\
\mathcal{L}_{\rm VJP} &= \sum_{a=1}^{7} \frac{c_a}{M_V}\,\mathcal{O}^a_{\rm VJP} \ , \qquad \mathcal{L}_{\rm VVP} = \sum_{a=1}^{4} d_a\,\mathcal{O}^a_{\rm VVP} \ .
\end{aligned} \tag{2.35}$$

For the computation of the $\langle VVP\rangle$ Green function one can also consider the inclusion of a multiplet of pseudoscalar resonances. As we shall see in Section 5.2.3, if

one considers a multiplet of vector and pseudoscalar resonances only, one cannot simultaneously match the OPE behaviour and the Brodsky–Lepage condition. For the sake of completeness we give its expression here. We now have to consider odd–intrinsic–parity operators comprising all possible vertices involving two vector and one pseudoscalar resonances (VVP), vertices with one vector resonance, one external vector source and one pseudoscalar resonance (VJP), and vertices with two vector external sources and one pseudoscalar (JJP).

$$\begin{aligned}
\mathcal{O}_{VJP} &= \varepsilon_{\mu\nu\alpha\beta} \left\langle \left\{ f_+^{\mu\nu},\, V^{\alpha\beta} \right\} P \right\rangle , \qquad \mathcal{O}_{VVP} = \varepsilon_{\mu\nu\alpha\beta} \left\langle \left\{ V^{\mu\nu},\, V^{\alpha\beta} \right\} P \right\rangle , \\
\mathcal{O}_{JJP} &= \varepsilon_{\mu\nu\alpha\beta} \left\langle \left\{ f_+^{\mu\nu},\, f_+^{\alpha\beta} \right\} P \right\rangle .
\end{aligned} \tag{2.36}$$

Finally we consider the Lagrangian including two multiplets of vector meson resonances, ρ and ρ'.

$$\mathcal{L}_V^{\text{even}} = \frac{F_V}{2\sqrt{2}} \langle\, V_1^{\mu\nu} f_{+\,\mu\nu} \rangle + \frac{F_V'}{2\sqrt{2}} \langle\, V_2^{\mu\nu} f_{+\,\mu\nu} \rangle , \tag{2.37}$$

$$\begin{aligned}
\mathcal{L}_V^{\text{odd}} &= \sum_{i=1}^{7} \frac{c_i}{M_{V_1}} \mathcal{O}^i_{V_1 JP} + \sum_{i=1}^{7} \frac{c_i'}{M_{V_2}} \mathcal{O}^i_{V_2 JP} + \sum_{i=1}^{4} d_i \, \mathcal{O}^i_{V_1 V_1 P} \\
&\quad + \sum_{i=1}^{4} d_i' \, \mathcal{O}^i_{V_2 V_2 P} + \sum_{n=a,b,c,d,e} d_n \, \mathcal{O}^n_{V_1 V_2 P} + d_f \, \mathcal{O}^f_{V_1 V_2 J} ,
\end{aligned} \tag{2.38}$$

Operators $\mathcal{O}_{V_i JP}$ and $\mathcal{O}_{V_i V_i P}$ were already given in Eqs. (2.33) and (2.34) and for the last part of the Lagrangian there are two subsets of pieces [43]:

- $V_1 V_2 P$ terms, which contain vertices with Goldstone and two vector resonances from different multiplets:

$$\begin{aligned}
\mathcal{O}^a_{V_1 V_2 P} &= \varepsilon_{\mu\nu\rho\sigma} \langle \{ V_1^{\mu\nu}, V_2^{\rho\alpha} \} \nabla_\alpha u^\sigma \rangle , \qquad \mathcal{O}^b_{V_1 V_2 P} = \varepsilon_{\mu\nu\rho\sigma} \langle \{ V_1^{\mu\alpha}, V_2^{\rho\sigma} \} \nabla_\alpha u^\nu \rangle , \\
\mathcal{O}^c_{V_1 V_2 P} &= \varepsilon_{\mu\nu\rho\sigma} \langle \{ \nabla_\alpha V_1^{\mu\nu}, V_2^{\rho\alpha} \} u^\sigma \rangle , \qquad \mathcal{O}^d_{V_1 V_2 P} = \varepsilon_{\mu\nu\rho\sigma} \langle \{ \nabla_\alpha V_1^{\mu\alpha}, V_2^{\rho\sigma} \} u^\nu \rangle , \\
\mathcal{O}^d_{V_1 V_2 P} &= \varepsilon_{\mu\nu\rho\sigma} \langle \{ \nabla^\sigma V_1^{\mu\nu}, V_2^{\rho\alpha} \} u_\alpha \rangle .
\end{aligned} \tag{2.39}$$

- $V_1 V_2 J$ terms, with two vector resonances from different multiplets and one pseudoscalar external source:

$$\mathcal{O}^f_{V_1 V_2 J} = i \, \varepsilon_{\mu\nu\rho\sigma} \langle \{ V_1^{\mu\nu}, V_2^{\rho\sigma} \} \chi_- \rangle . \tag{2.40}$$

Chapter 3

The $1/N_C$ expansion II: Baryons

3.1 Introduction

Baryons are colour singlets made up of quarks (no antiquark). Since in the $SU(N_C)$ gauge group the Levi–Civitá symbol has N_C indices, a baryon is an N_C–quark state,

$$B = \frac{1}{\sqrt{N_C\,!}}\,\epsilon_{i_1 i_2 \ldots i_{N_C}}\, q^{i_1} q^{i_2} \cdots q^{i_{N_C}}\,. \tag{3.1}$$

Quarks forming a baryon have all different colours, since the indices of the ϵ–symbol must be all different for it to be non–zero. Since quarks are fermions they must obey Fermi–Dirac statistics; the ϵ–symbol is totally antisymmetric and hence the baryon must be completely symmetric in the rest of quantum numbers: spin and flavour.

Baryon masses grow linearly with N_C, and hence they become infinitely heavy for $N_C \to \infty$. For massless quarks, the only dimensionful parameter of QCD is $\Lambda_{\rm QCD}$, hence

$$M_B \sim N_C\,\Lambda_{\rm QDC}\,. \tag{3.2}$$

The number of quarks in a baryon grows as N_C does, but its size is governed by $\Lambda_{\rm QCD}$, which is $\mathcal{O}(1)$. Therefore baryons become more and more dense as N_C grows. The $1/N_C$ expansion for baryons will give us a deep connection between QCD and two popular models: non–relativistic quark model and Skyrme model.

For the elaboration of this chapter I have followed Refs. [11, 14, 44].

3.2 Counting rules for baryons

Let us draw a propagating baryon as N_C incoming lines with colours arranged in order, $1 \cdots N_C$, and the outgoing N_C quark lines as a permutation of $1 \cdots N_C$. Let us first concentrate in the counting of the baryon propagator. It is convenient to derive the counting rules for connected diagrams. For this purpose, the incoming and outgoing quark lines are to be treated as ending on independent vertices, so that the connected piece of Fig. 3.1 (a) is Fig. 3.1 (b). A connected piece that contains n

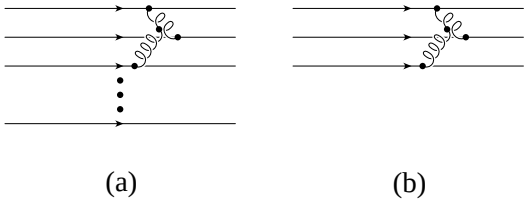

Figure 3.1: Self–interaction of a baryon and its connected piece.

quark lines will be referred to as an n–body interaction. The colours of the outgoing lines in an n–body interaction are a permutation of the n incoming quarks. One can relate n quarks connected graphs for baryons interactions with vacuum planar diagrams with a single quark in the outermost edge, by cutting the quark loop in n different places, and setting the colour of each quark line with that of an incoming (outgoing) quark in the baryon. Curiously, dominant "planar" diagrams are not necessarily flat when written on a sheet of paper.

An n–body interaction is of order N_c^{1-n}, since planar quark diagrams are of order N_C and n index sums over quark colour have been eliminated by cutting n fermion lines. But there are $N_C(N_C-1)\cdots(N_C-n+1)/n! \sim \mathcal{O}(N_C^n)$ ways to choose n lines out of N_C quarks, and so the net effect of an n–body interaction is order N_C for any n. Diagrams with m disconnected pieces are of order N_C^m, and this should not be surprising. Since the baryon mass increases with N_C, baryons are very heavy and we can concentrate only on their static properties. In particular baryons are always in their rest frame ($\vec{p}_B = 0$), and so the propagator we are looking for reads

$$e^{-\,i\,M_B\,t} \;=\; 1 \;-\; i\,M_B\,t \;-\; \frac{M_B^2\,t^2}{2} \;+\; \cdots\,, \tag{3.3}$$

where the 1 corresponds to the quarks propagating without interactions. So, since $M_B \sim \mathcal{O}(N_C)$, each term has a different N_C scaling and corresponds to the contributions with different numbers of disconnected pieces.

The N_C–counting rules can be extended to baryon matrix elements of a colour singlet such as $\langle\, B \,|\, \bar{q}\,\Gamma q \,|\, B \,\rangle$. It has N_C terms because it can be inserted in any of the quark lines, as shown in Fig. 3.2. In general we will assume $\langle\, B \,|\, \bar{q}\,\Gamma q \,|\, B \,\rangle \leq \mathcal{O}(N_C)$, because cancellations among the different insertions can occur. In general, an n–body operator has matrix elements $\leq \mathcal{O}(N_C^n)$.

With the previous result we deduce that the baryon–meson coupling (Fig. 3.3) constant g is $\leq \sqrt{N_C}$, since the normalized interpolating field for creating a meson is $1/\sqrt{N_C}\,\bar{q}\,\Gamma q$. The baryon–meson scattering amplitude is $\leq \mathcal{O}(1)$. Two possible contributions are shown in Fig. 3.4 : the two mesonic operators must be inserted into the same quark line, diagram (a), to preserve energy (the baryon is static and hence it remains static after the interaction takes place), or a gluon must be exchanged between the two lines, diagram (b). In general the amplitude for Baryon + meson $\to$ Baryon + n mesons is $\leq N_C^{(1-n)/2}$, and hence each meson insertion is accompanied by a $1/\sqrt{N_C}$ suppression factor as for the purely mesonic sector.

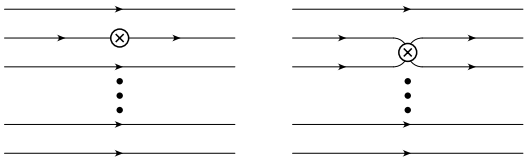

Figure 3.2: Baryon matrix elements of a one–body interaction and a two–body interaction.

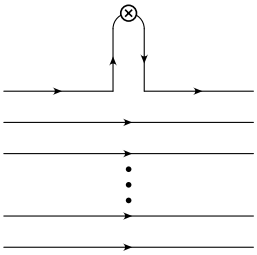

Figure 3.3: Diagram of baryon–meson coupling.

An observation due to Witten is that the N_C–counting rules derived in this section are the same as in a field theory with coupling constant $1/\sqrt{N_C}$, where mesons are fundamental fields and baryons are solitonic solutions.

3.3 Consistency conditions

The simplest way to derive the non–trivial consistency conditions is to consider baryon–meson scattering at low (fixed) energy, in the chiral limit, and derive the conditions for pion–nucleon couplings. The only assumptions needed are that both the baryon mass and g_A are of order N_C, as they are, since that is the counting for one–body operators.

One can extend the formalism of χPT in Chapter 1 to accommodate also baryons. We are not going to discuss the details here, but quote the needed elements. Since

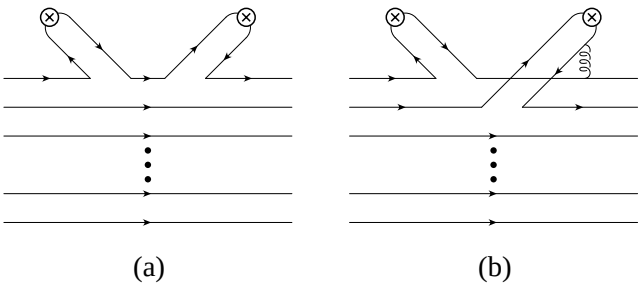

Figure 3.4: Diagrams for baryon–meson scattering.

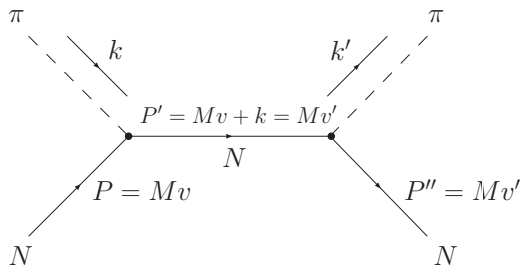

Figure 3.5: Momentum of the particles involved in pion–nucleon scattering.

we are considering static baryons our Lagrangian will have only one baryon and one antibaryon field. The most general such Lagrangian with the lowest number of derivatives is (two flavours) [45]

$$\mathcal{L}_B \;=\; \bar{\Psi}\left(i\not{D} - M + \frac{g_A}{2}\,\gamma_\mu\,\gamma_5\,u^\mu\right)\Psi \;\doteq\; \bar{\Psi}\left[i\not{D} - M + \frac{g_A}{2}\,\gamma_\mu\,\gamma_5\,t^i\left(a_i^\mu - \frac{\partial^\mu \pi^i}{F}\right)\right]\Psi\,, \tag{3.4}$$

where $t^i = \sigma^i/2$ and Ψ is a column matrix with the proton and neutron Dirac fields. With this Lagrangian we can study the axial–vector matrix element of nucleons and also the pion–nucleon vertex. After relating them we get :

$$\begin{aligned} \left\langle B \,\middle|\, \bar{q}\,t^i\gamma_\mu\,\gamma_5\,q \,\middle|\, B \right\rangle \;&=\; g_A\bar{\Psi}\left(t^i\gamma_\mu\,\gamma_5\right)\Psi \sim \mathcal{O}(N_C)\,, \\ \mathcal{L}_{\pi-N} \;=\; -\frac{\partial^\mu\pi^i}{F}\left\langle B \,\middle|\, \bar{q}\,t^i\gamma_\mu\,\gamma_5\,q \,\middle|\, B \right\rangle \;&\sim\; -\frac{\vec{\nabla}\pi^i}{F}\left\langle B \,\middle|\, \bar{q}\,t^i\,\vec{\gamma}\,\gamma_5\,q \,\middle|\, B \right\rangle\,, \end{aligned} \tag{3.5}$$

The pion–nucleon vertex is order $\sqrt{N_C}$, as stems from the counting for F and g_A, already discussed. The baryon acts as a heavy static source for the scattering of mesons at low energies. The absorption of the incoming meson by the heavy baryon results in an intermediate baryon state which is off–shell by a four–momentum of order unity. The momentum of an intermediate meson can be written as

$$P \;=\; M\,v + k \;=\; M\,v'\,, \tag{3.6}$$

where v is the velocity of the incoming baryon (and hence $v^2 = 1$) and k is the incoming pion momentum. The $M\,v$ piece is $\mathcal{O}(N_C)$ while k is order one, so the intermediate baryon four velocity

$$v' \;=\; v \;+\; \mathcal{O}\left(\frac{1}{N_C}\right)\,, \tag{3.7}$$

is equal to the initial baryon four–velocity in the large–N_C limit. So recoil effects are of order $1/N_C$ and can be neglected. In this limit, the incident and emitted mesons have the same energy, since there is no transfer to the infinitely heavy baryon, but

the three–momentum of the meson changes in the scattering process. Using the heavy–quark techniques, we can write the heavy baryon propagator as

$$\frac{\not{P} + M}{P^2 - M^2} \to \frac{i}{k \cdot v} \left(\frac{1 + \not{v}}{2} \right) , \tag{3.8}$$

which does not involve the baryon mass and is manifestly $\mathcal{O}(1)$. In the rest frame of the baryon $v^\mu = (1, \vec{0})$ the propagator projects out the two large components of the baryon Dirac spinor, and Eq. (3.8) reduces to the non–relativistic propagator i/E, with E the initial and final meson energy. As shown in Eq. (3.5) the time component of the axial–vector current between two nucleons at rest vanishes (non–relativistic reduction). We then define

$$\left\langle B \left| \bar{q}\, t^a\, \gamma^i\, \gamma_5\, q \right| B \right\rangle \equiv g\, N_C \left\langle B \left| X^{ia} \right| B \right\rangle , \tag{3.9}$$

where $\langle B \,|\, X^{ia} \,|\, B \rangle$ and g are $\mathcal{O}(1)$. The coupling constant g has been factored out so that the normalization of X^{ia} can be chosen to simplify future expressions. Since the non–relativistic reduction allows us to write matrix elements in terms of the two component spinors, $|\, B \,\rangle$ on the right–hand side represents one of the four possible states $p^\uparrow$, $p^\downarrow$, $n^\uparrow$ and $n^\downarrow$, and X^{ia} is a 4×4 matrix defined upon those states, that has a finite $N_C \to \infty$ limit :

$$X^{ia} \;=\; X_0^{ia} \;+\; \frac{X_1^{ia}}{N_C} \;+\; \frac{X_2^{ia}}{N_C^2} \;+\; \cdots , \tag{3.10}$$

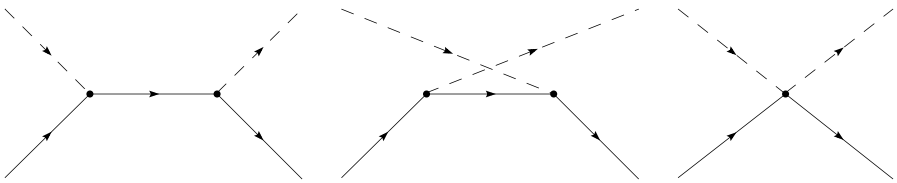

Figure 3.6: Diagrams for the baryon–meson scattering. The third diagram is suppressed by $1/N_C$.

The leading contribution to pion–nucleon scattering is from the pole graphs in Fig. 3.6, which contributes at order E provided the intermediate state is degenerate (same mass) with the initial and final states. The scattering amplitude for the process $\pi^a(k) + B(q) \to \pi^b(k') + B'(q')$ is :

$$-\, i\, k^i\, k'^j\, \frac{N_C^2\, g^2}{F^2 E} \left\langle B' \left| \left[X^{ia},\, X^{jb} \right] \right| B \right\rangle , \tag{3.11}$$

Apparently this amplitude is $\mathcal{O}(N_C)$ and it violates both unitarity and the power counting rules derived in Section 3.2. This means that large–N_C QCD with a multiplet of nucleons with $I = J = 1/2$ is an inconsistent field theory unless some nice

cancellation occurs. There must be other intermediate states that cancel the N_C order of Eq. (3.11) to make it $\mathcal{O}(1)$. This leads to the consistency condition, derived in Refs. [46, 47]

$$\left[X^{ia},\, X^{jb}\right] \,\leq\, \mathcal{O}\left(\frac{1}{N_C}\right)\,, \qquad \left[X_0^{ia},\, X_0^{jb}\right] \,=\, 0\,. \tag{3.12}$$

Since X^{ia} is an isospin triplet spin–one operator it must satisfy the following algebra relations

$$\begin{aligned} \left[J^i,\, X^{jb}\right] \,&=\, i\,\epsilon_{ijk}\,X^{kb}\,, \qquad \left[T^a,\, X^{ib}\right] \,=\, i\,f_{abc}\,X_0^{ic}\,, \\ \left[T^a,\, T^b\right] \,&=\, i\,f_{abc}\,T^c \;\;, \qquad \left[J^i,\, J^j\right] \,=\, i\,\epsilon_{ijk}\,J^k\,. \end{aligned} \tag{3.13}$$

In general we can consider the case of n_f flavours. Eqs. (3.12) and (3.13) constitute a contracted $SU(2\,n_f)_c$ algebra. It is useful to compare the $SU(2\,n_f)_c$ algebra with the $SU(2\,n_f)$ algebra. The only new relation is

$$\left[G^{ia},\, G^{jb}\right] \,=\, \frac{i}{2\,n_f}\,\epsilon_{ijk}\,\delta_{ab}\,J^k \,+\, \frac{i}{4}\,f_{abc}\,\delta_{ij}\,T^c \,+\, \frac{i}{2}\,\epsilon_{ijk}\,d_{abc}\,G^{kc}\,. \tag{3.14}$$

Then we can identify

$$X^{ia} \,\equiv\, \lim_{N_C\to\infty}\,\frac{G^{ia}}{N_C}\,. \tag{3.15}$$

that accurately reproduces Eq. (3.12), and is known as the contraction of a Lie algebra. The usual spin and flavour algebra of baryons is then extended to a spin–flavour algebra in the large–N_C limit when X^{ia} is included in the algebra. Note that a spin–flavour symmetry which mixes internal and space–time symmetries can emerge for large–N_C baryons because the baryon field is static in the large–N_C limit. Then there is no violation of the Coleman–Mandula theorem [48], since the baryon is non–relativistic. While we have just shown that the large–N_C limit of QCD has a contracted $SU(2\,n_f)$ symmetry in the baryonic sector, we have not shown it for finite N_C, and there is no reason to believe this is true (even if the quark model does).

It is easy to show that the large–N_C predictions for the pion–baryon coupling ratios are the same as those obtained in either the skyrme or the non–relativistic quark model, because both models also have a contracted $SU(2\,n_f)$ algebra in this limit. There are then two natural approaches to the study of the spin–flavour algebra of baryons, two different explicit representations of the $N_C \to \infty$ $SU(2\,n_f)_c$ algebra. One can solve the consistency conditions by constructing the irreducible representations of the $SU(2\,n_f)_c$ algebra, using standard techniques from the theory of induced representations, that can be shown to be infinitely dimensional. This is very closely related to the Skyrme model. One can also construct solutions considering N_C an odd and large but finite number, using quark operators (quark representation), an approach that is closely related to the non–relativistic quark model. Basically, as

we will see, the solution to the consistency conditions allows to express the matrix element of a QCD operator in terms of unknown coefficients and operators of the contracted algebra. Whereas the Skyrme representation uses X_0^{ia} as the spin–flavour generator, the quark representation makes use of G^{ia}. The operators X_0^{ia} and G^{ia}/N_C only differ at subleading powers of $1/N_C$, and so, to a given order in $1/N_C$ results expressed in both basis only differ by higher order $1/N_C$ corrections. In this thesis we will concentrate on the quark representation.

3.4 Large–N$_C$ baryon representations

Figure 3.7: $SU(2\,n_f)$ representation of the ground state baryons. The Young tableau has N_C boxes.

We will discuss briefly the irreducible representations of the ground–state baryons for an arbitrary number of flavours n_f in the quark representation. The totally symmetric representation for $SU(2\,n_f)$, Fig. 3.7, has baryons with spin $\frac{1}{2}$, $\frac{3}{2}$, ... $\frac{N_C}{2}$, transforming as the flavour representations shown in Table 3.1. For $n_f = 2$ states can be identified by its spin and isospin as $I = J = \frac{1}{2}$, $\frac{3}{2}$, ... $\frac{N_C}{2}$. For three flavours, weight diagrams look a bit complicated. We show in Fig. 3.8 an example for spin $\frac{1}{2}$. In general, weight diagrams for spin J have one edge with $a = 2\,J + 1$ weights and another with $b = (N_C + 2)/2 - J$. The dimension of the irreducible representation is $a\,b\,(a+b)/2$. The multiplicity starts by one in the edge of the polygon and increases one unit as we move inwards till we reach the shape of a triangle. From that moment on multiplicity remains constant.

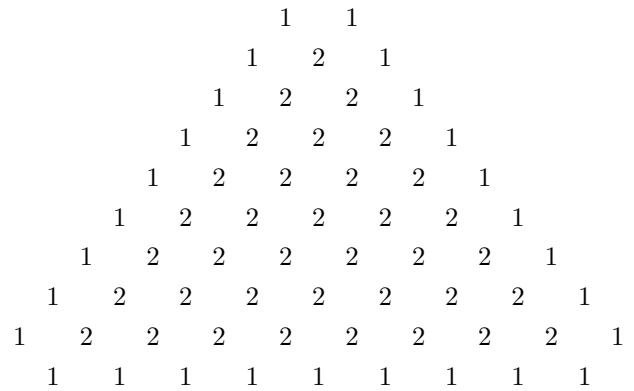

Figure 3.8: Weight diagram for the spin–$\frac{1}{2}$ representation. In this particular example $N_C = 17$. Numbers denote the multiplicity of the states.

$SU(2)$	$SU(n_f)$
$\frac{1}{2}$	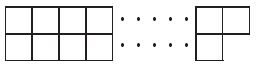
$\frac{3}{2}$	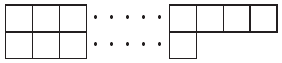
.	.
.	.
.	.
$\frac{N_C-2}{2}$	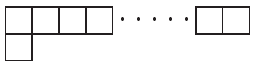
$\frac{N_C}{2}$	

Table 3.1: Decomposition of the  representation. All Young tableaux have N_C boxes.

3.5 Quark representation

In this section we present the explicit realization of the $SU(2\,n_f)$ algebra in the quark representation and express the QCD matrix elements in terms of the algebra operators. In this representation q does not denote the QCD fermionic field, but an annihilation field. These fields do not depend on position (since the spatial dependence of the quark wave function is irrelevant for the computation of static baryon matrix elements of the ground state baryons) and follow commutation relations (antisymmetry is carried by colour quantum number). The quark field has three labels, corresponding to spin (i, j), flavour (α, β)[1] and quark line (l, m):

$$\left[q_l^{\alpha i},\, q_{m\beta}^{\dagger j}\right] \;=\; \delta_\beta^\alpha\, \delta^{ij}\, \delta_{lm}\,. \tag{3.16}$$

The $SU(2n_f)$ algebra generators are

$$\begin{aligned}
J^i &= \sum_{l=1}^{N_C} q_l^\dagger \left(\frac{\sigma^i}{2}\otimes 1\right) q_l\,, && (1,0)\\
T^a &= \sum_{l=1}^{N_C} q_l^\dagger \,(1\otimes t^a)\, q_l\,, && (0,\mathrm{adj})\\
G^{ia} &= \sum_{l=1}^{N_C} q_l^\dagger \left(\frac{\sigma^i}{2}\otimes t^a\right) q_l\,, && (1,\mathrm{adj})
\end{aligned} \tag{3.17}$$

[1]The spin and flavour indices in the fundamental representation are not to be confused with the indices in the adjoint representation of the algebra generators.

where in brackets the transformation properties under the spin and $SU(n_f)$ subgroups are shown. The notation we are following is

$$q^\dagger \, (A \otimes B) \, q \; = \; q^{\dagger \alpha i} \, A^{ij} \, B^\beta_\alpha \, q^j_\beta \, . \tag{3.18}$$

It is immediate to demonstrate with the help of Eq. (3.16) that operators (3.17) fulfill the algebraic relations (3.13) and (3.14). It is important not to confuse the one–body operator G^{ia} with the two–body operator $J^i \, T^a$

$$\begin{aligned} G^{ia} &= \sum_{l=1}^{N_C} q_l^\dagger \left(\frac{\sigma^i}{2} \otimes t^a \right) q_l \, , \\ J^i \, T^a &= \sum_{l,m}^{N_C} \left(q_l^\dagger \, \frac{\sigma^i}{2} \, q_l \right) \left(q_m^\dagger \, t^a \, q_m \right) \, . \end{aligned} \tag{3.19}$$

The static baryon matrix element of a QCD m–body operator can be written as a $1/N_C$ expansion in terms of products of operators in Eq. (3.17) times incalculable coefficients :

$$\mathcal{O}^m_{\rm QCD} \; = \; N_C^m \sum_{n,l,k} c_n \, \frac{1}{N_C^n} \, (J^i)^l \, (T^a)^k \, (G^{ia})^{n-l-k} \, . \tag{3.20}$$

The N_C^m prefactor appears due to the fact that an m–body operator has matrix elements of order $\leq N_C^m$. The $1/N_C^n$ factor is present because each generator is accompanied by a $1/N_C$ factor. The expansion (much as happens with the OPE, to be discussed in Chapter 4) includes only operators transforming in the same way as the QCD operator under the $SU(2) \otimes SU(n_f)$ group. The coefficients c_n parametrize the unknown non–perturbative QCD dynamics, and admit an expansion in $1/N_C$ starting at order one. For finite N_C the sum on n runs for $0 \leq n \leq N_C$. The subleading terms in c_n are generated by non–planar diagrams or quark loops. Let us discuss Eq. (3.20) for a one body operator. Then $n = 1$ corresponds to the insertion of the operator on the different quark lines, $n = 2$ would correspond to the insertion of the operator plus one–gluon exchange, $n = 3$ two gluon exchanges, and so on. Each exchange brings a $1/N_C$ factor from the two couplings, and this justifies the $1/N_C^n$ factor.

Matrix elements of the J^i operator are in general of order N_C, but we will assume that physical baryons have spin of order unity. However, matrix elements of T^a and G^{ia} operator are in general of order N_C and in principle, even for spin values of order one, their value can be of order N_C. For two flavours, $I = J$ and then we it is straightforward to have order unity matrix elements for the I^a operators.

At first sight all terms in the expansion (3.20) are equally important, since an n–body interaction has a coefficient of order $1/N_C^n$ and matrix elements of n–body interactions are of order N_C^n. So it seems that we cannot truncate the series and hence we do not have any predictive power. However for baryons of spin $\mathcal{O}(1)$ operators with polynomials containing more factors of J are systematically suppressed

in $1/N_C$ and the operator expansion can be truncated at various orders in the $1/N_C$ expansion. In addition there are operator identities which allow one to simplify the general expansion (3.20) and drop certain terms as subleading in $1/N_C$. The $1/N_C$ expansion for low spin baryons is predictive because not all spin–flavour structures appear at a given order in $1/N_C$.

3.6 Operator identities

Before entering the discussion of the operator identities, let us write the $SU(2\,n_f)$ generator properly normalized. If we want the algebra matrices of the group Λ^A to satisfy, as usual, $\mathrm{Tr}\,\Lambda^A\Lambda^B = \frac{1}{2}\delta^{AB}$, and our spin j^i and flavour t^a matrices satisfy $\mathrm{Tr}\,j^i j^j = \frac{1}{2}\delta^{ij}$ and $\mathrm{Tr}\,t^a t^b = \frac{1}{2}\delta^{ab}$, respectively [2], we have to write Λ^A as

$$\begin{aligned} \frac{j^i \otimes \mathbb{1}}{\sqrt{n_f}}\,, \qquad & J^i \to \frac{J^i}{\sqrt{n_f}}\,, \\ \frac{\mathbb{1} \otimes t^a}{\sqrt{2}}\,, \qquad & T^a \to \frac{T^a}{\sqrt{2}}\,, \\ \sqrt{2}\left(j^i \otimes T^a\right)\,, \qquad & G^{ia} \to \sqrt{2}\,G^{ia}\,, \end{aligned} \tag{3.21}$$

that corresponds to rescale the quark representation operators as shown in Eq. (3.21). Only symmetric products (anticommutators) of baryon spin–flavour generators occur, because antisymmetric products (commutators) reduce to linear combinations of lower–body operators by the $SU(2\,n_f)$ Lie algebra relations. Not all of the n–th order operator products correspond to independent operators. Let us discuss the identities among the different operators.

We can write n–body operators in to different ways : as the multilineal product of several one–body operators (the algebra generators) or as the normal–ordered product of this multilineal. The former case reads

$$\mathcal{O}^n \;=\; \mathcal{M}(J^i, T^a, G^{ia})\,, \tag{3.22}$$

with $\mathcal{M}$ an nth order monomial; the normal–ordered product reads

$$\mathcal{O}'^n \;=\; q^\dagger_{j_1\beta_1}\ldots q^\dagger_{j_n\beta_n}\mathcal{T}^{(i_1\alpha_1)\ldots(i_n\alpha_n)}_{(j_1\beta_1)\ldots(j_n\beta_n)}\,q^{i_1\alpha_1}\ldots q^{i_n\alpha_n}\,. \tag{3.23}$$

In this case each quark operator acts on a different quark line, and that is why we have omitted such label, and then the order of the creation of annihilation operators is unimportant (they commute because the quark line label is always different). $\mathcal{T}$ represents a spin and flavour tensor, and independent n–body operators correspond to tensors completely symmetric and traceless. It must be totally symmetric because it acts on ground state baryons, that are completely symmetric (any tensor

[2] In the following, indices A, B, ... will denote adjoint $SU(2\,n_f)$ indices, a, b, ... $SU(n_f)$ and i, j, ... spin indices.

with mixed symmetry vanish identically upon actuation on a baryon) and traceless because non–vanishing traces reduce to lower–body operators.

Baryon matrix elements of operator products of the spin–flavour generators are easy to evaluate, but the classification of independent operator products is nontrivial. When operators are written in normal ordered form, it is not easy to identify the spin and flavour quantum numbers of the operator and baryon matrix elements are not simple to calculate. However it is straightforward to identify redundant operators, since they correspond to tensors with non–vanishing traces (they reduce to lower–body operators) or non completely symmetric (vanish on the ground baryon representation).

The general structure of the identities is that certain m–body operators can be reduced to linear combinations of n–body operators, where $m > n$. Since n–body operators acting on an N_C baryon state are generically of order N_C^n the coefficient of the n–body operator is typically of order N_C^{m-n}. The operator identities have an elegant group theoretical structure, written in terms of $SU(2\,n_f)$ invariants, and have been derived for an arbitrary number of flavours n_f.

3.6.1 Zero– and one–body operators

There is only one such operator, the identity operator $\mathbb{1}$, having matrix elements of $\mathcal{O}(1)$. It transforms under $SU(2) \otimes SU(n_f)$ as a singlet. There is no identity at this level.

The one body operators transform under $SU(2\,n_f)$ as the tensor product of a quark and antiquark representation :

$$\left(\overline{\square} \otimes \square\right) = 1 + \text{adj} = 1 + T^\alpha_\beta \,, \tag{3.24}$$

where T^α_β is a traceless tensor transforming as the adjoint representation. There is then only one identity at this level, and it is the trivial identity

$$q^\dagger q \;=\; \sum_{l=1}^{N_C} q_l^\dagger q_l \;=\; N_C\,\mathbb{1}\,, \tag{3.25}$$

stating that $q^\dagger q$ is the number operator. This identity must be understood as acting on a baryon state.

An important result of Ref. [14] is that the only non–trivial operator identities which are required are those which reduce 2–body operators to linear combinations of 1– or 0–body operators. All identities for n–body operators with $n > 2$ can be obtained by recursively application the 2–body identities. So next section constitutes the all–important set of reduction rules.

3.6.2 Two–body identities

The non–trivial identities occur among two–body operators. The two–body operators transform as the tensor product of a two–quark and two–antiquark tensor

state :

$$\left(\overline{\square\square}\otimes\square\square\right) = 1 + \text{adj} + \bar{s}s = 1 + T^{\alpha}_{\beta} + T^{(\alpha_1\alpha_2)}_{(\beta_1\beta_2)}\,, \tag{3.26}$$

where $T^{(\alpha_1\alpha_2)}_{(\beta_1\beta_2)}$ is a traceless symmetric in upper and lower indices tensor. This tensor representation will be referred to as the $\bar{s}s$ representation (this is not, of course, standard notation). So Eq. (3.26) tells us that we can eliminate a linear combination of two–body operators that transforms as a singlet and another linear combination that transforms as the adjoint representation.

We can compare this decomposition with the symmetric decomposition of two adjoint representations :

$$(\text{adj}\otimes\text{adj})_S \;=\; 1 + \text{adj} + \bar{a}a + \bar{s}s\,, \tag{3.27}$$

where $\bar{a}a = T^{[\alpha_1\alpha_2]}_{[\beta_1\beta_2]}$ transforms as a traceless tensor which is antisymmetric in its upper and lower indices. Of course this representation vanishes upon actuation on the baryon ground state and constitutes the last set of two–body identities.

The linear combination of two–body operator transforming as a singlet must be necessarily of the form $\left\{q^{\dagger}\Lambda^A q,\, q^{\dagger}\Lambda^A q\right\}$, and it is related to one Casimir operator. Let us calculate explicitly, as an example, its value acting on a baryon state [3]

$$\begin{aligned} 2\,q^{\dagger}\Lambda^A q\,q^{\dagger}\Lambda^A q \;&=\; 2\sum_{r,s} q^{\dagger}_{r\alpha}\left(\Lambda^A\right)^{\alpha}_{\beta} q^{\beta}_{r}\, q^{\dagger}_{s\gamma}\left(\Lambda^A\right)^{\gamma}_{\delta} q^{\delta}_{s} = 2\left(\Lambda^A\right)^{\alpha}_{\beta}\left(\Lambda^A\right)^{\gamma}_{\delta}\sum_{r,s} q^{\dagger}_{r\alpha}\, q^{\beta}_{r}\, q^{\dagger}_{s\gamma}\, q^{\delta}_{s} \\ &=\; \sum_{r,s} q^{\dagger}_{r\alpha}\, q^{\beta}_{r}\, q^{\dagger}_{s\beta}\, q^{\alpha}_{s} \;-\; \frac{1}{2\,n_f}\,N_C^2\,, \end{aligned} \tag{3.28}$$

where we have used the Fierz identity Eq. (2.6). It is convenient to split the sum in the last equality of Eq. (3.28) into a sum over $s = r$ and a sum over $s \neq r$:

$$\sum_{r} q^{\dagger}_{r\alpha}\, q^{\beta}_{r}\, q^{\dagger}_{r\beta}\, q^{\alpha}_{r} \;=\; 2\,n_f\,N_C\,, \tag{3.29}$$

where we have used that the normal ordered version of the sum vanishes because the annihilation operators acting on the same quark line produces a null result. For the other sum we can treat q_r and $q^{\dagger}_s$ as commuting objects since they act on different quark lines

$$\sum_{r\neq s} q^{\dagger}_{r\alpha}\, q^{\beta}_{r}\, q^{\dagger}_{s\beta}\, q^{\alpha}_{s} \;=\; \sum_{r\neq s} q^{\dagger}_{r\alpha}\, q^{\alpha}_{r}\, q^{\dagger}_{s\beta}\, q^{\beta}_{s} \;=\; N_C\,(N_C - 1)\,, \tag{3.30}$$

where we have used that that the baryon state is symmetric in spin–flavour. Putting all the contributions together we arrive at

$$\{q^{\dagger}\Lambda^A q,\, q^{\dagger}\Lambda^A q\} \;=\; N_C\,(N_C + 2\,n_f)\left(1 - \frac{1}{2\,n_f}\right)\mathbb{1}\,, \tag{3.31}$$

[3] For this derivation is convenient to use a label for the quark line and to collect the spin and flavour labels in a single one with $2\,n_f$ possible values.

that can be written in terms of the spin–flavour operators as

$$2\left\{J^i,\,J^i\right\}+n_f\left\{T^a,\,T^a\right\}+4\,n_f\left\{G^{ia},\,G^{ia}\right\}\,=\,N_C\,(N_C+2\,n_f)\,(2\,n_f-1)\;. \quad (3.32)$$

The linear combination of two–body operators transforming as the adjoint must be necessarily of the form $d^{ABC}\{q^\dagger\Lambda^B q,\,q^\dagger\Lambda^C q\}$, because a similar structure with an f symbol would reduce to commutators. By a manipulation parallel to that leading to the singlet identity, we can show that

$$d^{ABC}\,\{q^\dagger\Lambda^B q,\,q^\dagger\Lambda^C q\}\,=\,2\,(N_C+n_f)\left(1-\frac{1}{n_f}\right)\,q^\dagger\Lambda^A q\,, \quad (3.33)$$

where one has to use the identity

$$d^{ABC}\,\left(\Lambda^A\right)^\alpha_\beta\left(\Lambda^B\right)^\gamma_\delta\,=\,-\,\frac{1}{2\,n_f}\left[\delta^\alpha_\beta\left(\Lambda^C\right)^\gamma_\delta+\left(\Lambda^C\right)^\alpha_\beta\,\delta^\gamma_\delta\right]+\frac{1}{2}\left[\delta^\alpha_\delta\left(\Lambda^C\right)^\gamma_\beta+\left(\Lambda^C\right)^\alpha_\delta\,\delta^\gamma_\beta\right]\,. \quad (3.34)$$

Of course one can write Eq. (3.33) in terms of the spin–flavour operators, and the explicit relations can be found in Table 3.2.

The rest of the identities follow from the fact that the $\bar{a}a$ representation is zero upon actuation on the baryons. Their derivation is more involved and we will not discuss it in this thesis. The complete set of identities can be found in Table 3.2 or Ref. [14]. Many simplifications occur for the values $n_f = 2, 3$. By means of the operator identities one can choose a set of independent 2–body operators. The choice of the appropriate set translates into two operator reduction rules :

- Three flavours : *All operator products in which two flavour indices are contracted using δ^{ab}, f^{abc} or d^{abc}, or two spin indices on G's are contracted using δ^{ij} or ϵ^{ijk} can be eliminated.*

- Two flavours : *All operators in which two spin or isospin indices are contracted with a δ or ϵ symbol can be eliminated with the exception of $\vec{J}^2$.*

Note that for two flavours $\vec{J}^{\,2}=\vec{I}^{\,2}$ on ground state baryons.

3.7 Flavour symmetry breaking

An additional complication for the three flavour case is that $SU(3)_V$ flavour symmetry corrections are comparable in size with $1/N_C$ corrections and then we cannot neglect symmetry breaking effects if going beyond the leading order in $1/N_C$. Fortunately, this flavour symmetry breaking can be perturbatively introduced in the $1/N_C$ expansion in a combined series, producing a nice pattern in the spin–flavour breaking, not dominated by neither symmetry breaking nor $1/N_C$ effects.

Since the $1/N_C$ only covers operators of N_C–bodies, the expansion in symmetry breaking can only be extended to the (N_C-n) order for baryonic matrix elements of n–body QCD operators.

3.8 Useful relations for spin–flavour operators

In this section we briefly give a non–exhaustive list of relations that are very useful for the computation of matrix elements of spin–flavour operator between ground state baryons

$$
\begin{aligned}
T^8 &= \frac{1}{2\sqrt{3}}(N_C - 3\,N_s)\,, & T^3 &= \frac{1}{2}\,(N_u - N_d)\,,\\
G^{i8} &= \frac{1}{2\sqrt{3}}(J^i - 3\,J^i_s)\,, & G^{i3} &= \frac{1}{2}\,\left(J^i_u - J^i_d\right)\,,\\
T^{3+\frac{8}{\sqrt{3}}} &= T^Q\,, & J^i\,G^{i8} &= \frac{1}{\sqrt{12}}\left(3\,\vec{I}^{\,2} - \vec{J}^{\,2} - 3\,\vec{J}^{\,2}_s\right)\,,\\
J^i\,G^{i3} &= \frac{1}{4}\left(\vec{J}^{\,2}_u - \vec{J}^{\,2}_d + V^2 - U^2\right)\,, & \frac{J^i\,G^{ia}}{\vec{J}^{\,2}} &= \frac{2}{3}\left(T^a + \frac{1}{2}\,\{T^a, N_s\}\right)\,. \qquad (3.35)
\end{aligned}
$$

The complete set of the actuation of the spin–flavour operators on the octet of spin–$\frac{1}{2}$ baryons, together with its wave functions in the completely spin–flavour representation can be found in Ref. [49].

3.9 Vector and axial–vector form factors.

In this section we will apply the large–N_C rules for a particular example, that will be of phenomenological interest in Chapter 5. We anticipate here the definition of those form factors. Let B and b be two spin–$\frac{1}{2}$ octet baryons connected by the flavour matrix $\frac{\lambda^a}{2}$. We will be concerned with the matrix elements

$$
V^{\mu a} \equiv \langle\, b \,|\, \overline{q}\,\gamma^\mu t^a q \,|\, B\,\rangle\,, \quad A^{\mu a} \equiv \langle\, b \,|\, \overline{q}\,\gamma^\mu\gamma_5 t^a q \,|\, B\,\rangle\,, \qquad (3.36)
$$

governing the weak decay of the B baryon into b plus a pair of leptons. We are only capable of calculating static properties of baryons, and this implies that both B and b are at rest, that is, there is no three–momentum $\vec{q}$ transfer to the vector and axial–vector currents. This is equivalent to the non–relativistic reduction of the matrix elements (3.36), and no momentum dependence will be determined. Moreover, since all octet baryons have similar mass, not only the three–momentum but the four–momentum q^μ will be zero, and hence we will determine the form factors at $q^2 = 0$. The non–relativistic reduction implies

$$
V^{\mu a} \to V^{0a} = \left\langle\, b \,\middle|\, \overline{q}\,\gamma^0\, t^a\, q \,\middle|\, B\,\right\rangle\,, \quad A^{\mu\, a} \to A^{ia} = \left\langle\, b \,\middle|\, \overline{q}\,\gamma^i\,\gamma_5\, t^a\, q \,\middle|\, B\,\right\rangle\,. \qquad (3.37)
$$

So, under the $SU(2) \otimes SU(3)$ group the vector current transforms as $(0, 8)$ and the axial vector as $(1, 8)$. These transformation properties will, to a large extent, determine its operator expansion. Let us parametrize these form factors in the $1/N_C$ and symmetry breaking expansion.

$2\{J^i,J^i\} + n_f\{T^a,T^a\} + 4\,n_f\{G^{ia},G^{ia}\}$ $= N_C(N_C+2\,n_f)(2\,n_f-1)$	$(0,0)$
$d^{abc}\{G^{ia},G^{ib}\} + \frac{2}{n_f}\{J^i,G^{ic}\} + \frac{1}{4}d^{abc}\{T^a,T^b\}$ $= (N_C+n_f)\left(1-\frac{1}{n_f}\right)T^c$	$(0,\mathrm{adj})$
$\{T^a,G^{ia}\} = (N_C+n_f)\left(1-\frac{1}{n_f}\right)J^i$	$(1,0)$
$\frac{1}{n_f}\{J^k,T^c\} + d^{abc}\{T^a,G^{kb}\} - \epsilon^{ijk}f^{abc}\{G^{ia},G^{jb}\}$ $= 2(N_C+n_f)\left(1-\frac{1}{n_f}\right)G^{kc}$	$(1,\mathrm{adj})$
$4\,n_f\left(2-n_f^2\right)\{G^{ia},G^{ia}\} + 3\,n_f^2\{T^a,T^a\} + 4\left(1-n_f^2\right)\{J^i,J^i\} = 0$	$(0,0)$
$4\,n_f(2-n_f)\{G^{ia},G^{ia}\} + 3\,n_f^2\{T^a,T^a\} + 4\left(1-n_f^2\right)\{J^i,J^i\} = 0$	$(0,\mathrm{adj})$
$4\{G^{ia},G^{ib}\} = -3\{T^a,T^b\} \qquad (\bar{a}a)$	$(0,\bar{a}a)$
$4\{G^{ia},G^{ib}\} = \{T^a,T^b\} \qquad (\bar{s}s)$	$(0,\bar{s}s)$
$\epsilon^{ijk}\{J^i,G^{jc}\} = f^{abc}\{T^a,G^{kb}\}$	$(1,\mathrm{adj})$
$d^{abc}\{T^a,G^{kb}\} = \left(1-\frac{2}{n_f}\right)\left(\{J^k,T^c\} - \epsilon^{ijk}f^{abc}\{G^{ia},G^{jb}\}\right)$	$(1,\mathrm{adj})$
$\epsilon^{ijk}\{G^{ia},G^{jb}\} = f^{acg}\,d^{bch}\{T^g,G^{kh}\} \qquad (\bar{a}s+\bar{s}a)$	$(1,\bar{a}s+\bar{s}a)$
$\{T^a,G^{ib}\} = 0 \qquad (\bar{a}a)$	$(1,\bar{a}a)$
$\{G^{ia},G^{ja}\} = \frac{1}{2}\left(1-\frac{1}{n_f}\right)\{J^i,J^j\} \qquad (J=2)$	$(2,0)$
$d^{abc}\{G^{ia},G^{jb}\} = \left(1-\frac{2}{n_f}\right)\{J^i,G^{jc}\} \qquad (J=2)$	$(2,\mathrm{adj})$
$\{G^{ia},G^{jb}\} = 0 \qquad (J=2,\bar{a}a)$	$(2,\mathrm{adj})$

Table 3.2: $SU(2\,n_f)$ identities. Some of the identities must be projected onto a given channel. The second column gives the transformation properties of the identities under $SU(2)\otimes SU(n_f)$.

3.9.1 Vector form factor

Let us first concentrate on the operator expansion in the limit of exact symmetry. There is one one–body operator and one two–body operator

$$\mathcal{O}_1^a = T^a\,, \qquad \mathcal{O}_2^a = \{J^i,G^{ia}\} = 2\,J^i\,G^{ia}\,, \tag{3.38}$$

we have to stop our expansion at three–body operators. There is only one such operator

$$\mathcal{O}_3^a = \left\{\vec{J}^2,T^a\right\} = 2\,\vec{J}^2\,T^a\,, \tag{3.39}$$

that in the case of octet–to–octet transitions is equivalent to $\mathcal{O}_3^a = \frac{3}{2}T^a$ and hence can be absorbed in $\mathcal{O}_1^a$ (the coefficient of both operators in undetermined). Since in the limit of exact $SU(3)_V$ symmetry vector current is conserved, we can use this

additional information to calculate the unknown coefficients : $c_1 = 1$ and $c_2 = 0$, and then

$$V^{0a} \,=\, T^a \,. \tag{3.40}$$

Let us include now the $SU(3)_V$ breaking effects. As we shall see in Chapter 5, Eq. (5.57), symmetry breaking effects transform as $(0,8)$, and so we must compute the tensor product of irreducible representations

$$(0,8)\otimes(0,8) \,=\, (0,1)\oplus(0,8)\oplus(0,8)\oplus(0,10)\oplus(0,\overline{10})\oplus(0,27)\,, \tag{3.41}$$

for first order symmetry breaking corrections. Due to the Ademollo–Gatto theorem, to be discussed in Chapter 5, first order symmetry breaking corrections are null, and so we must compute second order effects. This amounts to the calculation of the tensor product $(0,8)\otimes(0,8)\otimes(0,8)$, and results in all the irreducible representations of Eq. (3.41) and the new ones $(0,35)$ and $(0,64)$. Among all those representations we must keep only those transforming under time reversal in the same way as V^{0a} does, and so we have :

- $(0,0)$: only two operators

$$\mathcal{O}_0 \,=\, 1\,, \qquad \mathcal{O}_2 \,=\, \vec{J}^{\,2}\,, \tag{3.42}$$

  but again, for octet–to–octet transitions $\mathcal{O}_2 = \frac{3}{4}$ and can be absorbed in $\mathcal{O}_0$. When it corresponds to a two–body operator we have to multiply it by an $SU(3)$ invariant tensor with two adjoint indices, namely δ^{ab}. One index must be set to 8 to account for the symmetry breaking, and then δ^{a8} is zero for our transitions. If it corresponds to a three–body operator, it must be accompanied by $d^{a88} = -1/\sqrt{3}\,\delta^{a8}$, again zero for our transitions. So those operators do not play any röle in our analysis. The number of 8's in an operator indicates the order of the symmetry breaking.

- $(0,8)$: those operators have been considered in Eq. (3.38). Since they correspond to first order symmetry breaking, will appear as $d^{ab8}\,\mathcal{O}^b_{1,2}$.

- $(0,27)$: There are two– and three–body operators, corresponding to first– and second–order symmetry breaking effects

$$\begin{aligned}
\mathcal{O}_2^{ab} &= \{T^a, T^b\}\,, \\
\mathcal{O}_3^{ab} &= \{T^a, \{J^i, G^{ib}\}\} \,+\, \{T^b, \{J^i, G^{ia}\}\} \\
&= 2\,\{T^a, J^i\,G^{ib}\} \,+\, 2\,\{T^b, J^i\,G^{ia}\}\,,
\end{aligned} \tag{3.43}$$

  and they will appear as $\mathcal{O}^{a8}_{2,3}$ and $d^{ab8}\,\mathcal{O}^{b8}_{2,3}$.

- $(0,10+\overline{10})$: there is one three–body operator, corresponding to second–order symmetry breaking effects [the two–body $(0,10+\overline{10})$ operators are reducible]

$$\begin{aligned}
\mathcal{O}_{\bar{3}}^{ab} &= \{T^a, \{J^i, G^{ib}\}\} \,-\, \{T^b, \{J^i, G^{ia}\}\} \\
&= 2\,\{T^a, J^i\,G^{ib}\} \,-\, 2\,\{T^b, J^i\,G^{ia}\}\,,
\end{aligned} \tag{3.44}$$

  and contributes as $\mathcal{O}^{a8}_{\bar{3}}$ and $d^{ab8}\,\mathcal{O}^{b8}_{\bar{3}}$.

- $(0,64)$: there is one three–body operator [there is no $(0,64)$ in $(0,8)\otimes(0,8)$]
$$\mathcal{O}_3^{abc} = \{T^a,\{T^b,T^c\}\}\,, \tag{3.45}$$
contributing as $\mathcal{O}_3^{a88}$.

In principle one has to subtract from the higher dimension representation operators those terms corresponding to lower dimension representations. However, in practice, these lower dimension terms already appear in our expansion and can be reabsorbed in those. The $(0,35)$ and $(0,10+\overline{10})$ irreducible representations are odd under time–reversal and hence do not contribute (V^{0a} is T–even). With all that, to second order in symmetry breaking we can write

$$\begin{aligned} V^{0a} &= (1+\epsilon\,a_1)\,T^a + \epsilon\,a_2\,\frac{1}{N_C}\{J^i,G^{ia}\} + \epsilon\,b_1 d^{ab8}\,T^b + \\ &\epsilon\,b_2\,\frac{1}{N_C}\,d^{ab8}\{J^i,G^{ib}\} + \epsilon\,a_4\,\frac{1}{N_C}\{T^a,T^8\} + \\ &\epsilon\,a_5\,\frac{1}{N_C^2}\left(\{T^a,\{J^i,G^{i8}\}\} + \{T^8,\{J^i,G^{ia}\}\}\right) + \\ &\epsilon\,a_6\,\frac{1}{N_C^2}\left(\{T^a,\{J^i,G^{i8}\}\} - \{T^8,\{J^i,G^{ia}\}\}\right) + \\ &\epsilon^2\,b_4\,\frac{1}{N_C}\,d^{ab8}\{T^b,T^8\} + \epsilon^2\,a_7\,\frac{1}{N_C^2}\{T^a,\{T^8,T^8\}\} + \\ &\epsilon^2\,b_5\,\frac{1}{N_C^2}\,d^{ab8}\left(\{T^b,\{J^i,G^{i8}\}\} + \{T^8,\{J^i,G^{ib}\}\}\right) + \\ &\epsilon^2\,b_6\,\frac{1}{N_C^2}\,d^{ab8}\left(\{T^b,\{J^i,G^{i8}\}\} - \{T^8,\{J^i,G^{ib}\}\}\right)\,. \end{aligned} \tag{3.46}$$

We can rewrite this expression for our transitions in terms of N_s and J_s^i. We have to demand that $\Delta S = 0$ transitions have no symmetry violation, since isospin symmetry is unbroken

$$\begin{aligned} V^{0a} &= T^a\,, & \Delta S &= 0\,, \\ V^{0a} &= (1+v_1)\,T^a + v_2\,\{T^a,N_s\} + v_3\,\{T^a,-I^2+\vec{J}_s^{\,2}\}, & |\Delta S| &= 1\,. \end{aligned} \tag{3.47}$$

In Table 3.3 we depict the matrix elements of the operators in front of the unknown coefficients for the vector current.

3.9.2 Axial–vector form factor

Let us first concentrate on the unbroken symmetry operators. There are one–, two– and three–body operators

$$\begin{aligned} \mathcal{O}_1^{ia} &= G^{ia}\,, & \mathcal{O}_2^{ia} &= \epsilon^{ijk}\{J^i,G^{ka}\} = i\left[\vec{J}^{\,2},G^{ia}\right]\,, \\ \mathcal{D}_2^{ia} &= J^i\,T^a\,, & \mathcal{D}_3^{ia} &= \{J^i,\{J^j,G^{ja}\}\} = 2\,\{J^i,J^j\,G^{ja}\}\,, \\ \mathcal{O}_3^{ia} &= \{\vec{J}^{\,2},G^{ia}\} - \frac{1}{2}\,\{J^i,\{J^j,G^{ja}\}\} = \{\vec{J}^{\,2},G^{ia}\} - \{J^i,J^j\,G^{ja}\}\,. \end{aligned} \tag{3.48}$$

Transition	1	v_1	v_2	v_3
$n \to p$	1	0	0	0
$\Sigma^\pm \to \Lambda$	0	0	0	0
$\Lambda \to p$	$-\sqrt{\frac{3}{2}}$	$-\sqrt{\frac{3}{2}}$	$-\sqrt{\frac{3}{2}}$	0
$\Sigma^- \to n$	-1	-1	-1	2
$\Xi^- \to \Lambda$	$\sqrt{\frac{3}{2}}$	$\sqrt{\frac{3}{2}}$	$3\sqrt{\frac{3}{2}}$	$\sqrt{6}$
$\Xi^- \to \Sigma^0$	$\frac{1}{\sqrt{2}}$	$\frac{1}{\sqrt{2}}$	$\frac{3}{\sqrt{2}}$	0
$\Xi^0 \to \Sigma^+$	1	1	3	0

Table 3.3: Matrix elements for the vector form factor

There is only one additional operator, $\{\vec{J}^{\,2}, G^{ia}\}$ that for octet–to–octet transitions can be absorbed in $\mathcal{O}_1^{ia}$. The operators $\mathcal{D}_n^{ia}$ connect only states with the same spin, whereas $\mathcal{O}_{n>2}^{ia}$ connect only states with different spin. Hence they do not contribute to our processes. Furthermore, $\mathcal{O}_2^{ia}$ is even under time reversal and do not contribute ($A^{i\,a}$ is T–odd). Then we have

$$A^{ia} \,=\, a_1\,\mathcal{O}_1^{ia} \,+\, a_2\,\frac{1}{N_C}\,\mathcal{D}_2^{ia} \,+\, a_3\,\frac{1}{N_C^2}\,\mathcal{D}_3^{ia}\,. \tag{3.49}$$

We are now in position to drop terms subleading in $1/N_C$. Since in general T^a/N_C and G^{ia}/N_C matrix elements can be order unity, the suppression is controlled by the J^i/N_C matrix elements : operators with more J^i elements are suppressed. Then $\mathcal{O}_1^{ia}$ and $\mathcal{D}_2^{ia}$ are of the same order in the counting, but $\mathcal{D}_3^{ia}$ is suppressed. Then at leading order we have

$$A^{ia} \,=\, a_1\,G^{ia} + a_2\,\frac{J^i\,T^a}{N_C}\,. \tag{3.50}$$

Let us study the symmetry breaking corrections. In this case we will only consider the first order effects, since there is no Ademollo–Gatto theorem for the axial–vector current.

- $(1,0)$: there is one one–body operator

$$\mathcal{O}_1^i \,=\, J^i\,, \tag{3.51}$$

  that will appear as $\delta^{a8}\,\mathcal{O}_1^i$ and hence it is zero for our transitions

- $(1,8)$: we have those of the unbroken case, that will appear as $d^{ab8}\,\mathcal{O}_1^{ib}$ and $d^{ab8}\,\mathcal{D}_2^{ia}$ (D_3^{ia} is already suppressed in $1/N_C$).

Transition	$a, \tilde{a}$	$b, \tilde{b}$	c_1	c_2	c_3	c_4	ρ
$n \to p$	$\frac{5}{3}$	1	0	0	0	0	1
$\Sigma^\pm \to \Lambda$	$\sqrt{\frac{2}{3}}$	0	0	0	$\sqrt{\frac{8}{3}}$	0	0
$\Lambda \to p$	$-\sqrt{\frac{3}{2}}$	$-\sqrt{\frac{3}{2}}$	$-\sqrt{\frac{3}{2}}$	$-\sqrt{\frac{3}{2}}$	$-\sqrt{\frac{3}{2}}$	$-\sqrt{\frac{3}{2}}$	0
$\Sigma^- \to n$	$\frac{1}{3}$	-1	$\frac{1}{3}$	-1	$\frac{1}{3}$	$\frac{1}{3}$	0
$\Xi^- \to \Lambda$	$\frac{1}{\sqrt{6}}$	$\sqrt{\frac{3}{2}}$	$\frac{1}{\sqrt{6}}$	$\sqrt{\frac{3}{2}}$	$\sqrt{\frac{3}{2}}$	$\frac{7}{\sqrt{6}}$	0
$\Xi^- \to \Sigma^0$	$\frac{5}{3\sqrt{2}}$	$\frac{1}{\sqrt{2}}$	$\frac{5}{3\sqrt{2}}$	$\frac{1}{\sqrt{2}}$	$\frac{5}{\sqrt{2}}$	$\frac{1}{\sqrt{2}}$	0
$\Xi^0 \to \Sigma^+$	$\frac{5}{3}$	1	$\frac{5}{3}$	1	5	1	0

Table 3.4: Matrix elements for the axial–vector form factor.

- $(1, 10 + \overline{10})$: we have one two–body operator

$$\begin{aligned} \mathcal{O}_2^{iab} &= \{G^{ia}, T^b\} - \{G^{ib}, T^a\} - \frac{2}{3} f^{abc} f^{cgh} \{G^{ig}, T^h\} \\ &= \{G^{ia}, T^b\} - \{G^{ib}, T^a\} - \frac{2}{3} \left[\vec{J}^{\,2}, [T^b, G^{ia}]\right] . \end{aligned} \tag{3.52}$$

  The last term vanishes for octet–to–octet transitions. It will appear as $\mathcal{O}_2^{ia8}$.

- $(1, 27)$: there is one operator (we do not bother subtracting the lower dimension operators, since they are absorbed in other representations)

$$\mathcal{O}_{2,27}^{iab} = \{G^{ia}, T^b\} + \{G^{ib}, T^a\} . \tag{3.53}$$

  It will appear as $\mathcal{O}_{2,27}^{ia8}$.

With that information, we can write A^{ia} at first order in $1/N_C$ and symmetry breaking

$$\begin{aligned} A^{ia} &= \left(a\,\delta^{ab} + \epsilon\, c_1\, d^{ab8}\right) G^{ib} + \left(b\,\delta^{ab} + \epsilon\, c_2\, d^{ab8}\right) \frac{J^i T^b}{N_C} + \epsilon\, c_3\, \frac{\{G^{ia}, N_s\}}{N_C} \\ &= a\, G^{ia} + b\, J^i\, T^a + \Delta^a (c_1\, G^{ia} + c_2\, J^i\, T^a) + c_3\, \{G^{ia}, N_s\} + c_4\, \{T^a, J_s^i\} , \end{aligned} \tag{3.54}$$

where Δ^a is 0 for $a = 1, 2, 3, 8$ and 1 for $a = 4, 5, 6, 7$. For $|\Delta S| = 1$ transitions $\Delta^a = 1$ and 0 for $\Delta S = 0$. For the latter we have then

$$\begin{aligned} A^{ia}_{|\Delta S|=1} &= \tilde{a}\, G^{ia} + \tilde{b}\, J^i\, T^a + c_3\, \{G^{ia}, N_s\} + c_4\, \{T^a, J_s^i\} , \\ \tilde{a} &= a + c_1 , \\ \tilde{b} &= b + c_2 . \end{aligned} \tag{3.55}$$

Since we are interested only in one transition with $\Delta S = 0$, namely neutron decay into proton, we only need an additional parameter for our analysis

$$- \langle\, p \,|\, (c_1\, G^{ia} + c_2\, J^i\, T^a) \,|\, n \,\rangle \;\equiv\; \rho\,. \tag{3.56}$$

In Table 3.4 we depict the matrix elements of the operators in front of the unknown coefficients for the axial–vector current.

Chapter 4

Green functions of QCD

4.1 Introduction

As already pointed out in Chapter 1, the QCD Lagrangian (1.1) does not have hadrons (which are the particles we indeed observe as asymptotic free states at low energies) as degrees of freedom, but rather quarks and gluons. It does not make much sense then to compute amplitudes having these fundamental particles as asymptotic states, since we do not gain any insight on hadronic dynamics. Instead it is better to compute Green functions (GFs for short) of composite operators (that is, operators having more than one field in the same space–time point). We must choose composite operators having the same quantum numbers as the hadronic state we want to study, as they qualify as interpolating fields in the sense of the LSZ reduction formula, having non–vanishing matrix element between the vacuum and the hadronic state: $\langle\, H_J^a \,|\, J_\Gamma^b \,|\, 0 \,\rangle \neq 0$. In the case of mesonic states quark bilinear currents are the suitable composite operators, and a very detailed discussion about them was given in Section 1.2 [see Eqs. (1.7), (1.12) and (1.13)].

Since these currents have dimension three, we can introduce them into the QCD Lagrangian *via* dimension–one external sources [see Eq. (1.21)], as was explained in Chapter 1. In this way the extended QCD Lagrangian is still renormalizable. We can treat the external sources as bosonic fields (spinless for scalar and pseudoscalar, and spin–one for the rest of the currents) which are not quantized. Accordingly they cannot propagate and only appear as current insertions in GFs and form factors. In fact we can write Feynman rules for the coupling of the quark current to the external source: given the generic extended Lagrangian

$$\mathcal{L}_{\rm QCD}^{\rm ext} \doteq : \bar{q}(x)\,\Gamma\,\frac{\lambda^a}{2}\,q(x) :\, S_\Gamma^a\,, \tag{4.1}$$

each current insertion is accompanied by the matrix $i\,\Gamma\,\frac{\lambda^a}{2}$ as shown in Fig. 4.1. From now on we will assume that all operators are normal–ordered and will drop the symbol "$: \cdots :$" everywhere. Analogous Feynman rules can be derived for χPT and RχT in the presence of external sources.

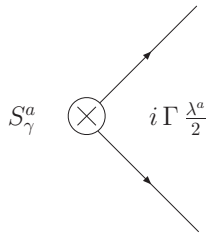

Figure 4.1: Feynman diagram of an external source insertion for quark–gluon degrees of freedom.

At very low energies (long distances) $E \ll m_\rho$ GFs can be computed as a perturbative series in the (small) momentum carried by the current and the quark masses (although we will set them to zero). At high energies (short distances) the QCD currents in the GF approach each other and one can expand their product as a tower of local operators, in the Wilson operator product expansion (OPE). In momentum space this is tantamount to an expansion in inverse powers of momenta, only valid in the deep Euclidean region $-p^2 \gg m_\rho^2$. At intermediate energies one can only rely on the expansion of QCD in powers of $1/N_C$, as discussed in Chapter 2. This region is populated by hadronic resonances driving the strong dynamics. One is then able to perform a matching of the three regimes and thus to estimate the values of the LECs present in the χPT Lagrangian. In this chapter we will calculate all two–point GFs in the three regimes: χPT to $\mathcal{O}(p^4)$ accuracy, RχT at leading $1/N_C$ precision and OPE up to and including dimension six operators, and including leading α_s corrections in the Wilson coefficient of the$\langle\bar{q}q\rangle$ operator.

The power of EFTs is enhanced by matching onto the more fundamental theory in a region where both descriptions are sensible, and running down with the renormalization group equations (RGE) to a scale when the EFT is useful. This results into a resummation of large logarithms that would otherwise spoil the perturbative expansion. This matching between χPT and RχT is straightforward since up to a certain mass scale Λ_χ the spectrum of both EFTs coincide, and the heavy particles can be formally integrated out of the action. However the situation drastically changes when matching RχT onto QCD, because the spectrum no longer has any particle in common. The reason for it is that we are going through the chiral phase transition. One is then forced to compare GFs computed in the different EFTs in momentum regions where their domain of validity overlap.

This matching relation is better understood for the so called order parameter of the chiral symmetry breaking GFs (order parameters for short). These GFs have zero Wilson coefficient for the identity operator (that is, the purely perturbative contribution) to all orders in α_s in the chiral limit, and hence, as we shall see, its main contribution stems form the $\langle\bar{q}q\rangle$ condensate. Since this operator is the responsible for the chiral symmetry breaking those GFs encode essential information for a better understanding of confinement. As a result, two–point GFs order parameter do not have subtractions in their dispersion relations (in the chiral limit). Thus

they are fully determined by its spectral function, which is of course an observable. In this sense these GFs can be regarded as observables, and a direct matching of their expression in the different theories (that is, in different energy domains) is meaningfull. For two–point GFs we will match all GFs (even those not being order parameters of the chiral symmetry breaking) to the OPE result, within different ansätze (MHA or including the full tower of resonances).

This method has been used for two–point GFs including several orders of α_s corrections [50], but only at leading order for three–point GFs [41, 42, 51–53]. In Section 4.13.1 we will match the $\langle VVP \rangle$ GF with two multiplets of vector meson resonances. It is the purpose of some sections of this chapter to push the matching up to $\mathcal{O}(\alpha_s)$. Unfortunately the $\mathcal{O}(\alpha_s)$ corrections to the $\langle \bar{q}q \rangle$ Wilson coefficient $C_{\langle \bar{q}q \rangle}$ for three–point GFs are not known, and we will concentrate on their computation, relegating the matching to forthcoming works. Finally, we will use the $\langle VT \rangle$ GF to illustrate that within the MHA one cannot match the OPE result when radiative corrections are taken into account.

Throughout this chapter we will assume the chiral limit of QCD. For the elaboration of this chapter I have followed Refs. [1, 54–58].

4.2 Definitions of Green functions and Ward identities

The formal definition of the GF of n–currents follows:

$$\Pi_{J_1 \cdots J_n}(p_1 \cdots p_{n-1}) \, = \, i^{n-1} \int \prod_{j=1}^{n-1} \mathrm{d}^4 x_j \, e^{i \sum_{k=1}^{n-1} x_k \cdot p_k} \, \langle \, 0 \, | \, \mathrm{T}\{ J_1(x_1) \cdots J_n(0) \} | \, 0 \, \rangle \, , \tag{4.2}$$

where the i^{n-1} factor is included by convention and ensures that Feynman rules for external currents can be applied thoroughly. It is important to remark that the $|\, 0 \,\rangle$ state is the true non–perturbative QCD vacuum (the one which is not annihilated by the axial generators) in contrast with the perturbative one. We will discuss its nature in the next sections. It is customary to design the non–perturbative vacuum as $|\, \Omega \,\rangle$, but we will not adopt this notation. In this chapter we will compute GFs in the chiral limit, what implies that both vector and axial–vector currents are conserved and that $SU(3)_V$ symmetry is exact. We will exploit these two features. Some of the material covered in this section can be found in Refs. [51, 59].

For those GFs having at least either one vector or one axial–vector current, we can derive the so called Ward identities, being a consequence of their null divergence. For bosonic operators time–ordering requires currents with bigger time components to appear to the left. For example for two currents

$$\mathrm{T}\{ J_1(x) \, J_2(0) \} \, = \, \theta(x^0) \, J_1(x) \, J_2(0) \, + \, \theta(-x^0) \, J_2(0) \, J_1(x) \, , \tag{4.3}$$

and similar for more currents. With this definition we can calculate the following derivatives:

$$\begin{aligned}
\partial_\mu T\{J_1^\mu(x)\,J_2(0)\} &= \mathrm{T}\{\partial_\mu J_1^\mu(x)\,J_2(0)\} + \delta(x^0)\,[J_1^0(x),\,J_2(0)]\,, \\
\partial_\mu T\{J_1^\mu(x)\,J_2(y)\,J_3(0)\} &= \mathrm{T}\{\partial_\mu J_1^\mu(x)\,J_2(y)\,J_3(0)\} \\
&\quad + \delta(x^0-y^0)\,T\{[J_1^0(x),\,J_2(y)]\,J_3(0)\} \\
&\quad + \delta(x^0)\,T\{[J_1^0(x),\,J_3(0)]\,J_2(y)\}\,. \qquad (4.4)
\end{aligned}$$

On the other hand, we can relate derivatives with contractions with one momentum

$$i^n \int \prod_{j=1}^{n-1} \mathrm{d}^4x_j\, e^{i\sum_{k=1}^{n-1} x_k\cdot p_k} \left(\partial_{j\mu} + i\,p_{j\mu}\right) \langle\,0\,|\,\mathrm{T}\{J_1^\mu(x_1)\cdots J_n(0)\}\,|\,0\,\rangle = 0\,. \qquad (4.5)$$

The commutator of two quark currents can be easily computed using the identity [1]

$$\begin{aligned}
&\delta(x^0-y^0)\left[\left(\bar q\,\frac{\lambda^a}{2}\,\Gamma_1 q\right)(x),\left(\bar q\,\frac{\lambda^b}{2}\,\Gamma_2 q\right)(y)\right] = \\
&\delta^4(x-y)\,\bar q(x)\left\{\Gamma_1\,\gamma_0\,\Gamma_2\frac{\lambda^a}{2}\frac{\lambda^b}{2} - \Gamma_2\,\gamma_0\,\Gamma_1\frac{\lambda^b}{2}\frac{\lambda^a}{2}\right\} q(x)\,, \qquad (4.6)
\end{aligned}$$

from where we obtain the well–known current algebra relations:

$$\begin{aligned}
&\delta(x^0-y^0)\left[V_0^a(x),V_\mu^b(y)\right] = \delta(x^0-y^0)\left[A_0^a(x),A_\mu^b(y)\right] = i\,f^{abc}\,V_\mu^c(x)\,\delta^{(4)}(x-y)\,, \\
&\delta(x^0-y^0)\left[V_0^a(x),A_\mu^b(y)\right] = \delta(x^0-y^0)\left[A_0^a(x),V_\mu^b(y)\right] = i\,f^{abc}\,A_\mu^c(x)\,\delta^{(4)}(x-y)\,, \\
&\delta(x^0-y^0)\left[V_0^a(x),S^b(y)\left\{P^b(y)\right\}\right] = i\,f^{abc}\,S^c(x)\left\{P^c(x)\right\}\,\delta^{(4)}(x-y)\,, \\
&\delta(x^0-y^0)\left[A_0^a(x),S^b(y)\{P^b(y)\}\right] = -i\left[\frac{2}{n_f}\,\delta^{ab}P(x)\{S(x) \right. \\
&\qquad\qquad \left. + d^{abc}P^c(x)\{S^c(x)\}\delta^{(4)}(x-y)\right]\,, \\
&\delta(x^0-y^0)\left[A_0^a(x),T_{\mu\nu}^b(y)\right] = -\frac{i}{2}\,\epsilon_{\mu\nu\alpha\beta}\left[\frac{1}{n_f}\,T^{\alpha\beta}(x) + d^{abc}\,T^{c\,\alpha\beta}(x)\right]\delta^{(4)}(x-y)\,. \\
&\delta(x^0-y^0)\left[V_0^a(x),T_{\mu\nu}^b(y)\right] = i\,f^{abc}\,T_{\mu\nu}^c(x)\,\delta^{(4)}(x-y)\,, \qquad (4.7)
\end{aligned}$$

Let us apply this to two–point GFs:

$$\begin{aligned}
p^\mu\left(\Pi_{VV\,[AA]}\right)_{\mu\nu}^{ab}(p) &= -i\,f^{abc}\,\langle\,0\,|\,V_\nu^c(0)\,|\,0\,\rangle = 0\,, \\
p^\mu\left(\Pi_{VT}\right)_{\mu\,\nu\alpha}^{ab}(p) &= -i\,f^{abc}\,\langle\,0\,|\,T_{\nu\alpha}^c(0)|\,0\,\rangle = 0\,, \qquad (4.8)
\end{aligned}$$

where the right–hand side vanishes because vacuum is Lorentz invariant and flavourless. Let us study separately the $\langle AP\rangle$ GF. From Lorentz invariance and $SU(3)_V$ symmetry we can write

$$\left(\Pi_{AP}\right)_\mu^{ab}(p) = i\,\delta^{ab}\,\Pi_{AP}(p^2)\,p_\mu\,, \qquad (4.9)$$

[1] Schwinger terms will be omitted in this thesis.

and then

$$p^\mu \left(\Pi_{AP}\right)^{ab}_{\mu}(p) = i\,\delta^{ab}\,p^2\,\Pi_{AP} \;=\; i\,\frac{2}{n_f}\,\delta^{ab}\,\langle\,0\,|\,S(0)|\,0\,\rangle = \;2\,i\,\delta^{ab}\,\langle\bar{q}q\rangle\,, \tag{4.10}$$

from where we can identify $\Pi_{AP} = 2\,\langle\bar{q}q\rangle\,/p^2$. Thus the $\langle AP\rangle$ is fully saturated by one pion exchange in the chiral limit:

$$\left(\Pi_{AP}\right)^{ab}_{\mu}(p) \;=\; 2\,i\,\delta^{ab}\,\frac{\langle\bar{q}q\rangle}{p^2}\,p_\mu\,. \tag{4.11}$$

The only remaining two–point GFs are $\langle SS\rangle$, $\langle PP\rangle$ and $\langle TT\rangle$. The rest can be shown to vanish due to discrete symmetries. Due to Eqs. (4.8) plus other symmetry considerations we can write

$$\begin{aligned}
\left(\Pi_{VV\,[AA]}\right)^{ab}_{\mu\nu}(p) &= \delta^{ab}\,(p_\mu p_\nu - p^2 g_{\mu\nu})\,\Pi_{VV\,[AA]}(p^2)\,,\\
\left(\Pi_{VT}\right)^{ab}_{\mu,\nu\rho}(p) &= i\,\delta^{ab}\,(p^\rho g^{\mu\nu} - p^\nu g^{\mu\rho})\,\Pi_{VT}(p^2)\,,\\
\Pi^{ab}_{SS\,(PP)}(p^2) &= \delta^{ab}\,\Pi_{SS\,(PP)}(p^2)\,,\\
\left(\Pi_{TT}\right)^{ab}_{\mu\nu;\alpha\beta}(p) &= -\,2\,q^2\delta^{ab}\left[\Pi^{-}_{TT}(p^2)\,\Omega^{L}_{\mu\nu;\alpha\beta} - \Pi^{+}_{TT}(p^2)\,\Omega^{T}_{\mu\nu;\alpha\beta}\right],
\end{aligned} \tag{4.12}$$

where $\Omega^{L,T}$ are defined in Appendix C.

In general one always has $\Pi^{ab}_{ij}(p) \;=\; \delta^{ab}\,\Pi_{ij}(p)$ and also $\Pi_{ij}(p) \;=\; \pm\,\Pi_{ij}(-\,p)$ where the $-$ sign corresponds to $\langle AP\rangle$ and $\langle VT\rangle$ and $+$ to the rest. One can define the correlators of the chirality currents defined in Eq. (1.13) which, as for the $\langle AP\rangle$ and $\langle VT\rangle$ GFs, are order parameters:

$$\begin{aligned}
\Pi_{LR}(p^2) &= \Pi_{VV}(p^2) - \Pi_{AA}(p^2)\,,\\
\Pi_{SS-PP}(p^2) &= \Pi_{SS}(p^2) \;- \Pi_{PP}(p^2)\,,\\
\Pi^{\Delta}_{TT}(p^2) &= \Pi^{+}_{TT}(p^2) \;- \Pi^{-}_{TT}(p^2)
\end{aligned} \tag{4.13}$$

Let us turn now our attention to the three–point GFs. For these we will not consider the tensor source and will only concentrate on order parameter GFs. Among those, we will discard order parameters that are the difference of two GFs which are not (e.g. $\langle VVV\rangle - \langle VAA\rangle$). Bearing in mind that the GF made out of an octet and a singlet current is zero, that Π_{VS}, Π_{AS} and Π_{VP} are identically null and the result of Eq. (4.11), we obtain:

$$\begin{aligned}
p^\mu(q^\nu)\left(\Pi_{VVP\,(AAP)\,[VAS]\,\{VVS\}}\right)^{abc}_{\mu\nu}(p,q) &= 0\,,\\
p^\mu(q^\nu)\left(\Pi_{AAS}\right)^{ab}_{\mu\nu}(p,q) &= -\,2\,d^{abc}\;\langle\bar{q}q\rangle\;\frac{q_\nu}{q^2}\left(\frac{p_\mu}{p^2}\right),\\
p^\mu\left(\Pi_{VAP}\right)^{ab}_{\mu\nu}(p,q) &= -\,2\,\langle\bar{q}q\rangle\;f^{abc}\left[\frac{r_\nu}{r^2} + \frac{q_\nu}{q^2}\right],\\
q^\nu\left(\Pi_{VAP}\right)^{ab}_{\mu\nu}(p,q) &= \langle\bar{q}q\rangle\;f^{abc}\,\frac{r_\mu}{r^2}\,,
\end{aligned} \tag{4.14}$$

where we have defined the four–momentum $r = -(p+q)$ associated with the third current. These results rely on the fact that the $\langle AP \rangle$ GF is fully determined by the chiral Ward identity Eq. (4.11), and they must be satisfied in any sensible description of the strong interactions. The right hand sides of Eqs. (4.14) are proportional to the quark condensate and this has deep implications. For instance in RχT it means that once we contract with one momenta, only the pion pole can survive. In the OPE they also have deep implications : the contribution of higher dimension condensates vanishes when contracting with one external momenta, and since there is no α_s factor all radiative corrections to the $\langle \bar{q} q \rangle$ Wilson coefficient beyond leading order must also vanish when the contraction is done.These relations together with discrete symmetries and $SU(3)_V$ invariance determine for the odd–intrinsic–parity sector

$$\left(\Pi^{\mu\nu}_{VVP\,(AAP)\,[VAS]}\right)^{abc}(p,q) \;=\; \varepsilon_{\mu\nu\alpha\beta}\, p^\alpha q^\beta d^{abc}\, \Pi_{VVP\,(AAP)\,[VAS]}\left(p^2,q^2,r^2\right)\,. \qquad (4.15)$$

In addition Bose symmetry requires

$$\Pi_{VVP\,(AAP)}(p^2,q^2,r^2) \;=\; \Pi_{VVP\,(AAP)}(q^2,p^2,r^2)\,, \qquad (4.16)$$

The even–intrinsic–parity sector can be split into a subset of GFs being rank–two Lorentz tensors :

$$\begin{aligned}
\left(\Pi^{\mu\nu}_{VVS}\right)^{abc}\left(p^2,q^2,r^2\right) &= d^{abc}\left[P^{\mu\nu}(p,q)\,\mathcal{F}_{VVS}\left(p^2,q^2,r^2\right)\right. \\
&\quad \left. + Q^{\mu\nu}(p,q)\,\mathcal{G}_{VVS}\left(p^2,q^2,r^2\right)\right]\,, \\
\left(\Pi^{\mu\nu}_{AAS}\right)^{abc}\left(p^2,q^2,r^2\right) &= d^{abc}\left[2\,\langle\bar{q}q\rangle\,\frac{p^\mu q^\nu}{q^2p^2} + P^{\mu\nu}(p,q)\,\mathcal{F}_{AAS}\left(p^2,q^2,r^2\right)\right. \\
&\quad \left. + Q^{\mu\nu}(p,q)\,\mathcal{G}_{AAS}\left(p^2,q^2,r^2\right)\right]\,, \\
\left(\Pi^{\mu\nu}_{VAP}\right)^{abc}\left(p^2,q^2,r^2\right) &= 2\,f^{abc}\left\{-\langle\bar{q}q\rangle\left[\frac{(p+2\,q)^\mu\,q^\nu}{q^2r^2} - \frac{g^{\mu\nu}}{r^2}\right] + P^{\mu\nu}(p,q)\right. \\
&\quad \left. \times\,\mathcal{F}_{VAP}\left(p^2,q^2,r^2\right) + Q^{\mu\nu}(p,q)\,\mathcal{G}_{VAP}\left(p^2,q^2,r^2\right)\right\}\,,
\end{aligned} \qquad (4.17)$$

and the Lorentz scalar subset :

$$\Pi^{abc}_{SSS\,(SPP)} \;=\; d^{abc}\,\Pi_{SSS\,(SPP)}(p^2,q^2,r^2)\,, \qquad (4.18)$$

where the transverse tensors $P^{\mu\nu}$ and $Q^{\mu\nu}$ are defined as

$$\begin{aligned}
P^{\mu\nu}(p,q) &= q^\mu p^\nu - (p\cdot q)\,g^{\mu\nu}\,, \\
Q^{\mu\nu}(p,q) &= p^2\,q^\mu q^\nu + q^2\,p^\mu p^\nu - (p\cdot q)\,p^\mu q^\nu - p^2q^2\,g^{\mu\nu}\,.
\end{aligned} \qquad (4.19)$$

Again Bose symmetry requires

$$\begin{aligned}
\mathcal{F}\left[\,\mathcal{G}\,\right]_{VVS\,(AAS)}\left(p^2,q^2,r^2\right) &= \mathcal{F}\left[\,\mathcal{G}\,\right]_{VVS\,(AAS)}\left(q^2,p^2,r^2\right)\,, \\
\Pi_{SPP}(p^2,q^2,r^2) &= \Pi_{SPP}(p^2,r^2,q^2)\,,
\end{aligned} \qquad (4.20)$$

and Π_{SSS} is invariant under any relabeling of the three squared momenta.

4.3 Dispersion relations for two–point Green functions

It was shown by Källén and Lehmann [61] that two–point GFs obey *dispersion relations*. Dispersion relations follow from the analytic properties of $\Pi(q^2)$ as a complex function of q^2, the only energy–momentum invariant appearing in a two–point function. In full generality $\Pi(q^2)$ is an analytic function in the entire complex q^2–plane except for a cut in the real axis $0 \leq q^2 \leq \infty$.

The general proof of dispersion relations is the main topic of this section. We first deduce them for scalar currents J_α and J_β, and generalize the discussion for the rest of the currents afterwards. The only requirement is that the two currents are hermitian and the key point is to insert a complete set of states between them, using the Parseval identity

$$\begin{aligned} \mathcal{I} &= \sum_{n,s} \int \frac{\mathrm{d}^3\vec{q}_1 \cdots \mathrm{d}^3\vec{q}_n}{2^{4n}\,\pi^{3n}\,E_1 \cdots E_n} \mid n \rangle \langle\, n \mid \;=\; \sum_{n,s} \int \frac{\mathrm{d}^4 p}{(2\pi)^4}\, \mathrm{d}Q_n\, \theta(p^0) \mid n \rangle \langle\, n \mid \\ &\equiv \sum_{n,s} \int \frac{d^4 p}{(2\,\pi)^4}\, \frac{\mathrm{d}^3\vec{q}_1 \cdots \mathrm{d}^3\vec{q}_n}{2^{4(n-1)}\,\pi^{3n-4}\,E_1 \cdots E_n}\, \theta(p^0)\, \delta^{(4)}(p - p_n) \mid n \rangle \langle\, n \mid , \end{aligned} \tag{4.21}$$

where the sum runs over all possible multiparticle states and all possible polarizations, $\mathrm{d}Q_n$ is the n–particle phase space, $E_i = \sqrt{\vec{p}_i^{\,2} + m_i^2}$ is the on–shell energy of the particle and $p_n = \sum q_i$ is the total four–momentum of the n particles. Since all particles in the sum are on–shell, $p^2 \geq 0$ (timelike) and $p^0 > 0$ (future oriented). The second condition is enforced by $\theta(p^0)$ and we can enforce the first one by a slight modification of Eq. (4.21)

$$\mathcal{I} = \sum_{n,s} \int_0^\infty \mathrm{d}t \int \frac{\mathrm{d}^4 p}{(2\,\pi)^4}\, \mathrm{d}Q_n\, \delta(p^2 - t)\, \theta(p^0) \mid n \rangle \langle\, n \mid . \tag{4.22}$$

Poincaré invariance relates any operator to its value at the origin,

$$\mathcal{O}(x) \;=\; e^{i\,P\cdot x}\, \mathcal{O}(0)\, e^{-\,i\,P\cdot x} . \tag{4.23}$$

Having in mind that vacuum carries zero four–momentum it follows

$$\begin{aligned} \left\langle\, 0 \,\middle|\, J_\alpha(0)\, J_\beta^\dagger(0) \,\right|\, 0 \,\right\rangle &= \sum_{n,s} \int_0^\infty \mathrm{d}t \int \frac{\mathrm{d}^4 p}{(2\,\pi)^4}\, \mathrm{d}Q_n\, \delta(p^2 - t)\, \theta(p^0) \langle\, 0 \mid J_\alpha(0) \mid n \,\rangle \langle\, 0 \mid J_\beta(0) \mid n \,\rangle^* \\ &\equiv \int_0^\infty \mathrm{d}t \int \frac{\mathrm{d}^4 p}{(2\,\pi)^3}\, \delta(p^2 - t)\, \theta(p^0)\, \rho_{\alpha\beta}(p^2) , \end{aligned} \tag{4.24}$$

where we have defined the spectral function

$$\rho_{\alpha\beta}(p^2) \;=\; \frac{1}{(2\,\pi)} \sum_{n,s} \int \mathrm{d}Q_n \,\langle\, 0 \mid J_\alpha(0) \mid n \,\rangle \langle\, 0 \mid J_\beta(0) \mid n \,\rangle^* . \tag{4.25}$$

It follows immediately $\rho_{\alpha\beta}(p^2) = \rho_{\beta\alpha}(p^2)^*$, and so, if we specialize to $\alpha = \beta$, $\rho_{\alpha\alpha}(p^2) \equiv \rho(p^2) = \rho(p^2)^* \geq 0$, the spectral function is real and positive definite. For this particular case we have

$$\begin{aligned}\langle\, 0 \,|\, \mathrm{T}\{J(x)\, J(0)\} \,|\, 0 \,\rangle &= \int_0^\infty \mathrm{d}t \int \frac{\mathrm{d}^4 p}{(2\,\pi)^3}\, \delta(p^2 - t)\, \theta(p^0)\, \rho(t)\, \left[e^{-\,i\,p\cdot x}\theta(x^0) + e^{i\,p\cdot x}\theta(-x^0)\right] \\ &= -\,i \int_0^\infty \mathrm{d}t\, \rho(t) \int \frac{\mathrm{d}^4 p}{(2\,\pi)^4}\, \frac{e^{-\,i\,p\cdot x}}{t - p^2 + i\,\epsilon}\,, \end{aligned} \tag{4.26}$$

where we have used the definition of the Feynman propagator, or instead the integral expression for the Heavyside function

$$\theta(x) \,=\, \frac{1}{2\,\pi\,i} \int \mathrm{d}w\, \frac{e^{i\,w\,x}}{w - i\,\epsilon}\,. \tag{4.27}$$

Finally in momentum space we have our final expression

$$\Pi(p^2) \,=\, i \int \mathrm{d}^4 x\, e^{i\,p\cdot x}\, \langle\, 0 \,|\, \mathrm{T}\{J(x)\, J(0)\} \,|\, 0 \,\rangle \,=\, \int_0^\infty \mathrm{d}t\, \rho(t)\, \frac{1}{t - p^2 + i\,\epsilon}\,. \tag{4.28}$$

The last goal is to relate the spectral function $\rho(q^2)$ with the imaginary part of $\Pi(q^2)$. This is easy using the widely known formula

$$\frac{1}{x - x_0 \pm i\,\epsilon} \,=\, P\left(\frac{1}{x - x_0}\right) \,\mp\, i\,\pi\,\delta(x - x_0)\,, \tag{4.29}$$

in Eq. (4.28) to obtain $\rho(q^2) = \dfrac{1}{\pi}\,\mathrm{Im}\,\Pi(q^2)$. So the imaginary part is positive. Then our dispersion relation is complete:

$$\Pi(p^2) \,=\, \int_0^\infty \mathrm{d}t\, \frac{1}{\pi}\,\mathrm{Im}\,\Pi(t)\, \frac{1}{t - p^2 + i\,\epsilon}\,. \tag{4.30}$$

As an example we will compute the spectral function for the single–particle intermediate state a

$$\begin{aligned}\frac{1}{\pi}\,\mathrm{Im}\,\Pi(p^2) \;&=\; \int \frac{\mathrm{d}^3 \vec{q}}{2\,E_p}\, |\langle\, 0 \,|J(0)|\, a \,\rangle|^2\, \delta^4(p - q) \,=\, |\langle\, 0 \,|J(0)|\, a \,\rangle|^2\, \frac{1}{2\,E_q}\, \delta(E_p - p^0) \\ &=\; |\langle\, 0 \,|J(0)|\, a \,\rangle|^2\, \delta(p^2 - m_a^2)\,. \end{aligned} \tag{4.31}$$

We can derive Eq. (4.30) using Cauchy's theorem for $\Pi(q^2)$ bearing in mind that it is analytic in the full q^2–plane except for a branch cut in the real positive axis, starting in the first multiparticle threshold of the sum in Eq. (4.25). Then we perform a contour integral as shown in Fig. 4.2 (a) and then deform it as in Fig. 4.2 (b).

$$\Pi(q^2) \,=\, \frac{1}{2\,\pi\,i} \oint_C \mathrm{d}t\, \frac{\Pi(t)}{t - q^2} \,=\, \frac{1}{2\,\pi\,i} \oint_{|t|=R} \mathrm{d}t\, \frac{\Pi(t)}{t - q^2} \,+\, \frac{1}{2\,\pi\,i} \int_0^\infty \mathrm{d}t\, \frac{\Pi(t + i\,\epsilon) - \Pi(t - i\,\epsilon)}{t - q^2}\,, \tag{4.32}$$

assuming that $\Pi(t)$ falls sufficiently rapidly for $t \to \infty$ the first integral is zero, and using Schwartz's reflection principle

$$\Pi(t + i\,\epsilon) - \Pi(t - i\,\epsilon) \;=\; 2\,i\,\mathrm{Im}\,\Pi(t + i\,\epsilon)\,, \tag{4.33}$$

we recover Eq. (4.30). But, what happens if the first integral is not zero? We can perform n–derivatives in $\Pi(q^2)$ to make it converge,

$$\left(\frac{\mathrm{d}}{\mathrm{d}q^2}\right)^n \Pi(q^2) \;=\; \frac{n!}{2\,\pi\,i}\oint_C \mathrm{d}t\,\frac{\Pi(t)}{(t-q^2)^{n+1}}\,, \tag{4.34}$$

each derivative is known as a subtraction. In general, if in the $q^2 \to \infty$ limit $\Pi(q^2) \sim q^{2n}\log q^2$, then $n+1$ subtractions are needed. When such subtractions are performed, Eq. (4.30) is modified to

$$\begin{aligned}\Pi(q^2) \;&=\; \int_0^\infty \mathrm{d}t\,\frac{1}{\pi}\,\mathrm{Im}\,\Pi(t)\,\frac{1}{t - q^2 + i\,\epsilon} \;+\; \sum_{j=0}^{n-1} a_j\,q^{2j} \\ &=\; q^{2n}\int_0^\infty \mathrm{d}t\,\frac{1}{\pi}\,\mathrm{Im}\,\Pi(t)\,\frac{1}{t^n(t - q^2 + i\,\epsilon)} \;+\; \sum_{j=0}^{n-1} b_j\,q^{2j}\,. \end{aligned} \tag{4.35}$$

Any of the $a_j(b_j)$ is a subtraction point [for instance $b_0 = \Pi(0)$], generically divergent.

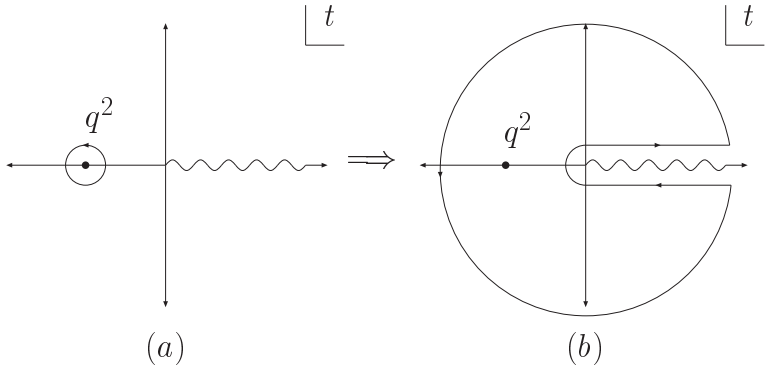

Figure 4.2: Contour integral yielding the dispersion relation for two–point functions.

However it seems that in the first derivation of the dispersion relation there was no room for subtractions. In fact there is : in Eq. (4.24) we have commuted the sum and the integral, and this can only be done if the sum is convergent.

Let us close this section with the derivation of dispersion relations for conserved vector currents. In this case Lorentz invariance and current conservation implies

$$\begin{aligned}&\frac{1}{(2\,\pi)}\sum_n \int \mathrm{d}Q_n\,\langle\,0\,|J^\mu(0)|\,n\,\rangle\,\langle\,0\,|J^\nu(0)|\,n\,\rangle^*\,\delta^{(4)}(p - p_n) = \rho_J(p^2)\,(p^\mu p^\nu - p^2 g^{\mu\nu})\,, \\ &-\frac{1}{3\,p^2}\,\frac{1}{(2\,\pi)}\sum_n \int \mathrm{d}Q_n\,\langle\,0\,|J^\mu(0)|\,n\rangle\,\langle\,0\,|J_\mu(0)|\,n\,\rangle^*\,\delta^{(4)}(p - p_n) = \rho_J(p^2) \geq 0\,,\end{aligned} \tag{4.36}$$

and again $\rho_J(p^2) = \rho_J(p^2)^* > 0$. Plugging this into the time–ordered product we get

$$\begin{aligned}\left\langle\, 0 \,\middle|\, \mathrm{T}\{J^\mu(x)\, J^{\nu\,\dagger}(0)\}\,\middle|\, 0 \,\right\rangle &= \int_0^\infty \mathrm{d}t \int \frac{\mathrm{d}^4p}{(2\,\pi)^3}\, \delta(p^2 - t)\, \theta(p^0)\, \rho_J(t) \\ &\times (p^\mu p^\nu - p^2 g^{\mu\nu}) \left[e^{-\,i\,p\cdot x}\theta(x^0) + e^{i\,p\cdot x}\theta(-x^0)\right] \\ &= i\int_0^\infty \mathrm{d}t\, \rho_J(t)\, \left(\partial^\mu\partial^\nu - \partial^2\, g^{\mu\nu}\right) \int \frac{\mathrm{d}^4p}{(2\,\pi)^4}\, \frac{e^{-\,i\,p\cdot x}}{t - p^2 + i\,\epsilon}\,, \\ &= -\,i\int_0^\infty \mathrm{d}t\, \rho(t) \int \frac{\mathrm{d}^4p}{(2\,\pi)^4}\, \frac{e^{-\,i\,p\cdot x}}{t - p^2 + i\,\epsilon}\, (p^\mu p^\nu - p^2 g^{\mu\nu})\,, \end{aligned} \tag{4.37}$$

were Schwinger terms have been omitted. Fourier transforming, identifying the scalar GF and using Eq. (4.29) we arrive at

$$\begin{aligned}\Pi_{JJ}(p^2) &= \int_0^\infty \mathrm{d}t\, \frac{1}{\pi}\, \mathrm{Im}\,\Pi_{JJ}(t)\, \frac{1}{t - p^2 + i\,\epsilon} + \sum_{j=0}^{n-1} a_j\, q^{2j}\,, \\ \frac{1}{\pi}\,\mathrm{Im}\,\Pi_{JJ}(t) &= -\,\frac{1}{3\,p^2}\,(2\,\pi) \sum_n \int \mathrm{d}Q_n\, \left\langle\, 0\,|J^\mu(0)|\, n\,\right\rangle \left\langle\, 0\,|J_\mu(0)|\, n\,\right\rangle^*\,, \end{aligned} \tag{4.38}$$

were again possible subtractions have been included. Similar expressions can be found for more complex GFs.

Before we close this section we should address one last point : kinematical singularities in dispersion relations. This topic is closely linked to the physical meaning of subtractions. Let us first discuss the $\langle SS\rangle$ GF as an illustration. As we shall see, in the deep Euclidean it diverges as $q^2\log(-\,q^2)$ and hence it needs two subtractions. However we also learn from perturbative QCD that only one of the two subtractions is unphysical, and so one could perfectly define the function $\widetilde{\Pi}_{SS} = \frac{1}{q^2}\Pi_{SS}$ that must be subtracted only once, being such subtraction genuinely unphysical. By doing so one is generating at low q^2 a kinematical singularity, since we know from χPT that at such momentum Π_{SS} behaves like a constant. This is not a major problem, and we must simply have to modify Eq. (4.34) to account for a second residue

$$\left(\frac{\mathrm{d}}{\mathrm{d}q^2}\right)^n \Pi(q^2) = \frac{n!}{2\,\pi\,i}\oint_C \mathrm{d}t\, \frac{\Pi(t)}{(t - q^2)^{n+1}} + (-1)^n \frac{1}{q^{2(n+1)}} \lim_{q^2\to 0} q^2\, \Pi(q^2)\,, \tag{4.39}$$

where now the contour C in the t complex plane must enclose both $t = q^2$ and $t = 0$. After integrating n times the dispersion relation reads

$$\Pi(q^2) = \int_0^\infty \mathrm{d}t\, \frac{1}{\pi}\, \mathrm{Im}\,\Pi(t)\, \frac{1}{t - q^2 + i\,\epsilon} + \frac{1}{q^2} \lim_{q^2\to 0} q^2\, \Pi(q^2) + \sum_{j=0}^{n-1} a_j\, q^{2j}\,, \tag{4.40}$$

where we insist once more that $\lim_{q^2\to 0} q^2\,\Pi(q^2)$ is a physical constant, typically related to a chiral LEC. In this case, obviously one cannot pick $q^2 = 0$ as the subtraction point, since the GF is not defined there. This singularity should never

be confused with a pion pole : it is not, and so it will never be present in the spectral function $\rho(t)$. So the two options for writing a dispersion relation for $\langle SS\rangle$ are either "over–subtract" and bear in mind that only one subtraction is unphysical, or divide by q^2 and take into account the kinematical singularity as an additional pole. For the case of $\langle PP\rangle$ we indeed have a pion pole and so if we define $\widetilde{\Pi}_{PP} = \frac{1}{q^2}\Pi_{PP}$ in the chiral limit its spectral function would read $\rho_\pi(t) = F^2\,\frac{1}{t}\,\delta(t)$, which is not well defined.

Something similar happens with the $\langle TT\rangle$ GF. With the definition of Eq. (4.12) $\Pi^{\pm}_{TT}$ need only one (unphysical) subtraction, but on the other hand they have a kinematical singularity at $q^2 = 0$. In this case chiral symmetry predicts that the residues of the longitudinal and transversal correlators at zero momentum are related : $\lim_{q^2\to 0} q^2\,\Pi^{\pm}_{TT}(q^2) = \mp\,\Lambda_3$.

4.4 Wilson's Operator Product Expansion (OPE)

We often find ourselves needing to know how a GF behaves when the four–momentum brought in by one operator tends to infinity. If an operator product such as $J_\alpha(x)J_\beta(0)$ were analytic in x^μ, then its Fourier transform would decrease exponentially as the Fourier variable k goes to infinity. The leading terms in the high–momentum limit of the Fourier transform arise from the singularities of the operator product as the space–time arguments approach one another.

Wilson [15] hypothesized that the singular part as $x \to y$ of the product of two operators is given by a sum over other local operators

$$\lim_{x\to y} \mathcal{O}_\alpha(x,\mu)\,\mathcal{O}_\beta(y,\mu) \;=\; \sum_j C_j^{\alpha\beta}(x-y,\mu)\,\mathcal{O}_j(y,\mu)\,, \tag{4.41}$$

were $C_j^{\alpha\beta}$ are singular c–number functions known as the Wilson coefficients and $\mathcal{O}_j$ are local operators of increasing dimension d_j. These local operators $\mathcal{O}_j(y)$ must have the same global symmetry quantum numbers of the product $\mathcal{O}_\alpha\,\mathcal{O}_\beta$, but are otherwise unrestricted. In the case of QCD, aside from the identity $\mathbb{1}$ these operators are constructed from quark and gluon fields and we will consider them as normal–ordered. By dimensional analysis the mass–dimension of the Wilson coefficients is $d_{\alpha,\beta;j} = d_\alpha + d_\beta - d_j$ and thus naïvely its singular part behaves as $\sim (x-y)^{-\,d_\alpha - d_\beta + d_j}$. So as the dimension of $\mathcal{O}_j$ increases its numerical influence rapidly decreases. Hence it is safe to truncate this expression at a finite order. A relation like (4.41) holds also for commutators or time–ordered products, and the latter are the ones we are interested in. In general operators such as $\mathcal{O}_\alpha$, $\mathcal{O}_\beta$ or $\mathcal{O}_j$ have anomalous dimension and then must be defined at a certain renormalization scale μ. This scale is then also present in the Wilson coefficients modifying the simple power–counting argument. In principle non–analytic functions are likely to occur. The remarkable thing of the OPE is that it is an operator relation : then the Wilson coefficients are universal

and do not depend on the particular matrix element

$$\lim_{x\to y} \langle\, A \,|\, \mathrm{T}\{\mathcal{O}_\alpha(x,\mu)\,\mathcal{O}_\beta(y,\mu)\}\,|\, B\,\rangle \;=\; \sum_j C_j^{\alpha\beta}(x-y,\mu)\;\langle\, A\,|\mathcal{O}_j(y,\mu)|\, B\,\rangle\;. \quad (4.42)$$

When taking matrix elements, not all the operators entering the OPE will give a non–zero contribution.

The standard proof of the OPE was given in perturbation theory in 1970 by Zimmerman [62], but it is believed that it also remains valid under non–perturbative effects. In [1] a non–perturbative (but less rigorous) proof based on path–integral is given. We will not enter in the details of the calculations, but merely state the result. Basically it is proved that the vacuum expectation value of the time–ordered product of $n+m$ operators when the space–time arguments of n operators tend to a common space–time point x which is far from the space–time points of the remaining m operators can be expanded as follows:

$$\lim_{x_1\cdots x_i\to x} \langle\, 0 \,|\, \mathrm{T}\{\mathcal{O}_1(x_1)\cdots\mathcal{O}_n(x_n)\,\mathcal{B}_1(y_1)\cdots\mathcal{B}_m(y_m)\}\,|\, 0\,\rangle \;=$$
$$\sum_k C_k^{1\cdots n}(x-x_1,\cdots,x-x_n)\,\langle\, 0 \,|\, \mathrm{T}\{\mathcal{O}_k(x)\,\mathcal{B}_1(y_1)\cdots\mathcal{B}_m(y_m)\}\,|\, 0\,\rangle \quad , \quad (4.43)$$

now the idea is to use the $\mathcal{B}_j$ fields as interpolating functions for particles in the spirit of the LSZ formula on both sides of Eq. (4.43). Since the nature and number of these fields is arbitrary, in principle we can interpolate any particle in the spectrum, and so

$$\lim_{x_1\cdots x_i\to x} \langle\, A \,|\, \mathrm{T}\{\mathcal{O}_1(x_1)\cdots\mathcal{O}_n(x_n)\}\,|\, B\,\rangle \;=\; \sum_k C_k^{1\cdots n}\,(x-x_1,\cdots,x-x_n)\langle\, A\,|\mathcal{O}_k(x)|\, B\,\rangle\,, \quad (4.44)$$

since the states A and B are arbitrary, we are facing an operator identity

$$\lim_{x_1\cdots x_i\to x} T\{\mathcal{O}_1(x_1)\cdots\mathcal{O}_n(x_n)\} \;=\; \sum_k C_k^{1\cdots n}(x-x_1,\cdots,x-x_n)\,\mathcal{O}_k(x)\,. \quad (4.45)$$

Fourier transforming we write the OPE into momentum space

$$\lim_{p_1\cdots p_{n-1}\to\infty} i^{n-1}\int\prod_{j=1}^{n-1}\mathrm{d}^4x_j\,e^{i\sum_{k=1}^{n-1}x_k\cdot p_k}\,\mathrm{T}\{\mathcal{O}_1(x_1)\cdots\mathcal{O}_n(0)\} \;=$$
$$\sum_k i^{n-1}\left[\int\prod_{j=1}^{n-1}\mathrm{d}^4x_j\,e^{i\sum_{k=1}^{n-1}x_k\cdot p_k}C_k^{1\cdots n}(x_1\cdots x_{n-1})\right]\mathcal{O}_k(0) \;=$$
$$\sum_k C_k^{1\cdots n}(p_1\cdots p_{n-1})\,\mathcal{O}_k(0)\,, \quad (4.46)$$

At this point a comment is in order. At the sight of the previous equation it seems clear that the $x^\mu\to 0$ limit is dual to the $p^\mu\to\infty$, but for this to be true we must require in addition that p is space–like ($p^2<0$), that is the OPE has its validity only in the deep Euclidean region $p^2\to-\infty$.

4.5 Callan–Symanzik equation in the OPE

As explained in Section 4.4, composite operators made out of the product of several fields in the same space–time point, due to renormalization need to be defined at some scale μ[2]. In the renormalization programme of QCD, also all fields and constants in the Lagrangian must be defined at a certain scale. One then distinguishes between bare and renormalized fields and parameters, related multiplicatively as follows:

$$\begin{aligned} q_B(x) &= Z_{2F}^{\frac{1}{2}}\, q(x)\,, \qquad G^a_{B\mu}(x) = Z_G^{\frac{1}{2}}\, G^a_\mu(x)\,, \\ \mathcal{M}_B &= Z_m\, \mathcal{M}\,, \qquad\qquad g_{sB} = Z_g\, g_s\,, \end{aligned} \tag{4.47}$$

where the mass will be treated as a small parameter, and will be eventually set to zero. Whereas bare quantities do not depend on any renormalization scale, renormalized ones do. In $D = 4-2\,\epsilon$ dimensions, g_s has dimension ϵ, and so we will define $\alpha_s(\mu) \equiv \mu^{-2\,\epsilon} g_s^2/(4\,\pi)$. Operators made out of the product of several fields at the same space–time need additional multiplicative renormalization (it is not enough to renormalize the fields they are made of)

$$J^a_B = \bar{q}_B(x)\,\Gamma\,\frac{\lambda^a}{2}\,q_B(x)\,, \qquad J^a_R = \frac{1}{Z_J}\,J^a_B = \frac{Z_{2F}}{Z_J}\,\bar{q}(x)\,\Gamma\,\frac{\lambda^a}{2}\,q(x)\,. \tag{4.48}$$

Let us introduce all these definitions in the extended QCD Lagrangian (1.21)

$$\begin{aligned} \mathcal{L}_{QCD} &= Z_{2F}\,\bar{q}\,(i\not{D} - Z_m\,\mathcal{M})\,q - \frac{1}{4}\,Z_G\,G^a_{\mu\nu}G^{\mu\nu}_a + \mathcal{L}_{FP} + \mathcal{L}_{GF} + \mathcal{L}_{ext}\,, \\ D_\mu &= \partial_\mu - i\,Z_g\,Z_G^{\frac{1}{2}}\,g_s\,G^a_\mu\,T^a\,,\; G^{\mu\nu}_a = Z_G^{\frac{1}{2}}\left(\partial_\mu G^a_\nu - \partial_\nu G^a_\mu\right) + Z_g\,Z_G\,f^{abc}g_s G^a_\mu\,G^b_\nu, \\ \mathcal{L}_{ext} &= \sum_\Gamma \bar{q}_B(x)\,\Gamma\,\frac{\lambda^a}{2}\,q_B(x)\,\mathcal{J}^a_B = \frac{Z_{2F}}{Z_\Gamma}\,\bar{q}(x)\,\Gamma\,\frac{\lambda^a}{2}\,q(x)\,\mathcal{J}^a\,, \end{aligned} \tag{4.49}$$

All Feynman rules must be read from the renormalized Lagrangian. For example, the propagators, condensates and source insertions are:

$$S(p) \to \frac{1}{Z_{2F}}\,\frac{i}{\not{p}}\,, \qquad \langle\bar{q}q\rangle \to \frac{1}{Z_{2F}\,Z_m}\,\langle\bar{q}q\rangle(\mu)\,, \qquad \mathcal{J}^a \to i\,\frac{Z_{2F}}{Z_J}\,\frac{\lambda^a}{2}\,\Gamma\,, \tag{4.50}$$

respectively. Actually, it is the GF of renormalized currents what is finite under renormalization[3]. It is not difficult to find a general formula for the Z_Γ factor at one loop

$$Z_\Gamma\,\Gamma = \left(1 - \frac{1}{\hat{\epsilon}}\,\frac{C_F}{4}\,\frac{\alpha_s}{\pi}\right)\Gamma + \frac{1}{\hat{\epsilon}}\,\frac{C_F}{16}\,\frac{\alpha_s}{\pi}\,\gamma^\mu\,\gamma^\nu\,\Gamma\,\gamma_\nu\,\gamma_\mu + \mathcal{O}\left(\alpha_s^2\right)\,, \tag{4.51}$$

[2] In some cases one also needs to define the operator unambiguously, which often requires more than defining them at particular a scale.

[3] Actually this is not exactly true, since GFs needing subtractions in their dispersion relations have a divergence in the identity Wilson coefficient that cannot be regularized with the above procedure. For the rest of the divergences, it is however enough to use the renormalization procedure outlined in this section.

where the Dirac algebra must be performed in *four* dimensions. Let us recall the definition of the γ_m function together with the expressions for all the Z factors at leading order :

$$\begin{aligned} Z_{2F} &= 1 - a\,\frac{C_F}{4}\,\frac{\alpha_s}{\pi}\,\frac{1}{\hat{\epsilon}} + \mathcal{O}\left(\alpha_s^2\right)\,, \quad Z_m \,=\, Z_{S(P)}^{-1} \,=\, 1 - \frac{3\,C_F}{4}\,\frac{\alpha_s}{\pi}\,\frac{1}{\hat{\epsilon}} + \mathcal{O}\left(\alpha_s^2\right)\,, \\ Z_T &= 1 - \frac{1}{\hat{\epsilon}}\,\frac{\alpha_s}{\pi}\,\frac{C_F}{4} + \mathcal{O}\left(\alpha_s^2\right)\,, \quad Z_{V(A)} \,=\, 1\,, \quad \gamma_m(\alpha_s) \,=\, -\,\frac{\mu}{m}\,\frac{\mathrm{d}m}{\mathrm{d}\mu}\,, \end{aligned} \tag{4.52}$$

As previously stated, QCD currents need to be defined at a certain renormalization scale, as they consist on the product of several fields at the same space–time point. In other words, renormalized QCD currents depend on the scale, or "run"; this motivates the definition of their anomalous dimension, [4]

$$\mu\,\frac{\mathrm{d}J_R(\mu)}{\mathrm{d}\mu} = -\,\gamma_J\,J_R(\mu) \,=\, -\,\frac{1}{Z_J(\mu)}\,\mu\,\frac{\mathrm{d}Z_J(\mu)}{\mathrm{d}\mu}\,J_R(\mu)\,. \tag{4.53}$$

The anomalous dimension depends on the coupling α_s, and in perturbation theory has an expansion

$$\gamma_\Gamma(a_s) \,=\, \gamma_\Gamma^{(1)}\,\frac{\alpha_s}{\pi} + \gamma_\Gamma^{(2)}\,\left(\frac{\alpha_s}{\pi}\right)^2 + \gamma_\Gamma^{(3)}\,\left(\frac{\alpha_s}{\pi}\right)^3 + \ldots\,.$$

Vector and axial–vector currents have zero anomalous dimension. This is a general result that stems from the fact that in the chiral limit both currents are conserved. In the $\overline{\mathrm{MS}}$ scheme that we follow in this thesis the renormalization procedure is mass independent and so the result holds for non–zero quark masses. Similarly one can show that the quantities $m_q\,S^a$ and $m_q\,P^a$ are also independent of μ (if the currents are normal–ordered), whence it follows $\gamma_S \,=\, \gamma_P \,=\, -\,\gamma_m$. For the tensor current there is no such simple relation and we will calculate γ_T at leading order in α_s. The general formula for the one–loop order anomalous dimension stems directly from Eq. (4.51) and reads :

$$\gamma_\Gamma^{(1)}\,\Gamma \,=\, \frac{C_F}{2}\left(\Gamma \,-\, \frac{1}{4}\,\gamma^\mu\,\gamma^\nu\,\Gamma\,\gamma_\nu\,\gamma_\mu\right)\,, \tag{4.54}$$

where again the Dirac algebra must be performed in four dimensions. For the tensor current its value is

$$\gamma_T^{(1)} \,=\, \frac{C_F}{2} \,=\, \frac{2}{3} \approx \frac{N_C}{4}, \tag{4.55}$$

where the approximation corresponds to the large–N_C limit. We are now in condition to discuss the Callan–Symanzik equation (often also known as the renormalization

[4] In this discussion we will assume no mixing between operators.

group equation or RGE). The relation of the time–ordered products of bare and renormalized currents read

$$\left(\prod_{i=1}^{n} Z_i\right) \mathrm{T}\{\mathcal{O}_1^R(x_1)\cdots\mathcal{O}_n^R(x_n)\} \;=\; T\{\mathcal{O}_1^B(x_1)\cdots\mathcal{O}_n^B(x_n)\}\,. \tag{4.56}$$

The right–hand side is a bare object, and hence scale independent. Applying one derivative with respect to μ to the above expression we find [5]

$$\left(\sum_{i=1}^{n}\gamma_i + \mu\,\frac{\mathrm{d}}{\mathrm{d}\mu}\right) \mathrm{T}\{\mathcal{O}_1^R(x_1)\cdots\mathcal{O}_n^R(x_n)\} \;=\; 0\,. \tag{4.57}$$

This very same equation must be satisfied once the OPE is applied for any of the terms entering the expansion

$$\begin{aligned} -\mu\,\frac{\mathrm{d}}{\mathrm{d}\mu}\left[C_k^{1\cdots n}(x-x_1,\cdots,x-x_n)\,\mathcal{O}_k(x)\right] \;&=\\ \left\{\left[-\mu\,\frac{\mathrm{d}}{\mathrm{d}\mu}+\gamma_k\right] C_k^{1\cdots n}(x-x_1,\cdots,x-x_n)\right\}\mathcal{O}_k(x) \;&=\\ \left(\sum_{i=1}^{n}\gamma_i\right) C_k^{1\cdots n}(x-x_1,\cdots,x-x_n)\,\mathcal{O}_k(x) \quad &, \end{aligned} \tag{4.58}$$

and so

$$\begin{aligned} \left[-\mu\,\frac{\mathrm{d}}{\mathrm{d}\mu} \;+\; \gamma_k \;-\sum_{i=1}^{n}\gamma_i\right] C_k^{1\cdots n} \;&=\; 0\,,\\ \left[-\mu\,\frac{\partial}{\partial\mu} \;+\; \beta(\alpha_s)\,\frac{\partial}{\partial\alpha_s} \;+\; m(\mu)\,\gamma_m(\alpha_s)\,\frac{\partial}{\partial m} \;+\; \gamma_k \;-\sum_{i=1}^{n}\gamma_i\right] C_k^{1\cdots n} \;&=\; 0\,, \end{aligned} \tag{4.59}$$

where we have used the chain rule to separate the explicit μ dependence from that encoded in parameters of the Lagrangian. This last expression constitutes the Callan–Symanzik equation for the Wilson coefficients of the OPE. If we specialize for the cases under study in this thesis, many simplifications occur. Since we are working in the chiral limit, there is no quark mass term, and since we work at most to the $\mathcal{O}(\alpha_s)$ precision, the β term does not contribute. We will only compute gluonic corrections of the quark condensate Wilson coefficient:

$$\left[-\mu\,\frac{\partial}{\partial\mu} \;-\; \gamma_m \;-\sum_{i=1}^{n}\gamma_i\right] C_{\langle\bar{q}q\rangle}^{1\cdots n} \;=\; 0\,, \tag{4.60}$$

where we have used that the product $m_q : \bar{q}q :$ has no running, or equivalently that $\gamma_{\langle\bar{q}q\rangle} = \gamma_S = -\,\gamma_m$.

[5] This argument is spoiled if the GF needs subtractions, that is it does not correspond to a physical quantity. GFs made of quark bilinear currents that are order parameter never need subtractions.

4.6 QCD sum rules

The physical vacuum of QCD is not the vacuum state that one uses in perturbation theory. Physical effects discussed in Chapter 1 such as spontaneous chiral symmetry breaking and confinement do not appear in an order by order perturbation treatment of QCD (even if we consider *all* such orders). Then one might wonder *how the perturbative QCD results get modified by non–perturbative effects at long distances*. We shall see that non–perturbative effects manifest in GFs evaluated at large momentum transfer as inverse power corrections of the squared momenta.

In this section we will apply the OPE to QCD GFs. Then we only have to take vacuum expectation value of both sides of Eq. (4.46). Naïvely one could think that since the operators appearing in the right–hand side of the OPE are normal ordered, their vacuum expectation value must be zero and thus only the identity operator would contribute, giving then the usual perturbative result. However, this would only be true for the "perturbative" vacuum. The non–perturbative QCD vacuum is by no means trivial, and the vacuum expectation value of normal–ordered operators is in general non–vanishing due to long–distance effects. They are known as *vacuum condensates*. The Wilson coefficients are calculable perturbatively and admit an expansion in powers of α_s.

In fact it is known that the need of non–perturbative power corrections to GFs can be "hinted" from what emerges already in perturbation theory when renormalon effects are studied, as discussed in [55].

This idea was pioneered by the ITEP group [16] and consists on an explicit separation of long– and short–distance effects. The short–distance effects are encoded in the Wilson coefficients and the long–distance ones in the condensates. This splitting of scales must be performed at some arbitrary scale μ high enough to make a perturbative calculation reliable. This is reflected in the μ dependence of both the Wilson coefficient and the condensate. So the Wilson coefficient covers the interactions corresponding to $-q^2 < \mu^2$ and the condensates parametrize effects due to $-q^2 > \mu^2$. Whereas the former depend on the specific GF under study, the latter are universal parameters. In principle these condensates are calculable in QCD and depend only on the parameters of the Lagrangian, but as happens with the chiral LECs, their computation is only abordable with either models (instanton based) or lattice QCD. Our approach will be to consider the condensates as phenomenological parameters to fit. In practice, using the standard methods of Feynman diagrams, an explicit separation of distances is impossible in the quark–gluon diagrams. One is then forced to take into account both the soft parts of perturbative diagrams and the long–distance condensate effects simultaneously. This yields a certain amount of double counting, which is, fortunately, numerically insignificant, because the condensate contributions turn out to be much larger that the soft "tails" of perturbative diagrams.

However, one cannot calculate in the OPE an arbitrary number of power corrections. As demonstrated in [16] there is a critical dimension at which non–perturbative effects cause the OPE to break down. We will not enter in the details

of this phenomenon, but will restrict ourselves to the first orders.

To close this section we give a list of the condensates that we are going to consider in this thesis

$$\langle\bar{q}q\rangle \ , \ \alpha_s \left\langle G^a_{\mu\nu}G^{\mu\nu}_a\right\rangle \ , \ g_s \left\langle\bar{q}\,\sigma_{\mu\nu}G^{\mu\nu}q\right\rangle \ , \ \left\langle\bar{q}\,\Gamma\,\lambda^a q\,\bar{q}\,\Gamma\,\lambda^a q\right\rangle \ , \tag{4.61}$$

4.7 First OPE applications

In this section we will use the results derived in Section 4.4 to obtain relations between two– and three–point GFs when high momentum limits are taken. Of course, in the language of Fourier transformations this limit is dual to the small coordinate limit when momentum and coordinate are conjugate to each other. Some of the topics discussed in this section can be found in Ref. [51]. To start with, let us reduce the time–ordered product of three currents when the limit of one coordinate tending to another is taken

$$\lim_{x\to 0} T\{J_1(x)\,J_2(y)\,J_3(0)\} = T\{T\{J_1(x)\,J_3(0)\}J_2(y)\}\,. \tag{4.62}$$

Thus the time–ordered product of three operators reduces to the time–ordered product of the time–ordered of two of them with the third one, when the appropriate limit is taken. Next we consider the OPE for two currents at $\mathcal{O}(\alpha_s^0)$. Defining $h^{abc} = 4\,\mathrm{Tr}\big[T^a\,T^b\,T^c\big] = d^{abc} + i\,f^{abc}$ we find:

$$\begin{aligned}\lim_{x\to y} T\left\{J_1^a(x)J_2^b(y)\right\} \ &= \ \frac{N_C\,\delta^{ab}}{2}\int\frac{\mathrm{d}^4p\,\mathrm{d}^4q}{(2\,\pi)^8}\,e^{-i(p-q)(x-y)}\,\frac{\mathrm{Tr}[\not{p}\,\Gamma_2\,\not{q}\,\Gamma_1]}{p^2q^2}\\ &+\frac{i}{8}\int\frac{\mathrm{d}^4q}{(2\,\pi)^4}\,e^{-iq(x-y)}\sum_\Gamma\frac{c_\Gamma}{q^2}\left\{\frac{\delta^{ab}}{n_f}\,(\bar{q}\,\Gamma\,q)\,(x)\,\mathrm{Tr}[\,(\Gamma_2\,\Gamma\,\Gamma_1-\Gamma_1\,\Gamma\,\Gamma_2)\,\not{q}\,]\right.\\ &\left.+\left(\bar{q}\,\Gamma\,\frac{\lambda^c}{2}\,q\right)(x)\big(h^{abc}\,\mathrm{Tr}[\,\Gamma_2\,\Gamma\,\Gamma_1\,\not{q}\,]\ -\ h^{acb}\,\mathrm{Tr}[\,\Gamma_1\,\Gamma\,\Gamma_2\,\not{q}\,]\big)\right\}\end{aligned} \tag{4.63}$$

$$\begin{aligned}\lim_{x\to y} T\left\{J_1^a(x)J_2^b(y)\right\} \ &= \ -\frac{N_C\,\delta^{ab}}{8\,\pi^2}\,\frac{1}{(x-y)^8}\,\mathrm{Tr}\,[\,\Gamma_1(\not{x}-\not{y})\Gamma_2(\not{x}-\not{y})]\\ &+\frac{i}{16\,\pi^2}\sum_\Gamma\frac{c_\Gamma}{(x-y)^3}\left\{\frac{\delta^{ab}}{n_f}\,(\bar{q}\,\Gamma\,q)\,(x)\,\mathrm{Tr}\,[\,(\Gamma_2\,\Gamma\,\Gamma_1-\Gamma_1\,\Gamma\,\Gamma_2)\,(\not{x}-\not{y})]\right.\\ &\left.+\left(\bar{q}\,\Gamma\,\frac{\lambda^c}{2}\,q\right)(x)\big(h^{abc}\,\mathrm{Tr}\,[\,\Gamma_2\,\Gamma\,\Gamma_1\,(\not{x}-\not{y})]\ -\ h^{acb}\,\mathrm{Tr}\,[\,\Gamma_1\,\Gamma\,\Gamma_2\,(\not{x}-\not{y})]\big)\right\}\ ,\end{aligned} \tag{4.64}$$

where we have written the result both in momentum and position spaces. We denote generically

$$J_i^a(x) \ =: \bar{q}(x)\,\Gamma_i\,\frac{\lambda^a}{2}\,q(x) :\ . \tag{4.65}$$

Γ	$\mathbb{1}_{4\times 4}$	$i\,\gamma_5$	γ_μ	$\gamma_\mu\,\gamma_5$	$\sigma_{\mu\nu}$
c_Γ	1	-1	1	-1	$\frac{1}{2}$

Table 4.1: Fierz identity in the Dirac algebra.

The first term corresponds to the perturbative part and in general needs to be subtracted, and the second is obtained after applying the Fierz identity in both flavour and Dirac spaces

$$\delta_{\alpha\beta}\,\delta_{\gamma\delta} \;=\; 2\left(\frac{\lambda^a}{2}\right)_{\alpha\gamma}\left(\frac{\lambda^a}{2}\right)_{\beta\delta} + \frac{1}{n_f}\,\delta_{\alpha\gamma}\,\delta_{\beta\delta}\,, \quad \delta_{ij}\,\delta_{kl} \;=\; \frac{1}{4}\sum_\Gamma c_\Gamma\,\Gamma_{ik}\,\Gamma_{jl}\,. \tag{4.66}$$

The Γ matrices span a basis of the Dirac algebra, and their expression can be found in Table 4.1 together with the values for the c_Γ coefficients. For order parameter GFs the perturbative term vanishes, whereas the second one does so for the rest.

As a first application of Eq. (4.64) we can compute the leading order of both the perturbative term and quark condensate contribution to two–point GFs in the OPE [6]

$$\begin{aligned}\lim_{p\to\infty}\Pi^{ab}_{12}(p) \;&=\; i\,\frac{N_C\,\delta^{ab}}{2}\int\frac{\mathrm{d}^4\ell}{(2\,\pi)^4}\,\frac{\mathrm{Tr}\,[\Gamma_1\not{\ell}\,\Gamma_2\,(\not{\ell}-\not{p}\,)]}{\ell^2(\ell-p)^2}\\ &\quad+\frac{\langle\bar{q}q\rangle}{8\,p^2}\,\delta^{ab}\,\mathrm{Tr}\,([\Gamma_1,\Gamma_2]\,\not{p}\,)+\mathcal{O}\left(p^{-2}\right)\,,\end{aligned} \tag{4.67}$$

where either the first or the second term survive depending on the nature of the GF. The integral in the first term can be explicitly calculated with the help of the expressions in Appendix G and after properly regularized we find

$$\begin{aligned}\lim_{p\to\infty}\Pi^{ab}_{12}(p) \;&=\; \frac{N_C\,\delta^{ab}}{12\,(4\,\pi)^2}\left\{\frac{p^2}{2}\,\mathrm{Tr}\,[\,\Gamma_1\,\gamma^\alpha\,\Gamma_2\,\gamma_\alpha]\left[\frac{1}{\hat{\epsilon}}+\frac{8}{3}-\log\left(-\frac{p^2}{\mu^2}\right)\right]\right.\\ &\quad\left.+\,\mathrm{Tr}\,[\,\Gamma_1\not{p}\,\Gamma_2\not{p}\,]\left[\frac{1}{\hat{\epsilon}}+\frac{5}{3}-\log\left(-\frac{p^2}{\mu^2}\right)\right]\right\}+\mathcal{O}\left(p^0\right)\,.\end{aligned} \tag{4.68}$$

The Feynman diagram leading to this result is depicted in Fig 4.3 (a).

Applying this formula to the set of GFs not being order parameter we obtain

$$\begin{aligned}\Pi_{SS\,(PP)}(p^2) \;&=\; \frac{N_C\,p^2}{(4\,\pi)^2}\left[\frac{1}{\hat{\epsilon}}+2-\log\left(-\frac{p^2}{\mu^2}\right)\right]+\mathcal{O}\left(p^{-2}\right)\,,\\ \Pi_{VV\,(AA)}(p^2) \;&=\; \frac{2}{3}\,\frac{N_C}{(4\,\pi)^2}\left[\frac{1}{\hat{\epsilon}}+\frac{5}{3}-\log\left(-\frac{p^2}{\mu^2}\right)\right]+\mathcal{O}\left(p^{-4}\right)\,,\\ \Pi^{\pm}_{TT}(p^2) \;&=\; \frac{N_C}{3(4\,\pi)^2}\left[\frac{1}{\hat{\epsilon}}+\frac{8}{3}-\log\left(-\frac{p^2}{\mu^2}\right)\right]+\mathcal{O}\left(p^{-4}\right)\,,\end{aligned} \tag{4.69}$$

[6] The statement $\mathcal{O}(p^n)$ must be understood as $\mathcal{O}(\lambda^n)$ having written $p^\mu=\lambda\,n^\mu$ with $n^2=-1$. If more than one momenta appear in the limit, we will understand $p_i^\mu=\lambda\,n_i^\mu$, $n_i^2=-1$ with the same λ for all i.

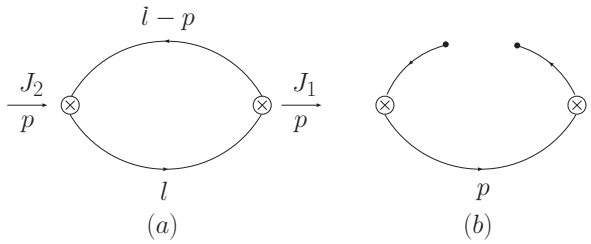

Figure 4.3: Feynman diagrams of: (a) the perturbative term and (b) the quark condensate, for a two–point GF at $\mathcal{O}(\alpha_s^0)$.

And doing so with the ones being order parameter we get

$$\Pi_{AP}(p^2) \,=\, 2\,\frac{\langle\bar{q}q\rangle}{p^2}\,, \qquad \Pi_{VT}(p^2) \,=\, \frac{\langle\bar{q}q\rangle}{p^2} + \mathcal{O}\left(p^{-6}\right)\,. \tag{4.70}$$

and the corresponding Feynman diagram is drawn in Fig 4.3 (b). One has to multiply this diagram by a factor of two because the counterclockwise contribution coincides with the clockwise one. Notice that for the case of $\langle AP\rangle$ we recover the result obtained in Eq. (4.11), which we know is the exact solution.

As a second application, we obtain the following set of relations:

$$\begin{aligned}
\lim_{p\to\infty}\Pi^{abc}_{123}(p,q) &= \frac{1}{8\,p^2}\sum_{i=1}^{8} c_\Gamma\Pi_{2\Gamma}(q)\big(h^{abc}\mathrm{Tr}\left[\Gamma_1\Gamma\Gamma_3\not{p}\right] - h^{acb}\mathrm{Tr}\left[\Gamma_3\Gamma\Gamma_1\not{p}\right]\big)\,,\\
\lim_{q\to\infty}\Pi^{abc}_{123}(p,q) &= -\frac{1}{8\,q^2}\sum_{i=1}^{8} c_\Gamma\Pi_{1\Gamma}(p)\big(h^{abc}\mathrm{Tr}\left[\Gamma_3\Gamma\Gamma_2\not{q}\right] - h^{acb}\mathrm{Tr}\left[\Gamma_2\Gamma\Gamma_3\not{q}\right]\big)\,,\\
\lim_{p\to\infty}\Pi^{abc}_{123}(p,-r-p) &= -\frac{1}{8\,p^2}\sum_{i=1}^{8} c_\Gamma\Pi_{3\Gamma}(r)\big(h^{abc}\mathrm{Tr}\left[\Gamma_1\Gamma\Gamma_3\not{p}\right] - h^{acb}\mathrm{Tr}\left[\Gamma_3\Gamma\Gamma_1\not{p}\right]\big),
\end{aligned} \tag{4.71}$$

where in the last expression we have used the fact that $\Pi_{ij}(p) = \Pi_{ji}(-p)$. We can now particularize Eq. (4.71) to the different three–point GFs.

$$\begin{aligned}
\lim_{q\to\infty}\Pi_{SSS\,(SPP)}(p^2,q^2,(p+q)^2) &= \mathcal{O}(q^{-2})\,,\\
\lim_{p\to\infty}\Pi_{SPP}(p^2,q^2,(p+q)^2) &= -8\,\langle\bar{q}q\rangle\,\frac{p\cdot q}{p^2\,q^2} \,+\, \mathcal{O}(p^{-2})\,,\\
\lim_{q\to\infty}\Pi_{VVP\,(VAS)}(p^2,q^2,(p+q)^2) &= -2\,\frac{\Pi_{VT}(p^2)}{q^2} \,+\, \mathcal{O}(q^{-3})\,, \qquad (4.72)\\
\lim_{p\to\infty}\Pi_{VVP\,(AAP)}(p^2,(r+p)^2,r^2) &= -2\,\frac{\langle\bar{q}q\rangle}{p^2\,r^2} \,+\, \mathcal{O}(p^{-3})\,, \qquad (4.73)\\
\lim_{p\to\infty}\Pi_{AAP\,(VAS)}(p^2,q^2,(p+q)^2) &= \lim_{p\to\infty}\Pi_{VAS}(p^2,(r+p)^2,r^2) \,=\, \mathcal{O}(p^{-3})\,,
\end{aligned}$$

$$
\begin{aligned}
\lim_{p\to\infty} \mathcal{F}_{VVS}(p^2,q^2,(p+q)^2) &= 2\,\frac{\Pi_{VT}(q^2)}{p^2} + \mathcal{O}(p^{-3})\,, \\
\lim_{q\to\infty} \mathcal{G}_{VVS\,(AAS)\,[VAP]}(p^2,q^2,(p+q)^2) &= \lim_{q\to\infty} \mathcal{F}_{AAS}(p^2,q^2,(p+q)^2) = \mathcal{O}(q^{-4})\,, \\
\lim_{p\to\infty} \mathcal{F}_{VVS}(p^2,(r+p)^2,r^2) &= \lim_{p\to\infty} \mathcal{G}_{VAP}(p^2,q^2,(p+q)^2) = \mathcal{O}(p^{-4})\,, \\
\lim_{p\to\infty} \mathcal{G}_{VVS}(p^2,(r+p)^2,r^2) &= \mathcal{O}(p^{-6})\,, \\
\lim_{p\to\infty} \mathcal{F}_{AAS\,(VAP)}(p^2,q^2,(p+q)^2) &= \mathcal{O}(p^{-3})\,, \\
\lim_{q\to\infty} \mathcal{F}_{VAP}(p^2,q^2,(p+q)^2) &= \frac{\Pi_{VT}(p^2)}{q^2} + \mathcal{O}(q^{-4})\,, \qquad (4.74)
\end{aligned}
$$

And in addition we have

$$
\lim_{p\to\infty} \mathcal{F}_{AAS}(p^2,(r+p)^2,r^2) - p^2\,\mathcal{G}_{AAS}(p^2,(r+p)^2,r^2) = \mathcal{O}(p^{-4})\,, \qquad (4.75)
$$

and

$$
\begin{aligned}
\lim_{p\to\infty} \mathcal{F}_{VAP}(p^2,(r+p)^2,r^2) &= -\frac{\langle\bar{q}q\rangle}{p^2}\left[\mathcal{F}^{(0)}(r^2) + \frac{p\cdot r}{p^2}\,\mathcal{F}^{(1)}(r^2) + \mathcal{O}(p^{-2})\right], \\
\lim_{p\to\infty} \mathcal{G}_{VAP}(p^2,(r+p)^2,r^2) &= -\frac{\langle\bar{q}q\rangle}{p^4}\left[\mathcal{G}^{(0)}(r^2) + \frac{p\cdot r}{p^2}\,\mathcal{G}^{(1)}(r^2) + \mathcal{O}(p^{-2})\right], \qquad (4.76)
\end{aligned}
$$

together with

$$
\mathcal{F}^{(0)}(r^2) - \mathcal{G}^{(0)}(r^2) = \frac{1}{r^2}\,, \qquad \mathcal{F}^{(1)}(r^2) - \mathcal{G}^{(1)}(r^2) + \mathcal{G}^{(0)}(r^2) = \frac{2}{r^2}\,. \qquad (4.77)
$$

4.8 $C_{\langle\bar{q}q\rangle}$ for three–point Green functions at $\mathcal{O}(\alpha_s^0)$

As already discussed in the introduction of this chapter, the $\langle\bar{q}q\rangle$ condensate plays a special röle since it is believed to be driving the spontaneous breaking of chiral symmetry. Moreover, since we are considering only order parameter GFs, there is no perturbative contribution and the quark condensate is the first OPE term. We recall the reader that the Wilson coefficient for two–point GFs has been already calculated in the previous section.

The easiest way to compute the Wilson coefficient for the quark condensate operator is a direct application of the Wick theorem leaving a pair of quark fields uncontracted and using the identity

$$
\left\langle \bar{q}^a_{i\alpha}(0) q^b_{j\beta}(0) \right\rangle = \frac{1}{4\,N_C}\,\delta^{ab}\,\delta_{ij}\,\delta_{\alpha\beta}\,\langle\bar{q}q\rangle\,, \qquad (4.78)
$$

where a, b are flavour indices, i, j are Dirac indices and α, β are colour indices. A more efficient method to obtain $C_{\langle\bar{q}q\rangle}$ is to use the plane wave method, which exploits the fact that the OPE is an operator relation. The Feynman diagrams corresponding

to this contribution are depicted in Fig. 4.4. In fact one has to consider the same diagrams with the fermionic charge flowing counterclockwise. We will define

$$\begin{aligned}
\Pi^{\rm OPE}_{SSS(SPP)}(p^2,q^2,r^2,\mu) &= C^{SSS(SPP)}_{\langle\bar{q}q\rangle}(p^2,q^2,r^2,\mu)\langle\bar{q}q\rangle(\mu)+\cdots\,,\\
\Pi_{VVP(AAP)[VAS]}(p^2,q^2,r^2,\mu) &= C^{VVP(AAP)[VAS]}_{\langle\bar{q}q\rangle}(p^2,q^2,r^2)\,\langle\bar{q}q\rangle(\mu)+\cdots\,,\\
\mathcal{F}[\mathcal{G}]_{VVS(AAS)[VAP]}(p^2,q^2,r^2,\mu) &= C^{VVS(AAS)[VAP]}_{\mathcal{F}[\mathcal{G}]\langle\bar{q}q\rangle}(p^2,q^2,r^2)\,\langle\bar{q}q\rangle(\mu)+\cdots\,.
\end{aligned} \tag{4.79}$$

It is not difficult to find a general formula for this Wilson coefficient. We obtain:

$$\begin{aligned}
C^{abc}_{\langle\bar{q}q\rangle\,123} &= -\frac{1}{16}\left\{\frac{1}{p^2\,q^2}\left(h^{abc}\,{\rm Tr}\left[\,\Gamma_1\Gamma_2\not{q}\,\Gamma_3\not{p}\,\right]+h^{acb}\,{\rm Tr}\left[\,\Gamma_2\Gamma_1\not{p}\,\Gamma_3\not{q}\,\right]\right)\right.\\
&\quad+\frac{1}{p^2\,r^2}\left(h^{abc}\,{\rm Tr}\left[\,\Gamma_3\Gamma_1\not{p}\,\Gamma_2\not{r}\,\right]+h^{acb}\,{\rm Tr}\left[\,\Gamma_1\Gamma_3\not{r}\,\Gamma_2\not{p}\,\right]\right)\\
&\quad\left.+\frac{1}{q^2\,r^2}\left(h^{abc}\,{\rm Tr}\left[\,\Gamma_2\Gamma_3\not{r}\,\Gamma_1\not{q}\,\right]+h^{acb}\,{\rm Tr}\left[\,\Gamma_2\Gamma_3\not{q}\,\Gamma_1\not{r}\,\right]\right)\right\},
\end{aligned} \tag{4.80}$$

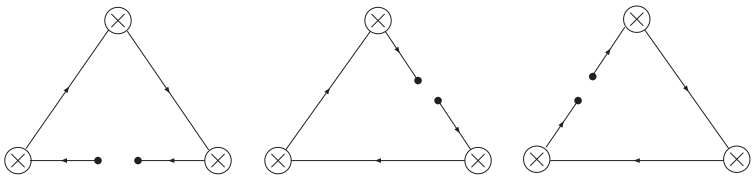

Figure 4.4: $\mathcal{O}(\alpha_s^0)$ contributions to the quark condensate operator for three–point functions.

Applying Eq. (4.80) to the functions we are interested in we get:

$$\begin{aligned}
C^{SSS}_{\langle\bar{q}q\rangle}(p^2,q^2,r^2) &= -\,2\,\frac{\lambda\,(p^2,q^2,r^2)}{p^2\,q^2\,r^2}\,, & C^{SPP}_{\langle\bar{q}q\rangle}(p^2,q^2,r^2) &= 2\,\frac{p^4-(q^2-r^2)^2}{p^2\,q^2\,r^2}\,,\\
C^{VVP}_{\langle\bar{q}q\rangle}(p^2,q^2,r^2) &= -\,\frac{p^2+q^2+r^2}{p^2\,q^2\,r^2}\,, & C^{AAP\,(VAS)}_{\langle\bar{q}q\rangle}(p^2,q^2,r^2) &= \frac{r^2-p^2\mp q^2}{p^2\,q^2\,r^2}\,,\\
C^{VVS\,(AAS)}_{\mathcal{F}\,\langle\bar{q}q\rangle}\left(p^2,q^2,r^2\right) &= \frac{p^2+q^2\pm r^2}{p^2\,q^2\,r^2}\,, & C^{VAP}_{\mathcal{F}\,\langle\bar{q}q\rangle}\left(p^2,q^2,r^2\right) &= -\,\frac{p^2-q^2-r^2}{p^2\,q^2\,r^2}\,.\\
C^{VVS\,(AAS)\,[VAP]}_{\mathcal{G}\,\langle\bar{q}q\rangle}\left(p^2,q^2,r^2\right) &= 2\,\frac{1}{p^2\,q^2\,r^2}\,,
\end{aligned} \tag{4.81}$$

4.9 Hard–gluon corrections to the quark condensate

In this section we will compute the $\mathcal{O}(\alpha_s)$ corrections to the Wilson coefficient corresponding to the first non–perturbative operator: $\langle\bar{q}q\rangle$. In the case of order

parameter of the chiral symmetry breaking GFs this first operator is the leading one, and so it is relevant to calculate its first order gluonic corrections. Yet another motivation for computing the $\mathcal{O}(\alpha_s)$ corrections to $C_{\langle\bar{q}q\rangle}$ is to make the QCD running coincide both in the OPE and RχT.

Let us now consider the case of the Π_{SSS} GF. In the OPE it gets its first contribution from $\langle\bar{q}q\rangle$, and at leading order its Wilson coefficient is μ–independent. On the RχT side the situation is a bit different. It is well known that each scalar and pseudoscalar current insertion in a chiral theory is accompanied by a $\langle\bar{q}q\rangle$ factor, so

$$\Pi_{SSS}^{\mathrm{OPE}} \,=\, C_{\langle\bar{q}q\rangle}(p,q)\,\langle\bar{q}q\rangle(\mu)\,, \qquad \Pi_{SSS}^{\mathrm{R}\chi\mathrm{T}} \,=\, \widetilde{\Pi}(p,q)\,\langle\bar{q}q\rangle(\mu)^3\,, \tag{4.82}$$

and apparently we cannot match one onto the other because the μ dependence is different. What it is happening is that whereas for $C_{\langle\bar{q}q\rangle}$ we restrict our calculation to the leading order, RχT includes all α_s orders in a non–perturbative fashion. But if we take into account the RGE for the Wilson coefficient Eq. (4.86), Eq. (4.82) becomes meaningful and in principle the matching could be performed.

We will first discuss the case of two–point GFs and concentrate later in the three–point case.

4.9.1 Two–point functions

We start reviewing the derivation of the α_s corrections for $C_{\langle\bar{q}q\rangle}$ in the case of two–point GFs which are order parameter. In this simple scenario we will discuss the appearance of infrared (IR) divergences and the renormalization of $\langle\bar{q}q\rangle$. The only GF that we can consider is the $\langle VT\rangle$, since the $\langle AP\rangle$ is fully determined by the Ward identities and does not receive any contribution (in Ref. [60] this has been explicitly checked to the one loop level). The diagrams that contribute to this order are shown in Fig. 4.5 (each diagram is accompanied by a factor of two as discussed in Section 4.7).

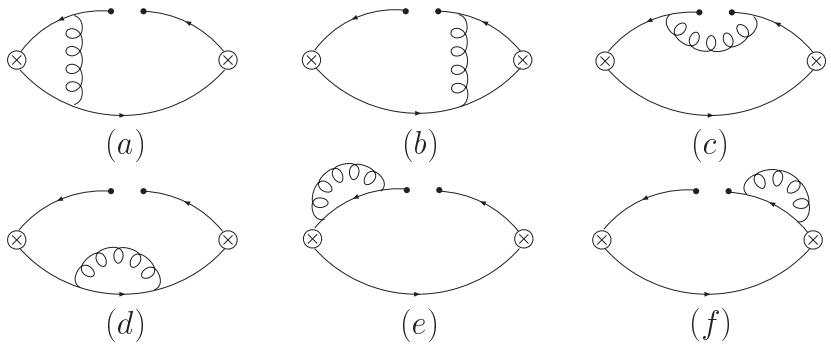

Figure 4.5: Gluonic corrections to the quark condensate.

The first thing one should observe is that diagrams (c), (e) and (f) of Fig. (4.5) are infrared divergent since they involve gluons attached to quark lines with zero

momentum. The same diagrams contribute to Π^{μ}_{AP} and Eq. (4.11) shows that it is free from IR divergences. So they cancel when adding the six diagrams, and something similar must occur for the $\langle VT\rangle$ GF. Since these divergences cancel at the end we might choose any method to regularize them. A first option, more intuitive, is to give the quark (or the gluon) a small mass, and in this way the divergence will manifest itself as $\log(m)$. This method is analytically more involved and gets terrible for three–point GFs. We will adopt the dimensional regularization method which simplifies the computations notoriously. The problem with this method is that one loses the possibility of distinguishing the ultraviolet (UV) divergences from the IR ones. The divergences will manifest, as usual, as $1/\hat{\epsilon}$ and $\log(\mu)$. In this scheme diagrams (e) and (f) are zero: they are scaleless and convert the IR divergences of (c) into UV ones. So we are left with diagram (c) as the only one potentially problematic. For this diagram (computed in an arbitrary gauge) we obtain in the $\overline{\rm MS}$ scheme:

$$\mathcal{M}^{(c)}_{VT} \;=\; -\,\frac{\alpha_s}{\pi}\frac{C_F}{4}\frac{\langle\bar{q}q\rangle}{p^2}\left\{(a+3)\left[\frac{1}{\hat{\epsilon}}-\log\left(-\frac{p^2}{\mu^2}\right)\right]+a+1\right\}\,. \tag{4.83}$$

As we see, by itself this diagram is still gauge dependent, which means that the other diagrams are required in order to obtain a gauge–invariant result. The divergence in the expression has the form $\frac{1}{\hat{\epsilon}}\frac{(3+a)}{4}\frac{\alpha_s}{\pi}\frac{C_F}{2}$ and together with the tree–level amplitude we get the structure:

$$\begin{aligned}\langle\bar{q}q\rangle\left(1-\frac{1}{\hat{\epsilon}}\frac{(3+a)}{4}\frac{\alpha_s}{\pi}C_F\right) &= \langle\bar{q}q\rangle\, Z_m\, Z_{2F} \;=\; \langle\bar{q}_B\, q_B\rangle\, Z_m \\ &= \frac{m_B}{m_R(\mu)}\,\langle\bar{q}_B\, q_B\rangle = \langle\bar{q}q\rangle_R\,(\mu)\,. \end{aligned}\tag{4.84}$$

We have used the fact that the product $m\,\langle\bar{q}q\rangle$ is a renormalization group invariant quantity and so the divergence is absorbed in the renormalization of the condensate. Summing up all diagrams, taking into account Eq. (4.84), including the wave function renormalization of the quark fields and the renormalization of the tensor current we find

$$\Pi^{\rm OPE}_{VT}(p^2) \;=\; \frac{\langle\bar{q}q\rangle\,(\mu)}{p^2}\left\{1+\frac{\alpha_s}{\pi}\,C_F\left[\log\left(-\frac{p^2}{\mu^2}\right)-1\right]\right\}+\,\mathcal{O}(\alpha_s^2,p^{-4})\,, \tag{4.85}$$

which is of course independent of the a parameter as required by gauge invariance, constituting a good check for our calculation[7]. For N_C flavours $C_F=\frac{N_C^2-1}{2N_C}\approx\frac{N_C}{2}$ where the approximation corresponds to the large–N_C limit. As a last comment, let us write the Wilson coefficient Callan–Symanzik equation,

$$\left[-\,\mu\,\frac{\partial}{\partial\mu}\;-\;\gamma_m\;-\gamma_T\right]C^{VT}_{\langle\bar{q}q\rangle} \;=\; \left[-\,\mu\,\frac{\partial}{\partial\mu}\;-\,2\,\frac{\alpha_s}{\pi}\,C_F\right]C^{VT}_{\langle\bar{q}q\rangle} \;=\; 0\,, \tag{4.86}$$

[7] All calculations in this chapter have been performed in an arbitrary gauge. The dependence into the gauge parameter a cancels in all our final results.

which is identically satisfied by Eq. (4.85).

4.9.2 Three–point functions

We turn now our attention to the three–point functions which are of great interest for different reasons. First, unlike the two–point ones, there is a quite big amount of them that are order parameter of the chiral symmetry breaking. Second, in the framework of RχT they involve vertices among resonances and so it is useful to learn how they interact. Third, there are a lot of $\mathcal{O}(p^6)$ χPT LECs that can be determined with these GFs [41]. And fourth, by means of the LSZ reduction formula we can relate the GFs with form factors entering the calculation of many interesting hadronic observables.

The expressions of the α_s corrections to $C_{\langle\bar{q}q\rangle}$ for the three–point GFs are quite involved and their explicit form is relegated to Appendix D. There are two reasons for this complexity : first, they involve three Lorentz invariants p^2, q^2 and r^2, and second (and specially for VVS, AAS and VAP) they involve different Lorentz structures that mix with each other under quantum corrections.

The diagrams contributing to the hard gluonic corrections for the three–point functions when the quark condensate is between the first and second currents are shown in Fig. 4.6. Of course, the same kind of corrections must be considered for the other two insertions of the quark condensate and the reverse fermionic flow terms. Diagrams (h), (i) and (j) are analogous to those in Fig. 4.5 (c), (e) and (f), respectively. Diagrams (d) and (e) are IR and UV safe, even though they have gluons attached to zero momentum quark lines. Much as we did in Section 4.9.1, we regularize both type of divergences in dimensional regularization, renormalize the quark condensate as in Eq. (4.84) and after summing up all diagrams IR divergences will cancel out. The rest of the (UV) divergences are absorbed in counterterms as usual and this renders a finite (but in general scale dependent) result.

Loop corrections manifest themselves as logarithms, dilogarithms and constant pieces. In general we will have the following decomposition :

$$C^{\alpha_s}_{\langle\bar{q}q\rangle} = \frac{\alpha_s}{\pi}\frac{C_F}{8}\left[L_p \log\left(-\frac{p^2}{\mu^2}\right) + L_q \log\left(-\frac{q^2}{\mu^2}\right) + L_r \log\left(-\frac{r^2}{\mu^2}\right) + L_d\, C_0 + L_c\right], \tag{4.87}$$

where L_i are μ–independent meromorphic functions of the squared external momenta. This simple structure arises because in the chiral limit all internal lines, either quark or gluon, are massless. C_0 collects all dilogarithms and its explicit expression reads :

$$\begin{aligned} C_o\left(p^2,q^2,r^2\right) &= -\,i\,(4\pi)^2 \int \frac{\mathrm{d}^4k}{(2\pi)^4}\,\frac{1}{k^2(p+k)^2(q-k)^2} \\ &= \frac{1}{\sqrt{\lambda}}\left\{\mathrm{Li}_2\left(-\frac{\lambda+q^2+p^2-r^2}{\lambda-q^2-p^2+r^2}\right) - \mathrm{Li}_2\left(-\frac{\lambda-q^2-p^2+r^2}{\lambda+q^2+p^2-r^2}\right)\right. \end{aligned}$$

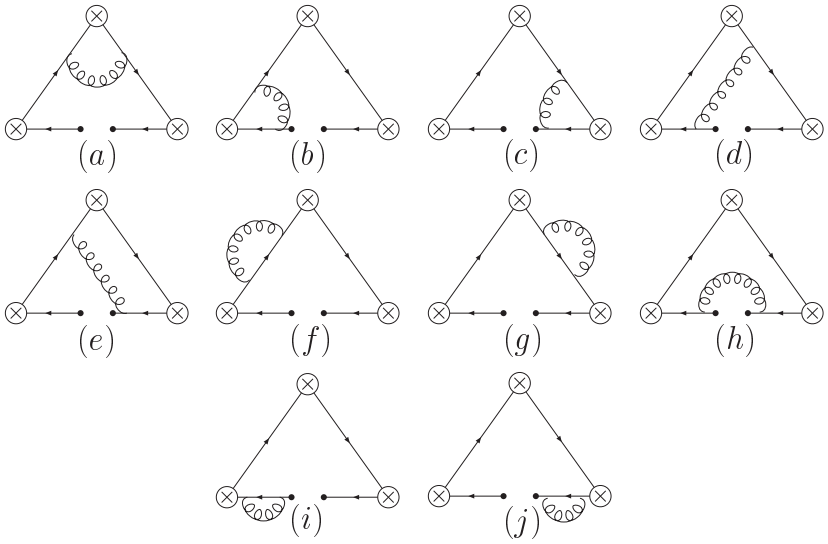

Figure 4.6: Gluonic corrections to Fig. (4.4)

$$+\mathrm{Li}_2\left(-\frac{\lambda+q^2+r^2-p^2}{\lambda-q^2-r^2+p^2}\right)-\mathrm{Li}_2\left(-\frac{\lambda-q^2-r^2+p^2}{\lambda+q^2+r^2-p^2}\right)$$
$$+\mathrm{Li}_2\left(-\frac{\lambda+r^2+p^2-q^2}{\lambda-r^2-p^2+q^2}\right)-\mathrm{Li}_2\left(-\frac{\lambda-r^2-p^2+q^2}{\lambda+r^2+p^2-q^2}\right)\Bigg\}, \quad (4.88)$$

where λ is the well known Källén function $\lambda\,(p^2,q^2,r^2)=\left(p^2+q^2-r^2\right)^2-4\,p^2q^2$. The μ dependence of $C_{\langle\bar{q}q\rangle}$ corresponds then to

$$-\,\mu\,\frac{\partial}{\partial\mu}\,C_{\langle\bar{q}q\rangle}\;=\;\frac{\alpha_s}{\pi}\frac{C_F}{4}\,(L_p+L_q+L_r)\,. \quad (4.89)$$

For the $\langle VVP\rangle$, $\langle AAP\rangle$, $\langle VAS\rangle$, $\langle VVS\rangle$, $\langle AAS\rangle$ and $\langle VAP\rangle$ GFs the total anomalous dimension is $\gamma=\gamma_S$ and the Callan–Symanzik equation for their Wilson coefficient is trivial

$$\frac{\partial}{\partial\mu}\,C^{VVP[S]\,(AAP[S])\,\{VAS[P]\}}_{\langle\bar{q}q\rangle}\;=\;0\,, \quad (4.90)$$

having no μ–dependence. For the rest of the GFs, $\langle SSS\rangle$ and $\langle SPP\rangle$, $\gamma=3\,\gamma_S$ and the RGE is also rather simple:

$$\left[-\mu\,\frac{\partial}{\partial\mu}\;+\;2\,\gamma_m\right]C^{SSS\,(SPP)}_{\langle\bar{q}q\rangle}\;=\;0\,. \quad (4.91)$$

It is better to study the odd–intrinsic–parity sector ($\langle VVP\rangle$, $\langle AAP\rangle$ and $\langle VAS\rangle$) at once. The Feynman diagram for any of the three GFs has the same value up to a $\pm\,i$ factor. The same applies to the rest of sectors. Here a technical comment is in order. Since we work in dimensional regularization, there is a question how to treat

γ_5. In all our computations we have employed a fully anticommuting γ_5. Either two γ_5's appear in a trace and can be cancelled before taking the trace, or, in the odd–parity sector, we can first perform the γ contractions before taking the trace, and are then left with traces of only four γ–matrices and a γ_5 which are unambiguous.

As we saw in Eq. (4.17) each rank–two even–intrinsic–parity GF ($\langle VVS\rangle$, $\langle AAS\rangle$ and $\langle VAP\rangle$) decomposes into two scalar functions, $\mathcal{F}$ and $\mathcal{G}$. At lowest order the determination of these two scalar functions is straightforward, but once we go beyond this level their direct computation turns out to be rather complicated. Instead we will concentrate on the determination of linear combinations of these factors, obtained by taking the appropriate traces in Eq. (4.17) [those traces that do not reduce to a Ward identity] :

$$\begin{aligned}
g_{\mu\nu}\,\Pi^{\mu\nu}_{VVS} &= \frac{3}{2}\left(p^2+q^2-r^2\right)\mathcal{F}_{VVS} - \left(\frac{\lambda}{4}+3\,p^2q^2\right)\mathcal{G}_{VVS}\,,\\
q_\mu\,p_\nu\,\Pi^{\mu\nu}_{VVS} &= \frac{1}{4}\,\lambda\left[-\mathcal{F}_{VVS}+\frac{1}{2}\left(p^2+q^2-r^2\right)\mathcal{G}_{VVS}\right]\,,\\
g_{\mu\nu}\,\Pi^{\mu\nu}_{AAS} &= \frac{3}{2}\left(p^2+q^2-r^2\right)\mathcal{F}_{AAS} - \left(\frac{\lambda}{4}+3\,p^2\,q^2\right)\mathcal{G}_{AAS} + \langle\bar{q}q\rangle\,\frac{(r^2-p^2-q^2)}{p^2\,q^2}\,,\\
q_\mu\,p_\nu\,\Pi^{\mu\nu}_{AAS} &= \frac{1}{4}\,\lambda\left[-\mathcal{F}_{AAS}+\frac{1}{2}\left(p^2+q^2-r^2\right)\mathcal{G}_{AAS}\right] + \langle\bar{q}q\rangle\,\frac{(r^2-p^2-q^2)^2}{2\,p^2\,q^2}\,,\\
g_{\mu\nu}\,\Pi^{\mu\nu}_{VAP} &= \frac{3}{2}\left(p^2+q^2-r^2\right)\mathcal{F}_{VAP} - \left(\frac{\lambda}{4}+3\,p^2\,q^2\right)\mathcal{G}_{VAP} + \langle\bar{q}q\rangle\,\frac{5\,q^2+p^2-r^2}{q^2\,r^2}\,,\\
q_\mu\,p_\nu\,\Pi^{\mu\nu}_{VAP} &= \frac{1}{4}\,\lambda\left[-\mathcal{F}_{VAP}+\frac{1}{2}\left(p^2+q^2-r^2\right)\mathcal{G}_{VAP}\right] - \langle\bar{q}q\rangle\,\frac{(r^2-p^2)^2-q^4}{2\,q^2\,r^2}\,.
\end{aligned} \tag{4.92}$$

These traces have the same symmetry properties under exchange of momenta as $\mathcal{F}$ and $\mathcal{G}$, due to Bose symmetry. Once they are known we can reconstruct the total GFs inverting Eq. (4.92).

The analytic expressions for L_p, L_q, L_r, L_c, and L_d can be found in Appendix D.

4.10 Soft–gluon corrections : the $\langle\bar{q}\,\sigma_{\mu\nu}\,G^{\mu\nu}q\rangle$ operator

In this section we calculate the next non–perturbative correction to the $\langle VT\rangle$ GF. We will compute the corresponding Wilson coefficient only at leading order in α_s. The operator $\langle\bar{q}\,\sigma_{\mu\nu}\,G^{\mu\nu}q\rangle$ has dimension five and represents interactions due to a soft quark pair and a soft gluon from the vacuum. One can of course calculate this coefficient directly using Wick's theorem, but in this way many diagrams are infrared divergent constituting a redefinition of the $\langle\bar{q}q\rangle$ condensate itself, as shown in Fig. 4.7 (a). There is, however, a smart procedure for computing soft–gluonic corrections without confronting such difficulties, the so called *background field method*.

This idea was originally proposed by Fock [63] and Schwinger [64] and rediscovered by a number of people [65, 66]. In this method one introduces an external gauge field $G^a_\mu(x)$ into the QCD Lagrangian with the following gauge condition (Schwinger or fixed point gauge):

$$(x - x_0)^\mu G^a_\mu(x) \,=\, 0\,, \tag{4.93}$$

where x_0 is an arbitrary but fixed point in space–time that can be eventually set to the origin. The gauge field can be then directly expressed in terms of gauge covariant derivatives

$$G_\mu = \int_0^1 \alpha\,\mathrm{d}\alpha\, G_{\nu\mu}(\alpha\, x)\, x^\nu = \frac{1}{2}\, x^\nu G_{\nu\mu}(0) + \cdots\,. \tag{4.94}$$

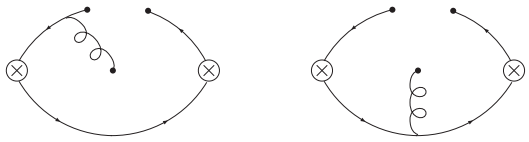

Figure 4.7: Diagrams of the mixed quark-gluon condensate: (a) Infrared divergent diagram renormalizing the $\langle\bar{q}q\rangle$ condensate, (b) contribution to the quark–gluon condensate coming from the background gluons.

Gluonic corrections can now be calculated by considering that our virtual quarks and gluons propagate into this background field, being propagators modified (in fact we will only need the modification of the quark propagator). This modified propagator in momentum space and for massless quarks reads

$$S_F(p) = \frac{i}{\not p} \,-\, \frac{i}{4}\, g_s\, G_{\mu\nu}(0) \frac{1}{p^4} \{\sigma^{\mu\nu}, \not p\} \,+\, \frac{i}{3}\, g_s\, D_\alpha G_{\mu\nu}(0)\, \frac{\not p\, \gamma^\mu\, \not p}{p^6}\, (\gamma^\nu\, \not p\, \gamma^\alpha \,+\, \gamma^\alpha\, \not p\, \gamma^\nu) \,+\, \cdots\,, \tag{4.95}$$

and its diagrammatic representation is shown in Fig. 4.8. It is also simple to express the quark propagator in coordinate space, what makes computations easier

$$\begin{aligned} S_F(x) \;&=\; s_0(x)\, \not x \,-\, i\, g_s\, G_{\mu\nu}(x)\, s_1(x) \{\not x\,, \sigma^{\mu\nu}\} \,+\, \cdots\,, \\ s_0(x) \;&=\; \frac{i}{2\,\pi^2}\, \frac{1}{x^4}\,, \qquad s_1(x) \,=\, \frac{1}{32\,\pi^2}\, \frac{1}{x^2}\,. \end{aligned} \tag{4.96}$$

The only missing ingredient for the computation of gluonic corrections is the following integral

$$\int \frac{\mathrm{d}^4 x}{x^{2n}}\, e^{iq\cdot x} = \begin{cases} i\, \dfrac{(-1)^n\, 2^{\,4-2n}\, \pi^2}{\Gamma(n-1)\Gamma(n)}\, q^{2(n-2)} \log(-\,q^2)\,, & n \geq 2 \\ -\, i\, \dfrac{4\,\pi^2}{q^2} \qquad\qquad\qquad\qquad\quad , & n = 1 \end{cases}\,. \tag{4.97}$$

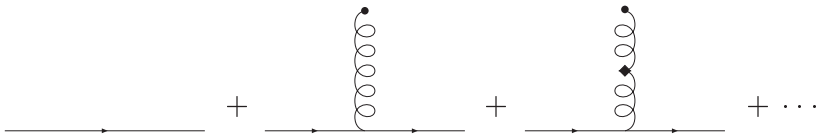

Figure 4.8: Quark propagator in a background of gluon fields.

But the Wilson coefficient of the $\langle \bar{q}\,\sigma_{\mu\nu}\,G^{\mu\nu}q\rangle$ operator does not only come from soft background gluons, but also from the expansion of the quark condensate in diagrams like Fig. 4.3 (b). So, after applying Wick's theorem, one has to consider

$$\left\langle \bar{q}^a_{i\alpha}(x) q^b_{j\beta}(0)\right\rangle \;=\; \frac{1}{4\,N_C}\,\delta^{ab}\,\delta_{ij}\,\delta_{\alpha\beta}\left(\langle\bar{q}q\rangle \;+\; \frac{1}{16}\,x^2\,g_s\,\langle\bar{q}\,\sigma_{\mu\nu}\,G^{\mu\nu}q\rangle\right) \;+\;\cdots\,. \tag{4.98}$$

For the computation of the contribution from gluons coming from the background one has to take into account that

$$\langle\,\bar{q}_i(0)\,G^{\mu\nu}(0)\,q_j(0)\rangle \;=\; \frac{1}{48}\,\langle\,\bar{q}\,\sigma_{\mu\nu}\,G^{\mu\nu}q\rangle\,(\sigma^{\mu\nu})_{ji}\;. \tag{4.99}$$

Let us now concentrate on the computation of the Wilson coefficient for a generic two–point GF. The first contribution coming from the expansion of the quark condensate gives

$$C^{(1)}_{\langle\bar{q}\,\sigma_{\mu\nu}\,G^{\mu\nu}q\rangle} \;=\; g_s\,\frac{\delta^{ab}}{32}\,\frac{\mathrm{Tr}\left([\,\Gamma_1,\Gamma_2]\,\not{p}\,\right)}{p^4}\,, \tag{4.100}$$

whereas the second one, coming from a diagram like the one in Fig. 4.7 gives

$$C^{(2)}_{\langle\bar{q}\,\sigma_{\mu\nu}\,G^{\mu\nu}q\rangle} \;=\; g_s\,\frac{\delta^{ab}}{384\,p^4}\mathrm{Tr}\left[\{\not{p}\,,\sigma^{\mu\nu}\}\,(\Gamma_2\,\sigma_{\mu\nu}\,\Gamma_1 - \Gamma_1\,\sigma_{\mu\nu}\,\Gamma_2)\right]\,. \tag{4.101}$$

It is reassuring to check that for the $\langle AP\rangle$ GF, both contributions exactly cancel, as the Ward identity demands. For $\langle VT\rangle$ we obtain [adding also Eq. (4.85)]:

$$\Pi^{\mathrm{OPE}}_{VT}(p^2) \;=\; \frac{\langle\bar{q}q\rangle}{p^2}\left\{1 \;+\; \frac{\alpha_s}{\pi}\,C_F\left[\log\left(-\,\frac{p^2}{\mu^2}\right) \;-\; 1\right]\right\} \;+\; \frac{g_s}{3}\,\frac{\langle\bar{q}\,\sigma_{\mu\nu}\,G^{\mu\nu}q\rangle}{p^4}\,. \tag{4.102}$$

4.11 Soft gluon corrections: the $\langle G^a_{\mu\nu}G^{\mu\nu}_a\rangle$ operator

We will now consider the first non–perturbative correction to the two–point GFs that are not order parameters. These are purely gluonic corrections due to the interactions of the hard quarks with the vacuum gluons. For its computation it is better to use once more the background field method in position space. The corresponding Feynman diagrams are shown in Fig. 4.9 and the expression for arbitrary currents of its Wilson coefficient is

$$C_{\langle G^a_{\mu\nu}G^{\mu\nu}_a\rangle} \;=\; \frac{\delta^{ab}\alpha_s}{3072\,\pi\,p^2}\left(g_{\mu\nu} - \frac{p_\mu p_\nu}{p^2}\right)\mathrm{Tr}\left[\{\gamma^\mu,\sigma^{\alpha\beta}\}\Gamma_2\{\gamma^\nu,\sigma_{\alpha\beta}\}\Gamma_1\right]\,. \tag{4.103}$$

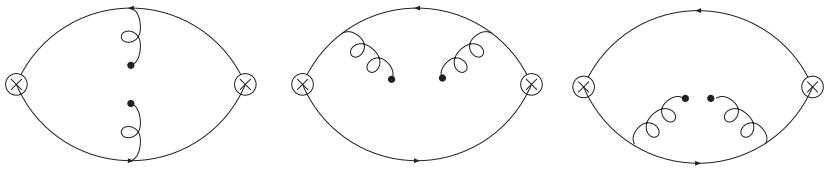

Figure 4.9: Gluon condensate Feynman diagrams.

In particular, for the different GFs we obtain :

$$C^{VV\,(AA)}_{\langle G^a_{\mu\nu}G^{\mu\nu}_a\rangle} = \frac{\alpha_s}{24\,\pi\,p^4}\,, \quad C^{SS\,(PP)}_{\langle G^a_{\mu\nu}G^{\mu\nu}_a\rangle} = \frac{\alpha_s}{4\,\pi\,p^2}\,, \quad C^{TT^{\pm}}_{\langle G^a_{\mu\nu}G^{\mu\nu}_a\rangle} = \frac{\alpha_s}{48\,\pi\,p^4}\,. \tag{4.104}$$

4.12 The four–quark operator $\langle \bar{q}\,\Gamma\,\lambda^a q\,\bar{q}\,\Gamma\,\lambda^a q\rangle$

This operator is specially important because it is the first non–perturbative contribution that distinguishes $\langle VV\rangle$ from $\langle AA\rangle$, $\langle SS\rangle$ from $\langle PP\rangle$ and $\langle TT\rangle^+$ from $\langle TT\rangle^-$. However, there are additional contributions of the same order in $1/p^2$ that vanish when taking the differences of the GFs mentioned before. We are not going to calculate them in detail here.

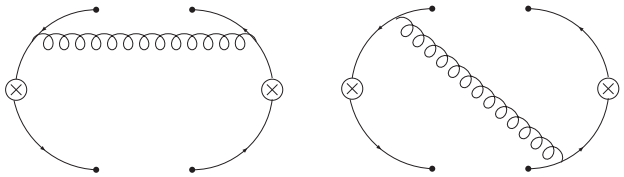

Figure 4.10: Four–quark condensate contribution.

Even though we are calculating corrections involving one gluon (see Fig. 4.10), the background field method is no longer useful for two reasons : first, the gluon is a virtual, hard gluon and it is not taken into account in the modified quark propagator (it comes from the QCD action); second, we are integrating over three space–time points x (were the first current is defined) y and z (the two hard–gluon insertions). The most efficient way to calculate the Wilson coefficient is the plane wave method in combination with the Fierz identity (4.66).

In fact there is not only one operator but rather five, one per each independent Dirac matrix (no summation over flavour index implied) :

$$\mu_S = \left\langle \bar{q}\,\frac{\lambda^a}{2}q\,\bar{q}\,\frac{\lambda^a}{2}q\right\rangle\,, \qquad \mu_P = \left\langle \bar{q}\,\frac{\lambda^a}{2}\,i\,\gamma_5\,q\,\bar{q}\,\frac{\lambda^a}{2}\,i\,\gamma_5\,q\right\rangle\,,$$

$$\mu_V = \left\langle \bar{q}\,\frac{\lambda^a}{2}\,\gamma_\mu\,q\,\bar{q}\,\frac{\lambda^a}{2}\,\gamma^\mu q\right\rangle\,, \qquad \mu_A = \left\langle \bar{q}\,\frac{\lambda^a}{2}\,\gamma_\mu\,\gamma_5\,q\,\bar{q}\,\frac{\lambda^a}{2}\,\gamma^\mu\,\gamma_5\,q\right\rangle$$

$$\mu_T \;=\; \left\langle\, \bar q\, \frac{\lambda^a}{2}\, \sigma_{\mu\nu}\, q\, \bar q\, \frac{\lambda^a}{2}\, \sigma^{\mu\nu}\, q \,\right\rangle\,, \tag{4.105}$$

where λ^a are color matrices of the $SU(N_C)$ group. All those contributions stem from diagrams like those depicted in Fig. (4.10). The general formula for the Wilson coefficient is easily obtained and reads

$$C_{\mu_\Gamma} \;=\; \delta^{ab}\, \frac{g_s^2}{p^6}\, c_\Gamma\, g_s^2\, \mathrm{Tr}(\not p\,[\,\Gamma_1\Gamma, \gamma_\mu])\, \mathrm{Tr}\,(\not p\,[\gamma_\mu\,\Gamma\,\Gamma_2 - \Gamma_2\,\Gamma\,\gamma_\mu])\,. \tag{4.106}$$

For the different functions it renders

$$C^{VV(AA)}_{A(V)} \;=\; \frac{2\,g_s^2}{p^6}\,, \qquad C^{SS(PP)}_{T} \;=\; \pm\,\frac{4\,g_s^2}{p^4}\,, \qquad C^{TT^\pm}_{S(P)} \;=\; \pm\,\frac{4\,g_s^2}{p^6}\,. \tag{4.107}$$

Since very little is known about the numeric value of the four–quark condensates, an approximation only valid in the strict large–N_C limit is normally assumed. It is known as the vacuum saturation hypothesis and it basically assumes that the intermediate state giving the main contribution when inserting a Parseval identity is precisely the vacuum

$$\begin{aligned}
\langle\, \bar q\, \Gamma_1\, \frac{\lambda^a}{2}\, T^A\, q\, \bar q\, \Gamma_2\, \frac{\lambda^b}{2}\, T^B\, q\,\rangle \;&=\; \sum_n \langle\, 0\,|\,\bar q\,\Gamma_1\,\frac{\lambda^a}{2}\,T^A\,q\,|\,n\,\rangle\,\langle\, n\,|\,\bar q\,\Gamma_2\,\frac{\lambda^a}{2}\,T^B\,q\,|\,0\,\rangle \\
&\approx\; \langle\, 0\,|\,\bar q\,\Gamma_1\,\frac{\lambda^a}{2}\,T^A\,q\,|\,0\,\rangle\,\langle\, 0\,|\,\bar q\,\Gamma_2\,\frac{\lambda^a}{2}\,T^B\,q\,|\,0\,\rangle \\
&=\; -\,\frac{\langle\bar q q\rangle^2}{64\,N_C^2}\,\delta^{ab}\,\delta^{AB}\,\mathrm{Tr}[\,\Gamma_1\Gamma_2\,]\,,
\end{aligned} \tag{4.108}$$

and certainly it makes sense since large–N_C QCD favours contributions with as less number of intermediate particles as possible. Eq. (4.108) leads to tremendous simplifications in the calculation and, in particular, it reduces the five independent operators in Eq. (4.105) to only one, namely $\langle\bar q q\rangle^2$. The general expression for the Wilson coefficient of that operator is

$$C_{\langle\bar q q\rangle^2} \;=\; \frac{g_s^2\,C_F}{16\,N_C\,p^6}\,\left\{\mathrm{Tr}\,[\gamma_\mu \not p\,\Gamma_2\gamma^\mu \not p\,\Gamma_1] + \mathrm{Tr}\,[\not p\,\gamma_\mu\Gamma_2 \not p\,\gamma^\mu\Gamma_1] - 8\,\mathrm{Tr}\,[\,\Gamma_1\Gamma_2]\right\}\,, \tag{4.109}$$

and its value for the GFs under study is

$$C^{VV\,(AA)}_{\langle\bar q q\rangle^2} \approx \pm\,\frac{g_s^2}{2\,p^6}\,, \qquad C^{SS\,(PP)}_{\langle\bar q q\rangle^2} \approx \mp\,\frac{3\,g_s^2}{p^4}\,, \qquad C^{TT^\pm}_{\langle\bar q q\rangle^2} \approx \mp\,\frac{g_s^2}{4\,p^6}\,, \tag{4.110}$$

where we perform the approximation $C_F \approx N_C/2$ because the vacuum saturation hypothesis is only valid in the strict large–N_C limit. However, several tests seem to indicate that the vacuum saturation hypothesis is quite inaccurate, and in certain condensates the deviation is about 100%. We will assume that this error does not change the sign.

4.13 Calculation in χPT

In this section we calculate some GFs in the opposite regime : the low energy region. The basic ideas of χPT and the operators needed for these calculations have been covered in Chapter 1. Again we will assume the chiral limit.

4.13.1 Three–point Green function : $\langle$VVP$\rangle$

For this function and bearing in mind the application it will be used for (see Chapter 5), we will concentrate only on the leading $1/N_C$ term of the $\mathcal{O}(p^4)$ result. So there will be no logarithms. The leading term is produced by the WZW anomalous term in Eq. (1.78), giving rise to a piece proportional to N_C, and the next corrections are produced by the odd–intrinsic–parity $\mathcal{L}_{(6)}$ Lagrangian (1.79). The result reads

$$\Pi^{\chi\mathrm{PT}}_{VVP} \,=\, B_0 \left(64\, \widetilde{C}^W_7 \,-\, 16\, \widetilde{C}^W_{22}\, \frac{p^2+q^2}{r^2} \,-\, \frac{N_C}{4\,\pi^2\, r^2} \right) + \,\mathcal{O}\big(p^2, N_C^0\big)\ , \qquad (4.111)$$

and the Feynman diagrams leading to it are shown in Fig. 4.11.

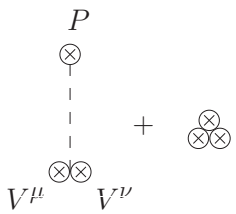

Figure 4.11: $\langle VVP\rangle$ GF in χPT.

4.13.2 Two–point Green functions

For this simple case we will perform the calculations to the next–to–leading order in both the chiral and $1/N_C$ expansions. So we will in principle find chiral logarithms. The three possible contributions are drawn in Fig. 4.12. To $\langle AA\rangle$ and $\langle PP\rangle$ only Fig. 4.12 (a) and (c) contribute, for $\langle VV\rangle$ and $\langle SS\rangle$ only 4.12 (b) and (c), for $\langle VT\rangle$ only 4.12 (b) and (c) and for $\langle TT\rangle$ only 4.12 (c) :

$$\begin{aligned}
\Pi^{\chi PT}_{VV}(p^2) \;&=\; -\,2\,L^r_{10} - 4\,H^r_1 + \frac{1}{32\,\pi^2}\left[\frac{5}{3} - \log\left(-\frac{p^2}{\mu^2}\right)\right]\ ,\\
\Pi^{\chi PT}_{AA}(p^2) \;&=\; -\,\frac{F^2}{p^2} - 4\,H^r_1 + 2\,L^r_{10}\,,\\
\Pi^{\chi PT}_{SS}(p^2) \;&=\; B_0^2\left\{32\left(L^r_8 + \frac{H^r_2}{2}\right) + \frac{5}{24\,\pi^2}\left[1 - \log\left(-\frac{p^2}{\mu^2}\right)\right]\right\}\ ,\\
\Pi^{\chi PT}_{PP}(p^2) \;&=\; -\,4\,B_0^2\left[\frac{F^2}{p^2} + 8\left(L^r_8 - \frac{H^r_2}{2}\right)\right]\ ,
\end{aligned}$$

$$\Pi_{VT}(p^2) = -\Lambda_1(\mu) + \frac{p^2\,\Lambda_2(\mu)}{F^2}\left\{-\frac{\widetilde{\Omega}_{94}(\mu)}{2} + \frac{1}{64\,\pi^2}\left[C' + \frac{5}{3} - \log\left(-\frac{p^2}{\mu^2}\right)\right]\right\},$$

$$\Pi_{TT}^{\pm(\chi\mathrm{PT})}(p^2) = \pm\frac{\Lambda_3}{p^2} \pm \Omega_{51} \mp \frac{\Omega_{53}}{2} - \frac{H_{118}}{8}. \qquad (4.112)$$

It is interesting to stress the fact that in the chiral limit and at next–to–leading order the $\langle TT\rangle$ GF does not get any logarithmic correction. This is so because the tensor source is $\mathcal{O}(p^2)$ and appears for the first time $\mathcal{L}_{(4)}$. So the one–loop corrections is formed with two vertices from $\mathcal{L}_{(4)}$, which is already $\mathcal{O}(p^8)$.

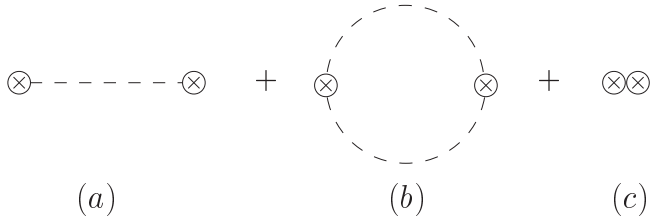

Figure 4.12: Two–point GFs in χPT.

4.14 Calculation in RχT

In this section we will calculate some GFs in the large–N_C limit. The many simplifications occurring in this limit where already exposed in Chapter 2. Whereas in Section 4.4 we used quark and gluon degrees of freedom, the calculations will now be performed with hadronic degrees of freedom. All these features are implemented in the RχT Lagrangian of Sections 2.6.2 and 2.8. The expressions obtained will have validity (in principle) in all energy domains. We will restrict ourselves to the MHA approximation, that is, considering only the minimal number of resonances needed to satisfy several constraints. Use of quark–hadron duality is done when comparing the results of this section with those of Section 4.4.

4.14.1 Three–point Green function : $\langle$VVP$\rangle$

Our purpose is now to build a representation of the $\langle VVP\rangle$ GF which is valid at all energies. In particular we have already calculated its expression in the asymptotic energy region, including hard–gluonic corrections to the leading order condensate $\langle\bar{q}q\rangle$. For our ansatz it suffices to consider only the $\mathcal{O}(\alpha_s^0)$ quark condensate contribution. Our parametrization has to reproduce this behaviour for large values of the momenta. In addition, we also have to enforce the conditions of Eq. (4.72) when only one momentum is large. In the very low energy region, the GF has to satisfy the constraints of chiral symmetry encoded in χPT that can be read from Eq. (4.111). In addition to these constraints on the $\langle VVP\rangle$ GF there is also a requirement that

we will enforce in any hadronic form factor of vector or axial–vector QCD currents. It is known [67] that the leading perturbative contribution, within QCD, to the spectral functions of both vector and axial–vector correlators is constant. Then it comes out, as a heuristic deduction, that any of the infinite hadron contributions to the spectral functions should vanish at high transfer of momentum. This implies, in order, that hadron form factors of those currents should behave smoothly at high energy [68, 69]. Incidentally this feature coincides with the known Brodsky–Lepage condition on form factors (derived from a partonic framework) [70]. Specifically the condition, in our case, reads:

$$\lim_{r^2\to 0,\, q^2\to\infty} r^2\, \Pi_{VVP}(0, q^2, r^2) \;=\; 0\;. \tag{4.113}$$

Our task is to construct a function for $\langle VVP\rangle$ that satisfies, at least, the conditions defined above. In general the large–N_C predictions allows us to parametrize Π_{VVP} with meromorphic functions (*i.e.* functions with real poles as singularities) with poles in the corresponding resonances propagating between the QCD currents. In general we have then

$$\Pi_{VVP} \;=\; \frac{\sum_{n=0}^{3+m-1} P_n(p^2, q^2, r^2)}{\prod_{i,j=1}^{3,m}(p_i^2 - m_j^2)}\,, \tag{4.114}$$

where m_j are the masses of the resonances that couple to the current $J_i = V, P$, and $p_i^2 = p^2, q^2, r^2$ is the momentum flowing from this current. P_n is the most general nth order monomial in p^2, q^2 and r^2:

$$P_n \;=\; \sum_{k=0}^{n}\sum_{l=0}^{k} c_{n-k,k-l,l}(r^2)^{n-k}(q^2)^{k-l}(p^2)^l\,. \tag{4.115}$$

Bose symmetry requires that $c_{kml} = c_{klm}$.

In Ref. [42] a Lagrangian theory, including one multiplet of vector resonances only, was designed in order to obtain an expression for Π_{VVP} that satisfied all conditions but for the one in Eq. (4.113). Indeed the fact that only one multiplet of vector resonances was not enough in order to satisfy all short–distance constraints for this GF was already noticed [51] with the use of a parametric *ansatz*. It is already well known [51, 71] that the MHA is more involved if we want that our representation of the GF satisfies both OPE and the Brodsky–Lepage requirements. To see that let us use (4.114) for this ansatz:

$$\Pi_{VVP}^{\rm res}\,(p^2, q^2, r^2) \;=\; \frac{c_{000} + c_{100}\, r^2 + c_{010}\,(p^2 + q^2)}{(M_V^2 - q^2)\,(M_V^2 - p^2)\, r^2}\,. \tag{4.116}$$

Matching to OPE requires $c_{100} = c_{010} = -\,B_0\, F^2$ whereas the Brodsky–Lepage would imply $c_{010} = 0$, thence these two requirements cannot be satisfied at the same time.

The obvious extension is to extend our spectrum by including also a multiplet of pseudoscalar resonances in the construction of the Π_{VVP} function. Although it can be shown that indeed this parametrization satisfies conditions in Eqs. (4.111,4.81,4.113), it fails to meet the OPE condition in Eq. (4.73)[8]. Eq. (4.114)

[8] Constraints in Eq. (4.72) are, in this case, undetermined.

reads for this ansatz:

$$\Pi^{\rm res}_{VVP}\,(p^2,q^2,r^2) \;=\; \frac{1}{(M_V^2-q^2)\,(M_V^2-p^2)\,r^2\,(M_P^2-r^2)}\big[c_{000}+c_{100}\,r^2+c_{010}\,(p^2+q^2) + c_{200}\,r^4+c_{020}\,(p^4+q^4)+c_{110}\,r^2(p^2+q^2)+c_{011}\,p^2\,q^2\big]\;. \quad (4.117)$$

After matching this result with the OPE we get

$$c_{020} \;=\; c_{011} \;=\; 0\,, \quad c_{200} \;=\; c_{110} \;=\; B_0\,F^2\,, \qquad (4.118)$$

whereas the Brodsky–Lepage condition implies $c_{010}=0$, and so they do not clash. However when we try to satisfy Eq. (4.73) we find that instead of a pion pole we have a pseudoscalar resonance pole

$$\lim_{\lambda\to\infty}\,\Pi^{res}_{VVP}((\lambda p)^2,(q-\lambda p)^2,q^2) \;\simeq\; 2\,\frac{B_0F^2}{\lambda^2}\,\frac{1}{p^2}\,\frac{1}{M_P^2-q^2}\;+\;\cdots\,. \qquad (4.119)$$

It is not difficult to relate this problem to the fact that the $\langle AP\rangle$ correlator in the chiral limit is saturated by one pion exchange [60].

It can be seen that all conditions are met if we consider in the spectrum of the $\langle VVP\rangle$ GF two non–degenerated multiplets of vector resonances, together with the Goldstone pseudoscalar mesons. Then the *ansatz* would read [40]:

$$\Pi^{res}_{VVP} \;=\frac{1}{(M_{V_1}^2-q^2)\,(M_{V_1}^2-p^2)\,(M_{V_2}^2-q^2)\,(M_{V_2}^2-p^2)\,r^2}\;\big[\,c_{000}\;+\;c_{100}\,r^2\;+\;c_{200}\,r^4 + c_{010}\,(p^2+q^2)\;+\;c_{020}\,(q^4+p^4)\;+\;c_{011}\,p^2\,q^2+c_{110}\,r^2(p^2+q^2) + c_{300}\,r^6\;+\;c_{030}\,(p^6+q^6)\;+\;c_{021}\,p^2\,q^2(p^2+q^2)\;+\;c_{111}\,r^2\,p^2\,q^2 + c_{120}\,r^2(p^4+q^4)\;+\;c_{210}\,r^4(p^2+q^2)\,\big]\;. \qquad (4.120)$$

The chiral symmetry behaviour (4.111) gives

$$c_{000} \;=\; B_0\,M_{V_1}^4\,M_{V_2}^4\,\frac{N_C}{4\,\pi^2}\,, \qquad (4.121)$$

and the OPE matching demands

$$c_{300}=c_{030} \;=\; c_{120} \;=\; c_{210} \;=\; 0\;, \quad c_{021}=c_{111} \;=\; -\,B_0\,F^2\;. \qquad (4.122)$$

Finally the Brodsky–Lepage behaviour on the vector form factor, defined by condition (4.113), fixes one additional parameter, namely:

$$c_{020} \;=\; 0\,. \qquad (4.123)$$

Our ansatz, with all these constraints, satisfies also the OPE conditions in Eqs. (4.73).

The study of the $\langle VVP\rangle$ GF along the lines outlined in this section can also be carried out within a resonance Lagrange theory instead of a parametric representation as given by Eq. (4.120). We collect this procedure in Appendix E.

4.14.2 Two–point Green functions

For the case of the two point GFs, the parameters appearing in the large–N_C limit are only masses and decay constants. The definition of the latter follow:

$$\begin{aligned}
\langle\, 0 \,|\, V^a_\mu(0) \,|\, \rho^b_n(p,\lambda)\rangle &\doteq \delta^{ab}\, F_{Vn}\, m_{Vn}\, \epsilon^{(\lambda)}_\mu\,, \\
\langle\, 0 \,|\, T^a_{\nu\rho}(0) \,|\, \rho^b_n(p,\lambda)\rangle &\doteq i\,\delta^{ab}\, F^T_{Vn}(\mu)\,(\epsilon^{(\lambda)}_\nu p_\rho - \epsilon^{(\lambda)}_\rho p_\nu)\,, \\
\langle\, 0 \,|\, T^a_{\nu\rho}(0) \,|\, b^b_n(p,\lambda)\rangle &\doteq i\,\delta^{ab}\, F^T_{B\,n}(\mu)\,\varepsilon_{\nu\rho\mu\sigma}\,\epsilon^\mu_{(\lambda)}\,p^\sigma\,, \\
\langle\, 0 \,|\, A^a_\mu(0) \,|\, a^b_n(p,\lambda)\rangle &\doteq \delta^{ab}\, F_{A\,n}\, m_{A\,n}\, \epsilon^{(\lambda)}_\mu\,, \\
\langle\, 0 \,|\, S^a(0) \,|\, s^b_n(p)\rangle &\doteq 4\,\sqrt{2}\,\delta^{ab}\, B_0(\mu)\, c_{mn}\,, \\
\langle\, 0 \,|\, P^a(0) \,|\, p^b_n(p)\rangle &\doteq 4\,\sqrt{2}\,\delta^{ab}\, B_0(\mu)\, d_{mn}\,.
\end{aligned} \tag{4.124}$$

The scale dependence of the $F^T_V(\mu)$ and $F^T_B(\mu)$ in Eq. (4.124) [much as happens with $B_0(\mu)$] reflects the fact that the tensor current has a non–vanishing anomalous dimension. In the literature it is also common to work with the lowercase decay constants f_{Vn}, f^T_{Vn} and f^T_{Bn}, which are related to the uppercase ones in a trivial way: $f_{Vn} = -\sqrt{2}\,F_{Vn}$, $f^T_{Vn} = -\sqrt{2}\,F^T_{Vn}$, $f^T_{Bn} = -\sqrt{2}\,F^T_{Bn}$. Also, for future convenience we introduce the parameter ξ_n, defined as

$$\xi_n \;=\; \frac{f^T_{Vn}}{f_{Vn}} \;=\; \frac{F^T_{Vn}}{F_{Vn}}\,. \tag{4.125}$$

In the strict large–N_c limit two–point functions are saturated by the single–particle exchange of an infinite number of stable mesons. Therefore, the spectral functions above take the simple forms

$$\begin{aligned}
\frac{1}{\pi}\,\mathrm{Im}\,\Pi_{VV}(t) &= \sum_n F^2_{Vn}\,\delta(t-m^2_{Vn}), \qquad \frac{1}{\pi}\,\mathrm{Im}\,\Pi^+_{TT}(t) = \sum_n \left(F^T_{Bn}\right)^2\delta(t-m^2_{Bn}), \\
\frac{1}{\pi}\,\mathrm{Im}\,\Pi^-_{TT}(t) &= \sum_n \left(F^T_{Vn}\right)^2\,\delta(t-m^2_{Vn}), \; \frac{1}{\pi}\,\mathrm{Im}\,\Pi_{VT}(t) = \sum_n F_V F^T_{Vn} m_{Vn}\,\delta(t-m^2_{Vn}), \\
\frac{1}{\pi}\,\mathrm{Im}\,\Pi_{AA}(t) &= \sum_n (F_{An})^2\,\delta(t-m^2_{An}), \quad \frac{1}{\pi}\,\mathrm{Im}\,\Pi_{SS}(t) = 32\,B_0^2 \sum_n c^2_{mn}\,\delta(t-m^2_{Sn}), \\
\frac{1}{\pi}\,\mathrm{Im}\,\Pi_{PP}(t) &= 32\,B_0^2 \sum_n d^2_{mn}\,\delta(t-m^2_{Pn}).
\end{aligned} \tag{4.126}$$

In this section we will consider only the first multiplet for each set of quantum numbers, and apply the matching to the short–distance behaviour (OPE). The expression for the two–point GFs in the antisymmetric formalism read:

$$\begin{aligned}
\Pi^{\mathrm{R}\chi\mathrm{T}}_{VV}(p^2) &= \frac{F_V^2}{m_V^2-p^2} - \frac{F_B^2}{m_B^2} - 2\,\tilde{L}_{10} - 4\,\tilde{H}_1\,, \\
\Pi^{\mathrm{R}\chi\mathrm{T}}_{AA}(p^2) &= -\frac{F^2}{p^2} + \frac{F_A^2}{m_A^2-p^2} - 4\,\tilde{H}_1 + 2\,\tilde{L}_{10}\,,
\end{aligned} \tag{4.127}$$

$$
\begin{aligned}
\Pi_{SS}^{\mathrm{R}\chi\mathrm{T}}(p^2) &= 32\,B_0^2\left[\frac{c_m^2}{m_S^2-p^2}+\left(\tilde{L}_8+\frac{\tilde{H}_2}{2}\right)\right]\,,\\
\Pi_{PP}^{\mathrm{R}\chi\mathrm{T}}(p^2) &= -32\,B_0^2\left[-\frac{d_m^2}{m_P^2-p^2}+\frac{F^2}{8\,p^2}+\left(\tilde{L}_8-\frac{\tilde{H}_2}{2}\right)\right]\,,\\
\Pi_{VT}^{\mathrm{R}\chi\mathrm{T}}(p^2) &= \frac{F_V\,F_V^T\,m_V}{m_V^2-p^2}-\frac{F_B\,F_B^T}{2\,m_B}-\tilde{\Lambda}_1\,,\\
\Pi_{TT}^{-\,\mathrm{R}\chi\mathrm{T}}(p^2) &= \frac{(F_V^T)^2}{m_V^2-p^2}-\frac{1}{p^2}\left[(F_B^T)^2-(F_V^T)^2-\tilde{\Lambda}_3\right]+\frac{1}{2}\left(\tilde{\Omega}_{51}-\frac{\tilde{H}_{118}}{8}\right)\,,\\
\Pi_{TT}^{+\,\mathrm{R}\chi\mathrm{T}}(p^2) &= \frac{(F_B^T)^2}{m_B^2-p^2}+\frac{1}{p^2}\left[(F_B^T)^2-(F_V^T)^2-\tilde{\Lambda}_3\right]-\frac{1}{2}\left(\tilde{\Omega}_{51}+\frac{\tilde{\Omega}_{52}}{2}+\frac{\tilde{H}_{118}}{8}\right)\,,
\end{aligned}
$$

A matching to short distances implies

$$
\begin{aligned}
&\tilde{L}_{10}=-\frac{F_B^2}{4\,m_B^2}\,, && F_V^2\,-\,F_A^2=F^2\,, && m_V^2\,F_V^2\,=F_A^2\,m_A^2\,,\\
&\tilde{L}_8\,=\,0\,, && 8\,(c_m^2\,-\,d_m^2)\,=\,F^2\,, && c_m^2\,m_S^2\,-\,d_m^2\,m_P^2=\frac{3\,\pi\,\alpha_s}{4}\,F^4\,,\\
&\tilde{\Lambda}_1(\mu)\,=\,-\frac{F_B\,F_{BT}(\mu)}{2\,m_B}\,, && 2\,\tilde{\Lambda}_3\,=\,(F_B^T)^2\,-\,(F_V^T)^2\,, && F_V\,F_V^T(\mu)=\frac{F^2\,B_0(\mu)}{m_V}\,,\\
&F_V^T(\mu)\,m_V\,=\,F_B^T(\mu)\,m_B\,, && \tilde{\Omega}_{51}\,+\,\frac{\tilde{\Omega}_{52}}{4}\,=\,0\,. &&
\end{aligned}
\tag{4.128}
$$

In particular this fixes $\Lambda_1=-\frac{F_V\,F_V^T}{m_V}=\frac{F^2B_0}{m_V^2}$. In addition we can match the quartic condensate to obtain

$$
\begin{aligned}
F_V^2\,m_V^2\left(m_A^2-m_V^2\right) &= 4\,\pi\,\alpha_s\,F^4\,B_0^2(\mu) \;>\; 0\,,\\
\left[F_V^T(\mu)\right]^2\,m_V^2\left(m_B^2-m_V^2\right) &= 2\,\pi\,\alpha_s\,F^4\,B_0^2(\mu) \;>\; 0\,.
\end{aligned}
\tag{4.129}
$$

The results above deserve some comments. In this MHA approximation we predict that $m_A > m_V$ and $m_B > m_V$, but we cannot say anything similar for m_S and m_P. Phenomenology supports this picture, and of course there are more sophisticate theoretical methods that also conclude the same. It is remarkable that the aforementioned kinematical singularity in $\langle TT\rangle$ is playing the same röle as that of the pion pole in $\langle PP\rangle$ and $\langle AA\rangle$. Had it been zero, $m_V=m_B$, in clear contradiction with experimental determinations. B mesons only play a röle in GFs involving tensor currents (and also in the tensor form factor of the pions). Matching to short–distance QCD implies that the contributions of B mesons on $\langle VV\rangle$ and $\langle VT\rangle$ must be compensated with local counterterms from the chiral Lagrangian. This was first noticed in Ref. [39], and as we saw in Chapter 2, in the Proca formalism B mesons decouple from the vector current. In the case of $\langle VT\rangle$ and in this MHA approximation, the matching to short distances fully determines the product F_VF_{VT}.

It is worth calculating the $\langle TT\rangle$ GF in the Proca formalism, where for simplicity we ignore the $\mathcal{O}(p^6)$ χPT contributions

$$\begin{aligned}\Pi_{TT}^{-\,\mathrm{R}\chi\mathrm{T}}(p^2) &= \frac{(F_V^T)^2}{m_V^2-p^2}+\frac{\tilde\Lambda_3^P}{q^2}\,, \quad \Pi_{TT}^{+\,\mathrm{R}\chi\mathrm{T}}(p^2) = \frac{(F_B^T)^2}{m_B^2-p^2}-\frac{\tilde\Lambda_3^P}{p^2}\,,\\ \Pi_{TT}^{\Delta(\mathrm{res})}(p^2) &= \frac{(F_B^T)^2}{m_B^2-p^2}-\frac{(F_V^T)^2}{m_V^2-p^2}-\frac{2\,\tilde\Lambda_3^P}{p^2}\,, \end{aligned} \tag{4.130}$$

in this case the longitudinal part of the propagator does not "pollute" the GFs with kinematical singularities. In this formalism the matching to short distances implies $2\,\tilde\Lambda_3^P=(F_V^T)^2-(F_B^T)^2$. Either in antisymmetric or Proca formalism, once we impose short–distance matching we obtain the same result, namely:

$$\Pi_{TT}^{\Delta(\mathrm{res})}(p^2) = \frac{m_V^2(F_V^T)^2}{p^2}\left(\frac{1}{m_B^2-p^2}-\frac{1}{m_V^2-p^2}\right). \tag{4.131}$$

This result fixes the Λ_3 chiral LEC and its sign:

$$\begin{aligned}\Lambda_3 &= \frac{1}{2}\,m_V^2(F_V^T)^2\left(\frac{1}{m_B^2}-\frac{1}{m_V^2}\right)=\frac{F^4\,B_0^2(\mu)}{2\,F_V^2}\left(\frac{1}{m_B^2}-\frac{1}{m_V^2}\right)\\ &= \frac{1}{4}\,F^2\,B_0^2(\mu)\left(\frac{1}{m_B^2}-\frac{1}{m_V^2}\right) < 0\,,\end{aligned} \tag{4.132}$$

where in the second step we have used one relation of Eqs. (4.128) and in the last we used $F_V=\sqrt{2}\,F$, which comes from assuming unsubtracted dispersion relations for both the pion electromagnetic form factor and the axial form factor in radiative pion decay [13] and has been shown to be satisfied in sum rule analysis of vector and axial channels.

As a last comment, in Eq. (4.128) several relations have scale dependence. In some cases the scale dependence on the left– and right–hand sides coincide, making the matching μ–independent. But in some other cases the dependence is not the same, and it seems that the matching condition is different for different values of μ. In fact what is happening is that our calculation in the OPE is truncated in the number of loops (in fact, it has no loops at all), and so we do not generate the explicit μ dependence that makes the anomalous dimensions of left– and right–hand sides coincide, at least formally.

4.15 Can we match the MHA to the OPE at $\mathcal{O}(\alpha_s)$?

In this section we shall see that even if the MHA does not suffice to match order parameter GFs to the the OPE when radiative corrections to the quark–condensate Wilson coefficient are taken into account, [that is we cannot match Eqs. (4.85) and (4.127)] we can make a refinement of the matching at tree–level.

Since the $\langle VT\rangle$ GF in the chiral limit does not need to be subtracted, it is completely determined by its spectral function. Then it can be regarded as an observable

and thus we can directly match its expression in different approximations, such as OPE and RχT. However, we still have the problem that the tensor current requires renormalization, and thus, the $\langle VT\rangle$ GF is scale and scheme dependent. This renormalization dependence would then be reflected in a scale dependent coupling of the tensor current to vector mesons $F_V^T(\mu)$ on the hadronic side. Since we prefer to work with hadronic quantities which are explicitly scale independent, another possibility is to multiply $F_V^T(\mu)$ by an appropriate scale factor $R_T(\mu)$, which results in a scale independent tensor decay constant $\hat{F}_V^T$. This is analogous to the definition of scale–invariant B–factors, which parametrize hadronic matrix elements of four–quark operators, in the case of weak hadronic decays, see `e.g.` [72]. Therefore, we define

$$\begin{aligned}
\hat{f}_V^T &\equiv f_V^T(\mu)\, R_T(\mu) \equiv f_V^T(\mu)\, \exp\left\{-\int^{a_s(\mu)} \frac{\gamma_T(a_s)}{\beta(a_s)}\, \mathrm{d}a_s\right\} \\
&= f_V^T(\mu)\, [a_s(\mu)]^{-\gamma_T^{(1)}/\beta_1}\left[1-\left(\frac{\gamma_T^{(2)}}{\beta_1}-\frac{\beta_2\,\gamma_T^{(1)}}{\beta_1^2}\right)a_s(\mu)+\mathcal{O}(a_s^2)\right] \\
&\overset{N_f=3}{=} f_V^T(\mu)\, [a_s(\mu)]^{-\frac{4}{27}}\left[1-\frac{337}{486}\,a_s(\mu)+\mathcal{O}(a_s^2)\right]. \qquad (4.133)
\end{aligned}$$

The anomalous dimension of the tensor current is known up to order α_s^3 [73,74], and thus one could even extend Eq. (4.133). However, at the order considered here this does not make sense, since we only stay at the next–to–leading order level.

$$\gamma_T^{(2)} = \frac{C_F}{144}(257\,N_C - 117\,C_F - 26\,n_f) = \frac{179}{36} \approx \frac{397}{576}\,N_C^2\,,$$

were the exact number corresponds to three colours and flavours, and the approximation to the large–N_C limit. For our numerics we also need the $\beta^{(2)}$ function [75]:

$$\beta^{(2)} = \frac{17}{12}\,N_C^2 - \frac{1}{4}\,C_F\,n_f - \frac{5}{12}\,N_C\,n_f = 8 \approx \frac{17}{12}\,N_C^2\,.$$

Now multiplying our result (4.85) for the Green function with the scale factor $R_T(\mu)$, it is a trivial exercise to convince oneself that $R_T(\mu)\,\Pi_{VT}^{\mathrm{OPE}}(p^2,\mu)$ is scale independent at the considered order. Nevertheless, it should be kept in mind that it still depends on the renormalization scheme, for example on the scheme in which $\langle\bar{q}q\rangle$ is renormalized.

In principle, since the next–to–leading order result for the $\langle VT\rangle$ GF contains a logarithm in the dynamical variable p^2, let us strongly emphasize that an infinite tower of resonances would be required for a sound matching to the RχT. Still, as a simple–minded approach, we will next consider the aforementioned minimal hadronic ansatz (MHA). This amounts to the assumption that a single resonance is enough to correctly describe the physics in a certain energy regime. In Ref. [40] the matching for the $\langle VT\rangle$ GF was performed at $\mathcal{O}(\alpha_s^0)$, and here we will include

the $\mathcal{O}(\alpha_s)$ corrections. Again multiplying the GF with the scale factor in order to obtain a scale–invariant quantity, the hadronic ansatz reads:

$$R_T(\mu)\,\Pi_{VT}^{\mathrm{R}\chi\mathrm{T}}(p^2) \;=\; \frac{F_V\,\hat{F}_V^T\,m_V}{m_V^2-p^2}\,. \tag{4.134}$$

Eq. (4.134) is in principle assumed to be valid at all energies at leading order in $1/N_C$, since it incorporates chiral symmetry and the correct high–energy behaviour. It can be expanded in inverse powers of p^2, permitting a direct comparison with the OPE in Eq. (4.85). However while Eq. (4.127) is explicitly scale independent, (4.85) contains a logarithm which compensate the running of the tensor source and the quark condensate.

To perform the matching in practice, we choose a particular matching point and scale. First of all, to sum up the logarithm, we will employ the scale $\mu^2 = -\,p^2 \equiv M^2$. Then, M^2 should be large enough so that only keeping the first term in the OPE is a good approximation, while it should not be too large so that only putting one resonance on the hadronic side is reasonable. From these considerations, we would conclude, that M should be in the range 1–2 GeV. For the matching relation, we then find

$$F_V\,\hat{F}_V^T\,m_V \;=\; -\,[a_s(M^2)]^{-\frac{4}{27}\left\{\frac{3}{22}\right\}}\,\langle\bar{q}q\rangle(M^2)\left[1-\frac{985}{486}\left\{\frac{8357}{11616}\,N_C\right\}\,a_s(M^2)\right]\,, \tag{4.135}$$

where in the curly brackets, we have also included the numbers corresponding to the large–N_C limit. Eq. (4.135) can be viewed as a refinement over the analogous estimate of Ref. [40].

Let us finally come to a numerical analysis of Eq. (4.135). Employing the central values $F_V = 156\,\mathrm{MeV}$ and $M_V = 775\,\mathrm{MeV}$, as well as the value for the quark condensate $\langle\bar{q}q\rangle(2\,\mathrm{GeV}) = -\,(267\,\mathrm{MeV})^3$ [76], we obtain

$$\hat{F}_V^T \;=\; 138 \pm 40\ \mathrm{MeV}\,, \tag{4.136}$$

where the quoted uncertainty dominantly results from a variation of the matching scale M in the range 1–2 GeV, and to a lesser extent from either taking the renormalization–group coefficients in full QCD, or the large–N_C limit. The large matching–scale dependence of our result reflects the imperfection of the matching. At a scale of 1 GeV, the scale dependent vector–meson tensor coupling reads: $F_V^T(1\,\mathrm{GeV}) = 118 \pm 33\,\mathrm{MeV}$. Given the large uncertainties from the matching scale, this finding is in surprising agreement to the leading order result $F_V^T(1\,\mathrm{GeV}) = 117\,\mathrm{MeV}$ [40] and to determinations of the tensor coupling F_V^T from QCD sum rules and lattice QCD of Refs. [77–80].

For the tree–point GFs one cannot even get rid of logarithms (and dilogarithms) by a convenient choice of the μ scale and hence the full spectrum of resonances should be considered as well.

4.16 Matching to the OPE with an infinite number of resonances

In this section we will obtain a quantitative prediction of the large–N_C limit in the sector of vector mesons. In particular, we will show that perturbative QCD alone sets a relation between the couplings of vector mesons to the vector and tensor currents. This power of prediction is due to the exceptional status of the two–point correlators Π_{VV}, Π_{TT} and Π_{VT}. As we saw in Section 4.14.2 $J^{PC} = (1^{--})$ ρ–like mesons are exchanged in the three correlators, a situation that strongly constrains and, as we will show, sets a distinct pattern for the decay constants of vector resonances in the large–N_C limit. To the best of our knowledge, no similar self–constrained set of correlators exists for particles other than vector resonances. This system of correlators was first discussed in [81], where, in their words, the (1^{--}) vector meson sector was 'bootstrapped'. However in their analysis they ignored the kinematical singularity of the $\Pi^{\pm}_{TT}$ GFs at $q^2 = 0$ and hence their results should be read with care.

So far, when comparing the OPE results of Section 4.4 with the calculations of Section 4.14 we have restricted ourselves to the MHA approximation. Since we were interested in GFs being order parameter of the chiral symmetry breaking, the Wilson coefficient of the identity operator in the OPE was identically zero. This implied that at leading order in gluonic corrections there was no logarithm to worry about, and then the OPE was simply a pure expansion in inverse powers of the momentum. Since in the large–N_C limit GFs are described by meromorphic functions of the resonances, the high–momentum limit of those expressions is precisely in inverse powers of the momentum. So the matching procedure was straightforward, even when considering only one multiplet of resonances.

But one might wonder what kind of information is obtained by matching the large–N_C resonance expression onto the perturbative parton logarithm, *i.e.*, for functions that are not order parameters. Having a finite number of multiplets, we can only obtain a series in inverse powers of the momentum. It is then impossible to match a logarithm and one is forced to introduce an infinite number of them (as explained in Chapter 2). If we have an infinite number of resonances of increasing mass, the process of taking the high–momentum limit and the sum over an infinite number of terms no longer commute. This can be seen as follows: let n be an integer number labeling the resonances with equal quantum numbers ordered by increasing mass; when expanding in $1/p^2$ no matter how large is p^2, there will be in the spectrum an integer n_Λ such that $m^2_{n_\Lambda} > |p^2|$, and then for $n \geq n_\Lambda$ we cannot expand in $1/p^2$. So we have first to sum up the infinite number of resonances, and afterwards, perform the $1/p^2$ expansion.

But, how can we deal with this? We can trade the infinite for integrals over the resonance counting index n with the use of Euler–Maclaurin theorem

$$\sum_{n=0}^{N} f(n) \;=\; \int_0^{N+1} f(n)\, dn \;+\; \frac{1}{2}\left\{f(0) \;-\; f(N+1)\right\} \;+$$

$$+\sum_{n=1}^{\infty}\frac{B_{2n}}{(2\,n)!}\left\{f^{(2n-1)}(N+1)\,-\,f^{(2n-1)}(0)\right\}\,, \qquad (4.137)$$

that is nothing more than the familiar trapezoidal rule for numerical integrations. This idea was pioneered by a series of authors [82, 83] and recently in Ref. [50] the method has been extended to include radiative corrections. In Ref. [84] an attempt to estimate the error committed by the truncation of the infinite tower was done.

Let us apply this formula to the case of the $\langle VV\rangle$ correlator, and generalize it latter for the rest:

$$\Pi_{VV}(p^2)\,=\,\sum_{n=0}^{N}\frac{F_{Vn}^2}{m_{Vn}^2-p^2}\,=\,\int_0^{N+1}\mathrm{d}n\,\frac{F_{Vn}^2}{m_{Vn}^2-\,p^2}\,+\,\cdots\,, \qquad (4.138)$$

where the dots stand for the terms subleading in inverse powers of p^2 that will contribute to higher order terms in the OPE. Let us concentrate on the integral and split it in the following way

$$\int_0^{N+1}\mathrm{d}n\,\frac{F_{Vn}^2}{m_{Vn}^2-\,p^2}\,=\,\int_{n_\Lambda}^{N+1}\mathrm{d}n\,\frac{F_{Vn}^2}{m_{Vn}^2-\,p^2}\,+\,\int_0^{n_\Lambda}\mathrm{d}n\,\frac{F_{Vn}^2}{m_{Vn}^2-\,p^2}\,, \qquad (4.139)$$

where n_Λ is a large but finite number, defined such that for an arbitrarily large $|p^2|$, $-p^2 > m_{Vn_\Lambda}^2$. By using n_Λ, we have split the integral keeping the contribution that will match the parton model logarithm of perturbative QCD [*cf*, Eqs. (4.69)]. We expect that for $n \gtrsim n_\Lambda$ the masses and decay constants follow a regular pattern in n. The remaining piece can therefore be safely expanded in inverse powers of the momentum and together with the omitted terms determines the OPE condensates; it is in general model dependent. We are left with the first integral, where the cutoff N will eventually be sent to infinity. Whatever the precise form of F_{Vn} and m_{Vn} may take, the integral has to match the parton model logarithm of Eq. (4.69). By looking at Eq. (4.139) one concludes that for highly excited resonances

$$\begin{aligned} F_{Vn}^2\,&=\,A_V^2\,\frac{\mathrm{d}m_{Vn}^2}{\mathrm{d}n}\,, \qquad (F_{Vn}^T)^2\,=\,A_V^{T\,2}\,\frac{\mathrm{d}m_{Vn}^2}{\mathrm{d}n}\,,\\ F_{A\,n}^2\,&=\,A_A^2\,\frac{\mathrm{d}m_{A\,n}^2}{\mathrm{d}n}\,, \qquad F_{B\,n}^2\,=\,A_B^2\,\frac{\mathrm{d}m_{B\,n}^2}{\mathrm{d}n}\,, \end{aligned} \qquad (4.140)$$

for both vector and tensor decay constants, and correspondingly with axial–vector and pseudovector resonances. Actually, this is the only possibility if we want to ensure the right high energy behaviour.

The scaling of the vector and tensor form factors makes possible to convert the integral in Eq. (4.139) over the radial excitation number n into an integral over the mass. The integration is performed trivially yielding:

$$\Pi_{VV\,(TT)}^{(-)}(q^2)\,\doteq\,(A_V^{(T)})^2\int_{m_{n_\Lambda}^2}^{m_{N+1}^2}\mathrm{d}m^2\frac{1}{m^2-q^2}\,=\,(A_V^{(T)})^2\log\left(\frac{m_{N+1}^2-q^2}{m_{n_\Lambda}^2-q^2}\right)\,, \qquad (4.141)$$

and analogously for Π_{AA} and Π^+_{TT}. It is important to stress that the limits $N \to \infty$ and $q^2 \to \infty$ do not commute. The former must be taken in first place, and together with the requirement $\lim_{n\to\infty} m_n = \infty$ the parton model logarithm is reproduced. So our first prediction is that vector masses grow to infinity as n does. Moreover, imposing that the quark–gluon picture is dual to the hadronic one, we obtain

$$A_V^2 \,=\, A_A^2 \,=\, \frac{N_C}{24\,\pi^2}\,, \quad A_B^2 \,=\, A_T^2 \,=\, \frac{N_C}{48\,\pi^2} \longrightarrow \lim_{n\to\infty} \xi_n^2 = \frac{1}{2}\,. \tag{4.142}$$

The definition of ξ_n can be found in Eq. (4.125). Incidentally, note that for the determination of ξ_n no use was made of the b mesons entering Π^+_{TT}. In order to relate both parity sectors in Π_{TT}, additional assumptions on the spectrum would have to be made. For instance, if some relation between m_{Vn} and m_{Bn} were specified, a prediction for f^T_{Vn}/f_{Bn} would then follow.

For the case of scalar and pseudoscalar correlators, the OPE result in Eqs. (4.69) has $\sim p^2 \log p^2$, and so we have to perform the following manipulation to the resonance propagator

$$\frac{c^2_{m\,n}}{m^2_{Sn} - p^2} \,=\, \frac{c^2_{m\,n}}{m^2_{Sn}} \,+\, \frac{c^2_{m\,n}}{m^2_{Sn}}\,\frac{p^2}{m^2_{Sn} - p^2}\,, \tag{4.143}$$

and similarly for the pseudoscalar correlator. Then we obtain

$$c^2_{m\,n} \,=\, A_S^2\,\frac{\mathrm{d}m^4_{Sn}}{\mathrm{d}n}\,, \qquad d^2_{m\,n} \,=\, A_P^2\,\frac{\mathrm{d}m^4_{Pn}}{\mathrm{d}n}\,, \tag{4.144}$$

and again matching to the perturbative result fixes $B_0^2\,A_S^2 = B_0^2\,A_P^2 = \frac{N_C}{32\,\pi^2}$. In this case the anomalous dimensions in both sides of the equality do not match. Indeed we already faced the same situation for $F^T_{Vn}(\mu)$.

4.16.1 Sign alternation in ξ_n

So far we have been able to fix the magnitude of ξ_n from the asymptotic behaviour of Π_{VV} and Π^-_{TT}. However, it turns out that even the sign can be predicted. To show this we turn our attention to the crossed–correlator Π_{VT}. In this case, the Euler–MacLaurin theorem takes the form

$$\Pi_{VT}(p^2) \,=\, 2\sum_{n=0}^{N} \frac{F^2_{Vn}\,\xi_n\,m_{Vn}}{m^2_{Vn} - p^2} \,=\, 2\int_{n_\Lambda}^{N+1} \mathrm{d}n\,\frac{F^2_{Vn}\,\xi_n\,m_{Vn}}{m^2_{Vn} - p^2} + \cdots\,. \tag{4.145}$$

With the help of our previous combined analysis of Π_{VV} and Π^-_{TT} we can also transform Eq. (4.145) into an integral over the mass. Taking the limit $N \to \infty$ we obtain

$$\Pi_{VT}(q^2) \,=\, -\,\frac{N_C}{24\sqrt{2}\,\pi}\,\sqrt{-\,q^2} + \mathcal{O}(q^{-2})\,. \tag{4.146}$$

However, in order to comply with the short distance behaviour, it should *converge* as q^{-2}. The only possibility left is to allow for an alternate series, with ξ_n showing a pattern of alternation in sign [9]. Note that, unlike $\Pi_{VV\,(AA)}$, $\Pi^{\pm}_{TT}$ and $\Pi_{SS\,(PP)}$, Π_{VT} is not positive definite: the corresponding spectral function in Eq. (4.126) can contain both positive and negative contributions.

The most general situation that complies with QCD is the presence of some cancellations for high–resonance contributions, no matter how they are arranged. So we need an infinite number of positive contributions v^+, with cut–off N^+ and an infinite number of negative ones v^- with cut–off N^-. So one consequence is that not all vector mesons are alike. Let us show that this general scenario does not contradict QCD. We will have to find a representation for the GF such that the result is independent of the cut–offs $N^{\pm}$ for $N^{\pm} \to \infty$. An unsubtracted dispersion relation does not satisfy this basic requirement, and so we will addopt a once (over–) subtracted one. For highly excited states, for both v^+ and v^- we have

$$F_{Vn^{\pm}}\,\xi_{n^{\pm}} \;=\; \pm\,\frac{N_C}{24\sqrt{2}\pi^2}\,\frac{\mathrm{d}m^2_{Vn^{\pm}}}{\mathrm{d}n}\,. \tag{4.147}$$

The once subtracted dispersion relation reads

$$\Pi_{VT}(p^2) = p^2 \int \mathrm{d}t\,\frac{1}{t(t-p^2)}\,\frac{1}{\pi}\,\mathrm{Im}\,\Pi_{VT}(t) - \Lambda_1\,,. \tag{4.148}$$

Imposing that this GF must vanish for $q^2 \to \infty$ we get the following sum rule

$$\Lambda_1 \;=\; \lim_{p^2\to\infty} p^2 \int \mathrm{d}t\,\frac{1}{t(t-p^2)}\,\frac{1}{\pi}\,\mathrm{Im}\,\Pi_{VT}(t)\,. \tag{4.149}$$

Eq. (4.148) leads to

$$\begin{aligned}\Pi_{VT}(p^2) \;&\doteq\; \frac{N_C\,p^2}{24\sqrt{2}\pi^2}\left(\int_{m_{n^+_\Lambda}}^{m_{N^+}} \mathrm{d}n\,\frac{1}{m^2-p^2} - \int_{m_{n^-_\Lambda}}^{m_{N^-}} \mathrm{d}n\,\frac{1}{m^2-p^2}\right)\\ &=\; \frac{N_C\,p^2}{24\sqrt{2}\pi^2}\left(\int_{m_{N^-}}^{m_{N^+}} \mathrm{d}n\,\frac{1}{m^2-p^2} + \int_{m_{n^+_\Lambda}}^{m_{n^-_\Lambda}} \mathrm{d}n\,\frac{1}{m^2-p^2}\right)\,.\end{aligned} \tag{4.150}$$

The first integral vanishes when taking the limits $N^{\pm} \to \infty$ in an independent (uncorrelated) way (that is, the limit is defined); the second integral involves only the finite quantities and so can be safely expanded in inverse powers of p^2. Then we comply with the OPE because there are only integer powers of p^2 and the series starts with $1/p^2$ terms.

[9] Note that ξ_n is a real number because f_V and f_V^T are defined to be real, so this is indeed the only possible scenario. To the best of our knowledge, the first instance of alternating contributions in the hadronic spectrum was found in Ref. [85] in the context of $e^+e^- \to$ hadrons.

The simplest (and most natural) scenario consists of a regular pattern of sign–alternating contributions. For this particular scenario, consistency with perturbative QCD leads to the prediction

$$\xi_n = (-1)^n \, |\xi_n| \, , \qquad |\xi_n| = \frac{1}{\sqrt{2}} \simeq 0.71 \, , \tag{4.151}$$

for highly excited ρ–like vector meson resonances. Interestingly, the ξ parameter has been recently computed in the lattice for the $\rho(770)$ meson [79, 80, 86]. Quite remarkably, the value reported is $\xi_\rho = 0.72(2)$ for $\mu = 2\,\mathrm{GeV}$ [10]. In Section 5.2.9 we shall see that either sum rules or RχT within the minimal hadronic ansatz get similar answers.

This result is extremely interesting, suggesting that ξ_n may be a constant independent of the resonance excitation number. Therefore, one would like to assess what is the range of validity of the pattern shown in Eq. (4.151). Incidentally, one would also like to identify the specific realization of opposite–sign contributions. Note that strictly speaking, short distances only demand that some cancellations between high–resonance contributions have to take place in Π_{VT}. It would certainly look odd if the alternation started at some energy scale $\mu \sim m_{\rho_{\bar{n}}}$, but it cannot be ruled out. However, if this were the case, some triggering dynamical mechanism at this scale should be invoked. The natural thing to expect is that a regular pattern of sign–flipping contributions be a feature of the whole meson tower.

So far we have been dealing with large–N_C QCD. A more ambitious and interesting issue is to check whether the result of Eq. (4.151) and the conjectured opposite–sign pattern we advocate as its most natural realization has anything to do with QCD. In the following section we will see that sum rules nicely comply with this picture.

4.16.2 Comparison with QCD spectral sum rules

In order to test the ideas of the previous section, we will consider a set of sum rules. We will start with the Π_{VV} and Π^-_{TT} correlators and afterwards consider Π_{VT}.

We choose as hadronic ansätze the following functions,

$$\begin{aligned}
\frac{1}{\pi} \, \mathrm{Im} \, \Pi^-_{TT}(t) &= \xi^2_\rho F^2_\rho \delta(t - m^2_\rho) + \xi^2_{\rho\prime} F^2_{\rho\prime} \delta(t - m^2_{\rho\prime}) + \frac{1}{3} \frac{N_c}{(4\,\pi)^2} \, \kappa_V \, \theta(t - \bar{s}_0) \, , \\
\frac{1}{\pi} \, \mathrm{Im} \, \Pi_{VV}(t) &= F^2_\rho \delta(t - m^2_\rho) + F^2_{\rho\prime} \delta(t - m^2_{\rho\prime}) + \frac{2}{3} \frac{N_c}{(4\,\pi)^2} \, \kappa_T \, \theta(t - s_0) \, ,
\end{aligned} \tag{4.152}$$

consisting of two isolated single poles, corresponding to the $\rho(770)$ and $\rho(1450)$ plus a continuum, whose onset is determined by the parameters s_0 and $\bar{s}_0$, which in

[10] In a recent paper [40] this ratio was also determined for $\mu = 1\,\mathrm{GeV}$, the value reported being $\xi_\rho = 0.75(14)$. Sum rules also obtain similar results [77, 78]. Incidentally, in the ENJL model [87] one also finds $\xi_\rho = 1/\sqrt{2}$.

general are different. The factors in front of the theta terms have been chosen so as to match the parton model logarithms. The parameters κ_T, κ_V are given by

$$\kappa_T(\mu) \,=\, 1 \,+\, \frac{\alpha_s(\mu)}{3\,\pi}\left(\frac{7}{3} \,+\, 2\,\log\frac{t}{\mu^2}\right)\,, \qquad \kappa_V \,=\, 1 \,+\, \frac{\alpha_s(\mu)}{\pi}\,. \tag{4.153}$$

They represent the first–order α_s correction to the perturbative contribution, the former also accounting for the fact that the tensor current has a non–vanishing anomalous dimension.

Using once subtracted dispersion relations and expanding the result in inverse powers of momenta and matching onto the OPE result one finds

$$\begin{aligned}
F_\rho^2 + F_{\rho\prime}^2 - \frac{2}{3}\frac{N_c}{(4\,\pi)^2}\,\kappa_V\,s_0 &= 0\,,\\
\xi_\rho^2\,F_\rho^2 + \xi_{\rho\prime}^2\,F_{\rho\prime}^2 + \Lambda_3 - \frac{1}{3}\frac{N_c}{(4\,\pi)^2}\,\kappa_2\,\bar{s}_0 &= 0\,,\\
F_\rho^2\,m_\rho^2 + F_{\rho\prime}^2\,m_{\rho\prime}^2 - \frac{1}{3}\frac{N_c}{(4\,\pi)^2}\,\kappa_V\,s_0^2 &= -\,\frac{1}{24\,\pi}\,\langle\alpha_s G^{\mu\nu}G_{\mu\nu}\rangle,\\
\xi_\rho^2\,F_\rho^2\,m_\rho^2 + \xi_{\rho\prime}^2\,F_{\rho\prime}^2\,m_{\rho\prime}^2 - \frac{1}{6}\frac{N_c}{(4\,\pi)^2}\,\kappa_4\,\bar{s}_0^2 &= \frac{1}{48\,\pi}\,\langle\alpha_s G^{\mu\nu}G_{\mu\nu}\rangle,
\end{aligned} \tag{4.154}$$

where κ_2 and κ_4 are given by

$$\kappa_2(\bar{s}_0) \,=\, 1 + \frac{1}{9}\frac{\alpha_s(\sqrt{\bar{s}_0})}{\pi}\,, \qquad \kappa_4(\bar{s}_0) \,=\, 1 + \frac{4}{9}\frac{\alpha_s(\sqrt{\bar{s}_0})}{\pi}\,. \tag{4.155}$$

Notice that above the renormalization point was chosen to be $\mu^2 = \bar{s}_0$.

As already noticed in Ref. [88], α_s corrections in the vector channel induce at most a 8% change in the decay constants and will be dismissed. For the tensor channel, the equations above show that the α_s correction in the sum rules is extremely small. For instance, at $\bar{s}_0 = 1.5$ GeV^2, they represent less than 2% for κ_2 and about 6% for κ_4. Therefore, the perturbative corrections in α_s can be safely neglected.

For the numerical analysis, we will take as inputs the masses, $m_\rho = 770$ MeV and $m_{\rho\prime} = 1440$ MeV, and the gluon condensate. Due to the existing uncertainty, we will choose it to lie in the range $\langle\alpha_s G^{\mu\nu}G_{\mu\nu}\rangle = (0.001 - 0.021)\,\pi$ GeV^4, which includes both the values extracted from charmonium sum rules and τ decays [89]. Additionally, we will use the relation $F_\rho = \sqrt{2}\,F$. With $F = 92$ MeV, one obtains $F_\rho = 131$ MeV. Finally, we will further impose $\xi_\rho^2 = 0.5$, in accord with the lattice determination. Notice that in the sum rules we have included the Λ_3 term. However, lacking any estimate of the parameter, for our numerical analysis we will set $\Lambda_3 = 0$, as commonly assumed in the literature.

Solving Eqs. (4.154) for $F_{\rho\prime}$, s_0, $\bar{s}_0$ and $\xi_{\rho\prime}$, one finds

$$\begin{aligned}
\sqrt{s_0} &= (1.64 \pm 0.02)\,\text{GeV}\,, \qquad \sqrt{\bar{s}_0} = (1.59 \pm 0.02)\,\text{GeV}\,,\\
F_{\rho\prime} &= (129 \pm 4)\,\text{MeV}\,, \qquad \xi_{\rho\prime} = (0.95 \pm 0.05)\,\xi_\rho\,,
\end{aligned} \tag{4.156}$$

where the errors quoted are due to the variation of the gluon condensate. Note that both s_0 and $\bar{s}_0$ yield reasonable values, *i.e.*, they satisfy $m_{\rho(1440)} < \sqrt{s_0} \sim \sqrt{\bar{s}_0} < m_{\rho(1750)}$.

The following comments are in order:

- Lower values of the gluon condensate, typical in analysis of τ decays, favor $\xi_{\rho\prime} \sim \xi_\rho$. In particular, notice that a vanishing gluon condensate, not excluded by τ decay analyses, implies $\xi_{\rho\prime} = \xi_\rho$ (together with $s_0 = \bar{s}_0$).
- Eqs. (4.154) provide a solution only for the narrow range 126 MeV $\leq f_\rho \leq$ 133 MeV. Interestingly, the range complies with the relation $F_\rho^2 \simeq 2\,F^2$.

In order to test our conjectured pattern of signs we have to consider Π_{VT}. Our spectral ansatz will be the following:

$$\frac{1}{\pi}\,\mathrm{Im}\,\Pi_{VT}(t) \;=\; \xi_\rho\,F_\rho^2\,m_\rho\,\delta(t-m_\rho^2) \;+\; \xi_{\rho\prime}\,F_{\rho\prime}^2\,m_{\rho\prime}\,\delta(t-m_{\rho\prime}^2)\,, \tag{4.157}$$

Inserting the last expression and the OPE of Eq. (4.102) into the dispersion relation, equating powers of q^2 on both sides we get

$$\begin{aligned} -\,\langle\bar{q}q\rangle &= \xi_\rho\,F_\rho^2\,m_\rho + \xi_{\rho\prime}\,F_{\rho\prime}^2\,m_{\rho\prime}\,, \\ -\,\frac{g_s}{3}\langle\bar{q}\,\sigma_{\mu\nu}\,G^{\mu\nu}q\rangle &= \xi_\rho\,F_\rho^2\,m_\rho^3 + \xi_{\rho\prime}\,F_{\rho\prime}^2\,m_{\rho\prime}^3\,, \end{aligned} \tag{4.158}$$

upon solving these equations for ξ_ρ and $\xi_{\rho\prime}$ we find

$$\begin{aligned} \xi_{\rho\prime} &= \frac{\langle\bar{q}q\rangle m_\rho^2}{F_{\rho\prime}^2\,m_{\rho\prime}(m_{\rho\prime}^2-m_\rho^2)}\left[1-\frac{\lambda}{m_\rho^2}\right]\,, \\ \xi_\rho &= -\,\frac{\langle\bar{q}q\rangle m_{\rho\prime}^2}{F_\rho^2\,m_\rho(m_{\rho\prime}^2-m_\rho^2)}\left[1-\frac{\lambda}{m_{\rho\prime}^2}\right]\,, \end{aligned} \tag{4.159}$$

where

$$\lambda \;=\; \frac{g_s}{3}\,\frac{\langle\bar{q}\,\sigma_{\mu\nu}\,G^{\mu\nu}q\rangle}{\langle\bar{q}q\rangle}\,, \tag{4.160}$$

is the ratio between the mixed and the quark condensates. In view of Eqs. (4.159) there are three possible scenarios, depending on the magnitude of λ (recall that the quark condensate is negative):

- $\lambda < m_\rho^2$, leading to alternation in sign, with positive ξ_ρ;
- $m_\rho^2 < \lambda < m_{\rho\prime}^2$, where both ξ_ρ and $\xi_{\rho\prime}$ are positive;
- $\lambda > m_{\rho\prime}^2$, leading to alternation in sign but with a negative ξ_ρ.

The last possibility is in clear contradiction with the lattice result and can be readily excluded. Independent sum rule analyses [90] indeed concluded that

$$\lambda = 0.22\,\mathrm{GeV}^2\,, \tag{4.161}$$

so that the mixed condensate is small enough and leads to alternation in sign. (Incidentally, notice that arbitrarily large negative values of λ would have also led to this scenario). Note that the small value of the mixed condensate in the second equation forces the alternation in sign, whereas the quark condensate fixes the contribution of the $\rho(770)$ to be positive.

More sophisticated sum rules have confirmed the pattern of alternating contributions in Π_{VT} [91]. However, a word of caution should be issued on the quantitative values of the parameters extracted from such sum rules. We already pointed out in the previous section that the presence of a mass factor multiplying each resonance contribution in Eq. (4.157) spoils the convergence of the series. As a result, the sum rules are not stable under addition of new resonance states in the spectral function. However, Eqs. (4.159) distinctly show that there has to be some negative contribution to outweight the $\rho(770)$ contribution.

4.16.3 Discussion

A remarkable property of QCD in the large–N_C limit is that the qualitative characteristics of hadrons emerge naturally from imposing quark–hadron duality consistency conditions on the correlators of the theory. This very general analysis does not rely on the particular flavour or Dirac structure of the correlators. Therefore, any relation between a certain subset of correlators may turn out to yield additional useful constraints on the spectrum of large–N_C QCD.

From a combined analysis of three correlators we concluded that, for highly excited states, $F^T_{Vn}/F_{Vn} \sim (-1)^n |F^T_{Vn}/F_{Vn}|$, where $|F^T_{Vn}/F_{Vn}| = 1/\sqrt{2}$. The ratio of decay constants is fixed by the Dirac structure of the currents and equals the ratio of the leading perturbative behaviour of Π_{VV} and Π_{TT}, while the alternate character is required to ensure the convergence of Π_{VT}.

We find this result particularly beautiful. It is a really striking prediction which relies only on the simultaneous high–energy consistency of the correlators. In this sense, the previous result can be rendered as a high–energy theorem of large–N_C QCD. Our analysis was restricted to light–flavour vector mesons, but similar predictions should be obtained for mesons with heavy flavours.

A natural issue to address at this point is whether this pattern, valid for highly excited mesons in the large–N_c limit, resembles QCD. The lattice recently computed the ratio of the $\rho(770)$ decay constants, with the result $F^T_\rho/F_\rho = 0.72(2)$. The agreement is certainly impressive, and it seems suggestive to entertain the scenario of n–independent decay constant ratios for the ρ–meson radial excitations. We tested this possibility with QCD sum rules and the pattern is qualitatively reproduced. Corrections due to light quark masses and the anomalous dimension of the tensor current have not been considered.

Chapter 5

Phenomenological applications

5.1 Weak decays

In this chapter we are going to discuss some applications of the methods we have studied in this thesis. By phenomenological we mean computations that can be directly compared with the experimental data.

We will be concerned by the phenomenology of particle decays mediated by weak interactions. Most of the particles decay due to the weak force, and this certainly makes sense, because it is the only known interaction that couples particles within one family (electron with neutrino, up with down quark), and also mixes the different families (in the quark sector). It is in this sense that this thesis deals with the topic of flavour–dynamics.

If gauge interactions only coupled particles with themselves (we will call then diagonal interactions), such as QED or QCD, particles would not be able to decay because a particle cannot decay into itself (this statement is true for fundamental particles, not for composite particles such as hadrons or atoms). This special feature of the weak interactions is linked with the spontaneous symmetry breakdown of a *local* gauge symmetry known as the Higgs mechanism. It is this breakdown what provides fundamental particles with non–zero masses, and gives rise to the known Higgs boson. The details of this mechanism are not going to be discussed in this thesis (a nice review can be found for instance in Refs. [3, 57, 92, 93]). We will however, comment the results that we need for our computations.

The standard model of electroweak interactions has three gauge particles, each one associated with one force. As discussed in Chapter 1, the gluon mediates the strong interactions (QCD) and is a massless spin–one boson. The photon is also massless, and governs the electromagnetic interactions. The fact that these particles are massless points that the corresponding symmetry is unbroken. The weak interactions are mediated by two particles, one neutral boson Z coupled to all particles in a diagonal way, and the charged W particle, the one that couples the two weak partners and the different families among themselves. These three particles are far from being massless, in fact $m_W \sim m_Z \sim 90\,\mathrm{GeV}$. At the energies we are working, we can integrate out of the action these particles, along with the heavy quarks.

Then we are left with four–fermion local interactions (non–renormalizable). Since we are interested in the leptonic decay of hadrons we will write only this piece of the weak Lagrangian. A fundamental feature of the flavour changing weak interactions is that they only involve left–handed currents [3]

$$\begin{aligned} \mathcal{L}_W &= -\frac{G}{\sqrt{2}}\,(J_\mu\,L^\mu + \text{h.c.})\,, \\ L^\mu &= \overline{e}\,\gamma^\mu(1-\gamma_5)\,\nu_e\,, \qquad\qquad J^\mu = V^\mu - A^\mu\,, \\ V^\mu &= V_{ud}\,\overline{u}\,\gamma^\mu\,d + V_{us}\,\overline{u}\,\gamma^\mu\,s\,, \quad A^\mu = V_{ud}\,\overline{u}\,\gamma^\mu\,\gamma_5\,d + V_{us}\,\overline{u}\,\gamma^\mu\,\gamma_5\,s\,. \end{aligned} \tag{5.1}$$

G is the Fermi constant, L^μ and J^μ denote the leptonic and hadronic currents, respectively; V^μ and A^μ stand for the vector and axial–vector currents. V_{ud} and V_{us} are the CKM matrix elements [94, 95], that can be chosen to be real [96], and to a very good approximation satisfy $|V_{ud}|^2 + |V_{us}|^2 = 1$, or equivalently $V_{ud} = \sin\theta_c$, $V_{us} = \cos\theta_c$, being θ_c the Cabibbo angle. The hadronic currents can be written in terms of the Noether currents as

$$V^\mu = V_{ud}\,V_\mu^{1+i2} + V_{us}\,V_\mu^{4+i5}\,, \qquad A^\mu = V_{ud}\,A_\mu^{1+i2} + V_{us}\,A_\mu^{4+i5}\,. \tag{5.2}$$

Whereas the leptonic part is always trivial, and can be analysed perturbatively, the quark current deserves a specific treatment. Even if the effective Lagrangian (5.1) is written in terms of quarks, we know that the effective degrees of freedom are hadrons, and so we are facing a non–perturbative problem. For the case of pseudoscalar mesons decaying weakly into a pair of leptons, only the axial current has a non–vanishing matrix element with the vacuum, and the problem simplifies somehow. But if the pseudoscalar is decaying into a pair of leptons *plus* a photon (involving then the electromagnetic interactions), then both vector and axial–vector currents play a röle. The same can be said if a baryon is decaying into another baryon and a couple of leptons. These two last "pathologic" cases are the ones to be discussed in this chapter.

5.2 Radiative pion decay

5.2.1 Introduction

The radiative decay of the pion is a suitable process to be analysed within χPT. This framework provides the structure of the relevant form factors through: i) a polynomial expansion in momenta, essentially driven by the contributions of heavier degrees of freedom that have been integrated out, and ii) the required chiral logarithms generated by the loop expansion and compelled by unitarity. Both contributions correspond to the chiral expansion in p^2/M_V^2 and p^2/Λ_χ^2, respectively, where $\Lambda_\chi \sim 4\,\pi F$ [25]. Hence their magnitude is, in principle, comparable. The chiral logarithms have thoroughly been studied in later years up to and including $\mathcal{O}(p^6)$ both in $SU(2)$ [97] and $SU(3)$ [98, 99].

However the size of the polynomial contributions is more controversial. They involve short–distance dynamics through the chiral low–energy constants (LECs) of the χPT Lagrangian and their determination from QCD is a difficult non–perturbative problem. Phenomenology and theoretical arguments suggest that the main röle is played by the physics at the scale M_V, *i.e.* the physics of low–lying resonances. This assumption, widely known as resonance saturation of the LECs in χPT, implies that the structure of the form factors is given by the pole dynamics of resonances and this hint works well in all known cases.

Because $m_\pi \ll M_V$, it is expected that the structure of the form factors in pion decays should be less relevant and, accordingly, the approach provided by χPT should be good enough even when only the first terms of the chiral expansion are included. This is the case of the radiative pion decay, namely $\pi \to \ell\,\nu_\ell\,\gamma$, $\ell = \mu,\, e$, where constant form factors (that correspond to the leading order contribution in the chiral expansion) have widely been employed in the analyses of data. However the PIBETA collaboration [100] showed that a strong discrepancy between theory and experiment arises for the branching ratio of the process in a specific region of the electron and photon energies. Lately the same collaboration, after their 2004 analysis, concludes that the discrepancy has faded away [101]. Curiously enough this decay has a persistent story of deceptive comparisons between theory and experiment [102] that have prompted the publication of proposals beyond the Standard Model (SM) to account for the variance [103–107]. Between these it has received particular attention the possibility of allowing a tensor contribution that could explain the discrepancy by interfering destructively with the Standard Model prescription though showing some inconsistency with the corresponding tensor contribution in nuclear β decay [108]. Related with this issue it is essential, seeking to discern the presence of a new physics contribution to the radiative decay of the pion, to provide an accurate profile of the involved form factors within QCD.

In order to settle the Standard Model description of the vector and axial–vector form factors participating in $\pi \to \ell\,\nu_\ell\,\gamma$ decays we study, in this section, the structure provided by the lightest meson resonances. This is very much relevant on the experimental side because high–statistics experiments as PIBETA [101] already are able to determine, for instance, the slopes of the form factors involved in these decays.

5.2.2 Radiative pion decay : vector and axial–vector form factors

The amplitude that describes the $\pi^+ \to \ell^+\nu_\ell\,\gamma$ process can be split into two different contributions :

$$M(\pi^+ \to \ell^+\nu_\ell\,\gamma) \;=\; M_{IB} \;+\; M_{SD}\;.$$

Here M_{IB} is the inner bremsstrahlung (IB) amplitude where the photon is radiated by the electrically charged external legs, either pion or lepton; consequently the interaction is driven by the axial–vector current. M_{SD} is the structure–dependent

(SD) contribution where the photon is emitted from intermediate states generated by strong interactions. In this later case both vector and axial–vector form factors arise from the hadronization of the QCD currents within the Standard Model.

Because $\pi^+ \to e^+\nu_e$ is helicity suppressed, the IB contribution to its radiative counterpart suffers the same inhibition and, consequently, the electron case is the appropriate channel to uncover the non–perturbative SD amplitude. Contrarily, the $\pi^+ \to \mu^+\nu_\mu\gamma$ decay is fairly dominated by IB. As a consequence the $\pi^+ \to e^+\nu_e\gamma$ is of great interest to investigate the hadronization of the currents contributing to the SD amplitudes that are driven, within the Standard Model, by the vector $[F_V(q^2)]$ and axial–vector $[F_A(q^2)]$ form factors defined by :

$$\begin{aligned} \left\langle \gamma \,|\, \overline{u}\,\gamma_\alpha\, d \,|\, \pi^- \right\rangle &= -\frac{e}{M_{\pi^+}}\,\varepsilon^{\beta *}\,F_V(q^2)\,\varepsilon_{\alpha\beta\mu\nu}\,r^\mu\,p^\nu\,, \\ \left\langle \gamma \,|\, \overline{u}\,\gamma_\alpha\,\gamma_5\, d \,|\, \pi^- \right\rangle &= i\,\frac{e}{M_{\pi^+}}\,\varepsilon^{\beta *}\,F_A(q^2)\,[(r\cdot p)\,g_{\alpha\beta} - p_\alpha r_\beta] + i\,e\,\varepsilon^*_\alpha\,\sqrt{2}\,F\,, \end{aligned} \tag{5.3}$$

where r and p are the pion and photon momenta, respectively, $q^2 = (r-p)^2$ and e is the electric charge of the electron. The second term in the matrix element of the axial–vector current corresponds to the pion pole contribution (which coupling is given by the decay constant of the pion F) to the IB amplitude.

Form factors drive the hadronization of QCD currents and embed non–perturbative aspects that we still do not know how to evaluate from the underlying strong interaction theory. Their determination is all–important in order to disentangle those aspects. It is reasonable to assume, as has been common lore in the literature on this topic, that hadronic resonance states should dominate the structure of form factors and, accordingly, meromorphic functions with poles in the relevant resonances coupled to the corresponding channels have been extensively proposed in order to fit hadronic data. This procedure by itself is, however, not fully satisfactory because it does not impose known QCD constraints.

On one side chiral symmetry of massless QCD drives the very low–energy region of form factors. Hence the latter have to satisfy its constraints in this energy domain. On the other, one can also demand that form factors in the resonance energy region should match short–distance QCD properties.

In the following we apply these techniques in order to determine the Standard Model description of the vector and axial–vector form factors in the radiative pion decay. Their definition, given by Eq. (5.3), illustrates the fact that they follow from three–point GFs of the corresponding QCD currents. The proper GF in this case, namely $\langle VVP\rangle$ and $\langle VAP\rangle$, happen to be order parameters of the spontaneous breaking of chiral symmetry hence free of perturbative contributions in the chiral limit. This is a key aspect required by our procedure. Hence we consider in this article their study in the chiral limit, that otherwise should provide the dominant features. In the following we handle the GF in order to provide a description constrained by QCD and then we will work out the form factors.

5.2.3 Vector form factor

For the determination of the vector form factor defined by Eq. (5.3) we will use the LSZ formula (valid in the chiral limit)

$$F_V(q^2) = \frac{\sqrt{2}\, M_{\pi^+}}{6\, F B_0} \lim_{p^2, r^2 \to 0} r^2\, \Pi_{VVP}(p^2, q^2, r^2)\,,$$

on the $\langle VVP \rangle$ GF determined in Eq. (4.120) to obtain:

$$F_V(q^2) \;=\; \frac{M_{\pi^+}}{3\sqrt{2}\, B_0\, F\, M_{V_1}^2\, M_{V_2}^2}\, \frac{c_{000} + c_{010}\, q^2}{(M_{V_1}^2 - q^2)\,(M_{V_2}^2 - q^2)}\,, \tag{5.4}$$

and we observe that only one parameter, c_{010}, has not been fixed by our procedure. The expression for the vector form factor in the radiative pion decay given by Eq. (5.4) is the most general one that satisfies the short–distance constraints specified above. As the transferred momenta in the $\pi^+ \to e^+\, \nu_e\, \gamma$ process is small by comparison with the mass of the lightest vector meson resonance, $q^2 \ll M_V^2$, it is appropriate to perform the relevant expansion until first order in q^2. Using the result for c_{000} given by Eq. (4.121) it gives:

$$F_V(q^2) = F_V(0)\, \left[1 \,+\, \lambda_V\, \frac{q^2}{M_{\pi^+}^2} \,+\, \mathcal{O}(q^4) \right]\,, \tag{5.5}$$

where $\lambda_V = \Lambda^V_{N_C \to \infty} + \Lambda^V_{1/N_C} + \cdots$ admits an expansion in $1/N_C$ and

$$\begin{aligned} F_V(0) \;&=\; \frac{\sqrt{2}\, N_C\, M_{\pi^+}}{24\, \pi^2 F}\,, \\ \Lambda^V_{N_C \to \infty} \;&=\; \frac{M_{\pi^+}^2}{M_{V_1}^2} + \frac{M_{\pi^+}^2}{M_{V_2}^2} + M_{\pi^+}^2\, \frac{c_{010}}{c_{000}}\,. \end{aligned} \tag{5.6}$$

We must compare our value[1] for $F_V(0) \simeq 0.0271$ with the result coming from $\Gamma(\pi^0 \to \gamma\,\gamma)$ and CVC, $F_V(0) = 0.0261(9)$, and with the recent experimental fit by the PIBETA collaboration, $F_V(0) = 0.0259(18)$ [109]. We recall that our result for the vector form factor (5.4) arises from a large–N_C procedure where a model of the $N_C \to \infty$ has been implemented, namely the cut in the spectrum. At $q^2 \ll M_V^2$ this form factor has been studied up to $\mathcal{O}(p^6)$ in χPT [97, 98]. At $\mathcal{O}(p^4)$ the Wess–Zumino Lagrangian determines $F_V(0)$ as given in Eq. (5.6). Higher chiral order corrections to this result vanish in the chiral limit, accordingly their size is suppressed over the leading order by powers of M_π^2/M_V^2 or M_π^2/Λ_χ^2 that are tiny. Indeed, using the $\mathcal{O}(p^6)$ odd–intrinsic–parity Lagrangian $\mathcal{L}_6^W$ worked out in Ref. [33], this modification to $F_V(0)$ is proportional to a low–energy constant as $M_{\pi^+}^2\, C_7^W$, that also contributes to the $\pi^0 \to \gamma\,\gamma$ decay. From the latter one obtains [110] $C_7^W \simeq (0.013 \pm 1.17) \times 10^{-3}\,\mathrm{GeV}^{-2}$, *i.e.* compatible with zero.

[1] In the following numerical determinations we will use $F = 0.0924\,\mathrm{GeV}$, $M_\pi = 0.138\,\mathrm{GeV}$, $M_K = 0.496\,\mathrm{GeV}$, $M_{\pi^0} = 0.135\,\mathrm{GeV}$,$M_{\pi^+} = 0.140\,\mathrm{GeV}$ and $M_{V_1} = M_{\rho(770)} = 0.775\,\mathrm{GeV}$.

The slope λ_V arises at $\mathcal{O}(p^6)$ with the usual two features: the local operator O_{22}^W in $\mathcal{L}_6^W$ provides the $N_C \to \infty$ contribution:

$$\Lambda^{\chi PT}_{N_C\to\infty} \;=\; \frac{64\,\pi^2}{N_C}\, M^2_{\pi^+}\, C_{22}^{Wr}(\mu)\,, \tag{5.7}$$

and a one–loop calculation provides the chiral logs that correspond to the next–to–leading order in the $1/N_C$ expansion [98]:

$$\Lambda^{\chi PT}_{1/N_C} \;=\; -\,\frac{M^2_{\pi^+}}{48\,\pi^2 F^2}\left[1+\log\left(\frac{M^2_\pi}{\mu^2}\right)\right]\,. \tag{5.8}$$

There is another process directly related with the $\langle VVP\rangle$ GF, namely $\pi \to \gamma\,\gamma^*$; hence it should be related with the radiative pion decay. Indeed within the assumptions that carried us to $F_V(q^2)$ in Eq. (5.4), the momenta structure for the $\pi \to \gamma\,\gamma^*$ decay should be the same, though with different normalization. In consequence the $\Lambda^V_{N_C\to\infty}$ slope in Eq. (5.6) is the same for both processes.

The $\pi^0 \to \gamma\, e^+e^-$ amplitude can be expressed by:

$$\mathcal{M}_{\pi\to\gamma\gamma^*} \;=\; \mathcal{M}_{\pi\to\gamma\gamma}\,\left[1\;+\;\lambda_\gamma\,\frac{q^2}{M^2_{\pi^0}}\;+...\right]\,, \tag{5.9}$$

where $q^2 = (p_{e^+} + p_{e^-})^2$. The slope arises at $\mathcal{O}(p^6)$ in χPT and it is [111][2]:

$$\lambda_\gamma \;=\; \frac{64\,\pi^2}{N_C}\, M^2_{\pi^0}\, C_{22}^{Wr}(\mu) \;-\; \frac{M^2_{\pi^0}}{96\,\pi^2 F^2}\left[2+\log\left(\frac{M^2_\pi M^2_K}{\mu^4}\right)\right]\,. \tag{5.10}$$

Fortunately it has been measured rather accurately [112], $\lambda_\gamma = 0.032 \pm 0.004$ and then we can input this measure to determine the LEC $C_{22}^W(\mu)$ obtaining:

$$C_{22}^{Wr}(M_\rho) \;=\; 7.0^{+1.0}_{-1.5}\times 10^{-3}\,\mathrm{GeV}^{-2}\,, \tag{5.11}$$

where the error includes also the incertitude of the renormalization point μ between M_ρ and 1 GeV. Coming back to the slope of $F_V(q^2)$ we get:

$$\lambda_V \;=\; 0.041^{+0.004}_{-0.007}\,, \tag{5.12}$$

that compares well with the recent PIBETA measurement $\lambda_V = 0.070 \pm 0.058$ [109].

By comparing now $\Lambda^V_{N_C\to\infty}$ in Eq. (5.6) and $\Lambda^{\chi PT}_{N_C\to\infty}$ in Eq. (5.7) we can provide a determination for the undetermined parameter in the GF and then give a full prescription for the $F_V(q^2)$ form factor in Eq. (5.4). For the mass of the first multiplet of vector resonances we take $M_{\rho(770)}$ and for the second $M_{\rho(1450)} = 1.459$ GeV:

$$\frac{c_{010}}{c_{000}} \;=\; (-\,0.7 \pm 0.3)\,\mathrm{GeV}^{-2}\,. \tag{5.13}$$

[2]Notice that one–loop $\mathcal{O}(p^6)$ χPT contributions, encoded in $\Lambda^{\chi PT}_{1/N_C}$, coincide in $\pi \to e\,\nu_e\gamma$ and $\pi \to \gamma\,\gamma^*$ in the $SU(2)$ limit.

Notice that the size of this parameter is of the same order that the other two terms in $\Lambda^V_{N_C\to\infty}$. With this result we end the construction of the vector form factor in radiative pion decays in the large–N_C limit given by Eq. (5.4).

It is interesting to compare our results with those in Ref. [42]. As commented above the construction of the $\langle VVP\rangle$ GF in those references was carried out using only one multiplet of vector resonances, hence the vector form factor in radiative pion decay did not satisfy the constraint in Eq. (4.113). With this setting they are able to give a full prediction for the leading contribution to the slope λ_V, namely,

$$\Lambda^{1R}_{N_C\to\infty} \;=\; \frac{M^2_{\pi^+}}{M^2_V}\left[1-\frac{4\,\pi^2 F^2}{N_C\,M^2_V}\right]\,. \tag{5.14}$$

Using $M_V = M_\rho$ they get $\Lambda^{1R}_{N_C\to\infty}\simeq 0.027$ to be compared with $\Lambda^V_{N_C\to\infty} = 0.028\pm 0.006$ from our analysis above.

5.2.4 Axial–vector form factor

We now come back to the axial–vector form factor defined by Eq. (5.3) . In order to determine the $F_A(q^2)$ form factor we follow an analogous procedure to the one outlined before for the vector form factor. The LSZ formula then reads:

$$F_A(q^2) \;=\; \frac{\sqrt{2}\,M_{\pi^+}}{B_0\,F}\lim_{p^2,r^2\to 0} r^2\,\mathcal{F}(p^2,q^2,r^2)\,. \tag{5.15}$$

A detailed study of this GF was performed in Ref. [52]. One of the conclusions achieved was that the inclusion of one multiplet of vector, axial–vector and pseudoscalar resonances (together with the pseudoscalar mesons) was enough to satisfy the matching to the OPE of the $\langle VAP\rangle$ GF at leading order. Moreover the analogous to the Brodsky–Lepage condition (4.113), in this case, was also satisfied, *i.e.* the resulting axial–vector form factor $F_A(q^2)$ behaves smoothly at high q^2. Hence we obtain, for $N_C\to\infty$ with a cut spectrum:

$$F_A(q^2) \;=\; \frac{\sqrt{2}\,F\,M_{\pi^+}}{M^2_A-q^2}\left(\frac{M^2_A}{M^2_V}-1\right)\,, \tag{5.16}$$

At $q^2\ll M^2_A$ we may resort again to χPT [97,99] with the expansion:

$$F_A(q^2) \;=\; F_A(0)\left[1+\lambda_A\,\frac{q^2}{M^2_{\pi^+}}+...\right]\,. \tag{5.17}$$

Both terms, $F_A(0)$ and slope, satisfy an expansion in $1/N_C$, for instance $\lambda_A = \Lambda^A_{N_C\to\infty}+\Lambda^A_{1/N_C}+\cdots$. From our result above we get:

$$\begin{aligned} F_A(0) \;&=\; \sqrt{2}\,F\,M_{\pi^+}\left(\frac{1}{M^2_V}-\frac{1}{M^2_A}\right)\,,\\ \Lambda^A_{N_C\to\infty} \;&=\; \frac{M^2_{\pi^+}}{M^2_A}\,. \end{aligned} \tag{5.18}$$

	Experiment [101]	$SU(2)$ Ref. [97]	$SU(3)$ Ref. [99]	Our work
$F_V(0)$	0.0258(18)	0.0271	0.0272	0.0271
λ_V	0.070(58)	0.044	0.045	0.041
$F_A(0)$	0.0121(18)	0.0091	0.0112	exp. input
λ_A	not measured	0.0034	~ 0	0.0197(19)

Table 5.1: Comparison of theoretical and experimental determinations for the low–energy expansion of vector and axial–vector form factors. The PIBETA determination assumes that the axial–vector form factor is constant, *i.e.* it does not consider a slope.

$F_A(q^2)$ arises first at $\mathcal{O}(p^4)$ with a constant local contribution from the χPT Lagrangian, namely:

$$F_A^{(4)}(q^2) \,=\, 4\sqrt{2}\,\frac{M_{\pi^+}}{F}\,(L_9^r + L_{10}^r)\,. \tag{5.19}$$

The next corrections appear at $\mathcal{O}(p^6)$ in the chiral expansion [99]. One of them results from local operators of the $\mathcal{O}(p^6)$ chiral Lagrangian that, in the chiral limit, only contribute to λ_A:

$$\lambda_A^{(6)}|_{N_C\to\infty} \,=\, \frac{M_{\pi^+}^2}{L_9^r + L_{10}^r}\left[C_{78}^r - 2\,C_{87}^r + \frac{1}{2}\,C_{88}^r\right]\,. \tag{5.20}$$

There is also a subleading term, in the large–N_C expansion, that comes from one–loop diagrams involving the $\mathcal{O}(p^4)$ chiral Lagrangian. However it only affects $F_A(0)$ and it is zero in the chiral limit. The third correction is sub–subleading and results from two–loop diagrams evaluated with the $\mathcal{O}(p^2)$ chiral Lagrangian. The latter contributes both to $F_A(0)$ and λ_A. All local additions, $F_A^{(4)}(q^2)$ and $\lambda_A^{(6)}|_{N_C\to\infty}$, correspond to our result in Eq. (5.18), *i.e.* $N_C \to \infty$, when LECs are saturated by resonance contributions [52]. Though the full $\mathcal{O}(p^6)$ chiral result is rather cumbersome, the authors of Ref. [99] have provided a numerical expression for the renormalization scale $\mu = M_\rho$. The conclusion is that, in the chiral limit, subleading contributions to the slope are negligible. Notwithstanding it is relevant to emphasize that both χPT results of Refs. [97, 99] use models to evaluate the resonance contributions to the $\mathcal{O}(p^6)$ local terms and, accordingly, their final conclusion is tamed by this estimate.

We turn now to give our numerical results. Contrarily to what happens in the vector case, where the lightest vector resonance mass in the $N_C \to \infty$ limit is well approximated by the $\rho(770)$ mass, the axial–vector mass in that limit (M_A) differs appreciably from the lightest multiplet of these resonances, namely $a_1(1260)$. The result $M_A = \sqrt{2}\,M_V$ was obtained in Ref. [13] by imposing several short–distance constraints on the couplings of the resonance Lagrangian. Lately [68, 69] it has been noticed that the inclusion of NLO effects in the large–N_C expansion points out to

$M_A \leq \sqrt{2}\, M_V$. These results are rather different from the mass of the lightest axial–vector meson determined experimentally $M_A \simeq 1.230\,\mathrm{GeV} \simeq M_{a(1260)}$ [113] but it is important to remind that this resonance is rather wide.

Our strategy is the following: we will use the experimental value of $F_A(0)$ as given in Tab. 5.2.4 to determine M_A through Eq. (5.18); then we provide a prediction for λ_A. We find [3]:

$$M_A \,=\, 998\,(49)\,\mathrm{MeV}\,, \qquad \lambda_A \,=\, 0.0197\,(19)\,, \tag{5.21}$$

where the error stems only from the experimental uncertainty in $F_A(0)$. Notice that this result satisfies $M_A \leq \sqrt{2}\, M_V \simeq 1096\,\mathrm{MeV}$.

5.2.5 Theory versus Experiment

We are now ready to compare our results with other theoretical settings and experimental determinations. In Tab. 5.2.4 we compare our outcome for the low–energy expansion of the form factors with the one provided by $\mathcal{O}(p^6)$ χPT and the recent PIBETA published values.

As $F_V(0)$ is ruled by the Wess–Zumino anomaly all the theoretical results agree for this parameter. Leading corrections to this value are driven by the pion mass and as a result happen to be tiny [42]. This is also reflected in the excellent comparison with the experimental determination. The agreement is also good for the slope of the vector form factor, considering the large error of the experimental value.

The axial–vector form factor does not arise a similar consensus. As indicated above χPT can only predict reliably all loop contributions [up to $\mathcal{O}(p^4)$ in the even–intrinsic–parity and $\mathcal{O}(p^6)$ in the odd–intrinsic–parity sectors] while higher order loops involve the couplings of local operators. Moreover tree–level $\mathcal{O}(p^4)$ (5.19) and $\mathcal{O}(p^6)$ (5.20) terms can only be determined in different models for resonance saturation contributions. The excellent agreement between the χPT results and the experimental determination of $F_A(0)$ is, indeed, not a major issue as the axial–vector form factor in radiative pion decay is the main phenomenological source [4] to fix the value of L_{10}^r . It happens that $F_A^{(4)}(0)$ arises from a strong cancellation between the L_9^r and L_{10}^r LECs and, in consequence, it is very sensitive to the chosen value for L_{10}^r. In terms of resonance saturation this sensitivity moves to the value of the axial–vector mass M_A input in the numerical determination. The value of $L_{10}^r \simeq -\,5.5 \times 10^{-3}$, used by Ref . [99], arises for $M_A \simeq 1\,\mathrm{GeV}$.

Our model of large–N_C gives the leading result for the axial–vector form factor parameters and there are leading Goldstone–mass driven contributions that we have not considered. In the χPT framework these $\mathcal{O}(p^6)$ corrections arise from the LECs and, a priory, it is difficult to estimate their contribution due to our lack of reliable knowledge on those low–energy couplings. However it has been pointed out [99] that

[3] It is important to notice that the value of $F_A(0)$ measured by the PIBETA experiment assumes no slope for the axial–vector form factor. We should repeat this exercise when λ_A is included.

[4] L_9^r is rather well determined from the phenomenology (squared charge radius of the pion) and its numerical value agrees nicely with resonance saturation.

the röle of LECs is unimportant in the $\mathcal{O}(p^6)$ corrections. As the subleading loop contributions are also tiny, it is concluded that λ_A is not sizeable and $F_A(0)$ is ruled by the leading $\mathcal{O}(p^4)$ contribution by far.

However using as input the experimental value of $F_A(0)$ we find a large value for λ_A. As subleading $1/N_C$ loop contributions seem to be tiny our leading result shows a clear discrepancy with the estimates of tree–level contributions performed in the chiral framework [97,99]. It would be very much interesting to have an experimental determination of λ_A in order to disentangle the different resonance models.

5.2.6 Beyond SM : Tensor form factor

As pointed out in Section 5.2.1, the history of the radiative decay of the pion accumulates a few clashes between theory and experiment. It seems though that, after the latest analysis by the PIBETA collaboration, the landscape has very much soothed. However it has become customary to investigate possible contributions beyond the Standard Model in order to appease alleged discrepancies. Between the latter the possible röle played by a tensor form factor has thoroughly been studied [103–107].

The new short–distance interaction can be written in terms of quark and lepton currents and it reads :

$$\mathcal{L}_T \;=\; \frac{G_F}{2\sqrt{2}}\, V_{ud}\, F_T\, \left[\, \bar{q}\, \sigma_{\mu\nu}\, (1-\gamma_5)\, q\, \right]\, \left[\, \bar{\ell}\, \sigma^{\mu\nu}\, (1-\gamma_5)\, \nu_\ell\, \right]\, , \tag{5.22}$$

where F_T is an adimensional parameter measuring the strength of the new interaction. Because of the identity (1.14) we can write (5.22) as :

$$\mathcal{L}_T \;=\; -\,\frac{G_F}{\sqrt{2}}\, V_{ud}\, F_T\, \left[\, \bar{q}\, \sigma_{\mu\nu}\, \gamma_5\, q\, \right]\, \left[\, \bar{\ell}\, \sigma^{\mu\nu}\, (1-\gamma_5)\, \nu_\ell\, \right]\, . \tag{5.23}$$

In the Standard Model the later structure, a tensor–like quark–lepton interaction, arises from loop corrections to the tree–level amplitudes and gives a tiny value for $F_T \sim 10^{-8}$ [104]. More sizeable contributions could come from New Physics models. Leptoquark exchanges, for instance, could give $F_T \sim 10^{-3}$ [105], while SUSY contributions provide $F_T \sim 10^{-4} - 10^{-5}$ [104] for light supersymmetric partners.

The hadronization of the tensor current, at very low transfer of momenta, is driven by the constant f_T defined by :

$$\left\langle \gamma \,|\, \bar{u}\, \sigma_{\mu\nu}\, \gamma_5\, d \,|\, \pi^- \right\rangle \;=\; -\,\frac{e}{2}\, f_T\, (p_\mu\, \epsilon_\nu - p_\nu\, \epsilon_\mu)\, , \tag{5.24}$$

where p is the photon momentum [5]. The determination of f_T involves QCD in its non–perturbative regime and, consequently, is a non–trivial task. We will come back to this issue in the next Subsection.

[5] There is in fact another Lorentz structure contributing to this matrix element but it carries higher orders in momenta. If the latter is included f_T acquires a dependence in the squared of the transferred momenta, *i.e.* $f_T(q^2)$. See Section 5.2.8 for a detailed evaluation of both form factors.

$E_{e^+}^{\min}$	$E_{\gamma}^{\min}$	$\theta_{e\gamma}^{\min}$	exp	no slopes	with slopes	$SU(2)$	$SU(3)$
50	50	–	2.614(21)	2.78(38)	2.81(38)	2.46(35)	2.72(38)
10	50	40°	14.46(22)	14.81(54)	15.08(58)	14.73(53)	15.00(37)
50	10	40°	37.69(46)	37.69(98)	38.41(103)	37.51(94)	38.17(103)

Table 5.2: Comparison of the theoretical predictions and the experimental data for $\mathcal{R}_Q = 10^8\, R_Q$ for constant form factors and different predictions of the q^2 dependence. All energies are measured in MeV.

It is possible to obtain the product $\mathcal{T} = F_T\, f_T$ from the analyses of different processes. Hence from some previous discrepancy in the $\pi \to e\,\nu_e\gamma$ process it is found that $\mathcal{T}_\pi = -\,(5.6 \pm 1.7) \times 10^{-3}$ [103], while from the introduction of a Gamow–Teller term in the amplitude of nuclear β–decay [108] gives $\mathcal{T}_N = (1.8 \pm 1.7) \times 10^{-3}$.

5.2.7 $\langle$VT$\rangle$ Green function: the tensor form factor

If we want to extract information on the value of F_T from experimental data, we need a reliable QCD–based determination of the hadronic tensor form factor. Using LSZ and at leading order in the pion mass we can express the matrix element (5.24) as follows [6]:

$$\left\langle \gamma \,|\, \bar{u}\,\sigma_{\mu\nu}\,\gamma_5\, d\,|\,\pi^-\right\rangle = \frac{i}{\sqrt{2}\,F}\left\langle \gamma \,\middle|\, \bar{u}\,\sigma_{\mu\nu}\,u + \bar{d}\,\sigma_{\mu\nu}\,d \,\middle|\, 0\right\rangle = -\,i\,\frac{\sqrt{2}\,e}{3\,F}\,\Pi_{VT}(0)(p_\mu\,\epsilon_\nu - p_\nu\,\epsilon_\mu), \tag{5.25}$$

where in the last step we have used again the LSZ reduction formula applied to the $\langle VT\rangle$ correlator. Then we have:

$$f_T \;=\; i\,\frac{2\sqrt{2}}{3\,F}\,\Pi_{VT}(0)\,. \tag{5.26}$$

The correlator has been calculated in Chapter 4 and after imposing matching to the OPE result we get:

$$\Pi_{VT}(q^2) \;=\; -\,i\,\frac{B_0\,F^2}{M_V^2 - q^2}\,. \tag{5.27}$$

Using Eq. (5.27) in Eq. (5.26) yields:

$$f_T \;=\; \frac{2\sqrt{2}\,B_0\,F}{3\,M_V^2}\,. \tag{5.28}$$

An educated guess can be obtained by writing $B_0\,F \;=\; -\,\langle\bar{q}q\rangle_0\,/F$ and using the estimate $\left\langle\bar{\psi}\psi\right\rangle_0(1\,\mathrm{GeV}) = -\,(242 \pm 15\,\mathrm{MeV})^3$ [76].

[6] See Appendix A.2 for a derivation of this expression.

Another parameter of interest is the susceptibility of the quark condensate χ_z defined by the vacuum expectation value of the tensor current in the presence of an external source $Z_{\mu\nu}$ [114, 115]:

$$\langle\, 0 \,|\, \bar{q}\, \sigma_{\mu\nu}\, q \,|\, 0 \,\rangle_Z \;=\; g_\psi\, \chi_z\, \langle \bar{q} q \rangle_0\; Z_{\mu\nu}\,. \tag{5.29}$$

In our case we consider the magnetic susceptibility χ given by an external electromagnetic field as:

$$\left\langle\, \gamma \,|\, \bar{u}\, \sigma_{\mu\nu}\, u + \bar{d}\, \sigma_{\mu\nu}\, d \,|\, 0 \,\right\rangle \;=\; -\, i\, e\, (e_u + e_d)\; \chi\; \langle \bar{q} q \rangle_0\; F_{\mu\nu}\,, \tag{5.30}$$

with $e_u = 2/3$ and $e_d = -\,1/3$. Using the first equality of Eq. (5.25) we get:

$$f_T \;=\; -\,\frac{\sqrt{2}}{3}\,\chi\, B_0 F\,, \tag{5.31}$$

and comparing with Eq. (5.28) we obtain:

$$\chi \;=\; -\,\frac{2}{M_V^2} \;\simeq\; -\,3.3\,\mathrm{GeV}^{-2}\,. \tag{5.32}$$

There are several determinations of the magnetic susceptibility that provide a range that runs from $\chi = -\,(8.16 \pm 0.41)\,\mathrm{GeV}^{-2}$ [114] up to $\chi \simeq -\,2.7\,\mathrm{GeV}^{-2}$ [77].

5.2.8 q^2–dependence of the tensor form factor

As mentioned in Section 5.2.7 there are two form factors involved in the hadronic tensor matrix element

$$\begin{aligned}\left\langle\, \gamma \,|\, \bar{u}\, \sigma_{\mu\nu}\, \gamma_5\, d \,|\, \pi^- \right\rangle \;&=\; -\,\frac{e}{2}\, f_T(q^2)\, (p_\mu\, \epsilon_\nu - p_\nu\, \epsilon_\mu) \\ &\quad -\,\frac{e}{2}\, g_T(q^2)\, [\, \epsilon \cdot q\, (p^\mu\, q^\nu - p^\nu\, q^\mu) + q \cdot p\, (q^\mu\, \epsilon^\nu - q^\nu\, \epsilon^\mu)]\,,\end{aligned} \tag{5.33}$$

where p is the photon momentum and q the transferred momentum by the tensor current. To generate the second Lorentz structure one needs operators of higher order in the chiral expansion, such as

$$Y_{93} \;=\; \langle \nabla_\mu t_+^{\mu\nu}\, \nabla^\alpha f_{+\alpha\nu} \rangle\,, \tag{5.34}$$

of Ref. [23] that can be found in Appendix B. In the framework of resonance chiral theory one needs in addition of the operators in (2.24) the basis of odd–intrinsic–parity operators of Eqs. (2.34) and (2.35). These new contributions do not modify result of the $f_T = f_T(0)$. The result reads:

$$f_T(q^2) \;=\; \frac{\sqrt{2}\, F_V^T}{3\, F\, M_V} \left\{ 2\, F_V - \left[4\sqrt{2}\, M_V\, (c_1 - c_2 - c_5 + 2c_6) + 8\, F_V\, d_3\, \frac{q^2}{M_V^2 - q^2} \right] \right\}\,,$$

$$g_T(q^2) = \frac{8\,F_V^T}{3\,F\,M_V^2}\left[\frac{2\,M_V^2-q^2}{M_V^2-q^2}(c_1-c_2-c_5)+2\,\frac{M_V^2}{M_V^2-q^2}\,c_6-2\,c_7 + \sqrt{2}\,\frac{F_V}{M_V}\left(\frac{M_V^2}{M_V^2-q^2}\,d_3+d_4\right)\right]. \quad (5.35)$$

The spectral function of the tensor–tensor currents correlator to which the amplitude in Eq. (5.33) contributes behaves as a constant at high q^2 and leading order in α_s [81]. Hence the $f_T(q^2)$ and $g_T(q^2)$ form factor should exhibit a smooth behaviour, vanishing at large transferred momentum.

Imposing that the $f_T(q^2)$ form factor vanishes at large momentum we get the constraint:

$$c_1-c_2-c_5-2\,c_6 = -\frac{\sqrt{2}}{4}\frac{F_V}{M_V}\,(1+4\,d_3)\,. \quad (5.36)$$

The same procedure with $g_T(q^2)$ gives:

$$c_1-c_2-c_5-2\,c_7 = -\sqrt{2}\,\frac{F_V}{M_V}\,d_4\,. \quad (5.37)$$

Interestingly enough these constraints fully determine both form factors:

$$f_T(q^2) = \frac{2\sqrt{2}\,F_V^T\,F_V}{3\,F}\,\frac{M_V}{M_V^2-q^2}\,,$$
$$g_T(q^2) = -\,\frac{f_T(q^2)}{M_V^2}\,. \quad (5.38)$$

Notice that the contribution of the $g_T(q^2)$ form factor to the matrix element under study is fairly suppressed, typically $\mathcal{O}(q^2/M_V^2)$ over the $f_T(q^2)$ contribution.

5.2.9 Lattice data and sum rules

The last years have witnessed and increasing attention to the determination of matrix elements of tensor quark currents. For instance, together with the QCD sum rules technique [77, 78], lattice has also performed evaluations of amplitudes involving the tensor current and a vector resonance [79, 80].

The F_V coupling can be obtained from the measured $\Gamma(\rho^0\to e^+e^-)$ [112]. We obtain $F_V \simeq 156\,\text{MeV}$ with an expected tiny error[7]. Then from Eq. (4.128) and using the value of the quark condensate quoted above we get:

$$F_V^T\,(1\,\text{GeV}) = 117\pm 22\,\text{MeV}\,, \quad (5.39)$$

[7] The vector coupling can also be determined from short–distance analyses within resonance theory [52], giving $f_V^2 = 2\frac{F^2M_A^2}{M_A^2-M_V^2}$, that translates into $f_V = 207\,(15)\,\text{MeV}$ for $M_A = 998\,(49)\,\text{MeV}$ (5.21), in excellent agreement with the quoted phenomenological result.

where the error collects only the uncertainty in the value of $\langle\bar{\psi}\psi\rangle_0$. Our result is in excellent agreement with those coming from QCD sum rules : $F_\rho^T = 113(7)$ MeV [77] and $F_\rho^T = 111(4)$ MeV [78].

Lattice evaluations determine the ratio with the vector coupling. From our results we get

$$\frac{F_V^T}{F_V}(1\,\mathrm{GeV}) \;=\; 0.75 \pm 0.14\,, \tag{5.40}$$

to be compared with the quenched value [79, 80], run down to $\mu = 1$ GeV :

$$\frac{F_\rho^T}{F_\rho}(1\,\mathrm{GeV}) \;=\; 0.74 \pm 0.03\,. \tag{5.41}$$

Finally from the later result and the phenomenological value of F_V lattice provides the determination :

$$F_\rho^T\,(1\,\mathrm{GeV}) \;=\; 164 \pm 7\,\mathrm{MeV}\,, \tag{5.42}$$

to compare with our figure in Eq. (5.39).

5.2.10 Analysis of the photon spectrum in the radiative pion decay

The PIBETA experiment has thoroughly measured the photon spectrum in the radiative decay of the pion [100]. Though the results of that reference seemed to confirm a serious discrepancy with theoretical determinations, an ensuing analysis of more data and the refinement of systematic errors [101, 109] has brought a close agreement between Theory and Experiment.

The experimental available data amounts to the branching ratio of the radiative pion decay integrated in different subregions (Q) of the final state phase space :

$$R_Q \;=\; \frac{1}{\Gamma_{\pi\to e\,\nu}} \int_Q dQ_3 \sum_\lambda |\mathcal{M}(E_e, E_\nu)|^2\;, \tag{5.43}$$

where the sum runs over the polarizations of the final particles. The three regions and the experimental results are shown in Tab. 5.2.

We test the predictions ruled by our determination for the hadronic form factors with the experimental data, ignoring first a possible tensor interaction, and compare them with other theoretical settings. In order to achieve the accuracy required by the experimental information higher order radiative corrections to the decay [116] must be included and they have been implemented in our analysis. The numerical input for vector and axial–vector form factors is given in Tab. 5.2.4.

In the fourth column of Tab. 5.2 the latest experimental data are given; in the fifth and sixth we show the results provided by our analysis. We study the numerical impact of the momenta dependence of the form factors by setting the slopes to zero

and we conclude that it is tiny : the q^2 dependence tends to increase the central value of R but the modification is by far within the errors. The last two columns bring the results yielded by two– and three–flavour two–loop χPT calculations. The evaluation of the errors for the theoretical predictions is ruled by those in the form factors. The estimate of the latter has been done in the following way : we assume no error coming from the slopes (since their numerical impact is very poor); to the vector form factor we assign the same error as that of the experimental determination $\sim 7\%$ and to the axial–vector form factor we attach the error of the experimental input. Finally the error given for the χPT calculations only considers the scale dependence that is a tiny 5%.

We conclude then that the corrections induced by the q^2 dependence of vector and axial–vector form factors are numerically negligible unless the theoretical error is reduced. For this we would need a better determination of vector and, specially, axial–vector form factors at $q^2 = 0$. When comparing our results with experimental data, we see that our predictions are in agreement with previous estimates.

As a final exercise we use the experimental data to fit the value of $\mathcal{T} = F_T f_T$ defined above. In order to reach this purpose we use the experimentally fitted values for the hadronic inputs $F_V(0)$ and $F_A(0)$, and our results for the slopes λ_V and λ_A. Finally, to extract the value of the F_T coupling from the fit, we use our determination for the tensor form factor f_T. The value that we obtain is compatible with zero and its order of magnitude is compatible with that dictated by SUSY :

$$F_T \;=\; (1 \pm 14) \times 10^{-4} \,. \tag{5.44}$$

5.2.11 Conclusions

Radiative pion decay has been a continuous source of debate between theoretical predictions and experimental determinations. Nevertheless the latest analysis by the PIBETA Collaboration seems to bring a close agreement between both sides.

In this thesis we have performed a detailed analysis of the structure–dependent amplitudes contributing to $\pi \to e\,\nu_e\gamma$. The q^2 dependence of vector and axial–vector form factors, driven by the Standard Model, has been rigorously constructed through the study of the $\langle VVP\rangle$ and $\langle VAP\rangle$ GFs, by matching meromorphic *ansätze* with their leading OPE contributions. Moreover we have also required that our form factors are soft at high transfer of momenta. Hence we obtain the most general (and simple) functions that satisfy all those constraints. The appropriate structure of the form factors requires a double vector resonance pole for the vector form factor and a single axial–vector resonance pole for the axial–vector form factor. After a small momenta expansion we compare our results with those of χPT and while in the vector sector we find complete agreement, our slope for the axial–vector form factor is much larger than the one provided by modelizations of local terms in the chiral framework.

The röle of a tensor contribution to the radiative pion decay has customarily been taken into account in order to analyse the experimental results. We use those

in order to fix the size of the contribution and we find that it is compatible with zero. Incidentally we have given a prediction for F_V^T that measures the coupling of a vector resonance $J^{PC} = 1^{--}$ to the tensor current. Our results agree well with determinations from QCD sum rules and quenched lattice.

We conclude that the Standard Model is able to embody the experimentally known features of the radiative pion decay. As it happens with other decays involving non–perturbative strong effects, the rather large size of the numerical incertitudes generated by our lack of knowledge of this QCD regime shows that this process is, at present, unsuitable for the search of New Physics.

5.3 V_{us} from hyperon semileptonic decay

5.3.1 Introduction

Accurate determinations of the quark mixing parameters are of fundamental importance to test the flavour structure of the Standard Model. In particular, the unitarity of the CKM matrix [94, 95] has been tested to the 0.2% level [3, 117] with the precise measurement of its first–row entries $|V_{ud}|$ and $|V_{us}|$ [119]. At that level of precision, a good control of systematic uncertainties becomes mandatory. In fact, the existence of small deviations from unitarity has been a long–standing question for many years [120].

Recently, there have been many relevant changes to this unitarity test, which have motivated a very alive discussion. While the standard $|V_{ud}|$ determination from superallowed nuclear beta decays remains stable, $|V_{ud}| = 0.97418 \pm 0.00026$ [117], the information from neutron decay is suffering strong fluctuations, due to conflicting data on the axial coupling g_A measured through decay asymmetries [112] and the large decrease of the neutron lifetime by more than $6\,\sigma$ obtained in the most recent precision measurement [121].

On the other side, the $K \to \pi\, l\, \nu$ branching ratios have been found to be significantly larger than the previously quoted world averages. Taking into account the recently improved calculation of radiative and isospin–breaking corrections [122–124], the new experimental data from BNL–E865 [125], KTeV [126], NA48 [127] and KLOE [128] imply [129].

$$|V_{us}\, f_+^{K^0\pi^-}(0)| \;=\; 0.21661 \pm 0.00047\,. \tag{5.45}$$

In the $SU(3)_V$ limit, vector current conservation guarantees that the K_{l3} form factor $f_+^{K^0\pi^-}(0)$ is equal to one. Moreover, the Ademollo–Gatto theorem [130, 131] states that corrections to this result are at least of second order in $SU(3)$ breaking. They were calculated long time ago, at $O(p^4)$ in Chiral Perturbation Theory, by Leutwyler and Roos [132] with the result $f_+^{K^0\pi^-}(0) = 0.961 \pm 0.008$. Using the calculated two–loop chiral corrections [133, 134], two recent estimates of the $O(p^6)$ contributions obtain the updated values $f_+^{K^0\pi^-}(0) = 0.974 \pm 0.011$ [135] and $f_+^{K^0\pi^-}(0) = 0.984 \pm 0.012$ [53], while a lattice simulation in the quenched approximation gives the result

$f_+^{K^0\pi^-}(0) = 0.960 \pm 0.005_{\rm stat} \pm 0.007_{\rm syst}$ [136] (the quoted lattice systematic error does not account for quenching effects, which are unfortunately unknown). Taking $f_+^{K^0\pi^-}(0) = 0.974 \pm 0.012$, one derives from K_{l3} :

$$|V_{us}| \;=\; 0.2233 \pm 0.0028\,. \tag{5.46}$$

An independent determination of $|V_{us}|$ can be obtained from the Cabibbo–suppressed hadronic decays of the τ lepton [137]. The present data implies [138] $|V_{us}| = 0.2208 \pm 0.0034$. The uncertainty is dominated by experimental errors in the τ decay distribution and it is expected to be significantly improved at the B factories. $|V_{us}|$ can be also determined from $\Gamma(K^+ \to \mu^+\nu_\mu)/\Gamma(\pi^+ \to \mu^+\nu_\mu)$ [139], using the lattice evaluation of the ratio of decay constants f_K/f_π [140]; one gets $|V_{us}| = 0.2219 \pm 0.0025$.

The $|V_{us}|$ determination from hyperon decays is supposed to be affected by larger theoretical uncertainties, because the axial–vector form factors contributing to the relevant baryonic matrix elements are not protected by the Ademollo–Gatto theorem. Thus, it suffers from first–order $SU(3)_V$ breaking corrections. Moreover, the second–order corrections to the leading vector–current contribution are badly known. In spite of that, two recent analyses of the hyperon decay data claim accuracies which, surprisingly, are competitive with the previous determinations :

$$|V_{us}| \;=\; 0.2250 \pm 0.0027\,, \qquad \text{Ref. [141]} \tag{5.47}$$

$$|V_{us}| \;=\; 0.2199 \pm 0.0026\,, \qquad \text{Ref. [142]} \tag{5.48}$$

Although they use basically the same data, the two analyses result in rather different central values for $|V_{us}|$ and obtain a qualitatively different conclusion on the pattern of $SU(3)$ violations. While the fit of Ref. [141] finds no indication of $SU(3)_V$ breaking effects in the data, Ref. [142] claims sizeable second–order symmetry breaking contributions which increase the vector form factors over their $SU(3)_V$ predictions. Clearly, systematic uncertainties seem to be underestimated.

In order to clarify the situation, we have performed a new numerical analysis [143] of the semileptonic hyperon decay data, trying to understand the differences between the results (5.47) and (5.48).

5.3.2 Theoretical Description of Hyperon Semileptonic Decays

The semileptonic decay of a spin–$\frac{1}{2}$ hyperon, $B_1 \to B_2\, l^-\bar\nu_l$, involves the hadronic matrix elements of the vector and axial–vector currents :

$$\begin{aligned}
\langle B_2(p_2)|\, V^\mu\, |B_1(p_1)\rangle &= \bar u(p_2)\left[f_1(q^2)\,\gamma^\mu + i\,\frac{f_2(q^2)}{M_{B_1}}\,\sigma^{\mu\nu}q_\nu + \frac{f_3(q^2)}{M_{B_1}}\,q^\mu\right] u(p_1)\,, \\
\langle B_2(p_2)|\, A^\mu\, |B_1(p_1)\rangle &= \bar u(p_2)\left[g_1(q^2)\,\gamma^\mu + i\,\frac{g_2(q^2)}{M_{B_1}}\,\sigma^{\mu\nu}q_\nu + \frac{g_3(q^2)}{M_{B_1}}\,q^\mu\right] \gamma_5\, u(p_1)\,,
\end{aligned} \tag{5.49}$$

$B_1 \to B_2$	$n \to p$	$\Lambda \to p$	$\Sigma^- \to n$	$\Xi^- \to \Lambda$	$\Xi^- \to \Sigma^0$	$\Xi^0 \to \Sigma^+$
$C_F^{B_2 B_1}$	1	$-\sqrt{\frac{3}{2}}$	-1	$\sqrt{\frac{3}{2}}$	$\frac{1}{\sqrt{2}}$	1
$C_D^{B_2 B_1}$	1	$-\frac{1}{\sqrt{6}}$	1	$-\frac{1}{\sqrt{6}}$	$\frac{1}{\sqrt{2}}$	1

Table 5.3: Clebsh–Gordan coefficients for octet baryon decays.

where $q = p_1 - p_2$ is the four–momentum transfer. Since the corresponding $V - A$ leptonic current satisfies $q^\mu L_\mu \sim m_l$, the contribution of the form factors $f_3(q^2)$ and $g_3(q^2)$ to the decay amplitude is suppressed by the charged lepton mass m_l. Therefore, these two form factors can be safely neglected in the electronic decays which we are going to consider.

In the limit of exact $SU(3)_V$ symmetry, we can use the Clebsh–Gordan theorem

$$\left\langle B^a \left| \mathcal{J}^b \right| B^c \right\rangle \, = \, F_{\mathcal{J}} \, f_{abc} \, + \, D_{\mathcal{J}} \, d_{abc} \, , \tag{5.50}$$

and then the current matrix elements among the different members of the baryon octet are related [144]:

$$\begin{aligned} f_k^{\rm sym}(q^2) \;\; &= \;\; C_F^{B_2 B_1} \, F_k(q^2) \, + \, C_D^{B_2 B_1} \, D_k(q^2) \, , \\ g_k^{\rm sym}(q^2) \;\; &= \;\; C_F^{B_2 B_1} \, F_{k+3}(q^2) \, + \, C_D^{B_2 B_1} \, D_{k+3}(q^2) \, , \end{aligned} \tag{5.51}$$

where $F_k(q^2)$ and $D_k(q^2)$ are reduced form factors and $C_F^{B_2 B_1}$ and $C_D^{B_2 B_1}$ are well–known Clebsh–Gordan coefficients. The conservation of the vector current implies $F_3(q^2) = D_3(q^2) = 0$. Moreover, the electromagnetic current belongs to the same octet of vector currents, and from general principles such as Lorentz and gauge invariance it is known that

$$\left\langle \, b \, \right| J^\mu_{\rm em} \left| \, B \, \right\rangle \, = \, \overline{u}_b(p_b) \left[F_1(q^2) \, \gamma^\mu + \frac{i \, F_2(q^2) \, \sigma^{\mu\nu}}{2 \, m_B} \, q_\nu \right] u_B(p_B) \, , \tag{5.52}$$

with $F_1(0) = Q_{\rm em}$ and $2\,F_2(0) = g_\mu - 2$. Then the values at $q^2 = 0$ of the vector form factors are determined by the electric charges and the anomalous magnetic moments of the two nucleons, $\mu_p = 1.792847351\,(28)$ and $\mu_n = -\,1.9130427\,(5)$ [112]:

$$F_1(0) = 1 \, , \quad D_1(0) = 0 \, , \quad F_2(0) = - \left(\mu_p + \frac{1}{2} \, \mu_n \right) \, , \quad D_2(0) = \frac{3}{2} \, \mu_n \, . \tag{5.53}$$

The values at $q^2 = 0$ of the two reduced form factors determining $g_1(q^2)$ are the usual F and D parameters: $F_4(0) = F$, $D_4(0) = D$. $SU(3)_V$ symmetry also implies a vanishing "weak–electricity" form factor $g_2(q^2)$, because charge conjugation does not allow a $\mathcal{C}$–odd g_2 term in the matrix elements of the neutral axial–vector currents A^3_μ and A^8_μ, which are $\mathcal{C}$–even.

The available kinematic phase space is bounded by $m_e^2 \leq q^2 \leq (M_{B_1} - M_{B_2})^2$. Thus, q^2 is a parametrically small $SU(3)$ breaking effect. Since the form factor $f_2(q^2)$ appears multiplied by a factor q_ν, it gives a small contribution to the decay rate. To $O(q^2)$ accuracy, which seems sufficient to analyse the current data, the only momentum dependence which needs to be taken into account is the one of the leading form factors $f_1(q^2)$ and $g_1(q^2)$:

$$f_1(q^2) \approx f_1(0) \left(1 + \lambda_1^f \frac{q^2}{M_{B_1}^2}\right), \qquad g_1(q^2) \approx g_1(0) \left(1 + \lambda_1^g \frac{q^2}{M_{B_1}^2}\right). \quad (5.54)$$

Moreover, $f_2(0)$ and $g_2(0)$ can be fixed to their $SU(3)_V$ values, because any deviations from the symmetry limit would give a second–order symmetry breaking effect. Therefore, the form factor $g_2(q^2)$ can be neglected.

The slopes λ_1^f and λ_1^g are usually fixed assuming a dipole form regulated by the mesonic resonance with the appropriate quantum numbers [145,146]:

$$\begin{aligned} f_1(q^2) &= \frac{f_1(0)}{\left(1 - \frac{q^2}{M_V^2}\right)^2}, \quad \lambda_1^f = \frac{2M_{B_1}^2}{M_V^2}, \\ g_1(q^2) &= \frac{g_1(0)}{\left(1 - \frac{q^2}{M_A^2}\right)^2}, \quad \lambda_1^g = \frac{2M_{B_1}^2}{M_A^2}. \end{aligned} \quad (5.55)$$

Previous analyses have adopted the mass values $M_V = 0.97$ GeV [141,142,144–146] and $M_A = 1.25$ GeV [141,145] or $M_A = 1.11$ GeV [142,144,146]. We will analyse the systematic uncertainties associated with these inputs.

It is useful to define the ratio of the physical value of $f_1(0)$ over the $SU(3)_V$ prediction $C_F^{B_2B_1}$:

$$\tilde{f}_1 = f_1(0)/C_F^{B_2B_1} = 1 + \mathcal{O}(\epsilon^2). \quad (5.56)$$

Due to the Ademollo–Gatto theorem [130,131], $\tilde{f}_1$ is equal to one up to second–order $SU(3)$ breaking effects.

The transition amplitudes for hyperon semileptonic decays have been extensively studied, using standard techniques. We will not repeat the detailed expressions of the different observables, which can be found in Refs. [142,145–147]. In order to make a precision determination of $|V_{us}|$, one needs to include the effect of radiative corrections [146,148–150]. To the present level of experimental precision, the measured angular correlation and angular spin–asymmetry coefficients are unaffected by higher–order electroweak contributions. However, these corrections are sizeable in the total decay rates. To a very good approximation, their effect can be taken into account as a global correction to the partial decay widths: $\Gamma \sim G_F^2 |V_{us}|^2 (1 + \delta_{\rm RC})$. The Fermi coupling measured in μ decay, $G_F = 1.16637\,(1) \cdot 10^{-5}$ GeV^{-2} [112], absorbs some common radiative contributions. The numerical values of the remaining corrections $\delta_{\rm RC}$ can be obtained from Ref. [146].

5.3.3 The Ademollo–Gatto theorem

Before studing the $SU(3)_V$ breaking effects in the $1/N_C$ framework, it is convenient to discuss a general theorem that will give us hints about the symmetry breaking pattern. It is known as the Ademollo–Gatto theorem and it applies to vector currents, not only in the hyperon sector, but also for mesons.

As already discussed in Chapter 1, the symmetry breaking effects come entirely from the mass difference between the up/down quark (that will be regarded as degenerate) and the strange quark. We can write the quark mass matrix (denoting $m_u = m_d \equiv \hat{m}$) as

$$\mathcal{M} \,=\, \frac{1}{3}\,(m_s + \hat{m})\,\mathbb{1} \,+\, \frac{1}{\sqrt{3}}\,(m_s + \hat{m})\,\frac{\lambda^8}{2}\,, \tag{5.57}$$

where the first term is symmetry conserving [an $SU(3)_V$ singlet] and the second one is symmetry violating, and transforms as an octet (adjoint representation). Moreover, it is proportional to the flavour generator T^8. The adimensional parameter ϵ giving the order of the symmetry breaking can be estimated as

$$\epsilon \,\sim\, \frac{m_s}{\Lambda_{\rm QCD}} \sim \frac{1}{3}\,. \tag{5.58}$$

Using the commutation relations for the vector charges mediating $\Delta S = 1$ transitions at equal times we get

$$\begin{aligned} \left[Q^{4+i\,5}, Q^{4-i\,5}\right] \;&=\; Q^3 + \sqrt{3}\,Q^8 = Q^{\rm em} + Y\,, \\ Y \;&=\; \frac{2}{\sqrt{3}}\,Q^8\,, \end{aligned} \tag{5.59}$$

where Y corresponds to the hypercharge operator. Since $\partial^\mu V^{3,8}_\mu = 0$ even for different quark masses, the right–hand side, and correspondingly the left–hand side, are time independent. Let us take the matrix element of Eq. (5.59) for a spin–$\frac{1}{2}$ baryon B with mass m_B and three–momentum $\vec{p}_B$

$$\begin{aligned} &\left(Q^{\rm em} + Y\right)_B \langle B(p_B)\,|B(p_B)\rangle \,= \\ &-\left|\langle\, b\,|Q^{4+i\,5}|B(p_B)\rangle\right|^2 \,+\, \sum_m{}^{\!\sim}\, \left|\langle\, m\,|Q^{4-i\,5}|B(p_B)\rangle\right|^2 - \sum_n{}^{\!\sim}\, \left|\langle\, n\,|Q^{4+i\,5}|B(p_B)\rangle\right|^2 \\ &\qquad\qquad =\, -\left|\langle\, b\,|Q^{4+i\,5}|B(p_B)\rangle\right|^2 + \mathcal{O}(\epsilon^2)\,, \end{aligned} \tag{5.60}$$

where b is the only octet baryon connected to B through $Q^{4+i\,5}$, and m, n are decuplet baryons. The second and third terms of Eq. (5.60) are $\mathcal{O}(\epsilon^2)$, because in the exact $SU(3)$ limit $\langle\, n\,|Q^{4+i\,5}|B(p_B)\rangle = 0$, and so it must be $\mathcal{O}(\epsilon)$. The covariant normalization for particles reads

$$\langle B(p_B)\,|\,B(p_B)\rangle \,=\, 2\,E_B(2\,\pi)^3\,\delta^{(3)}(0)\,, \tag{5.61}$$

and will be used latter. From the first term in Eq. (5.60) we get

$$\begin{aligned}
\langle\, b,p,\lambda\,|Q^{4+i5}|B(p_B)\rangle \;&=\; \int \mathrm{d}^3\vec{x}\,\langle\, b,p,\lambda\,|\,\overline{u}(x)\,\gamma^0\,s(x)\,|B(p_B)\rangle \\
&= \int \mathrm{d}^3\vec{x}\,\langle\, b,p,\lambda\,|\,e^{iP\cdot x}\,\overline{u}(0)\,\gamma^0\,s(0)\,e^{-iP\cdot x}\,|B(p_B)\rangle \\
&= \int \mathrm{d}^3\vec{x}\,e^{iq\cdot x}\langle\, b,p,\lambda\,|\,\overline{u}(0)\,\gamma^0\,s(0)\,|B(p_B)\rangle \\
&= \int \mathrm{d}^3\vec{x}\,e^{iq\cdot x}\,\overline{u}(p,\lambda)\left[f_1(q^2)\,\gamma^0 + \frac{i\,f_2(q^2)\sigma^{0\nu}}{2m_B}\,q_\nu + \frac{f_3(q^2)}{m_B}\,q^0\right]u(p_B) \\
&= (2\,\pi)^3\delta^{(3)}(\vec{q})\,\overline{u}(p,\lambda)\left[f_1(q_0^2)\,\gamma^0 + \frac{f_3(q_0^2)}{m_B}\,q^0\right]u(p_B) \\
&\doteq (2\,\pi)^3\delta^{(3)}(\vec{q})\,f_1(q_0^2)\,u^\dagger(p,\lambda)\,u(p_B) + \mathcal{O}(\epsilon^2)\,. \qquad (5.62)
\end{aligned}$$

where we drop the f_3 factor because it is $\mathcal{O}(\epsilon)$ and as we will see $q^0 \sim \mathcal{O}(\epsilon)$. Lorentz invariance enforces $q^2 = (q^0)^2$ in the rest frame of the baryons. With that, summing over polarizations and integrating over the phase space we obtain

$$\begin{aligned}
&\sum_\lambda \int \frac{\mathrm{d}^3\vec{p}}{(2\,\pi)^3 2\,E}\left|\langle\, b,p,\lambda\,|\,Q^{4+i5}\,|B(p_B)\rangle\right|^2 \\
&= \sum_\lambda \int \frac{\mathrm{d}^3\vec{p}}{2\,E}\,(2\pi)^3\,\delta^{(3)}(\vec{q})\,\delta^{(3)}(\vec{q})\,f_1^2(q^2)\,\overline{u}(p_B)\,\gamma^0\,u(p,\lambda)\,\overline{u}(p,\lambda)\,\gamma^0\,u(p_B) \\
&= \int \frac{\mathrm{d}^3\vec{p}}{2\,E}\,(2\,\pi)^3\,\delta^{(3)}(\vec{q})\,\delta^{(3)}(\vec{0})\,f_1^2(q^2)\,\overline{u}(p_B)\,(\not{p}^\dagger\; + m_b)\,u(p_B) \\
&= \int \frac{\mathrm{d}^3\vec{p}}{2\,E}\,(2\,\pi)^3\,\delta^{(3)}(\vec{q})\,\delta^{(3)}(\vec{0})\,f_1^2(q^2)\,\overline{u}(p_B)\left\{(E_B+E)\gamma^0 + (m_b - m_B)\right]u(p_B)\,, \\
&= \frac{(2\,\pi)^3}{E_b}\,\delta^{(3)}(\vec{0})\left[E_B(E_B+E_b) + m_B(m_b-m_B)\right]\,, \qquad (5.63)
\end{aligned}$$

where we understand $E_B = \sqrt{\vec{p}_B^{\,2} + m_B^2}$, $E = \sqrt{\vec{p}^{\,2} + m_b^2}$ and $E_b = \sqrt{\vec{p}_B^{\,2} + m_b^2}$. We have used

$$\begin{aligned}
\not{p}_b \;&=\; E\,\gamma^0 \;-\; \vec{p_b}\cdot\vec{\gamma}\,, \\
\not{p}_b^\dagger \;&=\; E\,\gamma^0 \;+\; \vec{p_b}\cdot\vec{\gamma}\,, \\
\left(E_B\,\gamma^0 \;-\; \vec{p_B}\cdot\vec{\gamma}\right)u(p_B) \;&=\; m_B\,u(p_B)\,. \qquad (5.64)
\end{aligned}$$

We will consider the phenomenologically interesting rest frame of the B baryon $\vec{p}_B = 0$, and hence $E_B = m_B$, $E_b = m_b$. In this frame $q^2 = (q^0)^2 = (m_B - m_b)^2 \sim \mathcal{O}(\epsilon^2)$. Eq. (5.63) reduces to

$$\sum_\lambda \int \frac{\mathrm{d}^3\vec{p}}{(2\,\pi)^3 2\,E}\left|\langle\, b,p,\lambda\,|\,Q^{4+i5}\,|B(p_B)\rangle\right|^2 \;=\; 2\,m_B(2\pi)^3\delta^{(3)}(\vec{0})\,f_1^2(0) + \mathcal{O}(\epsilon^2)\,. \qquad (5.65)$$

	$\Lambda \to p\, e^- \overline{\nu}_e$	$\Sigma^- \to n\, e^- \overline{\nu}_e$	$\Xi^- \to \Lambda\, e^- \overline{\nu}_e$	$\Xi^- \to \Sigma^0 e^- \overline{\nu}_e$	$\Xi^0 \to \Sigma^+ e^- \overline{\nu}_e$
$\mathcal{R}$	3.161 ± 0.058	6.88 ± 0.24	3.44 ± 0.19	0.53 ± 0.10	0.93 ± 0.14
$\alpha_{e\nu}$	-0.019 ± 0.013	0.347 ± 0.024	0.53 ± 0.10		
α_e	0.125 ± 0.066	-0.519 ± 0.104			
α_ν	0.821 ± 0.060	-0.230 ± 0.061			
α_B	-0.508 ± 0.065	0.509 ± 0.102			
A			0.62 ± 0.10		
g_1/f_1	0.718 ± 0.015	-0.340 ± 0.017	0.25 ± 0.05	1.287 ± 0.158	1.32 ± 0.22

Table 5.4: Experimental data on $|\Delta S| = 1$ hyperon semileptonic decays [112]. R is given in units of 10^6 s^{-1}.

Comparing Eqs. (5.60), (5.61) and (5.65) we obtain

$$f_1(0)^2 \;=\; -\,(Q^{\rm em} + Y)_B + \mathcal{O}(\epsilon^2)\,, \qquad f_1(0) \;=\; f_1^{\rm sym}(0) + \mathcal{O}(\epsilon^2)\,. \tag{5.66}$$

Last equation is equivalent to Eq. (5.56).

5.3.4 g_1/f_1 analysis

	$\Lambda \to p$	$\Sigma^- \to n$	$\Xi^- \to \Lambda$	$\Xi^0 \to \Sigma^+$
$\lvert\tilde{f}_1\, V_{us}\rvert$	0.2221 (33)	0.2274 (49)	0.2367 (97)	0.216 (33)

Table 5.5: Results for $|\tilde{f}_1\, V_{us}|$ obtained from the measured rates and $g_1(0)/f_1(0)$ ratios. The quoted errors only reflect the statistical uncertainties.

The experimentally measured observables in hyperon semileptonic decays [112] are given in Table 5.4, which collects the total decay rate R, the angular correlation coefficient $\alpha_{e\nu}$ and the angular–asymmetry coefficients α_e, α_ν, α_B, A and B. The precise definition of these quantities can be found in Refs. [145, 146]. Also given is the ratio $g_1(0)/f_1(0)$, which is determined from the measured asymmetries.

The simplest way to analyse [141] these experimental results is to use the measured values of the rates and the ratios $g_1(0)/f_1(0)$. Taking for $f_2(0)$ the $SU(3)_V$ predictions, this determines the product $|\tilde{f}_1\, V_{us}|$. Table 5.5 shows the results obtained from the four available decay modes. The differences with the values given in Ref. [141] are very small; the largest one is due to the slightly different value of the $\Xi^0 \to \Sigma^+ e^- \bar{\nu}_e$ branching ratio [151]. The four decays give consistent results (χ^2/d.o.f. = 2.52/3), which allows one (assuming a common value for $\tilde{f}_1$) to derive a combined average

$$|\tilde{f}_1\, V_{us}| \;=\; 0.2247 \pm 0.0026\,. \tag{5.67}$$

This number agrees (assuming $\tilde{f}_1 = 1$) with the value in Eq. (5.47).

The quoted uncertainty only reflects the statistical errors and does not account for the unknown $SU(3)_V$ breaking contributions to $\tilde{f}_1 - 1$, and other sources of theoretical uncertainties such as the values of $f_2(0)$ and $g_2(0)$ [$SU(3)_V$ has been assumed], or the momentum dependence of $f_1(q^2)$ and $g_1(q^2)$. We will estimate later on the size of all these effects. For the moment, let us just mention that changing the dipole ansatz for $f_1(q^2)$ and $g_1(q^2)$ to a monopole form, the central value in (5.67) increases to 0.2278, with a χ^2/d.o.f. = 3.24/3.

The agreement among the four determinations in Table 5.5 has been claimed to be a strong indication that $SU(3)_V$ breaking effects are indeed small [141]. Note, however, that first–order symmetry breaking corrections in the ratio $g_1(0)/f_1(0)$ are effectively taken into account, since we have used the experimental measurements. What Table 5.5 shows is that the fitted results are consistent, within errors, with a common $\tilde{f}_1$ value for the four hyperon decays. The deviations of $\tilde{f}_1$ from one are of second order in symmetry breaking, but unfortunately even their sign seems controversial [152–155].

5.3.5 $1/N_C$ Analysis of $SU(3)_V$ Breaking Effects

As explained in Chapter 3, the $1/N_C$ expansion of QCD provides a framework to analyse the spin–flavour structure of baryons [14, 156], which can be used to investigate the size of $SU(3)_V$ breaking effects through a combined expansion in $1/N_C$ and $SU(3)_V$ symmetry breaking. A detailed analysis, within this framework, of $SU(3)_V$ breaking in hyperon semileptonic decays was performed in Refs. [142, 144], and we performed an explicit calculation in Chapter 3, where all relevant formulae can be found. To avoid unnecessary repetition we will only show explicitly the most important ingredients which have been used in the recent $|V_{us}|$ determination of Ref. [142].

At $q^2 = 0$ the hadronic matrix elements of the vector current are governed by the associated charge or $SU(3)$ generator. In the limit of exact $SU(3)$ flavour symmetry, $V^{0a} = T^a$ to all orders in the $1/N_C$ expansion, where T^a are the baryon flavour generators. The $SU(3)$ symmetry breaking corrections to V^{0a} have been computed to second order [144, 157]. For the hyperon $|\Delta S| = 1$ decays that we are considering, the final result can be written in the form [144] of Eq. (3.47) which we repeat here :

$$V^{0a} \; = \; (1 + v_1)\, T^a + v_2 \, \{T^a, N_s\} + v_3 \, \left\{T^a, - I^2 + J_s^2\right\} \; , \tag{5.68}$$

where N_s counts the number of strange quarks, I denotes the isospin and J_s the strange quark spin. The parameters v_i constitute a second–order effect in agreement with the Ademollo–Gatto theorem [130, 131].

The $1/N_C$ expansion for the axial–vector current was studied in Refs. [14, 158]. For the hyperon $|\Delta S| = 1$ decay modes, one can write the result in a simplified form which accounts for first–order symmetry breaking effects [142, 144] of Eq. (3.55)

Decay	$g_1(0)$	$\tilde{f}_1$
$n \to p$	$\frac{5}{3}\,\tilde{a} + \tilde{b} + \rho$	1
$\Lambda \to p$	$-\sqrt{\frac{3}{2}}\,\left(\tilde{a} + \tilde{b} + c_3 + c_4\right)$	$1 + v_1 + v_2$
$\Sigma^- \to n$	$\frac{1}{3}\,(\tilde{a} + c_3 + c_4) - \tilde{b}$	$1 + v_1 + v_2 - 2v_3$
$\Xi^- \to \Lambda$	$\frac{1}{\sqrt{6}}\,(\tilde{a} + 7\,c_4) + \sqrt{\frac{3}{2}}\,\left(\tilde{b} + c_3\right)$	$1 + v_1 + 3\,v_2 + 2\,v_3$
$\Xi^- \to \Sigma^0$	$\frac{5}{3\sqrt{2}}\,(\tilde{a} + 3\,c_3) + \frac{1}{\sqrt{2}}\,\left(\tilde{b} + c_4\right)$	$1 + v_1 + 3\,v_2$
$\Xi^0 \to \Sigma^+$	$\frac{5}{3}\,\tilde{a} + \tilde{b} + 5\,c_3 + c_4$	$1 + v_1 + 3\,v_2$

Table 5.6: Parameterization of $g_1(0)$ and $\tilde{f}_1$ to first and second order, respectively, in symmetry breaking [144]. The neutron decay involves an additional parameter ρ, not included in (5.69).

which for the reader's convenience we repeat here:

$$\frac{1}{2}\,A^{ia} \;=\; \tilde{a}\,G^{ia} + \tilde{b}\,J^i\,T^a + c_3\,\left\{G^{ia}, N_s\right\} + c_4\,\left\{T^a, J^i_s\right\}\;. \tag{5.69}$$

The coefficients $\tilde{a} \equiv a + c_1$ and $\tilde{b} \equiv b + c_2$ reabsorb the effect of two additional operators considered in Ref. [144]. These operators generate an additional contribution to neutron decay, which we parametrize as $\rho = -\left(\frac{5}{3}\,c_1 + c_2\right)$. Table 5.6 shows the resulting values of $g_1(0)$ and $\tilde{f}_1$ for the relevant decay modes, in terms of the parameters $\tilde{a}$, $\tilde{b}$, c_3, c_4, ρ, v_1, v_2 and v_3.

In the strict $SU(3)_V$ symmetry limit, $c_i = v_i = 0$, *i.e.* $\tilde{f}_1 = 1$ while the values of $g_1(0)$ are determined by two parameters a and b, or equivalently by the more usual quantities $D = a$ and $F = \frac{2}{3}\,a + b$. A 3–parameter fit to the hyperon decay data gives the results shown in Table 5.7. Column 2 uses directly the measured values of the different rates and asymmetries, while in column 3 the asymmetries have been substituted by the derived $g_1(0)/f_1(0)$ values in Table 5.4. Both procedures give consistent results, but the direct fit to the asymmetries has a worse $\chi^2/\text{d.o.f.} = 3.09$ (2.36 for the $g_1(0)/f_1(0)$ fit). These χ^2 values indicate the need for $SU(3)_V$ breaking corrections. The fitted parameters agree within errors with the ones obtained in Ref. [142], although our central value for $|V_{us}|$ is $1\,\sigma$ smaller. For the F and D parameters, we obtain:

$$F = 0.462 \pm 0.011\,, \qquad D = 0.808 \pm 0.006\,, \qquad F + D = 1.270 \pm 0.015\,. \tag{5.70}$$

The last number, can be compared with the value of $g_1(0)/f_1(0)$ measured in neutron decay: $\left[\,g_1(0)/f_1(0)\right]_{n\to p} = D + F = 1.2695 \pm 0.0029$ [112]. Using the $|V_{ud}|$ value determined from superallowed nuclear beta decays and the neutron lifetime quoted by the Particle Data Group [112], a more precise value, $\left[g_1(0)/f_1(0)\right]_{n\to p} = 1.2703 \pm 0.0008$, has been derived in Ref. [118].

	$SU(3)$ symmetric fit		1st-order symmetry breaking	
	Asymmetries	$g_1(0)/f_1(0)$	Asymmetries	$g_1(0)/f_1(0)$
$\|V_{us}\|$	0.2214 ± 0.0017	0.2216 ± 0.0017	0.2266 ± 0.0027	0.2239 ± 0.0027
$\tilde{a}$	0.805 ± 0.006	0.810 ± 0.006	0.69 ± 0.03	0.72 ± 0.03
$\tilde{b}$	-0.072 ± 0.010	-0.081 ± 0.010	-0.071 ± 0.010	-0.081 ± 0.011
c_3			0.026 ± 0.024	0.022 ± 0.023
c_4			0.047 ± 0.018	0.049 ± 0.018
χ^2/d.o.f.	40.23/13	14.15/6	18.09/11	2.15/4

Table 5.7: Results of different fits to the semileptonic hyperon decay data.

Including first–order $SU(3)$ breaking effects in $g_1(0)$, the fit has two more free parameters. The fitted values are given in the last two columns of Table 5.7. The effect of $SU(3)_V$ breaking manifests through a value of $\tilde{a}$ lower than a [*i.e.* $c_1 = -0.10 \pm 0.03 \neq 0$, taking a from the $SU(3)_V$ fits], and the non–zero value of c_4. The fit to the asymmetries has again a worse χ^2/d.o.f. = 1.64 than the $g_1(0)/f_1(0)$ fit (χ^2/d.o.f. = 0.54) and gives a $1\,\sigma$ higher value of $|V_{us}|$. Taking $|V_{us}|$ from the best fit, its central value is about $1\,\sigma$ higher than the value obtained with exact $SU(3)_V$ symmetry. These results agree within errors with the corresponding fits in Ref. [142].

One can repeat the fits including also the neutron decay, which introduces the additional parameter ρ. Taking $V_{ud} = 0.97418 \pm 0.00026$ [117], this gives a sizeable measure of $SU(3)_V$ breaking, $\rho = 0.16 \pm 0.05$. The other parameters remain unchanged.

Ref. [142] presents the results of another fit, including second–order $SU(3)_V$ breaking effects in $\tilde{f}_1$ through the parameters v_i. The final value quoted for $|V_{us}|$ comes in fact from this fit, where $|V_{us}|$, v_1, v_2 and v_3 are fitted simultaneously (together with $\tilde{a}$, $\tilde{b}$, c_3 and c_4), obtaining a very good χ^2/d.o.f. = 0.72/2 = 0.36. We cannot understand the meaning of this numerical exercise. While it is indeed possible to fit the data with the parameters given in Ref. [142], one can obtain an infinite amount of different parameter sets giving fits of acceptable quality, because there is a flat χ^2 distribution in this case. This can be easily understood looking to the last column in Table 5.6. From the four analysed $|\Delta S| = 1$ hyperon semileptonic decays, one could only determine the global factor $|V_{us}\,(1 + v_1 + v_2)\,|$, v_2 and v_3. It is not possible to perform separate determinations of $|V_{us}|$ and v_1 because, as shown in Eq. (5.68), the contribution to the vector current of the flavour generator T^a is always multiplied by the same global factor $(1 + v_1)$.

To assess the possible size of these second–order effects, we have also performed a 7–parameter fit to the data. The results are shown in Table 5.8. Once more, the fit to

	2^{nd}-order symmetry breaking	
	Asymmetries	$g_1(0)/f_1(0)$
$\lvert(1+v_1+v_2)\ V_{us}\rvert$	0.2280 ± 0.0034	0.2220 ± 0.0038
$\tilde{a}$	0.69 ± 0.03	0.74 ± 0.04
$\tilde{b}$	-0.075 ± 0.010	-0.083 ± 0.011
c_3	0.03 ± 0.03	0.02 ± 0.03
c_4	0.04 ± 0.02	0.04 ± 0.02
v_2	0.01 ± 0.03	0.04 ± 0.03
v_3	-0.004 ± 0.013	-0.013 ± 0.014
χ^2/d.o.f.	16.5/9	0.53/2

Table 5.8: Second order fits to the semileptonic hyperon decay data.

the asymmetries has a worse χ^2/d.o.f. and gives a larger value for $|V_{us}\,(1+v_1+v_2)\,|$. The fitted values are consistent with the results in Table 5.7 from the first–order fit. Within the present experimental uncertainties, the 7–parameter fit is not able to clearly identify any non–zero effect from second–order $SU(3)_V$ breaking. Notice, that in this numerical exercise one is only considering second–order contributions to $\tilde{f}_1$, while $g_1(0)$ is still kept at first order. Unfortunately, it is not possible at present to perform a complete second–order analysis, owing to the large number of operators contributing to the axial current at this order.

Comparing the results from all fits, it seems safe to conclude that the $g_1(0)/f_1(0)$ ratios are less sensitive to $SU(3)_V$ breaking than the asymmetries. Therefore, we will take as our best estimate the corresponding first–order result in Table 5.7,

$$|\tilde{f}_1\, V_{us}| \,=\, 0.2239 \pm 0.0027\,. \tag{5.71}$$

This number is in good agreement with the simplest phenomenological fit in Eq. (5.67) and could give a very adequate estimate of $|V_{us}|$, once the systematic uncertainties are properly included.

5.3.6 Systematic Uncertainties

In our analysis the lepton masses, and therefore the form factors $f_3(q^2)$ and $g_3(q^2)$, have been neglected. This approximation does not introduce any relevant uncertainty at the present level of experimental accuracy. The errors associated with radiative corrections have been already taken into account in the fits, together with the experimental uncertainties. At first order in symmetry breaking, the main source

Parameter	$SU(3)_V$ symmetric fit		1^{st}–order $SU(3)_V$ breaking	
	Asymmetries	$g_1(0)/f_1(0)$	Asymmetries	$g_1(0)/f_1(0)$
$f_2^{\Lambda\to p} = 2.40 \pm 0.20$	$^{-0.0001}_{+0.0001}$	$^{-0.0001}_{+0.0001}$	$^{+0.0001}_{-0.0000}$	$^{-0.0002}_{+0.0001}$
$f_2^{\Sigma^-\to n} = -2.32 \pm 0.28$	$^{-0.0001}_{+0.0000}$	$^{+0.0001}_{-0.0000}$	$^{+0.0000}_{-0.0000}$	$^{-0.0001}_{+0.0000}$
$f_2^{\Xi^-\to\Lambda} = 0.178 \pm 0.030$	$^{+0.0000}_{-0.0000}$	$^{+0.0000}_{-0.0000}$	$^{+0.0000}_{-0.0000}$	$^{+0.0000}_{-0.0000}$
$f_2^{\Xi^-\to\Sigma^0} = -3.2 \pm 0.6$	$^{+0.0000}_{-0.0000}$	$^{+0.0000}_{-0.0000}$	$^{+0.0000}_{-0.0000}$	$^{+0.0000}_{-0.0000}$
$f_2^{\Xi^0\to\Sigma^+} = -4.4 \pm 0.8$	$^{+0.0000}_{-0.0000}$	$^{+0.0000}_{-0.0000}$	$^{+0.0000}_{-0.0000}$	$^{+0.0000}_{-0.0000}$
$M_A = 1.10 \pm 0.09$	$^{+0.0001}_{-0.0001}$	$^{+0.0001}_{-0.0001}$	$^{+0.0001}_{-0.0001}$	$^{+0.0001}_{-0.0001}$
$M_V = 0.91 \pm 0.07$	$^{+0.0005}_{-0.0006}$	$^{+0.0004}_{-0.0005}$	$^{+0.0002}_{-0.0002}$	$^{+0.0005}_{-0.0006}$
Total systematic error	0.0006	0.0004	0.0002	0.0006

Table 5.9: Parametric uncertainties of the V_{us} determination from hyperon decays

of parametric uncertainties comes from the numerical values of $f_2(0)$ and the slopes λ_1^f and λ_1^g governing the low–q^2 behaviour of the form factors $f_1(0)$ and $g_1(0)$.

Since the $f_2(q^2)$ contribution to the decay amplitude appears multiplied by q_ν, which is already a parametrically small $SU(3)$ breaking effect, at $\mathcal{O}(\epsilon)$ the value of $f_2(0)$ can be fixed in the $SU(3)$ limit from the proton and neutron magnetic moments [see Eq. (5.53)]. However, what appears in the vector matrix elements (5.49) are the ratios $f_2(q^2)/M_{B_1}$. The $SU(3)_V$ limit can either be applied to $f_2(0)$ or $f_2(0)/M_{B_1}$, because the baryon masses are the same for the whole octet multiplet in the limit of exact $SU(3)_V$ symmetry. Taking the physical baryon masses, the numerical results would be obviously different. In order to estimate the associated uncertainty in $f_2(0)$ we will vary its value within the range obtained with these two possibilities.

The slopes λ_1^f and λ_1^g are determined from electroproduction and neutrino scattering data with nucleons, which are sensitive to the flavour–diagonal vector and axial–vector form factors in the $Q^2 = -q^2 > 0$ region. The obtained distributions are well fitted with dipole parametrizations $G_{V,A}(Q^2) = G_{V,A}(0)/\left(1 + Q^2/M_{V,A}^2\right)^2$, with $M_V^0 = (0.84 \pm 0.04)\,\text{GeV}$ and $M_A^0 = (1.08 \pm 0.08)\,\text{GeV}$ [145]. Extrapolating these functional forms to $q^2 > 0$, one gets a rough estimate of the needed hyperon form factor slopes in the $SU(3)$ limit. To account for $SU(3)$ breaking, one usually modifies the parameters M_V and M_A in a rather naïve way, adopting the values $M_V = M_V^0\,(m_{K^*}/m_\rho) = 0.98\,\text{GeV}$ and $M_A = M_A^0\,(m_{K_1}/m_{a_1}) = 1.12\,\text{GeV}$. To estimate the systematic uncertainty associated with λ_1^f and λ_1^g, we adopt these dipole parametrizations, varying the values of the vector and axial–vector mass parameters between $M_{V,A}^0$ and $M_{V,A}$. As mentioned in previous sections, a monopole parametrization could lead to a significative shift of the fitted V_{us} value; however, in this case one should take different values for the parameters $M_{V,A}$, in order to fit the $q^2 < 0$ data.

Reference	$\Lambda \to p$	$\Sigma^- \to n$	$\Xi^- \to \Lambda$	$\Xi^- \to \Sigma^0$	$\Xi^0 \to \Sigma^+$
DHK'87 [152] (quark model)	0.987	0.987	0.987	0.987	0.987
Sch'95 [153] (quark model)	0.976	0.975	0.976	0.976	
Kr'90 [154] (chiral loops)	0.943	0.987	0.957	0.943	
AL'93 [155] (chiral loops)	1.024	1.100	1.059	1.011	
LKM [159] (chiral loops)	0.943	1.028	0.989	0.944	

Table 5.10: Theoretical predictions for $\tilde{f}_1$.

In Table 5.9 we show the sensitivity of the resulting V_{us} value to these parametric uncertainties. Columns 2 and 3 give the induced systematic errors in the 3–parameter [$SU(3)$ symmetric] fits, while columns 4 and 5 contain the corresponding numbers for the 5–parameter fits including first–order $SU(3)$ breaking in $g_1(0)$. In both cases, we indicate separately the estimates obtained for the fits to the asymmetries and the $g_1(0)/f_1(0)$ fits. The numbers in the table show that the vector slope λ_1^f is the dominant source of parametric uncertainty. In any case, these uncertainties are much smaller than the statistical errors of the corresponding fits.

At second order, one should take into account the unknown value of $g_2(0)$ and the $\mathcal{O}(\epsilon^2)$ corrections to $f_1(0)$ and $g_1(0)$. There exist a few estimates of $f_1(0)$ using quark models and baryon chiral Lagrangians. Unfortunately, they give rather different results as shown in Table 5.10. The quark–model calculations agree with the naïve expectation that $SU(3)_V$ corrections should be negative, *i.e.* $\tilde{f}_1 < 1$ [152,153]. In contrast, the chiral–loop estimates obtain large corrections with opposite signs : while Ref. [155] finds values for $\tilde{f}_1$ which are larger than one for all analysed decays, Ref. [154] gets results more consistent with the quark–model evaluations. The two references use slightly different chiral techniques, and are probably taking into account different sets of Feynman diagram contributions. Ref. [159] is the latest χPT calculation. They use the infrared regularization scheme, which is a relativistic formulation that preserves chiral counting. However they do not take into account the effect of the spin–$\frac{3}{2}$ decuplet and hence their results should be read with care. In Ref. [160] the heavy baryon formalism is used, but it is found that the contributions of the spin–$\frac{3}{2}$ decuplet spoil the convergence of the chiral series. Clearly, a new and more complete calculation is needed.

Nothing useful is known about $g_2(0)$ and the needed $\mathcal{O}(\epsilon^2)$ corrections to $g_1(0)$. However, $g_2(0)$ is not expected to give a sizeable contribution, while $g_1(0)/f_1(0)$ can be directly taken from experiment using the phenomenological fit of previous sections. In fact, the experimental $g_1(0)/f_1(0)$ ratios given in Table 5.4 assume already $g_2(0) = 0$. Thus, the value of $\tilde{f}_1$ constitute the main theoretical problem for an accurate determination of V_{us} from hyperon decays. Although corrections to the $SU(3)_V$ symmetric value are of $\mathcal{O}(\epsilon^2)$, it has been argued that they are numerically enhanced by infrared–sensitive denominators [144, 155]. In the absence of a reliable theoretical calculation, and in view of the estimates shown in Table 5.10, we adopt

the common value

$$\tilde{f}_1 \;=\; 0.99 \pm 0.02\,, \tag{5.72}$$

for the five decay modes we have studied. While the two quark model estimates are in the range $\tilde{f}_1 = 0.98 \pm 0.01$, the disagreement between the two chiral calculations expands the interval of published results to $\tilde{f}_1 = 1.02 \pm 0.08$. However, for some decay modes such as $\Sigma^- \to n\, e^- \bar{\nu}_e$ one can show that $\tilde{f}_1$ should indeed be smaller than one, as naïvely expected [141, 161]. This disagrees with the results obtained in Ref. [155]. Our educated guess in (5.72) spans the whole interval of quark model results, allowing also for higher values of $\tilde{f}_1$ within a reasonable range. Applying this correction to our best estimate in Eq. (5.71), gives the final result:

$$|V_{us}| \;=\; 0.226 \pm 0.005\,. \tag{5.73}$$

5.3.7 V_{ud} from Neutron Decay

A recent reanalysis of radiative corrections to the neutron decay amplitude has given the updated relation [118, 162]:

$$|V_{ud}| \;=\; \left(\frac{4908\ (4)\ \mathrm{sec}}{\tau_n\ (1 + 3\, g_A^2)} \right)^{1/2}\,. \tag{5.74}$$

Using $V_{ud} = 0.97418 \pm 0.0005$, Ref. [118] derives the Standard Model prediction for the axial coupling

$$g_A \;\equiv\; g_1(0)/f_1(0) \;=\; 1.2703 \pm 0.0008\,, \tag{5.75}$$

which is more precise than the direct measurements through neutron decay asymmetries.

In order to extract V_{ud} from (5.74), using as inputs the measured values of the neutron lifetime and g_A, one would need to clarify the present experimental situation. The Particle Data Group [112] quotes the world averages

$$\tau_n = (885.7 \pm 0.8)\,\mathrm{s}\,, \qquad\qquad g_A = 1.2695 \pm 0.0029\,, \tag{5.76}$$

which implies

$$|V_{ud}| \;=\; 0.9745 \pm 0.0019\,. \tag{5.77}$$

However, the most recent measurement of the neutron lifetime [121] has lead to a very precise value which is lower than the world average by $6.5\,\sigma$,

$$\tau_n \;=\; (878.5 \pm 0.7 \pm 0.3)\,\mathrm{s}\,. \tag{5.78}$$

Taking g_A from (5.76), this would imply a $2\,\sigma$ higher $|V_{ud}|$:

$$|V_{ud}| \;=\; 0.9785 \pm 0.0019\,. \tag{5.79}$$

Source	K_{l3} [53, 122–128, 132–136]	K_{l2} [139, 140]	τ [137, 138]	Hyperons
$\lvert V_{us}\rvert$	0.2233 ± 0.0028	0.2219 ± 0.0025	0.2208 ± 0.0034	0.226 ± 0.005

Table 5.11: Determinations of V_{us}.

Actually, the PDG value of g_A in (5.76) comes from an average of five measurements which do not agree among them ($\chi^2 = 15.5$, confidence level $= 0.004$). If one adopts the value obtained in the most recent and precise experiment [163],

$$g_A = 1.2739 \pm 0.0019\,, \tag{5.80}$$

one gets the results:

$$|V_{ud}| = \begin{cases} 0.9717 \pm 0.0013 \\ 0.9757 \pm 0.0013 \end{cases} . \tag{5.81}$$

5.3.8 Summary

At present, the determinations of $|V_{ud}|$ and $|V_{us}|$ from baryon semileptonic decays have large uncertainties and cannot compete with the more precise information obtained from other sources.

Hyperon semileptonic decays could provide an independent determination of $|V_{us}|$, to be compared with the ones obtained from kaon decays or from the Cabibbo–suppressed τ decay width. However, our theoretical understanding of $SU(3)_V$ breaking effects constitutes a severe limitation to the achievable precision. We have presented a new numerical analysis of the available data, trying to understand the discrepancies between the results previously obtained in Refs. [141] and [142], and the systematic uncertainties entering the calculation.

The $1/N_C$ expansion of QCD is a convenient theoretical framework to study the baryon decay amplitudes and estimate the size of $SU(3)_V$ breaking effects. From the comparison of fits done at different orders in symmetry breaking, one can clearly identify the presence of a sizeable $SU(3)_V$ breaking at first order. However, the present uncertainties are too large to pin down these effects at second order.

One can use the measured decay rates and $g_1(0)/f_1(0)$ ratios to perform a rather clean determination of $|\tilde{f}_1\, V_{us}|$. However it is impossible to disentangle V_{us} from $\tilde{f}_1$ without additional theoretical input. The Ademollo–Gatto theorem guarantees that $\tilde{f}_1 = 1 + \mathcal{O}(\epsilon^2)$, but it has been argued that the second–order $SU(3)$ corrections to $\tilde{f}_1 = 1$ are numerically enhanced by infrared–sensitive denominators [144, 155]. The existing calculations, using quark models or baryon chiral perturbation theory, give contradictory results and signal the possible presence of sizable corrections. Adopting as an educated guess the value $\tilde{f}_1 = 0.99 \pm 0.02$, we find our final result in Eq. (5.73).

Table 5.11 compares the hyperon determination of V_{us}, with the results obtained from other sources. The present hyperon value has the largest uncertainty. To get a competitive determination one would need more precise experimental information and a better theoretical understanding of $\tilde{f}_1$, beyond its symmetric value. The average of all determinations is

$$|V_{us}| \;=\; 0.2225 \pm 0.0016\,. \tag{5.82}$$

Without the information from hyperon semileptonic decays, the average would be 0.2221 ± 0.0016. Taking $|V_{ud}| = 0.97418 \pm 0.00026$, from superallowed nuclear beta decays [117], the resulting first–row unitarity test gives (the $|V_{ub}|$ contribution is negligible) :

$$|V_{ud}|^2 + |V_{us}|^2 + |V_{ub}|^2 \;=\; 0.9985 \pm 0.0009\,. \tag{5.83}$$

Thus, the unitarity of the quark mixing matrix is satisfied at the $1.7\,\sigma$ level.

Chapter 6

Dispersion relations and unitarity

6.1 Introduction

The failure of early attempts to apply perturbative quantum field theory to the strong and weak nuclear forces led theorists by the late sixties to attempt the use of the analyticity and unitarity of scattering amplitudes as a way of deriving general non–perturbative results that would not depend on any particular field theory. This started with a revival of interest in dispersion relations.

Even before quantum field theory (QFT for short) was regarded as the theory capable of describing a relativistic quantum theory of particles (at least at low energies [1]), some of the basic ingredients (S–matrix, scattering amplitudes, ...) and their properties (unitarity, crossing, ...) where already known, or at least conjectured. In fact QFT provides a method of calculating these basic ingredients, and of course with its axiomatic properties. However, in most (if not all) of the cases the QFT calculation is of perturbative nature (by perturbative we mean any kind of organization allowing to drop some terms as subleading, and not necessarily an expansion in the coupling constant), and then some of the properties of the S–matrix are only satisfied at the perturbative level (it is well known that the absorptive part of an amplitude appears for the first time at one loop, and not at tree level).

So some times it is good to "forget" for a while the goods of QFT and derive general expressions for the S–matrix elements or the scattering amplitudes (for instance, dispersion relations), and afterwards combine these relations with QFT results to obtain the maximum information possible. In the case of non–perturbative dynamics where the information is rather scarce, these relations (of non–perturbative nature) are an essential tool for the QCD practitioner.

In this chapter we use axiomatic field theory together with χPT to derive bounds on the chiral LECs and to constrain the predictions for the production of mesons in two photon reactions. For writing some of the technical aspects of this chapter I have followed [57, 164, 165].

6.2 Unitarity and partial wave decomposition

Unitarity is the simplest and more fundamental requirement that any sensible theory must fulfill. Basically it is equivalent to the quantum mechanical principle of "probability conservation". Of course, in a relativistic quantum theory particles are created and destroyed all the time, and so the quantum mechanics concept of "probability" loses its meaning. Instead one must require that the probability of finding any final state $|\, i \,\rangle$ out of the collision of several particles $|\alpha\rangle$ must be 100% :

$$1 = \sum_i |\langle\, i \,|\, S \,|\, \alpha \,\rangle|^2 = \sum_i \langle\, \alpha \,|\, S \,|\, i \,\rangle\langle\, i \,|\, S^\dagger |\, \alpha \,\rangle = \langle\, \alpha \,|\, SS^\dagger \,|\, \alpha \,\rangle\,, \tag{6.1}$$

and also that the probability of finding a given final state $|\, \alpha \,\rangle$ when trying with all possible initial states $|\, i \,\rangle$ must be one : $\langle\, \alpha \,|\, SS^\dagger \,|\, \alpha \,\rangle = 1$ for any state $|\, \alpha \,\rangle$. If now we write $|\, \alpha \,\rangle = a_1\, |\alpha_1\rangle + a_2\, |\alpha_2\rangle$ with $|\alpha_1\rangle \neq |\alpha_2\rangle$ and $a_1^2 + a_2^2 = 1$ we obtain

$$1 \;=\; 1 \;+\; a_1^* a_2 \langle\, \alpha_1 \,|\, SS^\dagger \,|\, \alpha_2 \,\rangle \;+\; a_1 a_2^* \langle\, \alpha_2 \,|\, SS^\dagger \,|\, \alpha_1 \,\rangle\,. \tag{6.2}$$

Since this must be satisfied for arbitrary a_1, a_2, necessarily $\langle\, \alpha_1 \,|\, SS^\dagger \,|\, \alpha_2 \,\rangle = 0$. This relation together with Eq. (6.1) enables us to write the unitarity requirement as an operator identity :

$$SS^\dagger \;=\; S^\dagger S \;=\; \mathbb{1}\,. \tag{6.3}$$

It is customary to separate the trivial part of the S–matrix describing the probability of the particles not to interact at all from the so called T–matrix, encoding the dynamics :

$$S \;=\; \mathbb{1} \;+\; i\,T\,. \tag{6.4}$$

Moreover, since the S–matrix must commute with the generators of the Poincaré group, when the initial and final states have well defined total momentum P_i and P_f it must have an overall momentum conservation Dirac delta function, that can be factored out as well :

$$\langle\, P_f \,|\, T \,|\, P_i \,\rangle \;=\; (2\,\pi)^4\, \delta^{(4)}(P_f - P_i)\, \mathcal{M}\,, \tag{6.5}$$

being $\mathcal{M}$ the reduced matrix element. Inserting Eq. (6.4) into (6.3) we obtain

$$-\,i\left(T - T^\dagger\right) \;=\; T^\dagger\, T\,. \tag{6.6}$$

Let us consider the scattering process of two particles into two particles, and let us insert a Parseval identity in the right–hand side of Eq. (6.6)

$$-\,i\,[\mathcal{M}(k_1 k_2 \to p_1 p_2) - \mathcal{M}(p_1 p_2 \to k_1 k_2)^*] \;=\; \sum_f \int \mathrm{d}Q_f\, \mathcal{M}(k_1 k_2 \to f)\mathcal{M}(p_1 p_2 \to f)^*\,, \tag{6.7}$$

Of course time reversal invariance (if it applies) requires $\mathcal{M}\,(p \to k) = \mathcal{M}\,(k \to p)$. Let us assume now that the identity of the initial and final states is the same, and also that $p_i = k_i$ (forward scattering). Then Eq. (6.7) reduces to the so called *Optical theorem*

$$\mathrm{Im}\,\mathcal{M}(k_1 k_2 \to k_1 k_2) \;=\; \lambda(s, m_1^2, m_2^2)\,\sigma_{\rm tot}(k_1 k_2 \to \mathrm{all}) > 0\,. \tag{6.8}$$

The diagrammatic representation of this equation is shown in Fig. 6.1. Although this expression is very interesting by itself, it only applies for the specific case of forward scattering. It would be desirable to have a similar expressions for more general situations. In fact one can write unitarity relations like in Eq. (6.8) for the partial wave amplitudes. We can characterize the initial and final states by the value of the total spin of the two particles, its total energy and two angles defining the orientation of the three–momentum (the option we have used so far). Without lose of generality we can choose the initial state momenta to point in the z direction. Another possible choice (corresponding to another complete set of commuting operators) is the value of the spin of the two particles, its total energy, the value of the total angular momentum J and its third component M. It is convenient to separate the uninteresting center of mass three–momentum :

$$\begin{aligned} |\,\vec{p}_1, \vec{p}_2;\; s_1, s_2\rangle &= |\vec{P}\,\rangle \otimes |E, \theta, \phi; s_1, s_2\rangle\;, \\ |\vec{P}, E, J, M;\; s_1, s_2\rangle &= |\vec{P}\,\rangle \otimes |E, J, M; s_1, s_2\rangle\;, \end{aligned} \tag{6.9}$$

The two basis are related by (we label the total energy in the center of mass frame by E)

$$\begin{aligned} |E, \theta, \phi; s_1, s_2\rangle &= \sum_{JM} c_J\, \mathcal{D}^{(J)}_{M,\mu}(\phi, \theta, -\phi)\, |E, J, M; s_1, s_2\rangle\;, \\ |E, J, M; s_1, s_2\rangle &= c_J \int \mathrm{d}\Omega\, \mathcal{D}^{(J)\,*}_{M,\mu}(\phi, \theta, -\phi)\, |E, \theta, \phi; s_1, s_2\rangle\;, \\ \mu &= \mu_1 - \mu_2\,, \\ c_J &= \sqrt{\frac{2\,J+1}{4\,\pi}}\,, \end{aligned} \tag{6.10}$$

where $\mathcal{D}^{(J)}_{M,\mu}$ are the usual rotation matrices. Matrix elements of the T–matrix taken with states of definite angular momentum are known as partial waves

$$\begin{aligned} \langle E', J', M'; s_1', s_2' \,|\, T \,|\, E, J, M; s_1, s_2\rangle &= (4\,\pi)(2\pi)^4 \delta_{JJ'} \delta_{MM'} \delta(E - E')\, \mathcal{M}^J_{12\to 1'2'}(E)\,, \\ \langle E', \Omega; s_1', s_2' \,|\, T \,|\, E, 0; s_1, s_2\rangle &= (2\,\pi)^4 \delta(E - E')\, \mathcal{M}_{12\to 1'2'}(E, \Omega)\,, \end{aligned} \tag{6.11}$$

and the two decompositions of the T–matrix are related

$$\begin{aligned} \mathcal{M}_{12\to 1'2'}(E, \Omega) &= \sum_J (2\,J+1)\, \mathcal{D}^{(J)\,*}_{\mu,\mu'}(\phi, \theta, -\phi)\, \mathcal{M}^J_{12\to 1'2'}(E)\,, \\ \mathcal{M}^J_{12\to 1'2'}(E) &= (2\,J+1) \int \mathrm{d}\Omega\, \mathcal{D}^{(J)}_{\mu,\mu'}(\phi, \theta, -\phi)\, \mathcal{M}_{12\to 1'2'}(E, \Omega)\,. \end{aligned} \tag{6.12}$$

The first relation of Eq. (6.12) is known as the partial wave decomposition of the scattering amplitude. Taking matrix elements of Eq. (6.6) with angular momentum eigenstates, and inserting a Parseval identity, expressed in the angular momentum basis, we obtain (the sum over final states includes integrations and sum over polarizations)

$$\mathcal{M}^J_{12\to 1'2'}(E) \,-\, \mathcal{M}^J_{1'2'\to 12}(E)^* \,=\, i \sum_f \mathcal{M}^J_{f\to 1'2'}(E)\, \mathcal{M}^J_{12\to f}(E)^* \,, \tag{6.13}$$

where f is a multiparticle state with total energy E and total angular momentum J. If the identity (and hence spin) of the initial and final states coincide we obtain the optical theorem for partial wave amplitudes

$$2\,\mathrm{Im}\,\mathcal{M}^J_{12\to 12}(E) \,=\, \sum_f \left|\mathcal{M}^J_{12\to f}(E)\right|^2 > 0 \,, \tag{6.14}$$

and when inserting this result back into Eq. (6.12) we get

$$2\,\mathrm{Im}\,\mathcal{M}_{12\to 12}(E) \,=\, \sum_{J,f} (2\,J+1)\, \mathcal{D}^{(J)*}_{\mu,\mu'}(\phi,\theta,-\phi)\, \left|\mathcal{M}^J_{12\to f}(E)\right|^2 \tag{6.15}$$

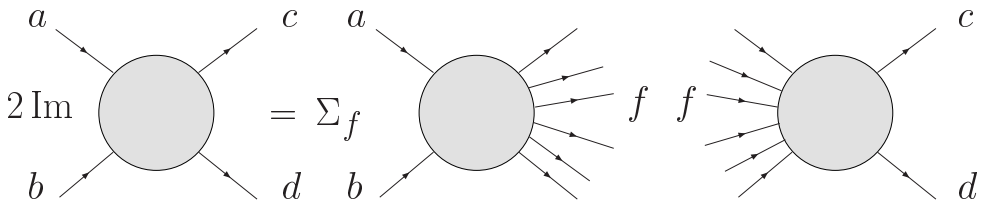

Figure 6.1: Diagrammatic representation of the optical theorem.

To close this section we will comment on the concepts of crossing symmetry and analyticity. Crossing symmetry states that (for simplicity we will assume spinless particles) given the reaction $a\,b \to c\,d$ described by the matrix element $\mathcal{M}_{ab\to cd}(s,t)$ being s, t and u the usual Mandelstam variables [1] defined as

$$\begin{aligned}
s &= (p_a + p_b)^2 = (p_c + p_d)^2 \qquad & s &> (m_a + m_b)^2 \,, \\
t &= (p_a - p_c)^2 = (p_b - p_d)^2 \qquad & t &< \mathrm{Min}\left[(m_a - m_c)^2,\, (m_b - m_d)^2\right] \,, \\
u &= (p_a - p_d)^2 = (p_b - p_c)^2 \qquad & u &< \mathrm{Min}\left[(m_a - m_d)^2,\, (m_b - m_c)^2\right] \,,
\end{aligned} \tag{6.16}$$

satisfying the on–shell constraint

$$s \,+\, t \,+\, u \,=\, m_a^2 \,+\, m_b^2 \,+\, m_c^2 \,+\, m_d^2 \,, \tag{6.17}$$

[1] For the definition of the Mandelstam variables the ordering of the initial and final state particles is important. For instance $\mathcal{M}_{ab\to dc}(s,t) = \mathcal{M}_{ab\to cd}(s,u)$.

the crossed channel reactions (see Fig. 6.2) are described by the same matrix element as follows : $\mathcal{M}_{ac\to bd}(s,t) = \mathcal{M}_{ab\to cd}(t,s)$, $\mathcal{M}_{ad\to cb}(s,t) = \mathcal{M}_{ab\to cd}(u,t)$.

Analyticity states that, if we regard the amplitude $\mathcal{M}(s,t)$ as a function of the complex variables s and t, the amplitude is analytic everywhere in the complex $s-t$ space except for a number of isolated points, due to single particle exchange and branch cuts along the real axis, necessary for unitarity to be satisfied. So all the branch cuts overlap and we have a single branch cut, its branch point coinciding with the first possible intermediate state. The rest of branch cuts are dictated by *crossing symmetry*. The physical amplitudes are defined for certain (real) values of s and t with a certain prescription, acceptable for all the crossed channels. The three physical regions are non–overlapping, and out of them the amplitude is defined by analytic continuation. So physical amplitudes are boundaries of the same analytic function $\mathcal{M}(s,t)$. This statement can be translated to the partial wave amplitudes $\mathcal{M}^J(s)$. Let us keep in mind that one partial wave amplitude from the s–channel receives contributions from *all* the partial waves defined in the t– or u–channels.

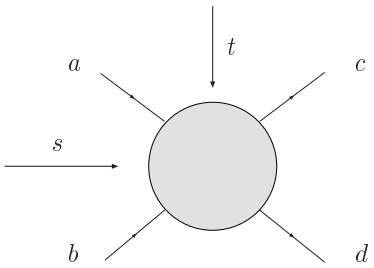

Figure 6.2: Graphic representation of the s and t crossed channels.

6.3 The linear sigma model

In this section we introduce and discuss the $SU(2)$ linear sigma model of Gell–Mann and Levy [166]. This model was originally developed as a toy model for nuclear forces, describing the nucleon–pion interactions. It incorporates in an specific way the breakdown of chiral symmetry. Here we will concentrate only in the scalar sector of the model. For this section I have followed Refs. [92, 93, 167].

In linear sigma models, basic fields are assumed to belong to linear representations of the chiral group G. We will consider representations of low dimensions, playing the main röle at low energies. Then one builds the most general Lagrangian being renormalizable and chiral invariant. For denoting the irreducible representations of G we will use the notation (m,n), being m and n the dimension of the corresponding left and right $SU(2)$ subgroups [note that $SU(2)$ is a real group]. The fundamental left– and right–handed fields χ_L, χ_R are fermionic. They transform under G as $(2,1)$ and $(1,2)$: $\chi'_{LR} = g_{LR}\,\chi_{LR}$. Under parity, of course $\chi_L \leftrightarrow \chi_R$. The

Dirac representations $\psi = \chi_R + \chi_L$ and $\gamma_5\,\psi = \chi_R - \chi_L$ transform as $(2,1)+(1,2)$ and are parity eigenstates.

Of particular importance is the (chiral) four–vector representation, that can be built out of the fundamental ones

$$B_\alpha \;=\; \chi_R^\dagger\,\tau_\alpha\,\chi_L\,, \tag{6.18}$$

where $\tau_\alpha = (\mathbb{1}, \tau_i)$ are the Pauli matrices acting on the isospin indices. The basic transformation rule of B_α under an infinitesimal chiral transformation is

$$\begin{aligned} B_0 \;&\to\; B_0 \,+\, i\,\vec{a}\cdot\vec{B}\,,\\ \vec{B} \;&\to\; \vec{B} \,+\, \vec{v}\times\vec{B} \,+\, i\,B_0\,\vec{a}\,, \end{aligned} \tag{6.19}$$

where we have written the chiral transformation Eq. (1.4) as

$$g \;=\; \exp\left[\,i\,(\vec{v}-\vec{a})\cdot\vec{\tau},\, i\,(\vec{v}+\vec{a})\cdot\vec{\tau}\,\right]. \tag{6.20}$$

Eq. (6.19) implies that the group $SU(2)\otimes SU(2)$ is isomorphic to $O(4)$. The four–vector B_α is not a parity eigenstate: $B_\alpha^{\mathcal{P}} = B_\alpha^\dagger$. We can form the appropriate combinations with definite parity

$$\begin{aligned} \sigma_\alpha \;&=\; \chi_R^\dagger\,\tau_\alpha\chi_L + \chi_L^\dagger\,\tau_\alpha\chi_R \;=\; \bar{\psi}\,\tau_\alpha\,\psi\,,\\ \pi_\alpha \;&=\; i\,(\chi_R^\dagger\,\tau_\alpha\chi_L - \chi_L^\dagger\,\tau_\alpha\chi_R) \;=\; \bar{\psi}\,\tau_\alpha\,i\,\gamma_5\,\psi\,, \end{aligned} \tag{6.21}$$

and so there are two chiral four–vectors of (Lorentz) scalars and pseudoscalars. Their infinitesimal transformations under G are

$$\begin{aligned} \sigma_0 \;&\to\; \sigma_0 + \vec{\pi}\cdot\vec{a}\,,\\ \vec{\sigma} \;&\to\; \vec{\sigma} + \vec{v}\times\vec{\sigma} + \pi_0\,\vec{a}\,,\\ \pi_0 \;&\to\; \pi_0 - \vec{\sigma}\cdot\vec{a}\,,\\ \vec{\pi} \;&\to\; \vec{\pi} + \vec{v}\times\vec{\pi} - \sigma_0\,\vec{a}\,, \end{aligned} \tag{6.22}$$

from these we see that there are two invariants in quadratic form: $\sigma_0^2 + \vec{\pi}^{\,2}$ and $\pi_0^2 + \vec{\sigma}^{\,2}$. Since in nature there are three degenerate negative–parity states (pions) we will adopt the first combination as the basic building block. It constitutes the length of a four–vector $(\sigma_0, \vec{\pi})$ in notation of the $O(4)$ group. We will identify $\sigma_0 \equiv \sigma$ and, in order to have a more direct connection with the chiral group G we will group the particles in the matrix [2]

$$\Sigma \;=\; \sigma + i\,\vec{\tau}\cdot\vec{\pi}\,, \tag{6.23}$$

which reproduces the transformation rules (6.22) if it transforms under G as $\Sigma' = g_L\Sigma\,g_R^\dagger$ (of course the choice $\Sigma = \pi_0 + i\,\vec{\tau}\cdot\vec{\sigma}$ is transformed in a similar way with

[2] By a field redefinition the Σ matrix can be cast into the form $\Sigma = \sigma\,\exp(i\frac{\vec{\tau}\cdot\vec{\pi}}{v})$. Then $\Sigma\,\Sigma^\dagger = \sigma^2$ and the pion dynamics is entirely contained in the kinetic term.

$L \leftrightarrow R$). Now, since $\Sigma\,\Sigma^\dagger = \Sigma^\dagger\,\Sigma = (\sigma^2 + \vec{\pi}^{\,2})\,\mathbb{1}$ and $\det\Sigma = \sigma^2 + \vec{\pi}^{\,2}$ it follows that $\Sigma\,\Sigma^\dagger$ is $\sqrt{\sigma^2 + \vec{\pi}^{\,2}}$ times a unitary unimodular matrix, and that $\sigma^2 + \vec{\pi}^{\,2}$ is the only possible chiral invariant. So the most general invariant Lagrangian is

$$\begin{aligned}
\mathcal{L} &= \frac{1}{4}\left\langle \partial_\mu\Sigma\,\partial^\mu\Sigma^\dagger\right\rangle - V(\sigma^2+\vec{\pi}^2) = \frac{1}{4}\left\langle \partial_\mu\Sigma\,\partial^\mu\Sigma^\dagger\right\rangle + \frac{\mu^2}{4}\left\langle \Sigma\,\Sigma^\dagger\right\rangle - \frac{g}{16}\left\langle \Sigma\,\Sigma^\dagger\right\rangle^2 \\
&= \frac{1}{4}\left\langle \partial_\mu\Sigma\,\partial^\mu\Sigma^\dagger\right\rangle - \frac{g}{16}\left(\left\langle \Sigma\,\Sigma^\dagger\right\rangle - 2\,v^2\right)^2 \\
&= \frac{1}{2}\left(\partial_\mu\sigma\,\partial^\mu\sigma + \partial_\mu\vec{\pi}\,\partial^\mu\vec{\pi}\right) - \frac{g}{4}\left[(\sigma^2+\vec{\pi}^{\,2}) - v^2\right]^2 , \qquad (6.24)
\end{aligned}$$

with $v^2 = \mu^2/g$. If $\mu^2 < 0$ the symmetry is realized *a la* Wigner–Weyl, and all particles have a common mass of $\sqrt{-\mu^2}$. For $\mu^2 > 0$ the symmetry is realized *a la* Nambu–Goldstone and the Lagrangian exhibits the phenomenon of spontaneous symmetry breaking. This last possibility is the one concerning us.

The vacuum, which has the lowest energy is expected to be static and uniform ($\partial_\mu\bar{\phi}_i = 0$), and so the energy minimum satisfies $\partial V/\partial\phi_i = 0$. The minimum condition is [3]

$$\sigma^2 + \vec{\pi}^{\,2} = v^2 , \qquad (6.25)$$

and so we have an infinite number of configurations with minimum energy. Now we can use our freedom to make chiral transformations to rotate any vacuum expectation value into the σ direction. If the minimum has a non–vanishing component in a pion direction, it does not have definite parity, contradicting nature. So that without any loss of generality we can assume

$$\langle\sigma\rangle = v , \qquad \langle\,\vec{\pi}\,\rangle = 0 , \qquad (6.26)$$

and perturb around the vacuum. Thus we define the shifted field and the shifted matrix

$$\sigma' = \sigma - v , \quad \Sigma' = \Sigma - v\,\mathbb{1} , \qquad (6.27)$$

in which the Lagrangian reads

$$\begin{aligned}
\mathcal{L} &= \frac{1}{4}\left\langle \partial_\mu\Sigma'\,\partial^\mu\Sigma'^\dagger\right\rangle - \frac{g}{16}\left(\left\langle \Sigma'\,\Sigma'^\dagger\right\rangle + v\left\langle \Sigma' + \Sigma'^\dagger\right\rangle\right)^2 \qquad (6.28) \\
&= \frac{1}{2}\left(\partial_\mu\sigma'\,\partial^\mu\sigma' - m_\sigma^2\,\sigma'^2 + \partial_\mu\vec{\pi}\cdot\partial^\mu\vec{\pi}\right) - \frac{g}{4}\left(\sigma'^2+\vec{\pi}^{\,2}\right)^2 - \sqrt{\frac{g}{2}}\,m_\sigma\,\sigma'\left(\sigma'^2+\vec{\pi}^{\,2}\right) ,
\end{aligned}$$

with $m_\sigma^2 = 2\,\mu^2 = 2\,g\,v^2$. The new Lagrangian (6.28) do not have the full $SU(2)\otimes SU(2) \approx O(4)$ symmetry any more, but possesses a remnant $SU(2)\approx O(3)$ symmetry. So, as expected from the Goldstone theorem, there appear in the theory three

[3] In the form $\Sigma = \sigma\,\exp(i\frac{\vec{\tau}\cdot\vec{\pi}}{F})$ the minimum condition reads directly $\sigma^2 = v^2$ and $\Sigma' = (v+\sigma)\,\exp(i\frac{\vec{\tau}\cdot\vec{\pi}}{v})$.

massless spin–zero particles, the Goldstone bosons. The σ scalar particle, however, has acquired a non–vanishing mass.

As discussed in Chapter 1, in the real world the $SU(2)\otimes SU(2) \approx O(4)$ symmetry is also explicitly broken by the mass term of the u and d quarks. Assuming that isospin is preserved by this mass term (that is, $m_u = m_d$) the linear sigma model Lagrangian is only invariant under $SU(2) \approx O(3)$. So, we must introduce a term violating chiral symmetry but preserving isospin symmetry (and of course, being renormalizable and hermitian). The simplest choice is to add to Eq. (6.24) a term like $\left\langle \Sigma + \Sigma^\dagger \right\rangle$ (analogous to an external magnetic field):

$$\mathcal{L} = \frac{1}{4}\left\langle \partial_\mu \Sigma\, \partial^\mu \Sigma^\dagger \right\rangle + \frac{\mu^2}{4}\left\langle \Sigma\, \Sigma^\dagger \right\rangle - \frac{g}{16}\left\langle \Sigma\, \Sigma^\dagger \right\rangle^2 + \beta \left\langle \Sigma + \Sigma^\dagger \right\rangle \,. \tag{6.29}$$

When trying to find the minimum of the potential, we find that there is no degeneracy in the vacuum state as in Eq. (6.25) any more. Now the minimum condition imposes $\langle \vec{\pi} \rangle = 0$ and $\langle \sigma \rangle = v$, where v must satisfy the third order equation

$$\mu^2\, v \,-\, g\, v^3 \,+\, 4\,\beta \,=\, 0\,. \tag{6.30}$$

We can use Eq. (6.30) in order to write the Lagrangian in a more apparent way

$$\mathcal{L} = \frac{1}{4}\left\langle \partial_\mu \Sigma'\, \partial^\mu \Sigma'^\dagger \right\rangle - \frac{g}{16}\left(\left\langle \Sigma'\, \Sigma'^\dagger \right\rangle - 2\, v^2\right)^2 - \frac{\beta}{v}\left\langle \Sigma'\, \Sigma'^\dagger \right\rangle + \beta \left\langle \Sigma' + \Sigma'^\dagger \right\rangle , \tag{6.31}$$

and after writing the Lagrangian in terms of the excitations around the true vacuum one gets:

$$\begin{aligned} \mathcal{L} \;&=\; \frac{1}{4}\left\langle \partial_\mu \Sigma'\, \partial^\mu \Sigma'^\dagger \right\rangle - \frac{g}{16}\left(\left\langle \Sigma'\, \Sigma'^\dagger \right\rangle + v \left\langle \Sigma' + \Sigma'^\dagger \right\rangle\right)^2 - \frac{\beta}{v}\left\langle \Sigma'\, \Sigma'^\dagger \right\rangle \\ &=\; \frac{1}{2}\left(\partial_\mu \sigma'\, \partial^\mu \sigma' - m_\sigma^2\, \sigma'^2 + \partial_\mu \vec{\pi} \cdot \partial^\mu \vec{\pi} - m^2\, \vec{\pi} \cdot \vec{\pi}\right) - \frac{g}{4}\left(\sigma'^2 + \vec{\pi}^{\,2}\right)^2 \\ &\quad - \sqrt{\frac{g\,(m_\sigma^2 - m^2)}{2}}\, \sigma' \left(\sigma'^2 + \vec{\pi}^{\,2}\right) \,, \end{aligned} \tag{6.32}$$

where we have used the following relations and definitions:

$$\mu^2 \,=\, \frac{m_\sigma^2 - 3\, m^2}{2}\,, \quad v^2 \,=\, \frac{m_\sigma^2 - m^2}{2\, g}\,, \quad \beta \,=\, \frac{m^2}{4}\sqrt{\frac{m_\sigma^2 - m^2}{2\, g}}\,. \tag{6.33}$$

By means of a tree level matching with χPT we can relate the g constant with the pion decay constant [4]

$$g \,=\, \frac{m_\sigma^2 - m^2}{2\, F^2}\,, \tag{6.34}$$

[4]Note that in Ref. [9] the relation $2\,g = m_\sigma^2/F_\pi^2$ is used. However we identify F_π with the vacuum expectation value of the σ field v, which can be shown to coincide with the pion decay constant at leading order. In addition, in the non-linear parametrization of the LSM the pion fields are collected in the exponential matrix $\exp(i\,\vec{\tau}\cdot\vec{\pi}/v)$, which compares well with χPT after the identification $F_\pi = v$ is made. Finally, m_σ depends on the pion mass but at leading order the combination $m_\sigma^2 - m^2$ does not. Although in practice this choice does not affect the results of Eq. (6.60) and the discussion of this section, we prefer to use the notation of Ref. [182].

which allows us the write the Lagrangian as

$$\begin{aligned}\mathcal{L} &= \frac{1}{2}\left(\partial_\mu\sigma'\,\partial^\mu\sigma' - m_\sigma^2\,\sigma'^{\,2} + \partial_\mu\vec{\pi}\cdot\partial^\mu\vec{\pi} - m^2\,\vec{\pi}^{\,2}\right) \\ &\quad - \frac{m_\sigma^4}{F^4}\left(\sigma'^{\,2}+\vec{\pi}^{\,2}\right)^2 - \frac{m_\sigma}{F}\sqrt{(m_\sigma^2-m^2)}\,\sigma'\left(\sigma'^{\,2}+\vec{\pi}^{\,2}\right)\,. \end{aligned} \tag{6.35}$$

Let us calculate the minimum value $\frac{m_\sigma^2}{m^2}$ can achieve. From (6.33)

$$\frac{m_\sigma^2}{m^2} = 1 + \frac{g\,v^3}{2\,\beta}\,, \tag{6.36}$$

and then could naïvely think that for $g \to 0$ $\frac{m_\sigma^2}{m^2} \to 1$ but this is not true because from (6.30) follows that $g\,v^3 - 4\,\beta \geq 0$, and so $\beta \to 0$ as g does. Defining $g\,v^3 = 4\,\beta + g'\,v^3$, we always fulfill the minimum condition for $g' > 0$. Rewriting (6.36) we get

$$\frac{m_\sigma^2}{m^2} = 3 + \frac{g'\,v^3}{2\beta}\,, \qquad \Longrightarrow \qquad \frac{m_\sigma^2}{m^2} \geq 3\,. \tag{6.37}$$

where the limit is achieved for $g' \to 0^+$.

As a last comment, all the derivations we have done for finding the minimum of the potential are only valid at tree level. If one is to perform a one–loop calculation, the minimum condition has to be derived imposing a vanishing σ one–point function, as discussed in Appendix H.

6.4 Bounds on chiral LECs from dispersion relations

Low energy pion dynamics, particularly elastic pion–pion scattering encodes useful information about the confining dynamics of the strong interactions. The pions (and kaons) are the pseudo Goldstone bosons associated with the spontaneous breakdown of the chiral symmetry in QCD, a purely non–perturbative phenomenon.

As explained in Chapter 1, the standard technique to study the pion dynamics at very low energies as a series expansion in powers of the momentum and the quark masses is Chiral Perturbation Theory (χPT). It is formulated in terms of a Lagrangian whose only degrees of freedom are pions and which incorporates the symmetries of QCD, including spontaneously broken chiral symmetry. It also has all the usual benefits of a Lagrangian formalism.

At lowest order the physical observables are determined it terms of two parameters, namely the pion decay constant F and the pion (and kaon) mass m_π (m_K). The determination of their values from the experimental data is very precise. If one wants to go beyond the lowest order, a number of LECs l_i or L_i, not fixed by symmetries must be included. The grow of low energy constants (LECs for short)

is even more dramatic in the theory with three flavours [$SU(3)$ case] because the Cayley–Hamilton relations are less restrictive than for the $SU(2)$ theory. These can be determined by fitting to experimental data (for the best determination see Refs. [168,169]) or estimated by vector–meson dominance as discussed in Chapter 2 (see also [13, 170]), but both methods have large uncertainties.

An alternative formulation of $\pi\,\pi$ (and $\pi\,K$) scattering can be obtained based only on axiomatic principles of quantum field theory, such as analyticity, unitarity and crossing symmetry. This allows one to obtain relations between observable quantities that must hold, regardless of the theory used for the description of the phenomenon under study. Of course, one of the usual benefits of an effective theory approach is that many of these principles are automatically satisfied by the scattering amplitudes computed using the effective theory. Nevertheless, there is still useful information missing in the effective theory approach, and one obtains interesting results by studying the constraints imposed by axiomatic principles on the effective Lagrangian. Analyticity and unitarity can be exploited to write the well known dispersion relations for the scattering amplitudes. These, together with crossing symmetry, can be converted into positivity conditions on scattering amplitudes, which in turn, can be combined with the χPT predictions to give bounds on the $\bar{l}_1$ and $\bar{l}_2$ LECs in the chiral Lagrangian at $\mathcal{O}(p^4)$ [171]. We will extend this study also to the $SU(3)$ case, in which the kaon and eta particles also appear in the Lagrangian, to obtain bounds for L_1, L_2 and L_3 [172].

Two–flavour χPT was combined with axiomatic principles in Ref [173], which analysed constraints on s and p partial wave amplitudes in the framework of dispersion relations. The analysis was done in χPT at the one–loop level. In Ref. [174] this study was extended to cover all three isospin amplitudes of $\pi\,\pi$ scattering at the two–loop level in χPT. The best bounds were found for positivity conditions on full amplitudes (in contrast with partial wave amplitudes), and we follow this approach in the present work. However, we find inconsistencies in the domain of applicability of the positivity constraints used in Ref. [174] which will be explained in Section 6.4.1. Similar bounds where first found in Ref. [170] in the context of the Froissart–Gribov representation for the scattering lengths. More recently, in Ref. [175], the very same bounds of Ref. [170] were rediscovered using the same procedure as in Ref. [174] but using a more restricted domain of validity (in the Mandelstam plane) of the positivity constraint. References [170,175] both used one–loop χPT amplitudes. We show that the methods of Ref. [170] and Refs. [174, 175] are equivalent, and we improve the bounds by properly using the domain of validity considered in Ref. [174], which is bigger than that considered in Ref. [175].

To our knowledge the first attempt to confront dispersion relations with three–flavour χPT to bound linear combinations of LECs was Ref. [176]. However, in this early work, the contribution from chiral logarithms in the $\mathcal{O}(p^4)$ amplitude was ignored. This simplification becomes exact in the limit of infinite number of colours, but for a numerical analysis better results are obtained maintaining also chiral loops. In Ref. [176] it was only possible to assert that certain linear combinations of LECs were positive, and no information about the scale at which these

LECs were evaluated could be obtained.

In Ref. [177] a different approach was followed for putting bounds on some χPT parameters. QCD inequalities on Green functions of quark bilinear currents were used to obtain relations (inequalities) that involve light quark masses, the quark condensate and some LECs. With our method we are insensitive to the quark mass and condensate, since these are lowest order quantities and our analysis starts at $\mathcal{O}(p^4)$. On the other hand, since our study relies on scattering amplitudes, we only make use of the chiral Lagrangian when vector, axial–vector and pseudoscalar sources are switched off (one always needs the scalar source for giving masses to the pseudo–Goldstone bosons). In fact we can only give bounds for the $\mathcal{O}(p^4)$ LECs of operators containing only pseudo-Goldstone fields, L_1, L_2 and L_3, and so our results do not overlap with theirs.

The LSM Lagrangian is renormalizable and thus has a reduced (finite) number of parameters compared with the most general chiral Lagrangian. It shares the same symmetries as χPT but has an additional (σ) particle in its spectrum. If the σ mass is sufficiently greater than that of the pions, it can be formally integrated out of the action, leaving behind the χPT Lagrangian, with all the LECs having specific values which can be predicted in terms of the finite number of parameters of the LSM.

The values for $\bar{l}_1$ and $\bar{l}_2$ predicted by the LSM do not satisfy the dispersion relation bounds for low values of the σ mass. We will demonstrate that the LSM is perfectly consistent with the dispersion relation bounds and that the apparent contradiction results because for low values of the σ mass, integrating out the σ is not valid, or equivalently, that higher order terms in the chiral expansion cannot be neglected.

It is the purpose of Section 6.4.2 to generalize those results to the $SU(3)$ theory, and in particular to extend the method to cover the situation of different masses [this is, considering $SU(3)_V$ symmetry breaking]. In this way we will find out if for three flavours χPT suffers the same anomaly as the linear sigma model.

Since χPT consists on an expansion in both the external momenta and quark masses, the coefficients of the expansion (that is, the LECs) cannot depend on either of them. This means that LECs do not depend on the pseudo–Goldstone bosons masses. In other words the value of chiral LECs in our universe with $m_s \neq m_u = m_d$ is the same as in "another" universe in which the symmetry is unbroken, $m_u = m_d = m_s$. It is common lore in the literature, for instance, to consider massless quarks for estimating the values of some LECs, but this limit is not suitable for a dispersion relation analysis. The most straightforward generalization of the method used for $\pi\,\pi$ is thus to consider the exact $SU(3)_V$ limit in which there are only five independent amplitudes.

The bounds derived in this limit have two drawbacks: first, it is not clear what common mass should be adopted for the degenerate octet, what is essential to compare our bounds with the values obtained by fitting the experimental data (usually displayed at the $\mu = m_\rho$ scale); second, the results are not very challenging. In order to assess these two problems we will repeat our analysis with the physical values for the K and η masses. In this case the dispersive integrals will imply positivity

conditions only under more severe conditions. Once these are addressed the new bounds turn out to be much more restrictive, and remarkably the central values of the fitted LEC values lie precisely on the border dictated by axiomatic principles.

6.4.1 SU(2) bounds

Dispersion relations for $\pi\,\pi$ scattering

In this section, we find the region of the Mandelstam $s-t$ plane in which the $\pi\,\pi$ scattering amplitude is analytic, and derive the corresponding dispersion relations.

We begin by briefly reviewing a few properties of $\pi\,\pi$ scattering. For further details the reader is referred, for instance, to Ref. [178]. The three pionic states can be labeled either by $I_3 = -1,\, 0,\, 1$ or by Cartesian indices $a = 1,\, 2,\, 3$. Both sets of states are linearly related between them and to the physical pion states:

$$\begin{aligned} \left|\,\pi^{\pm}\,\right\rangle &= \frac{1}{\sqrt{2}}\left(\left|\,\pi^{1}\,\right\rangle \mp \left|\pi^{2}\right\rangle\right), \qquad \left|\,\pi^{0}\,\right\rangle = \left|\,\pi^{3}\,\right\rangle, \\ \left|\,1,\pm 1\,\right\rangle &= \mp\left|\,\pi^{\pm}\,\right\rangle, \qquad\qquad \left|\,1,0\,\right\rangle = \left|\,\pi^{0}\,\right\rangle, \end{aligned} \tag{6.38}$$

where $|\,\pi^{a}\,\rangle$ denotes the Cartesian basis, and $|\,1,I_3\,\rangle$ denotes the isospin basis states. Isospin invariance implies that there are only three linearly independent scattering amplitudes in the $I = 0, 1, 2$ channels, and crossing symmetry relates them to each other, so they can all be described by a single function of s and t. In the Cartesian basis we can write the Chew–Mandelstam formula

$$T(a\,b \to c\,d) \;=\; A(s,t,u)\,\delta^{ab}\delta^{cd} \,+\, A(t,s,u)\,\delta^{ac}\delta^{bd} \,+\, A(u,t,s)\,\delta^{ad}\delta^{bc}\,. \tag{6.39}$$

Crossing symmetry implies $A(x,y,z) = A(x,z,y) \equiv A(x,y) = A(x, 4\,m^2 - x - y)$ where m is the pion mass. The function A is related to the isospin amplitudes through

$$T^{0}(s,t) \,=\, 3\,A(s,t) + A(t,s) + A(u,s)\,,\; T^{1,2}(s,t) \,=\, A(t,s) \mp A(u,s)\,. \tag{6.40}$$

The $I = 0, 2$ amplitudes are symmetric under the exchange of the final states, whereas the $I = 1$ is antisymmetric: $T^{(0,2)}(s,t) = T^{(0,2)}(s,u)$, $T^{1}(s,t) = -\,T^{1}(s,u)$.

The isospin amplitudes in the different kinematic channels are also linearly related. For our present purposes, we only need the relation with the crossed u–channel. This follows directly from Eq. (6.40) and can be conveniently displayed in matrix notation

$$T^{\,I}(s,t) \;=\; C_u^{II'} T^{\,I'}(u,t)\,,\; C_u^{II'} C_u^{I'J} \,=\, \delta_{IJ}\,,\; C_u \,=\, \frac{1}{6}\begin{pmatrix} 2 & -\,6 & 10 \\ -\,2 & 3 & 5 \\ 2 & 3 & 1 \end{pmatrix}, \tag{6.41}$$

where, as expected, the crossing–matrix C_u is its own inverse. $T^{\,I}(s,t)$ is the scattering amplitude with isospin I in the s–channel, and $T^{\,I'}(u,t)$ is the amplitude with isospin I' in the u–channel.

Axiomatic principles can be used to show that scattering amplitudes are analytic in the full complex s plane except for possible isolated points, due to single particle exchange, and branch cuts, due to unitarity. For our purposes we only need to know the position s_0 of the first branch point along the real axis of the complex s plane. There is then a branch cut along the real s–axis for $s \geq s_0$. Any other singularities along the real s–axis will be along this cut. The remaining branch cuts will be determined by crossing symmetry.

Let us concentrate on the s channel keeping t fixed. Unitarity ensures that for real s, the scattering amplitude only develops an imaginary part above the lowest mass threshold of possible intermediate states [5]. In our case the threshold corresponds to two–pion states, *i.e.* $s_0 = 4\,m^2$. This means that above the production threshold (for physical amplitudes) the scattering amplitude is complex. Since below threshold, the amplitude is real and analytic away from the real axis, it follows from the Schwarz reflection principle that $T^*\,(s + i\,\epsilon) = T\,(s - i\,\epsilon)$ and hence $T\,(s + i\,\epsilon) - T\,(s - i\,\epsilon) = 2\,i\,\mathrm{Im}\,T\,(s + i\,\epsilon) \neq 0$. This means there must be a branch point at $s = 4\,m^2$, and a discontinuity in the amplitude along the real axis for $s > 4\,m^2$. We will choose the branch cut to run along the real s axis, because as already explained, the other branch points due to higher mass thresholds (`e.g.` four–pion state $s_1 = 16\,m^2$) or singularities due to single–particle states (`e.g.` ρ exchange $s_\rho = m_\rho^2$) will lie along it. We conclude that our amplitude is non–analytic for $s > 4\,m^2$, regardless of the value of t. The amplitude must also reproduce the singularities in the crossed channels, so it is non–analytic for $s, t, u > 4\,m^2$. The region in the $s - t$ plane where the amplitude is analytic is limited to the inside of the triangle defined by the conditions $s,\, t \leq 4\,m^2$, $s + t \geq 0$. $4\,m^2$ is referred to as the normal threshold, associated to the production of two pions. In Refs. [173, 175] it is assumed that the amplitude is only analytic between the normal threshold and the abnormal threshold, corresponding to $s,\, t,\, u = 0$. The region delimited by the condition $0 < s,\, t,\, u < 4\,m^2$ is known as the Mandelstam triangle (see Fig. 6.3).

However it has been proved [164] using very general arguments that rely on perturbation theory to all orders (i.e. that are true for every single Feynman diagram), that the amplitude becomes non–analytic only above the normal threshold, and that nothing particular happens at $s = 0$. The region bounded by $s, t, u < 4\,m^2$ is the larger triangle shown in Fig. 6.3. This is the main difference between our method and that of Ref. [175]. We use analyticity in a larger domain, and so obtain more restrictive conditions on the scattering amplitude. Ref. [174] uses the same analyticity domain as we do. However, in their numeric computations, they include points outside this region, which is not justified.

The derivation of the dispersion relation is quite straightforward and is very nicely explained, for instance, in Ref. [165]. For our derivation we consider t as a

[5] Above threshold, the physical scattering amplitude is defined as the value given by approaching the cut from above, $T^{\mathrm{phys}}(s, t) = T(s + i\,\epsilon, t)$, with $\epsilon \to 0$. This corresponds to the Feynman $i\,\epsilon$ prescription for propagators

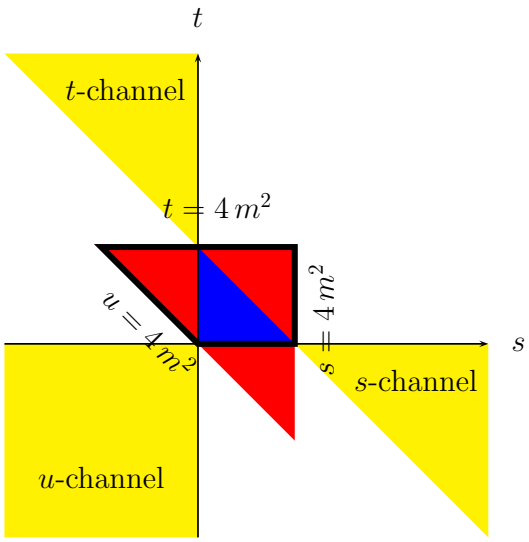

Figure 6.3: Mandelstam plane for $\pi\,\pi$ scattering. The small triangle in the center is the Mandelstam triangle. The big triangle is the region free from singularities. The outer dashed regions denote the physical regions for the three crossed channels, and the inner dashed region corresponds to the area $\mathcal{A}$ in which the positivity conditions are defined.

fixed parameter. We can then use Cauchy's theorem to write

$$T^I(s,t) \;=\; \frac{1}{2\,\pi\,i}\oint_\gamma \mathrm{d}x\,\frac{T^I(x,t)}{x-s}\,, \tag{6.42}$$

wherever the amplitude is analytic in a neighborhood (in s) of the point (s,t), and where the contour γ encloses the point $x = s$ [see Fig. 6.4 (a)].

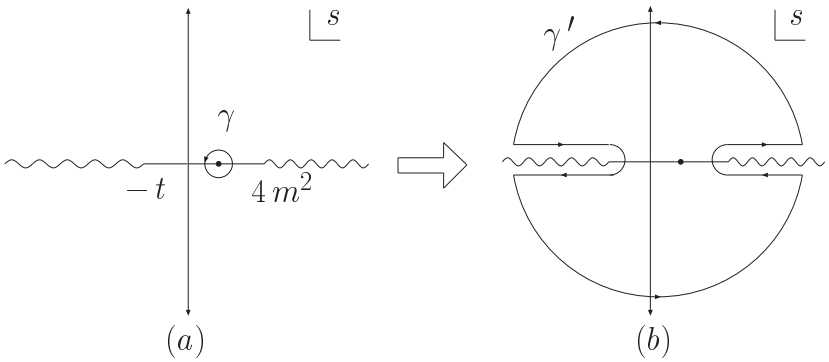

Figure 6.4: Contour integrals leading to the fixed t dispersion relations.

Then $t \leq 4\,m^2$, and if $s > 0$, we have to use $s \to s + i\,\epsilon$, as already mentioned. From the results of Ref. [164] we infer that fixed–t dispersion relations hold for

$t < 4\,m^2$, but using solely axiomatic principles it can be shown (Ref. [179]) that they are at least valid in the interval $-28\,m^2 \leq t \leq 4\,m^2$, which will be adequate for our purposes. For fixed t, we have along the real s–axis a right–hand branch cut for $s > 4\,m^2$ and a left–hand branch cut for $s < -t$. The γ contour in Eq. (6.42) can be deformed into γ', as shown in Fig. 6.4 (b) in order to express the integral in terms of the discontinuity of the amplitude along the real axis. In order to do this, the amplitude must fall sufficiently rapidly that the contribution from the contour at infinity vanishes. If it does not, we can perform n derivatives (subtractions) to increase the convergence at infinity,

$$\frac{\mathrm{d}^n}{\mathrm{d}s^n} T^I(s,t) \;=\; \frac{n!}{2\pi i} \oint_\gamma \mathrm{d}x\, \frac{T^I(x,t)}{(x-s)^{n+1}}\,. \tag{6.43}$$

For large enough n that the contour at infinity does not contribute, one finds after some straightforward manipulations that

$$\frac{\mathrm{d}^n}{\mathrm{d}s^n} T^I(s,t) \;=\; \frac{n!}{\pi} \int_{4\,m^2}^{\infty} \mathrm{d}x \left[\frac{\delta^{II'}}{(x-s)^{n+1}} + (-1)^n\, \frac{C_u^{II'}}{(x-u)^{n+1}} \right] \mathrm{Im}\, T^{I'}(x + i\,\epsilon, t)\,. \tag{6.44}$$

The first term is from the discontinuity across the right–hand cut. The second term is from the discontinuity across the left–hand cut, rewritten using crossing symmetry and Eq. (6.41) to relate the s–channel discontinuity in the unphysical region $s < 0$ to the u–channel discontinuity in the physical region.

The best constraint comes from using Eq. (6.44) with the smallest possible value of n. The Froissart bound [180] fixes the minimum number of subtractions needed for pion–pion scattering to $n = 2$. Clearly, if we restrict ourselves to $s < 4\,m^2$ and $s + t > 0$, both denominators in Eq. (6.44) are positive, and if n is an even number (for instance, in our case $n = 2$) the relative sign is also positive, except for the sign of $C_u^{II'}$.

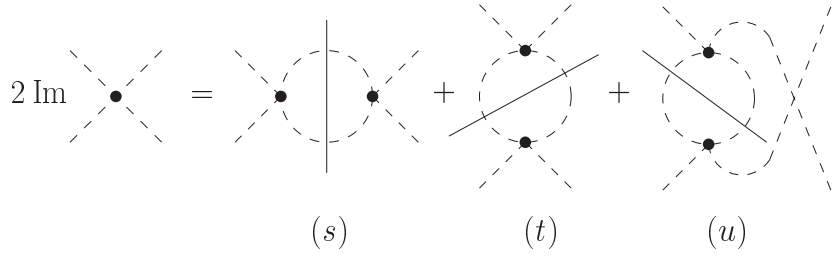

Figure 6.5: Lowest mass branch points in the three crossed channels, corresponding to the physical threshold of two–pion production .

Bounds implied by the dispersion relation

Each isospin amplitude admits a partial wave expansion. In the case of spin–zero particles, the amplitude depends only on the scattering angle θ, defined as the angle

between the three–momenta of the first initial and final pions, in the center of mass frame. Specializing Eq. (6.12) to spin–zero particles, taking $\phi = 0$ and using $\mathcal{D}^J_{00}(\phi, \theta, -\phi) = P_l(\cos\theta)$ we get :

$$T^I(s,t) \,=\sum_{\ell=0}^{\infty}(2\,\ell+1)\,f^I_\ell(s)P_\ell(\cos\theta) \,=\sum_{\ell=0}^{\infty}(2\,\ell+1)\,f^I_\ell(s)P_\ell\left(1+\frac{2\,t}{s-4\,m^2}\right)\,, \tag{6.45}$$

where $f^I_\ell(s)$ denotes the partial wave amplitudes. The optical theorem implies

$$\mathrm{Im}\, f^I_\ell(s) \;=\; s\,\beta(s)\,\sigma^I_\ell(s) \;\geq\; 0\,, \tag{6.46}$$

where $\beta(s) = \sqrt{1-\frac{4\,m^2}{s}}$ is the velocity of the pions in the center of mass frame, and σ^I_ℓ are the partial–wave cross–sections in a given isospin channel. Equation (6.46) gives

$$\mathrm{Im}\, T^I(s,t) \,=\sum_{\ell=0}^{\infty}(2\,\ell+1)s\,\beta(s)\,\sigma^I_\ell(s)P_\ell\left(1+\frac{2\,t}{s-4\,m^2}\right)\,. \tag{6.47}$$

The partial wave expansion of the absorptive part converges in the large Lehmann–Martin ellipse, which, when projected onto real s translates into the interval $-4\,m^2 < s < 60\,m^2$. We also need to make sure the absorptive part is positive. In Eq. (6.44), the region of integration is $s > 4\,m^2$, and as pointed out in Ref. [173], since $P_\ell(z) > 1$ for $z > 1$ for all ℓ, if we restrict ourselves to $t > 0$, each partial wave contribution to the imaginary part is positive and so the full imaginary part is itself positive. As noted in Ref. [175], one can find certain linear combinations $\sum a_I\,T^I$ with $a_I \geq 0$, $\sum a_I\,C^{IJ}_u\,T_J \equiv \sum_J b_J\,T_J$ with $b_J = \sum_I a_I\,C^{IJ}_u \geq 0$. For these linear combinations, the two terms in brackets in Eq. (6.44) give a positive contribution. Hence, for these linear combinations, in the region $\mathcal{A}$ defined as s, $t < 4\,m^2$, $t > 0$ and $s + t > 0$ (see Fig. 6.3) the right–hand side of Eq. (6.44) for $n = 2$ is also positive.

There are three linear combinations which satisfy the positivity condition, corresponding to the physical processes $\pi^0\pi^0 \to \pi^0\pi^0$, $\pi^+\pi^+ \to \pi^+\pi^+$ and $\pi^+\pi^0 \to \pi^+\pi^0$. In matrix notation we can write

$$0 \;\leq\; C^{I\,J}_{\rm pos}\,\frac{\mathrm{d}^2}{\mathrm{d}s^2}T^J[\,(s,t)\in\mathcal{A}\,]\,,\qquad C_{\rm pos} \;=\; \begin{pmatrix} \frac{1}{3} & 0 & \frac{2}{3} \\ 0 & \frac{1}{2} & \frac{1}{2} \\ 0 & 0 & 1 \end{pmatrix}\,. \tag{6.48}$$

These results are in fact expected and can be deduced without any mention of isospin amplitudes. The optical theorem ensures that for processes with the same initial and final particles $a + b \to a + b$, the imaginary part of each partial wave is positive definite. The crossed u–channel for those processes has equal initial and final states as well, $a + \bar{b} \to a + \bar{b}$, so for such processes, the imaginary part along

the right– and left–hand cuts will be always positive. The positivity conditions for the three processes are

$$0 \leq \frac{\mathrm{d}^2}{\mathrm{d}s^2} T\left(\pi^0\pi^0 \to \pi^0\pi^0\right)[\,(s,t) \in \mathcal{A}\,], \quad 0 \leq \frac{\mathrm{d}^2}{\mathrm{d}s^2} T\left(\pi^+\pi^0 \to \pi^+\pi^0\right)[\,(s,t) \in \mathcal{A}\,],$$
$$0 \leq \frac{\mathrm{d}^2}{\mathrm{d}s^2} T\left(\pi^+\pi^+ \to \pi^+\pi^+\right)[\,(s,t) \in \mathcal{A}\,], \tag{6.49}$$

corresponding to $\frac{2}{3}\,T^{(2)}(s,t) + \frac{1}{3}\,T^{(0)}(s,t)$, $\frac{1}{2}\,T^{(2)}(s,t) + \frac{1}{2}\,T^{(1)}(s,t)$ and $T^{(2)}(s,t)$, respectively.

Bounds for $\mathbf{l_1}$ and $\mathbf{l_2}$ in χPT : choice of the most stringent point

It is simple to convert the conditions displayed in Eq. (6.49) into bounds for chiral LECs. The region $\mathcal{A}$ covers a very low energy domain, and is below the $2\,\pi$ threshold in any of the three crossed channels. In this range of energies one expects the chiral expansion to work well, so we will approximate the right–hand side of Eq. (6.49) by the χPT result at $\mathcal{O}(p^4)$.

Since the χPT amplitude is derived from a local Lagrangian, it automatically respects the principles of crossing symmetry, unitarity and analyticity. One could naïvely argue that the positivity constraints should also be automatically satisfied, but this is not necessarily true. As noted in Ref. [173], χPT is an expansion in low momenta, so the amplitude has polynomial behaviour (up to logarithms) and grows as s^2 or even worse at higher orders, violating the Froissart bound. As a result, the positivity constraints provide additional information beyond χPT, and give restrictions on the LECs.

The χPT leading order amplitude is linear in s and t and so vanishes on taking the second derivative; the next–to–leading order amplitude does not. The $\mathcal{O}(p^4)$ amplitude can be found in Ref. [9, 18], and its second derivative depends only on two LECs : $\bar{l}_1$ and $\bar{l}_2$ in the $SU(2)_L \otimes SU(2)_R$ chiral Lagrangian. The amplitude can be split into polynomial terms quadratic in momenta and masses, and chiral logarithms. The former contain the LECs and their second derivatives yield energy independent terms; the latter depend only on momenta and masses, are independent of the $\mathcal{O}(p^4)$ LECs, and give energy dependent contributions to the second derivative. The general structure of the bound can thus be written as

$$\sum_{i=1}^{2} \alpha_{ji}\,\bar{l}_i \;-\; f_j[\,(s,t) \in \mathcal{A}\,] \;\geq\; 0 \quad j \;=\; 1,2,3\,, \tag{6.50}$$

where α_{ji} are real coefficients and $f_j(s,t)$ are functions obtained from chiral logarithms and LEC–independent polynomial terms, and j labels each one of the processes in Eq. (6.49). The most stringent restriction is obtained for those values of (s,t) that maximize $f_j(s,t)$ inside the region $\mathcal{A}$:

$$\sum_{i=1}^{2} \alpha_{ji}\,\bar{l}_i \;\geq\; f_j[\,(s,t) \in \mathcal{A}\,]\,\Big|_{\max}\,. \tag{6.51}$$

Process	LECs	Maximum position	Bound	Fit to Expt
$\pi^0\pi^0 \to \pi^0\pi^0$	$\bar{l}_1 + 2\,\bar{l}_2$	$s = 0$	$\geq \frac{157}{40} = 3.925 \pm 0.4$	8.2 ± 0.6
$\pi^+\pi^0 \to \pi^+\pi^0$	$\bar{l}_2$	$s = 0$	$\geq \frac{27}{20} = 1.350 \pm 0.4$	4.3 ± 0.1
$\pi^+\pi^+ \to \pi^+\pi^+$	$\bar{l}_1 + 3\,\bar{l}_2$	$1.114\,m^2$	$\geq 5.604 \pm 0.4$	12.5 ± 0.7

Table 6.1: Bounds obtained by unitarity, crossing and analyticity and comparison with values extracted from a fit to the experimental data given in Ref. [168]. The error on the bound is an estimate of the $\mathcal{O}(p^6)$ terms.

It is important to estimate possible corrections to the bounds in Eq. (6.51) coming from $\mathcal{O}(p^6)$ terms in the amplitude. The computation of the $\pi\,\pi$ scattering amplitude at this level of precision was performed in Ref. [181], and can be split into three pieces: two–loop terms (double chiral logarithms), that only depend on m and F_π; one–loop terms (single chiral logarithms), that depend linearly on several $\mathcal{O}(p^4)$ LECs (not only l_1 and l_2); and tree–level terms, that depend on $\mathcal{O}(p^6)$ LECs. In Ref. [174], Eq. (6.50) was calculated with the corresponding $\mathcal{O}(p^6)$ amplitude for $\pi^0\pi^0$ and $\pi^+\pi^0$ at $s = 0$, $t = 4\,m^2$. Unfortunately the corresponding $\mathcal{O}(p^6)$ LECs are badly known (resonance saturation estimates are usually used), and the chiral LECs we want to bound, l_1 and l_2, appear again in the one–loop terms. In addition the rest of LECs in the one–loop terms are symmetry breaking operators, and hence appear always multiplied by the pion mass. As a result, their numerical values are poorly known. So we have only control over the two–loop terms. To get an educated guess for the error from the $\mathcal{O}(p^6)$ terms, we will multiply the value of the purely two–loop correction by a factor of three. To be more conservative we will adopt as a common error for the three bounds, the biggest of these, which is 0.4.

There is one last issue to be discussed before we show our results. It is well known that the scalar one–loop two–point function is not smooth at threshold (for instance its imaginary part is zero below threshold but non–zero above). Its first and second derivatives tend to infinity when we approach threshold from below. So in order for the positivity condition to hold, the coefficients in front of these first and second derivatives must always be positive below threshold. This is indeed the case in all processes under study in our work.

We find that the maximum of $f_j(s,t)$ is always achieved for $t = 4\,m^2$, regardless of the process (i.e. for $j = 1, 2, 3$); the value for s does depend on the particular process. The maximum of f_j is at $s = 0$ for $j = 1, 2$. For $j = 3$, the maximum was found numerically to be at $s = 1.114\,m^2$. Our results are summarized in Table 6.1 together with a comparison with the values for the experimentally fitted LECs $\bar{l}_1 = -0.4 \pm 0.6$ and $\bar{l}_2 = 4.3 \pm 0.1$ from Ref. [168]. In Fig. 6.6, we plot the allowed region in the $\bar{l}_1 - \bar{l}_2$ space parameter, together with the experimentally fitted value.

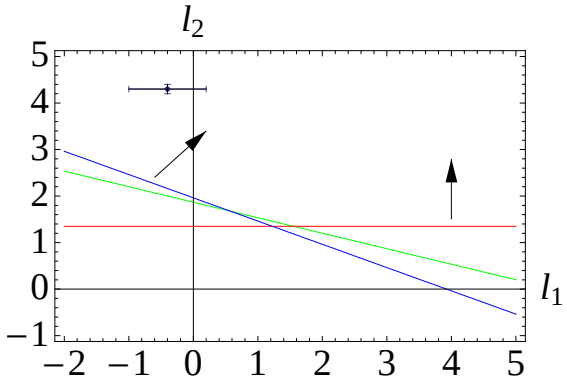

Figure 6.6: The $\bar{l}_1 - \bar{l}_2$ region allowed by the positivity conditions is shown. The three lines correspond to the three bounds in Table 6.1. We also show the experimentally fitted values of Ref. [168] with their error.

Comparison with previous analyses

As mentioned in Section 6.4, there are several studies in the literature that combine χPT with axiomatic principles. In this section we compare with previous results and point out the advantages of the method used here.

In Ref. [173] only the $\pi^0\pi^0$ amplitude was considered, and so only bounds on $\bar{l}_1 + 2\,\bar{l}_2$ could be obtained. From the requirement that the s–wave amplitude has a minimum in the interval $1.217 \leq s/m^2 \leq 1.697$ they obtain $\bar{l}_1 + 2\,\bar{l}_2 \geq 3.32 \pm 0.85$. This value is less restrictive than our bound, and in addition has a much bigger uncertainty. From the once subtracted dispersion relation of the full $\pi^0\pi^0$ amplitude they obtain $\bar{l}_1 + 2\,\bar{l}_2 \geq 3.3 \pm 2.5$ which has a very large error, and is weaker than our bound. Using the Froissart–Gribov representation for the d–wave partial amplitude, they obtained our value for the bound, but since a reliable estimate of its error was not found, this result was not taken into account in the final results in Ref. [173].

In Ref. [170], the Froissart–Gribov representation for the d–wave scattering lengths was used to derive positivity conditions. In this way they reproduce our results for $\bar{l}_1 + 2\,\bar{l}_2$ and $\bar{l}_2$, with no errors quoted. In the next section we demonstrate that this method is equivalent to ours for the particular point $s = 0$, $t = 4\,m^2$.

In Ref. [174], the analysis of Ref. [173] was repeated, requiring a minimum of the s–wave amplitude in the same interval as above, $1.217 \leq s/m^2 \leq 1.697$. Surprisingly Ref. [174] obtained a much more stringent bound, $\bar{l}_1 + 2\,\bar{l}_2 \geq 6.16$ (no error quoted). In view of the discussion in both papers, it is our believe that Ref. [173] gives the correct answer. The main analysis of Ref. [174] uses the same method that we do, and in the same domain $\mathcal{A}$. They argue that the most stringent point necessarily lies on the $2\,s + t = 4\,m^2$ line, but we do not see why this should be true. In fact, we explicitly find that for the $\pi^+\pi^+$ amplitude it is not on this line. Furthermore, Ref. [174] only display the bounds at $s = 0$ ($t = 4\,m^2$), where we get the same results for $\bar{l}_1 + 2\,\bar{l}_2$ and $\bar{l}_2$, and at $s = -\,4\,m^2$ ($t = 12\,m^2$), where the bounds are much more

restrictive. The result $\bar{l}_1 + \bar{l}_2 \geq 4.914$ quoted in Ref. [174] at $s = -4\,m^2$ ($t = 12\,m^2$) is violated by the experimentally fitted values of Ref. [168]. Even though Ref. [174] uses the same domain $\mathcal{A}$ as our analysis, for the numerics they trespass outside this region. The bounds $\bar{l}_1 + 2\,\bar{l}_2 \geq 6.923$, $\bar{l}_2 \geq 2.01$ and $\bar{l}_1 + \bar{l}_2 \geq 4.914$ should not be trusted since the fixed–t dispersion relations are not valid for $t > 4\,m^2$.

Finally, in Ref. [175] the same method of Ref. [174] is used, but only in the Mandelstam triangle, which is why their bound for $\bar{l}_1 + 3\,\bar{l}_2$ is less restrictive than ours, and does not exclude any values for $\bar{l}_{1,2}$ not already excluded by the bounds on $\bar{l}_1 + \bar{l}_2$ and $\bar{l}_2$.

Relation between our method with scattering lengths

In this appendix we wish to demonstrate how the procedure followed in Ref. [170] is related to ours. Let us start by recalling the definition of the scattering lengths. From the partial wave decomposition of Eq. (6.45), one defines for each spin and isospin amplitude the scattering lengths a_ℓ^I

$$a_\ell^I \;=\; \lim_{s\to 4\,m^2} \frac{f_\ell^I(s)}{\left(\frac{s}{4} - m^2\right)^\ell}\,. \tag{6.52}$$

For even ℓ, the $I = 1$ scattering length must vanish because of Bose symmetry. In Ref. [170] these scattering lengths can be shown to satisfy the positivity conditions

$$a_2^0 \,+\, 2\,a_2^2 \,\geq\, 0\,, \qquad a_2^0 \,-\, a_2^2 \,\geq\, 0\,. \tag{6.53}$$

using the Froissart–Gribov representation:

$$a_2^I \;=\; \frac{16}{15\pi} \int_{4m^2}^\infty \frac{\mathrm{d}s}{s^3}\, \mathrm{Im}\, F_t^I\left(s, 4\,m^2\right). \tag{6.54}$$

It is not difficult to relate the scattering lengths to the ℓ–derivative of the total spin–I scattering amplitude:

$$a_\ell^I \;\;=\;\; \frac{4^\ell\,\ell\,!}{(2\,\ell+1)}\, \frac{\mathrm{d}^\ell T^I(4\,m^2,t)}{\mathrm{d}\,t^\ell}\bigg|_{t=0} \;=\; \frac{4^\ell\,\ell\,!}{(2\,\ell+1)}\, C_t^{II'}\, \frac{\mathrm{d}^\ell T^{I'}(s,4\,m^2)}{\mathrm{d}\,s^\ell}\bigg|_{s=0}\,, \tag{6.55}$$

where we have used a relation analogous to Eq. (6.41)

$$T^I(s,t) \,=\, C_t^{II'} T^{I'}(t,s)\,, \quad C_t^{II'} C_t^{I'J} \,=\, \delta_{IJ}\,, \quad C_t \,=\, \frac{1}{6}\begin{pmatrix} 2 & 6 & 10 \\ 2 & 3 & -5 \\ 2 & -3 & 1 \end{pmatrix}, \tag{6.56}$$

which follows from crossing symmetry in the t–channel.

For even ℓ and $I = 1$, Eq. (6.55) implies that the corresponding scattering length is identically zero. To see this, recall that $T^1(4\,m^2,t) = -\,T^1(4\,m^2,-t)$ by

Bose symmetry. Now, since the point $s = 0$, $t = 4\,m^2$ lies in the region $\mathcal{A}$, for $\ell = 2$ we know that certain linear combinations of the derivatives appearing in the last equality of Eq. (6.55) must be positive. Inverting Eq. (6.55) we obtain

$$\left.\frac{\mathrm{d}^2\,T^I(4\,m^2,t)}{\mathrm{d}\,t^2}\right|_{t=0} = \frac{5}{32}\,C_t^{I\,J}\,a_2^I\,. \tag{6.57}$$

Using Eq. (6.48) we obtain

$$C_{\rm pos}^{IJ}\,C_t^{JK}\,a_2^K \equiv C_a^{IJ}\,a_2^J \geq 0\,, \qquad C_a = \begin{pmatrix} 1 & 0 & 2 \\ 1 & 0 & -1 \\ 2 & -3 & 1 \end{pmatrix}, \tag{6.58}$$

and bearing in mind that $a_2^1 \equiv 0$ we immediately reproduce the result shown in Eq. (6.53) plus the linearly dependent relation $2\,a_2^0 + a_2^2 \geq 0$.

We have demonstrated that the method in Ref. [170] corresponds to using positivity at the $s = 0$, $t = 4\,m^2$ point in region $\mathcal{A}$ of the Mandelstam plane. This is why Ref. [170] did not find our third bound, which arises from $s = 1.114\,m^2$, $t = 4\,m^2$.

Unitarity relations for the linear sigma model

In Section 6.4.1, we substituted the χPT results into Eq. (6.49) and obtained bounds on some undetermined low–energy constants in the effective Lagrangian. One can repeat this exercise for theories in which the low–energy effective Lagrangian is calculable, to test the validity of the bounds. In this section we perform such an analysis for the linear sigma model.

The most straightforward method is to use the predictions of the LSM for $\bar{l}_1$ and $\bar{l}_2$ for the bounds displayed in Table 6.1. As already explained the LSM is invariant under the same symmetries as χPT, and so all operators obtained after integrating out the σ particle must belong to the χPT Lagrangian at some order in the chiral expansion. In Ref. [9] this computation was performed at the one–loop level and at $\mathcal{O}(p^4)$, the following result was obtained:

$$\bar{l}_1 = \frac{24\,\pi^2}{g} + \log\left(\frac{m_\sigma}{m}\right) - \frac{35}{6}\,, \qquad \bar{l}_2 = \log\left(\frac{m_\sigma}{m}\right) - \frac{11}{6}\,, \tag{6.59}$$

leading to the inequalities

$$\frac{24\,\pi^2}{g} + 3\,\log\left(\frac{m_\sigma}{m}\right) \geq \frac{437}{40}\,, \quad \log\left(\frac{m_\sigma}{m}\right) \geq \frac{191}{60}\,, \quad \frac{24\,\pi^2}{g} + 4\,\log\left(\frac{m_\sigma}{m}\right) \geq 19.94\,. \tag{6.60}$$

These results are obtained in weak–coupling perturbation theory to one–loop, and have corrections of order g from the two–loop graphs. The first and third relations of Eq. (6.60) are always satisfied for a weakly coupled theory on which Eq. (6.59)

rely, since the $24\,\pi^2/g$ term is larger than the other terms for small values g. Note that the coefficient of the $1/g$ term must have the correct sign for the inequality to be satisfied, which it does. The second relation does not involve an inverse power of the coupling constant, and is not satisfied for large enough values of m/m_σ. In particular, it is violated if $m_\sigma \lesssim 4.9\,m$. One way out of this contradiction is that the derivation of the inequality, which relies on the Froissart bound, is not valid. But it is not difficult to show that the LSM is a local renormalizable theory, and satisfies the Froissart bound. In the chiral limit $m \to 0$ and the bound is satisfied. The Goldstone boson is made massive by a symmetry breaking term (analogous to an external magnetic field). The strength of the symmetric breaking term must be increased to increase m. The symmetry breaking term also contributes to the σ mass, so another way out is if the region $m_\sigma/m \lesssim 4.9$ is not possible for any values of the parameters in the LSM. But as we explicitly showed in Section 6.3 any $m_\sigma/m \geq \sqrt{3}$ is allowed, and since $\sqrt{3} < 4.9$ there are allowed values for the mass ratio which violate the bound.

The loophole in the argument is that for low values of the σ mass, the higher $1/m_\sigma^2$ corrections become more important. Results in Table 6.1 rely on the fact that in χPT, the scattering amplitude can be safely truncated at $\mathcal{O}(p^4)$, which translates into the statement that the LSM amplitude can be truncated at $\mathcal{O}(m_\sigma^{-2})$. If m_σ is not big enough, this approximation receives sizable corrections and the chiral expansion breaks down. To violate the bound in the second of Eqs. (6.60) requires $m_\sigma \lesssim 4.9.1\,m$. The chiral expansion is formally an expansion in powers of m/m_σ, and the bound is violated when $m^2/m_\sigma^2 \sim 0.04$, a finite distance away from the origin. What is surprising is that this number, which is formally of order one, is numerically much smaller than one would have naively guessed.

As a first approach, we include the $1/m_\sigma^4$ corrections to the amplitude, and find

$$\log\left(\frac{m_\sigma^2}{m^2}\right) \geq \frac{191\,m_\sigma^4 - 734\,m_\sigma^2\,m^2 + 540\,m^4}{60\,(m^2 - m_\sigma^2)(3\,m^2 - m_\sigma^2)}\,. \tag{6.61}$$

Taking the limit $m_\sigma \to \infty$ we recover the second relation in Eq. (6.60). Solving Eq. (6.61) we find that the bounds are violated for $m_\sigma \lesssim 5\,m$, which is not satisfactory, but indicates that the $1/m_\sigma^2$ expansion is slowly converging, and the $1/m_\sigma^4$ term contribution moves the result in the direction of restoring the validity of the bound. To test the LSM bound we will apply directly Eq. (6.49), rather than the expanded form Eq. (6.59), to the LSM scattering amplitude prediction for the $\pi^+\pi^0 \to \pi^+\pi^0$ process. The second derivative of the tree–level amplitude for this process within the LSM vanishes, and so one needs the one–loop result. In Ref. [182] this calculation was performed using a mass–dependent subtraction scheme. The result is expressed in terms of finite two–, three– and four–point scalar one–loop integrals, which are then expanded in inverse powers of m_σ^2. We will use instead the numerical values for the full integral expressions. The renormalization procedure followed in Ref. [182] is perfectly acceptable for our computation, since the physical amplitudes are scheme independent. Most modern computations are done in the $\overline{\rm MS}$ scheme. In Appendix H we give the one–loop LSM amplitudes in the mass–independent $\overline{\rm MS}$

scheme, a result which does not appear in the literature.

The second derivative $\frac{\mathrm{d}^2}{\mathrm{d}s^2}T(s,4\,m^2)|_{s=0}$ for the $\pi^+\pi^0 \to \pi^+\pi^0$ process in the LSM is computed for any value of the m_σ/m ratio. The results are shown in Fig. 6.7, which clearly shows that the positivity condition is satisfied at the one–loop level in the LSM for any value of the σ mass bigger than the pion mass (even though it would suffice to be satisfied for $m_\sigma > \sqrt{3}\,m$). The apparent contradiction of Eq. (6.60) was only due to the poor convergence of the of the $1/m_\sigma^2$ expansion of the LSM amplitude for small m_σ. The non–linear sigma model (understood as the non–renormalizable effective field theory obtained by integrating the σ field out the LSM action) is consistent (i.e. obeys the axiomatic bounds) only if we (at least) include the $\mathcal{O}(p^8)$ contribution. well.

This should serve as a warning for the estimate of chiral LECs by resonance saturation. In such determinations, one starts with a chiral invariant Lagrangian with resonances as explicit degrees of freedom [13]. The values of the chiral LECs are obtained, as in the LSM, by functionally integrating out the hadronic resonances. The ratio $m_\rho/m \sim 5.5$ is much smaller than the value m_σ/m that makes the LSM chiral expansion fail. However we believe that since in the Lagrangians of [13], all LECs are already generated at tree–level, this anomalous behaviour is absent. In the LSM, l_2 is only generated at one–loop, which is why the middle inequality in Eq. (6.60) does not have a $1/g$ term, and has poor convergence in the $1/m_\sigma^2$ expansion.

At this point a natural question arises. Since $m_K/m \sim 3.5 < 5$ it could be inconsistent to integrate the kaon and eta out of the $SU(3)$ χPT action to obtain the $SU(2)$ chiral LECs. In fact using the L_1, L_2 and L_3 values of Ref. [169], we obtain $\bar{l}_1 = 5.64 \pm 0.84$ and $\bar{l}_2 = 1.95 \pm 0.23$ which do not agree well with the values quoted in Ref. [168], but are in agreement with our bounds. The additional complications that arise on imposing the positivity conditions to $SU(3)$ χPT are discussed in next section.

6.4.2 SU(3) bounds

In this section we will apply the same procedure as in Section 6.4.1 for the $SU(3)$ theory. As a first approximation we will consider the $SU(3)_V$ limit in which $m_u = m_d = m_s$ and thus the masses of the eight pseudo–Goldstone bosons are the same, and will be denoted by m. As already mentioned, the value of the chiral LECs cannot depend of the quark masses, and so bounds for LECs derived in a world with equal quark masses must also be satisfied in our own world. After this simple analysis we will extend the method to cover also the case of $m_u = m_d \neq m_s$.

SU(3) relations: coupling of two octets and irreducible amplitudes

In the limit we are considering the QCD Lagrangian exhibits an exact $SU(3)_V$ symmetry. Then particles are classified according to the different irreducible representations of this group (e.g. pGs belong to the real octet representation) and the

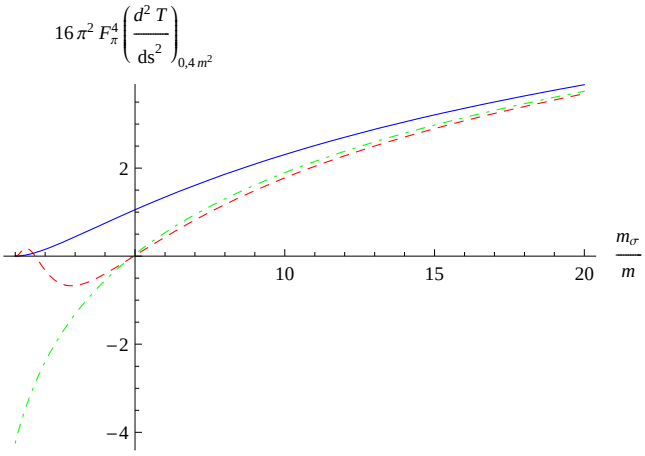

Figure 6.7: Plot of $16\,\pi^2 F_\pi^4\,\mathrm{d}^2T(s,4\,m^2)/\mathrm{d}s^2\big|_{s=0}$ in the linear sigma model for the $\pi^+\pi^0 \to \pi^+\pi^0$ process as a function of m_σ/m. The exact amplitude (blue) is positive for $m_\sigma > m$. The amplitude up to and including $1/m_\sigma^4$ terms (red, dashed), is positive for $m_\sigma > 5\,m$. The $\mathcal{O}(m_\sigma^{-2})$ amplitude (green, dotdashed) remains negative for $m_\sigma < 4.9\,m$.

Wigner–Eckart theorem drastically reduce the number of independent amplitudes to six. To see this we simply need to look at the Clebsch–Gordan decomposition of the direct product of two octets:

$$8 \otimes 8 \;=\; 27 \oplus 10 \oplus 10^* \oplus 8_1 \oplus 8_2 \oplus 1\,. \tag{6.62}$$

First we express the two–particle states as linear combinations of vectors with well defined total quantum numbers, belonging to different irreducible representations. We recall the $SU(3)$ quantum numbers for the octet mesons $|\mu, I, I_3, Y\rangle$:

$$\begin{aligned}
&|\,\pi^+\,\rangle = -\,|8,1,1,0\rangle\;, && |\,\pi^0\,\rangle = |8,1,0,0\rangle\;, && |\,\pi^-\,\rangle = |8,1,-1,0\rangle\;,\\
&|\,\eta\,\rangle = |8,0,0,0\rangle\;, && |\,K^+\,\rangle = \left|8,\frac{1}{2},\frac{1}{2},1\right\rangle\;, && |\,K^0\,\rangle = \left|8,\frac{1}{2},-\frac{1}{2},1\right\rangle\;,\\
&|\,\bar K^0\,\rangle = \left|8,\frac{1}{2},\frac{1}{2},-1\right\rangle\;, && |\,K^-\,\rangle = -\left|8,\frac{1}{2},-\frac{1}{2},-1\right\rangle\;,
\end{aligned} \tag{6.63}$$

and the relation between the Cartan and the physical states bases,

$$\begin{aligned}
&\left|\pi^\pm\right\rangle = \frac{1}{\sqrt{2}}\left(\left|\pi^1\right\rangle \mp i\left|\pi^2\right\rangle\right)\;, && \left|K^\pm\right\rangle = \frac{1}{\sqrt{2}}\left(\left|\pi^4\right\rangle \mp i\left|\pi^5\right\rangle\right)\;, && \left|\pi^0\right\rangle = \left|\pi^3\right\rangle\;,\\
&\left|K^0\right\rangle = \frac{1}{\sqrt{2}}\left(\left|\pi^6\right\rangle - i\left|\pi^7\right\rangle\right)\;, && \left|\bar K^0\right\rangle = \frac{1}{\sqrt{2}}\left(\left|\pi^6\right\rangle + i\left|\pi^7\right\rangle\right)\;, && |\,\eta\,\rangle = \left|\pi^8\right\rangle,
\end{aligned} \tag{6.64}$$

The general procedure to fully decompose the direct product of irreducible representations (which is in general reducible) into irreducible representations is explained

in Ref. [183], and we shall use its notation. Basically one must use the following general formula :

$$\begin{aligned}&\left|8,\, I^1,\, I_3^1,\, Y^1\right\rangle \otimes \left|8,\, I^2,\, I_3^2,\, Y^2\right\rangle = \\ &\sum_{I,\mu_\gamma} C\left(I^1,\, I^2,\, I \,\middle|\, I_3^1, I_3^2 I_3\right) C\left(\begin{array}{cc|c} 8 & 8 & \mu_\gamma \\ I^1\, Y^1 & I^2\, Y^2 & I\, Y \end{array}\right) \left|\mu_\gamma,\, I,\, I_3,\, Y\right\rangle . \quad (6.65)\end{aligned}$$

One can also calculate the inverted relation, what means that we express the vectors with well defined total quantum numbers belonging to different irreducible representations as linear combinations of two–particle states :

$$\begin{aligned}\left|\mu_\gamma,\, I,\, I_3,\, Y\right\rangle \;=\; &\sum_{I^1, I^2, I_3^1, I_3^2} C\left(I^1,\, I^2,\, I \,\middle|\, I_3^1, I_3^2 I_3\right) \times \quad (6.66)\\ &C\left(\begin{array}{cc|c} 8 & 8 & \mu_\gamma \\ I^1\, Y^1 & I^2\, Y^2 & I\, Y \end{array}\right) \left|8,\, I^1,\, I_3^1,\, Y^1\right\rangle \otimes \left|8,\, I^2,\, I_3^2,\, Y^2\right\rangle .\end{aligned}$$

Since we suppose that our QCD Lagrangian is invariant under the $SU(3)$ flavour group, we can make use of the identity

$$\left\langle \mu_1\, \nu_1 \,\middle|\, T \,\middle|\, \mu_2\, \nu_2 \right\rangle \;=\; F_{\mu_1} \delta_{\mu_1 \mu_2} \delta_{\nu_1 \nu_2} \,, \quad (6.67)$$

where μ labels the irreducible representation and ν labels one state inside a given irreducible representation. Using crossing symmetry one can show that two amplitudes are equal : $T_{10}(s,t,u) = T_{10^*}(s,t,u)$. One can also obtain the symmetry properties under the exchange of the final states ($t \leftrightarrow u$); two of the amplitudes are antisymmetric $T_{10(8_2)}(s,t) = -\,T_{10(8_2)}(s,u)$ and the rest are symmetric.

On the other hand one can find a representation analogous to the Chew–Mandelstam in $SU(3)$ [6]

$$\begin{aligned}T(ab \to cd) \;=\; &A_1(s,t,u)\, \delta^{ab}\delta^{cd} + A_2(s,t,u)\, \delta^{ac}\delta^{bd} + A_3(s,t,u)\, \delta^{ad}\delta^{bc} \\ &+ B_1(s,t,u)\, d^{abe} d^{cde} + B_2(s,t,u)\, d^{ace} d^{bde} \,. \quad (6.68)\end{aligned}$$

Eq. (6.68) has only five independent amplitudes, what is in perfect agreement with the aforementioned relation $T_{10} = T_{10^*}$. We also expect crossing symmetry to further reduce the number of independent functions. In case of having r irreducible representation amplitudes [$r = 3$ for $SU(2)$ and $r = 6$ for $SU(3)$] crossing symmetry implies that there are only $\frac{2\,r}{3}$ independent functions. This is easy to understand : the r irreducible functions T^I $I = 1, \ldots r$ translate into $3\,r$ degrees of freedom $T^I(s,t)$, $T^I(t,s)$ and $T^I(4\,m^2 - s - t, t)$ corresponding to the s, t and u crossed channels, respectively. Crossing symmetry implies $2\,r$ restrictions, since it relates the s–channel

[6] One must remember the $SU(3)$ identity $3\left(d^{abe}d^{cde} + d^{ace}d^{bde} + d^{ade}d^{bce}\right) = \delta^{ab}\delta^{cd} + \delta^{ac}\delta^{bd} + \delta^{ad}\delta^{bc}$ to make sure that the basis of tensors is minimal. One can also add four more structures of the type $f^{abe}d^{cde}$, but they clash after imposing crossing symmetry.

amplitudes with the t– and u–channel ones ($2\,r$ relations). So we end up with r independent degrees of freedom, which is equivalent to $\frac{r}{3}$ independent functions. So in $\pi\,\pi$ scattering there is only one independent function (e.g. the Chew–Mandelstam coordinate A) while for three flavours we are left with two independent functions. All in all for $SU(3)$ we can write the following crossing relations

$$T^I(s,t) = C_u^{II'} T^{I'}(u,t)\,, \quad T^I(s,t) = C_t^{II'} T^{I'}(t,s)\,, \quad C_{t(u)}^{II'} C_{t(u)}^{I'J} = \delta_{IJ}, \tag{6.69}$$

$$C_u = \begin{pmatrix} \frac{7}{40} & \frac{1}{6} & \frac{1}{5} & \frac{1}{3} & \frac{1}{8} \\ \frac{9}{40} & \frac{1}{2} & \frac{2}{5} & 0 & -\frac{1}{8} \\ \frac{27}{40} & 1 & -\frac{3}{10} & -\frac{1}{2} & \frac{1}{8} \\ \frac{9}{8} & 0 & -\frac{1}{2} & \frac{1}{2} & -\frac{1}{8} \\ \frac{27}{8} & -\frac{5}{2} & 1 & -1 & \frac{1}{8} \end{pmatrix}, \quad C_u = \begin{pmatrix} \frac{7}{40} & -\frac{1}{6} & \frac{1}{5} & -\frac{1}{3} & \frac{1}{8} \\ -\frac{9}{40} & \frac{1}{2} & -\frac{2}{5} & 0 & \frac{1}{8} \\ \frac{27}{40} & -1 & -\frac{3}{10} & \frac{1}{2} & \frac{1}{8} \\ -\frac{9}{8} & 0 & \frac{1}{2} & \frac{1}{2} & \frac{1}{8} \\ \frac{27}{8} & \frac{5}{2} & 1 & 1 & \frac{1}{8} \end{pmatrix}.$$

Bounds for the scattering amplitudes

In this section we apply the methods of Ref. [171] to the pseudoscalar–pseudoscalar scattering processes. The detailed derivation of the positivity conditions can be found in Section 6.4.1 and will not be repeated here.

We can write the following twice–subtracted dispersion relation

$$\frac{\mathrm{d}^2}{\mathrm{d}s^2} T^I(s,t) \;=\; \frac{2}{\pi} \int_{4m^2}^{\infty} \mathrm{d}x \left[\frac{\delta^{II'}}{(x-s)^3} + \frac{C_u^{II'}}{(x-u)^3} \right] \mathrm{Im}\, T^{I'}(x + i\epsilon, t)\,, \tag{6.70}$$

wherever (s,t) makes the amplitude analytic, that is $t \leq 4\,m^2$, $s + t \geq 0$ and if $s > 4\,m^2$ considering $s \to s + i\,\epsilon$, corresponding to the Feynman prescription for propagators. Again, if we restrict ourselves to $s < 4\,m^2$ and $s + t > 0$, both denominators in Eq. (6.70) are positive, and for several linear combinations $\sum a_I\, T^I$ with $a_I \geq 0$, $\sum a_I\, C_u^{IJ}\, T_J \equiv \sum_J b_J\, T_J$ with $b_J = \sum_I a_I\, C_u^{IJ} \geq 0$. These have positive imaginary part along the integral for $t > 0$, corresponding to physical processes with equal initial and final states. Of course, many different processes are related by $SU(3)$ symmetry and need to be considered only once. If a process can be expressed as a linear combination of other processes with positive coefficients it cannot be more restrictive that the processes separately, so it will be discarded. With all that we obtain the following set of positivity conditions:

$$\begin{aligned}
&\frac{\mathrm{d}^2}{\mathrm{d}s^2} T\left(\pi^+\pi^+ \to \pi^+\pi^+\right)[\,(s,t) \in \mathcal{A}\,] \geq 0\,, && \frac{\mathrm{d}^2}{\mathrm{d}s^2} T(\pi^0\pi^0 \to \pi^0\pi^0)[\,(s,t) \in \mathcal{A}\,] \geq 0\,, \\
&\frac{\mathrm{d}^2}{\mathrm{d}s^2} T(\pi^+\pi^0 \to \pi^+\pi^0)[\,(s,t) \in \mathcal{A}\,] \geq 0\,, && \frac{\mathrm{d}^2}{\mathrm{d}s^2} T(\eta\,\pi \to \eta\,\pi)[\,(s,t) \in \mathcal{A}\,] \geq 0\,, \\
&\frac{\mathrm{d}^2}{\mathrm{d}s^2} T(K\,\eta \to K\,\eta)[\,(s,t) \in \mathcal{A}\,] \geq 0\,, && \frac{\mathrm{d}^2}{\mathrm{d}s^2} T(K\pi^+ \to K\pi^+)[\,(s,t) \in \mathcal{A}\,] \geq 0\,,
\end{aligned} \tag{6.71}$$

where $\mathcal{A}$ is the closed region of the Mandelstam plane defined by $0 \leq t \leq 4\,m^2$, $s \leq 4\,m^2$, $s+t \geq 0$. Eq. (6.71) corresponds to the following linear combinations of irreducible amplitudes

$$T_{27}\,, \qquad \frac{27}{20}\,T_{27} + \frac{1}{5}\,T_{8_1} + \frac{1}{8}\,T_1\,, \qquad \frac{1}{2}\,T_{27} + \frac{1}{3}\,T_{8_2} + \frac{1}{5}\,T_{10}\,, \tag{6.72}$$
$$\frac{3}{10}\,T_{27} + \frac{1}{5}\,T_{8_1} + \frac{1}{2}\,T_{10}\,, \qquad \frac{9}{20}\,T_{27} + \frac{1}{20}\,T_{8_1} + \frac{1}{4}\,T_{8_2} + \frac{1}{4}\,T_{10}\,, \qquad \frac{1}{2}\,T_{27} + \frac{1}{2}\,T_{10}\,,$$

respectively.

Bounds for $\mathbf{L_1}$, $\mathbf{L_2}$ and $\mathbf{L_3}$.

It is straightforward now to convert the positivity conditions in Eq. (6.71) into bounds for chiral LECs, since the energy domain $\mathcal{A}$ is well inside the convergence radius of χPT. We simply plug into Eq. (6.71) the $\mathcal{O}(p^4)$ χPT prediction [the $\mathcal{O}(p^2)$ prediction vanishes when acting with two derivatives] for the different amplitudes and seek the most stringent point in $\mathcal{A}$. These amplitudes can be found in the literature but are collected and very nicely displayed in Ref. [184], which we follow. Upon second derivative they only depend on three LECs: L_1, L_2 and L_3. At one–loop the amplitudes explicitly depend on the chiral renormalization scale μ, but it is in fact canceled by the implicit μ dependence of the chiral LECs. We will adopt the value $\mu = m$ that greatly simplifies the expressions (as it is the only energy scale in the process). So we will get our bounds for L_1 and L_2 evaluated at that energy scale (L_3 does not get renormalized and thus it is μ independent). Our bounds have the following general expression

$$\alpha_{1i}\,L_1^r(m) + \alpha_{2i}\,L_2^r(m) + \alpha_{3i}\,L_3^r \geq f_i[\,(s,t) \in \mathcal{A}\,]\Big|_{\rm max}\,, \tag{6.73}$$

where f_i are functions obtained by isolating the LECs of the second derivative of the amplitude: it contains chiral logarithms and constant LEC–independent terms. For the processes $\pi^+\pi^+ \to \pi^+\pi^+$ and $K\,\pi^+ \to K\,\pi^+$ the minima are found for $s = 1.3684\,m^2$ and $s = 1.2593\,m^2$, respectively. For the rest of the processes it is found for $s = 0$.

If we are to compare our theoretical bounds with the fitted values we need to fix the common mass m to a physical value. The most conservative value is of course the pion mass m_π, since it is the lightest particle in the octet, but in principle any value low enough not to compromise the chiral expansion is equally good. We will adopt the two extreme values m_π and m_K for our analysis. The results are shown in Table 6.2.

If we consider the more realistic case of $m_s \neq m_u = m_d$ and use the physical value for the π and K states[7] the choice of m is absolutely transparent. This is discussed in the next section.

[7] In our analysis we will assume the Gell-Mann–Okubo formula for the masses: $m_\eta^2 = \frac{4}{3}m_K^2 - \frac{1}{3}m_\pi^2$.

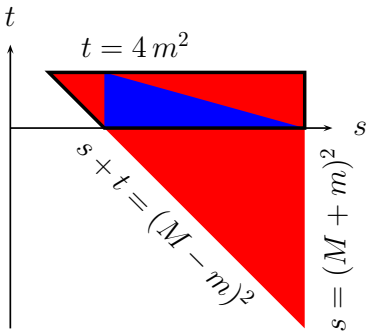

Figure 6.8: Scattering of particles with different masses. Inside the triangle the amplitude scattering is free from singularities. In the dashed region the unitarity condition applies.

Symmetry breaking corrections to the bounds

The first effect showing up when considering $m_\pi < m_K$ is that for several processes the unitarity branch cut might occur before reaching the physical threshold. This, as we discuss next, spoils the positivity condition.

Let us first obtain the analytic triangle for the present situation. We will consider only processes with equal initial and final states $a + b \to a + b$, of masses $m_a = M$ and $m_b = m$ $(M \geq m)$, since this ensures that the imaginary part of the partial wave amplitudes is positive. If the lowest mass intermediate state in that process is $c + d$, the amplitude is analytic for $s \leq (m_c + m_d)^2$. Analogously from the crossed channels we will obtain $t \leq (m_e + m_f)^2$ and $s + t \geq 2\,(m^2 + M^2) - (m_g + m_h)^2$. Of course the maximum [minimum] value for these three thresholds are $(m+M)^2$, $4\,m^2$ and $(M - m)^2$, respectively. Then the dispersion relation reads (now we directly consider physical processes)

$$\frac{\mathrm{d}^2}{\mathrm{d}s^2}\,T(s,t) \;=\; \frac{2}{\pi}\int_{(m_c+m_d)^2}^{\infty}\mathrm{d}x\,\frac{\mathrm{Im}\,T(x+i\epsilon,t)}{(x-s)^3} + \frac{2}{\pi}\int_{(m_g+m_h)^2}^{\infty}\mathrm{d}x\,\frac{\mathrm{Im}\,T_u(x+i\epsilon,t)}{(x-u)^3}\,, \tag{6.74}$$

wherever the amplitude is analytic. Here T_u is the amplitude corresponding to the u–channel $a + \bar{b} \to a + \bar{b}$, which has of course equal initial and final states, too. Both denominators are positive as far as $s \leq (m_c + m_d)^2$ and $s + t \geq 2\,(m^2 + M^2) - (m_g + m_h)^2$, and so up to this point there is nothing compromising the positivity condition. But still we have to make sure that the imaginary part remains positive along the two cuts. Expanding the amplitude T (and also T_u) in partial waves we get

$$T(s,t) \;=\; \sum_{\ell=0}^{\infty}(2\,\ell+1)\,f_\ell(s)P_\ell\left[1 + \frac{s\,t}{(s+m^2-M^2)^2 - 4\,m^2\,s}\right], \tag{6.75}$$

with $\mathrm{Im}\,f_\ell(s) \;=\; s\,\beta(s)\,\sigma_\ell(s)\,\theta\,[\,s - (m_c + m_d)^2\,] \;\geq\; 0$ and with $\theta\,[\,s - (m_g + m_h)^2\,]$ for the u–channel. So for getting a positive imaginary part each P_ℓ must be positive

along the corresponding cuts. Since $P_\ell(z) > 1$ for $z > 1$ for all ℓ it is enough to require

$$\frac{s\,t}{(s+m^2-M^2)^2-4\,m^2\,s} \geq 0 \qquad \text{for } s \geq (m_c+m_d)^2\,[\,(m_g+m_h)^2\,]\,. \tag{6.76}$$

Since for $s \to \infty$ Eq. (6.76) tends to t/s then we must require $t > 0$. Then for positive t Eq. (6.76) is only satisfied if $(M-m)^2 \geq s \geq (M+m)^2$. Thus if either (m_c+m_d) [or (m_g+m_h)] is less than $(M+m)$ the imaginary part between (m_c+m_d) [or (m_g+m_h)] and the physical threshold could turn negative, making the positivity condition invalid.

Summarising, *the positivity conditions hold for processes of the type $a+b \to a+b$ such that the lightest pair of particles that can arise off the scattering $a+b$ is precisely $a+b$, and analogously for $a+\bar{b}$.* Or in other words, for processes with equal initial and final states such that the imaginary part of the s– and u–channels starts at their physical production threshold. Moreover, the positivity condition is satisfied in the closed area of the Mandelstam plane $\mathcal{A}$ defined by $0 \leq t \leq 4\,m^2$, $s \leq (M+m)^2$ and $s+t \geq (M-m)^2$. As an additional bonus for breaking $SU(3)_V$ we have many independent amplitudes that are no longer related by symmetry. The final set of positivity conditions reads:

$$\begin{aligned}
&\frac{\mathrm{d}^2}{\mathrm{d}s^2}T\left(\pi^+\pi^+ \to \pi^+\pi^+\right)[\,(s,t)\in\mathcal{A}\,] \geq 0\,, \quad
\frac{\mathrm{d}^2}{\mathrm{d}s^2}T(\pi^0\pi^0 \to \pi^0\pi^0)[\,(s,t)\in\mathcal{A}\,] \geq 0\,,\\
&\frac{\mathrm{d}^2}{\mathrm{d}s^2}T(\pi^+\pi^0 \to \pi^+\pi^0)[\,(s,t)\in\mathcal{A}\,] \geq 0\,, \quad
\frac{\mathrm{d}^2}{\mathrm{d}s^2}T(\pi\,\eta \to \pi\,\eta)[\,(s,t)\in\mathcal{A}\,] \geq 0\,,\\
&\frac{\mathrm{d}^2}{\mathrm{d}s^2}T(K\,\pi^+ \to K\,\pi^+)[\,(s,t)\in\mathcal{A}\,] \geq 0\,,
\end{aligned} \tag{6.77}$$

where of course, the area $\mathcal{A}$ depends on each specific process. There are more processes satisfying the conditions stated above, but they give a less stringent bound for the same linear combination of LECs and so we will not show them. Again all minima are found at $t = 4\,m^2$. For the $\pi^+\pi^0$, $\pi\,\eta$ and $K\,\pi^+$ processes the minima are achieved for $s = 1.14384\,m^2$, $s = 16.0027\,m^2$ and $s = 4.78\,m^2$, respectively. For the remaining two processes, it is found at $s = 0$.

Results

In this section we discuss the bounds obtained for the different linear combinations of chiral LECs, and compare them with the values obtained by fitting observables to the experimental data. In Ref. [169] those values are given at the $\mu = m_\rho$ scale, so we will run our bounds to this scale to compare. The running equation for these LECs reads

$$L_i(\mu_1) - L_i(\mu_2) \;=\; -\,\frac{\Gamma_i}{16\,\pi^2}\log\left(\frac{\mu_1}{\mu_2}\right)\,, \quad \Gamma_1 \;=\; \frac{3}{32}\,, \quad \Gamma_2 \;=\; \frac{3}{16}\,, \tag{6.78}$$

and the values at the different scales are

$$\begin{aligned} L_1^r(m_\rho) &= (0.43\,[\,0.38\,]\pm 0.12)\times 10^{-3}\,, \quad L_2^r(m_\rho) = (0.73\,[\,1.59\,]\pm 0.12)\times 10^{-3}\,, \\ L_3 &= (-2.35\,[\,2.91]\pm 0.37)\times 10^{-3}\,. \end{aligned} \tag{6.79}$$

Those values were obtained from a fit to the available experimental data taking as theoretical input the $\mathcal{O}(p^6)$ χPT prediction. Since in our analysis we are using the $\mathcal{O}(p^4)$ amplitude it is instructive to compare our bounds with the values of the LECs obtained by fitting the $\mathcal{O}(p^4)$ χPT amplitude to the same data. Those can be found in Ref. [169] as well, and are displayed in Eq. (6.79) in brackets.

A very important issue is to estimate the error committed by truncating the amplitude at $\mathcal{O}(p^4)$. For the symmetric analysis this can be done in as in Ref. [171], that is, adopting as an educated guess three times the corrections of the $\mathcal{O}(p^6)$ amplitude due to chiral logarithms. When assuming $m = m_\pi$ the bounds are not very stringent, and the errors are rather small; experimental values are well within the bounds. However for $m = m_K$ the central values of the bounds greatly increase (that is, bounds tighten) and some experimental values apparently violate the bounds. But at the same time errors get multiplied by a factor of twelve. Thence the validity of the chiral expansion is not compromised.

For the symmetry breaking analysis the error cannot be estimated so straightforwardly. It is expected that the main corrections come from chiral LECs multiplied by the kaon mass. The $\mathcal{O}(p^6)$ computation of the $\pi\,\pi$ scattering amplitude in three-flavour χPT was performed in Ref. [185], and the $K\,\pi$ scattering at the same order can be found in Ref. [186]. We will adopt as an educated guess the correction due to the $\mathcal{O}(p^6)$ LECs, that is the $\mathcal{O}(p^6)$ tree–level piece. Unfortunately the $\mathcal{O}(p^6)$ LECs are unknown, so we will use the estimate given in Ref. [186], obtained by resonance saturation. In addition, to be more conservative, we will assume a common error for all the channels, the biggest of these, which is 3.0. This error is very large, of the same order as that of the symmetric analysis with $m = m_K$.

For the three $\pi\,\pi$ scattering processes we do not see large deviations of the corrected bounds (they increase around a 20%). However the estimated error due to higher order corrections greatly enhances due to terms proportional to the kaon mass. So we can conclude that the symmetric analysis is most convenient for these relations. Incidentally experimental values satisfy these three bounds. For $K\,\pi$ scattering the corrected bound is much worse. However for $\pi\,\eta$ scattering the increase of the corrected bound is great: 139%. In fact the experimentally fitted value is partially in conflict with the bound, but since the error of the bound is quite large, the validity of χPT is not compromised.

The bounds compare better to the values of the LECs obtained from an $\mathcal{O}(p^4)$ fit. It is quite easy to understand this. The bounds are to a large extent dominated by the value of L_2, since in the corresponding linear combinations it always appears multiplied by large coefficients (see second column of Table 6.2). In Eq. (6.79) we see that the value of L_2 in the $\mathcal{O}(p^4)$ fit is twice as big as in the $\mathcal{O}(p^6)$.

Results are displayed in Table 6.2. In the first column we show the corresponding linear combination of LECs for $\mathcal{O}(p^6)$ (up) and $\mathcal{O}(p^4)$ fits (down), in the second

column we display the corresponding linear combinations of the experimentally fitted values; in the third and fourth columns we display the bounds for the symmetric analysis assuming $m = m_\pi$ and $m = m_K$, respectively; in the last column we give the bounds obtained for broken $SU(3)_V$ symmetry.

$10^3\,\alpha_i\,L^i(m_\rho)$	Fit to exp.	bound $m = m_\pi$	bound $m = m_K$	bound $m_\pi \neq m_K$
$2L_1^r + 2L_2^r + L_3$	$-\,^{0.03}_{1.03} \pm 0.5$	$\geq -3.88 \pm 0.20$	$\geq 0.68 \pm 2.50$	$\geq -3.87 \pm 0.20$
L_2^r	$^{0.73}_{1.59} \pm 0.12$	$\geq -1.30 \pm 0.20$	$\geq 0.22 \pm 2.50$	$\geq -1.10 \pm 0.20$
$2L_1^r + 3L_2^r + L_3$	$^{0.70}_{2.62} \pm 0.6$	$\geq -4.88 \pm 0.20$	$\geq 1.20 \pm 2.50$	$\geq -4.29 \pm 0.20$
$12L_2^r + L_3$	$^{6.41}_{16.17} \pm 1.5$	$\geq -15.99 \pm 0.20$	$\geq 2.24 \pm 2.50$	-
$3L_2^r + L_3$	$^{-0.16}_{1.86} \pm 0.5$	$\geq -3.64 \pm 0.20$	$\geq 0.92 \pm 2.50$	$\geq -0.15 \pm 2.00$
$4L_2^r + L_3$	$^{0.57}_{3.45} \pm 0.6$	$\geq -4.70 \pm 0.20$	$\geq 1.38 \pm 2.50$	$\geq -14.75 \pm 2.00$

Table 6.2: Experimental values for linear combinations of the LECs [upstairs $\mathcal{O}(p^6)$ fit and downstairs $\mathcal{O}(p^4)$ fit] and their bounds.

6.4.3 Conclusions

There are non–trivial constraints which follow from unitarity, analyticity and crossing symmetry which must be satisfied by any relativistic quantum theory. There are some interesting and non–trivial constraints on low–energy effective theories which arise by imposing these constraints on the effective theory scattering amplitude.

In this work we have transformed the dispersion relations for the $\pi\,\pi$ scattering amplitude into positivity conditions for several processes, valid in a certain region of the Mandelstam plane below threshold. This region is in fact larger than the Mandelstam triangle, as commonly assumed. These positivity conditions can be converted into bounds for two LECs of the $SU(2)$ χPT Lagrangian. Our analysis leads to a stronger bound than those obtained previously, since we use positivity in a larger region of the Mandelstam plane. The values of the LECs extracted from experiment are consistent with the bounds derived in this paper.

One nice feature of the structure of the bounds is that it correlates two distinct pieces of the $\mathcal{O}(p^4)$ amplitude: LECs and chiral logarithms. Whereas the former is leading order in the $1/N_C$ counting and represents an expansion in $1/m_\rho^2 \sim (0.7\,\mathrm{GeV})^{-2}$ the latter is subleading in large–N_C and represents an expansion in $1/\Lambda_\chi^2 \sim (1.1\,\mathrm{GeV})^{-2}$ where $\Lambda_\chi \sim 4\,\pi F_\pi$ and F_π is the decay constant of the pion [25].

One can use Eq. (6.44) with $n = 4$ to obtain bounds for higher order LECs, using the amplitude up to order $\mathcal{O}(p^6)$. The $\mathcal{O}(p^4)$ LECs in the $\mathcal{O}(p^4)$ amplitude vanish on taking the fourth derivative but the one–loop $\mathcal{O}(p^4)$ chiral logarithmic terms do not. However, one–loop diagrams with one insertion of the $\mathcal{O}(p^4)$ LECs contribute

to terms of order p^6 times chiral logarithms, which do not vanish on taking the fourth derivative. The $\mathcal{O}(p^6)$ LECs also contribute to the fourth derivative. Thus one now gets inequalities involving the $\mathcal{O}(p^4)$ LECs and $\mathcal{O}(p^6)$ LECs plus $\mathcal{O}(p^4)$ chiral logarithms. In addition of having a lot of LECs we no longer compare terms of the same order in the chiral expansion.

We apply this program to χPT with three flavours and find bounds for L_1, L_2 and L_3. When the exact $SU(3)_V$ limit is considered the theory becomes slowly convergent if the common mass m for the multiplet of pGs is of the order of m_K (albeit it converges quickly for $m = m_\pi$). When the real values for the pion and kaon masses are employed the bounds become more stringent and in fact in one case the experimentally fitted values are partially in contradiction with the central value of the bound. However for this process the $\mathcal{O}(p^6)$ corrections are very large and so there is no contradiction.

The low–energy limit of the linear sigma model Lagrangian is a theory with spontaneous chiral symmetry breaking in which the LECs can be computed in terms of the coupling constant g of the LSM. The values of $\bar{l}_1$ and $\bar{l}_2$ for this model are in apparent violation of the positivity bounds for $m_\sigma \lesssim 4.9\, m$, while the range $m_\sigma > \sqrt{3}\, m$ can be realized in the LSM. We have shown that the apparent violation is an artifact of the truncation of the $1/m_\sigma^2$ corrections and that the LSM is consistent with the positivity conditions for $m_\sigma \geq m$.

6.5 Dipion production in two photon reactions

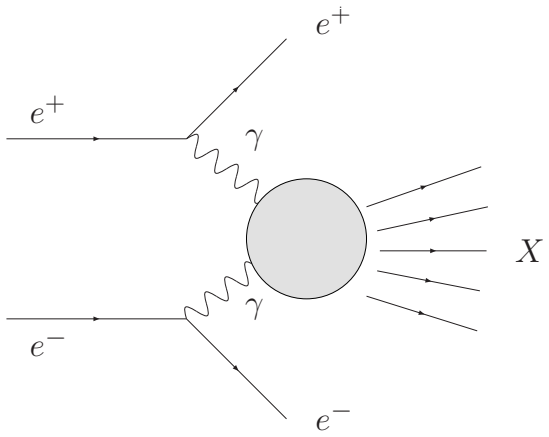

Figure 6.9: $e^+e^- \to e^+e^-\, X$ when dominated by two photon exchange.

In this section we discuss why two photon interactions are interesting and why, in particular for the $\gamma\,\gamma \to \pi^0\pi^0$ channel, the χPT prediction is not satisfactory enough for a sensible description. A more general approach, based in unitarity and analyticity is then mandatory, and we present here the basics of the formalism. We will derive a general parametrization for the two photon reaction amplitude

that preserves unitarity exactly and test the consistency of a particular model. For writing this section I have mainly followed Refs. [165, 187].

A beautiful feature of an e^+e^- machine is its ability to study two photon processes. The cross–section for $e^+e^- \to e^+e^- X$ is dominated by the exchange of two *almost real* photons, so that one can really extract information of $\gamma\gamma \to X$, where X is hadronic, as seen in Fig. 6.9.

At low momenta, $\pi\pi$, is the most abundantly produced hadronic final state. What this can teach can be seen by considering $\gamma\gamma \to \pi\pi$ from the t–channel point of view, where we think the photon scattering off a pion. At low energies, the photon, having long wavelenght sees the charged pions, but not the neutral, so the cross–section for $\gamma\gamma \to \pi^+\pi^-$ is large compared to that form $\pi^0\pi^0$, see Fig. 6.10. However, as the energy of the photon increases its wavelenght shortens it recognizes that the pions, whether charged or neutral, are made of the same charged constituents, namely quarks, and causes these to resonate.

In this section we will consider only the leading electromagnetic contribution (that is, amplitudes at order α_{em}), and all radiative corrections will be due to strong interactions.

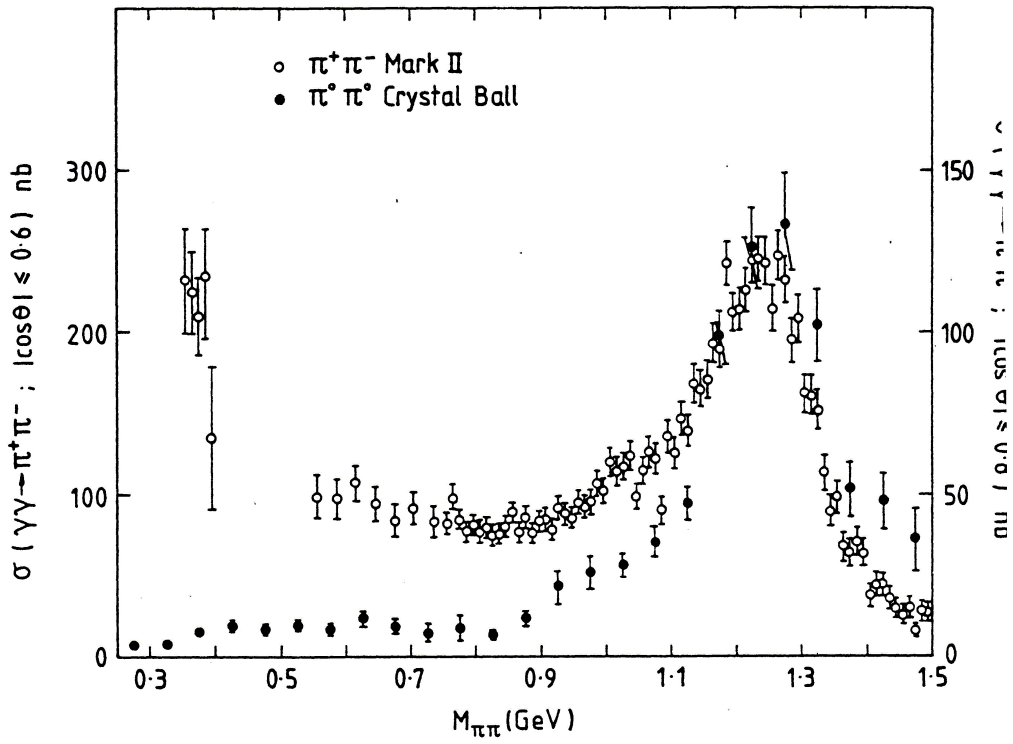

Figure 6.10: $\gamma\gamma \to \pi^+\pi^-$ (open circles, left–hand scale) for $|\cos\theta| < 0.6$ and the $\gamma\gamma \to \pi^0\pi^0$ cross–section (solid circles, right–hand scale) for $|\cos\theta| < 0.8$ as functions of s.

6.5.1 The pitfall of χPT

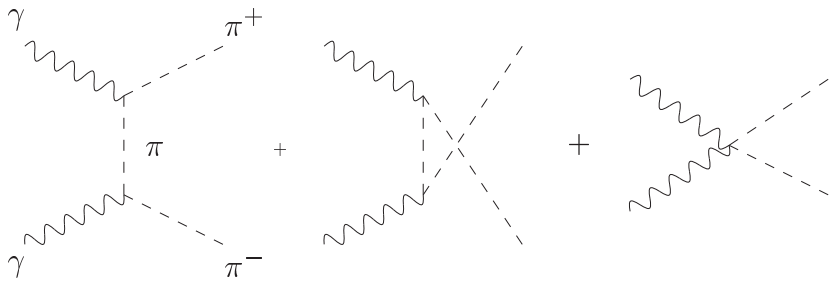

Figure 6.11: Born amplitude for the two photon reaction of charged pions.

At low energy, we can calculate the amplitude of $\gamma\gamma \to \pi^+\pi^-$ and $\gamma\gamma \to \pi^0\pi^0$ using the techniques explained in Chapter 1, χPT. For the charged channel, the leading contribution are tree–level diagrams, as shown in Fig. 6.11, that in the following will be referred to as the Born term $\mathcal{B}$. However, for the neutral case pions do not couple to photons directly and then the reaction takes place through loop diagrams, as shown in Fig. 6.12. Even though it is a general fact that loops need to be renormalized and in an effective field theory this implies the introduction of new parameters to be fixed, the neutral pion production is a remarkable exception. Since there is no Born term, the sum of all one–loop diagrams must be finite, and so we do not need any counterterm to get a finite answer. Moreover, there is no contribution from $\mathcal{L}^{(4)}$ to this process (no direct coupling of photons to two neutral pions) and then no new LECs appear in the scattering amplitude. The calculation of these diagrams was done long ago in Refs. [188, 189]. Another feature of this calculation is that it is purely S–wave (it has no angular dependence).

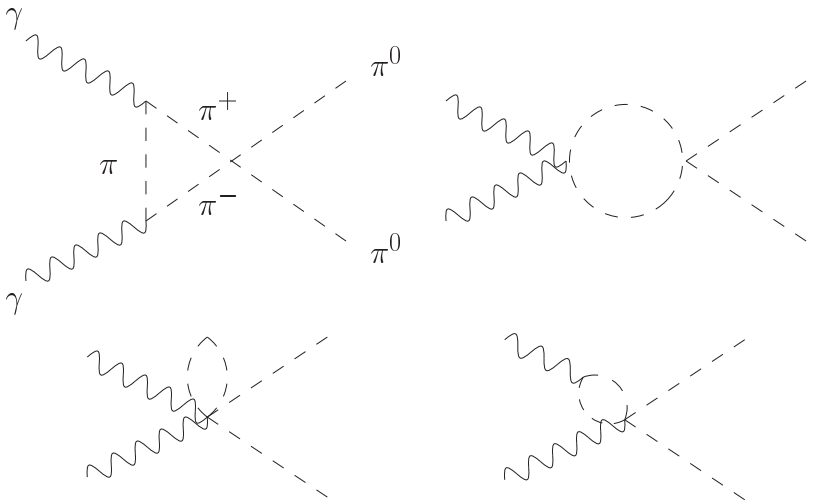

Figure 6.12: Lowest order contributions to $\gamma\gamma \to \pi^0\pi^0$ in χPT.

If we compare the clean prediction of χPT for the neutral channel with the experimental data, we become sorely disappointed, as shown in Fig. 6.13. Clearly, χPT predicts a cross–section of the same order of magnitude, but the shape is quite different. The data arise from threshold and are then essentially flat for hundreds of MeV, while χPT at lowest order gives an almost linearly increasing prediction.Of course, the prediction beyond one loop is expected to be modified at higher energies.

To attempt to resolve this puzzle, we need an independent way of modeling the amplitude for $\gamma\,\gamma \to \pi\,\pi$ and this will be discussed next.

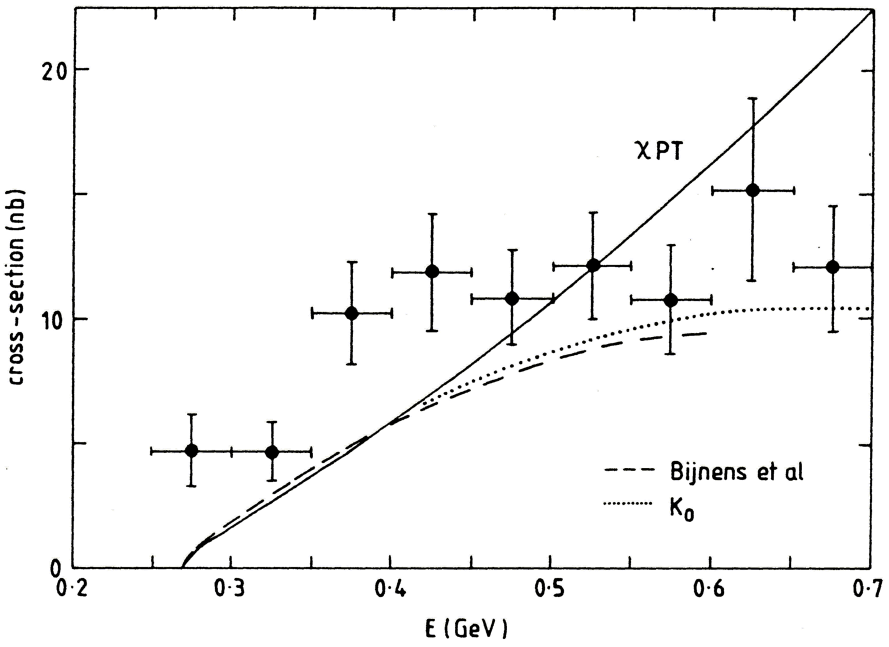

Figure 6.13: Integrated cross–section for $\gamma\,\gamma \to \pi^0\pi^0$ as a function of s. The dots are the experimental data. The line marked χPT is the prediction of the lowest order χPT [188, 189] and the dashed lines are corrections to this result.

6.5.2 Unitarity in meson–meson scattering

Before entering into the detailed discussion of the unitarity constraints for the dipion production, we will explain with some detail the very special case of $\pi\,\pi$ scattering. In principle one could think that we already exploited all the nice features implied by very first principles in Section 6.4, but if we restrict ourselves below the threshold production of four pions (or two kaons) we can further constrain the form of the scattering amplitude.

Let us first, for simplicity, discuss the case of $\pi\,\pi$ scattering below the two–kaon threshold. The unitarity requirement for the partial waves (6.14) implies only the

two–pion intermediate state. But of course there are always two possible intermediate states, $\pi^0\pi^0$ and $\pi^+\pi^-$ [8]. If instead of employing the physical states basis we use the isospin basis the only possible intermediate state must have the same isospin as the initial (and final) state (in this basis pions are identical particles and we have to include the 1/2 symmetry factor). Finally, let us write the specific form of the Parseval identity for two particles in the isospin and angular momentum basis

$$\mathcal{I}_2 \;=\; \frac{1}{2}\,\frac{1}{4\,\pi}\int \frac{\mathrm{d}^3\vec{p}_1}{2\,E_1}\,\frac{\mathrm{d}^3\vec{p}_2}{2\,E_2}\sum_{Ijm}\left|I,j,m\right\rangle\left\langle I,j,m\right| \;, \tag{6.80}$$

Inserting last expression in Eq. (6.14) we arrive at the condition [9]

$$\begin{aligned}\mathrm{Im}\,T^{I\,J}_{\pi\pi}(s) \;&=\; \rho_\pi(s)\left|T^{I\,J}_{\pi\pi}(s)\right|^2 \;,\\ \rho_\pi(s) \;&=\; \frac{\beta_\pi(s)}{32\,\pi}\,\theta(s-4\,m^2)\,,\;\beta_\pi(s) \;=\; \sqrt{1-\frac{4\,m^2}{s}}\,,\end{aligned} \tag{6.81}$$

where β is the velocity of the pions in the center of mass frame to which the angular momentum is referred. For the sake of clarity we will omit the spin and isospin indices. Of course Eq. (6.81) trivially leads to the relation

$$(\mathrm{Re}\,T)^2+\rho^2\,|T|^2 = |T|^2 \;. \tag{6.82}$$

It is easy to show that Eq. (6.81) completely fixes the imaginary part of the inverse of the scattering amplitude

$$\mathrm{Im}\,T^{-1}_{\pi\pi}(s) \;=\; -\,\rho_\pi(s)\,, \tag{6.83}$$

and this relation permits to write the most general parametrization for the scattering amplitude

$$T_{\pi\pi}(s) \;=\; \frac{T_{B\pi}(s)}{1-i\,\rho_\pi(s)\,T_{B\pi}(s)} \;=\; \frac{\sin\delta(s)}{\rho_\pi(s)}\,e^{i\delta(s)}\,, \tag{6.84}$$

where $T^{-1}_{B\pi}=\mathrm{Re}\,T^{-1}_{\pi\pi}$ is a real function. The second equality reflects the relation of the phase shift $\delta(s)$ and the modulus of the scattering amplitude. All these relations hold even above $4\,m_K^2$ for the $I=2$ case because there is no two–kaon state with such isospin.

Let us discuss now the case of production above the two–pion threshold. It is now better to consider at the same time three reactions: $\pi\,\pi\to\pi\,\pi$, $\pi\,\pi\to K\,K$ and $K\,K\to K\,K$, also for a given spin and isospin. Then we have

$$\mathrm{Im}\,T_{\pi\pi}(s) \;=\; \rho_\pi(s)\,|T_{\pi\pi}(s)|^2+\rho_K(s)\,|T_{KK}(s)|^2 \;,$$

[8] Since the neutral pions are identical particles, we have to include a 1/2 symmetry factor in the Parseval identity

[9] In this section, we reserve T for the matrix element of $\pi\,\pi$ interaction and F for two photon reactions.

$$\begin{aligned} \mathrm{Im}\, T_{\pi K}(s) &= \rho_\pi(s)\, T_{\pi\pi}(s)^*\, T_{\pi K}(s) + \rho_K(s)\, T_{\pi K}(s)^*\, T_{KK}(s)\,, \\ \mathrm{Im}\, T_{KK}(s) &= \rho_\pi(s)\, |T_{\pi K}(s)|^2 + \rho_K(s)\, |T_{KK}(s)|^2\,. \end{aligned} \tag{6.85}$$

These set of relations can be better gathered in matrix notation

$$\mathrm{Im}\, T = T\rho\, T^\dagger\,, \quad T \,=\, T^\top \,=\, \begin{pmatrix} T_{\pi\pi} & T_{\pi K} \\ T_{K\pi} & T_{KK} \end{pmatrix}\,, \quad \rho \,=\, \begin{pmatrix} \rho_\pi & 0 \\ 0 & \rho_K \end{pmatrix}\,. \tag{6.86}$$

It is easy to check that indeed $\mathrm{Im}\, T$ is a hermitian symmetric matrix, and hence real. Again Eq. (6.86) fully determines the imaginary part of T^{-1} (now it is the inverse of a matrix) and allows to write a general parametrization

$$\mathrm{Im}\,(T^{-1}) \,=\, -\,\rho\,, \quad T = (1 - i\, T_B\, \rho)^{-1}\, T_B = T_B (1 - i\, \rho\, T_B)^{-1}\,, \tag{6.87}$$

with $T_B^{-1} = \mathrm{Re}\,(T^{-1})$ a real matrix. We can derive two useful relations by inserting the identity $T = \mathrm{Re}\, T + i\, T\rho\, T^\dagger$ back into Eq. (6.86) and requiring $\mathrm{Im}\, T$ to be real:

$$\begin{aligned} T\rho\, T^\dagger &= (\mathrm{Re}\, T)\, \rho\, (\mathrm{Re}\, T) + T\rho\, T^\dagger\, \rho\, T\rho\, T^\dagger\,, \\ (\mathrm{Re}\, T)\, \rho\, T\rho\, T^\dagger &= \rho\, T\rho\, T^\dagger\,)\mathrm{Re}\, T)\,. \end{aligned} \tag{6.88}$$

The Lippmann–Schwinger equations are a theoretical field method to find scattering amplitudes satisfying unitarity exactly below the four–pion threshold. In matrix notation they read

$$T \,=\, V + VG\, T\,, \tag{6.89}$$

with $V = T$ at tree–level (hence it is real) and

$$VG\, T \,=\, \int \frac{\mathrm{d}^4 q}{(2\pi)^4}\, V(k,p;q)\, G(P,q)\, T(k,p;q)\,, \tag{6.90}$$

with $V(k,p;q)$ and $T(k,p;q)$ the off–shell total and tree–level amplitudes and G a diagonal matrix with entries

$$G_{ii} \,=\, \frac{1}{q^2 - m_i^2 + i\,\epsilon}\, \frac{1}{(q-P)^2 - m_i^2 + i\,\epsilon}\,, \tag{6.91}$$

being $P = p + k$, p and k the incoming particle momenta. Under the assumption $VG\, T \,\approx\, V\bar{G}(s)\, T$ (that is, the integral disappears) we arrive at the Bethe–Salpeter equations that have the trivial solution

$$T \,=\, V(1 - \bar{G}\, V)^{-1} \,\approx\, V(1 + \bar{G}\, V + \bar{G}\, V\bar{G}\, V + \cdots)\,, \tag{6.92}$$

satisfying unitarity exactly as far as $\mathrm{Im}\, \bar{G}(s) = \rho(s)$. Comparison of Eqs. (6.92) and (6.87) links V with T_B: $T_B = V(1 - \mathrm{Re}\, \bar{G}\, V)^{-1}$. These ideas are better understood in Fig. 6.14.

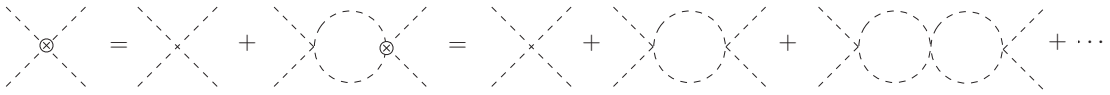

Figure 6.14: Diagrammatic representation of the Lippmann–Schwinger and Bethe–Salpeter equations. Crossed vertices correspond to the full amplitude whereas simple vertices represent tree–level couplings.

The combination of χPT and the Bethe–Salpeter equations is known as the Unitarized χPT or inverse amplitude method, see `e.g.` Ref. [190]. A particularly interesting application of the method is its extension to the three–body interactions. In Ref. [191] it was applied for the first time to the $N\,K\,\pi$ channel, in order to gain insight in the structure of the so called pentaquark hadron θ^+. The idea was (as it is common in the literature related to the inverse amplitude method) to seek for poles in the S–matrix, to be identified with (unstable) bound states with the same quantum numbers as the channel under study. Although the method used for the three–body interaction in Ref. [191] was rudimentary (refinements such as the Faddeev equations were ignored), the conclusion that the pentaquark was not a bound state of $N\,K\,\pi$ in S–wave was claimed.

6.5.3 General description of the two photon reaction

We consider dipion production out of two real photons below the four–pion threshold. It is well known that the amplitude for this process has two independent helicity components $\mathcal{F}_{++}$, $\mathcal{F}_{+-}$, which contribute incoherently to the unpolarized cross–section :

$$\frac{\mathrm{d}\sigma}{\mathrm{d}\Omega} \;=\; \frac{\beta_\pi}{128\,\pi^2 s}\left(\,|\mathcal{F}_{++}|^2 \;+\; |\mathcal{F}_{+-}|^2\,\right)\,, \tag{6.93}$$

and a similar formula for kaon production. The helicity amplitudes $\mathcal{F}_{++}$ and $\mathcal{F}_{+-}$ correspond to photon helicity differences of $\lambda = 0,\, 2$ respectively. These have partial wave expansions involving even $J \geq \lambda$, and from Eq. (6.12) with $\mu' = 0$, $\mu = \lambda = 0,\, 2$ we get :

$$\begin{aligned}
\mathcal{F}_{++}(s,\theta,\phi) &= e^2\sqrt{16\,\pi}\sum_{J\geq 0}\mathcal{F}_{J0}(s)\,Y_{J0}(\theta,\phi)\,,\\
\mathcal{F}_{+-}(s,\theta,\phi) &= e^2\sqrt{16\,\pi}\sum_{J\geq 2}\mathcal{F}_{J2}(s)\,Y_{J2}(\theta,\phi)\,,
\end{aligned} \tag{6.94}$$

where the factor of $e^2\sqrt{16\,\pi}$ has been taken out for convenience. With this normalization the integrated cross–section is

$$\sigma \;=\; 2\,\pi\,\alpha_{em}^2\frac{\beta_\pi}{s}\sum_{J\geq\lambda}|\mathcal{F}_{J\lambda}(s)|^2\;. \tag{6.95}$$

There is no interference among the different partial wave amplitudes in the total cross–section (6.95), but this is no longer true for the partially integrated cross–section.

Since isospin symmetry is not conserved by the electromagnetic interactions, any possible isospin two–pion state can emerge off the two photon collision. Since in the partial wave decomposition (6.94) only even partial waves take place, only the values $I = 0, 2$ are possible (Bose symmetry forbids odd values for I in the case of even partial waves). Since electric charge is, of course, conserved, the only possible final states have $I_z = 0$. Let us explore what can we learn from unitarity below the four–pion threshold. We remark that within electromagnetic interactions we are only interested in the $\mathcal{O}(\alpha_{em})$ terms, and so there are no virtual photon corrections. Thus the only possible intermediate states in Eq. (6.13) are hadrons, and the regime of energies we are interested in, two–hadron states. Let us first focus in pion production below the two–kaon production threshold, or equivalently the case of $I = 2$ pion production. Since time reversal is conserved by both electromagnetic and strong interactions we have

$$\mathrm{Im}\,\mathcal{F}_\pi \;=\; \rho_\pi\,\mathcal{F}_\pi^*\,T_{\pi\pi} \;=\rho_\pi\,\mathcal{F}_\pi\,T_{\pi\pi}^*\,, \tag{6.96}$$

where again we drop angular momentum and isospin indices. In the derivation of Eq. (6.96) we have taken into account that, even though isospin is not a symmetry of electromagnetism, and hence two particles of arbitrary total isospin can in principle be an intermediate state, the strong interaction rescattering forces its isospin to coincide with that of the final state. Let us compare Eq. (6.81) with Eq. (6.96): the first only involves $T_{\pi\pi}$, and constrains its strength, because it relates $T_{\pi\pi}$ with $T_{\pi\pi}^2$; the second relates $\mathcal{F}_\pi$ with $T_{\pi\pi}$, but it is linear in $\mathcal{F}_\pi$, and hence the strength of $\mathcal{F}_\pi$ is not constrained. Eq. (6.96) ensures that any resonance in $\pi\,\pi$ scattering also appears in the $\pi\,\pi$ two photon reaction and vice versa, as they must. One immediate consequence of Eq. (6.96) is that since $\mathrm{Im}\,\mathcal{F}_\pi$ is by definition real, the phase of $\mathcal{F}_\pi$ and $T_{\pi\pi}$ below $4\,m_K^2$ must coincide (Watson's final state interaction theorem [192]). This enables us to write the following relation

$$\mathcal{F}_\pi(s) \;=\; \alpha_\pi(s)\,T_{\pi\pi}(s)\,, \qquad \alpha_\pi \;=\; \frac{\mathcal{F}_\pi^*\,T_{\pi\pi}}{|T_{\pi\pi}|^2}\,. \tag{6.97}$$

with α_π a real function depending on the specific partial wave and isospin. The expression for α_π is obtained taking the imaginary part of Eq. (6.97) and using relations (6.96) and (6.81). Above the unitarity threshold, again unitarity is powerful, it says that $\mathcal{F}_\pi$ and T_π have the same right–hand cut structure. Our task is now to find the most general parametrization satisfying the constraints of unitarity for $\mathcal{F}_\pi(s)$. We will trial with and expression inspired in the Bethe–Salpeter equations and then prove that it is in fact unitarity preserving

$$\mathcal{F}_\pi \;=\; (\mathcal{F}_{B\pi} \;+\; \tilde{t}_\pi\,T_{\pi\pi})\,, \quad \mathcal{F}_{B\pi} \in \Re\,, \tag{6.98}$$

where $T_{\pi\pi}$ satisfies unitarity exactly. Taking the imaginary part of $\mathcal{F}_\pi^* T_{\pi\pi}$ and demanding it to be zero we obtain

$$\begin{aligned} \mathrm{Im}\,\tilde{t}_\pi &= \mathcal{F}_{B\pi}\,\rho_\pi\,, \\ \mathcal{F}_\pi^*\,T_{\pi\pi} &= \mathcal{F}_{B\pi}\,\mathrm{Re}\,T_{\pi\pi} + \mathrm{Re}\,\tilde{t}_\pi\,|T_{\pi\pi}|^2\,, \end{aligned} \tag{6.99}$$

Taking the imaginary part of Eq. (6.98) together with Eq. (6.99) we verify condition (6.96) and obtain an expression for α_π:

$$\alpha_\pi \;=\; \mathrm{Re}\,\tilde{t}_\pi \;+\; \mathcal{F}_{B\pi}\,\mathrm{Re}\,T_{\pi\pi}^{-1}\,. \tag{6.100}$$

Let us concentrate now in the production above the two–kaon threshold for $I = 0,\, 2$. Again it is interesting to study at the same time the kaon production: unitarity imposes

$$\begin{aligned} \mathrm{Im}\,\mathcal{F}_\pi &= \rho_\pi\,\mathcal{F}_\pi^*\,T_{\pi\pi} \;+\; \rho_K\,\mathcal{F}_K^*\,T_{K\pi}\,, \\ \mathrm{Im}\,\mathcal{F}_K &= \rho_\pi\,\mathcal{F}_\pi^*\,T_{\pi K} \;+\; \rho_K\,\mathcal{F}_K^*\,T_{KK}\,, \end{aligned} \tag{6.101}$$

and the reality of the imaginary parts requires

$$\begin{aligned} \mathcal{F}_\pi &= \alpha_\pi\,T_{\pi\pi} \;+\; \alpha_K\,T_{K\pi}\,, \\ \mathcal{F}_K &= \alpha_\pi\,T_{\pi K} \;+\; \alpha_K\,T_{KK}\,. \end{aligned} \tag{6.102}$$

Again it is most convenient to use matrix notation to group these equations

$$\mathrm{Im}\,\mathcal{F} \;=\; T\,\rho\,\mathcal{F}^* \;=T^\dagger\,\rho\,\mathcal{F}\,, \quad \mathcal{F} \;=\; T\,\alpha \quad \mathcal{F} \;=\; \begin{pmatrix} \mathcal{F}_\pi \\ \mathcal{F}_K \end{pmatrix} \quad \alpha \;=\; \begin{pmatrix} \alpha_\pi \\ \alpha_K \end{pmatrix}\,. \tag{6.103}$$

It is not difficult to find an expression for α as we did for α_π

$$\alpha \;=(T\,\rho\,T^\dagger)^{-1}\,T^\dagger\,\rho\,\mathcal{F}\,. \tag{6.104}$$

We have now to find the most general parametrization of the $\mathcal{F}$ matrix satisfying unitarity exactly. Our trial function is

$$\mathcal{F} \;=\; \mathcal{F}_B \;+\; T\,\tilde{t}\,. \tag{6.105}$$

By imposing that $T^\dagger\rho\,\mathcal{F}$ is a real matrix we easily obtain

$$\begin{aligned} \mathrm{Im}\,\tilde{t} &= \rho\,\mathcal{F}_B\,, \\ T^\dagger\,\rho\,\mathcal{F} &= T^\dagger\rho\,T\left(\mathrm{Re}\,\tilde{t} + \mathrm{Re}\,T^{-1}\,\mathcal{F}_B\right)\,, \\ \alpha &= \mathrm{Re}\,\tilde{t} + \mathrm{Re}\,T^{-1}\,\mathcal{F}_B\,. \end{aligned} \tag{6.106}$$

6.5.4 Schwinger–Dyson equations for the two photon reaction

Much as happens with unitary meson–meson scattering, there is a field theoretical method for exactly implementing unitarity in meson–meson production. Again to $\mathcal{O}(\alpha_{em})$ precision they read (in matrix notation)

$$\mathcal{F} = \mathcal{F}_B + T\,G\,\mathcal{F}_B\,. \tag{6.107}$$

Here $\mathcal{F}_B$ collects all the tree–level amplitudes, such as pion or resonance exchange, and so we can identify $\mathcal{F}_B \equiv \mathcal{H}$. Again $\mathcal{F}_B\,G\,T$ is an integral expression :

$$\mathcal{F}_B\,G\,T \;=\; \int \frac{\mathrm{d}^4 q}{(2\pi)^4}\,\mathcal{F}_B(k,p;q)\,G(P,q)\,T(k,p;q)\,, \tag{6.108}$$

with G defined in Eq. 6.91. If the same approximation leading to the Bethe–Salpeter equations in Section 6.5.2 is done, we arrive at the expression

$$\mathcal{F} \;=\; \mathcal{F}_B \;+\; T\,\bar{G}\,\mathcal{F}_B\,, \tag{6.109}$$

that satisfies unitarity exactly, as it is precisely of the form of Eq. (6.105) with $\tilde{t} = \bar{G}\,\mathcal{F}_B$. These ideas are diagrammatically explained in Fig. 6.15. The idea of using the Bethe–Salpeter equations for the meson production was used, for example, in Ref. [193]. We will see however, that despite the good description of the existing data, their amplitudes violate unitarity.

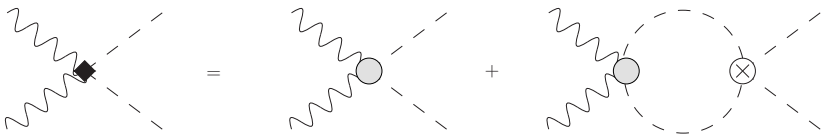

Figure 6.15: Diagrammatic picture of the Schwinger–Dyson equations. Diamond interactions means exact amplitude at $\mathcal{O}(\alpha_{em})$, gray circle means all tree–level electromagnetic contributions $\mathcal{H}$ (or $\mathcal{F}_B$) and crossed circle stands for the exact meson–meson amplitude.

6.5.5 Unitarity violation

Having in mind what we have exposed in the previous sections it will not be difficult to find criteria to test and measure unitarity violation in several models. We will concentrate in the unitary χPT extension as worked out in Ref. [193], and in particular discuss only the S–wave amplitude. In this paper basically a parametrization similar to that of Eq. (6.15) was used, with a particular model for $\mathrm{Re}\,\bar{G}$

$$\mathcal{F} \;=\; \mathcal{F}_B \;+\; T\,\bar{G}\,\tilde{\mathcal{F}}_B\,. \tag{6.110}$$

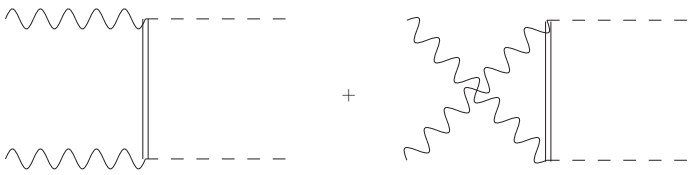

Figure 6.16: Resonance exchange contribution to $\mathcal{L}$ and to $\mathcal{F}_B$.

Their strong meson–meson scattering amplitude does satisfy unitarity exactly by construction, since it is of the form (6.92) with the same model for $\mathrm{Re}\,\bar{G}$, and V taken from tree–level χPT. The particular expressions can be found in Ref. [190] for $I = 0$ and Ref. [193] for $I = 2$. A feature of these amplitudes is that V has no resonance exchange. As long as $\tilde{\mathcal{F}}_B \neq \mathcal{F}_B$ unitarity is violated, and in fact we shall see that this situation happens for this model. Both $\mathcal{F}$ and $\mathcal{F}_B$ are built from χPT tree–level diagrams as in Fig. 6.11 and resonance exchange as in Fig. 6.16. In particular they consider ρ, ω and a_1 exchange in S–wave. These contributions were first introduced in a chiral invariant way in Ref. [194], but the rescattering effects were not considered. In the pure χPT sector (that is, no resonances) $\mathcal{F}^{\chi\mathrm{PT}} = \mathcal{F}_B^{\chi\mathrm{PT}}$ and hence this contribution does not violate unitarity. Problems arise when the resonance exchange is included, because its treatment is different in $\mathcal{F}$ and $\mathcal{F}_B$. While in the former the full resonance propagator is used, for the latter (that is, the one–loop computation) they contract the propagator to a single point: $1/(q^2 - M^2) \to -1/M^2$. Despite of the criticism that such contraction can receive from the field theoretical point of view, it also has the consequence of unitarity violation. So we have $\tilde{\mathcal{F}}_B = \mathcal{F} + \mathcal{O}(M^{-2})$ and unitarity is only satisfied at the $1/M^2$ level. Corrections will become important at energies comparable with the resonance mass.

We will define a function of s that measures the percentual unitarity violation. Since the $I = 0$ amplitude above threshold is a coupled channel but the $I = 2$ and the $I = 0$ below threshold consist of a single channel we will use a slightly different expression for each one. We will define our violation function as:

$$\Delta_I^{(1)} \;=\; 2\,\frac{\mathrm{Im}\,(F_I) - \rho_\pi\, F_I^*\, T_I}{\mathrm{Im}\,(F_I) + \rho_\pi\, F_I^*\, T_I}\,. \tag{6.111}$$

And for the two–channel case we define our violation function as:

$$\Delta_I^{(2)} \;=\; 2\,\frac{\mathrm{Im}\,(F_I) - \rho_\pi\, F_I^*\, T_I - \rho_K\, F_K^*\, T_{K\pi}}{\mathrm{Im}\,(F_I) + \rho_\pi\, F_I^*\, T_I + \rho_K\, F_K^*\, T_{K\pi}}\,. \tag{6.112}$$

It is immediate to realize that these two quantities are complex. So we will use their modulus as a measure of the unitarity violation. For the $I = 0$ channel we will define the violation function as Eq. (6.111) when we are below threshold and as Eq. (6.112) when we are above. The results are shown in Fig. 6.18. It can be seen that there are serious violations in the region near the mass of the resonances. The main contribution of this violation comes from ω exchange.

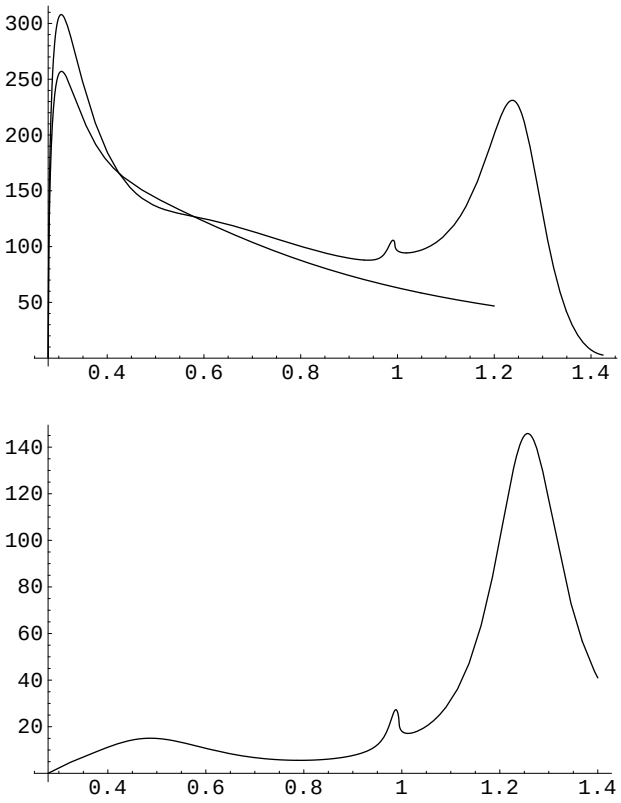

Figure 6.17: Predictions of Ref. [193] for the charged (up plot) and the neutral (down plot) pion production cross–sections. In the charged pion production plot we also show the born amplitude. The cross–section is measured in nanobarns as a function of the $\pi\,\pi$ invariant mass, in GeV.

6.5.6 Conclusions

Again we have experienced that the axiomatic principles of unitarity and crossing are a powerful tool for the description of meson–meson scattering and two photon processes. In particular, below the four–pion threshold, these principles severely constrain the behaviour of the scattering amplitudes. In the case of meson–meson scattering they link the phase shift with the modulus of the amplitude, constraining the strength of the interaction. For the two photon reaction, we obtain an interesting link between its amplitude and the meson–meson scattering amplitude. In particular it is easy to check that both amplitudes share the same right–hand cut structure and the same phase (Watson's theorem).

We have been able to find general parametrizations inspired in the Bethe–Salpeter equations that exactly satisfy unitarity. These parametrizations are then an excellent tool for testing if unitary is respected by some models, and if violated, how much.

We have applied this criteria to a model in which the χPT results are extended

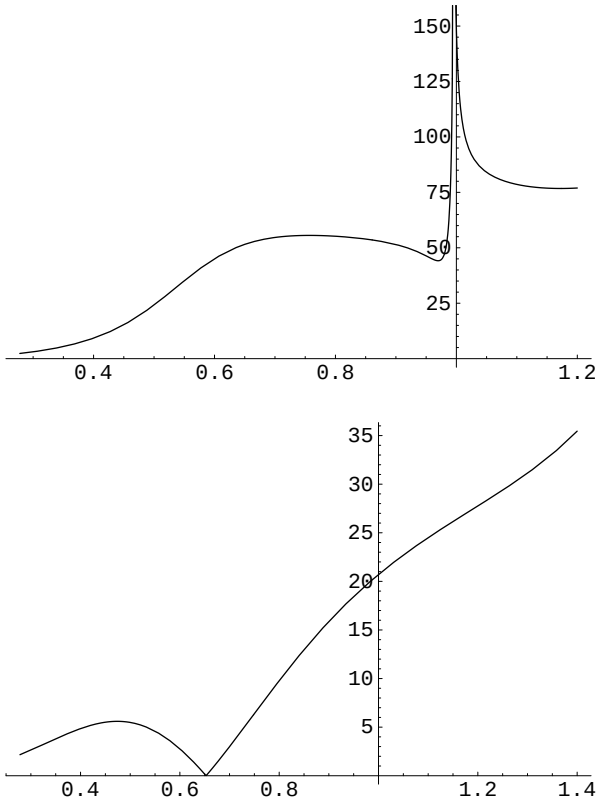

Figure 6.18: Unitarity violation function $|\Delta_I|$ for $I = 0$ pion production (up plot) and $I = 2$ (down plot). This function can be interpreted as a percentual violation, and it is plotted as a function of the invariant mass of the pions in GeV.

in a unitary way, and resonance exchange is considered in the tree–level term and the rescattering. This amounts to a particular modelization of some real parts, not fixed by unitarity.

A detailed study shows that the treatment of the resonance contributions lead in fact to unitarity violations. Despite the excellent description of the existing data obtained with such amplitudes, we have explicitly checked that unitarity is badly violated at intermediate energies.

We conclude then that a correct description of the experimental data is not sufficient to ensure a sensible description of the two photon reaction process.

Conclusions

Donat que el camp d'estudi d'esta tesi és prou ampli, no és fàcil obtindre una conclusió a nivell general. Es pot afirmar que s'han tractat tots els mètodes no pertorbatius aplicats al sector lleuger de QCD a excepció de càlculs en el reticle. Pot ser una conclusió que sí es pot extraure d'esta tesi és el paper fonamental que juga en els fenòmens no pertorbatius l'estudi conjunt dels diversos règims energètics. Anem però, a extraure les conclusions parcials més importants.

Teoria quiral de pertorbacions

Està més enllà de qualsevol dubte raonable el fet que χPT és la teoria dual de QCD en el règim d'energies molt baixes. En esta tesi hem fet una petita contribució al formalisme de χPT, incorporant la darrera font externa que mancava : la font tensorial. Hem estudiat les transformacions d'esta font sota les simetries de QCD, és a dir transformacions quirals, de paritat i conjugació de càrrega. Una particularitat de la font tensorial és que no té company quiral (no hi ha cap font "pseudotensorial"). L'estudi de les transformacions quirals ens ensenya que la font tensorial, que té sis components independents, es parteix en dos fonts de paritat oposada, cadascuna amb tres components independents. Por suposat cadascuna de les components és la companya quiral de l'altra. La font tensorial té associats alguns problemes conceptuals adicionals. En primer lloc no hi ha cap manera transparent d'assignar–li un contatge quiral. Per a la resta de les fonts açò era directe, ja que estan associades o bé a les transformacions quirals o bé al trencament explícit de la simetria quiral a través de les masses dels quarks. Ninguna d'estes situacions afecta a les fonts tensorials. Afortunadament estes fonts tan sols apareixen a funcions de Green i factors de forma, de manera que el seu contatge quiral és arbitrari. Diferents assignacions es tradueixen en la manera en què operadors amb diferent nombre de fonts tensorials s'organitzen en la base quiral, però no afecta els operadors que contribueixen a un ordre donat per a un càlcul específic. Per comoditat li assignem el mateix contatge que a la font escalar $t^{\mu\nu} \sim \mathcal{O}(p^2)$, de manera que tan sols tenim potències parelles al Lagrangià quiral. El segon problema té a veure amb la dimensió anòmala de la font tensorial. El corrent tensorial de QCD necessita una renormalització addicional a la pròpia dels camps de quarks que la formen. Este fenòmen es degut al fet de que tenim un producte de dos camps al mateix punt de l'espai–temps. Esta renormalització addicional fa que el corrent es tinga que definir a una certa escala, o

millor encara, que tinga una dependència explícita en l'escala de renormalització de QCD. Direm doncs que el corrent tensorial té dimensió anòmala no nul·la. Açò es tradueix en que la font tensorial també té dimensió anòmala. El Lagrangià de QCD no depén d'escala i per tant cadascun dels seus termes quan l'expresem (a energies baixes) en graus de llibertat hadrònics tampoc ho fa. La possibilitat més immediata és tractar amb $\tau^{\mu\nu} = b_0(\mu_{QCD})\, t^{\mu\nu}(\mu_{QCD})$ que no depén de μ_{QCD}, com a ent bàsic emprat per a la construcció del Lagrangià efectiu. La impossibilitat de determinar universalment la funció b_0 fa que tinguem que oblidar esta idea; la solució menys dolenta és considerar que les LECs que acompanyen a les fonts tensorials tenen una dependència amb μ_{QCD} que fa que el producte no depenga d'escala.

Determinació de $|\mathbf{V_{us}}|$

La determinació de paràmetres de la matriu CKM mitjançant desintegracions semileptòniques d'hiperons és independent de la determinació fent servir pions i kaons. Tindre determinacions independents és important ja que es poden detectars possibles errors i es millora l'estadística. En esta tesi hem estudiat els efectes del trencament de la simetria $SU(3)_V$ de sabor en la determinació de $|V_{us}|$ i els errors sistemàtics associats. El formalisme que hem triat és l'expansió de QCD en $1/N_C$. Al sector bariònic esta expansió es tradueix en unes condicions de consistència que determinen un àlgebra contreta d'spin–sabor. Podem per tant escriure propietats estàtiques de barions en termes dels generadors d'esta àlgegra. El teorema d'Ademollo–Gatto assegura que les correccions al factor de forma vectorial són de segon ordre en el trencament de simetria i per tant hem calculat fins este ordre en l'expansió combinada en $1/N_C$ i $m_s/\Lambda_{\rm QCD}$. Una de les conclusions més importants del nostre estudi és que no es poden ajustar les dades experimentals quan considerem trencament de simetria a segon ordre en el factor de forma vectorial i a primer ordre en el vector–axial: la funció χ^2 és plana i els diferents mímims no tenen significància estadística. El desconeiximent de les correccions al límit simètric del factor de forma vectorial són doncs la font principal d'error sistemàtic en la determinació de $|V_{us}|$.

Juntament amb la nostra determinació de $|V_{us}|$, emprant la determinació de $|V_{ud}|$ provinent de desintegracions nuclears i de la del neutró, podem comprobar que la unitarietat de la matriu CKM es satisfà al nivell de 1.5 σ.

Correccions de gluons durs a funcions de Green

Les funcions de Green que són paràmetres d'ordre del trencament espontàni de la simetria quiral són d'un interés especial per al coneixement de la física hadrònica. Com que estes funcions són exactament zero dins de teoria de pertorbacions, la seua existència es deu plenament al fenòmen del trencament espontani, que al mateix temps governa les interaccions dels hadrons a energies baixes. El seu estudi per a funcions de dos punts permet determinar les LECs del Lagrangià quiral d'ordre p^4 i les de tres punts fixen les constants d'ordre p^6. És l'empalmament amb el càlcul

realitzat en el marc de l'OPE a distàncies curtes el que fixa els coeficients. Estos estudis es fan en el límit de gran nombre de colors, però a més a l'ordre dominant en la constant d'acoblament α_s. Per a funcions de tres punts no hi ha en la literatura cap càlcul de correccions gluòniques al coeficient de Wilson associat al condensat de quarks. En esta tesi hem calculat estes correccions per a totes les funcions de Green paràmetre d'ordre de dos i tres punts. Els resultats són perfectament consistents i satisfan dues proves bàsiques. La primera és invariància gauge (el càlcul es realitza en un gauge arbitrari i la dependència en el paràmetre de gauge a cancela quan es sumen totes les contribucions). La segona es l'equació de Callan–Symanzic, és a dir, l'evolució dels coeficients de Wilson amb l'escala de renormalització de QCD. Les aplicacions fenomenològiques d'estos càlculs encara no s'han obtés.

Addicionalment en esta tesi s'han calculat els coeficients de Wilson associats als condensats gluonic, quatre quarks i mixte quark–gluó per a funcions de dos punts.

Desintegració radiativa del pio

Durant molt de temps la desintegració radiativa del pio ha estat una font de controvèrsia. Les dades experimentals es situaven a moltes desviacions estàndard de la predicció del SM, i per tant pareixia indicar la presència de nova física. En principi els procesos hadrònics a energies baixes no són sensibles a la física més enllà del SM, entre altres coses perquè la precisió en què es coneixen els paràmetres hadrònics no és massa gran. La nova interacció que es proposava per a curar este desacord entre teoria i experiment era precisament de tipus tensorial, i de fet es requeria un acoblament tan gran que ni tan sols SUSY la podia prediure. En esta tesi s'ha fet una anàlisi molt meticulosa d'este procés hadrònic. En primer lloc s'han incorporat al càlcul les dependències en el moment transferit dels factors de forma, cosa que sempre ha estat ignorada. Per al cas del factor de forma vectorial l'ansatz amb un sol multiplet de resonàncies vectorial és insuficient ja que no pot complir les condicions de Brodsky–Lepage. En el nostre treball hem inclós un segon multiplet i hem exigit totes les condicions de curtes distàncies per a determinar completament el factor de forma vectorial a través de la fórmula LSZ. En segon lloc, per tal de tindre en compte els efectes d'una possible interacció tensorial, s'ha de calcular l'element de matriu hadrònic corresponent de la manera més neta possible. El formalisme necessari per a este càlcul s'ha desenvolupat en esta tesi. En particular s'han empalmat la funció de Green $\langle VT \rangle$ calculada a χPT, RχT i l'OPE, de manera que tots els coeficients queden fixats. De la mateixa manera es pot calcular la dependència en moment dels factors de forma associats al corrent tensorial exigint bon comportament a distàncies curtes. Un altre cop tots els paràmetres queden fixats. La nostra anàlisi revela que la física més enllà del SM és compatible amb zero i el seu ordre de magnitut està d'acord amb SUSY.

Correladors vectorial i tensorial

Per a tindre una informació el més completa possible de la física relacionada amb les resonàncies vectorials cal fer un estudi conjunt dels correladors $\langle VV\rangle$, $\langle TT\rangle$ i $\langle VT\rangle$. Les resonàncies vectorials poden ser interpolades tant per corrents vectorials com tensorials, i per tant l'estudi més complet inclou totes les funcions de Green possibles amb estos dos corrents. A més el corrent tensorial també interpola resonàncies amb nombres quàntics $J^{PC} = 1^{+-}$. Les funcions de Green $\langle VV\rangle$ i $\langle TT\rangle$ no són paràmetres d'ordre, i per tant el seu terme pertorbatiu té una contribució logarítmica. Per a poder recuperar un logaritme a través d'una suma de funcions meromòrfiques (pols de masses de resonàncies) calen un nombre infinit de resonàncies, tal i com QCD per a un gran nombre de colors dicta. L'empalmament d'este logaritme amb la torre infinita de resonàncies ens determina com escalen les mases i les constants de desintegració per a nombres quàntics d'excitació radial (n) alts. Encara més, podem prediure exactament el quocient de les constants de desintegració vectorial sobre tensorial per a n gran. No obstant això, la funció de Green $\langle VT\rangle$ sí és un paràmetre d'ordre i per tant no té terme pertorbatiu ni logaritme. Este fet ens proporciona un resultat sorprenent : en exigir l'empalmament de la parametrització meromòrfica tenint en compte els resultats obtesos de l'estudi de les funcions de Green $\langle VV\rangle$ i $\langle TT\rangle$ obtenim que este quocient necessàriament té que alternar en signe. Este resultat ve suportat per estudis de regles de suma.

En incloure les fonts tensorials al Lagrangià de RχT conjuntament amb les resonàncies $J^{PC} = 1^{+-}$, es poden integrar funcionalment juntament amb les resonàncies vectorials i així obtindre prediccions per als acoblaments quirals.

Aplicacions d'unitarietat i analiticitat

El procés de dispersió de dos bosons de Goldstone a dos bosons de Goldstone (amb masses diferents de zero, però degenerats) és molt particular, ja que com que totes les partícules que intervenen al procés són les mateixes, simetria de creuament relaciona tots els canals possibles. Més encara, com que no hi ha partícules hadròniques de massa més lleugera, unitarietat lliga la part imaginària de l'amplitud de dispersió amb seccions eficaces, i a més el tall de discontinuïtat comença precisament al llindar de producció i no abans. Aquests trets, juntament amb el principi d'analiticitat, permeten escriure relacions de dispersió, és a dir, podem expresar l'amplitut de dispersió en un punt cinemàtic com una integral al llarg del tall de discontinuïtat. Dins d'un cert domini cinemàtic esta integral és definida positiva, de manera que l'amplitud de dispersió (més exactament, la seua segona derivada) és necessàriament positiva. A la regió cinemàtica en que açò és cert, els càlculs amb χPT són molt fiables (ràpida convergència), de tal manera que podem traduir aquesta condició de positivitat en restriccions per als valors de les constants quirals.

Este mètode pot generalitzar–se per al cas en què la simetria de sabor $SU(3)$ està trencada explícitament, de manera que les masses del kao, pio i eta són diferents.

Així doncs, per a certs procesos de dispersió, podem escriure relacions de positivitat que es tradueixen en cotes per a les constants d'energies baixes de la teoria amb tres sabors.

En esta tesi també hem emprat estes relacions de positivitat per a testejar la validesa del model sigma lineal amb dos sabors. Encara que en una primera anàlisi es poden trobar indicis d'inconsistències, un estudi més profund revela que realment no hi ha cap problema, i per tant el model és consistent amb els principis axiomàtics.

La producció de pions neutres en colisions de fotons és un procés de difícil descripció. A χPT la primera contribució no nul·la es dona a un loop i no conté cap LEC. L'acord d'este càlcul amb les dades experimental no és massa bo. Una descripció que tinga en compte el principi axiomàtic d'unitarietat de manera exacta és fonamental per a adequar–se més a la realitat. Per sota del llindar de producció de quatre partícules, el principi d'unitarietat constreny les amplituts de dispersió de fotons (i també de mesons) de manera dràstica. En esta tesi hem trobat les parametritzacions més generals que satisfan unitarietat de manera exacta, i les hem emprat per a testejar la validesa d'un model quiral. Les nostres conclusions són que encara que aquest model reprodueix les dades experimentals d'una manera més que acceptable, viola unitarietat d'una manera notòria, sent doncs aquesta descripció poc adequada.

Appendix A :

Cayley–Hamilton relations

The analysis in the main text to build the basis of operators has dealt with general $SU(n_f)$. In practice, however, one wants to specialize to the phenomenologically relevant cases, $n_f = 2$ and $n_f = 3$. The Cayley–Hamilton theorem states that any square $n \times n$ matrix A satisfies its own characteristic equation, $\chi_n(A) = 0$. This sets a relation between A and their invariants (traces and determinant). The form of the relation depends on the dimensionality n of the linear space. For instance,

$$\begin{aligned} \chi_2(A) \;=\; A^2 - \langle A\rangle A + (\det A)\,\mathbb{1}_{2\times 2} \;&=\; 0\,,\ (n=2)\,, \\ \chi_3(A) \;=\; A^3 - \langle A\rangle A^2 + \frac{\langle A\rangle^2 - \langle A^2\rangle}{2} A - (\det A)\,\mathbb{1}_{3\times 3} \;&=\; 0\,,\ (n=3)\,. \end{aligned} \tag{A.1}$$

One immediate consequence of the previous equations is that the determinant of any matrix is a function of its traces. We have implicitly used this information to write all chiral invariants solely in terms of traces. Solving the previous equations for the determinant, one finds

$$\begin{aligned} A^2 - \langle A\rangle A + \frac{\langle A\rangle^2 - \langle A^2\rangle}{2}\,\mathbb{1}_{2\times 2} \;&=\; 0\,, \\ A^3 - \langle A\rangle A^2 + \frac{\langle A\rangle^2 - \langle A^2\rangle}{2} A - \left[\frac{\langle A^3\rangle}{3} - \frac{\langle A^2\rangle\langle A\rangle}{2} - \frac{\langle A\rangle^3}{6}\right]\mathbb{1}_{3\times 3} \;&=\; 0\,. \end{aligned} \tag{A.2}$$

Cayley–Hamilton relations therefore set constraints between traces. For these constraints to be non–trivial, one has to build relations involving at least $n+1$ matrices. For instance, for $n = 2$ the quantity $\langle a\,\chi_2(b+c)\rangle$ gives

$$\langle a\,\{b,c\}\rangle - \langle a\rangle\langle b\,c\rangle - \langle b\rangle\langle c\,a\rangle - \langle c\rangle\langle a\,b\rangle + \langle a\rangle\langle b\rangle\langle c\rangle = 0 \tag{A.3}$$

whereas for $n = 3$, using $\langle a\,\chi_3(b+c+d)\rangle$ one ends up with

$$\begin{aligned} &\langle a\,b\,\{c,d\}\rangle + \langle a\,c\,\{b,d\}\rangle + \langle a\,d\,\{b,c\}\rangle - \langle a\,\{b,c\}\rangle\langle d\rangle - \langle a\,\{b,d\}\rangle\langle c\rangle - \langle a\,\{c,d\}\rangle\langle b\rangle \\ &\quad - \langle b\,\{c,d\}\rangle\langle a\rangle - \langle a\,b\rangle\langle cd\rangle - \langle a\,c\rangle\langle b\,d\rangle - \langle a\,d\rangle\langle b\,c\rangle + \langle a\rangle\langle b\rangle\langle c\,d\rangle + \langle a\rangle\langle c\rangle\langle b\,d\rangle \\ &\quad + \langle a\rangle\langle d\rangle\langle b\,c\rangle + \langle b\rangle\langle c\rangle\langle a\,d\rangle + \langle b\rangle\langle d\rangle\langle a\,c\rangle + \langle c\rangle\langle d\rangle\langle a\,b\rangle - \langle a\rangle\langle b\rangle\langle c\rangle\langle d\rangle \;=\; 0\,. \end{aligned} \tag{A.4}$$

In Table B.1 we have favored the terms with a minimum number of traces, bearing in mind that these are the dominant ones in a large–N_c expansion of the chiral Lagrangian.

A.1 SU(3)

For $n_f = 3$, use of Eq. (A.4) leads to the following relations,

$$\begin{aligned}
i\,\langle t_{+\mu\nu}\,[u^\mu,u^\alpha]\rangle\,\langle u_\alpha u^\nu\rangle\,[Y_6] &= Y_1 + 2\,Y_3 + Y_4 - Y_5\,,\\
i\,\langle t_{+\mu\nu} u_\alpha\rangle\,\langle u^\alpha u^\mu u^\nu\rangle\,[Y_7] &= Y_1 + Y_2 - \frac{1}{2}\,Y_5 - Y_8\,,\\
\langle t_{+\mu\nu}\rangle\,\langle t_+^{\mu\nu}\rangle\,\langle u_\alpha u^\alpha\rangle\,[Y_{21}] &= -\,4\,Y_9 - 2\,Y_{10} + Y_{14} + 2Y_{16} + 4\,Y_{19}\,,\\
\langle t_{+\mu\nu}\rangle\,\langle t_+^{\mu\alpha}\rangle\,\langle u_\alpha u^\nu\rangle\,[Y_{22}] &= -\,2\,Y_{11} - 2Y_{12} - Y_{13} + Y_{15} + Y_{17} + Y_{18} + 2\,Y_{20}\,,\\
\langle t_{-\mu\nu}\rangle\,\langle t_-^{\mu\alpha}\rangle\,\langle u_\alpha u^\nu\rangle\,[Y_{30}] &= -\,2\,Y_{23} - 2\,Y_{24} - Y_{25} + Y_{26} + Y_{27} + Y_{28} + 2\,Y_{29}\,,\\
\langle t_{+\mu\nu} u_\alpha\rangle\,\langle f_+^{\mu\nu} u^\alpha\rangle\,[Y_{63}] &= Y_{56} + Y_{57} - \frac{1}{2}\,Y_{61} - Y_{66}\,,\\
\langle t_{+\mu\nu} u_\alpha\rangle\,\langle f_+^{\mu\alpha} u^\nu\rangle\,[Y_{64}] &= Y_{58} + Y_{59} + Y_{60} - Y_{62} - Y_{65} - Y_{67}\,.
\end{aligned} \tag{A.5}$$

A.2 SU(2)

The relations derived in the previous section also hold for two flavours. In addition, repetitive use of Eq. (A.3) can be used to reduce monomials with multiple traces containing at least three chiral operators. We find

$$\begin{aligned}
i\,\langle t_{+\mu\nu}\,\{u_\alpha u^\alpha, u^\mu u^\nu\}\rangle\,[Y_1] &= 2\,Y_3\,,\\
i\,\langle t_{+\mu\nu}\,\{u_\alpha, u^\mu u^\alpha u^\nu\}\rangle\,[Y_4] &= -\,Y_2 - Y_3\,,\\
i\,\langle t_{+\mu\nu} u^\mu u^\nu\rangle\,\langle u_\alpha u^\alpha\rangle\,[Y_5] &= 2\,Y_3\,,\\
i\,\langle t_{+\mu\nu}\rangle\,\langle u_\alpha u^\alpha u^\mu u^\nu\rangle\,[Y_8] &= 0\,,\\
\langle t_{+\mu\nu} t_+^{\mu\nu}\rangle\,\langle u_\alpha u^\alpha\rangle\,[Y_{14}] &= 2\,Y_9\,,\\
\langle t_{+\mu\nu} t_+^{\mu\alpha}\rangle\,\langle u^\nu u_\alpha\rangle\,[Y_{15}] &= Y_{11} + Y_{12}\,,\\
\langle t_{+\mu\nu} u^\alpha\rangle\,\langle t_+^{\mu\alpha} u_\alpha\rangle\,[Y_{16}] &= Y_9 + Y_{10} - Y_{19}\,,\\
\langle t_{+\mu\nu} u^\alpha\rangle\,\langle t_+^{\mu\alpha} u_\nu\rangle\,[Y_{17}] &= Y_{12} + \frac{1}{2}\,Y_{13} - \frac{1}{2}\,Y_{20}\,,\\
\langle t_{+\mu\nu} u^\nu\rangle\,\langle t_+^{\mu\alpha} u_\alpha\rangle\,[Y_{18}] &= Y_{11} + \frac{1}{2}\,Y_{13} - \frac{1}{2}\,Y_{20}\,,\\
\langle t_{-\mu\nu} t_-^{\mu\alpha}\rangle\,\langle u^\nu u_\alpha\rangle\,[Y_{26}] &= Y_{23} + Y_{24}\,,\\
\langle t_{-\mu\nu} u^\alpha\rangle\,\langle t_-^{\mu\alpha} u_\nu\rangle\,[Y_{27}] &= Y_{24} + \frac{1}{2}\,Y_{25} - \frac{1}{2}\,Y_{29}\,,\\
\langle t_{-\mu\nu} u^\nu\rangle\,\langle t_-^{\mu\alpha} u_\alpha\rangle\,[Y_{28}] &= Y_{23} + \frac{1}{2}\,Y_{25} - \frac{1}{2}\,Y_{29}\,,
\end{aligned}$$

$$
\begin{aligned}
\langle t_{+\mu\nu}\rangle\,\langle t_+^{\mu\nu}\rangle\,\langle\chi_+\rangle\,[Y_{37}] &= -\,2\,Y_{31}+Y_{33}+2\,Y_{34}\,,\\
\langle t_{-\mu\nu}\rangle\,\langle t_+^{\mu\nu}\rangle\,\langle\chi_-\rangle\,[Y_{38}] &= -\,2\,Y_{32}+Y_{35}+2\,Y_{36}\,,\\
i\,\langle\chi_+\rangle\,\langle t_{+\mu\nu}u^\mu u^\nu\rangle\,[Y_{41}] &= \frac{1}{2}\,Y_{39}+Y_{40}\,,\\
i\,\langle t_{+\mu\nu}\rangle\,\langle\chi_+ u^\mu u^\nu\rangle\,[Y_{42}] &= \frac{1}{2}\,Y_{39}-Y_{40}\,,\\
i\,\langle\chi_-\rangle\,\langle t_{-\mu\nu}u^\mu u^\nu\rangle\,[Y_{45}] &= \frac{1}{2}\,Y_{43}+Y_{44}\,,\\
i\,\langle t_{-\mu\nu}\rangle\,\langle\chi_- u^\mu u^\nu\rangle\,[Y_{46}] &= \frac{1}{2}\,Y_{43}-Y_{44}\,,\\
\langle t_{+\mu\nu}f_+^{\mu\nu}\rangle\,\langle u_\alpha u^\alpha\rangle\,[Y_{61}] &= Y_{56}\,,\\
\langle t_{+\mu\nu}f_+^{\mu\alpha}\rangle\,\langle u^\nu u_\alpha\rangle\,[Y_{62}] &= \frac{1}{2}\,(Y_{58}+Y_{59})\,,\\
\langle t_{+\mu\nu}u^\nu\rangle\,\langle f_+^{\mu\alpha}u_\alpha\rangle\,[Y_{65}] &= \frac{1}{2}\,(Y_{59}+Y_{60})\,,\\
\langle t_{+\mu\nu}\rangle\,\langle f_+^{\mu\nu}u_\alpha u^\alpha\rangle\,[Y_{66}] &= 0\,,\\
\langle t_{+\mu\nu}\rangle\,\langle f_+^{\mu\alpha}\{u_\alpha,u^\nu\}\rangle\,[Y_{67}] &= 0\,,\\
\langle t_{+\mu\nu}f_+^{\mu\nu}\rangle\,\langle\chi_+\rangle\,[Y_{78}] &= Y_{73}-Y_{76}\,,\\
\langle t_{-\mu\nu}f_+^{\mu\nu}\rangle\,\langle\chi_-\rangle\,[Y_{79}] &= Y_{74}-Y_{77}\,,\\
i\,\langle t_-^{\nu\rho}\rangle\,\langle t_{+\mu\nu}h^\mu_{\ \rho}\rangle\,[Y_{82}] &= Y_{80}-Y_{81}\,,\\
i\,\langle t_{-\mu\nu}\rangle\,\langle f_-^{\nu\rho}f^\mu_{+\rho}\rangle\,[Y_{86}] &= Y_{85}\,,\\
i\,\langle t_-^{\nu\rho}\rangle\,\langle f_{-\mu\nu}t^\mu_{+\rho}\rangle\,[Y_{92}] &= Y_{89}-Y_{90}-Y_{92}-4\,Y_{119}\,,\\
i\,\langle\partial^\mu t_{-\mu\nu}\rangle\,\langle f_+^{\nu\rho}u_\rho\rangle\,[Y_{100}] &= Y_{97}\,,\\
i\,\langle\partial_\rho t_{-\mu\nu}\rangle\,\langle f_+^{\mu\nu}u^\rho\rangle\,[Y_{101}] &= Y_{98}\,,\\
i\,\langle\partial_\rho t_{-\mu\nu}\rangle\,\langle f_+^{\mu\rho}u^\nu\rangle\,[Y_{102}] &= Y_{99}\,,\\
i\,\langle t_{+\mu\nu}\rangle\,\langle\nabla_\lambda t_-^{\mu\nu}u^\lambda\rangle\,[Y_{109}] &= Y_{103}-Y_{106}\,,\\
i\,\langle t_{+\nu\lambda}\rangle\,\langle\nabla_\mu t_-^{\mu\nu}u^\lambda\rangle\,[Y_{110}] &= Y_{104}-Y_{107}\,,\\
i\,\langle t_{-\nu\lambda}\rangle\,\langle\nabla_\mu t_+^{\mu\nu}u^\lambda\rangle\,[Y_{111}] &= Y_{105}-Y_{108}\,,\\
i\,\langle t_{-\mu\nu}\rangle\,\langle h^{\nu\rho}f^\mu_{+\rho}\rangle\,[Y_{117}] &= Y_{116}\,. \qquad\qquad (A.6)
\end{aligned}
$$

Appendix B :

The $\mathcal{L}_6$ Lagrangian with tensor sources

monomial Y_i	$SU(n_f)$	$SU(3)$	$SU(2)$
$i\left\langle t_{+\mu\nu}\left\{u_\alpha u^\alpha, u^\mu u^\nu\right\}\right\rangle$	1	1	
$i\left\langle t_{+\mu\nu} u^\alpha u^\mu u^\nu u_\alpha\right\rangle$	2	2	1
$i\left\langle t_{+\mu\nu} u^\mu u_\alpha u^\alpha u^\nu\right\rangle$	3	3	2
$i\left\langle t_{+\mu\nu}\left\{u_\alpha, u^\mu u^\alpha u^\nu\right\}\right\rangle$	4	4	
$i\left\langle t_{+\mu\nu} u^\mu u^\nu\right\rangle\left\langle u_\alpha u^\alpha\right\rangle$	5	5	
$i\left\langle t_{+\mu\nu}\left[u^\mu, u^\alpha\right]\right\rangle\left\langle u_\alpha u^\nu\right\rangle$	6		
$i\left\langle t_{+\mu\nu} u_\alpha\right\rangle\left\langle u^\alpha u^\mu u^\nu\right\rangle$	7		
$i\left\langle t_{+\mu\nu}\right\rangle\left\langle u_\alpha u^\alpha u^\mu u^\nu\right\rangle$	8	6	
$\left\langle t_{+\mu\nu} t_+^{\mu\nu} u_\alpha u^\alpha\right\rangle$	9	7	3
$\left\langle t_{+\mu\nu} u_\alpha t_+^{\mu\nu} u^\alpha\right\rangle$	10	8	4
$\left\langle t_{+\mu\nu} t_+^{\mu\alpha} u_\alpha u^\nu\right\rangle$	11	9	5
$\left\langle t_{+\mu\nu} t_+^{\mu\alpha} u^\nu u_\alpha\right\rangle$	12	10	6
$\left\langle t_{+\mu\nu}\left(u^\nu t_+^{\mu\alpha} u_\alpha + u_\alpha t_+^{\mu\alpha} u^\nu\right)\right\rangle$	13	11	7
$\left\langle t_{+\mu\nu} t_+^{\mu\nu}\right\rangle\left\langle u_\alpha u^\alpha\right\rangle$	14	12	
$\left\langle t_{+\mu\nu} t_+^{\mu\alpha}\right\rangle\left\langle u^\nu u_\alpha\right\rangle$	15	13	

Table B.1: List of operators contributing to the $\mathcal{O}(p^6)$ Lagrangian

monomial Y_i	$SU(n_f)$	$SU(3)$	$SU(2)$
$\langle t_{+\mu\nu} u_\alpha \rangle \langle t_+^{\mu\nu} u^\alpha \rangle$	16	14	
$\langle t_{+\mu\nu} u_\alpha \rangle \langle t_+^{\mu\alpha} u^\nu \rangle$	17	15	
$\langle t_{+\mu\nu} u^\nu \rangle \langle t_+^{\mu\alpha} u_\alpha \rangle$	18	16	
$\langle t_{+\mu\nu} \rangle \langle t_+^{\mu\nu} u_\alpha u^\alpha \rangle$	19	17	8
$\langle t_{+\mu\nu} \rangle \langle t_+^{\mu\alpha} \{u_\alpha, u^\nu\} \rangle$	20	18	9
$\langle t_{+\mu\nu} \rangle \langle t_+^{\mu\nu} \rangle \langle u_\alpha u^\alpha \rangle$	21		
$\langle t_{+\mu\nu} \rangle \langle t_+^{\mu\alpha} \rangle \langle u_\alpha u^\nu \rangle$	22		
$\langle t_{-\mu\nu} t_-^{\mu\alpha} u_\alpha u^\nu \rangle$	23	19	10
$\langle t_{-\mu\nu} t_-^{\mu\alpha} u^\nu u_\alpha \rangle$	24	20	11
$\langle t_{-\mu\nu} \left(u^\nu t_-^{\mu\alpha} u_\alpha + u_\alpha t_-^{\mu\alpha} u^\nu\right) \rangle$	25	21	12
$\langle t_{-\mu\nu} t_-^{\mu\alpha} \rangle \langle u^\nu u_\alpha \rangle$	26	22	
$\langle t_{-\mu\nu} u_\alpha \rangle \langle t_-^{\mu\alpha} u^\nu \rangle$	27	23	
$\langle t_{-\mu\nu} u^\nu \rangle \langle t_-^{\mu\alpha} u_\alpha \rangle$	28	24	
$\langle t_{-\mu\nu} \rangle \langle t_-^{\mu\alpha} \{u_\alpha, u^\nu\} \rangle$	29	25	13
$\langle t_{-\mu\nu} \rangle \langle t_-^{\mu\alpha} \rangle \langle u_\alpha u^\nu \rangle$	30		
$\langle t_{+\mu\nu} t_+^{\mu\nu} \chi_+ \rangle$	31	26	14
$\langle t_{+\mu\nu} t_-^{\mu\nu} \chi_- \rangle$	32	27	15
$\langle t_{+\mu\nu} t_+^{\mu\nu} \rangle \langle \chi_+ \rangle$	33	28	16
$\langle t_{+\mu\nu} \chi_+ \rangle \langle t_+^{\mu\nu} \rangle$	34	29	17
$\langle t_{+\mu\nu} t_-^{\mu\nu} \rangle \langle \chi_- \rangle$	35	30	18
$\langle t_{+\mu\nu} \chi_- \rangle \langle t_-^{\mu\nu} \rangle$	36	31	19
$\langle t_{+\mu\nu} \rangle \langle t_+^{\mu\nu} \rangle \langle \chi_+ \rangle$	37	32	
$\langle t_{+\mu\nu} \rangle \langle t_-^{\mu\nu} \rangle \langle \chi_- \rangle$	38	33	
$i \langle t_{+\mu\nu} \{\chi_+, u^\mu u^\nu\} \rangle$	39	34	20

Table B.1: List of operators contributing to the $\mathcal{O}(p^6)$ Lagrangian

monomial Y_i	$SU(n_f)$	$SU(3)$	$SU(2)$
$i\langle t_{+\mu\nu}u^\mu\chi_+u^\nu\rangle$	40	35	21
$i\langle\chi_+\rangle\langle t_{+\mu\nu}u^\mu u^\nu\rangle$	41	36	
$i\langle t_{+\mu\nu}\rangle\langle\chi_+u^\mu u^\nu\rangle$	42	37	
$i\langle t_{-\mu\nu}\{\chi_-,u^\mu u^\nu\}\rangle$	43	38	22
$i\langle t_{-\mu\nu}u^\mu\chi_-u^\nu\rangle$	44	39	23
$i\langle\chi_-\rangle\langle t_{-\mu\nu}u^\mu u^\nu\rangle$	45	40	
$i\langle t_{-\mu\nu}\rangle\langle\chi_-u^\mu u^\nu\rangle$	46	41	
$\langle t_{-\mu\nu}(h^{\nu\rho}u_\rho u^\mu-u^\mu u_\rho h^{\nu\rho})\rangle$	47	42	24
$\langle t_{-\mu\nu}(h^{\nu\rho}u^\mu u_\rho-u_\rho u^\mu h^{\nu\rho})\rangle$	48	43	25
$\langle t_{-\mu\nu}(u_\rho h^{\nu\rho}u^\mu-u^\mu h^{\nu\rho}u_\rho)\rangle$	49	44	26
$\langle t_{-\mu\nu}\rangle\langle h^{\nu\rho}[u_\rho,u^\mu]\rangle$	50	45	27
$\langle\nabla_\rho t_{+\mu\nu}\nabla^\rho t_+^{\mu\nu}\rangle$	51	46	28
$\langle\nabla^\mu t_{+\nu\mu}\nabla_\rho t_+^{\nu\rho}\rangle$	52	47	29
$\langle\nabla_\mu t_-^{\mu\nu}\nabla^\rho t_{-\rho\nu}\rangle$	53	48	30
$\langle\partial_\rho t_{+\mu\nu}\rangle\langle\partial^\rho t_+^{\mu\nu}\rangle$	54	49	31
$\langle\partial^\mu t_{+\nu\mu}\rangle\langle\partial^\rho t_{+\rho}^{\nu}\rangle$	55	50	32
$\langle\partial^\mu t_{-\nu\mu}\rangle\langle\partial^\rho t_{-\rho}^{\nu}\rangle$	56	51	33
$\langle t_{+\mu\nu}\{f_+^{\mu\nu},u_\alpha u^\alpha\}\rangle$	57	52	34
$\langle t_{+\mu\nu}u_\alpha f_+^{\mu\nu}u^\alpha\rangle$	58	53	35
$\langle t_{+\mu\nu}(f_+^{\mu\alpha}u^\nu u_\alpha+u_\alpha u^\nu f_+^{\mu\alpha})\rangle$	59	54	36
$\langle t_{+\mu\nu}(f_+^{\mu\alpha}u_\alpha u^\nu+u^\nu u_\alpha f_+^{\mu\alpha})\rangle$	60	55	37
$\langle t_{+\mu\nu}(u^\nu f_+^{\mu\alpha}u_\alpha+u_\alpha f_+^{\mu\alpha}u^\nu)\rangle$	61	56	38
$\langle t_{+\mu\nu}f_+^{\mu\nu}\rangle\langle u_\alpha u^\alpha\rangle$	62	57	
$\langle t_{+\mu\nu}f_+^{\mu\alpha}\rangle\langle u^\nu u_\alpha\rangle$	63	58	
$\langle t_{+\mu\nu}u_\alpha\rangle\langle f_+^{\mu\nu}u^\alpha\rangle$	64		

Table B.1: List of operators contributing to the $\mathcal{O}(p^6)$ Lagrangian

monomial Y_i	$SU(n_f)$	$SU(3)$	$SU(2)$
$\langle t_{+\mu\nu} u_\alpha \rangle \langle f_+^{\mu\alpha} u^\nu \rangle$	65		
$\langle t_{+\mu\nu} u^\nu \rangle \langle f_+^{\mu\alpha} u_\alpha \rangle$	66	59	
$\langle t_{+\mu\nu} \rangle \langle f_+^{\mu\nu} u_\alpha u^\alpha \rangle$	67	60	
$\langle t_{+\mu\nu} \rangle \langle f_+^{\mu\alpha} \{u_\alpha, u^\nu\} \rangle$	68	61	
$\langle t_{-\mu\nu} [f_-^{\mu\nu}, u_\alpha u^\alpha] \rangle$	69	62	39
$\langle t_{-\mu\nu} (f_-^{\mu\alpha} u^\nu u_\alpha - u_\alpha u^\nu f_-^{\mu\alpha}) \rangle$	70	63	40
$\langle t_{-\mu\nu} (f_-^{\mu\alpha} u_\alpha u^\nu - u^\nu u_\alpha f_-^{\mu\alpha}) \rangle$	71	64	41
$\langle t_{-\mu\nu} (u^\nu f_-^{\mu\alpha} u_\alpha - u_\alpha f_-^{\mu\alpha} u^\nu) \rangle$	72	65	42
$\langle t_{-\mu\nu} \rangle \langle f_-^{\mu\alpha} [u_\alpha, u^\nu] \rangle$	73	66	43
$\langle t_{+\mu\nu} \{f_+^{\mu\nu}, \chi_+\} \rangle$	74	67	44
$\langle t_{-\mu\nu} \{f_+^{\mu\nu}, \chi_-\} \rangle$	75	68	45
$\langle t_{+\mu\nu} [f_-^{\mu\nu}, \chi_-] \rangle$	76	69	46
$\langle t_{+\mu\nu} \rangle \langle f_+^{\mu\nu} \chi_+ \rangle$	77	70	47
$\langle t_{-\mu\nu} \rangle \langle f_+^{\mu\nu} \chi_- \rangle$	78	71	48
$\langle t_{+\mu\nu} f_+^{\mu\nu} \rangle \langle \chi_+ \rangle$	79	72	
$\langle t_{-\mu\nu} f_+^{\mu\nu} \rangle \langle \chi_- \rangle$	80	73	
$i \left\langle t_{+\mu\nu} \left\{ t_-^{\nu\rho}, h^\mu_{\ \rho} \right\} \right\rangle$	81	74	49
$i \langle t_{+\mu\nu} \rangle \left\langle t_-^{\nu\rho} h^\mu_{\ \rho} \right\rangle$	82	75	50
$i \langle t_-^{\nu\rho} \rangle \left\langle t_{+\mu\nu} h^\mu_{\ \rho} \right\rangle$	83	76	
$i \left\langle t_{+\mu\nu} f_-^{\mu\rho} f_{-\rho}^{\nu} \right\rangle$	84	77	51
$i \left\langle t_{+\mu\nu} f_+^{\mu\rho} f_{+\rho}^{\nu} \right\rangle$	85	78	52
$i \left\langle t_{-\mu\nu} \left\{ f_-^{\nu\rho}, f_{+\rho}^{\mu} \right\} \right\rangle$	86	79	53
$i \langle t_{-\mu\nu} \rangle \left\langle f_-^{\nu\rho} f_{+\rho}^{\mu} \right\rangle$	87	80	

Table B.1: List of operators contributing to the $\mathcal{O}(p^6)$ Lagrangian

monomial Y_i	$SU(n_f)$	$SU(3)$	$SU(2)$
$i\left\langle t_{+\mu\nu}t_{+}^{\mu\rho}t_{+\rho}^{\nu}\right\rangle$	88	81	54
$i\left\langle t_{+\mu\nu}t_{-}^{\mu\rho}t_{-\rho}^{\nu}\right\rangle$	89	82	55
$i\left\langle f_{+\mu\nu}t_{+}^{\nu\rho}t_{+\rho}^{\mu}\right\rangle$	90	83	56
$i\left\langle f_{+\mu\nu}t_{-}^{\nu\rho}t_{-\rho}^{\mu}\right\rangle$	91	84	57
$i\left\langle t_{+\rho}^{\mu}\right\rangle\left\langle f_{-\mu\nu}t_{-}^{\nu\rho}\right\rangle$	92	85	58
$i\left\langle t_{-}^{\nu\rho}\right\rangle\left\langle f_{-\mu\nu}t_{+\rho}^{\mu}\right\rangle$	93	86	
$\left\langle \nabla_{\mu}t_{+}^{\mu\nu}\nabla^{\alpha}f_{+\alpha\nu}\right\rangle$	94	87	59
$i\left\langle \nabla_{\rho}t_{+\mu\nu}\left[h^{\mu\rho},u^{\nu}\right]\right\rangle$	95	88	60
$i\left\langle \nabla^{\mu}t_{+\mu\nu}\left[h^{\nu\rho},u_{\rho}\right]\right\rangle$	96	89	61
$i\left\langle \nabla^{\mu}t_{+\mu\nu}\left[f_{-}^{\nu\rho},u_{\rho}\right]\right\rangle$	97	90	62
$i\left\langle \nabla^{\mu}t_{-\mu\nu}\left\{f_{+}^{\nu\rho},u_{\rho}\right\}\right\rangle$	98	91	63
$i\left\langle \nabla_{\rho}t_{-\mu\nu}\left\{f_{+}^{\mu\nu},u^{\rho}\right\}\right\rangle$	99	92	64
$i\left\langle \nabla_{\rho}t_{-\mu\nu}\left\{f_{+}^{\mu\rho},u^{\nu}\right\}\right\rangle$	100	93	65
$i\left\langle \partial^{\mu}t_{-\mu\nu}\right\rangle\left\langle f_{+}^{\nu\rho}u_{\rho}\right\rangle$	101	94	
$i\left\langle \partial_{\rho}t_{-\mu\nu}\right\rangle\left\langle f_{+}^{\mu\nu}u^{\rho}\right\rangle$	102	95	
$i\left\langle \partial_{\rho}t_{-\mu\nu}\right\rangle\left\langle f_{+}^{\mu\rho}u^{\nu}\right\rangle$	103	96	
$i\left\langle \left\{\nabla_{\lambda}t_{-}^{\mu\nu},t_{+\mu\nu}\right\}u^{\lambda}\right\rangle$	104	97	66
$i\left\langle \left\{\nabla_{\mu}t_{+}^{\mu\nu},t_{-\nu\lambda}\right\}u^{\lambda}\right\rangle$	105	98	67
$i\left\langle \partial_{\lambda}t_{-}^{\mu\nu}\right\rangle\left\langle t_{+\mu\nu}u^{\lambda}\right\rangle$	106	99	68
$i\left\langle \partial_{\mu}t_{-}^{\mu\nu}\right\rangle\left\langle t_{+\nu\lambda}u^{\lambda}\right\rangle$	107	100	69
$i\left\langle \partial_{\mu}t_{+}^{\mu\nu}\right\rangle\left\langle t_{-\nu\lambda}u^{\lambda}\right\rangle$	108	101	70
$i\left\langle t_{+\mu\nu}\right\rangle\left\langle \nabla_{\lambda}t_{-}^{\mu\nu}u^{\lambda}\right\rangle$	109	102	
$i\left\langle t_{+\nu\lambda}\right\rangle\left\langle \nabla_{\mu}t_{-}^{\mu\nu}u^{\lambda}\right\rangle$	110	103	
$i\left\langle t_{-\nu\lambda}\right\rangle\left\langle \nabla_{\mu}t_{+}^{\mu\nu}u^{\lambda}\right\rangle$	111	104	

Table B.1: List of operators contributing to the $\mathcal{O}(p^6)$ Lagrangian

monomial Y_i	$SU(n_f)$	$SU(3)$	$SU(2)$
$\langle t_-^{\mu\nu}\,[\chi_{+\mu}, u_\nu]\rangle$	112	105	71
$\langle t_+^{\mu\nu}\,[\chi_{-\mu}, u_\nu]\rangle$	113	106	72
$i\,\langle t_{+\mu\nu} h^{\mu\alpha} h^{\nu}{}_{\alpha}\rangle$	114	107	73
$i\,\langle t_{+\mu\nu}\,[h^{\mu\alpha}, f_{-\alpha}^{\nu}]\rangle$	115	108	74
$i\,\langle t_{-\mu\nu}\,\{h^{\mu\alpha}, f_{+\alpha}^{\nu}\}\rangle$	116	109	75
$i\,\langle t_{-\mu\nu}\rangle\,\langle h^{\mu\alpha} f_{+\alpha}^{\nu}\rangle$	117	110	
Contact terms			
$\langle D_\mu t^{\mu\nu} D^\alpha t^\dagger_{\alpha\nu}\rangle$	118	111	76
$i\,\langle t^{\dagger\nu\rho} t^{\mu}{}_{\rho} F_{L\mu\nu} + t^{\nu\rho} t^{\dagger\mu}{}_{\rho} F_{R\mu\nu}\rangle$	119	112	77
$\langle t_{\mu\nu}\chi^\dagger F_R^{\mu\nu} + \chi t^\dagger_{\mu\nu} F_R^{\mu\nu} + t^\dagger_{\mu\nu}\chi F_L^{\mu\nu} + \chi^\dagger t_{\mu\nu} F_L^{\mu\nu}\rangle$	120	113	78

Table B.1: List of operators contributing to the $\mathcal{O}(p^6)$ Lagrangian

Appendix C :

The antisymmetric formalism

Although the antisymmetric tensor formalism for spin–one massive fields was already proposed at the end of 60's [195], its use was not regular until it was rediscovered in Ref. [9] in order to introduce the ρ resonance field in the chiral Lagrangian, Ecker *et al.* turned it into the usual way to work with spin–one resonances in RχT [13]. A very nice discussion about the different formalisms for spin one vector mesons can be found in Ref. [196], where the first order formalism is also discussed.

The most common formalism for the description of a spin–one massive particle is the Proca field R_μ. Since R_μ is a Lorentz vector it has four degrees of freedom, but a spin–one field has only three degrees of freedom. So the R_μ field must have a constraint, and it is given by the Lorentz transversality condition $\partial \cdot R = 0$. However the Proca Lagrangian

$$\begin{aligned} \mathcal{L}_{\rm Proca} &= -\frac{1}{4} R_{\mu\nu} R^{\mu\nu} + \frac{1}{2} M_R^2 R_\mu R^\mu \,, \\ R_{\mu\nu} &= \partial_\mu R_\nu - \partial_\nu R_\mu \,, \end{aligned} \tag{C.1}$$

automatically ensures the Lorentz condition because the equation of motion reads

$$\begin{aligned} &\partial_\mu R^{\mu\nu} + M_R^2 R^\nu = 0 \,, \\ &M_R^2 \, \partial_\mu R^\mu = 0 \,, \rightarrow \left(\partial^2 + M_R^2\right) R^\mu = 0 \,, \end{aligned} \tag{C.2}$$

the second equation is obtained calculating the divergence of the first one and when implemented back in the first we obtain that the Proca Lagrangian implies that each component of the Proca field satisfies the same Klein–Gordon equation subject to the Lorentz condition. Another way of seeing that indeed we have only two degrees of freedom is to notice that Eq. (C.1) is not the most general Lagrangian bilinear in the Proca field. In full generality one has $a\,\partial_\mu R_\nu \partial^\mu R^\nu + b\,\partial_\mu R_\nu \partial^\nu R^\mu$ but the choice $a = -b = -1/4$ removes one degree of freedom. The fact that Eq. (C.1) is built with $R_{\mu\nu}$ suggest that we can employ an antisymmetric tensor field to describe the spin–one massive particles. An antisymmetric tensor field has 6 independent components, hence we have to remove 3 degrees of freedom to correctly describe a spin–one particle.

In Ref. [197] it was proved that for antisymmetric tensor fields with mass there are (up to multiplicative factors and a total four divergence) only two possible Lagrangians of second order in derivatives, if one assumes the existence of a Klein–Gordon divisor. They correspond to having either the Lorentz condition or else a Bianchi identity satisfied by the fields. In the case of describing spin–one particles, one has these two possibilities, where $R_{\mu\nu} = -R_{\nu\mu}$,

1. The subsidiary condition is the Bianchi identity, i.e. $\epsilon^{\mu\lambda\rho\sigma}\partial_\lambda W_{\rho\sigma} = 0$, and W_{ik} are frozen, so the dynamical degrees of freedom are W_{i0}, where i runs over $i = 1, 2, 3$. Notice that there are 3 degrees of freedom, as it should be.

2. The subsidiary condition is now the Lorentz condition, that is, $\partial^\rho W_{\rho\nu} = 0$, and W_{i0} are frozen, so the three degrees of freedom are W_{ij}.

In order to get a better understanding on that, let us consider the most general Lagrangian with up to two derivatives built with an antisymmetric field $W_{\mu\nu}$:

$$\mathcal{L} \,=\, a\,\partial^\mu W_{\mu\nu}\partial_\rho W^{\rho\nu} \,+\, b\,\partial^\rho W_{\mu\nu}\partial_\rho W^{\mu\nu} \,+\, c\,W_{\mu\nu}W^{\mu\nu}\,, \tag{C.3}$$

where a, b and c are arbitrary constants. We have to choose these constants in such a way that three degrees of freedom are removed. Indeed, consider the EOM

$$a\,(\partial^\mu\partial_\sigma W^{\sigma\nu} \,-\, \partial^\nu\partial_\sigma W^{\sigma\mu}) \,+\, 2b\,\partial^\sigma\partial_\sigma W^{\mu\nu} \,-\, 2c\,W^{\mu\nu} \,=\, 0\,, \tag{C.4}$$

that can be split up into the time–spatial and spatial–spatial components :

$$\begin{aligned} (a+2\,b)\ddot{W}^{0i} \,+\, a\,\partial_l\dot{W}^{li} \,-\, a\,\partial^i\partial_l W^{l0} \,-\, 2\,(b\,\partial^2 \,+\, c)W^{0i} \;&=\; 0\,, \\ 2\,b\,\ddot{W}^{ik} \,+\, a\left[\partial^i(\dot{W}^{0k} \,+\, \partial_l W^{lk})\right] \,-\, 2\,(b\,\partial^2 \,+\, c)W^{ik} \;&=\; 0\,, \end{aligned} \tag{C.5}$$

where the dots denote time derivatives. For $a + 2\,b = 0$, the three fields W^{0i} do not propagate ($b = 0$ freezes the spatial–spatial components, on the contrary). The $W^{\mu\nu}$ propagator contains poles in $k^2 = -\,c/b$ and $k^2 = -\,2\,c/(a+2\,b)$, which disappear for $b = 0$, or $a + 2\,b = 0$, respectively. To maintain only one pole and reduce the number of degrees of freedom to three, we must choose among these two options, corresponding to the choices listed above. Because of historical reasons, the first option $b = 0$ has been chosen, and a and c are chosen to reproduce the pole corresponding to the particle mass, that is, $a = -\,1/2$, and $c = M^2/4$. Then, the Lagrangian [13] reads

$$\mathcal{L} \,=\, -\,\frac{1}{2}\,\partial^\mu W_{\mu\nu}\,\partial_\rho W^{\rho\nu} \,+\, \frac{1}{4}\,M^2\,W_{\mu\nu}W^{\mu\nu}\,, \tag{C.6}$$

from which the free–case EOM is

$$\partial^\mu\partial_\sigma W^{\sigma\nu} \,-\, \partial^\nu\partial_\sigma W^{\sigma\mu} \,+\, M^2\,W^{\mu\nu} \,=\, 0\,, \tag{C.7}$$

Notice that with the definition $W_\mu = \frac{1}{M}\,\partial^\nu W_{\nu\mu}$ (C.7) recovers the Proca equation of motion (C.2).

Now from (C.6) we can derive the propagator for the antisymmetric field [69]:

$$\int \mathrm{d}^4x\, e^{ik\,x}\,\langle\,0\,|\,\mathrm{T}\,\{W_{\mu\nu}(x),\,W_{\rho\sigma}(0)\}\,|\,0\,\rangle \;=\; \frac{2\,i}{M^2-q^2}\,\Omega^L_{\mu\nu,\rho\sigma} + \frac{2\,i}{M^2}\,\Omega^T_{\mu\nu,\rho\sigma}$$
$$= \frac{2\,i}{M^2-q^2}\left\{\mathcal{I}_{\mu\nu,\rho\sigma} - \frac{q^2}{M^2}\,\Omega^T_{\mu\nu,\rho\sigma}\right\}, \quad \text{(C.8)}$$

where the antisymmetric tensors (they are symmetric double 2–forms, and in general they have the structure $\mathcal{A}_{\mu\nu,\alpha\beta}$ being antisymmetric under $\mu \leftrightarrow \nu$ and $\alpha \leftrightarrow \beta$ but symmetric under $\mu\,\nu \leftrightarrow \alpha\,\beta$; they can be considered as symmetric operators acting on the space of antisymmetric 2–tensors)

$$\begin{aligned}
\Omega^L_{\mu\nu,\rho\sigma}(q) &= \frac{1}{2\,q^2}\,(g_{\mu\rho}q_\nu q_\sigma \,-\, g_{\rho\nu}q_\mu q_\sigma \,-\, (\rho \leftrightarrow \sigma))\;, \\
\Omega^T_{\mu\nu,\rho\sigma}(q) &= -\,\frac{1}{2\,q^2}\,\big(g_{\mu\rho}q_\nu q_\sigma \,-\, g_{\rho\nu}q_\mu q_\sigma \,-\, q^2 g_{\mu\rho}g_{\nu\sigma} \,-\, (\rho \leftrightarrow \sigma)\big)\;, \qquad \text{(C.9)}
\end{aligned}$$

denote *longitudinal* and *transverse* modes of propagation. The identity in the space of antisymmetric tensors is

$$\mathcal{I}_{\mu\nu,\rho\sigma} \;=\; \frac{1}{2}\,(g_{\mu\rho}g_{\nu\sigma} \,-\, g_{\mu\sigma}g_{\nu\rho})\;, \qquad \text{(C.10)}$$

and with that $\Omega^L_{\mu\nu,\rho\sigma}(q)$ and $\Omega^T_{\mu\nu,\rho\sigma}(q)$ are projection operators that satisfy the following properties:

$$\begin{aligned}
\Omega^T \,+\, \Omega^L \,=\, \mathcal{I}\,,\;\; \Omega^T\cdot\Omega^L \,=\, \Omega^L\cdot\Omega^T \,=\, 0\,, \\
\Omega^T\cdot\Omega^T \,=\, \Omega^T\,,\;\; \Omega^L\cdot\Omega^L \,=\, \Omega^L\,, \\
q^\mu\,\Omega^T_{\mu\nu,\rho\sigma}(q) \,=\, q^\nu\,\Omega^T_{\mu\nu,\rho\sigma}(q) \,=\, q^\rho\,\Omega^T_{\mu\nu,\rho\sigma}(q) \,=\, q^\sigma\,\Omega^T_{\mu\nu,\rho\sigma}(q) \,=\, 0\,, \\
\epsilon^{\mu\nu\alpha\beta}\,\epsilon^{\rho\sigma\xi\kappa}\,\Omega^T_{\mu\nu,\rho\sigma} \,=\, -\,4\,\Omega^{\alpha\beta,\xi\kappa}_L\,,\quad \epsilon^{\mu\nu\alpha\beta}\,\epsilon^{\rho\sigma\xi\kappa}\,\Omega^L_{\mu\nu,\rho\sigma} \,=\, -\,4\,\Omega^{\alpha\beta,\xi\kappa}_T\,, \\
\varepsilon^{\mu\nu\lambda\rho}\,\varepsilon_{\alpha\beta\lambda\rho} \,=\, -\,4\,\mathcal{I}^{\mu\nu\alpha\beta}\,. \qquad \text{(C.11)}
\end{aligned}$$

The propagator (C.8) corresponds to the normalization

$$\langle\,0\,|\,W_{\mu\nu}|\,W,p\,\rangle \;=\; \varepsilon_{\mu\nu} \;=\; \frac{i}{M}[\,p_\mu\varepsilon_\nu(p) \,-\, p_\nu\varepsilon_\mu(p)]\,. \qquad \text{(C.12)}$$

Thus, the summation over the physical vector polarizations $\varepsilon^\mu_{\lambda=1,2,3}$ for a massive vector ($\varepsilon\cdot p = 0$) yields:

$$\sum_\lambda \varepsilon^{\mu\nu}_\lambda\,\varepsilon^{\alpha\beta\,*}_\lambda \;=\; -\,\frac{2\,p^2}{M^2}\,\Omega^{\mu\nu,\alpha\beta}_L \qquad \text{(C.13)}$$

where we have used

$$\sum_\lambda \varepsilon^\mu_\lambda\varepsilon^{\nu\,*}_\lambda \;=\; -\,g^{\mu\nu} \,+\, \frac{p^\mu p^\nu}{M^2}\,. \qquad \text{(C.14)}$$

Appendix D :

Wilson coefficient $\mathbf{C}_{\langle\bar{\mathbf{q}}\mathbf{q}\rangle}$ at $\mathcal{O}(\alpha_s)$

In this appendix we give the expression to the α_s corrections for the quark condensate Wilson coefficients. We will split our results as shown in Eq. (4.87), in terms of coefficients multiplying logarithms, dilogarithms and polynomic terms. The results can be found in Table D.

$\langle SSS\rangle$	
L_p	$\frac{4}{p^2q^2r^2}\left[\,4\,p^4+q^4+r^4-6\,q^2\,r^2-3\,p^2\,(q^2+r^2)\right]$
L_q	$\frac{4}{p^2q^2r^2}\left[\,4\,q^4+p^4+r^4-6\,p^2\,r^2-3\,q^2\,(p^2+r^2)\right]$
L_r	$\frac{4}{p^2q^2r^2}\left[\,4\,r^4+q^4+p^4-6\,q^2\,p^2-3\,r^2\,(q^2+p^2)\right]$
L_d	$\frac{8}{p^2q^2r^2}\left[\,p^6+q^6+r^6-2\,p^4\,(q^2+r^2)-2\,q^4\,(p^2+r^2)-2\,r^4\,(p^2+q^2)\right]$
L_c	$\frac{8}{p^2q^2r^2}\left(-5\,p^4-5\,q^4-5\,r^4+14\,p^2\,r^2+14\,q^2\,p^2+14\,q^2\,r^2\right)$
$\langle SPP\rangle$	
L_p	$\frac{4}{p^2q^2r^2}\left[\,r^4+q^4-4\,p^4-3\,p^2\,(r^2+q^2)-6\,r^2\,q^2\,\right]$
L_q	$\frac{4}{p^2q^2r^2}\left[\,4\,q^4+r^4-p^4+3\,q^2\,(p^2-r^2)\right]$
L_r	$\frac{4}{p^2q^2r^2}\left[\,4\,r^4+q^4-p^4+3\,r^2\,(p^2-q^2)\right]$
L_d	$\frac{8}{p^2q^2r^2}\left[\,r^6+q^6-p^6-2\,p^2\,(r^4+q^4)+2\,(p^4-q^2\,r^2)\,(r^2+q^2)\right]$
L_c	$\frac{8}{p^2q^2r^2}\left(-5\,r^4-5\,q^4+5\,p^4+14\,r^2\,q^2\right)$
$\langle VVP\rangle$	
L_p	$\frac{2}{\lambda\,p^2q^2r^2}\left[\,p^6+r^2\,p^4+p^2\,q^2\,(5\,r^2+q^2)-2\,(r^2+q^2)\,(r^2-q^2)^2\right]$

Table D: α_s corrections to the Wilson coefficients for three–point GFs.

L_q	$\frac{2}{\lambda p^2q^2r^2}\left[q^6+r^2\,q^4+p^2\,q^2\,(5\,r^2+p^2)-2\,(r^2+p^2)\,(r^2-p^2)^2\right]$
L_r	$\frac{2}{\lambda p^2q^2r^2}\left[(p^2+q^2)\,(p^2-q^2)^2+4\,r^6-\,r^2\,(3\,p^2+q^2)\,(3\,q^2+p^2)-2\,r^4\,(q^2+p^2)\right]$
L_d	$\frac{4}{\lambda p^2q^2r^2}\,[\,2\,(p^4-3\,p^2q^2+q^4)\,r^4-2\,r^2\,(p^2+q^2)\,(p^4+q^4)$
	$-\,2\,r^6\,(p^2+q^2)+r^8+(p^2-q^2)^2\,(p^4+q^4-q^2\,p^2)\Big]$
L_c	$\frac{-2}{p^2q^2r^2}\,(p^2+q^2+4\,r^2)$
	$\langle AAP\rangle$
L_p	$\frac{2}{\lambda p^2q^2r^2}\left[p^6-3\,r^2\,p^4+p^2\,q^2\,(5\,r^2+q^2)+2\,(r^2-q^2)^3\right]$
L_q	$\frac{2}{\lambda p^2q^2r^2}\left[q^6-3\,r^2\,q^4+p^2\,q^2\,(5\,r^2+p^2)+2\,(r^2-p^2)^3\right]$
L_r	$\frac{2}{\lambda p^2q^2r^2}\left[-4\,r^6+6\,r^4\,(p^2+q^2)-r^2\,(q^2+3\,p^2)\,(p^2+3\,q^2)+(p^2-q^2)^2\,(p^2+q^2)\right]$
L_d	$\frac{4}{\lambda p^2q^2r^2}\,[\,2\,r^6\,(p^2+q^2)+6\,p^2\,q^2\,r^4-2\,r^2\,(p^2+q^2)\,(p^4+q^4)$
	$-\,r^8+(p^2-q^2)^2\,(p^4+q^4-q^2\,p^2)\Big]$
L_c	$\frac{-2}{p^2q^2r^2}\,(p^2+q^2-4\,r^2)$
	$\langle VA\,S\rangle$
L_p	$\frac{2}{\lambda p^2q^2r^2}\left[p^6+3\,p^4\,(2\,q^2-r^2)-p^2q^2\,(5\,r^2+q^2)+2\,(r^2+q^2)\,(r^2-q^2)^2\right]$
L_q	$\frac{2}{\lambda p^2q^2r^2}\,[-2\,p^6+(q^2+6\,r^2)\,p^4-(6\,q^4+6\,r^4-5\,q^2\,r^2)\,p^2-q^6+2\,r^6-q^4\,r^2\,]$
L_r	$\frac{2}{\lambda p^2q^2r^2}\,[\,p^6+7q^2\,p^2(q^2-p^2)-q^6-4\,r^6+2\,(3\,p^2+q^2)\,r^4-3\,(p^4-q^4)\,r^2\,]$
L_d	$\frac{4}{\lambda p^2q^2r^2}\Big[(3\,q^6+2\,r^2\,q^4+6\,r^4\,q^2+2\,r^6)\,p^2-(r^2-q^2)^2\,(r^4+q^4)$
	$+\;p^8-p^6\,(3\,q^2+2\,r^2)-2\,r^2\,q^2\,p^4\,]$
L_c	$\frac{-2}{p^2q^2r^2}\,(p^2-q^2-4\,r^2)$
	$g_{\mu\nu}\,\langle V^\mu V^\nu S\rangle$
L_p	$\frac{2}{p^2q^2r^2}\,[\,2\,(q^4-r^4)-p^4+p^2\,(r^2-3\,q^2)]$
L_q	$\frac{2}{p^2q^2r^2}\,[\,2\,(p^4-r^4)-q^4+q^2\,(r^2-3\,p^2)]$
L_r	$\frac{2}{p^2q^2r^2}\,[\,6\,p^2\,q^2+4\,r^4-p^4-q^4-r^2\,(p^2+q^2)]$
L_d	$\frac{4}{p^2q^2r^2}\,[\,2\,r^6-(r^4+p^4+q^4-3\,p^2\,q^2)\,(p^2+q^2)]$

Table D: α_s corrections to the Wilson coefficients for three–point GFs.

L_c	$\frac{4}{p^2q^2r^2}\,[\,3\,r^2(p^2+q^2-r^2)-4\,p^2\,q^2]$
$q_\mu\,p_\nu\,\langle V^\mu V^\nu S\rangle$	
L_p	$\frac{1}{q^2r^2}\,[\,q^2\,(2\,q^2-2\,p^2+r^2)-3\,r^2\,(p^2-r^2)]$
L_q	$\frac{1}{p^2r^2}\,[\,p^2\,(2\,p^2-2\,q^2+r^2)-3\,r^2\,(q^2-r^2)]$
L_r	$\frac{1}{p^2q^2}\,[3\,(p^4+q^4)-3\,r^2\,(p^2+q^2)-2\,p^2\,q^2]$
L_d	$\frac{2}{p^2q^2}\,[\,p^6-p^4\,r^2+(q^2-r^2)^2(q^2+r^2)-p^2\,r^2(4\,q^2+r^2)]$
L_c	$\frac{1}{q^2r^2p^2}\,(p^2+q^2-2\,r^2)\,\lambda$
$g_{\mu\nu}\,\langle A^\mu A^\nu S\rangle$	
L_p	$\frac{2}{p^2q^2r^2}\,\Big[\,2\,(q^2-r^2)^2-p^4+p^2\,(5\,r^2-3\,q^2)\Big]$
L_q	$\frac{2}{p^2q^2r^2}\,\Big[\,2\,(p^2-r^2)^2-q^4+q^2\,(5\,r^2-3\,p^2)\Big]$
L_r	$\frac{2}{p^2q^2r^2}\,[\,6\,p^2\,q^2-4\,r^4-p^4-q^4-r^2\,(p^2+q^2)]$
L_d	$-\frac{4}{p^2q^2r^2}\,[\,2\,r^6+(-3\,r^4+p^4+q^4-3\,p^2\,q^2)\,(p^2+q^2)]$
L_c	$\frac{4}{p^2q^2r^2}\,[\,3\,r^4-4\,p^2\,q^2-3\,r^2\,(q^2+p^2)]$
$q_\mu\,p_\nu\,\langle A^\mu A^\nu S\rangle$	
L_p	$\frac{1}{q^2r^2}\,[\,r^2\,(q^2-3\,p^2+3\,r^2)+2\,q^2\,(q^2-p^2)]$
L_q	$\frac{1}{p^2r^2}\,[\,r^2\,(p^2-3\,q^2+3\,r^2)-2\,p^2\,(q^2-p^2)]$
L_r	$\frac{1}{p^2q^2}\,[-2\,p^2\,q^2+3\,(p^4+q^4)-3\,r^2(p^2+q^2)]$
L_d	$\frac{2}{p^2q^2}\,[\,p^6-3\,p^4\,r^2+3\,p^2\,r^4+(q^2-r^2)^3]$
L_c	$\frac{1}{p^2q^2r^2}\,(p^2+q^2+2\,r^2)\,\lambda$
$g_{\mu\nu}\,\langle V^\mu A^\nu P\rangle$	
L_p	$\frac{2}{p^2q^2r^2}\,[\,2\,(q^4-r^4)+p^4-p^2\,(5\,r^2+q^2)]$
L_q	$\frac{2}{p^2q^2r^2}\,[\,p^2\,(q^2+4\,r^2)-2\,p^4-q^4-2\,r^4+q^2\,r^2]$
L_r	$\frac{2}{p^2q^2r^2}\,[\,p^4-q^4+4\,r^4+r^2\,(p^2-q^2)]$
L_d	$\frac{4}{p^2q^2r^2}\,[\,p^6-2\,q^2\,p^4+2\,p^2\,q^4-q^6+2\,r^6-r^4\,(3\,p^2+q^2)]$

Table D: α_s corrections to the Wilson coefficients for three–point GFs.

L_c	$\frac{12}{p^2 q^2}\,(q^2+p^2-r^2)$
$q_\mu\, p_\nu\, \langle V^\mu A^\nu P\rangle$	
L_p	$\frac{3}{q^2}\,(p^2+3\,q^2-r^2)$
L_q	$-\frac{3}{p^2}\,(3\,p^2+q^2-r^2)$
L_r	$\frac{3}{p^2 q^2}\,(q^2-p^2)\,(q^2+p^2-r^2)$
L_d	$-\frac{2}{p^2 q^2}\left[p^6-3\,r^2\,p^4+p^2\,r^2\,(2\,q^2+3\,r^2)-(q^2-r^2)^2\,(q^2+r^2)\right]$
L_c	$-\frac{1}{p^2 q^2 r^2}\,(p^2-q^2+2\,r^2)\,\lambda$

Table D: α_s corrections to the Wilson coefficients for three–point GFs.

Appendix E:

$\langle$VVP$\rangle$ from a Lagrangian

We used the meromorphic *ansatz* in Eq. (4.120) in order to determine the $\langle VVP\rangle$ Green function. To reach the same result one could also proceed starting with a Lagrangian like the one given by Resonance Chiral Theory RχT and collected in Eqs. (1.79), (2.37) and (2.38) to explicitly calculate the coefficients c_{klm} using the Lagrangian formalism. The result can be expressed as [40]:

$$
\begin{aligned}
\Pi_{VVP}^{R\chi T} \;=\; & -B_0 \left\{ 64\,\widetilde{C}_7^W - 16\,\widetilde{C}_{22}^W\,\frac{p^2+q^2}{r^2} + C\,\frac{1}{\left(M_{V_1}^2-p^2\right)\left(M_{V_1}^2-q^2\right)} - \frac{N_C}{4\,\pi^2 r^2} \right. \\
& + D\,\left(\frac{1}{M_{V_1}^2-p^2}+\frac{1}{M_{V_1}^2-q^2}\right) + \frac{1}{r^2}\left(\frac{E\,r^2+K\,p^2+G\,q^2}{M_{V_1}^2-p^2}\right. \\
& \left. + \frac{E\,r^2+K\,q^2+G\,p^2}{M_{V_1}^2-q^2}\right) + \frac{A' r^2 + B'\,(p^2+q^2)}{\left(M_{V_2}^2-p^2\right)\left(M_{V_2}^2-q^2\right) r^2} \\
& + C'\,\frac{1}{\left(M_{V_2}^2-p^2\right)\left(M_{V_2}^2-q^2\right)} + D'\,\left(\frac{1}{M_{V_2}^2-p^2}+\frac{1}{M_{V_2}^2-q^2}\right) \\
& + \frac{1}{r^2}\left(\frac{E' r^2+K' p^2+G' q^2}{M_{V_2}^2-p^2} + \frac{E' r^2+K' q^2+G' p^2}{M_{V_2}^2-q^2}\right) \\
& + \frac{1}{r^2}\left[\frac{A'' r^2+B'' p^2+H\,q^2}{\left(M_{V_1}^2-p^2\right)\left(M_{V_2}^2-q^2\right)} + \frac{A'' r^2+B'' q^2+H\,p^2}{\left(M_{V_2}^2-p^2\right)\left(M_{V_1}^2-q^2\right)}\right] \\
& \left. + \;C''\left[\frac{1}{\left(M_{V_1}^2-p^2\right)\left(M_{V_2}^2-q^2\right)} + \frac{1}{\left(M_{V_1}^2-q^2\right)\left(M_{V_2}^2-p^2\right)}\right]\right\}\,, \qquad \text{(E.1)}
\end{aligned}
$$

where

$$
\begin{aligned}
& A' = 8\,F_V^2\,(d_1-d_3)\,, \quad A'' = 8\,F_V'^2\,(d_1'-d_3')\,, \quad B = 8\,F_V^2\,d_3\,, \\
& B' = 8\,F_V'^2\,d_3'\,, \quad C = 64\,F_V^2\,d_2\,, \quad C' = 64\,F_V'^2\,d_2'\,, \quad D = -\,\frac{32\sqrt{2}\,F_V\,c_3}{M_{V_1}}\,, \\
& D' = -\,\frac{32\sqrt{2}\,F_V'\,c_3'}{M_{V_2}}\,, \quad E' = -\,\frac{4\sqrt{2}\,F_V'}{M_{V_2}}\,(c_1'+c_2'-c_5')\,,
\end{aligned}
$$

$$
\begin{aligned}
E &= -\frac{4\sqrt{2}\,F_V}{M_{V_1}}\,(c_1+c_2-c_5)\;, \quad K' = -\frac{4\sqrt{2}\,F_V'}{M_{V_2}}\,(-c_1'+c_2'+c_5'-2c_6')\;,\\
G &= -\frac{4\sqrt{2}\,F_V}{M_{V_1}}\,(c_1-c_2+c_5)\;, \quad G'' = 32\,F_V\,F_V'\,d_f\;,\\
H &= 4F_V\,F_V'\,(d_a+d_c-d_b)\;, \quad A'' = 4\,F_V\,F_V'\,(d_a+d_b-d_c)\;,\\
B'' &= 4\,F_V\,F_V'\,(d_b+d_c-d_a-2d_d)\;, \quad G' = -\frac{4\sqrt{2}\,F_V'}{M_{V_2}}\,(c_1'-c_2'+c_5')\;,\\
K &= -\frac{4\sqrt{2}\,F_V}{M_{V_1}}\,(-c_1+c_2+c_5-2c_6)\;,
\end{aligned}
\tag{E.2}
$$

The parametrization of Eq. (E.1) reflects its origin in the Feynman diagrams of Fig. E.1.

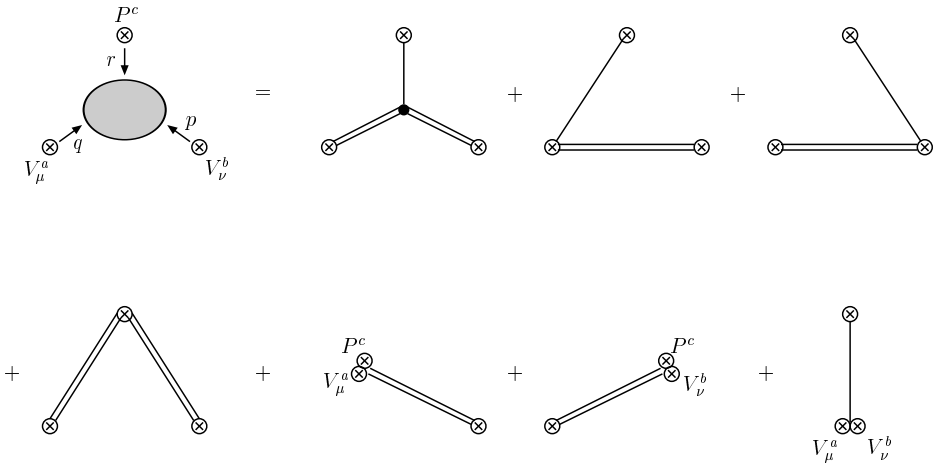

Figure E.1: Resonance contributions to the $\langle VVP\rangle$ Green function.

In terms of the parameters of our *ansatz* in Eq. (4.120) we obtain :

$$
\begin{aligned}
&c_{031} = -\,G-G'\;, \quad c_{022} = -\,2(K+K') - \frac{N_C}{4\,\pi^2}\;, \quad c_{121} = -\,D-D'-E-E'\\
&c_{120} = (D+E)M_{V_2}^2 + (D'+E')M_{V_1}^2\;, \quad c_{030} = GM_{V_2}^2 + G'M_{V_1}^2\;,\\
&c_{111} = A+A'+2\,A''+C+C'+2\,C''\\
&+2\left(M_{V_1}^2+M_{V_2}^2\right)(D+D'+E+E')\,,\\
&c_{021} = B+B'+B''+H+K\left(M_{V_1}^2+2M_{V_2}^2\right)+K'\left(2\,M_{V_1}^2+M_{V_2}^2\right)\\
&+\left(M_{V_1}^2+M_{V_2}^2\right)\left(G+G'+\frac{N_C}{4\,\pi^2}\right),\\
&c_{000} = -M_{V_2}^4M_{V_1}^4\,\frac{N_C}{4\,\pi^2}\;, \quad c_{030} = GM_{V_2}^2+G'M_{V_1}^2\;,\\
&c_{110} = -(D+E)M_{V_2}^4-(D'+E')M_{V_1}^4-(A+A''+C+C'')M_{V_2}^2\\
&-(A'+A''+C'+C'')M_{V_1}^2-2(D+D'+E+E')M_{V_1}^2M_{V_2}^2\;,
\end{aligned}
$$

$$
\begin{aligned}
&c_{011} = -2K\,M_{V_2}^4 - 2K'M_{V_1}^4 - \left(M_{V_1}^2 + M_{V_2}^2\right)^2 \frac{N_C}{4\,\pi^2} - 2(B+B'')M_{V_2}^2 \\
&- 2(K+K'+G+G')M_{V_1}^2 M_{V_2}^2\,, \\
&c_{020} = -G'M_{V_1}^4 - GM_{V_2}^4 - \left(K+K'+G+G'+\frac{N_C}{4\,\pi^2}\right) M_{V_1}^2 M_{V_2}^2 \\
&-(B'+B'')M_{V_1}^2 - (B+H)M_{V_2}^2\,, \\
&c_{010} = BM_{V_2}^4 + B'M_{V_1}^4 + (K'+G')M_{V_2}^2 M_{V_1}^4 + (K+G)M_{V_1}^2 M_{V_2}^4 \\
&(B''+H)M_{V_1}^2 M_{V_2}^2 + \left(M_{V_1}^2 + M_{V_2}^2\right) M_{V_1}^2 M_{V_2}^2 \frac{N_C}{4\,\pi^2}\,, \\
&c_{100} = (A'+C')M_{V_1}^4 + (A+C)M_{V_2}^4 + 2(A''+C'')M_{V_1}^2 M_{V_2}^2 \\
&+ 2(E'+D')M_{V_1}^4 M_{V_2}^2 + 2(E+D)M_{V_2}^4 M_{V_1}^2\,,
\end{aligned}
\tag{E.3}
$$

in units of $-B_0$. Chiral symmetry, implemented in our Lagrangian, brings features that with the *ansatz* had to be forced by hand. In this way we immediately find that $c_{300} = 0$ and $c_{210} = 0$. Moreover, as a bonus we also find $c_{200} = 0$. The rest of constraints are given in Eqs. (4.122,4.123). In addition we find five more relations:

$$
\begin{aligned}
\widetilde{C}_7^W \;&=\; \widetilde{C}_{22}^W \;=\; 0 \qquad G \,+\, G' \,=\, 0 \\
D \,+\, D' \,+\, E \,+\, E' \,&=\, 0 \qquad 2\,(K \,+\, K') \,=\, -\,\frac{N_C}{4\,\pi^2}\,.
\end{aligned}
\tag{E.4}
$$

After applying all the constraints coming from the OPE and Brodsky–Lepage asymptotic condition we obtain the following relations among the Lagrangian couplings:

$$
\begin{aligned}
&4\,c_3 + c_1 \;=\; 0\,, \quad 4\,c_3' + c_1' \;=\; 0\,, \quad c_1 - c_2 + c_5 \;=\; 0\,, \\
&c_5 - c_6 + \frac{F_V' M_{V_1}}{F_V M_{V_2}}\,(c_5' - c_6') = \frac{M_{V_1}}{F_V}\,\frac{N_C}{64\,\sqrt{2}\pi^2}\,, \\
&8\,F_V^2 d_3 + 8\,F_V'^2 d_3' + 8\,F_V F_V'(d_c - d_d) \\
&+ 8\,\sqrt{2}\,F_V' \frac{M_{V_2}^2 - M_{V_1}^2}{M_{V_2}}(c_5' - c_6') + M_{V_1}^2 \frac{N_C}{8\,\pi^2} \;=\; F^2\,, \\
&4\,F_V^2(d_1 + 8\,d_2) + 4\,F_V'^2(d_1' + 8\,d_2') + 4\,F_V F_V'(d_a + d_b - d_d + 8\,d_f) + \\
&4\,\sqrt{2}\,F_V' \frac{M_{V_2}^2 - M_{V_1}^2}{M_{V_2}}(c_5' - c_6') + M_{V_1}^2 \frac{N_C}{16\,\pi^2} \;=\; F^2\,, \\
&8\,M_{V_2}^2 F_V^2 d_3 + 8\,F_V'^2 M_{V_1}^2 d_3' + 4\,F_V F_V' \left[M_{V_1}^2(d_b + d_c - d_a - 2\,d_d)\right. \\
&\left. + M_{V_2}^2(d_a + d_c - d_b)\right] \;=\; -\,M_{V_1}^2 M_{V_2}^2 \frac{N_C}{8\,\pi^2}\,.
\end{aligned}
\tag{E.5}
$$

Appendix F :

LSZ formula for a soft pion

In this appendix we discuss the derivation of Eq. (5.25). Let us start defining three quark currents :

$$\begin{aligned} A_\pi^\mu(x) &= \bar{d}(x)\,\gamma^\mu\,\gamma_5\,u(x)\,, \\ T_5^{\mu\nu}(x) &= \bar{u}(x)\,\sigma^{\mu\nu}\,\gamma_5\,d(x)\,, \\ T_\pi^{\mu\nu} &= \bar{u}(x)\,\sigma^{\mu\nu}\,u(x) \,+\, \bar{d}(x)\,\sigma^{\mu\nu}\,d(x)\,. \end{aligned} \tag{F.1}$$

Then we can construct the following Green function that after partial integration can be expressed as :

$$\begin{aligned} \langle\gamma(p)\,|\,\partial_\alpha A^\alpha\,T_5^{\mu\nu}\,|\,0\,\rangle &\equiv i\int \mathrm{d}^4x\,e^{i\,r\cdot x}\,\langle\gamma(p)\,|\,T\,\{\partial_\alpha A_\pi^\alpha(x), T_5^{\mu\nu}(0)\}\,|\,0\,\rangle \\ &= r_\alpha\int \mathrm{d}^4x\,e^{i\,r\cdot x}\,\langle\gamma(p)\,|\,T\,\{A_\pi^\alpha(x), T_5^{\mu\nu}(0)\}\,|\,0\,\rangle \\ &- i\,\langle\gamma(p)\,|\,T_\pi^{\mu\nu}(0)|\,0\,\rangle \end{aligned} \tag{F.2}$$

We can relate this Green function to the $\langle\gamma(p)\,|\,\bar{u}\,\sigma_{\mu\nu}\,\gamma_5\,d\,|\,\pi^-(r)\rangle$ matrix element (5.22) through the LSZ formula :

$$\left\langle\gamma(p)\,|\,\bar{u}\,\sigma^{\mu\nu}\,\gamma_5\,d\,|\,\pi^-(r)\right\rangle \,=\, \lim_{r^2\to M_\pi^2}\frac{r^2-M_\pi^2}{\sqrt{2}\,F\,M_\pi^2}\,\langle\gamma(p)\,|\,\partial_\alpha A^\alpha\,T_5^{\mu\nu}|\,0\,\rangle\,. \tag{F.3}$$

Then the $\langle\gamma(p)\,|\partial_\alpha A^\alpha\,T_5^{\mu\nu}|\,0\,\rangle$ Green function must have a pole at $r^2 = M_\pi^2$. Since the second piece in (F.2) has no r–dependence it cannot have a pole, and this must come from the first term :

$$r_\alpha\int \mathrm{d}^4x\,e^{irx}\,\langle\gamma(p)\,|\,T\,\{A_\pi^\alpha(x), T_5^{\mu\nu}(0)\}\,|\,0\,\rangle \,\equiv\, \frac{1}{r^2-M_\pi^2}\,\mathcal{F}^{\mu\nu}(p,r)\,. \tag{F.4}$$

As the divergence of the axial current is zero in the chiral limit, the left–hand side must vanish for $M_\pi = 0$, what implies :

$$\mathcal{F}^{\mu\nu}(p,r)|_{M_\pi=0} \,=\, i\,r^2\,\langle\gamma(p)\,|T_\pi^{\mu\nu}(0)|\,0\,\rangle_{M_\pi=0}\,. \tag{F.5}$$

Finally, assuming that pion mass corrections are small, (F.3) yields the desired result :

$$\left\langle \gamma(p) \,|\, \bar{u}\, \sigma^{\mu\nu}\, \gamma_5\, d \,|\, \pi^-(r) \right\rangle \;=\; i\, \frac{1}{\sqrt{2}\, F}\, \left\langle \gamma(p) \,|\, T_\pi^{\mu\nu}(0) | \, 0 \, \right\rangle \;, \tag{F.6}$$

that is also the result that stems from the soft pion theorem.

Appendix G :

Loop functions

In this appendix we present expressions for one–, two– and three–point one–loop functions appearing in this thesis. The basic expressions are the scalar one loop amplitudes are defined as :

$$\begin{aligned} A_0(m^2) &\equiv \int \frac{\mathrm{d}^D\ell}{(2\,\pi)^D}\frac{1}{\ell^2-m^2}\,, \\ B_0(q^2,m_a^2,m_b^2) &\equiv \int \frac{\mathrm{d}^D\ell}{(2\,\pi)^D}\frac{1}{(\ell^2-m_a^2)\,[(\ell-q)^2-m_b^2]}\,, \\ C_0(p_1^2,p_2^2,p_3^2,m_a^2,m_b^2,m_c^2) &\equiv \int \frac{\mathrm{d}^D\ell}{(2\,\pi)^D}\frac{1}{(\ell^2-m_a^2)\,[(\ell-p_1)^2-m_b^2]\,[(\ell-p_2)^2-m_c^2]}\,, \end{aligned} \tag{G.1}$$

where $D = 4 - 2\,\epsilon$ is the space–time dimension and $p_3^2 = (p_1+p_2)^2$. The one–point amplitude has a simple expression :

$$A_0(m^2) \;=\; i\,\frac{m^2}{(4\,\pi)^2}\left[\frac{1}{\hat\epsilon}+1-\log\left(\frac{m^2}{\mu^2}\right)\right]\,, \tag{G.2}$$

where $1/\hat\epsilon = \mu^{-2\,\epsilon}/\epsilon - \gamma_E + \log(4\,\pi)$. The two point function is a bit more complicated. We display first the particular case of equal masses :

$$\begin{aligned} B_0(q^2,m^2,m^2) &= \frac{i}{(4\,\pi)^2}\left\{\frac{1}{\hat\epsilon}+2-\log\left(\frac{m^2}{\mu^2}\right)+\beta(q^2)\log\left[\frac{\beta(q^2)-1}{\beta(q^2)+1}\right]\right\}\,, \\ \beta(s) &= \sqrt{1-\frac{4\,m^2}{q^2}}\,, \end{aligned} \tag{G.3}$$

The function $-i\,B_0(q^2,m^2,m^2)$ is real for $q^2 < 4\,m^2$ and manifestly real for $s < 0$. For $0 < s < 4\,m^2$ it is convenient to express it in a way which is manifestly real :

$$B_0(q^2,m^2,m^2) \;=\; \frac{i}{(4\,\pi)^2}\left\{\frac{1}{\hat\epsilon}+2-\log\left(\frac{m^2}{\mu^2}\right)+2\,\bar\beta(q^2)\cot^{-1}\bar\beta(q^2)\right\}\,, \tag{G.4}$$

$$\bar{\beta}(s) \;=\; \sqrt{\frac{4\,m^2}{s}-1}\,.$$

If $s > 4\,m^2$ then $-\,i\,B_0(q^2,m^2,m^2)$ becomes complex,

$$B_0(q^2,m^2,m^2) \;=\; \frac{i}{(4\,\pi)^2}\left\{\frac{1}{\hat{\epsilon}}+2-\log\left(\frac{m^2}{\mu^2}\right)+\beta(q^2)\log\left[\frac{1-\beta(q^2)}{\beta(q^2)+1}\right]+i\,\pi\,\beta(q^2)\right\}. \tag{G.5}$$

For the general case of different masses we have :

$$\begin{aligned}
B_0(q^2,m_a^2,m_b^2) &= \frac{i}{(4\,\pi)^2}\left\{\frac{1}{\hat{\epsilon}}+1+\frac{1}{\Delta}\left[m_a^2\log\left(\frac{m_a^2}{\mu^2}\right)-m_b^2\log\left(\frac{m_b^2}{\mu^2}\right)\right]\right.\\
&\quad\left.+\left(\frac{\Delta}{q^2}-\frac{\Sigma}{\Delta}\right)\log\left(\frac{m_b^2}{m_a^2}\right)\right\}+\bar{B}_0(q^2,m_a^2,m_b^2)\,, \qquad\qquad (G.6)\\
\bar{B}_0(q^2,m_a^2,m_b^2) &= -\,\frac{1}{32\,\pi^2}\left\{\frac{\nu}{q^2}\log\left[\frac{(q^2+\nu)^2-\Delta^2}{(q^2-\nu)^2-\Delta^2}\right]\right\},\\
\nu &= \sqrt{[q^2-(m_a+m_b)^2]\,[q^2-(m_a-m_b)^2]}\,,\\
\Delta &= m_a^2-m_b^2\,,\quad \Sigma = m_a^2+m_b^2\,.
\end{aligned}$$

We know that this function should yield an imaginary part above threshold $q^2 > (m_a+m_b)^2$, but written as above this is not apparent. This expression it is not even satisfactory for the region $(m_a-m_b)^2 > q^2 > (m_a+m_b)^2$ where it develops a discontinuity. It has no problem, however, for $q^2 < (m_a-m_b)^2$. So it is better to split the definition of this function depending on the region we want to evaluate it :

$$\bar{B}_0 \;=\; \begin{cases}
-\,\dfrac{1}{32\,\pi^2}\left\{\dfrac{\nu}{q^2}\log\left[\dfrac{(q^2+\nu)^2-\Delta^2}{(q^2-\nu)^2-\Delta^2}\right]\right\} & q^2<(m_a-m_b)^2,\\[2ex]
-\,\dfrac{1}{32\,\pi^2}\left\{2\,\dfrac{\bar{\nu}}{q^2}\arctan\left[\dfrac{q^2-\Delta}{\bar{\nu}}\right]-2\,\dfrac{\bar{\nu}}{q^2}\arctan\left[\dfrac{q^2+\Delta}{\bar{\nu}}\right]\right\}, & \\
\qquad\qquad (m_a-m_b)^2<q^2<(m_b+m_b)^2, & \\[2ex]
-\dfrac{1}{32\,\pi^2}\left\{\dfrac{\nu}{q^2}\log\left[\dfrac{q^2+\nu-\Delta}{-\,q^2+\nu-\Delta}\right]-\dfrac{\nu}{q^2}\log\left[\dfrac{q^2+\nu+\Delta}{-\,q^2+\nu+\Delta}\right]\right\}, & \\
\qquad\qquad q^2>(m_b+m_b)^2, &
\end{cases} \tag{G.7}$$

with $\bar{\nu} = \sqrt{-\,[q^2-(m_a+m_b)^2]\,[q^2-(m_a-m_b)^2]}$. In addition to the scalar amplitudes it is also interesting to consider vector amplitudes for one– and two–point loops :

$$\int\frac{\mathrm{d}^D\ell}{(2\,\pi)^D}\frac{\ell^\mu}{\ell^2-m^2} \;=\; 0\,,$$

$$\int \frac{\mathrm{d}^D\ell}{(2\,\pi)^D}\frac{\ell^\mu}{(\ell^2-m_a^2)\,[(\ell-q)^2-m_b^2]} = \frac{q^\mu}{2\,q^2}\left[A_0(m_b^2)-A_0(m_a^2) + \left(m_a^2-m_b^2+p^2\right)B_0(q^2,m_a^2,m_b^2)\right] ,$$

$$\int \frac{\mathrm{d}^D\ell}{(2\,\pi)^D}\frac{\ell^\mu}{(\ell^2-m^2)\,[(\ell-q)^2-m^2]} = \frac{q^\mu}{2}\,B_0(q^2,m^2,m^2)\,. \tag{G.8}$$

In particular we are also interested in the massless one–loop integrals :

$$\begin{aligned}
A_0(0) &= 0\,,\\
B_0(q^2,0,0) &= \frac{i}{(4\,\pi)^2}\left[\frac{1}{\hat\epsilon}+2-\log\left(-\frac{q^2}{\mu^2}\right)\right] ,\\
C(p_1^2,p_2^2,p_3^2,0,0,0) &= \frac{i}{(4\,\pi)^2\,\lambda}\left\{\mathrm{Li}_2\left(-\frac{\lambda+p_2^2+p_1^2-p_3^2}{\lambda-p_2^2-p_1^2+p_3^2}\right)\right.\\
&\quad -\mathrm{Li}_2\left(-\frac{\lambda-p_2^2-p_1^2+p_3^2}{\lambda+p_2^2+p_1^2-p_3^2}\right)+\mathrm{Li}_2\left(-\frac{\lambda+p_2^2+p_3^2-p_1^2}{\lambda-p_2^2-p_3^2+p_1^2}\right)\\
&\quad -\mathrm{Li}_2\left(-\frac{\lambda-p_2^2-p_3^2+p_1^2}{\lambda+p_2^2+p_3^2-p_1^2}\right)+\mathrm{Li}_2\left(-\frac{\lambda+p_3^2+p_1^2-p_2^2}{\lambda-p_3^2-p_1^2+p_2^2}\right)\\
&\quad \left.-\mathrm{Li}_2\left(-\frac{\lambda-p_3^2-p_1^2+p_2^2}{\lambda+p_3^2+p_1^2-p_2^2}\right)\right\}\\
&\equiv \frac{i}{(4\,\pi)^2}\,C_0\left(p_1^2,p_2^2,p_3^2\right) ,
\end{aligned} \tag{G.9}$$

And also in loop amplitudes having some propagator squared or to the third power. Then we define

$$I\left(\alpha,\beta;q^2,0,0\right) \equiv \int \frac{\mathrm{d}^D\ell}{(2\,\pi)^D}\frac{1}{\ell^{2\alpha}(\ell-q)^{2\beta}} = I\left(\beta,\alpha;q^2,0,0\right) . \tag{G.10}$$

The explicit expression for some particular cases follow

$$\begin{aligned}
I\left(2,1,q^2,0,0\right) &= -\frac{i}{(4\,\pi)^2}\frac{1}{q^2}\left[\frac{1}{\hat\epsilon}-\log\left(-\frac{q^2}{\mu^2}\right)\right] ,\\
I\left(3,1,q^2,0,0\right) &= -\frac{i}{(4\,\pi)^2}\frac{1}{q^4}\,.
\end{aligned} \tag{G.11}$$

and also we provide the expression for the scalar three–point function with one propagator squared

$$\int \frac{\mathrm{d}^D\ell}{(2\,\pi)^D}\frac{1}{\ell^4(\ell-p_1)^2(\ell-p_2)^2} = \frac{-\,i}{(4\,\pi)^2}\frac{1}{p_1^2\,p_2^2}\left[\frac{1}{\hat\epsilon}-\log\left(-\frac{p_1^2}{\mu^2}\right) -\log\left(-\frac{p_2^2}{\mu^2}\right)+\log\left(-\frac{p_3^2}{\mu^2}\right)\right] , \tag{G.12}$$

where again $p_3 = -\,p_1 - p_2$. Finally, it is also useful to have explicit expressions for vector and tensor one–loop amplitudes for the one–, two– and three–point functions

in the massless case (with the possibility of having one propagator squared)

$$
\begin{aligned}
\int \frac{\mathrm{d}^D\ell}{(2\,\pi)^D}\frac{\ell^\mu}{\ell^2} &= 0\,,\\
\int \frac{\mathrm{d}^D\ell}{(2\,\pi)^D}\frac{\ell^\mu}{\ell^2(\ell-q)^2} &= \frac{q^\mu}{2}\,B_0(q^2,0,0) = \frac{i\,q^\mu}{2\,(4\,\pi)^2}\left[\frac{1}{\hat\epsilon}+2-\log\left(-\frac{q^2}{\mu^2}\right)\right]\,,\\
\int \frac{\mathrm{d}^Dl}{(2\,\pi)^D}\frac{\ell^\mu\ell^\nu}{\ell^2(\ell-q)^2} &= -\frac{1}{12}\frac{i\,q^2}{(4\,\pi)^2}\left[\frac{1}{\hat\epsilon}+\frac{8}{3}-\log\left(-\frac{q^2}{\mu^2}\right)\right]g^{\mu\nu}\\
&\quad+\frac{1}{3}\frac{i}{(4\,\pi)^2}\left[\frac{1}{\hat\epsilon}+\frac{13}{6}-\log\left(-\frac{q^2}{\mu^2}\right)\right]q^\mu q^\nu\,,\\
\int \frac{\mathrm{d}^Dl}{(2\,\pi)^D}\frac{\ell^\mu}{\ell^4(\ell-q)^2} &= \frac{i}{(4\,\pi)^2}\frac{q^\mu}{q^2}\,,\\
\int \frac{\mathrm{d}^Dl}{(2\,\pi)^D}\frac{\ell^\mu\ell^\nu}{\ell^4(\ell-q)^2} &= \frac{i}{(4\,\pi)^2}\frac{1}{4}\left\{\left[\frac{1}{\hat\epsilon}+2-\log\left(-\frac{q^2}{\mu}\right)\right]g^{\mu\nu}+2\,\frac{q^\mu q^\nu}{q^2}\right\}\,,
\end{aligned}
$$

$$
\begin{aligned}
\int \frac{\mathrm{d}^D\ell}{(2\,\pi)^D}\frac{\ell^\mu}{\ell^2(\ell-p_1)^2(\ell-p_2)^2} &= \frac{i}{(4\,\pi)^2\lambda}\left[C_1\left(p_1^2,p_2^2,p_3^2\right)\,p_1^\mu+C_1\left(p_2^2,p_1^2,p_3^2\right)\,p_2^\mu\right]\,,\\
C_1\left(p_1^2,p_2^2,p_3^2\right) &= \left(p_1^2+p_2^2-p_3^2\right)\log\left(\frac{p_1^2}{p_3^2}\right)-2p_2^2\log\left(\frac{p_2^2}{p_3^2}\right)\\
&\quad-p_2^2\left(p_3^2+p_1^2-p_2^2\right)C_0\left(p_1^2,p_2^2,p_3^2\right)\,,\\
\int \frac{\mathrm{d}^D\ell}{(2\,\pi)^D}\frac{\ell^\mu}{\ell^4(q-p_1)^2(q-p_2)^2} &= \frac{i}{(4\,\pi)^2\lambda}\left[\tilde C_1\left(p_1^2,p_2^2,p_3^2\right)\,p_1^\mu+\tilde C_1\left(p_2^2,p_1^2,p_3^2\right)\,p_2^\mu\right]\,,\\
\tilde C_1\left(p_1^2,p_2^2,p_3^2\right) &= \frac{(p_1^2+p_2^2-p_3^2)}{p_1^2}\log\left(\frac{p_2^2}{p_3^2}\right)-2\log\left(\frac{p_1^2}{p_3^2}\right)\\
&\quad-\left(p_2^2+p_3^2-p_1^2\right)C_0\left(p_1^2,p_2^2,p_3^2\right)\,,
\end{aligned}
\tag{G.13}
$$

once more, $p_3 = -\,p_1 - p_2$.

Appendix H :

Renormalization of the linear sigma model

In this appendix, we renormalize the linear sigma model at one–loop for finite pion mass. We will use the mass–independent $\overline{\rm MS}$ scheme, instead of the subtraction scheme of Ref. [182]. So our Lagrangian will be split into renormalized pieces and counterterms.

It is convenient to use the "primitive" set of parameters in the Lagrangian, namely g, μ and β and also to include explicitly the term linear in the σ field. Our Lagrangian is then written in terms of bare constants and fields. We then can reexpress the Lagrangian in terms of renormalized quantities and counterterms,

$$\mathcal{L} \;=\; \frac{1}{4}\left\langle \partial_\mu \Sigma\, \partial^\mu \Sigma^\dagger \right\rangle + \frac{\mu^2}{4}\left\langle \Sigma\, \Sigma^\dagger \right\rangle - \frac{g}{16}\left\langle \Sigma\Sigma^\dagger \right\rangle^2 + \beta\left\langle \Sigma + \Sigma^\dagger \right\rangle + \mathcal{L}_{c.t.}\,, \quad \text{(H.1)}$$

In the $\overline{\rm MS}$ scheme we will absorb in the counterterms the divergent pieces proportional to $\frac{1}{\hat{\epsilon}}$. Now we treat the counterterms as perturbations and then the non–perturbative part (kinetic term plus masses) must have the usual term with a positive mass squared. In other words, perturbation must be done around a minimum of the potential. This was already discussed in Section 6.3.

At tree–level, one can calculate the VEV directly from the Lagrangian by minimizing the potential. At one–loop, the most convenient procedure is to impose the condition that the one–point σ function identically vanishes, as shown in Fig. H.1. This ensures that we are considering quantum excitations around an extremum of the potential. It also implies that one–point functions (tadpoles) are zero in any graph, so we will not display this topology.

Let us start calculating the quantum corrections for the π and σ propagators, as shown in Fig. H.2. The pion propagator is diagonal in isospin, and thus proportional to δ^{ab}, which we drop . The renormalized one–loop contributions are

$$\begin{aligned} T^\pi &= \frac{g}{16\,\pi^2}\left[2\left(m_\sigma^2 - m^2\right) I_{\sigma\pi}(q^2) - 2\,m_\sigma^2\, A_\sigma + 2\,m^2 A_\pi\right]\,, \\ T^\sigma &= \frac{3\,g}{16\,\pi^2}\left(m_\sigma^2 - m^2\right)\left[I_{\pi\,\pi}(q^2) + 3\,I_{\sigma\sigma}(q^2)\right]\,, \end{aligned} \quad \text{(H.2)}$$

Figure H.1: One point σ function. Double line denotes σ particle and dashed line pions. It must vanish to ensure that perturbation theory is done around a minimum of the potential.

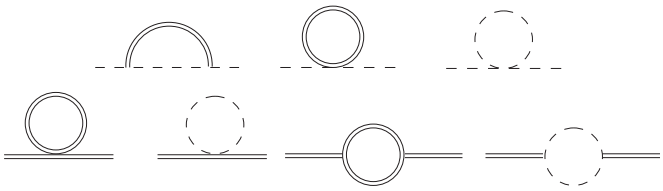

Figure H.2: One–loop diagrams for the π propagator.

where we have defined

$$
\begin{aligned}
A_\pi &= 1 - \log\left(\frac{m^2}{\mu^2}\right), \quad A_\sigma \,=\, 1 - \log\left(\frac{m_\sigma^2}{\mu^2}\right), \\
I_{\pi\,\pi}(q^2) &= A_\pi + 1 - \beta_\pi(q^2)\log\left(\frac{\beta_\pi(q^2)+1}{\beta_\pi(q^2)-1}\right), \\
I_{\sigma\sigma}(q^2) &= A_\sigma + 1 - \beta_\sigma(q^2)\log\left(\frac{\beta_\sigma(q^2)+1}{\beta_\sigma(q^2)-1}\right), \\
I_{\sigma\pi}(q^2) &= 1 + \frac{1}{m_\sigma^2 - m^2}\left[m_\sigma^2\, A_\sigma - m^2\, A_\pi\right] \\
&\quad + \frac{1}{2}\left(\frac{m_\sigma^2 - m^2}{s} - \frac{m_\sigma^2 + m^2}{m_\sigma^2 - m^2}\right)\log\left(\frac{m^2}{m_\sigma^2}\right) \\
&\quad - \frac{\nu(s)}{2\,s}\log\left\{\frac{[s+\nu(s)]^2 - (m_\sigma^2 - m^2)^2}{[s-\nu(s)]^2 - (m_\sigma^2 - m^2)^2}\right\}, \\
\beta_\pi(q^2) &= \sqrt{1 - \frac{4\,m^2}{q^2}}, \qquad \beta_\sigma(q^2) \,=\, \sqrt{1 - \frac{4\,m_\sigma^2}{q^2}}, \\
\nu(s) &= \sqrt{[s - (m_\sigma^2 + m^2)][s - (m_\sigma^2 - m^2)]},
\end{aligned}
\tag{H.3}
$$

From the renormalization of the propagators one can obtain the running of the g coupling constant

$$
\frac{\mu}{g}\,\frac{\mathrm{d}g}{\mathrm{d}\mu} \,=\, \frac{3}{2\,\pi^2}\,g\,, \tag{H.4}
$$

which ensures that observables are μ–independent.

Next we calculate the vertex correction to the $\sigma\,\pi\,\pi$ interaction, that is, the irreducible three–point function. This correction would affect, among other things,

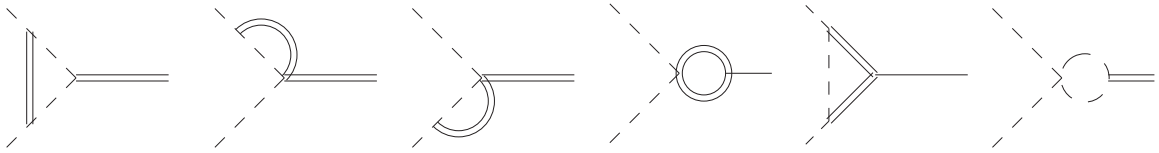

Figure H.3: Quantum corrections to the $\sigma - \pi\pi$ vertex.

the decay of the σ into two pions. The diagrams are shown in Fig. H.3. Since the σ is an isospin singlet, its coupling to the pair $\pi^a\,\pi^b$ must be proportional to δ^{ab} which again will not be displayed. The renormalized result then reads

$$\begin{aligned} T^{\sigma-\pi\,\pi} \;&=\; -\,2\,g\,v + \frac{g^2 v}{8\,\pi^2}\left[2\left(m_\sigma^2 - m^2\right)V_\sigma(s) + 6\left(m_\sigma^2 - m^2\right)V_\pi(s)\right. \\ &\quad \left. +\,4\,I_{\sigma\pi}(m^2) + 5\,I_{\pi\,\pi}(s) + 3\,I_{\sigma\sigma}(s)\right]\,, \end{aligned} \tag{H.5}$$

where we define three–point one–loop functions as

$$\begin{aligned} V_\sigma(s) \;=\; &-\frac{1}{s\,\beta_\pi(s)}\left\{2\,\mathrm{Li}_2\left[\frac{4\,m^2 - 2\,m_\sigma^2 + s\,(\beta_\pi(s)-1)}{8\,m^2 - 2\,m_\sigma^2 + s\,(3\beta_\pi(s)-2)}\right]\right. \\ &-2\,\mathrm{Li}_2\left[\frac{4\,m^2 - 2\,m_\sigma^2 + s\,(3\,\beta_\pi(s)-1)}{8\,m^2 - 2\,m_\sigma^2 + 2\,s\,(\beta_\pi(s)-1)}\right] \\ &-2\,\mathrm{Li}_2\left[-\frac{4\,m^2 - 2\,m_\sigma^2 + s\,(3\,\beta_\pi(s)-1)}{2\,m_\sigma^2\beta_\pi(s) + \frac{s m_\sigma^2}{2m^2}\,(3\,\beta_\pi(s)-1)\,(\beta_\pi(m^2)-1)}\right] \\ &-2\,\mathrm{Li}_2\left[\frac{1}{\beta_\pi(m_\sigma^2) + \frac{s}{4m^2}\,(3\,\beta_\pi(s)-1)\,(\beta_\pi(m_\sigma^2)-1)}\right] \\ &+\mathrm{Li}_2\left[\frac{1}{\beta_\pi(m_\sigma^2) + \frac{s}{4m^2}\,(\beta_\pi(s)-1)\,(\beta_\pi(m_\sigma^2)-1)}\right] \\ &-2\,\mathrm{Li}_2\left[-\frac{4\,m^2 - 2\,m_\sigma^2 + s\,(\beta_\pi(s)-1)}{2\,m_\sigma^2\beta_\pi(m_\sigma^2) + \frac{s m_\sigma^2}{2m^2}\,(\beta_\pi(s)-1)\,(\beta_\pi(m_\sigma^2)-1)}\right] \\ &\left.+\,\mathrm{Li}_2\left[\frac{\beta_\pi(s)-3}{(\beta_\pi(s)-1)\left[\beta_\pi(m_\sigma^2) + \frac{s}{4m^2}\,(3\,\beta_\pi(s)-1)\,(\beta_\pi(m_\sigma^2)-1)\right]}\right]\right\}\,, \end{aligned} \tag{H.6}$$

$$\begin{aligned} V_\pi(s) \;&-\; \frac{1}{s\,\beta_\pi(s)}\left\{2\,\mathrm{Li}_2\left[\frac{-2\,m_\sigma^2 + s\,(1-\beta_\pi(s))}{s - 2\,m_\sigma^2 + s\,\beta_\pi(s)\,(\beta_\sigma(s)-2)}\right]\right. \\ &-2\,\mathrm{Li}_2\left[\frac{-2\,m_\sigma^2 + s\,(1-3\,\beta_\pi(s))}{s - 2\,m_\sigma^2 + s\,\beta_\pi(s)\,(\beta_\sigma(s)-2)}\right] \\ &+2\,\mathrm{Li}_2\left[-\frac{2m_\sigma^2 + s\,(3\,\beta_\pi(s)-1)}{s + 2\,m_\sigma^2\beta_\pi(m_\sigma^2) - 3\,s\,\beta_\pi(s) + \frac{s m_\sigma^2}{m^2}\,(3\,\beta_\pi(s)-1)\,(\beta_\pi(m_\sigma^2)+1)}\right] \\ &\left.-2\,\mathrm{Li}_2\left[\frac{4\,m^2 - 2\,m_\sigma^2}{s + 2\,m_\sigma^2\beta_\pi(m_\sigma^2) - 3\,s\,\beta_\pi(s) + \frac{s m_\sigma^2}{2m^2}\,(3\,\beta_\pi(s)-1)\,(\beta_\pi(m_\sigma^2)+1)}\right]\right. \end{aligned} \tag{H.7}$$

$$+\,\mathrm{Li}_2\left[\frac{4\,m^2-2\,m_\sigma^2}{s+2\,m_\sigma^2\beta_\pi(m_\sigma^2)-s\,\beta_\pi(s)+\frac{s\,m_\sigma^2}{2m^2}\,(\beta_\pi(s)-1)\,(\beta_\pi(m_\sigma^2)+1)}\right]$$

$$+\,\mathrm{Li}_2\left[\frac{(4\,m^2-2\,m_\sigma^2)\,s\,(\beta_\pi(s)-3)}{s\,(\beta_\pi(s)-1)\left[s+2\,m_\sigma^2\,\beta_\pi(m_\sigma^2)-3\,s\,\beta_\pi(s)+\frac{s\,m_\sigma^2}{2m^2}\,(3\,\beta_\pi(s)-1)\,(\beta_\pi(m_\sigma^2)+1)\right]}\right] .$$

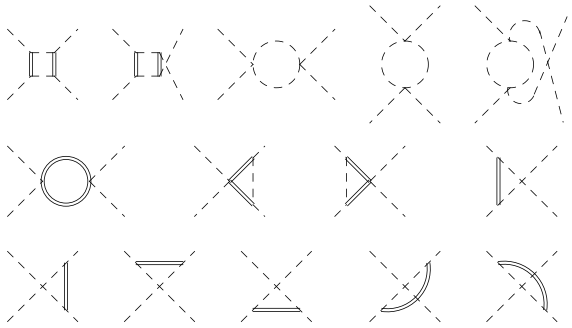

Figure H.4: Diagrams contributing to the 4–π irreducible Green Function.

The last set of diagrams to be considered are the corrections to the four–pion vertex, that is, the four–point irreducible function. Diagrams are shown in Fig H.4 and only contribute to the $\pi\,\pi$ scattering. The structure of the amplitude for the process $\pi^a\,\pi^b \to \pi^c\,\pi^d$ is identical to that of Eq. (6.39), and our result corresponds to $A(s,t,u)$. The renormalized result is

$$\begin{aligned} A^{4\pi} &= -2\,g+\frac{g^2}{8\pi^2}\left\{2\left(m_\sigma^2-m^2\right)^2\left[D(s,t)+D(s,u)\right]+V_\sigma(t)+V_\sigma(u)+I_{\sigma\sigma}(s)\right. \\ &\left.+4\left(m_\sigma^2-m^2\right)\left[V_\pi(s)+V_\sigma(s)\right]+7\,I_{\pi\,\pi}(s)+2\left[I_{\pi\,\pi}(t)+I_{\pi\,\pi}(u)\right]\right\}\,, \end{aligned} \tag{H.8}$$

where $D(s,t)$ is the scalar four–point one–loop function, or scalar box diagram, with all external momenta set to m^2 and two internal masses equal to m and the other two equal to m_σ, as can be deduced from Fig. H.4. Its expression is rather cumbersome and will not be displayed here, but it can be found for instance in Ref. [198].

All the pieces must be combined together to give the one–loop amplitude. First we recall the tree–level amplitude

$$A(s,t)_{\mathrm{tree-level}} = -\frac{g}{2}\,\frac{s-m^2}{s-m_\sigma^2}\,, \tag{H.9}$$

which reduces to the well known $\mathcal{O}(p^2)$ χPT result when the $m_\sigma \to \infty$ limit is taken. The renormalized one–loop amplitude is then

$$\begin{aligned} A(s,t)_{1-\mathrm{loop}} &= \frac{g^2}{8\,\pi^2}\left\{2\left(m_\sigma^2-m^2\right)^2\left[D(s,t)+D(s,u)\right]+V_\sigma(t)+V_\sigma(u)+I_{\sigma\sigma}(s)\right. \\ &\left.+4\left(m_\sigma^2-m^2\right)\left[V_\pi(s)+V_\sigma(s)\right]+7\,I_{\pi\,\pi}(s)+2\left[I_{\pi\,\pi}(t)+I_{\pi\,\pi}(u)\right]\right. \end{aligned}$$

$$
\begin{aligned}
&+ \frac{3\left(m_\sigma^2 - m^2\right)^2}{\left(m_\sigma^2 - s\right)^2}\left[I_{\pi\,\pi}(s) + 3\,I_{\sigma\sigma}(s) - 3\,A_\sigma\right] \\
&+ 2\,\frac{\left(m_\sigma^2 - m^2\right)}{s - m_\sigma^2}\left[2\left(m_\sigma^2 - m^2\right)V_\sigma(s) + 6\left(m_\sigma^2 - m^2\right)V_\pi(s)\right. \\
&\left. +\ 4\,I_{\sigma\pi}(m^2) + 5\,I_{\pi\,\pi}(s) + 3\,I_{\sigma\sigma}(s)\right]\Big\}\ , \qquad \text{(H.10)}
\end{aligned}
$$

and the total amplitude to one–loop is given by adding the two. It is μ–independent once we take into account the running coupling constant of Eq. (H.4).

Bibliography

[1] S. Weinberg, *"The Quantum Theory of Fields, Vol I: Foundations"* and *"Vol II: Modern Applications,"* Cambridge University Press (1995).

[2] A. Pich, "Aspects of quantum chromodynamics," arXiv:hep-ph/0001118.

[3] A. Pich, "The Standard Model of Electroweak Interactions," arXiv:0705.4264 [hep-ph].

[4] A. V. Manohar, "Effective field theories," arXiv:hep-ph/9606222.

[5] A. Pich, "Effective field theory," arXiv:hep-ph/9806303.

[6] J. Goldstone, "Field Theories With Superconductor Solutions," Nuovo Cim. **19** (1961) 154.

[7] S. R. Coleman, J. Wess and B. Zumino, "Structure Of Phenomenological Lagrangians. 1," Phys. Rev. **177** (1969) 2239;
C. G. Callan, S. R. Coleman, J. Wess and B. Zumino, "Structure Of Phenomenological Lagrangians. 2," Phys. Rev. **177** (1969) 2247.

[8] S. Weinberg, "Phenomenological Lagrangians," Physica A **96** (1979) 327.

[9] J. Gasser and H. Leutwyler, "Chiral Perturbation Theory To One Loop," Annals Phys. **158** (1984) 142;
J. Gasser and H. Leutwyler, "Chiral Perturbation Theory: Expansions In The Mass Of The Strange Quark," Nucl. Phys. B **250** (1985) 465;
J. Gasser and H. Leutwyler, "Low–energy Expansion for Meson Form-Factors," Nucl. Phys. B **250** (1985) 517.

[10] G. 't Hooft, "A Planar Diagram Theory For Strong Interactions", Nucl. Phys. B **72** (1974) 461;
G. 't Hooft, "A Two-Dimensional Model For Mesons", Nucl. Phys. B **75** (1974) 461.

[11] A. V. Manohar, "Large N QCD," arXiv:hep-ph/9802419.

[12] S. R. Coleman and E. Witten, "Chiral Symmetry Breakdown In Large N Chromodynamics," Phys. Rev. Lett. **45** (1980) 100.

[13] G. Ecker, J. Gasser, A. Pich and E. de Rafael, "The Role Of Resonances In Chiral Perturbation Theory," Nucl. Phys. B **321** (1989) 311;
G. Ecker, J. Gasser, H. Leutwyler, A. Pich and E. de Rafael, "Chiral Lagrangians For Massive Spin 1 Fields,"Phys. Lett. B **396** (1993) 205.

[14] R. F. Dashen, E. E. Jenkins and A. V. Manohar, "Spin flavor structure of large N_c baryons," Phys. Rev. D **51** (1995) 3697 [arXiv:hep-ph/9411234].

[15] K. G. Wilson,"Non-Lagrangian Models of Current Algebra," *Phys. Rev.* **179** (1969) 1499-1512.

[16] M. A. Shifman, A. I. Vainshtein and V. I. Zakharov, " QCD and Resonance Physics: Theoretical Foundations," *Nucl. Phys.* B **147** (1979) 385-447;
" QCD and Resonance Physics: Applications," *Nucl. Phys.* B **147** (1979) 448-418.

[17] T. Applequist and J. Carazone, "Infrared Singularities and Massive Fields," Phys. Rev. D **11** (1975) 2856.

[18] S. Scherer, "Introduction to chiral perturbation theory," Adv. Nucl. Phys. **27** (2003) 277 [arXiv:hep-ph/0210398].

[19] G. Ecker, "Chiral Perturbation Theory," Prog. Part. Nucl. Phys. **35** (1995) 1 [arXiv:hep-ph/9501357].

[20] D. J. Gross and F. Wilczek, "Ultraviolet Behavior Of Non-Abelian Gauge Theories," Phys. Rev. Lett. **30** (1973) 1343;
D. J. Gross and F. Wilczek, "Asymptotically Free Gauge Theories. 1," Phys. Rev. D **8** (1973) 3633;
D. J. Gross and F. Wilczek, "Asymptotically Free Gauge Theories. 2," Phys. Rev. D **9** (1974) 980.

[21] H. D. Politzer, "Reliable Perturbative Results for Strongs Interactions?," Phys. Rev. Lett. **30** (1973) 1346.

[22] H. Leutwyler, "On The Foundations Of Chiral Perturbation Theory," Annals Phys. **235** (1994) 165 [arXiv:hep-ph/9311274].

[23] O. Cata and V. Mateu, "Chiral Perturbation Theory with tensor sources," JHEP **0709** (2007) 078 arXiv:0705.2948 [hep-ph].

[24] C. Vafa and E. Witten, "Restrictions On Symmetry Breaking In Vector-Like Gauge Theories," Nucl. Phys. B **234** (1984) 173.

[25] A. Manohar and H. Georgi, "Chiral Quarks And The Nonrelativistic Quark Model," Nucl. Phys. B **234** (1984) 189.

[26] O. Cata and V. Mateu, "Novel patterns for vector mesons from the large-Nc limit," arXiv:0801.4374 [hep-ph].

[27] H. W. Fearing and S. Scherer, "Extension of the chiral perturbation theory meson Lagrangian to order p(6)," Phys. Rev. D **53** (1996) 315 [arXiv:hep-ph/9408346].

[28] J. Bijnens, G. Colangelo and G. Ecker, "The mesonic chiral Lagrangian of order p**6," JHEP **9902** (1999) 020 [arXiv:hep-ph/9902437];
J. Bijnens, G. Colangelo and G. Ecker, "Renormalization of chiral perturbation theory to order p**6," Annals Phys. **280** (2000) 100 [arXiv:hep-ph/9907333].

[29] C. Haefeli, M. A. Ivanov, M. Schmid and G. Ecker, "On the mesonic Lagrangian of order p^6 in chiral SU(2)," arXiv:0705.0576 [hep-ph].

[30] J. Wess and B. Zumino, "Consequences of anomalous Ward identities," Phys. Lett. B **37** (1971) 95.

[31] E. Witten, "Global Aspects Of Current Algebra," Nucl. Phys. B **223** (1983) 422.

[32] J. Bijnens, G. Ecker and J. Gasser, "Chiral perturbation theory," arXiv:hep-ph/9411232.

[33] J. Bijnens, L. Girlanda and P. Talavera, "The anomalous chiral Lagrangian of order p^6," Eur. Phys. J. C **23** (2002) 539 [arXiv:hep-ph/0110400].

[34] T. Ebertshauser, H. W. Fearing and S. Scherer, "The anomalous chiral perturbation theory meson Lagrangian to order p^6 revisited," Phys. Rev. D **65** (2002) 054033 [arXiv:hep-ph/0110261].

[35] A. Pich, "Colourless mesons in a polychromatic world," arXiv:hep-ph/0205030.

[36] S. Coleman, "1/N" in "Aspects of Symmetry", Cambridge University press, Cambridge, 1985.

[37] E. Witten, "Baryons In The 1/N Expansion," Nucl. Phys. B **160** (1979) 57.

[38] R. Kaiser and H. Leutwyler, "Large N_c in chiral perturbation theory," Eur. Phys. J. C **17** (2000) 623 [arXiv:hep-ph/0007101].

[39] G. Ecker and C. Zauner, "Tensor meson exchange at low energies," Eur. Phys. J. C **52** (2007) 315 arXiv:0705.0624 [hep-ph].

[40] V. Mateu and J. Portoles, "Form Factors in radiative pion decay," Eur. Phys. J. C **52** (2007) 325 arXiv:0706.1039 [hep-ph].

[41] V. Cirigliano, G. Ecker, M. Eidemuller, R. Kaiser, A. Pich and J. Portoles, "Towards a consistent estimate of the chiral low-energy constants," Nucl. Phys. B **753** (2006) 139 [arXiv:hep-ph/0603205].

[42] P. D. Ruiz-Femenia, A. Pich and J. Portoles, "Odd-intrinsic-parity processes within the resonance effective theory of QCD," JHEP **0307** (2003) 003 [arXiv:hep-ph/0306157];
P. D. Ruiz-Femenía, A. Pich and J. Portolés, "Phenomenology of the Green's function within the resonance chiral theory," Nucl. Phys. Proc. Suppl. **133** (2004) 215 [arXiv:hep-ph/0309345].

[43] P. D. Ruiz-Femenía, "Effective field theories for heavy and light fermions", PhD Thesis, University of Valencia (2003).

[44] E. E. Jenkins, "Large-N_c baryons," Ann. Rev. Nucl. Part. Sci. **48** (1998) 81 [arXiv:hep-ph/9803349].

[45] J. Gasser, M. E. Sainio and A. Svarc, "Nucleons With Chiral Loops," Nucl. Phys. B **307** (1988) 779.

[46] R. F. Dashen and A. V. Manohar, "Baryon - pion couplings from large N_c QCD," Phys. Lett. B **315** (1993) 425 [arXiv:hep-ph/9307241].

[47] J. L. Gervais and B. Sakita, "Large-N baryonic soliton and quarks," Phys. Rev. D **30** (1984) 1795.

[48] S. R. Coleman and J. Mandula, "All Possible Symmetries of the S Matrix," Phys. Rev. **159** (1967) 1251.

[49] V. Mateu "Ruptura de la simetría $SU(3)$ de sabor en desintegraciones semileptónicas de hiperones : Determinación de V_{us}," Treball d'Investigació Universitat de València (2005) (unpublished).

[50] J. Mondejar and A. Pineda, "Constraints on Regge models from perturbation theory," JHEP **0710** (2007) 061 arXiv:0704.1417 [hep-ph].

[51] M. Knecht and A. Nyffeler, "Resonance estimates of $O(p^6)$ low-energy constants and QCD short-distance constraints," Eur. Phys. J. C **21** (2001) 659 [arXiv:hep-ph/0106034].

[52] V. Cirigliano, G. Ecker, M. Eidemuller, A. Pich and J. Portoles, "The $\langle VAP\rangle$ Green function in the resonance region," Phys. Lett. B **596** (2004) 96 [arXiv:hep-ph/0404004].

[53] V. Cirigliano, G. Ecker, M. Eidemuller, R. Kaiser, A. Pich and J. Portoles, "The $\langle SPP\rangle$ Green function and SU(3) breaking in K(l3) decays," JHEP **0504** (2005) 006 [arXiv:hep-ph/0503108].

[54] P. Colangelo and A. Khodjamirian, "QCD sum rules: A modern perspective," [arXiv:hep-ph/0010175].

[55] E. de Rafael, "An introduction to sum rules in QCD," [arXiv:hep-ph/9802448].

[56] P. Pascual and R. Tarrach, "*QCD: Renormalization for the Practitioner*," Spriger (1984).

[57] M .E. Peskin and D. V. Shroder, *"An introduction to Quantum Field Theory*," Addison-Wesley (1995).

[58] L. J. Reinders, H. Rubinstein and S. Yazaki, "Hadron Properties From QCD Sum Rules," Phys. Rept. **127** (1985) 1.

[59] I. S. Gerstein and R. Jackiw, "Anomalies in ward identities for three-point functions," Phys. Rev. **181** (1969) 1955.

[60] M. Jamin and V. Mateu, "OPE-RchiT matching at order α_s: hard gluonic corrections to three-point Green functions," JHEP **0804** (2008) 040 arXiv:0802.2669 [hep-ph].

[61] G. Källén, Helv. Phys. Acta **25**, 417 (1952);
Lehmann, Nuoco Cimento **11**, 342 (1954).

[62] W. Zimmermann, "Normal products and the short distance expansion in the perturbation theory of renormalizable interactions," Annals Phys. **77** (1973) 570 [Lect. Notes Phys. **558** (2000) 278].

[63] V. A. Fock, Sov. Phys. **12** (1937) 404.

[64] J. Schwinger, *"Particles, Sources and Fields, Vol. II*" Addison-Wesley (1970).

[65] M. S. Dubonikov and A. V. Smilga, "Analitical Properties Of The Quark Polarization Operator In An External Selfdual Field," Nucl. Pyis. B **185** (1981) 109.

[66] V. A. Novikov, M. A. Shifman, A. I. Vainshtein and V. I. Zakharov, "Calculations In External Fields In Quantum Chromodynamics. Technical Review," Fortsch. Phys. **32** (1984) 585.

[67] E. G. Floratos, S. Narison and E. de Rafael, "Spectral Function Sum Rules In Quantum Chromodynamics. 1. Charged Currents Sector," Nucl. Phys. B **155** (1979) 115.

[68] I. Rosell, J. J. Sanz-Cillero and A. Pich, "Towards a determination of the chiral couplings at NLO in $1/N_c$: $L_8^r(\mu)$," JHEP **0701** (2007) 039 [arXiv:hep-ph/0610290].

[69] I. Rosell, "Quantum corrections in the resonance chiral theory," arXiv:hep-ph/0701248.

[70] G. P. Lepage and S. J. Brodsky, "Exclusive Processes In Perturbative Quantum Chromodynamics," Phys. Rev. D **22** (1980) 2157.

[71] J. Bijnens, E. Gamiz, E. Lipartia and J. Prades, "QCD short-distance constraints and hadronic approximations," JHEP **0304** (2003) 055 [arXiv:hep-ph/0304222].

[72] A. J. Buras, M. Jamin and P. H. Weisz, "Leading and Next-to-Leading QCD Corrections to epsilon parameter and $B_0 - \bar{B}_0$ Mising in the Presence of a Heavy Top Quark," Nucl. Phys. B **347** (1990) 491.

[73] D. J. Broadhurst and A. G. Grozin, "Matching QCD And Hqet Heavy - Light Currents At Two Loops And Beyond," Phys. Rev. D **52** (1995) 4082 [arXiv:hep-ph/9410240].

[74] J. A. Gracey, "Three loop $\overline{\rm MS}$ tensor current anomalous dimension in QCD," Phys. Lett. B **488** (2000) 175 [arXiv:hep-ph/0007171].

[75] T. van Ritbergen, J. A. M. Vermaseren and S. A. Larin, "The four-loop beta function in quantum chromodynamics," Phys. Lett. B **400**, 379 (1997) [arXiv:hep-ph/9701390].

[76] M. Jamin, "Flavour-symmetry breaking of the quark condensate and chiral corrections to the Gell-Mann-Oakes-Renner relation," Phys. Lett. B **538** (2002) 71 [arXiv:hep-ph/0201174].

[77] P. Ball, V. M. Braun and N. Kivel, "Photon distribution amplitudes in QCD," Nucl. Phys. B **649** (2003) 263 [arXiv:hep-ph/0207307].

[78] A. P. Bakulev and S. V. Mikhailov, "QCD vacuum tensor susceptibility and properties of transversely polarized mesons," Eur. Phys. J. C **17** (2000) 129 [arXiv:hep-ph/9908287].

[79] V. M. Braun, T. Burch, C. Gattringer, M. Gockeler, G. Lacagnina, S. Schaefer and A. Schafer, "A lattice calculation of vector meson couplings to the vector and tensor currents using chirally improved fermions," Phys. Rev. D **68** (2003) 054501 [arXiv:hep-lat/0306006].

[80] D. Becirevic, V. Lubicz, F. Mescia and C. Tarantino, "Coupling of the light vector meson to the vector and to the tensor current," JHEP **0305** (2003) 007 [arXiv:hep-lat/0301020].

[81] N. S. Craigie and J. Stern, "Sum Rules For The Spontaneous Chiral Symmetry Breaking Parameters Of QCD," Phys. Rev. D **26** (1982) 2430.

[82] M. Golterman and S. Peris, "Large-N_c QCD meets Regge theory: The example of spin-one two-point functions," JHEP **0101** (2001) 028 [arXiv:hep-ph/0101098].

[83] M. Golterman and S. Peris, "On the use of the operator product expansion to constrain the hadron spectrum," Phys. Rev. D **67** (2003) 096001 [arXiv:hep-ph/0207060].

[84] J. J. Sanz-Cillero, "Spin-1 correlators at large N_c: Matching OPE and resonance theory up to O(α_s)," Nucl. Phys. B **732**, 136 (2006) [arXiv:hep-ph/0507186].

[85] A. Bramon, E. Etim and M. Greco, "A Vector meson dominance approach to scale invariance," Phys. Lett. B **41**, 609 (1972).

[86] M. A. Donnellan *et al.*, "Lattice Results for Vector Meson Couplings and Parton Distribution Amplitudes," arXiv:0710.0869 [hep-lat].

[87] M. V. Chizhov, "Vector meson couplings to vector and tensor currents in extended NJL quark model," JETP Lett. **80** (2004) 73 [Pisma Zh. Eksp. Teor. Fiz. **80** (2004) 81] [arXiv:hep-ph/0307100].

[88] M. F. L. Golterman and S. Peris, "The 7/11 rule: An estimate of m_ρ/f_π," Phys. Rev. D **61** (2000) 034018 [arXiv:hep-ph/9908252].

[89] M. Davier, A. Hocker and Z. Zhang, "ALEPH tau spectral functions and QCD," Nucl. Phys. Proc. Suppl. **169** (2007) 22, [arXiv:hep-ph/0701170] ;
B. L. Ioffe and K. N. Zyablyuk, "Gluon condensate in charmonium sum rules with 3-loop corrections," Eur. Phys. J. C **27** (2003) 229; [arXiv:hep-ph/0207183];
F. J. Yndurain, "Gluon condensate from superconvergent QCD sum rule," Phys. Rept. **320** (1999) 287. [arXiv:hep-ph/9903457].

[90] V. M. Belyaev and B. L. Ioffe, "Determination Of Baryon And Baryonic Resonance Masses From QCD Sum Rules. 1. Nonstrange Baryons," Sov. Phys. JETP **56** (1982) 493 [Zh. Eksp. Teor. Fiz. **83** (1982) 876].

[91] I. I. Balitsky, A. V. Kolesnichenko and A. V. Yung, "On Vector Dominance In Sum Rules For Electromagnetic Hadron Characteristics. (In Russian)," Sov. J. Nucl. Phys. **41** (1985) 178 [Yad. Fiz. **41** (1985) 282].

[92] H. Georgi, "Weak Interactions And Modern Particle Theory," http://www.slac.stanford.edu/spires/find/hep/www?irn=1459899 *Menlo Park, Usa: Benjamin/cummings (1984) 165p*

[93] J. F. Donoghue, E. Golowich and B. R. Holstein, "Dynamics Of The Standard Model," Camb. Monogr. Part. Phys. Nucl. Phys. Cosmol. **2** (1992) 1.

[94] N. Cabibbo, "Unitary Symmetry and Leptonic Decays," Phys. Rev. Lett. **10** (1963) 531.

[95] M. Kobayashi and T. Maskawa, "CP Violation In The Renormalizable Theory Of Weak Interaction," Prog. Theor. Phys. **49** (1973) 652.

[96] A. Pich, "Flavourdynamics," [arXiv:hep-ph/9601202].

[97] J. Bijnens and P. Talavera, "$\pi \to l\nu\gamma$ form factors at two-loop," Nucl. Phys. B **489** (1997) 387 [arXiv:hep-ph/9610269].

[98] L. Ametller, J. Bijnens, A. Bramon and F. Cornet, "Semileptonic π and K decays and the chiral anomaly at one loop," Phys. Lett. B **303** (1993) 140 [arXiv:hep-ph/9302219].

[99] C. Q. Geng, I. L. Ho and T. H. Wu, "Axial-vector form factors for K(l2 γ) and π(l2 γ) at O(p^6) in chiral perturbation theory," Nucl. Phys. B **684** (2004) 281 [arXiv:hep-ph/0306165].

[100] E. Frlez *et al.*, "Precise measurement of the pion axial form factor in the $\pi^+ \to e^+\nu\gamma$ decay," Phys. Rev. Lett. **93** (2004) 181804 [arXiv:hep-ex/0312029].

[101] D. Počanić, talk given at the 5^{th} International Workshop on Chiral Dynamics, Theory and Experiment "Chiral Dynamics 2006", September 18th-22nd (2006), Durham (USA).

[102] V. N. Bolotov *et al.*, "The Experimental study of the $\pi^- \to e^-\bar{\nu}\gamma$ decay in flight," Phys. Lett. B **243** (1990) 308.

[103] A. A. Poblaguev, "On the $\pi \to e\nu\gamma$ decay sensitivity to a tensor coupling in the effective quark lepton interaction," Phys. Lett. B **238** (1990) 108.

[104] V. M. Belyaev and I. I. Kogan, "Supersymmetry and tensor coupling in $\pi^- \to e^-\bar{\nu}_e\gamma$ decay," Phys. Lett. B **280** (1992) 238;
Yu. Y. Komachenko, "Charged Higgs bosons in $\pi \to e\bar{n}u_e\gamma$ decay," Sov. J. Nucl. Phys. **55** (1992) 1384 [Yad. Fiz. **55** (1992) 2487].

[105] P. Herczeg, "On the question of a tensor interaction in $\pi \to e\bar{\nu}_e\gamma$ decay," Phys. Rev. D **49** (1994) 247.

[106] A. A. Poblaguev, "On the analysis of the $\pi \to e\nu\gamma$ experimental data," Phys. Rev. D **68** (2003) 054020 [arXiv:hep-ph/0307166].

[107] M. V. Chizhov, "Discovery of new physics in radiative pion decays?," Phys. Part. Nucl. Lett. **2** (2005) 193 [Pisma Fiz. Elem. Chast. Atom. Yadra **2N4** (2005) 7] [arXiv:hep-ph/0402105];
M. V. Chizhov, "New interactions in the radiative pion decay," [arXiv:hep-ph/0310203];
M. V. Chizhov, "Discovery of new physics in radiative pion decays?," Phys. Part. Nucl. Lett. **2** (2005) 193 [Pisma Fiz. Elem. Chast. Atom. Yadra **2N4** (2005) 7] [arXiv:hep-ph/0402105].

[108] P. A. Quin, T. E. Pickering, J. E. Schewe, P. A. Voytas and J. Deutsch, "Nuclear beta decay constraints on tensor contributions in $\pi \to e\nu\gamma$," Phys. Rev. D **47** (1993) 1247.

[109] M. A. Bychkov, talk given at the APS April Meeting-2007, April 14th-17th (2007), Jacksonville (USA).

[110] O. Strandberg, "Determination of the anomalous chiral coefficients of order p^6," arXiv:hep-ph/0302064.

[111] J. Bijnens, A. Bramon and F. Cornet, "Chiral Perturbation Theory For Anomalous Processes," Z. Phys. C **46** (1990) 599.

[112] W. M. Yao *et al.* [Particle Data Group], "Review of particle physics," J. Phys. G **33** (2006) 1.

[113] D. Gomez Dumm, A. Pich and J. Portoles, "$\tau \to \pi\pi\pi\nu_\tau$ decays in the resonance effective theory," Phys. Rev. D **69**, 073002 (2004) [arXiv:hep-ph/0312183].

[114] B. L. Ioffe and A. V. Smilga, "Nucleon Magnetic Moments And Magnetic Properties Of Vacuum In QCD," Nucl. Phys. B **232** (1984) 109.

[115] H. x. He and X. D. Ji, "QCD sum rule calculation for the tensor charge of the nucleon," Phys. Rev. D **54** (1996) 6897 [arXiv:hep-ph/9607408].

[116] E. A. Kuraev and Yu. M. Bystritsky, "Radiative corrections to radiative pi e2 decay," Phys. Rev. D **69** (2004) 114004 [arXiv:hep-ph/0310275].

[117] W. J. Marciano and A. Sirlin, Phys. Rev. Lett. **96** (2006) 032002 [arXiv:hep-ph/0510099].

[118] A. Czarnecki, W. J. Marciano and A. Sirlin, "Precision measurements and CKM unitarity," Phys. Rev. D **70** (2004) 093006 [arXiv:hep-ph/0406324].

[119] M. Battaglia *et al.*, "The CKM matrix and the unitarity triangle," [arXiv:hep-ph/0304132].

[120] W. J. Marciano and A. Sirlin, "Radiative Corrections To Beta Decay And The Possibility Of A Fourth Generation," Phys. Rev. Lett. **56** (1986) 22.

[121] A. Serebrov *et al.*, "Measurement of the neutron lifetime using a gravitational trap and a low-temperature Fomblin coating," Phys. Lett. B **605** (2005) 72 [arXiv:nucl-ex/0408009].

[122] V. Cirigliano, H. Neufeld and H. Pichl, "K(e3) decays and CKM unitarity," Eur. Phys. J. C **35** (2004) 53 [arXiv:hep-ph/0401173].

[123] V. Cirigliano, M. Knecht, H. Neufeld, H. Rupertsberger and P. Talavera, "Radiative corrections to K(l3) decays," Eur. Phys. J. C **23** (2002) 121 [arXiv:hep-ph/0110153].

[124] T. C. Andre, "Radiative corrections to K0(l3) decays," Annals Phys. **322** (2007) 2518 [arXiv:hep-ph/0406006].

[125] A. Sher *et al.*, "New, high statistics measurement of the $K^+ \to pi^0 e^+ \nu$ (K(e3)+) branching ratio," Phys. Rev. Lett. **91** (2003) 261802 [arXiv:hep-ex/0305042].

[126] T. Alexopoulos *et al.* [KTeV Collaboration], "A determination of the CKM parameter $|V_{us}|$," Phys. Rev. Lett. **93** (2004) 181802 [arXiv:hep-ex/0406001].

[127] A. Lai *et al.* [NA48 Collaboration], "Measurement of the branching ratio of the decay $K_L \to \pi^\pm e^\mp \nu$ and extraction of the CKM parameter $|V_{us}|$," Phys. Lett. B **602** (2004) 41 [arXiv:hep-ex/0410059].

[128] F. Ambrosino *et al.* [KLOE Collaboration], "Measurements of the absolute branching ratios for the dominant K_L decays, the K_L lifetime, and V_{us} with the KLOE detector," Phys. Lett. B **632** (2006) 43 [arXiv:hep-ex/0508027].

[129] V. Cirigliano, talk given at kaon 2005, http://diablo.phys.northwestern.edu/%7Eandy/conference.html.

[130] M. Ademollo and R. Gatto, "Nonrenormalization Theorem for the Strangeness Violating Vector Currents," Phys. Rev. Lett. **13** (1964) 264.

[131] R. E. Behrends and A. Sirlin, "Effect of mass splittings on the conserved vector current," Phys. Rev. Lett. **4** (1960) 186.

[132] H. Leutwyler and M. Roos, "Determination Of The Elements V_{us} And V_{ud} Of The Kobayashi-Maskawa Matrix," Z. Phys. C **25** (1984) 91.

[133] J. Bijnens and P. Talavera, "K(l3) decays in chiral perturbation theory," Nucl. Phys. B **669** (2003) 341 [arXiv:hep-ph/0303103].

[134] P. Post and K. Schilcher, "K(l3) form factors at order p^6 in chiral perturbation theory," Eur. Phys. J. C **25** (2002) 427 [arXiv:hep-ph/0112352].

[135] M. Jamin, J. A. Oller and A. Pich, "Order p^6 chiral couplings from the scalar K π form factor," JHEP **0402** (2004) 047 [arXiv:hep-ph/0401080].

[136] D. Becirevic *et al.*, "The $K \to \pi$ vector form factor at zero momentum transfer on the lattice," Nucl. Phys. B **705** (2005) 339 [arXiv:hep-ph/0403217].

[137] E. Gamiz, M. Jamin, A. Pich, J. Prades and F. Schwab, "Determination of m_s and $|V_{us}|$ from hadronic tau decays," JHEP **0301** (2003) 060 [arXiv:hep-ph/0212230].

[138] E. Gamiz, M. Jamin, A. Pich, J. Prades and F. Schwab, "V_{us} and m_s from hadronic tau decays," Phys. Rev. Lett. **94** (2005) 011803 [arXiv:hep-ph/0408044].

[139] W. J. Marciano, "Precise determination of $|V_{us}|$ from lattice calculations of pseudoscalar decay constants," Phys. Rev. Lett. **93** (2004) 231803 [arXiv:hep-ph/0402299].

[140] C. Aubin *et al.* [MILC Collaboration], "Light pseudoscalar decay constants, quark masses, and low energy constants from three-flavor lattice QCD," Phys. Rev. D **70** (2004) 114501 [arXiv:hep-lat/0407028].

[141] N. Cabibbo, E. C. Swallow and R. Winston, "Semileptonic hyperon decays," Ann. Rev. Nucl. Part. Sci. **53** (2003) 39 [arXiv:hep-ph/0307298];
"Semileptonic hyperon decays and CKM unitarity," Phys. Rev. Lett. **92** (2004) 251803 [arXiv:hep-ph/0307214].

[142] R. Flores-Mendieta, "V(us) from hyperon semileptonic decays," Phys. Rev. D **70** (2004) 114036 [arXiv:hep-ph/0410171].

[143] V. Mateu and A. Pich, "V(us) determination from hyperon semileptonic decays," JHEP **0510**, 041 (2005) [arXiv:hep-ph/0509045].

[144] R. Flores-Mendieta, E. E. Jenkins and A. V. Manohar, "SU(3) symmetry breaking in hyperon semileptonic decays," Phys. Rev. D **58** (1998) 094028 [arXiv:hep-ph/9805416].

[145] J. M. Gaillard and G. Sauvage, "Hyperon Beta Decays," Ann. Rev. Nucl. Part. Sci. **34** (1984) 351.

[146] A. García and P. Kielanowski, *The Beta Decay of Hyperons*, Lecture Notes in Physics Vol. 222 (Springer-Verlag, Berlin, 1985).

[147] V. Linke, "Leptonic decays of polarized baryons," Nucl. Phys. B **12** (1969) 669.

[148] A. Sirlin, "Universal Renormalization In Leptonic And Semileptonic Amplitudes," Phys. Rev. Lett. **32** (1974) 966.

[149] K. Toth, K. Szego and T. Margaritisz, "Radiative Corrections For Semileptonic Decays Of Hyperons: The 'Model Independent' Part," Phys. Rev. D **33** (1986) 3306.

[150] A. Martinez, J. J. Torres, R. Flores-Mendieta and A. Garcia, "Radiative corrections to the semileptonic Dalitz plot with angular correlation between polarized decaying hyperons and emitted charged leptons," Phys. Rev. D **63** (2001) 014025 [arXiv:hep-ph/0006279];
"Radiative corrections to the semileptonic Dalitz plot with angular correlation between polarized decaying and emitted hyperons," Phys. Rev. D **55** (1997) 5702.

[151] A. A. Affolder *et al.* [The KTeV E832/E799 Collaboration], "Observation of the decay $\Xi_0 \to \Sigma^+ e^- \bar{\nu}_e$," Phys. Rev. Lett. **82** (1999) 3751.

[152] J. F. Donoghue, B. R. Holstein and S. W. Klimt, "K-M Angles And SU(3) Breaking In Hyperon Beta Decay," Phys. Rev. D **35** (1987) 934.

[153] F. Schlumpf, "Beta decay of hyperons in a relativistic quark model," Phys. Rev. D **51** (1995) 2262 [arXiv:hep-ph/9409272].

[154] A. Krause, "Baryon Matrix Elements of the Vector Current in Chiral Perturbation Theory," Helv. Phys. Acta **63** (1990) 3.

[155] J. Anderson and M. A. Luty, "Chiral corrections to hyperon vector formfactors," Phys. Rev. D **47** (1993) 4975 [arXiv:hep-ph/9301219].

[156] R. F. Dashen, E. E. Jenkins and A. V. Manohar, "The $1/N_c$ expansion for baryons," Phys. Rev. D **49**, 4713 (1994) [Erratum-ibid. D **51**, 2489 (1995)] [arXiv:hep-ph/9310379].

[157] E. E. Jenkins and R. F. Lebed, "Baryon mass splittings in the $1/N_c$ expansion," Phys. Rev. D **52**, 282 (1995) [arXiv:hep-ph/9502227].

[158] J. Dai, R. F. Dashen, E. E. Jenkins and A. V. Manohar, "Flavor symmetry breaking in the $1/N_c$ expansion," Phys. Rev. D **53**, 273 (1996) [arXiv:hep-ph/9506273].

[159] A. Lacour, B. Kubis and U. G. Meissner, "Hyperon decay form factors in chiral perturbation theory," JHEP **0710** (2007) 083 arXiv:0708.3957 [hep-ph].

[160] G. Villadoro, "Chiral corrections to the hyperon vector form factors," Phys. Rev. D **74** (2006) 014018 [arXiv:hep-ph/0603226].

[161] H. R. Quinn and J. D. Bjorken, "Renormalization Of Weak Form-Factors, And The Cabibbo Angle," Phys. Rev. **171** (1968) 1660.

[162] A. Garcia, J. L. Garcia-Luna and G. Lopez Castro, "Neutron beta decay and the current determination of V(ud)," Phys. Lett. B **500** (2001) 66 [arXiv:nucl-th/0006037].

[163] H. Abele *et al.*, "Is the unitarity of the quark-mixing-CKM-matrix violated in neutron beta-decay?," Phys. Rev. Lett. **88**, 211801 (2002) [arXiv:hep-ex/0206058].

[164] R. J. Eden, P. V. Landshoff, D. I. Olive and J. C. Polkinghorne "*The Analitic S Matrix*," Cambridge University Press (1966).

[165] A. D. Martin and Spearman "Elementary particle theory" North Holland Publishing company (1970).

[166] M. Gell-Mann and M. Levy, "The Axial Vector Current In Beta Decay," Nuovo Cim. **16** (1960) 705.

[167] A. Hosaka and H. Toki "*Quarks, baryons and chiral symmetry*," World scientific (2001).

[168] G. Colangelo, J. Gasser and H. Leutwyler, "$\pi\,\pi$ scattering," Nucl. Phys. B **603** (2001) 125 [arXiv:hep-ph/0103088].

[169] G. Amoros, J. Bijnens and P. Talavera, "QCD isospin breaking in meson masses, decay constants and quark mass ratios," Nucl. Phys. B **602** (2001) 87 [arXiv:hep-ph/0101127].

[170] M. R. Pennington and J. Portoles, "The Chiral Lagrangian parameters, l_1, l_2, are determined by the ρ resonance," Phys. Lett. B **344** (1995) 399 [arXiv:hep-ph/9409426].

[171] A. V. Manohar and V. Mateu, "Dispersion Relation Bounds for $\pi\,\pi$ Scattering," Phys. Rev. D **77** (2008) 094019 arXiv:0801.3222 [hep-ph].

[172] V. Mateu, "Universal Bounds for SU(3) Low Energy Constants," Phys. Rev. D **77** (2008) 094020 arXiv:0801.3627 [hep-ph].

[173] B. Ananthanarayan, D. Toublan and G. Wanders, "Consistency Of The Chiral Pion Pion Scattering Amplitudes With Axiomatic Constraints," Phys. Rev. D **51** (1995) 1093 [arXiv:hep-ph/9410302].

[174] P. Dita, "Positivity constraints on chiral perturbation theory pion pion scattering amplitudes," Phys. Rev. D **59** (1999) 094007 [arXiv:hep-ph/9809568].

[175] J. Distler, B. Grinstein, R. A. Porto and I. Z. Rothstein, "Falsifying Models of New Physics via WW Scattering," Phys. Rev. Lett. **98** (2007) 041601 [arXiv:hep-ph/0604255].

[176] T. N. Pham and T. N. Truong, "Evaluation Of The Derivative Quartic Terms Of The Meson Chiral Lagrangian From Forward Dispersion Relation," Phys. Rev. D **31**, 3027 (1985).

[177] J. Comellas, J. I. Latorre and J. Taron, "Constraints On Chiral Perturbation Theory Parameters From QCD Inequalities," Phys. Lett. B **360** (1995) 109 [arXiv:hep-ph/9507258].

[178] J. L. Peterson, "The $\pi\,\pi$ Interaction," Yellow Report CERN 77-04 (1977).

[179] A. Martin, "Extension of the axiomatic analyticity domain of scattering amplitudes by unitarity. 1," Nuovo Cim. A **42** (1965) 930.

[180] M. Froissart, "Asymptotic behavior and subtractions in the Mandelstam representation," Phys. Rev. **123** (1961) 1053.

[181] J. Bijnens, G. Colangelo, G. Ecker, J. Gasser and M. E. Sainio, "Elastic $\pi\,\pi$ scattering to two loops," Phys. Lett. B **374** (1996) 210 [arXiv:hep-ph/9511397].

[182] D. Bessis and J. Zinn-Justin, "One-loop renormalization of the nonlinear sigma model," Phys. Rev. D **5** (1972) 1313.

[183] J. J. de Swart, "The Octet Model And Its Clebsch-Gordan Coefficients," Rev. Mod. Phys. **35**, 916 (1963).

[184] A. Gomez Nicola and J. R. Pelaez, "Meson meson scattering within one loop chiral perturbation theory and its Phys. Rev. D **65**, 054009 (2002) [arXiv:hep-ph/0109056].

[185] J. Bijnens, P. Dhonte and P. Talavera, "$\pi\,\pi$ scattering in three flavour ChPT," JHEP **0401** (2004) 050 [arXiv:hep-ph/0401039].

[186] J. Bijnens, P. Dhonte and P. Talavera, "π K scattering in three flavor ChPT," JHEP **0405** (2004) 036 [arXiv:hep-ph/0404150].

[187] M. R. Pennington, "Predictions for $\gamma\gamma \to \pi\pi$: What photons at DAPHNE will see,"

[188] J. Bijnens and F. Cornet, "Two Pion Production in Photon-Photon Collisions," Nucl. Phys. B **296** (1988) 557.

[189] J. F. Donoghue, B. R. Holstein and Y. C. Lin, "The Reaction $\gamma\gamma \to \pi^0\pi^0$ and Chiral Loops," Phys. Rev. D **37** (1988) 2423.

[190] J. A. Oller, E. Oset and J. Nieves, "Chiral Symmetry Approach to the f_0 (980) and a_0 (980) Resonances," arXiv:nucl-th/9601031.

[191] F. J. Llanes-Estrada, E. Oset and V. Mateu, "On the possible nature of the θ^+ as a K π N bound state," Phys. Rev. C **69** (2004) 055203 [arXiv:nucl-th/0311020].

[192] K. M. Watson, "Some general relations between the photoproduction and scattering of π mesons," Phys. Rev. **95**, 228 (1954).

[193] J. A. Oller and E. Oset, "Theoretical study of the $\gamma\gamma \to$ meson meson reaction," Nucl. Phys. A **629** (1998) 739 [arXiv:hep-ph/9706487].

[194] P. Ko, "Vector Meson Contributions to the Processes $\gamma\gamma \to \pi^0\pi^0$, $\pi^+\pi^-$, $K_L \to \pi^0\gamma\gamma$, and $K^+ \to \pi^+\gamma\gamma$," Phys. Rev. D **41** (1990) 1531.

[195] E. Kyriakopoulos, "Vector-Meson Interaction Hamiltonian," Phys. Rev. **183** (1969) 1318;
Y. Takahashi and R. Palmer, "Gauge-Independent Formulation Of A Massive Field With Spin One," Phys. Rev. D **1** (1970) 2974.

[196] K. Kampf, J. Novotny and J. Trnka, "On different Lagrangian formalisms for vector resonances within chiral perturbation theory," Eur. Phys. J. C **50** (2007) 385 [arXiv:hep-ph/0608051].

[197] A. Z. Capri, S. Kamefuchi and M. Kobayashi, "Lagrangians For Massive Totally Antisymmetric Tensor Fields," Prog. Theor. Phys. **74** (1985) 368;
A. Z. Capri, M. Kobayashi and Y. Ohnuki, "The Second Rank Tensor Field, A Systematic Study: Classification Of The Second Rank Tensor Field Theories," Prog. Theor. Phys. **77** (1987) 1484.

[198] A. Denner, U. Nierste and R. Scharf, "A Compact expression for the scalar one loop four point function," Nucl. Phys. B **367** (1991) 637.

Agraïments

Sempre és difícil escriure els agraïments d'una tesi, però al mateix temps una tesi no es pot considerar finalitzada si no s'escriuen. Aixíque anem-hi ...

En primer lloc, i com no podia ser de cap altra manera, vull agrair al meu director de tesi, Antonio Pich (Toni) el haver-me portat pel bon camí. Ell ha aconseguit que el que tan sols eren un bollit de idees al meu cap hagen acabat sent una tesi. Sempre ha sabut proposar temes interesants per a treballar i investigar, i quan no ha tingut temps ha sabut valorar e impulsar els meus propis projectes. Sempre ha sabut trobar una estona per a mi quan més em calia encara que la seva apretada agenda no ho permetés. Al seu costat he gaudit de la llibertat necessària i dels consells indispensables per a poder formar-me com a investigador.

En segon lloc, indiscutiblement, he de agrair a Jorge Portolés el incontable nombre d'hores que ha emprat per a ajudar-me en qualsevol cosa, desde recomanar bibliografia, aclarir dubtes, discutir idees o revisar documents (com aquesta tesi). Ha sigut un col·laborador impagable i ha sabut aconsellar-me sempre bé. Gran part d'esta tesi li la dec a ell.

En tercer lloc vull donar gràcies als meus col·aboradors, sense els quals aquesta tesi no seria mai el que és. Gràcies Oscar i Matthias. També he de estar agraït a aquelles persones que van acceptar que anara alguns mesos d'estància breu amb ells, com són els professors Michael Pennington (Durham), Aneesh V. Manohar (San Diego) i André Hoand (MPI Munich), i a les persones que allí vaig coneixer: David, Ivone i Karel a Durham; Mannie, Hanna i Rafael als Estats Units; i Julian, Carla, Daniela i Santi a Munich.

Els tres mesos passats a Trento també seran inoblidables per a mi. Vaig coneixer a molta gent allí, i de tots guarde un gran record. Gràcies a tots per aconseguir una atmosfera tant agradable, però gràcies especialment a Adam, Petr, Ciril i Chema, per estar sempre al meu costat.

Ha sigut també tot un plaer poder discutir de física amb altres estudiants de Toni, especialment amb Pedro, Juanjo i Natxo. Sempre és molt agradable trobar-me amb ells a conferències i workshops, i juntar-nos amb el Javi i el Jorge de Barcelona.

Durant quasi quatre anys he estat compartint despatx amb el Pablo, i crec sincerament que no podria haver-hi trobat cap altre company millor. Hem tingut una atmosfera de treball excel·lent i sempre hem sabut prendre un descans per a parlar o discutir de física quan calia. Tinc que estar-li especialment agraït al Pablo per totes les gestions burocràtiques que ha tingut que fer per a que esta tesi puguera ser llegida a temps (cosa que no ha estat gens trivial).

Gràcies també al professor Jiri Novotný per revisar la meua tesi encara sense ser membre del tribunal, i gràcies també per haver-me convidat a visitar-lo a l'Universitat de Praga.

A nivell personal he d'estar molt agraït a la meua dona Teresa, que ha sigut molt comprensiva amb mi quant he tingut que treballar fins tard bé perque tenia molta feina o tenia que discutir coses amb algú. Ella sempre ha cregut en mi, m'ha animat quan estava deprimit.

Finalment vull agrair als meus pares, Vicent i Trini, tot el suport que m'han donat sempre a nivell personal, per a aconseguir tot allò que m'he proposat. Ells sempre han cregut en mi i sempre m'han animat a que porte endavant els meus projectes. La seua labor com a pares i com a tutors ha segut part essencial de la meva formació com a persona.